

INTERNATIONAL COURT OF JUSTICE

DISPUTE OVER THE STATUS AND USE OF THE
WATERS OF THE SILALA

(CHILE v. BOLIVIA)

ADDITIONAL PLEADING OF THE
REPUBLIC OF CHILE

ANNEX 100 TO THE ADDITIONAL PLEADING AND
ANNEXES XV - XVI TO THE EXPERT REPORT

VOLUME 2 OF 2

16 SEPTEMBER 2019

VOLUME 2
LIST OF ANNEXES

ANNEX N°	TITLE	PAGE N°
ANNEX TO THE ADDITIONAL PLEADING		
Annex 100	100.1 Note from the Agent of the Republic of Chile to the Agent of the Plurinational State of Bolivia, 27 May 2019 (Original in English)	3
	100.2 Note from the Agent of the Plurinational State of Bolivia to the Agent of the Republic of Chile, 17 June 2019 (Original in English)	5
ANNEXES TO THE EXPERT REPORT		
Annex XV	Muñoz, J.F., Suárez, F., Sanzana, P. and Taylor, A., 2019. <i>Assessment of the Silala River Basin Hydrological Models Developed by DHI</i>	7
Annex XVI	SERNAGEOMIN (National Geology and Mining Service), 2019. <i>A Brief Review of the Geology presented in Annexes of the Rejoinder of the Plurinational State of Bolivia</i>	187

Annex 100

100.1 Note from the Agent of the Republic of Chile to the Agent
of the Plurinational State of Bolivia, 27 May 2019

100.2 Note from the Agent of the Plurinational State of Bolivia
to the Agent of the Republic of Chile, 17 June 2019

(Originals in English)



REPUBLICA DE CHILE
MINISTERIO DE RELACIONES EXTERIORES

27 May 2019

His Excellency
 Mr. Eduardo Rodríguez Veltzé
 Agent
 Plurinational State of Bolivia

Sir,

On behalf of the Government of the Republic of Chile, and with reference to the Dispute over the Status and Use of the Waters of the Silala (Chile v. Bolivia), I have the honour to refer to the Rejoinder filed by the Plurinational State of Bolivia on 15 May 2019 and, in particular, the sensitivity analysis conducted by the Danish Hydraulic Institute ("DHI") as reported in Annex 25 of the Rejoinder.

After consulting with its expert Prof. Howard Wheater, my Government wishes to convey that, in Prof. Wheater's expert opinion, the DHI sensitivity analysis model runs cannot be fully scrutinized without the relevant modelling data, including all model set-up, input and output files for all model runs that were reported in Annex 25 of the Rejoinder.

My Government requests submission of these modelling data that are essential to the analysis of DHI's recent results. It also requests that a copy of the data shall be formally deposited with the Registrar and be considered part of the record of the case. Finally, my Government suggests that the requested data shall be submitted promptly and no later than two weeks following receipt of this Note, to ensure their timely analysis by Chile's experts.

Attached you will find a letter from expert Prof. Howard Wheater, indicating the need for the requested information in order to complete the analysis of DHI's results.

Accept, Sir, the assurances of my highest consideration,

Ximena Fuentes Torrijo
 Agent of the Republic of Chile



EMBASSY OF THE PLURINATIONAL STATE OF BOLIVIA
The Hague – The Netherlands

EB.NL.-Cs- 31/2019

The Hague, 17 June 2019

Excellency
Mrs. Ximena Fuentes Torrijo
Agent of the Republic of Chile

Madam,

With reference to the case concerning the Dispute over the Status and Use of the Waters of the Silala (Chile v. Bolivia) and following my note dated 7 June 2019 regarding your request of the modelling data used by the Danish Hydraulic Institute (DHI) in the “Updating of the mathematical hydrological model scenarios of the Silala spring waters with: Sensitivity analysis of the model boundaries”, submitted in the Rejoinder of the Plurinational State of Bolivia as Annex 25, I hereby attach a USB containing the requested information.

Accept, Madam, the assurances of my highest consideration.

Eduardo Rodriguez Veltzé
Agent of the Plurinational State of Bolivia

Annex XV

Muñoz, J.F, Suárez, F., Sanzana, P. and Taylor, A., 2019.
Assessment of the Silala River Basin Hydrological Models
Developed by DHI

**ASSESSMENT OF THE SILALA RIVER BASIN HYDROLOGICAL MODELS
DEVELOPED BY DHI**

José Francisco Muñoz (PhD)

Professor, Pontificia Universidad Católica de Chile

Francisco Suárez (PhD)

Associate Professor, Pontificia Universidad Católica de Chile

Pedro Sanzana (PhD)

Project Manager, DICTUC S.A.

Adam Taylor (MSc)

Director, Groundwater Modelling Solutions Ltd., UK

María José Fuenzalida, Civil Engineer

Magdalena Lagos, Civil Engineer, MSc

Gonzalo Yáñez, Civil Engineer, MSc

August 2019

Annex XV

TABLE OF CONTENTS

1. INTRODUCTION.....	1
1.1 Objectives.....	4
1.2 Structure of the report.....	4
2. REVIEW OF BACKGROUND INFORMATION USED BY BOLIVIA FOR THE SILALA RIVER BASIN	5
2.1 Geological interpretation	12
3. WATER BALANCE MODEL (WBM)	20
3.1 Conceptual model.....	20
3.2 Numerical model	20
3.2.1 Boundary conditions	21
3.2.2 Water balance results	22
3.3 Main conclusions from the review of the WBM.....	23
4. NEAR FIELD MODEL (NFM)	24
4.1 Conceptual model.....	24
4.2 Numerical model	27
4.2.1 Topography of the NFM	28
4.2.2 Steady-state verification.....	34
4.2.3 Boundary conditions	35
4.2.4 Inconsistency between the Water Balance Model and the Near Field Model	36
4.2.5 Initial Potential Head of the Near Field – MIKE-SHE model	39
4.2.6 Surface water modelling	42
4.2.6.1 Surface flow calculation in the baseline scenario – MIKE-11	46
4.2.6.1.1 Downstream boundary condition	48
4.2.6.1.2 Manning coefficient and flow conditions	48
4.2.6.1.3 Channel geometry.....	52
4.2.6.1.4 Numerical instability in MIKE-11 model	56
4.2.6.2 Surface flow calculation in the No Canal and Undisturbed scenarios – MIKE-SHE Overland flow	58
4.2.7 Water balance results of the different scenarios modelled by DHI (2018).....	59
4.2.8 Summary of unreported differences between the DHI scenarios	63
5. CONCLUSIONS	65
6. REFERENCES.....	69
Appendix A	
Appendix B	
Appendix C	
Appendix D	

Annex XV

1. INTRODUCTION

The National Director of Borders and Boundaries (DIFROL) of the Ministry of Foreign Affairs, Mrs. Ximena Fuentes, asked professors José F. Muñoz and Francisco Suárez to review the study “*Study of the Flows in the Silala Wetlands and Springs System*”, commissioned by the Bolivian counterpart to the Danish Hydraulic Institute (DHI), and presented in the Bolivia’s Counter-Memorial (BCM) in 2018.

It was only after two requests that Bolivia provided Chile with the files used by DHI for the modelling reported in Bolivia’s Counter-Memorial, and these were received after Chile’s Reply (CR) of 15 February 2019 had been finalized. This report is based on the analysis of those files and complements and extends the previous analysis of DHI modelling, presented in Wheater and Peach, 2019 (CR, Vol.1, pp 85-154).

The focus of the DHI study was the surface water flow crossing the Chile-Bolivia international border in the Silala River, including the impacts of historical channelization. To analyze the hydrological behavior of the Silala River basin, DHI divided the study area into the Far Field and the Near Field:

- “The Near Field area covers all surface water features and immediate surroundings including springs, wetlands and canals” (BCM, Vol. 2, p. 367).
- The Far Field “is the full area contributing to the discharge through the springs and canals on the Bolivian territory” (BCM, Vol. 2, p. 328). The boundaries of the Far Field are uncertain, but a hydrological catchment was delineated by DHI (BCM, Vol. 2, p. 328; Figure 1-1). The Far Field catchment is roughly equivalent to the groundwater catchment described in the Chilean Reply (CR, Vol. 1, p. 105).

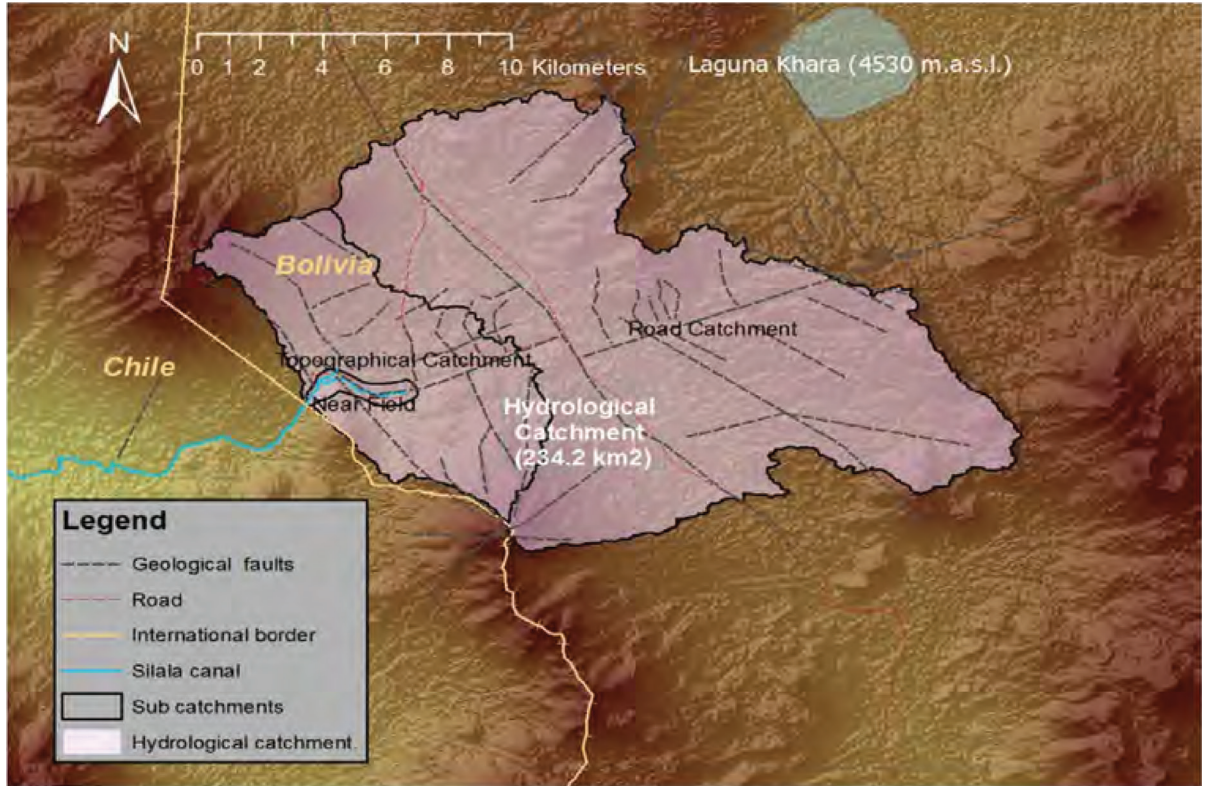


Figure 1-1. Hydrological catchment and Silala Near Field area defined in DHI (2018) (BCM, Vol. 2, p. 328).

DHI (2018) built three hydrological models: a Water Balance Model (WBM), a Near Field Model (NFM) and a Near Border Model (NBM). Each of these consists of a numerical model based on a conceptual model of the hydrological/hydrogeological processes. For the numerical models, DHI used an integrated groundwater/surface water model based on the MIKE-SHE model for coupled surface and groundwater flows. For one of the scenarios investigated (the Baseline scenario, representing current channelization) they also used the MIKE-11 modelling system for 1D open water flows.

The domain of each model is presented in Figure 1-2. The Water Balance Model covers the whole groundwater catchment of the Silala River upstream of the international border, excluding the area immediately adjacent to the wetlands. The excluded area is simulated in the Near Field Model. The Near Border Model covers the area of the Near Field Model between the confluence of the Orientales and Cajones tributaries and the international border. The NBM is not directly relevant to the main issues that remain in dispute between the parties and is therefore not considered further in this report.

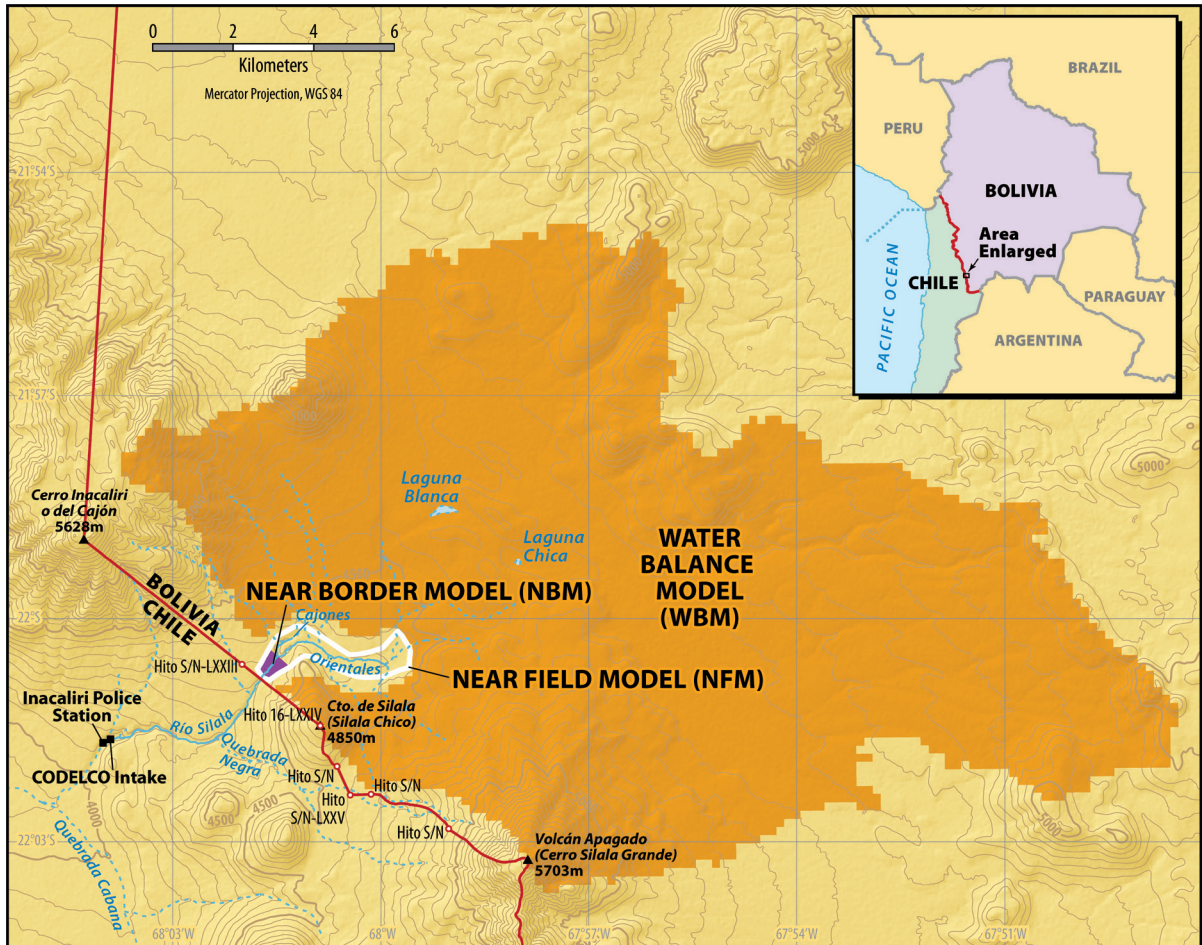


Figure 1-2. Domains covered by the three different DHI models.

The WBM was mainly used to estimate recharge and the available water resources in the Silala River Basin but was not used to assess surface or groundwater flow changes across the Chile-Bolivia international border. The NFM was used to compare scenarios with and without channelization and to quantify the influence of the channelization on the Silala River flow. The NBM was used by DHI to investigate infiltration from surface water to groundwater close to the border (between the confluence of the spring tributary channels and the border).

The NFM has been used to simulate various scenarios, in which the configuration of the model, and its inputs, are changed to evaluate the impact of the channelization. Three scenarios were used:

- i) Baseline: represents the current situation with channelization.
- ii) No Canal: represents the situation without channels.

- iii) Undisturbed: represents a ‘restored’ situation without channels and with assumed long-term development of wetland peat soils.

After the submission of the Bolivia's Counter-Memorial in 2018, Chile requested the data files of the three models. Two requests from Chile were necessary before DHI provided the requested files, which were received after Chile's Reply had been finalized. In this report, we review the DHI hydrological/hydraulic modelling in the light of this new information, in particular those aspects that deal with channelization impacts. The files provided by the Bolivian counterpart are specified in Appendix A.

Given its relevance to the continuing dispute between the Parties, the main focus of this report is a critical review of the Near Field Model, in which the impact of the channelization is evaluated using the three scenarios defined above. Additionally, we assess the consistency between the WBM and the NFM.

1.1 Objectives

The objectives of this study are therefore:

- To review the configuration, inputs, results and water balances of the Far Field and Near Field models.
- To carry out a critical review of the Near Field Model. Specifically, to evaluate whether the modelling approach is consistent with the available data and conceptual understanding of the Silala River basin and whether the scenarios selected are appropriate to represent the impacts of channelization.

1.2 Structure of the report

The structure of the remainder of this report is as follows: Section 2 presents relevant background information obtained from the Bolivian Counter-Memorial. Section 3 presents a brief review of the Water Balance Model, and in Section 4 the Near Field Model is analyzed in detail. In Section 5 the main conclusions are summarized and in Section 6 the references are presented.

2. REVIEW OF BACKGROUND INFORMATION USED BY BOLIVIA FOR THE SILALA RIVER BASIN

The background information collected by Bolivia and DHI for the hydrogeological study of the Silala River basin is presented in the BCM and associated annexes. A geological map of the entire basin is presented (BR, Complete Copies of Certain Annexes Vol.2, Annex 23.5 Appendix a, p.69, reproduced here as Figure 2-1). Also, the hydrological catchment delimitation is provided (BCM, Vol.2, p. 328, reproduced here as Figure 1-1), along with a Digital Elevation Model.

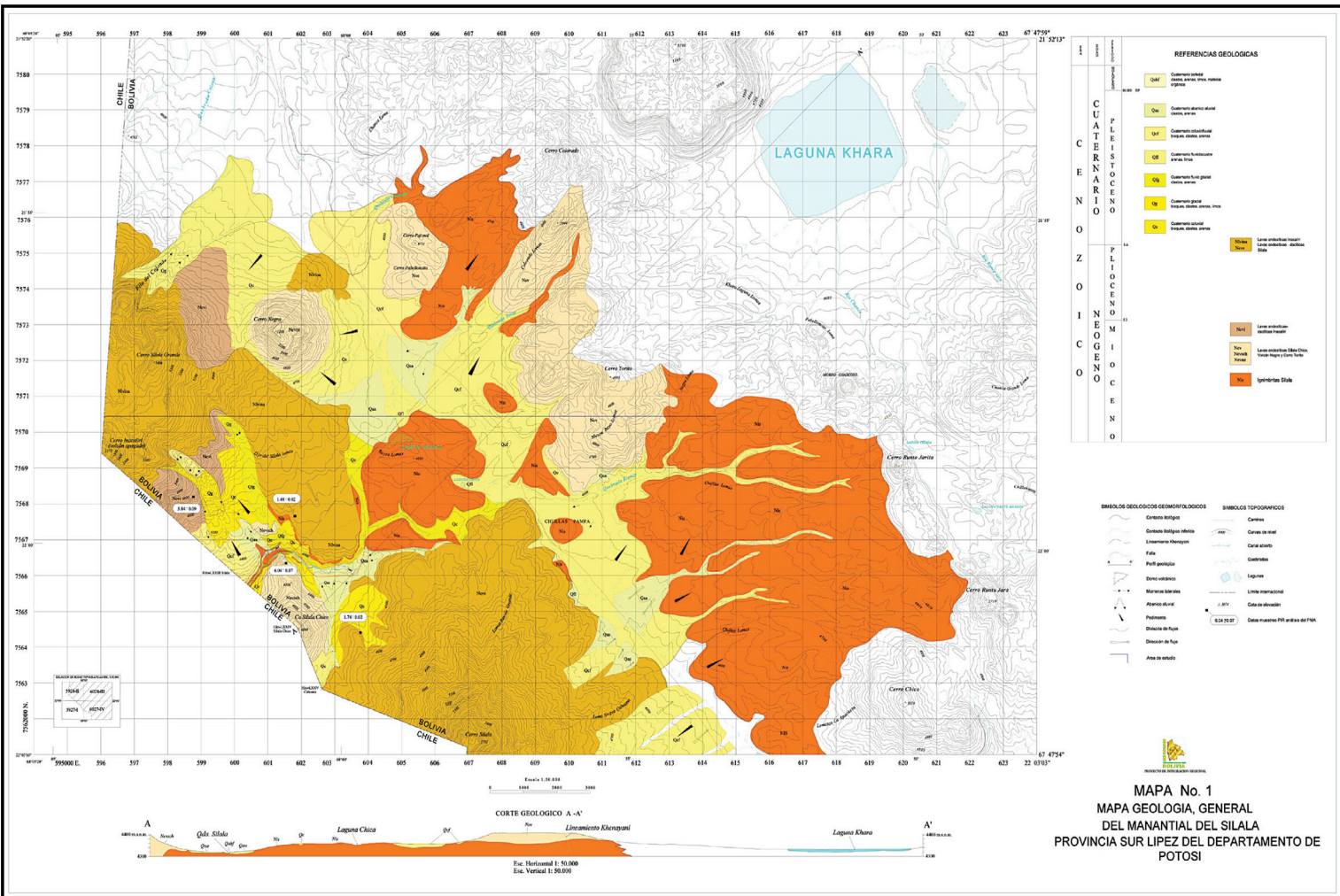


Figure 2-1. Geologic Map of the Silala Study Area (BR, Complete Copies of Certain Annexes, Vol. 2, Annex 23.5 Appendix a, p. 69). See also Figure 2-9 for larger legend

The Bolivian counterpart collected an extensive amount of field data in the Silala Near Field, including hydrogeological drilling and testing, surface flow, surface geological mapping, soil sampling in the wetlands and geophysical transect investigations.

For the hydrogeology study, presented in Annex F to the DHI Report (2018) (BCM, Vol. 4), wells and piezometers were drilled in the Silala Near Field. The locations of the boreholes and piezometers drilled are presented in Figure 2-2.



Figure 2-2. "Location of the boreholes and piezometers in the Silala Near Field" [Original Caption]. (BCM, Vol. 4, p. 25).

Water level monitoring was carried out by the Bolivian counterpart in these boreholes by taking manual measurements, typically on a daily basis. Groundwater level contours in the Silala Near Field, interpolated from piezometer wells, spring elevations, and wetland excavations for soil sampling, are presented in Figure 2-3, which is reproduced, together with the figure caption, from BCM, Vol.2, p. 293.¹ According to DHI (BCM, Vol. 4, p. 95) “[t]he contours reflect the interpretation of significant discharge to the Southern Wetlands from the north and northeast areas of the catchment as well as from recharge on Volcán Silala Grande”.

¹ The same figure, without the arrow, is also presented in BCM, Vol.4, p. 97.

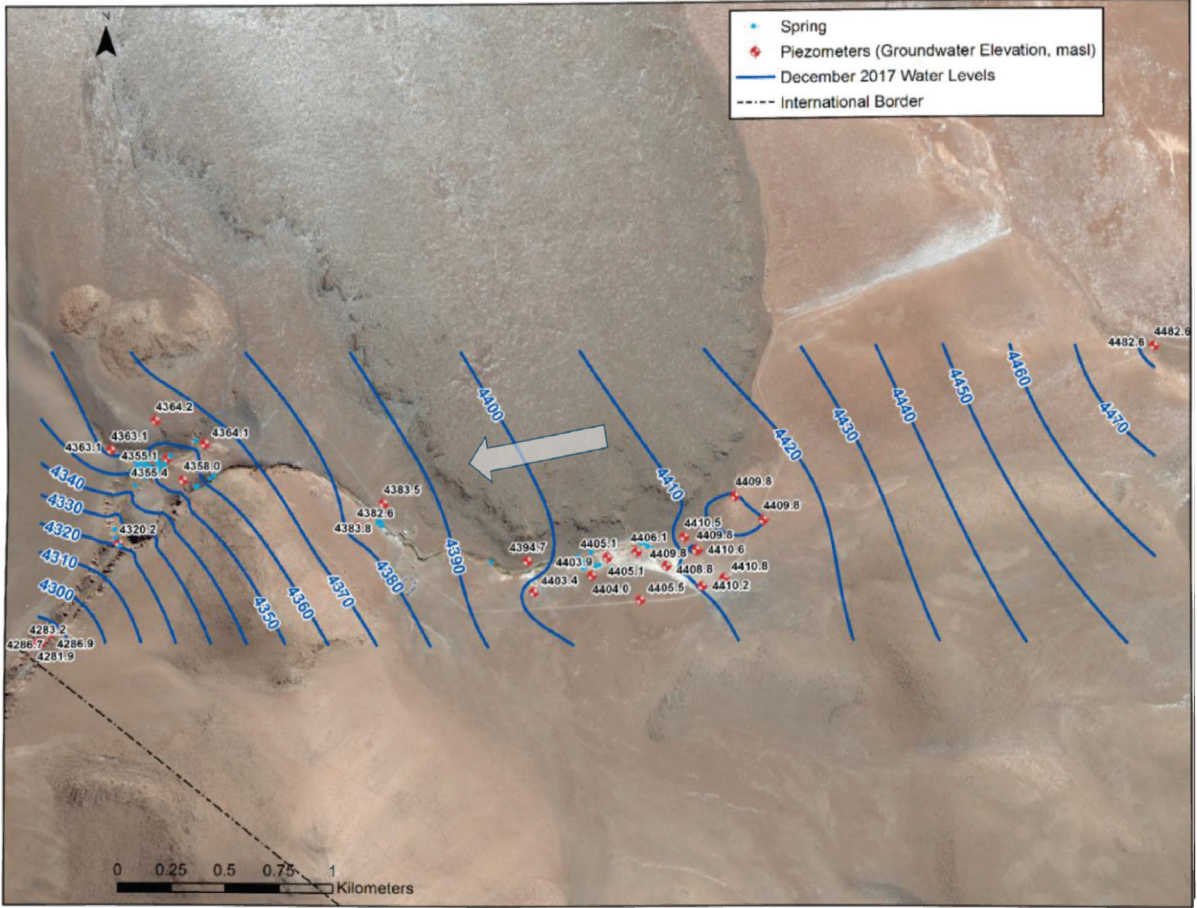
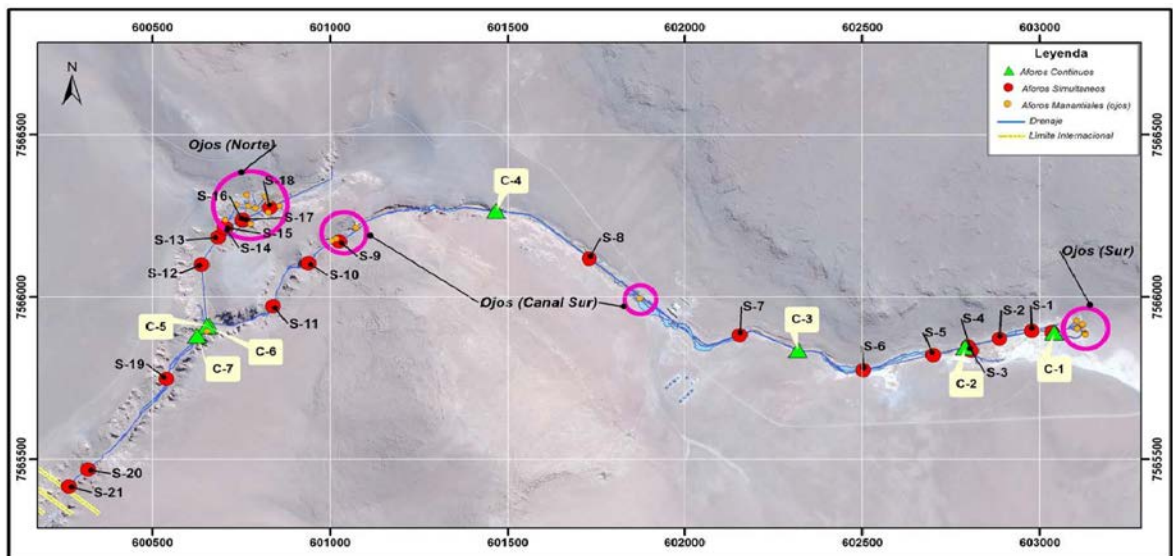


Figure 2-3. “Borehole locations and groundwater level contours in the Silala Near Field, interpolated from Piezometer wells spring elevations and wetlands excavations for soil sampling. N.B. the contouring away from the wetlands and the boreholes are uncertain”
 [Original Caption]. (BCM, Vol. 2, p. 293).

The surface flow study was presented in Annex C to the DHI Report, 2018 (BCM, Vol. 2, Annex 17). Its key objective was to quantify the flows in the Silala Near Field. For this study, simultaneous stream flow measurements were made at 21 locations and continuous flow records were collected at seven weirs (Figure 2-4).



*Figure 2-4. “Overview of flow measurement locations” [Original Caption].
(BCM, Vol. 2, p. 381).*

The DHI analysis of these measurements resulted in a conceptual understanding of the Near Field groundwater flows, which is reproduced in our Figure 2-5 and Figure 2-6. Figure 2-5 shows the conceptual model of the groundwater flows, where the overall flow directions proposed by DHI are shown by gray and blue arrows.

Additionally, the estimation of the diffuse groundwater inflow into the Silala River is presented in Table 2-1, which shows that an important part of the Silala River flow comes from diffuse groundwater inflows (as opposed to discrete spring flows). Specifically, an important diffuse inflow is observed between C-4 and C-5, which is a narrow gorge.

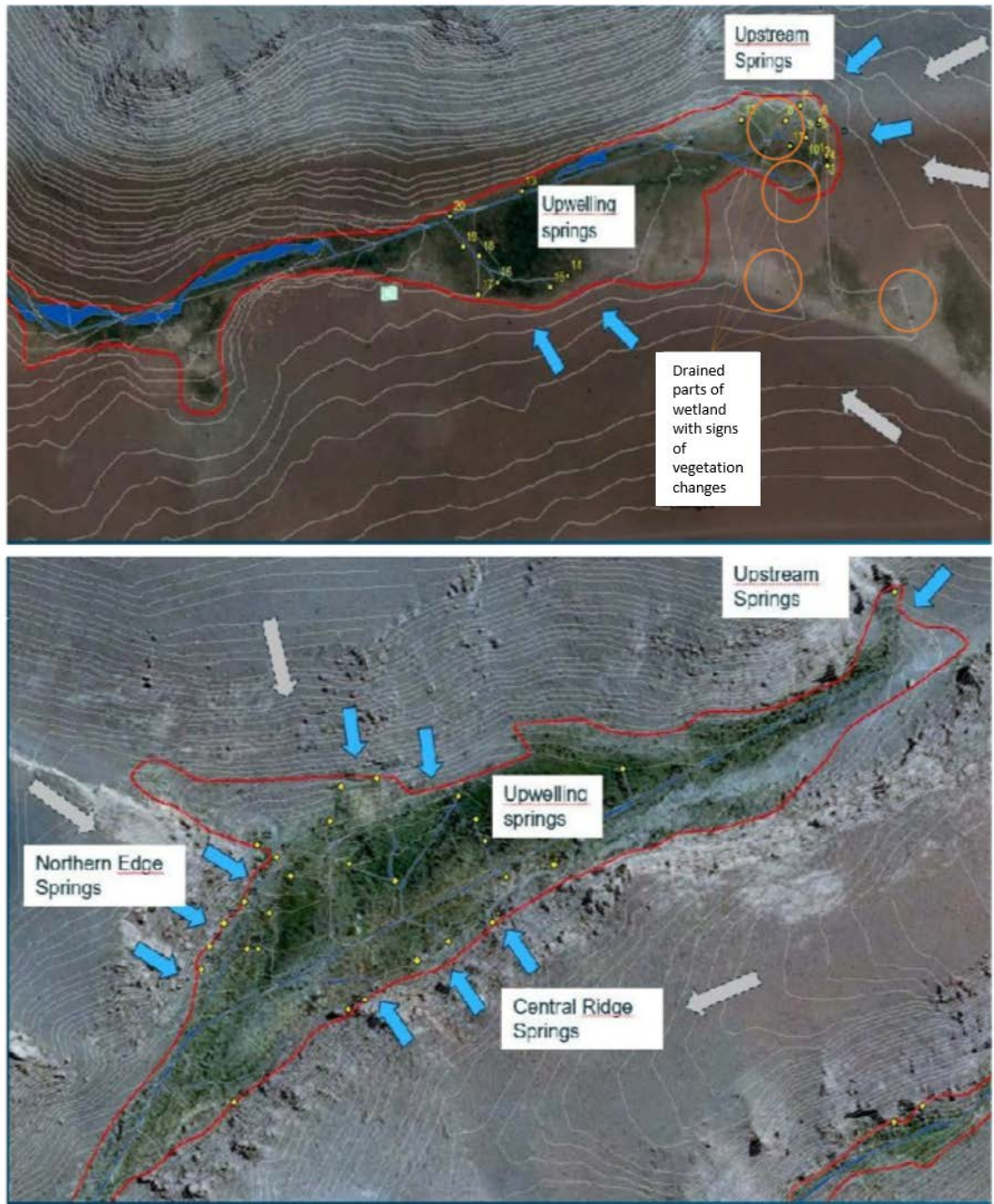


Figure 2-5. Southern (upper picture) and Northern (lower picture) wetlands “overview map showing extent (red polygon), canal network (blue line), springs (yellow dots) and overall flow directions by gray and blue arrows. Drained and drier wetland area with clear signs of vegetation changes are highlighted by orange circles” [part of the original caption]. (BCM, Vol. 2, p. 371).

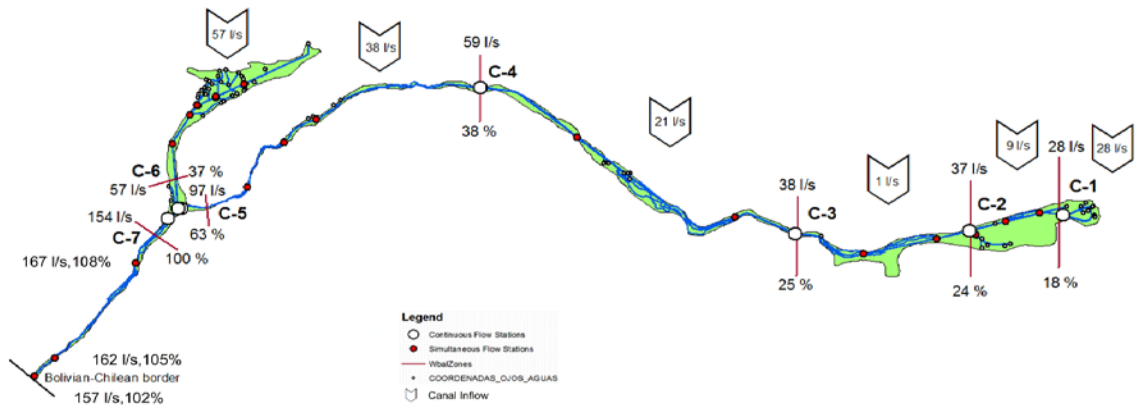


Figure 2-6. “Mapping of flows and net inflows based on simultaneous mean canal flow measurements (in l/s)” [Original Caption]. (BCM, Vol. 2, p. 391).

Section	Measured spring flow (l/s)	Measured Canal Flow (l/s)	Difference, canal-springs (l/s)
C1, springs 1-12 (Zone 2)	23.8	27.8	4.0
C2, springs 1-20 (Zone 2)	41.2	36.7	-4.5
C3, springs 1-21 (Zone 2)	41.2	38.0	-3.2
C4, springs 1-22 (Zone 3)	45.2	59.5	14.3
C5, springs 1-32 (Zone 4)	56.9	97.0	40.1
C6, springs 33-64 (Zone 1)	46.1	56.9	10.8
C5+C6, springs 1-64	103.0	154.0	51.0

Table 2-1. “Canal flows by section, accumulated upstream spring inflows and derived diffuse inflows [Difference, canal-springs]. The flows represent the average of all 10 measurement campaigns” [Original Caption]. (BCM, Vol. 2, p.386).

2.1 Geological interpretation

The Near Field modelling is based on the hydrogeological map generated by DHI (2018) (BCM, Vol. 4, p. 67), which is presented in Figure 2-7, and the definition of the hydrogeological units is presented in Table 2-2. In turn, the hydrogeological map is based on Bolivia's interpretation of the geology of the Silala River system, which is flawed in several respects. A detailed examination of the geological reports supporting the Bolivian Counter Memorial and presented in the Bolivian Rejoinder is available in SERNAGEOMIN (2019b) (**Chile's Additional Pleading (CAP), Vol.2, Annex XVI**).

Bolivian geologists (SERGEOMIN, 2017) have determined that in Bolivia the Ignimbrite succession can be divided into three distinct geological units (Nis-1, Nis-2 and Nis-3) (BR, Vol. 4, pp. 43-61), whereas in Chile only two ignimbrite units have been identified, in surface outcrops and borehole cores (SERNAGEOMIN 2017, 2019b and Arcadis, 2017). In the area of the Bolivian wetlands there may be, at depth, further ignimbrite units, but these have not been found in Chile.

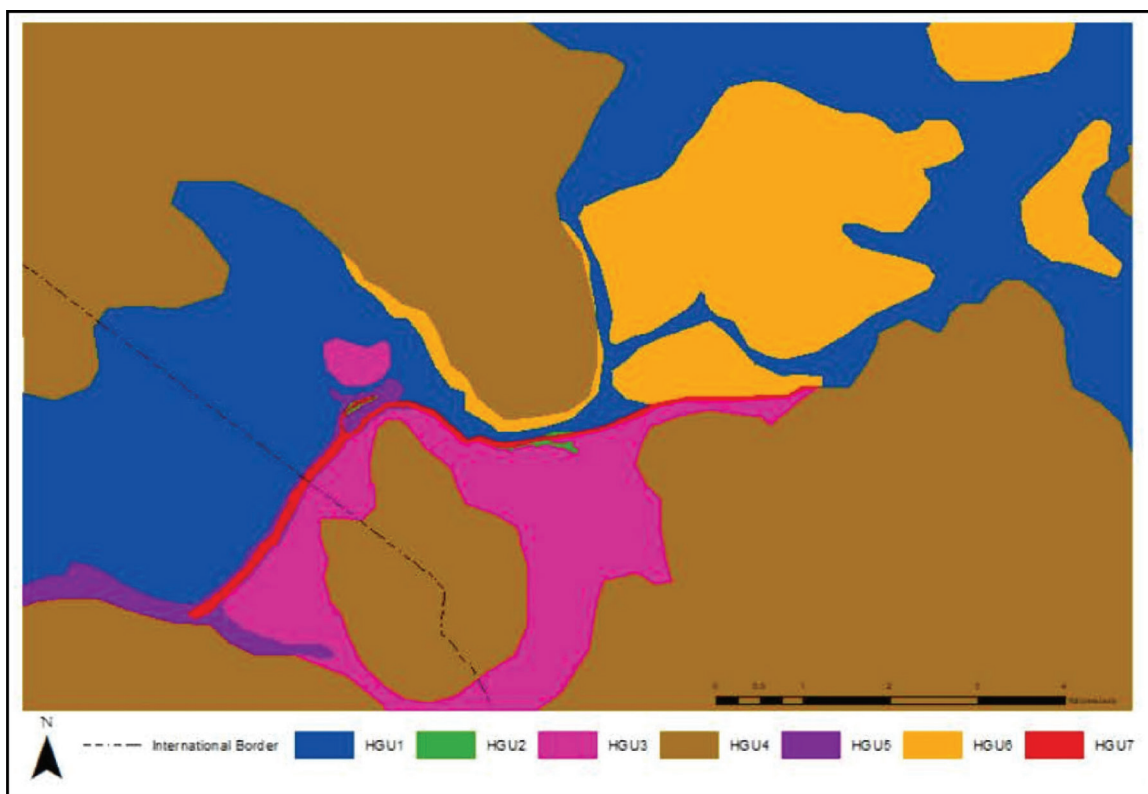


Figure 2-7. “Delineation of hydrogeological units (HGUs) in the Silala area” [part of the original caption]. (BCM, Vol 4, p. 67).

Hydrogeological Unit	Basic Lithology	Approximate Thickness (m)
HGU1	Colluvial and alluvial deposits	1 to 10 m
HGU2	Glacial deposits, sandy loams	1 to 10 m
HGU3	Weathered lava flows	1 to 30 m
HGU4	Felsic volcanic sequences	Up to 600 m
HGU6 Upper	Ignimbrite deposits with a high degree of welding	Up to 150 m
HGU5	Ignimbrite deposits with a low degree of welding	10 to 120 m
HGU6 Lower	Ignimbrite deposits with a high degree of welding	Up to 300 m; assumed to be 300 m in the model
HGU7	Fault zones believed important for groundwater flow	50 to 100 m wide, depth to base of ignimbrite (assumed)
HGU8	Volcanic neck of Silala Chico	650 to 760 m diameter; depth to base of ignimbrite

Table 2-2. Bolivian defined "Hydrogeological Units" [Original Caption] (BCM, Vol. 4, p. 65).

SERNAGEOMIN (2019a) (CR, Vol. 3, Annex XIV) have carried out a detailed analysis of the age and stratigraphic relationships of the Ignimbrites and Miocene volcanics that are found outcropping in the area of the Silala ravine in Bolivia and Chile. This work, without doubt, shows that the ignimbrite units defined in Chile, which can be traced northeast into Bolivia up the Silala ravine, are younger than the Miocene Volcanics that form the Silala Chico (Bolivian name) (Cerrito de Silala in Chile) and the small volcanic dome to the north of the Bofedales Norte (Cajones) wetland in Bolivia. These ignimbrite deposits overlie the less permeable Miocene volcanics. These ignimbrite deposits (Nis) and the Miocene volcanics (Nevsch) are clearly shown on the geological map of SERGEOMIN (2003) (reproduced here as Figure 2-1). In contrast, DHI (2018) shows, in pink on their figure, outcrops of “weathered lava flows” of thickness less than 30 m (see Table 2-2 and Figure 2-7) (BCM, Vol. 4, p. 67). Bolivia’s hydrogeological map and Bolivia’s geological map are compared in Figure 2-8. These weathered lava flows (HGU3) have been defined by DHI as “Chemically and mechanically weathered lava flows (see Table 3, DS-09). Characterized by areas where lavas extruded from the Inacaliri volcano (~1.5 Ma)” (BCM, Vol. 4, p. 65). Whereas the volcanic sequences of the Miocene (HGU4), which are called “Felsic volcanic sequences” by DHI (2018) (up to 600m thick) (see Table 2-2) (BCM, Vol. 4, p. 65), are compacted and of low permeability and considerably older. The area coloured pink on Figure 2-7 does not comprise weathered lava flows, so should not be assigned to HGU 3. Instead, the pink outcrop to the north of the Cajones ravine is a Miocene volcanic dome equivalent to what DHI (2018) calls Felsic Volcanic sequences and should be assigned to HGU 4. The remainder of the pink area on Figure 2-7 comprises outcrops of colluvial or alluvial deposits or is a part of the Miocene volcanic dome that makes up the Silala Chico (Bol) hill and should be assigned to HGU1 and HGU4 (see Figure 2-8). There are clearly errors in interpretation of the geological map, which have resulted in incorrect assignment of hydrogeological units.

These inconsistencies and errors in geological interpretation are in part demonstrated in the cross section at the bottom of Bolivia’s geological map (Figure 2-1), presented in Figure 2-9, which shows that SERGEOMIN (2003) interprets the Ignimbrite deposits (“Nis” shown in orange red) as extensively underlying (and therefore older than) the Miocene Volcanics (“Nevsch” shown in beige). The legend from this map, also presented in Figure 2-9, confirms this interpretation. According to the dating work undertaken by SERNAGEOMIN (2019a), this is clearly incorrect.

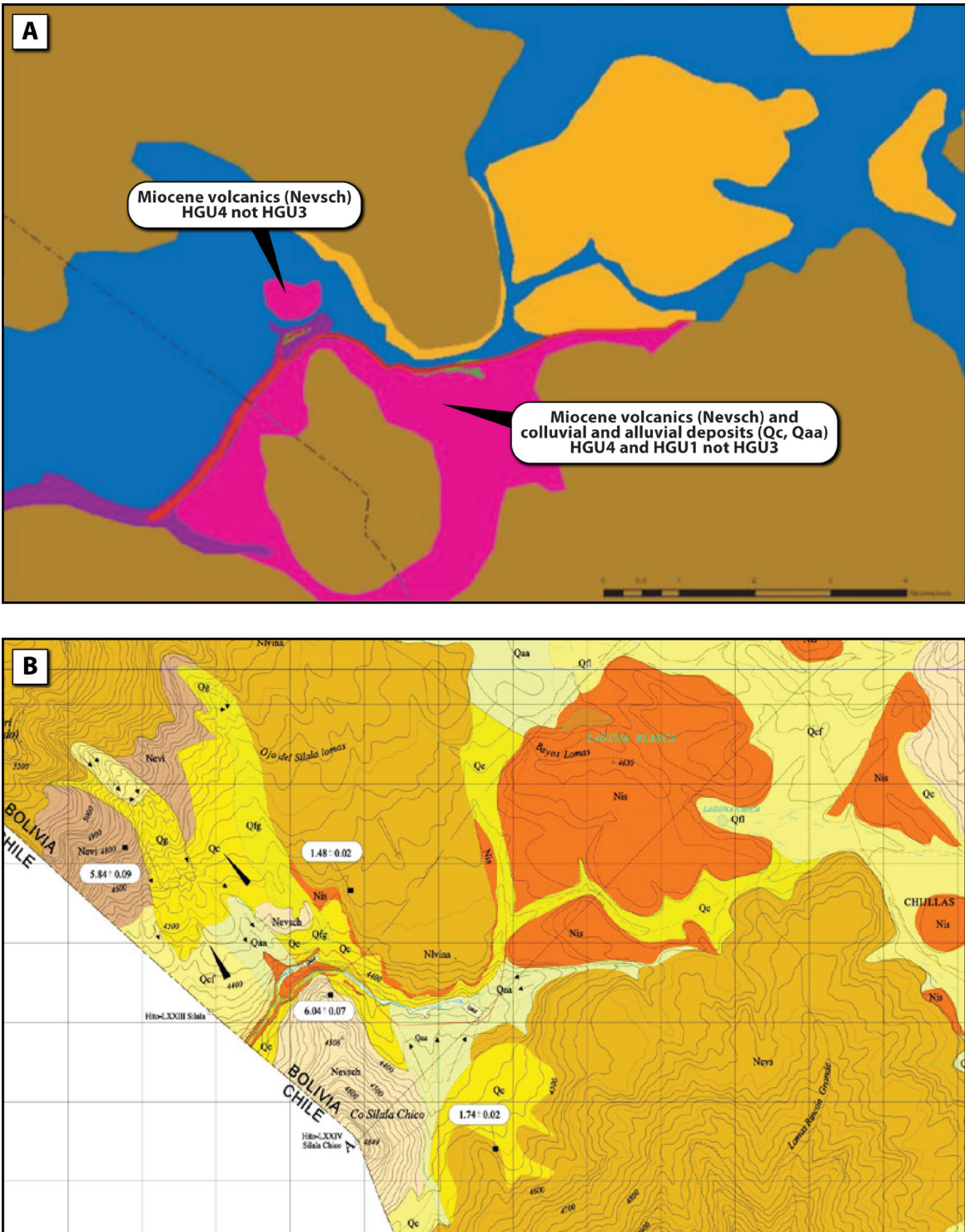


Figure 2-8. Comparison of (A) Bolivia's hydrogeological units (HGUs) (BCM, Vol 4, p. 67) and (B) surface geology in the Silala area. (BR, Complete Copies of Certain Annexes, Vol. 2, Annex 23.5 Appendix a, p. 69).

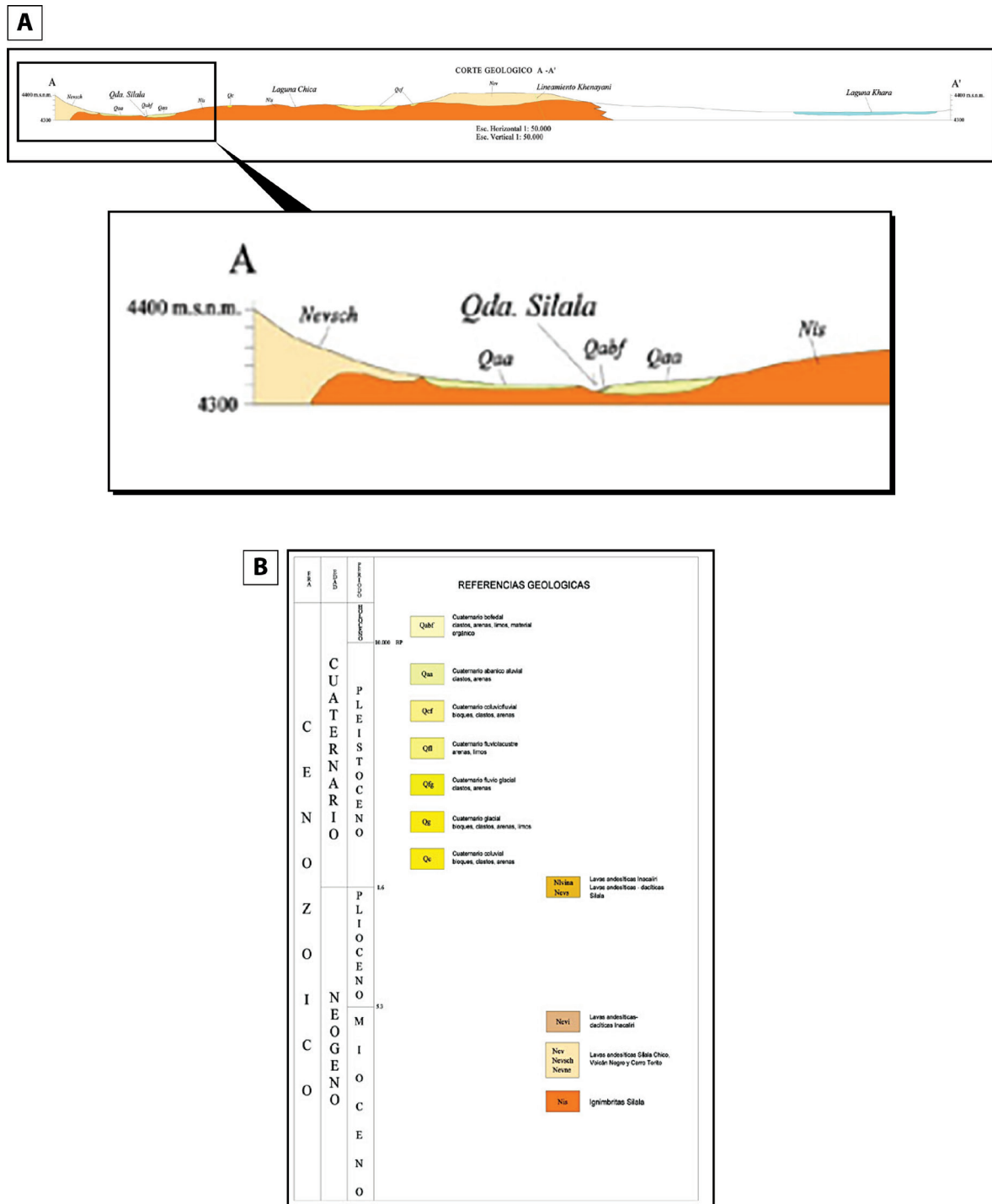


Figure 2-9. (A) Expanded view of the cross section and (B) legend from Bolivia's geological map reproduced at Figure 2-1. (BR, Complete Copies of Certain Annexes, Vol. 2, Annex 23.5 Appendix a, p. 69).

The importance of such errors and inconsistencies in the development of both a conceptual understanding of the hydrogeology and its representation in a numerical model is explained below.

The two ignimbrite units (named Silala (upper) and Cabana (lower) in Chile) are found beneath the Silala River ravine, but SERGEOMIN (Bolivia) (2003) does not recognize these units despite the fact that they occur close to the international border, where they have been observed by SERNAGEOMIN (Chile) (SERNAGEOMIN 2017, 2019b, Arcadis, 2017), the former in outcrop and both at depth in borehole core. The Silala Ignimbrite can be seen to cross the border in continuous outcrop and can be traced on satellite imagery upstream in the walls of the Silala ravine to the confluence of the Cajones and Orientales ravines.

These ignimbrite deposits are constrained by the (older) Miocene volcanics on each side (northwest and southeast) and at some depth (currently unknown). The surface gradient (as well as the ‘dip’ of the formations) changes from being relatively gentle upstream of this pinch-point, to noticeably steeper downstream. This supports the interpretation of the flow which deposited the ignimbrites being constrained by a narrow gap in the Miocene volcanics. This restriction in the cross-sectional area of the main ignimbrite aquifer will clearly impact the permeability and transmissivity distribution in any numerical groundwater flow model and the area where groundwater flow will be focused down-gradient into Chile. Groundwater flow to the south west into Chile will therefore be restricted to this narrow zone, rather than the much wider area shown by Bolivia in their conceptual cross-section (BCM, Vol. 4 p. 88). Since the permeability of the Miocene volcanics is much lower than that of the ignimbrite aquifer, it is unlikely that part of the groundwater flow bypasses the Near Field in the surrounding geological strata, as was modelled by DHI (2018). Figure 2-10 shows the groundwater level map used in definition of the boundary conditions of the Near Field Model. We have added a red arrow representing the implied flow direction; the HGU4 unit is shown by grey hatching. The piezometric contours in this figure, drawn by DHI, indicate groundwater in the ignimbrites flowing beneath the Miocene Volcanic (red arrow), whereas in reality this would not happen because the ignimbrites overlie the Miocene volcanics and groundwater flow would be funnelled through the narrow constriction delimited by the presence of the low permeability Miocene volcanics. This constriction must be taken into account in order to accurately represent the domain of groundwater flow, conceptually, or more pertinently in the construction of DHI’s NFM, or other models.

From experience from recent geological mapping (SERNAGEOMIN (Chile) 2017, 2019b), drilling and groundwater level measurements (Arcadis, 2017) Chile interprets two aquifer systems. One is a shallow aquifer found perched in Alluvial deposits and shallow weathered lavas and a second at depth in the Silala Ignimbrite (Chilean defined) but mostly found in the less welded and more permeable Cabana Ignimbrite (Chilean defined). The upper levels of the Silala Ignimbrite (Chilean defined) are highly welded and represent a confining or semi-confining layer above the Cabana Ignimbrite. It is therefore more appropriate to assess piezometric levels in the shallow aquifer and the deeper aquifer separately. A correct understanding of the hydrogeology leads to differences in the interpolation of the groundwater level data, and hence the current boundary conditions used for the NFM are incorrect.

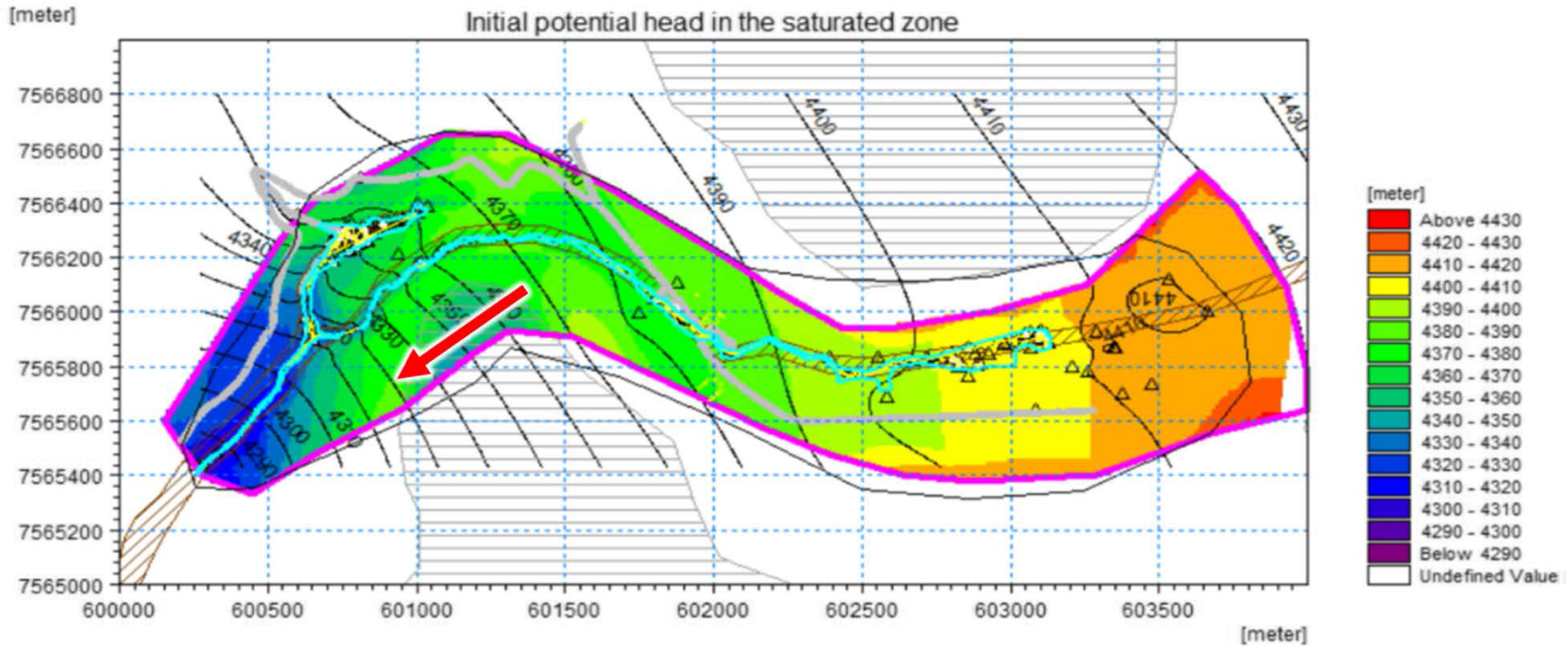


Figure 2-10. “Groundwater level maps used in definition of groundwater component boundary conditions” [Original Caption]. Black lines represent the piezometric contours, the polygons filled with grey lines represent the HGU4 unit. The added red arrow represents the implied groundwater flow through the HGU4 unit. (BCM, Vol. 5, p.19).

3. WATER BALANCE MODEL (WBM)

3.1 Conceptual model

To develop a conceptual model of the Far Field, limited data were available. Data from the Far Field area comprise a surface geology map, a single water level measurement in a borehole located approximately 2 km upstream of the Orientales wetland and soil sample analyses from six locations. According to DHI (BCM, Vol. 3, p. 471) the conceptual model of the Far Field (WBM) considered that groundwater recharge is driven by short-term precipitation events, often separated by long dry periods. And as noted by DHI (BCM, Vol. 3, p. 471), to correctly reproduce the recharge produced in this area, long-term dynamic simulation is necessary².

The hydrogeological conceptual model developed by DHI (BCM, Vol. 3, p. 472) considered that the main processes that affect the recharge and the available water resources in the Silala River basin are determined by precipitation, soil evaporation, infiltration and snow processes. The extent of the WBM was defined as the groundwater catchment (defined by DHI as the hydrological catchment) of the Silala River and was delineated using NASA's SRTM digital elevation model. Since the studied area is very dry, evaporation from the soil and infiltration through the upper soils and unsaturated zone of the aquifer to the underlying groundwater table are the main processes that determine the recharge to the catchment.

3.2 Numerical model

DHI's WBM is a transient numerical model that covers the Silala River hydrological catchment upstream of the Orientales and Cajones wetlands (Bolivian wetlands). The main purpose of developing this model was to estimate the overall recharge available to the Silala River basin and its groundwater catchment. This model covers an area of 228.7 km² (5,717 active cells of 200 x 200 m (BCM, Vol 3, p. 476)) (note that this differs from the area of 231.5 km² quoted in Section 2.2 of Annex E to the DHI (2018) report (BCM, Vol. 3, pp. 472-473)) and simulates the period between 01/02/1969 and 31/12/2016 (17,500 days) (not 1/1/1969 to 31/12/2016 as quoted in Section 2.5 of Annex E to the DHI report (BCM, Vol. 3, p. 477)).

Several versions of the WBM were provided (see Appendix A). The base case of the WBM model is described as "Silala_model_200m_v24.she" and does not include a saturated groundwater flow component. Only two versions of the WBM that simulate saturated groundwater flow as well as recharge were provided by DHI:

² We note that DHI's 48 year simulations do not represent the long-term for these groundwater systems. DHI (BCM, Vol.3, p. 491) estimate average groundwater travel times to be 1500 years.

- Silala_model_gw_200m_v12_final.she
- Silala_model_gw_200m_v12_final_tracer.she

In this report we review the first version because the second one was focused on estimating residence time for groundwater in the saturated zone, which is beyond the scope of this report.

3.2.1 Boundary conditions

The boundary conditions used to model the groundwater flow (saturated zone) in the WBM are presented in Figure 3-1. The model was constructed using a no-flow boundary condition across most of the model boundaries, with the exception of a fixed head boundary condition that permits water to exit the model domain towards the Bolivian wetlands (and to Chile). Thus, this fixed head boundary condition is located at the boundary of the NFM. The value of this boundary condition was defined as equal to the initial potential head at that boundary, therefore it is constant in time but it varies in space. It is important to mention that the southwestern no-flow boundary condition is not based on the DHI interpretation of the hydrogeology of the study area. Because the southwestern no-flow boundary condition is near the zone of interest, it is likely that it will have an impact on the simulated flows from the WBM towards the Bolivian wetlands. This issue was not assessed by DHI.

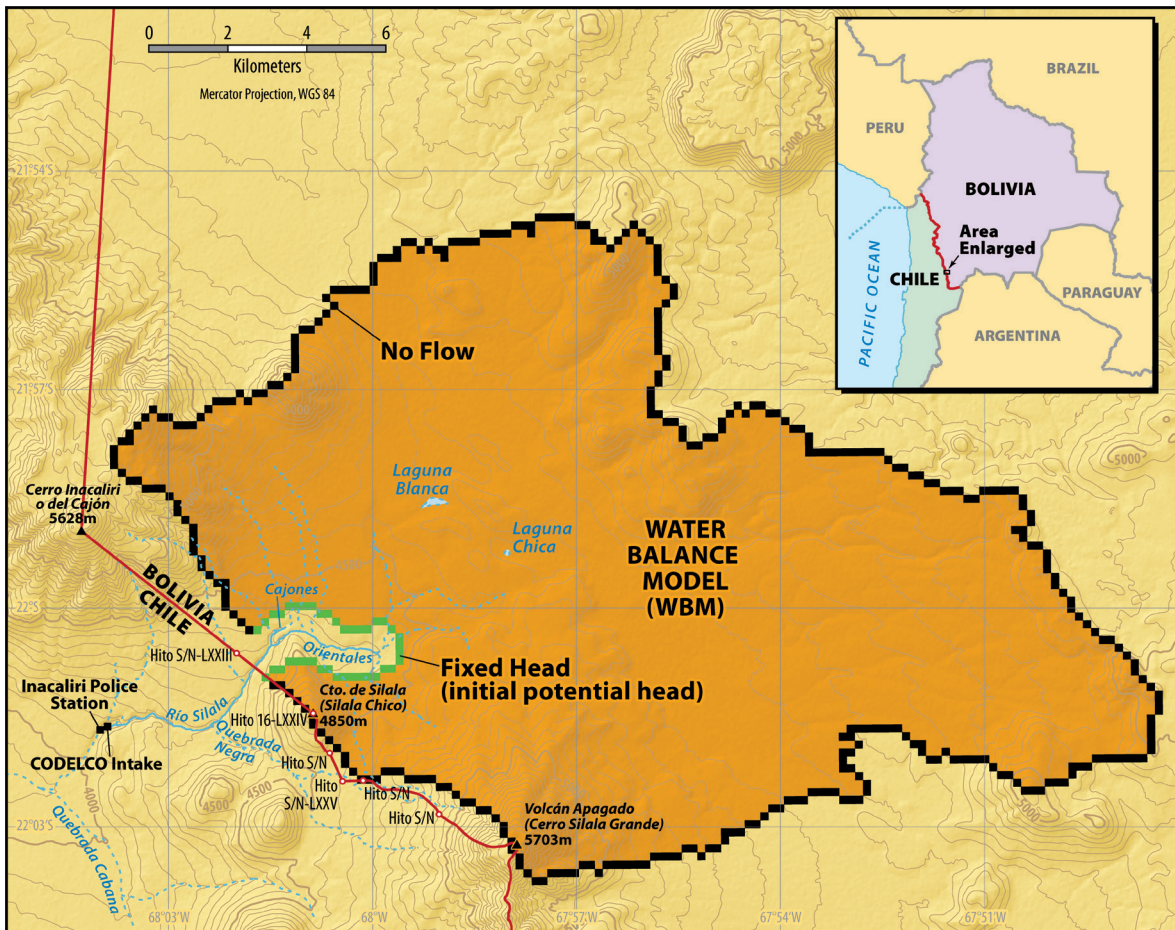


Figure 3-1. Boundary conditions of the “Water Balance Model”.

3.2.2 Water balance results

The water balance from the WBM, version Silala_model_gw_200m_v12_final.she, is presented in Table 3-1. This balance in cumulative millimeters was calculated using the water balance module of the MIKE-SHE model. The flows in mm/year and l/s were calculated using the simulation period (17,500 days, or just less than 48 years) and the area of the model’s active cells. This table shows that 198 l/s of groundwater exits the model through the fixed head boundary.

	Cumulative water depth (mm)	Average depth rate (mm/year)	Average flow rate (l/s)
Precipitation	-6023	-126	-911
Evapotranspiration	4854	101	734
Recharge (prec.-evap.)	-1170	-24	-177
Total storage change	-170	-4	-26
Net groundwater boundary outflow	1309	27	198
Error	-30	-1	-5

Table 3-1. Water balance from the “Water Balance Model” -
Silala_model_gw_200m_v12_final.she version.

The contributions from storage releases shown in Table 3-1 (which are consistent throughout the model period) indicate that the model has not reached a dynamic steady state (i.e. without long-term upward or downward trends in groundwater levels), which means that the model results are therefore still being influenced by the initial conditions and the estimated recharge is also affected by changes in storage. We also note that in DHI’s Provisional Report 3, Water balance of the basin and groundwater aquifer and update of measured flow (DHI 2017a, received by Chile in February 2019), recharge using the same model is estimated to be 56 mm/year (instead of the 24 mm/year shown in Table 3-1). No explanation has been provided by DHI for why the estimate was reduced in their final report. This Provisional Report 3 is attached to the present report as Appendix D.

3.3 Main conclusions from the review of the WBM

In this section a limited review of the main configuration of the WBM has been presented, primarily to set the context for the discussion of the NFM. The main conclusions of the review of the WBM are that the model has not reached steady state, so that the water balance is affected by changes in storage, and that the southwestern no-flow boundary condition is not based on DHI’s interpretation of the hydrogeology of the study area, instead it seems to be based, at least in part, on the geopolitical boundary between Bolivia and Chile.

4. NEAR FIELD MODEL (NFM)

4.1 Conceptual model

The Silala NFM covers the area immediately adjacent to the Bolivian wetlands upstream of the Chile-Bolivia international border (see Figure 4-1).

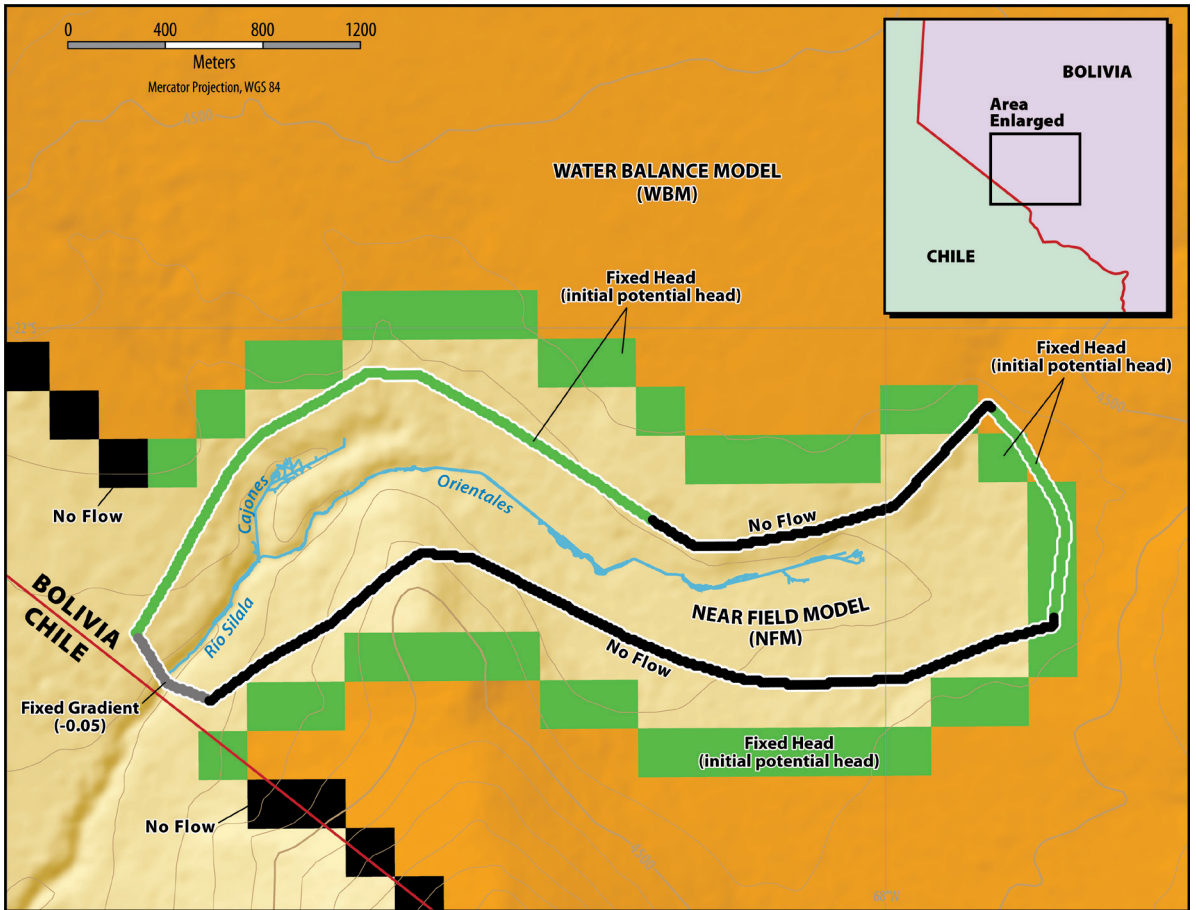


Figure 4-1. The area of Bolivia's Near Field Model. The green color represents Fixed Head boundary conditions, the black color represents No-Flow boundary conditions and the grey color represents Fixed Gradient boundary conditions.

Using the available piezometric information, DHI (BCM, Vol. 4, p. 97) proposed a piezometric map of the Silala Near Field area (see Figure 2-3). Analysis of DHI's piezometric map allows the direction of groundwater flow to be determined (groundwater flow directions are by definition perpendicular to the groundwater level contour lines). These directions are shown by our blue arrows in Figure 4-2A.

DHI's (2018) conceptual understanding of the groundwater system, as illustrated in their BCM figures reproduced in Figure 4-2B and C, shows that the groundwater flow

into the Cajones wetland (Bolivia's "northern wetland") comes from the North-North-West, North-West, North-East and South-East, and the flow into the Orientales wetland (Bolivia's "southern wetland") comes from the North-East and the South-East. In contrast, according to their piezometric map, water is entering the Near Field Model mainly through the North-East and is exiting the model through the South-West (see Figure 4-2A). Note that from interpretation of DHI's contours some of the water should also be exiting the Near Field Model through the southern No-Flow boundary of the model, a problem discussed further in section 4.2.3. The piezometric contours and the corresponding flow directions (Figure 4-2A) should be consistent with the groundwater flow directions presented in Figure 4-2B and C. However, when comparing the flow directions derived from Bolivia's piezometric contours and Bolivia's conceptual understanding, the flow directions obtained from DHI's groundwater level map do not correspond to those presented in Figure 4-2B and C. Therefore, the conceptual model of the NFM is based on conflicting interpretations of the data.

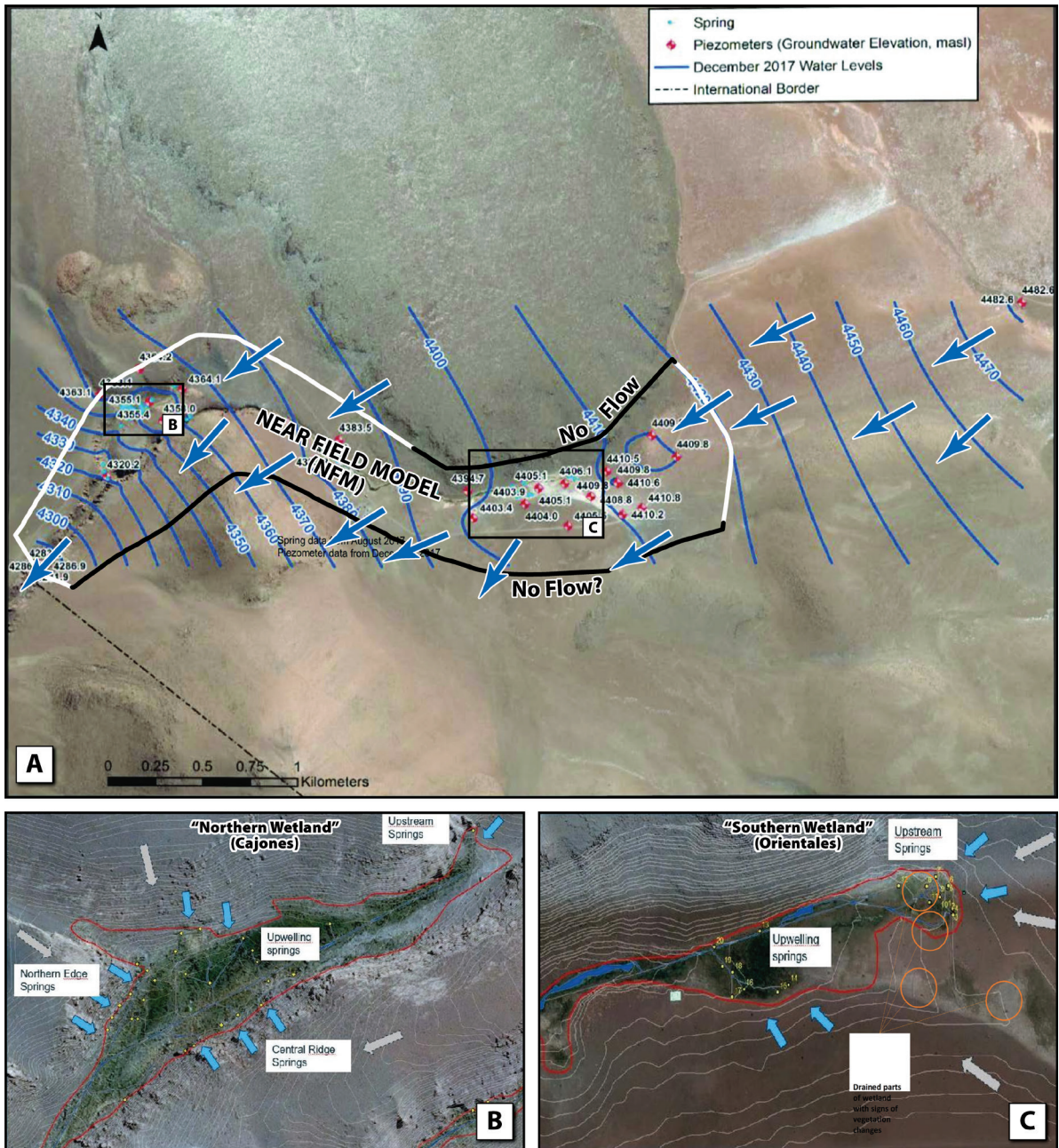


Figure 4-2. A) Groundwater level contours in the Silala NFM, interpolated from piezometer wells, spring elevations, and wetlands excavations for soil sampling (Adapted from BCM, Vol. 4, p. 97). The NFM domain is delimited by the polygon with a black and white border that shows in black the DHI no-flow boundaries and in white the boundaries through which water can pass. The blue arrows represent the direction of groundwater flow interpreted from the contour lines. B) Northern and C) Southern wetlands overall flow directions. (Adapted from BCM, Vol. 2, p. 371). Note: The text in the lower label of panel C is: "Drained part of wetland with signs of vegetation changes" (Muñoz et al., 2019).

Interpretation of the sparse groundwater level data is inevitably subject to uncertainty. However, given the existence of two distinct aquifers, a more realistic interpretation of the groundwater data would use two different piezometric maps, one for the shallow surficial aquifer and one for the deeper ignimbrite aquifer, and include adjustments to take into account the effects of gaining and losing reaches of the river and the presence of the low permeability formations, as discussed above. This more detailed approach would result in contours that are in places very different to those produced by DHI and would result in the definition of markedly different boundary conditions for the NFM.

4.2 Numerical model

DHI's NFM, as described in Annex G to DHI (2018) (BCM, Vol. 5, p. 13), is a transient model but with constant (steady-state) inputs. It covers the area immediately adjacent to the Orientales and Cajones wetlands (Bolivia's southern and northern wetlands, respectively), upstream of the Chile-Bolivia international border. The main purpose of this model was to determine the impacts of channelization on the Silala River flow. This model covers an area of 2.56 km² (25,632 active cells of 10 x 10 m) and was run for a period of 91 days.

The representation of the system was developed with the MIKE-SHE and MIKE-11 modelling software, for three scenarios, defined in Annex H to DHI (2018) (BCM, Vol. 5, pp. 67-70):

Baseline Scenario: The “Baseline” model represents the current configuration of the river system, including the historical wetland drainage channels and main river channelization. It includes coupled flow components for groundwater (3-D), unsaturated zone (1-D), evapotranspiration, overland flow (2-D) and channel flow (1-D).

No Canal Scenario: The “No Canal” scenario model is identical to the baseline model except that the 1-D channel flow (i.e. the MIKE-11 model) has been removed from the setup. The “No Canal” model thus includes coupled flow components for groundwater (3-D), unsaturated zone (1-D), evapotranspiration and overland flow (2-D).

Undisturbed Scenario: The “Undisturbed” scenario model³ is identical to the “No Canal” scenario model but the surface topography and unsaturated soil profile descriptions have been modified to represent the possible long term development of peat soils (of up to 60cm depth). The “Undisturbed” scenario model includes coupled flow

³ Variously referred to as the “Wetland restoration” scenario (BCM, Vol. 2, p. 303), the “Restored wetland” scenario (BCM, Vol. 5, p. 70), the “Wetland restoration (undisturbed)” scenario (BR, Vol. 5, p. 73), and the “Undisturbed” scenario (BR, Vol. 5, p. 73).

components for groundwater (3-D), unsaturated zone (1-D), evapotranspiration and overland flow (2-D).

The Baseline scenario was modelled using the MIKE-11 model (1D Surface water flow model) to represent the channel flow coupled with the MIKE-SHE model (integrated hydrological and groundwater model). The No Canal and Undisturbed scenarios were modelled using only the MIKE-SHE model. The lack of a MIKE-11 component for the No Canal and Undisturbed scenarios implies that there would be no surface water flow channels if the channelization was removed, which is incorrect. This conclusion has not been justified by DHI. In addition, the MIKE-SHE model is based on a coarser spatial resolution, which means that the routing of flow (as overland flow) in the No Canal and Undisturbed scenarios is not directly comparable to that of MIKE-11 used for the Baseline scenario.

4.2.1 Topography of the NFM

To study the comparability of the three scenarios developed by DHI (2018), a very basic requirement is to review the topography, or ground surface elevation, used in each of them. From this review, it was found that each of the three scenarios uses a different topography, and that the two models used in the Baseline scenario – MIKE-SHE and MIKE-11 – also use different topographies. The DHI (2018) report states that there is a change in topography between the No Canal and Undisturbed scenarios, and some small differences would be expected, given that long term growth of wetland peat soils is included. However there is no mention of differences between the topographies in the Baseline and No Canal scenarios.

For the Baseline scenario, the channel sections' topography (i.e., the Baseline MIKE-11 model) was constructed combining SENAMHI channel dimension surveys and digital surface model (DSM), which allows reference to this discretization as the closest to the real topography in the catchment. The Baseline scenario topography used by DHI (2018) in the Baseline MIKE-SHE model (which is different from the Baseline MIKE-11 topography), was obtained from a high resolution DEM “based on measurements taken during a drone flight in the last half of 2016 (IGM, 2016)” (BCM, Vol. 2, p. 325). Additionally, in both the No Canal and Undisturbed scenarios the topography of the natural terrain was also obtained by DEM data, but it was altered to remove the channel sections. The original files that contain the three MIKE-SHE topographies are:

- Baseline: xxx_topo_5m.dfs2
- No Canal: xxx_topo_5m_adj_v2.dfs2
- Undisturbed: xxx_topo_5m_undisturbed.dfs2

We extracted various cross sections from the MIKE-SHE topographies for comparison. The locations of these cross sections correspond to those used in the Baseline MIKE-11

model, so it is possible to compare the topography from both the Baseline MIKE-11 and the three MIKE-SHE models. Figure 4-3 and Figure 4-4 each show the ground surface elevation of two cross sections from the three scenarios modelled using MIKE-SHE and the ground elevation of the same sections in the Baseline MIKE-11 model. For an appropriate definition of topography, the three MIKE-SHE model cross sections should coincide, except where a small elevation difference (with a maximum of 0.6 m) is created due to assumed peat soil development. The MIKE-SHE model cross sections should also approximate the MIKE-11 cross sections, but with a coarser resolution. For all the cross sections presented in Figure 4-3 and Figure 4-4 and most of the reviewed cross sections, the Undisturbed scenario always overestimates the river bottom elevation. While it was expected that the Undisturbed topography would be higher than the others due to the assumed peat growth, the observed differences are much larger than expected. For example, the topography of the Undisturbed scenario in cross sections no. 3560 and 3370, shown in Figure 4-3, presents differences of almost 7 meters compared to the Baseline MIKE-11 channel bottom (cross section no. 3560) and of 3 meters compared to the Baseline MIKE-SHE topography (cross section 3370). The observed differences show that these three scenarios represent totally different topographies. The same issue is illustrated with the cross sections in Figure 4-4. These should be seen in the context of DHI's aim to show firstly the effect of the channels (the wetland drainage channels are generally less than 0.5 m deep, and the main channel depths less than 1 meter (see BCM, Vol.5, pp. 32-39)), and secondly, the scenario of peat growth, which increases existing peat depths by a maximum of 0.6 m (BCM Vol. 5, p. 70). The large and unrealistic topographic differences used by DHI are therefore much greater than the small changes to be studied, which indicates that the simulations of the different scenarios are neither equivalent nor comparable.

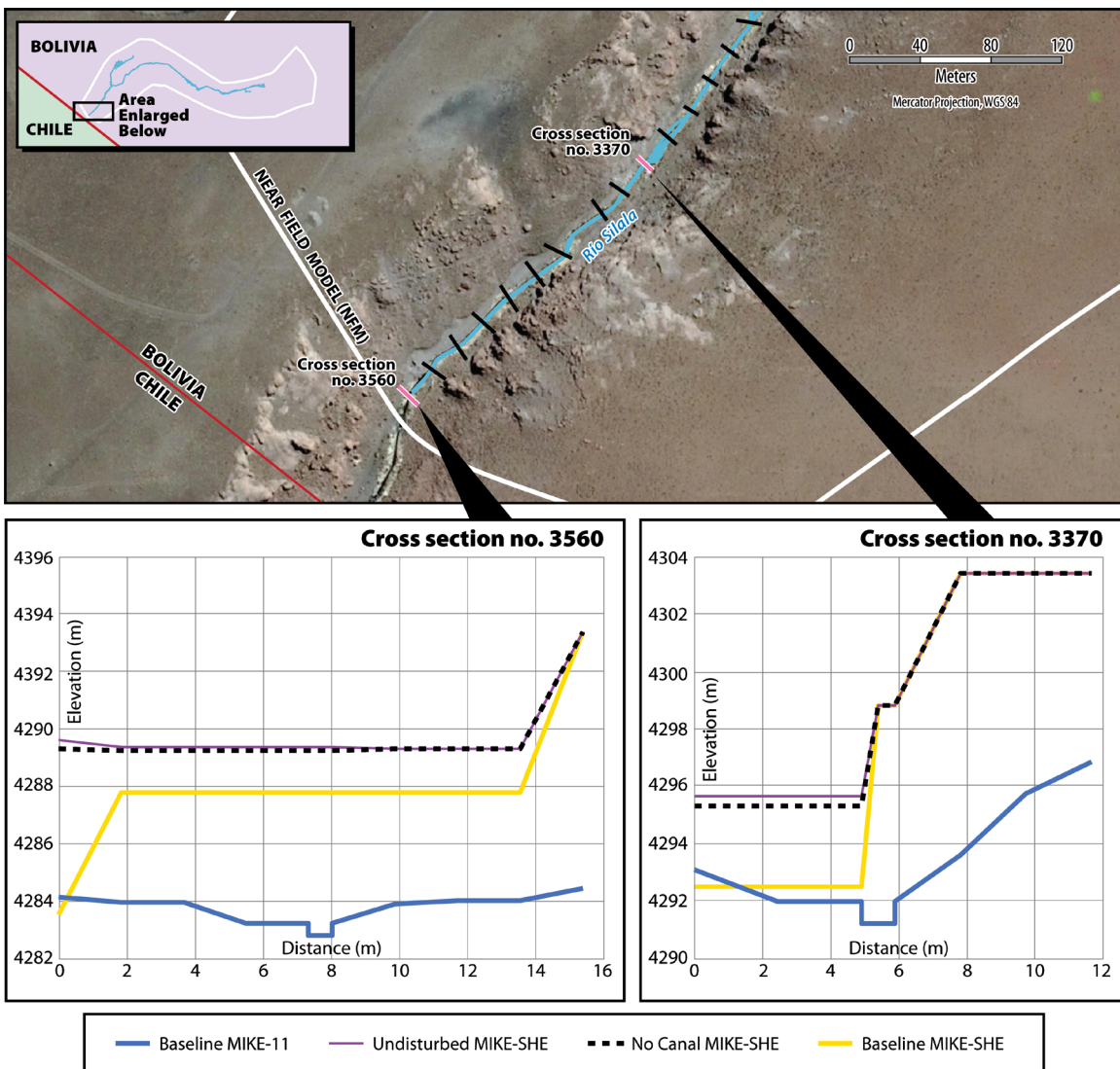


Figure 4-3. Ground surface elevations used in the Bolivian NFM model scenarios compared at two cross sections of the main channel near the international border.

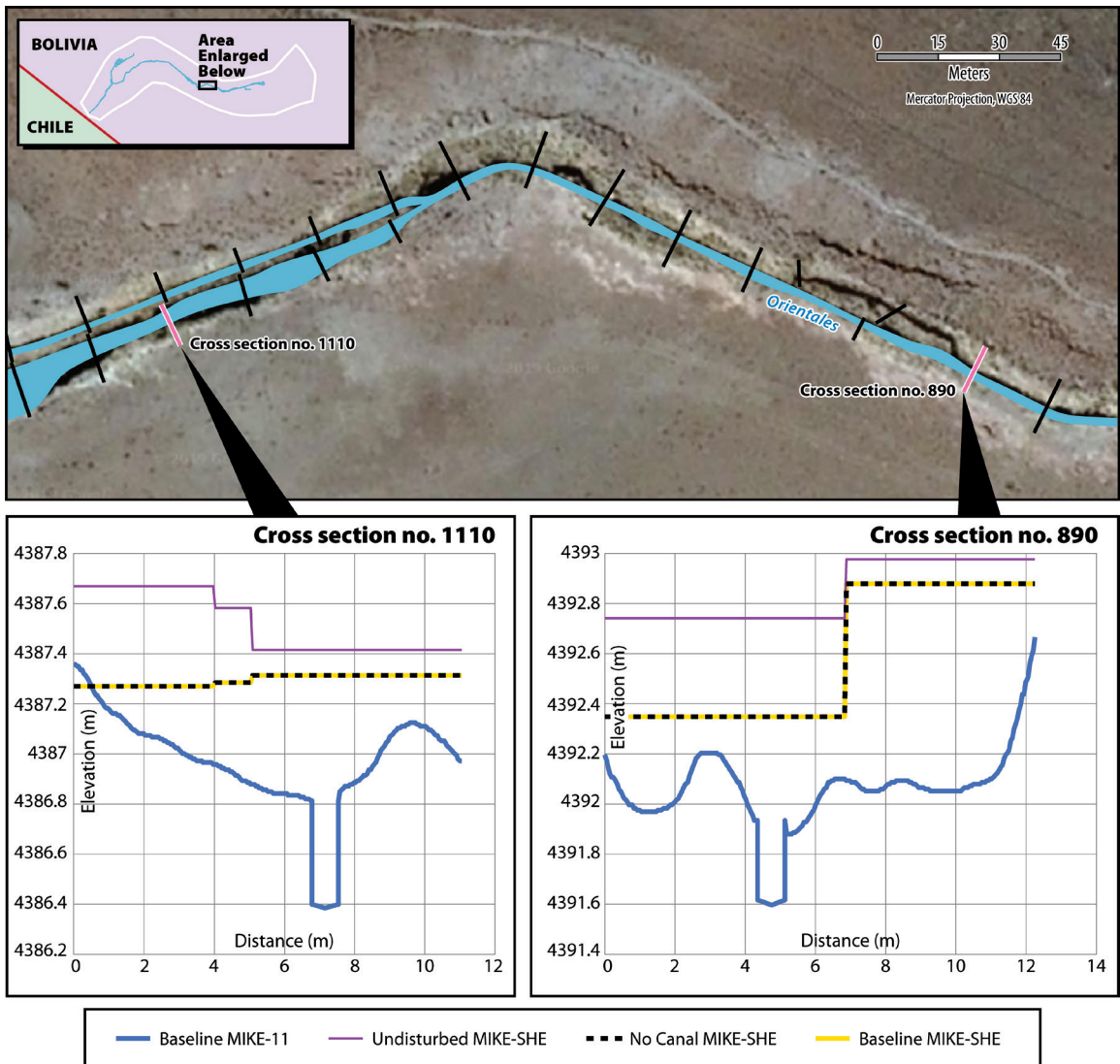


Figure 4-4. Ground surface elevations used in the Bolivian NFM model scenarios compared at two cross sections of the main channel in the Orientales wetland. Specifically, in these cross sections the Baseline and the No Canal topographies from the MIKE-SHE model coincide and the black dotted line obscures the yellow line.

Figure 4-5 shows the difference between the No Canal and the Undisturbed scenarios topographies. Here, differences between 0 and 0.4 meters are noted, which are reasonable and expected given that the scenario represents possible long term peat development.

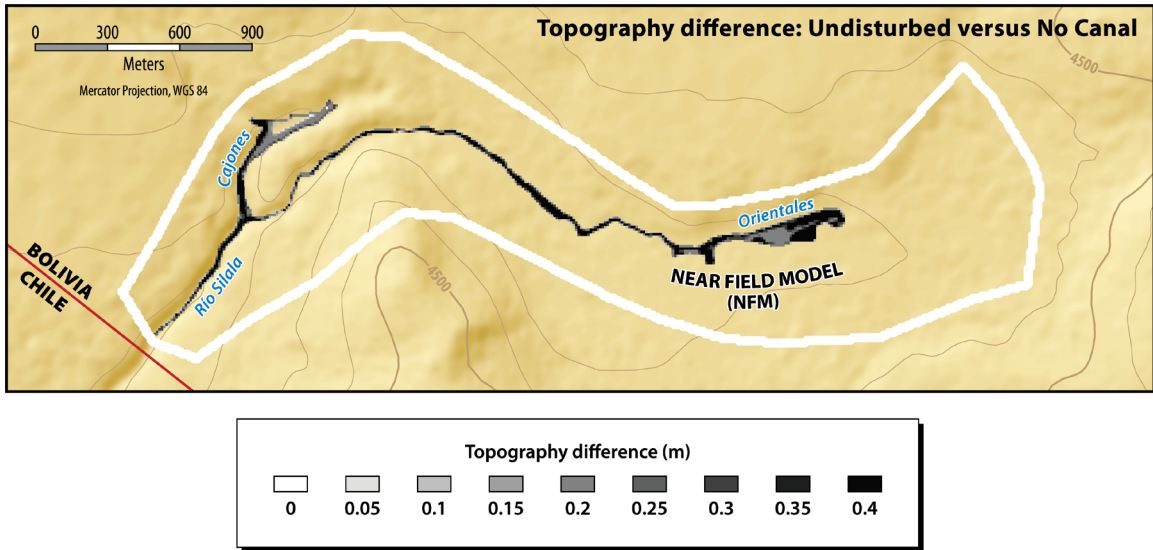


Figure 4-5. Difference between No Canal and Undisturbed model topographies.

Figure 4-6 shows, in plan view, the differences between the topography of the Baseline MIKE-SHE and the No Canal scenario in the NFM. As can be seen from this figure, differences in elevation (mostly over 1.5 m higher in the No Canal scenario) are large in comparison with the depths of the channels (typically 0.3 to 0.8 m). A plan view of the difference between Baseline MIKE-11 topography and any version of the MIKE-SHE topography has not been included because the MIKE-11 topographic information is linear, while the MIKE-SHE information is provided as a gridded digital elevation model (DEM). However, our analysis of individual MIKE-11 cross sections indicates that the differences are substantial (see Figure 4-3 and Figure 4-4).

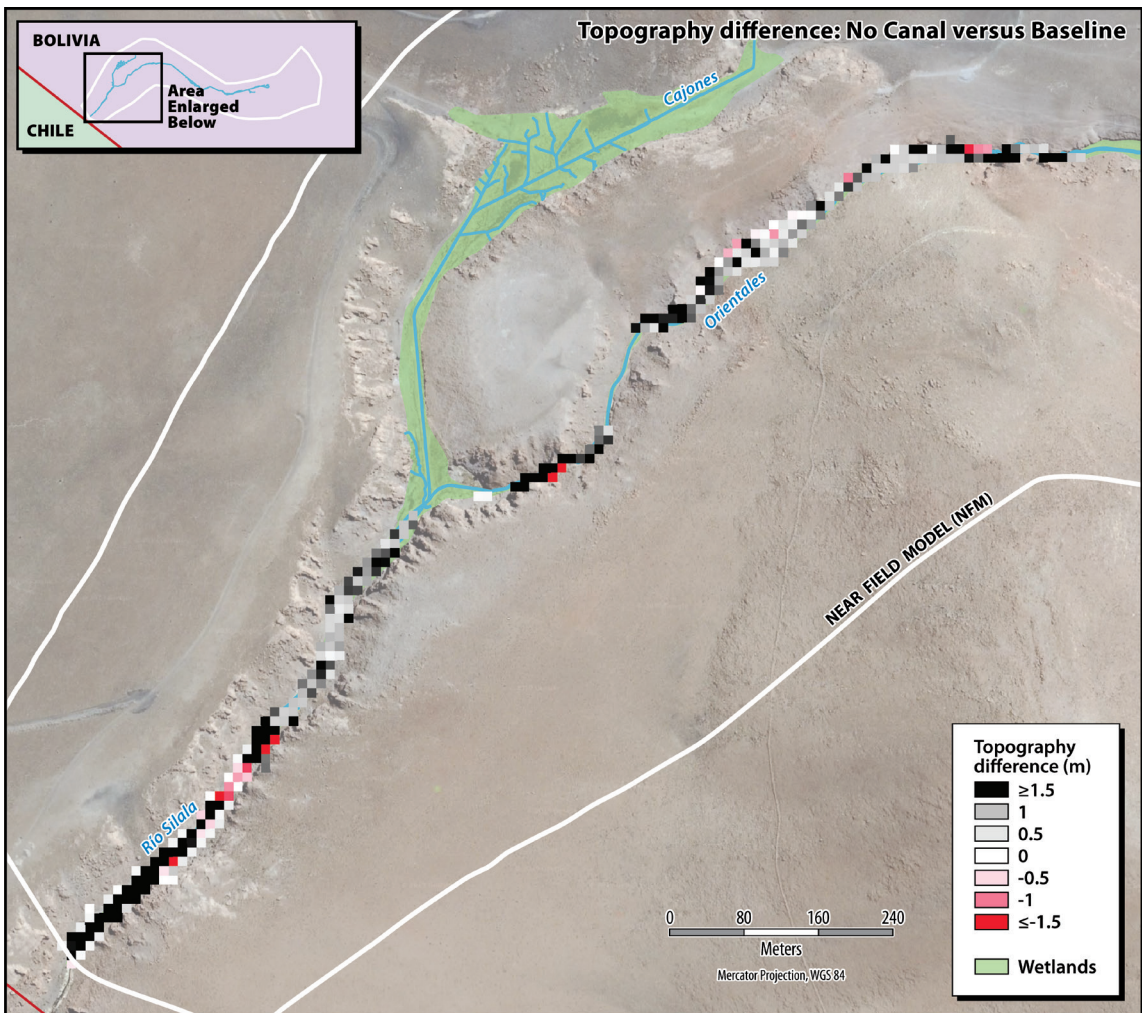


Figure 4-6. Difference between No Canal MIKE-SHE and Baseline MIKE-SHE topographies.

The very large differences between the topography used in the Baseline MIKE-SHE and Baseline MIKE-11 models, on the one hand, and the No Canal MIKE-SHE model, on the other, are not described in the DHI report. These differences, especially the differences of up to 7 m between the Baseline MIKE-11 and No Canal MIKE-SHE topographies shown at the downstream end of the catchment in Figure 4-3, mean that the No Canal scenario is not simply representing the removal of the channels, it also represents an increase in the level of the land surface on the Bolivian side of the border. This is an enormous change in ground level, equivalent to a structure the height of a two-story building spanning the width of the river valley and extending at least 200 m along the river.

Raising the ground surface in this way would reduce the amount of water that would be able to enter the surface water system from groundwater and increase the amount that would leak from the surface water system into groundwater.

In terms of the boundary conditions used by DHI in their model, the dramatic raising of the ground surface would also have the effect of increasing the groundwater heads at the inflow and outflow boundaries, which would in turn reduce the groundwater inflows to the model (from the fixed head boundaries), and increase the groundwater outflows (through the fixed gradient boundaries), leaving less water available to appear as surface water flow in their model.

As DHI's comparison of flows with and without the channels only refer to the surface water component of flow, artificially diverting from the surface water system to the groundwater system in this way gives a false impression of the influence of the channels.

These major differences between the Baseline and No Canal and Undisturbed scenarios are not described in any way in the DHI report. The failure to present this information in the Bolivia's Counter-Memorial leads to a comparison that is unjustified and incorrect, and exaggerates the effects that Bolivia is attempting to prove. At best, therefore, this is highly misleading for the Court.

4.2.2 Steady-state verification

The water balance from the Baseline scenario was examined to see if the model had reached a steady state. This is important as otherwise the model results will be influenced by the initial conditions, and the estimated flows will be affected because the water balance includes unrealistic changes in storage. A steady state condition means that the sum of the inflows is equal to the sum of the outflows, and any changes in groundwater storage should be negligible (i.e., groundwater levels have reached an equilibrium).

Figure 4-7 shows the flow rates to and from groundwater storage over time in the Baseline scenario. By the end of the simulation, there are still significant flows (4 l/s) coming out from groundwater storage. Therefore, the model had not reached a steady state at the end of the simulation period and the simulated flows are influenced by the model initial conditions and an associated error in the water balance.

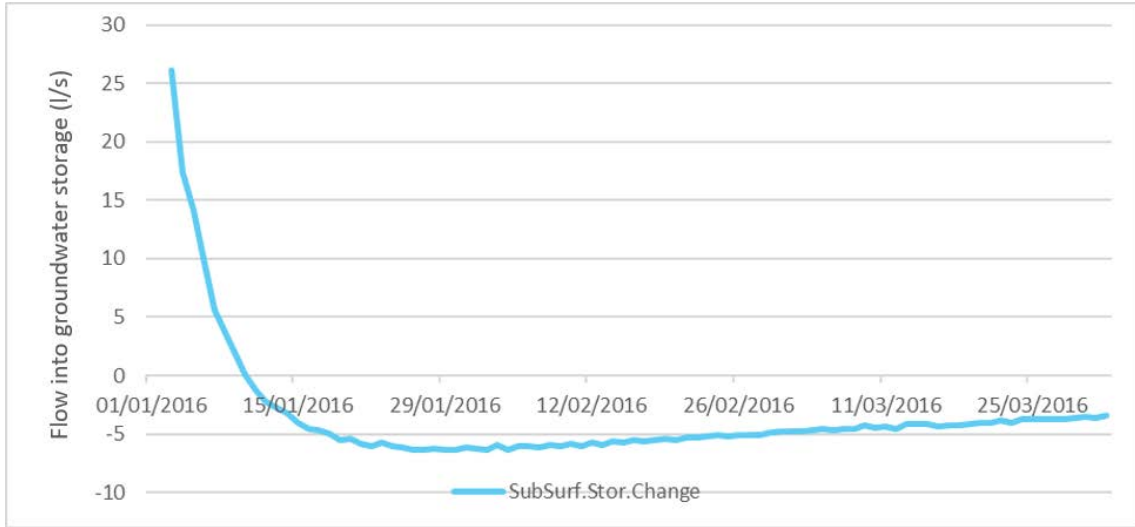


Figure 4-7. Flows into groundwater storage in the NFM, indicating that steady state has not been reached.

4.2.3 Boundary conditions

The distribution of boundary condition types is the same for the three scenarios of the NFM and is shown in Figure 4-8. Note that the NFM comprises three layers with depth (called by DHI in its NFM files Near Surface, Upper Silala Ignimbrite (Bol), and Lower Silala Ignimbrite (Bol))⁴. The same distribution of boundary condition types is used in each layer. Specifically, Figure 4-8 shows the boundary conditions of the Near Surface layer. The DHI model boundary conditions consist of three types (BCM, Vol. 5, p. 18):

- Fixed head: constant in time and equal to the Initial Potential Head (variable in space) in two borders, one at the eastern border and another at the northern border.
- No-Flow: one at the northern border and the whole southern border.
- Fixed gradient: equal to -0.05 at the western border. This gradient was obtained from Arcadis (2017).

DHI defined the boundary conditions using the piezometric map presented in Figure 2-3 (BCM, Vol. 2, p. 293). In Annex G to DHI (2018) (BCM, Vol. 5, p. 18), it is explained that a no-flow boundary is imposed where the head contour lines are perpendicular to the model boundary. Thus, the only flows entering the numerical model should be located where the piezometric lines are not perpendicular to the model borders. However, the boundary conditions are not consistent with the piezometric map presented by DHI (2018) in their conceptual model. As can be seen in Figure 4-2A, there should be flow exiting the model through the southern boundary, but instead, DHI

⁴ Note that the three scenarios of the NFM are not to be confused with the three depth layers in the model.

(2018) imposes a no-flow condition at that boundary. Additionally, the no-flow condition imposed on two boundaries of the model is an artificial condition, since there are no impermeable or very low permeability rocks at those boundaries (except where the Miocene volcanics outcrop to the southeast of the Cajones, but this is Chile's interpretation of the Geology, not Bolivia's). Consequently, both the conceptual and the numerical models are incorrect. The numerical model is not only based on a conceptual model that does not represent correctly the reality of the data presented, but also is not consistent with DHI's own conceptual model.

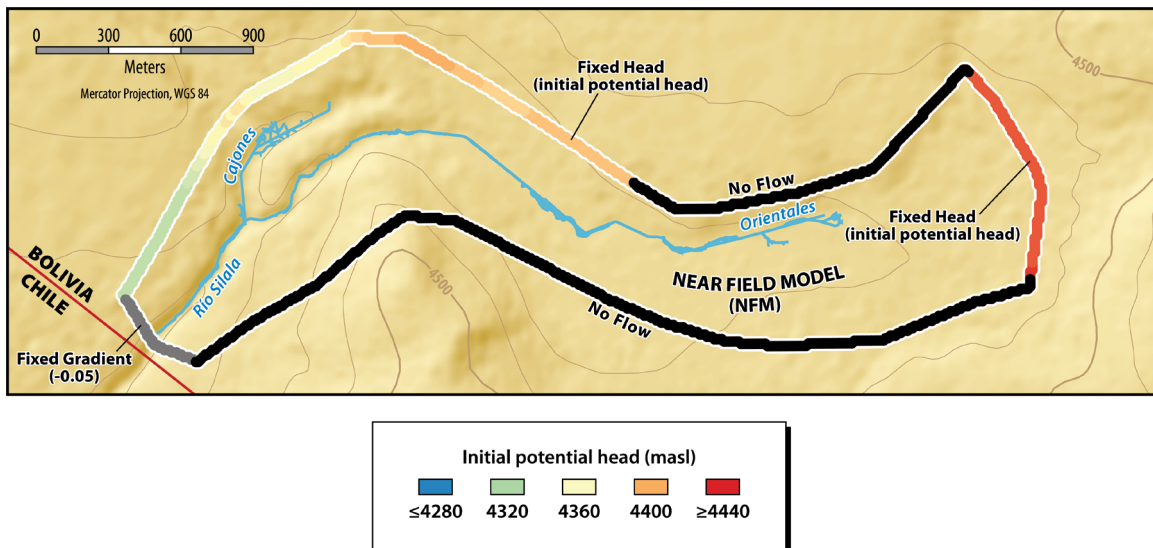


Figure 4-8: Near Field Model boundary conditions of the Near Surface layer. The same distribution of boundary condition types is used in each layer, but the Fixed Head boundary values change between layers. All three scenarios have the same boundary conditions.

4.2.4 Inconsistency between the Water Balance Model and the Near Field Model

Figure 4-9 shows the boundary conditions and the initial potential head contour lines of both the Water Balance Model and the Near Field Model (Baseline and No Canal scenarios). In both models the boundary conditions are shown by colour coding on the model boundary, and for the WBM they are also illustrated with arrows showing flow directions. The head contour lines are different for the two models. Also, when the head contours from the WBM are compared to the NFM boundary conditions, it is observed that there is an outflow from the WBM that should flow into the NFM through the northern No-Flow boundary (black arrow). Additionally, it is observed that a part of the WBM outflow is exiting the WBM model across the international border without

entering the NFM model (black arrow). Therefore, there is an inconsistency between the boundary conditions and the groundwater flow directions of the two models.

In addition to the inconsistencies between the flow directions at the boundaries of the two models, there are also inconsistencies between the flow rates. The 198 l/s that leaves the WBM (see Table 3-1) is not the same as the 212 l/s of groundwater flow that enters the Baseline NFM scenario (Table 4-4). Furthermore, the amounts of groundwater flow that enter the No Canal and Undisturbed scenarios of the NFM model (190 l/s and 185 l/s from Table 4-4) are reduced relative to the Baseline scenario. We note that the inflows to the near field model are determined by the model boundary conditions. The effect of this was extensively discussed in Chile's Reply (see Expert Report by Wheater and Peach, CR Vol.1, pp. 85-154) where it was shown that this will have exaggerated the effect of channelization and peat development, perhaps by a factor of 20. We reiterate here that the recharge to the wider groundwater catchment is unaffected by these localized effects, and that there is no explanation given by DHI for where the missing water has gone in these scenarios.

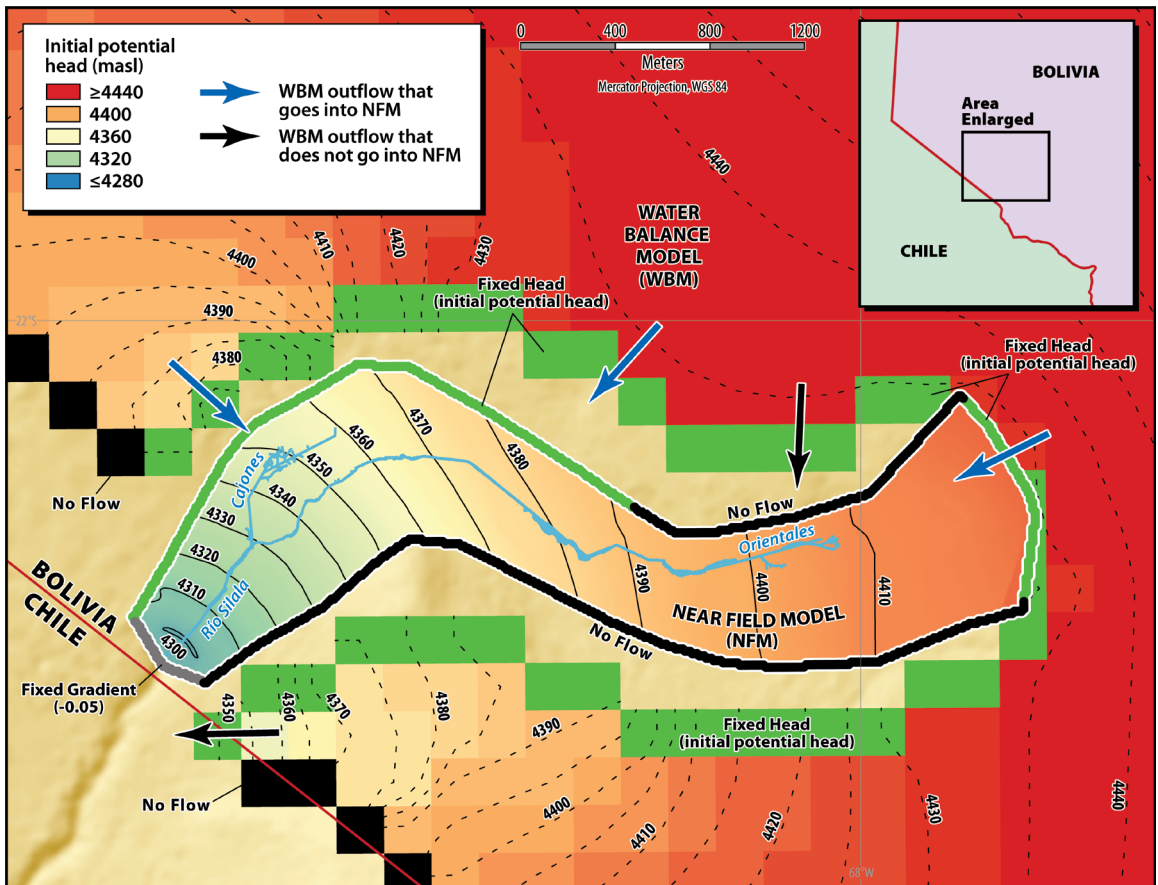


Figure 4-9. Boundary conditions and initial potential head contour lines of both Water Balance and Near Field models. Neither the contour lines nor the flow directions coincide in the two models.

4.2.5 Initial Potential Head of the Near Field – MIKE-SHE model

According to DHI (BCM, Vol. 5, p. 18), the initial potential head map was built using the information obtained in the field from manual measurements. We compared the initial potential heads of the Lower Silala Ignimbrite (Bolivia defined) layer (Computational layer n°3) for the Baseline and No Canal scenarios (which are the same) and the Undisturbed scenarios (Figure 4-10). The initial potential heads used by DHI (2018) in the Baseline scenario are the same as the No Canal scenario, but are different from the Undisturbed scenario. Given that these scenarios are supposed to be steady-state simulations and represent different physical configurations it would be reasonable for them to have different initial conditions. However, there is a methodological inconsistency as the same initial conditions are used for the Baseline and No Canal scenarios but not in the Undisturbed scenario, and there is no explanation given to support these differences. We also note that since none of the three simulations reached the steady-state condition (see Section 4.2.2), the initial groundwater heads influence the results of the simulations.

The differences between the initial potential heads in the Baseline/No Canal and the Undisturbed scenarios are shown in Figure 4-11, and vary between -18 m and +16.5 m. These very large imposed differences in the initial conditions mean that the three simulations are neither equivalent nor comparable. Figure 4-12 shows the difference between the final heads of the Baseline scenario and the No Canal and Undisturbed scenarios.

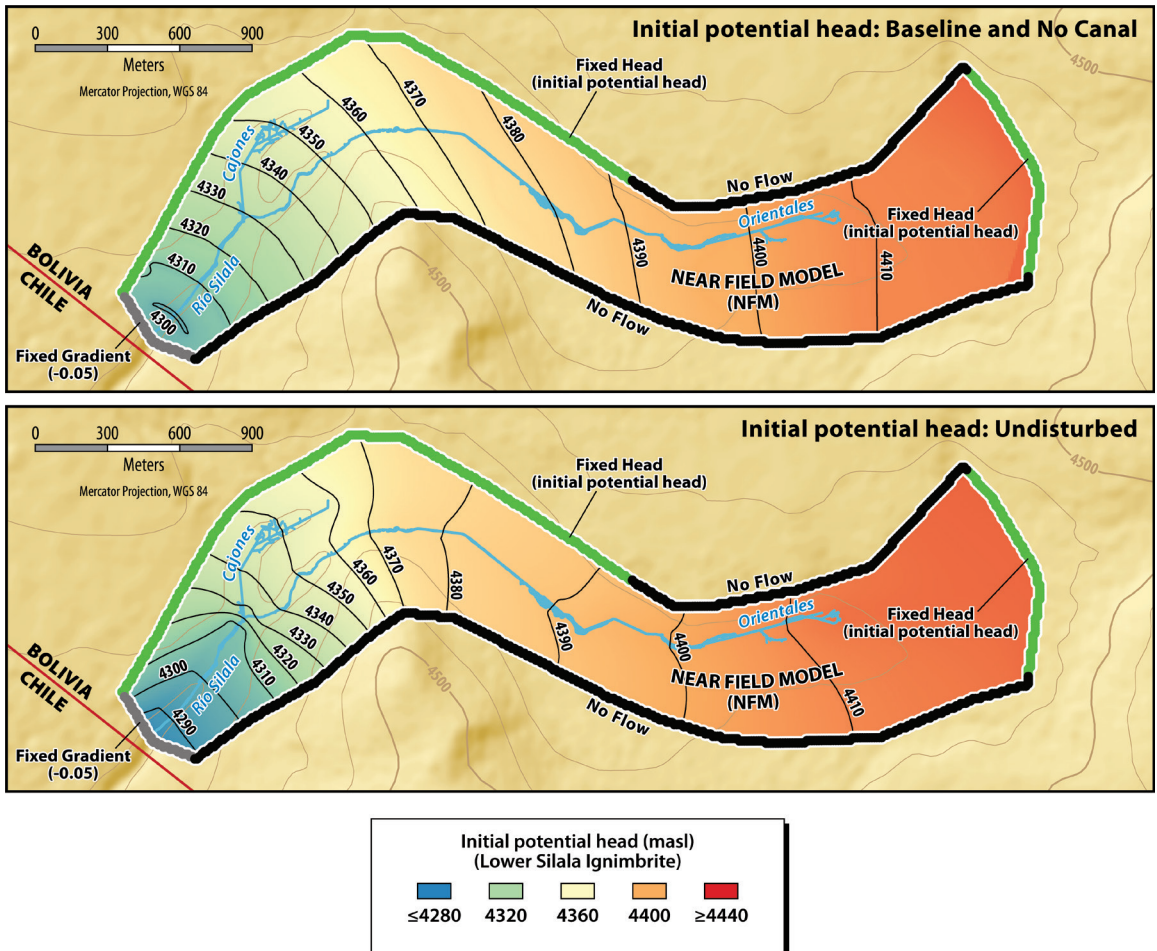


Figure 4-10. Initial potential head map and contour lines in the NFM.

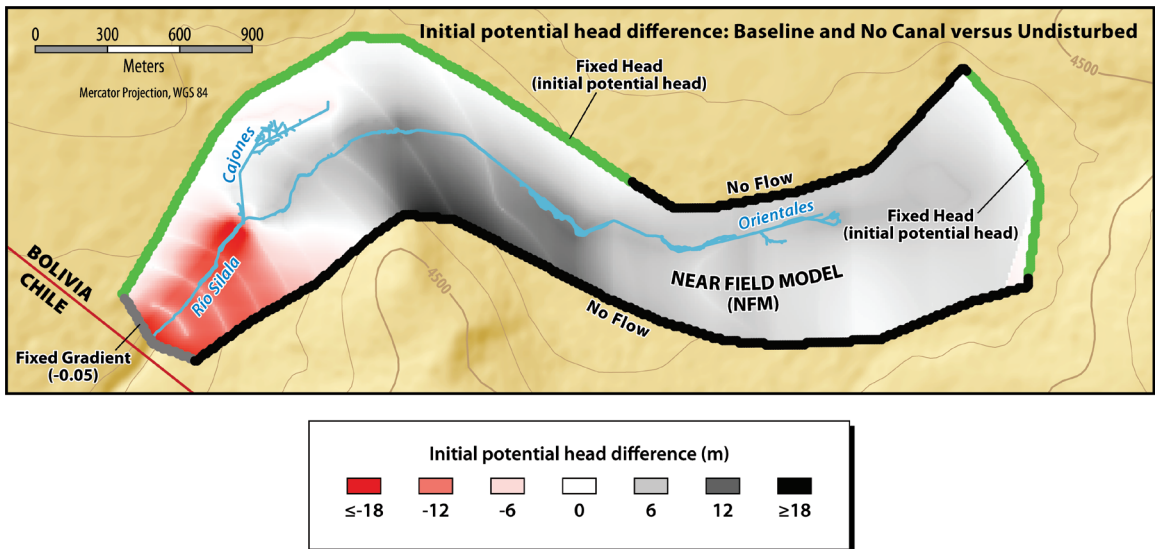


Figure 4-11. Initial potential head difference between the Baseline/No Canal scenarios and the Undisturbed scenario. Positive values correspond to locations where the initial potential head is higher in the Undisturbed scenario.

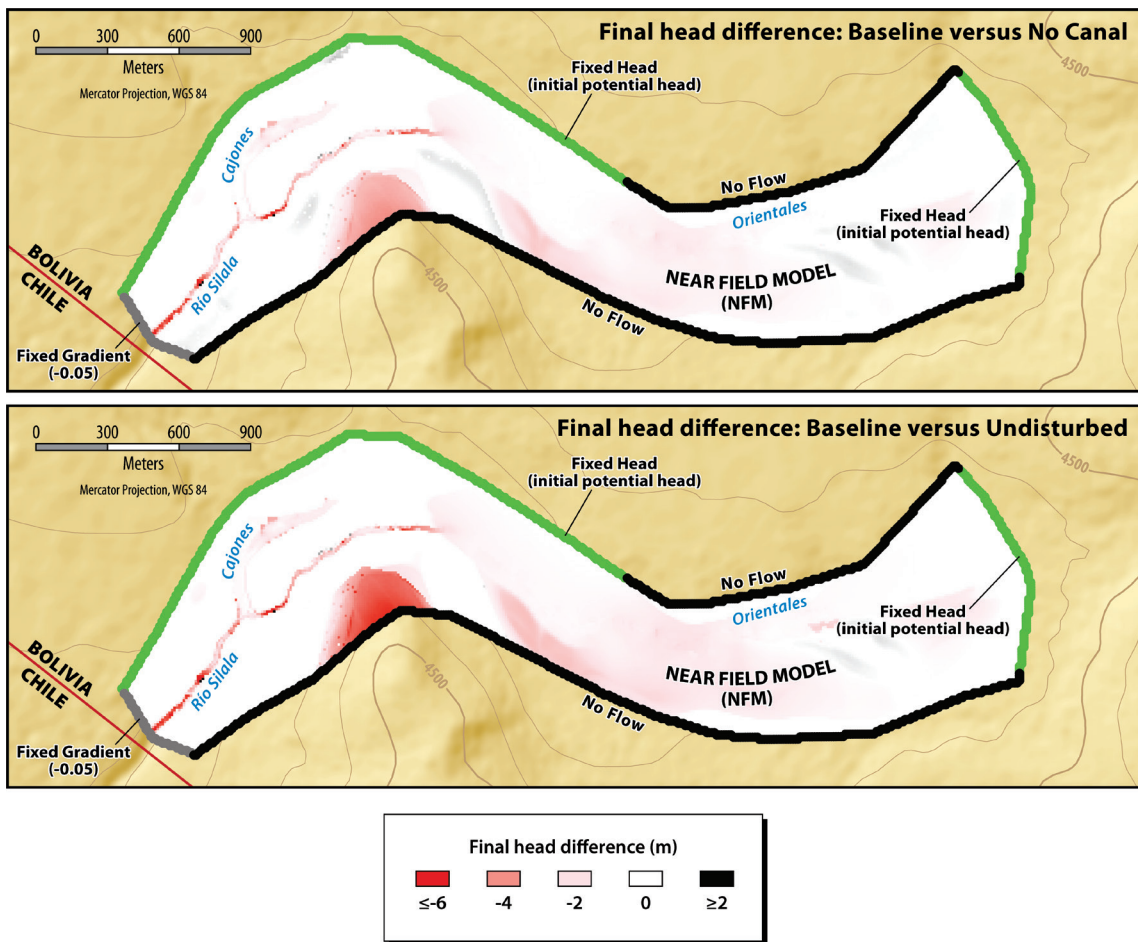


Figure 4-12. Final potential head difference between the Baseline and the No Canal scenarios (upper panel) and the Baseline and Undisturbed scenario (lower panel). Positive values correspond to locations where the final potential head is higher in the Baseline scenario.

4.2.6 Surface water modelling

In the Baseline scenario, the channel sections were represented explicitly in the MIKE-11 model, whereas in the No Canal and Undisturbed scenarios the MIKE-11 component of the model was removed and the natural river sections were not represented explicitly, meaning that the sections for the No Canal and Undisturbed scenarios have no natural channel(s). Figure 4-13 shows the MIKE-SHE and MIKE-11 topographies of the same cross-section. Also, when reviewing the model files, it was found that, to represent the wetland springs, there were local flow injections in all three scenarios. These inflows will hereinafter be referred to as “spring recharge”. This feature is inconsistent with the physical basis of the model, in which groundwater inflow to the Near Field is determined by the NFM fixed head inflow boundary conditions. It appears that

additional water has been created arbitrarily. This characteristic of the model is neither explained nor justified in DHI's report.

Table 4-1 summarizes the main aspects of river elements and the way that the “spring recharge” was modelled in the different scenarios.

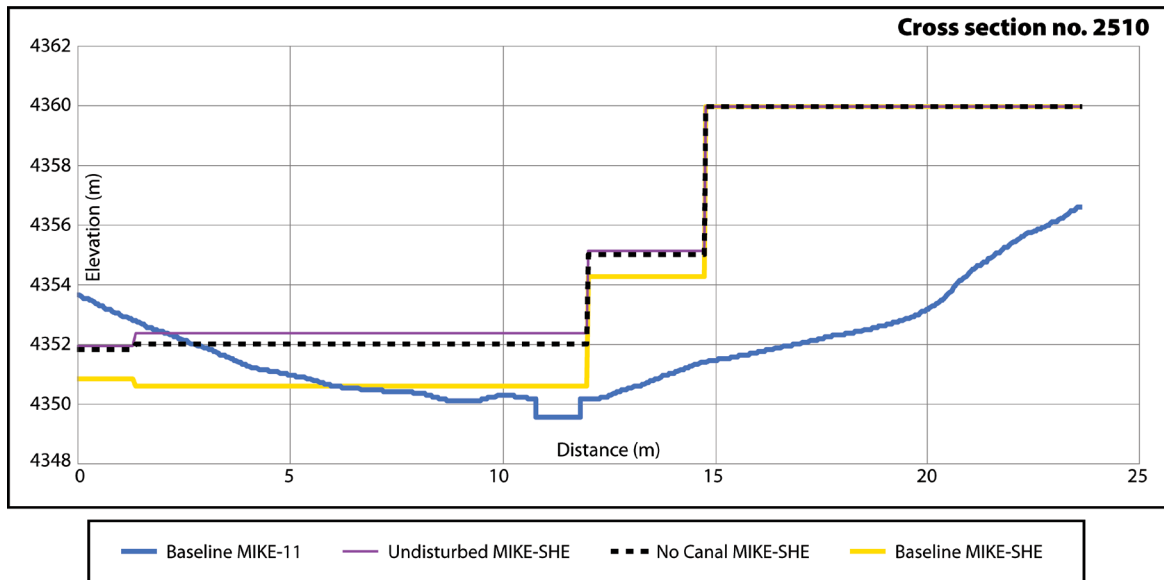


Figure 4-13. Representation of the channels in the different scenarios. The yellow, dotted black and purple lines represent the topography of the Baseline, No Canal and Undisturbed scenarios of the MIKE-SHE model, respectively. The blue line represents the channel section of the MIKE-11 model in the Baseline scenario. In the No Canal and Undisturbed scenarios, these channel sections were not represented explicitly.

Scenario	Hydrological Model	Canal or Natural/Undisturbed river section	River element	Spring Recharge	Elevation
Baseline	MIKE-SHE+MIKE-11	modelled by MIKE-11 – Dynamic Wave	Channel and banks	Local flow at headwaters and springs: 42 l/s	Topographical profiles
No Canal	MIKE-SHE	modelled as Overland Flow by MIKE-SHE – Diffusive Wave Approximation	Natural sections	Local Precipitation: 31 l/s (95 mm/in 91 days)	First Modification of Digital Elevation Model
Undisturbed	MIKE-SHE	modelled as Overland Flow by MIKE-SHE – Diffusive Wave Approximation	Restored sections	Local Precipitation: 31 l/s (95 mm/in 91 days)	Second Modification of Digital Elevation Model

Table 4-1. Summary of main aspects of river elements and the way that the spring recharge is modelled in the different scenarios.

As presented in Table 4-1, the spring recharge incorporated in the model is different for each scenario. In the Baseline scenario, a constant flow of 1 l/s at the headwater of each of 32 channels and at 10 springs in the MIKE-11 model is injected (a total of 42 l/s). Figure 4-14 shows the location of these inflows. In contrast, in the No Canal and Undisturbed scenarios, a total of 31 l/s (at 1 l/s or 2 l/s per spring cell) was injected into the MIKE-SHE model as *local precipitation* in a subset of the spring cells (Figure 4-15). The flow injected as precipitation in the No Canal and Undisturbed scenarios not only contributes to the overland flow (68%), but also part of this flow directly interacts with the saturated and the unsaturated zones (31%). This difference between the scenarios, which affects the distribution of surface water and groundwater outflows from the catchment, is not explained or justified by the DHI in its reports. The implications of this for DHI's water balances, and the supposed impacts of channelization, are discussed below in section 4.2.8.

It is important to mention that a sophisticated coupled surface water-groundwater model should be able to represent spring flows as interactions between groundwater and surface water: where the water table comes to surface, springs should appear in the groundwater model, representing discharge points for groundwater, and sources of surface water. It is unrealistic to represent the springs as anything other than interactions with groundwater and representing them as point sources of water injection as DHI have done is simply incorrect.

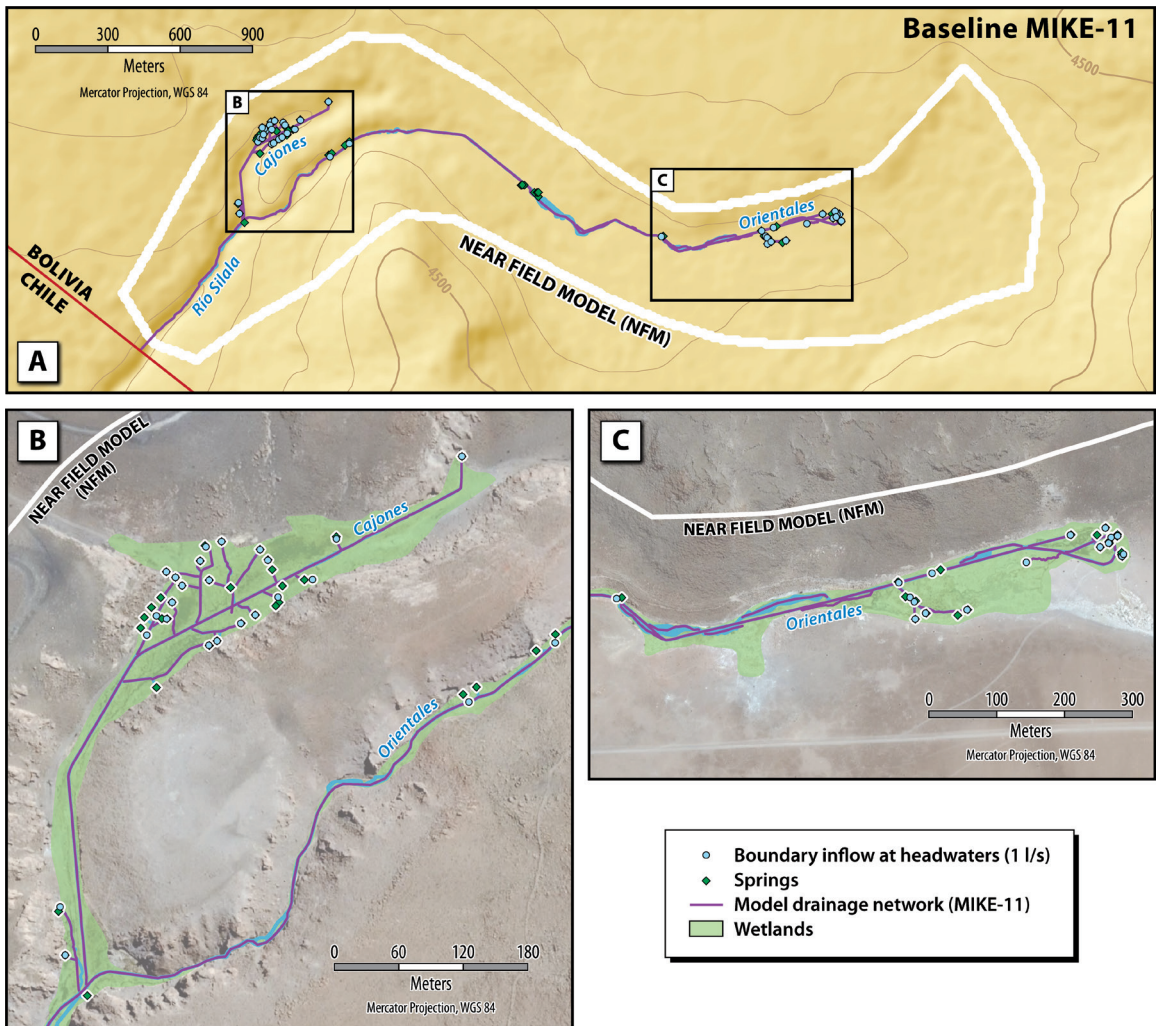


Figure 4-14. Constant inflow at each channel headwater node to model additional spring recharge for the Baseline MIKE-11 scenario, not as a result of interaction between the groundwater and surface water models

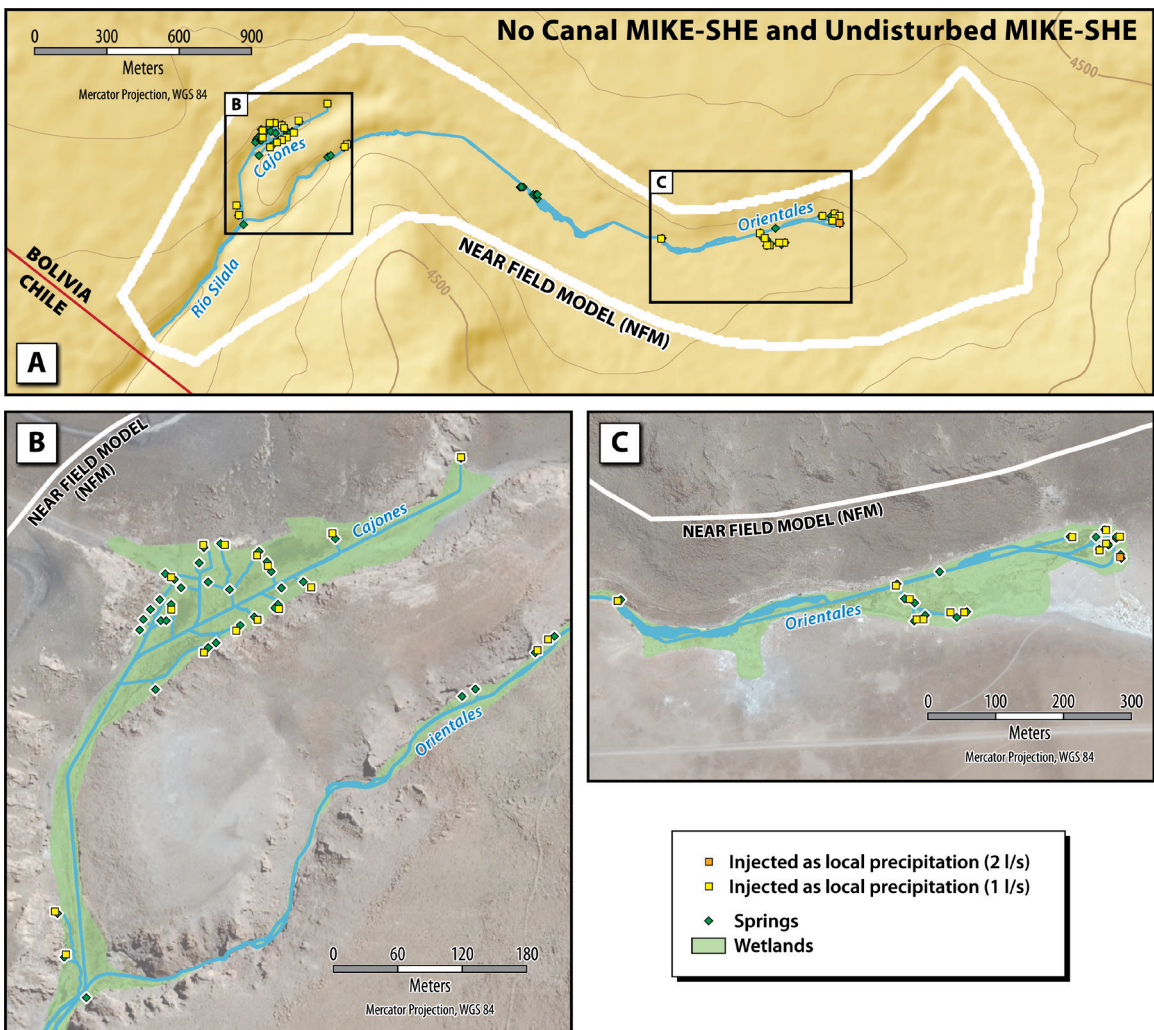


Figure 4-15. In the No Canal and Undisturbed scenarios, additional spring recharge is injected as “precipitation” into the spring cells, not as a result of the interaction between the surface and the groundwater in the coupled model MIKE-SHE.

4.2.6.1 Surface flow calculation in the baseline scenario – MIKE-11

To calculate the surface flows in the channels modelled in the Baseline scenario, the complete 1-D dynamic wave formulation of the Saint-Venant equations is solved using the MIKE-11 model. When coupling the MIKE-11 and the MIKE-SHE models, both the overland flow and groundwater flow modelled in MIKE-SHE are linked directly to MIKE-11 through MIKE-SHE Links (DHI, 2017b).

During a simulation, water levels within the coupled reaches are transferred from MIKE-11 to adjacent MIKE-SHE links. In turn, MIKE-SHE calculates the overland flow to each river link from neighboring grid squares and the river-aquifer exchange. These terms are fed back to the corresponding MIKE-11 as lateral inflows or outflows.

These flow transfers are directly dependent on the topography used for the MIKE-11 sections.

The MIKE-11 model was reviewed in detail. In the following sub-sections we present the results of the main channel reach between the Orientales and Cajones confluence and the last section of the MIKE-11 model (Figure 4-16).

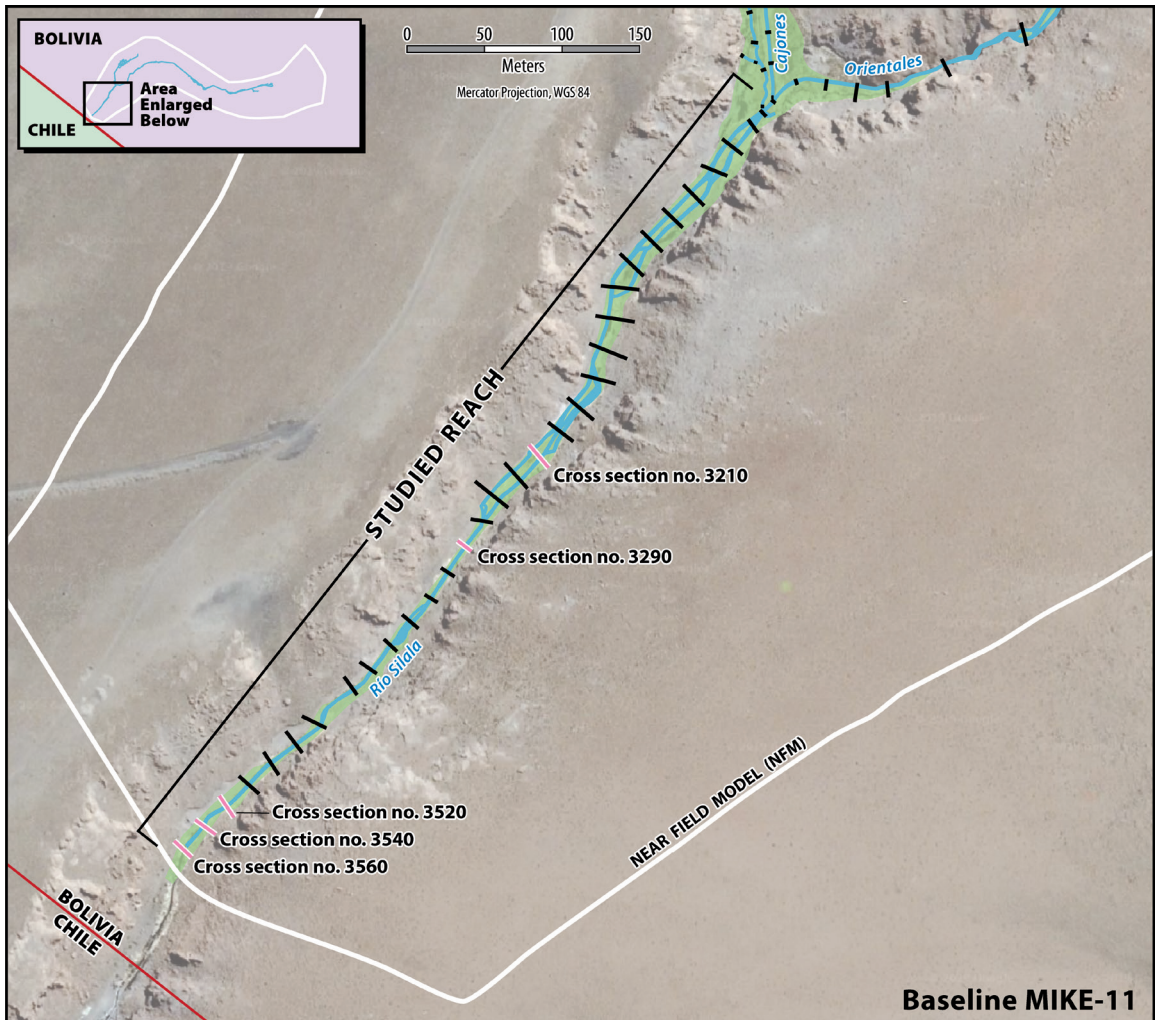


Figure 4-16. Reviewed reach and location of the cross sections (in pink lines) that are presented in the following sub-sections.

4.2.6.1.1 Downstream boundary condition

The discharge at the exit of the MIKE-11 Baseline scenario is calculated using a stage-discharge curve in the last section of the MIKE-11 model (3635, which is located near the international border outside the NFM boundaries), and the slope between the two last cross sections (3560 and 3635) is zero, which is unrealistic (Figure 4-17). This curve was defined to impose a critical flow condition, i.e., Froude number (Fr) equal to 1. The stage-discharge curve is then defined as the one in which Q and h meet $Fr = 1$:

$$Fr = 1 = \frac{Q(h)}{\sqrt{\frac{g \cdot A(h)^3}{T(h)}}}$$

where T is the width of the channel open surface, A is the cross sectional area of water in the channel and g is the acceleration of gravity.

This feature of the model is not explained or justified in the DHI report. The water level at the exit of the model in the last timestep is 4282.97 m.a.s.l., which corresponds to a flow of 150 l/s. This water depth is obtained after 91 days of simulation, where the steady state has not yet been reached in the integrated MIKE-SHE/MIKE-11 model.

When comparing the flow rates of the MIKE-11 model (150 l/s) with those of the MIKE-SHE water balance (143 l/s), a difference of 7 l/s is obtained (see Table 4-4 in Section 4.2.7), which is attributed to the use of the stage-discharge curve. The most significant aspect of this difference is that it was not reported in the DHI reports and that it results in an additional 7 l/s difference in flow rates between the Baseline and No Canal and Undisturbed scenarios, which is then reported as part of the impact of the channelization, when actually it is due to errors in the MIKE-11 modelling. The logical thing to do would be to compare the results of the MIKE-SHE models, instead of mixing the results of the MIKE-11 model in the Baseline scenario and the MIKE-SHE results in the No Canal and Undisturbed scenarios.

4.2.6.1.2 Manning coefficient and flow conditions

The Manning coefficient, n , which represents the hydraulic roughness of the channels, was found to be extremely high ($n = 0.200$).

Table 4-2 shows typical Manning coefficients. In the case of the Silala River, whose water flows through the channel, the expected values would be between 0.017 and 0.035 in the channelized reaches (minimum and maximum values for built masonry channels) and between 0.035 and 0.05 in the natural ones (minimum and maximum values for natural streams). Therefore, using a resistance of $n = 0.200$, which is representative of

the highest values recommended for flood plains covered by dense trees, is physically unrealistic.

Type of channel and description	Minimum	Normal	Maximum
B. Lined or Built-Up Channels			
B-2. Nonmetal			
g.- Masonry			
1. Cemented rubble	0.017	0.025	0.030
2. Dry rubble	0.023	0.032	0.035
D. Natural streams			
D-1. Minor streams (top width at flood stage 100 ft)			
a.- Streams on plain			
4. Clean, winding some pools and shoals, some weeds and stones	0.035	0.045	0.05
D-2. Flood plains			
d.-Trees			
1. Dense willows, summer, straight	0.110	0.150	0.200

Table 4-2. Typical Manning coefficients, n , for open channel flow for lined or built-up channels, natural streams and flood plains. The complete table is presented in Appendix B. Source: Chow (1959)

As a result of the high imposed value of the Manning coefficient, the normal depth of the channel is increased and the flow conditions are subcritical ($Fr < 1$) in almost all the cross sections, which does not coincide with what is observed in the field, i.e., supercritical flow conditions ($Fr > 1$). Subcritical conditions are observed when the flow is dominated by gravitational forces and behaves in a slow or stable manner, whereas a supercritical flow is dominated by inertial forces, and behaves in a fast or unstable way.

Considering the correct geometry of the last section of the river represented by the MIKE-11 model, i.e. a topographic slope of 5%, and a Manning coefficient of 0.035 (maximum value for built masonry channels), the normal depths of the cross section were calculated for the flow range reported by DHI (between 160 and 210 l/s), obtaining supercritical conditions (see Table 4-3). These results are consistent with field observations. However, DHI results show subcritical conditions (Froude number < 1) for most of the cross-sections, as shown in Figure 4-17. Hence, the results of DHI are unrealistic and conceptually inconsistent with the observed flow regime.

Discharge (l/s)	hc (m)	hn (m)	Froude (-)	Flow conditions
160	0.18	1.57	1.17	Supercritical
210	0.21	1.90	1.16	Supercritical

Table 4-3. Flow conditions in the Silala River at the international border. hc is the critical depth and hn is the normal depth of the Silala River at the international border. As hn is higher than hc, the normal flow condition is subcritical.

The resulting increase in the normal water depth (subcritical flow) due to the high Manning's n and the imposition of a critical flow in the last cross section affect the river-aquifer interactions, for example, more water than is realistic could be expected to infiltrate into the aquifer due to a larger hydraulic gradient between the river and the aquifer.

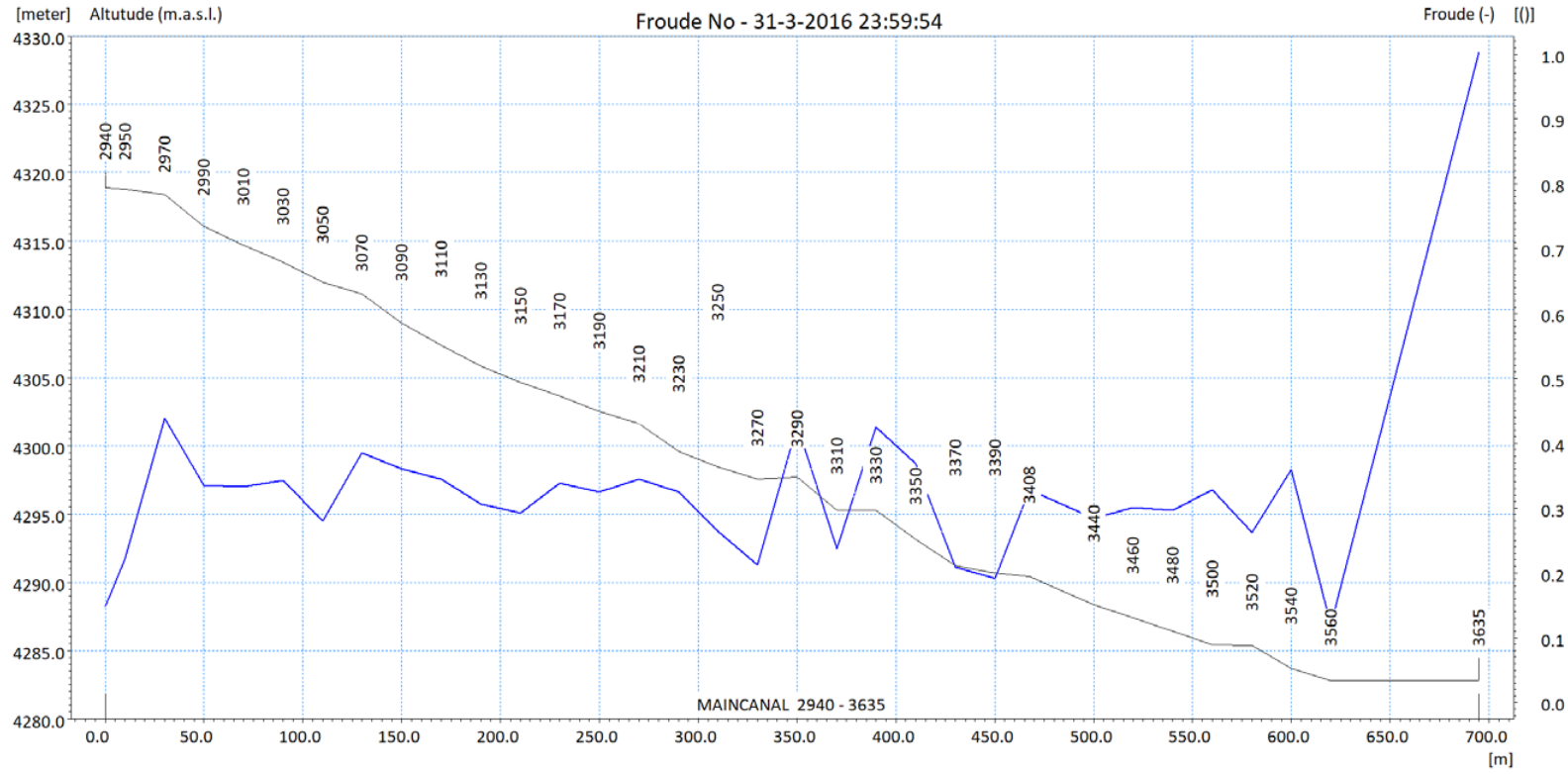


Figure 4-17. Froude number in the reach between the wetland confluence and the last section of the model. The vertical numbers represent the cross-section number, which is also the distance from the beginning of the main channel, located in the headwaters of the Orientales wetland and not shown in this profile. The x axis shows the distance from the beginning of the analyzed reach, which starts at 2940 m and ends at 3635 m of the MAINCANAL in MIKE-11.

4.2.6.1.3 Channel geometry

The channel geometry of the MIKE-11 model was also reviewed in depth. It was found that water at some of the cross sections does not flow through the main channel. Figure 4-18 shows the water level in the reach between the confluence of the Orientales and Cajones wetlands and the last section of the MIKE-11 model. Figure 4-19 shows some of the cross sections where the water does not flow through the main channel and Figure 4-16 shows the location of these sections. DHI (2018) provided no information related to the validity of the topography used in the Baseline MIKE-11 model. For instance, it is unclear why the main channel does not follow the bottom of the valley.

In two cross sections of the studied reach (between sections 2940 and 3625 of the main channel) the channel is simulated as being flooded and the water flows over the river banks (Figure 4-20). This behaviour does not represent the reality, where under an average flow condition the water only flows through the main channel.

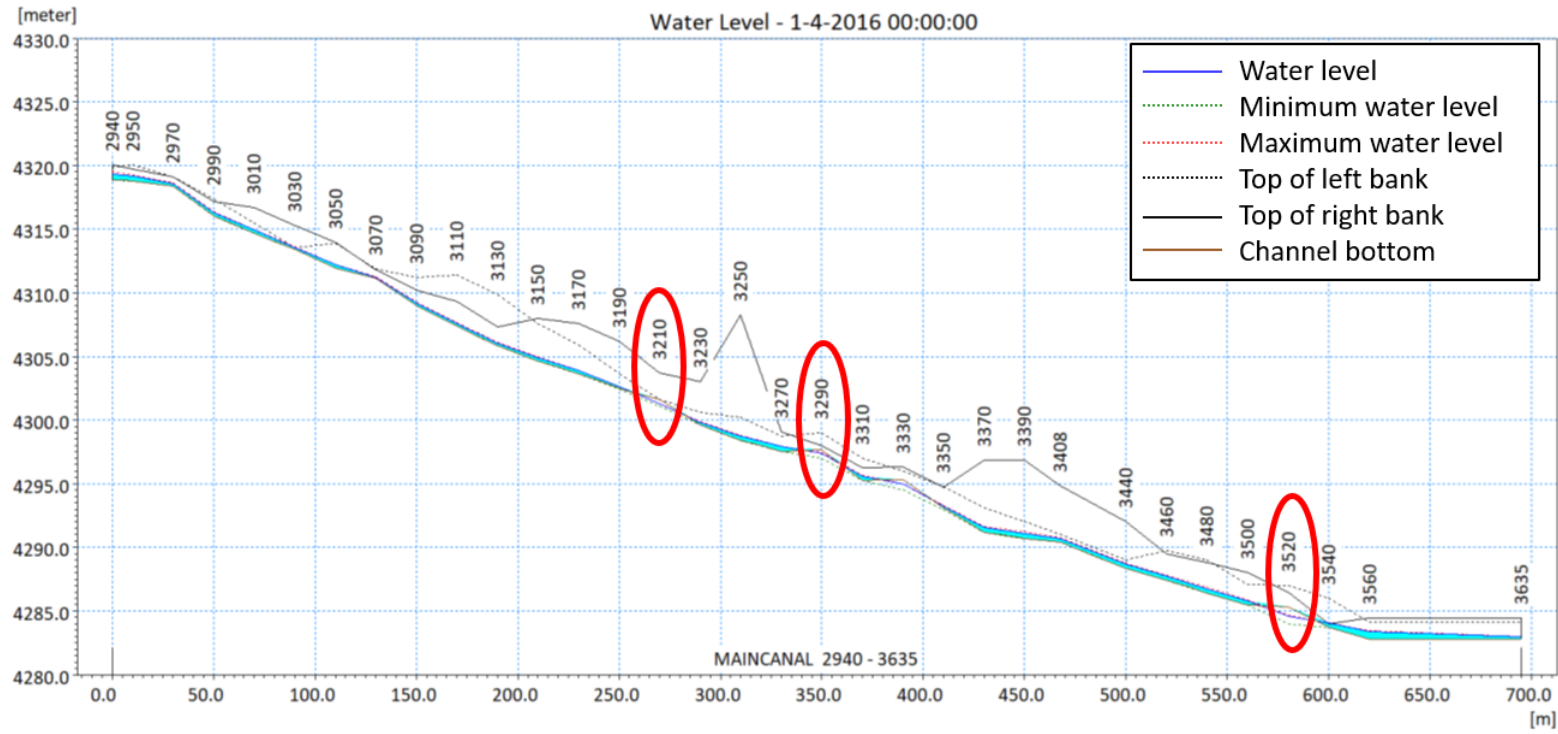


Figure 4-18. Water level in the reach between the confluence of the Orientales and Cajones wetlands and the last section of the MIKE-11 model. Some of the cross sections where water does not flow through the channel are depicted with a red circle (Figure 4-19).

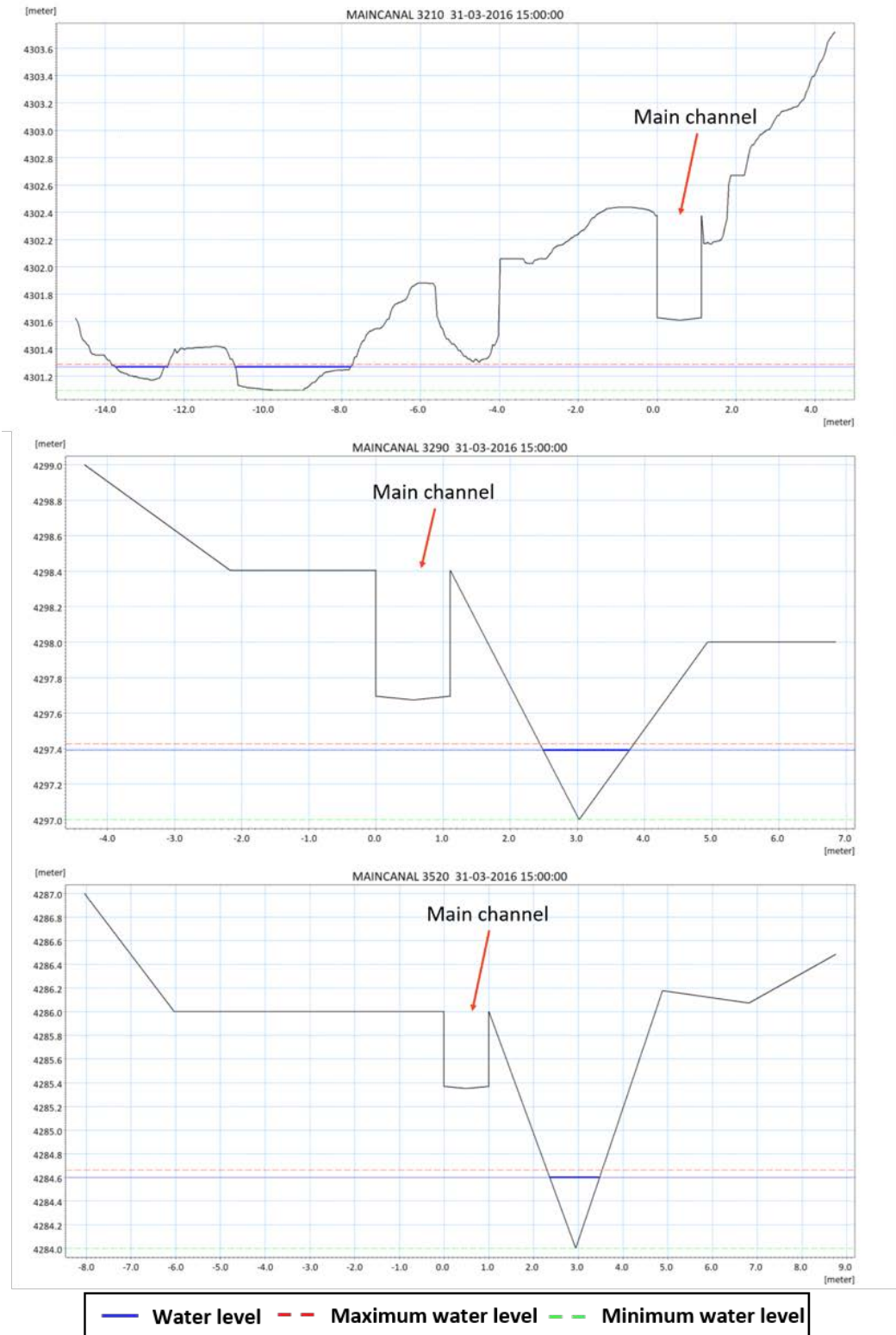


Figure 4-19. Some of the cross sections where the water does not flow through the main channel.

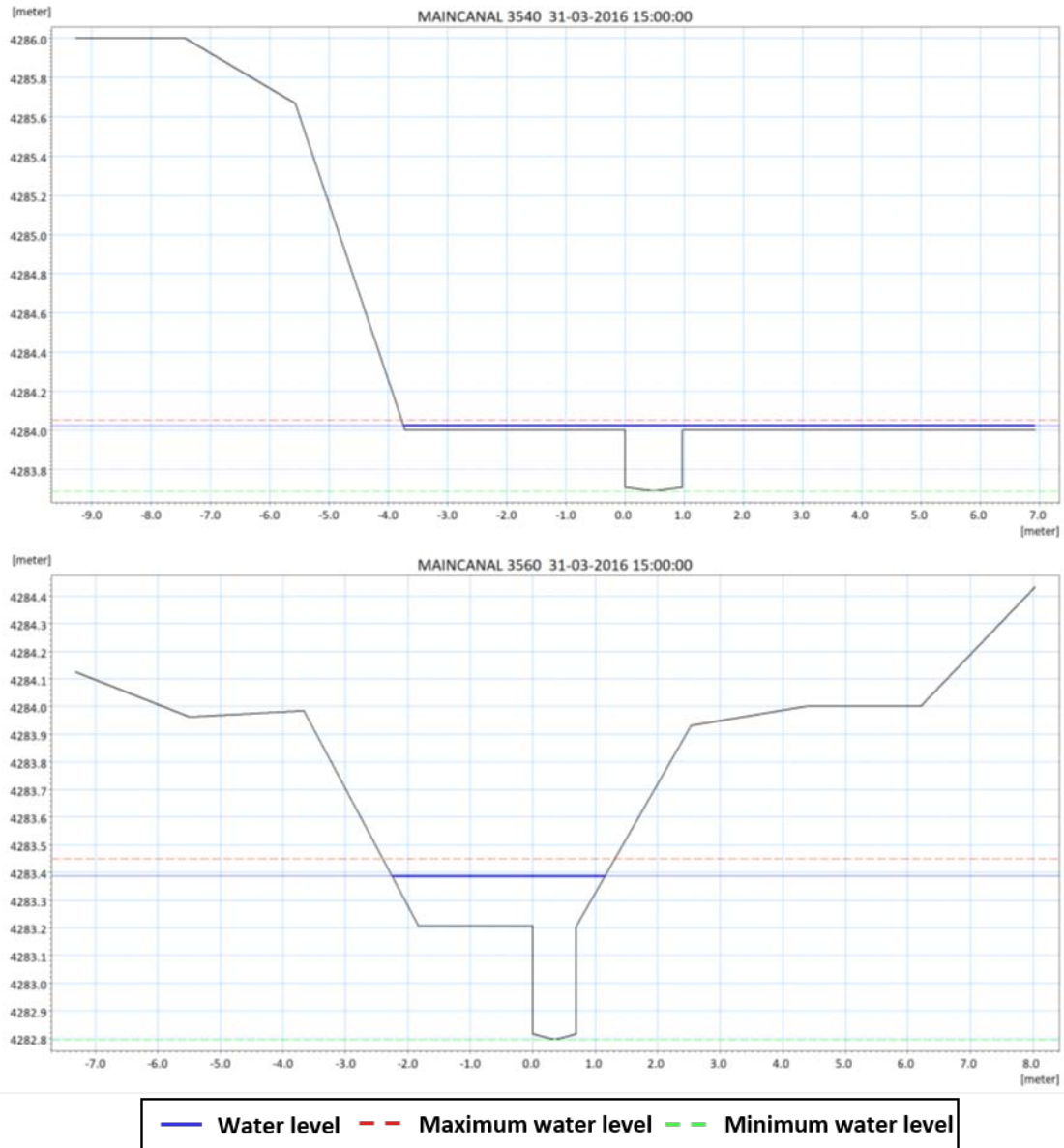


Figure 4-20. Cross sections were the channel is flooded.

4.2.6.1.4 Numerical instability in MIKE-11 model

When reviewing the Baseline MIKE-11 scenario results, errors were found in the DHI's hydraulic modelling:

- Abrupt changes in river flow were found at different points.
- There are flow variations along the river that never stabilize, even at the end of the simulated period. Figure 4-21 shows the flow variations at two points in the river throughout the simulation.

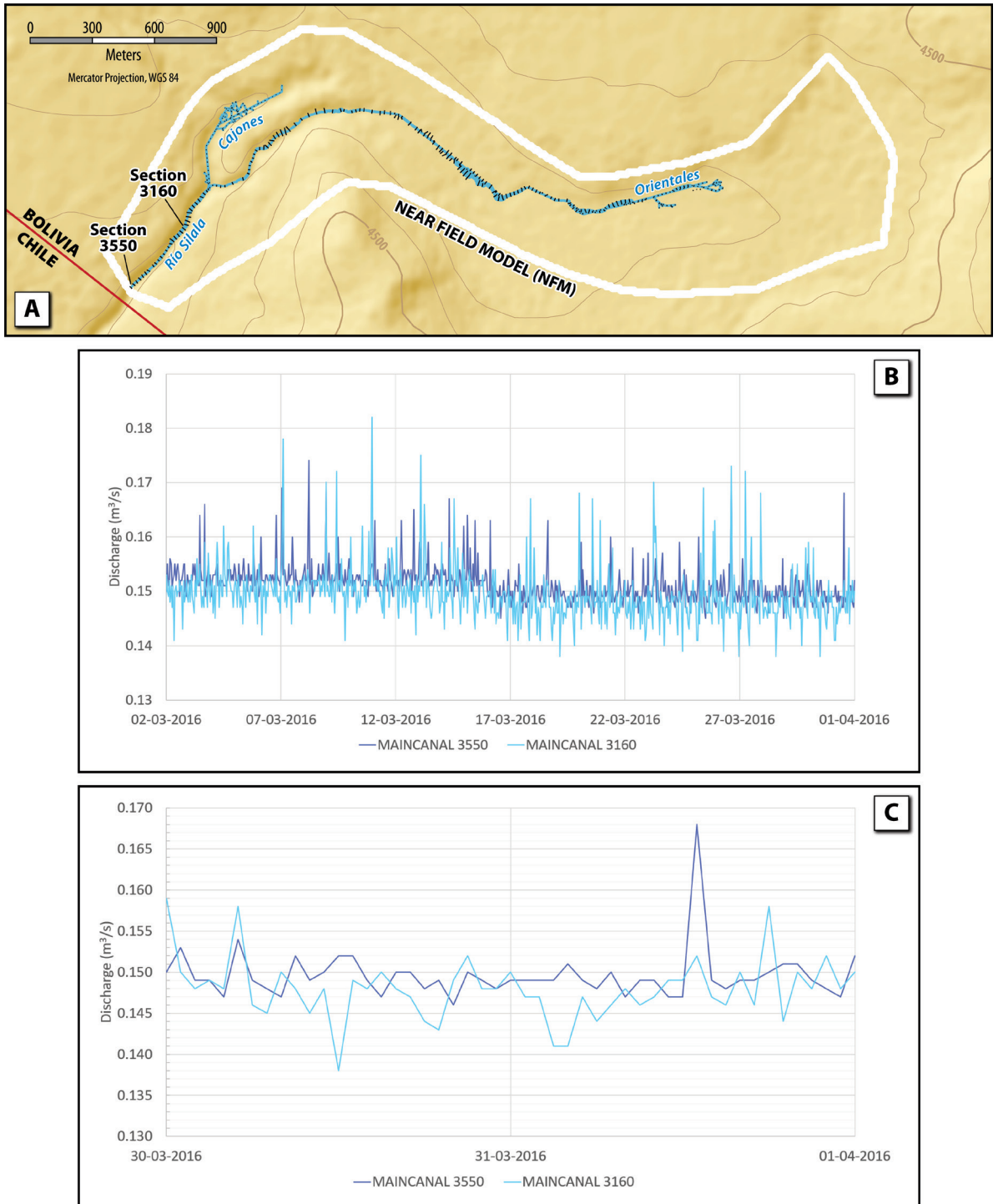


Figure 4-21. Flow variations in different sections of the reach between the Cajones and Orientales confluence and the international border. (A) Plan view of the NFM domain that depicts the locations of the two sections analyzed. (B) Discharge time series of the flow at sections 3550 and 3160. (C) Zoom into the last two days of the flow at sections 3550 and 3160.

4.2.6.2 Surface flow calculation in the No Canal and Undisturbed scenarios – MIKE-SHE Overland flow

The surface flow in both No Canal and Undisturbed scenarios was calculated as overland flow in the MIKE-SHE model: this is a quite different methodology to the Baseline scenario. The overland flow was calculated using the Diffusive Wave approximation of the Saint-Venant 2-D equations (Chow, 2010), and a different numerical scheme, which provides a less precise calculation of the surface flows (compared to the dynamic wave in Baseline scenario). It also uses a much coarser spatial resolution for the flow routing, as noted above. More specifically, in both the No Canal and Undisturbed scenarios there are no river channels identified, as opposed to the Baseline scenario, where the MIKE-11 module is used to transport the flow outside the basin, following the channel and ravine paths existing in the Silala basin. In reality in the absence of channelization, the overland flows would combine into numerous channels, which might change over time, and flow down the topographic gradient to the Silala ravine and thence across the border into Chile. Such braided stream channels are commonly seen in altiplano wetlands (see Figure 4-22). The use of the SHE overland flow algorithms therefore fails to represent the natural channel flow processes, and also provides a very different representation of the possible interactions between surface flow and groundwater, creating further modelling differences to confuse the scenario comparison.

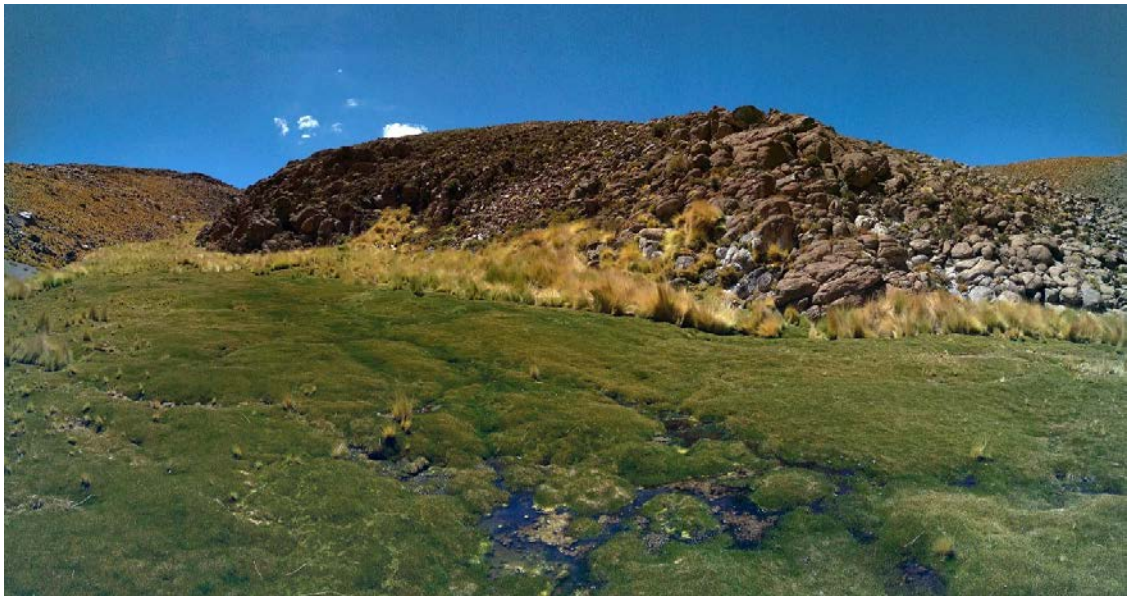


Figure 4-22. Photograph taken at the Quebrada Negra wetland that shows the overland flow combined into numerous channels.

4.2.7 Water balance results of the different scenarios modelled by DHI (2018)

Considering the aspects described in Table 4-1, we have reconstructed the water balance provided in Table 1 of Annex H to DHI (2018) (BCM, Vol. 5, p. 67). Table 4-4 shows the main aspects of the water balance obtained from the result files (.sheres) provided by DHI.

Table 4-5 presents the water balance reported in Table 1 of Annex H to the DHI Report (BCM, Vol. 5, p. 67). Given that the models presented by DHI (2018) are not at steady state (Section 4.2.2), the water balance calculations presented in Table 4-4 were obtained using the difference of the last two-time steps, which are the results that are closest to steady state.

As noted above, while groundwater inflow to the NFM is generated at the model boundaries, thus providing the water that should feed the springs, additional spring flows were represented in the Baseline scenario as point inflows to the channels (spring recharge), modelled using MIKE-11. In the No Canal and Undisturbed scenarios, these extra spring recharge were represented by point-source water injections entered as precipitation rates at each of the spring headwater cells. This precipitation is then processed by the overland flow module and a water balance in each cell is carried out. As mentioned above, none of this spring recharge comes from groundwater interaction, but instead is represented as water apparently created from nowhere, and with no explanation or justification provided by DHI. The discharges obtained by MIKE-11 (“Total river outflow (MIKE-11)” in Table 4-4) and MIKE-SHE (“Total river outflow (MIKE-SHE)” in Table 4-4) are different in part because neither of the two models have reached steady state, but mainly because of the numerical instabilities in the MIKE-11 modelling (see Section 4.2.6.1.4).

		Variables in mm/y			Variables in l/s		
		Baseline	No Canal	Undisturbed	Baseline	No Canal	Undisturbed
Inflow	Variable description	3131	2724	2656	254	221	216
Spring recharge	Boundary inflow in MIKE-11/ Precipitation in MIKE-SHE	-518	-382	-382	-42*	-31**	-31**
SubSurf.Bou.Inflow	Subsurface boundary inflow	-2613	-2342	-2275	-212	-190	-185
Storage change		44	5	64	4	0	5
SubSurf.Stor.Change	Subsurface storage change	-44	-5	-64	-4	0	-5
OL Stor.Change	Overland storage change	0	0	0	0	0	0
Total groundwater outflow		1311	1419	1442	106	115	117
SubSurf.Bou.Outflow	Subsurface boundary outflow	1311	1419	1442	106	115	117
Total river outflow (MIKE-SHE)		1766			143***		
Baseflow to river	Baseflow to river	1226	-	-	100	-	-
Baseflow from river	Baseflow from river	-112	-	-	-9	-	-
OL->River/MOUSE	Overland flow to river	134	-	-	11	-	-
Spring recharge	Boundary inflow (MIKE-11)	518	-	-	42	-	-
Total overland outflow (MIKE-SHE)		-	1159	1113	-	94	90
OL Bou.Outflow	Overland boundary outflow	-	1159	1113	-	94	90
Total river outflow (MIKE-11)		1847			150***		
Evapotranspiration		126	150	164	10	12	13
Total outflow		3283	2728	2718	267	222	221
Error		27	0	-2	2	0	0

Table 4-4. Detailed NFM water balance for the three scenarios, obtained from the results file provided by DHI. For the Baseline scenario, the MIKE-11 boundary inflows were considered as spring recharge and included in the Inflow component of the water balance. For the No Canal and Undisturbed scenarios, precipitation was considered as a point-source spring recharge and was included in the Inflow component of the water balance.

*42 l/s input at head waters sections in MIKE-11; **31 l/s injected as point-source precipitation in the MIKE-SHE model.

*** the 143 l/s reported as total river outflow (MIKE-SHE) is not the same as the 150 l/s reported as total river outflow (MIKE-11).

	Variables in mm/y			Variables in l/s		
	Baseline	No Canal	Undisturbed	Baseline	No Canal	Undisturbed
Inflow	3116	2722	2655	253	221	216
Storage change	49	12	64	4	1	5
Total groundwater outflow	1310	1418	1441	106	115	117
Total overland outflow (MIKE-SHE)	-	1159	1112	-	94	90
Total river outflow (MIKE-11)	1846	-	-	150	-	-
Evapotranspiration	125	150	164	10	12	13
Total outflow	3281	2727	2717	266	221	220
Error	25	0	-2	2	0	0

Table 4-5. Detailed NFM water balance for the three scenarios reported in Table I of Annex H of DHI's report.

We found an important inconsistency when DHI reported the impact of channelization on surface water flows. In the BCM, DHI states that removing the channels reduces the river flow by 31 to 40% relative to current conditions (BCM, Vol. 2, p. 303). Then, in Bolivia's Rejoinder, DHI reported that removing the channels reduces the river flow by 11% to 33% (BR, Vol. 5, p. 56). The highest values of flow reduction, i.e., the 40% and the 33%, were calculated using the same data from their model runs (Table 4-5), and comparing the Total overland flow (MIKE-SHE) from the Undisturbed scenario with the Total river outflow (MIKE-11) from the Baseline scenario. Nonetheless, the flow reduction percentages are different. The 40% flow reduction can be calculated from the values reported in Table 4-5. However, the 33% flow reduction was only replicated when incorporating 10 l/s of additional surface water flow in the Undisturbed scenario. The incorporation of this additional 10 l/s to the surface water flow was not explained in Bolivia's Rejoinder, but it was included in the Excel spreadsheet named "Water balance tables – Sensitivity Report.xls", which was delivered by DHI along with the files provided to support the Rejoinder modelling (Appendix C). The arbitrary inclusion of this additional surface water flow is wholly unexplained and thus, in addition to all the previous issues described before, the estimations of the impact of channelization on river flow are flawed.

Additionally, we disaggregated the water balance to estimate the groundwater flow that enters at each boundary in the Baseline model scenario. We calculated the water balance using the two sub-catchments that are presented in Figure 4-23. This figure also shows the results of the water balance of each sub-catchment. Taking into consideration the results of this analysis, most of the groundwater inflow comes from the northern boundary. When looking at the groundwater levels and contours presented in Figure 4-2, it would be expected that most of the inflow would come from the eastern boundary.

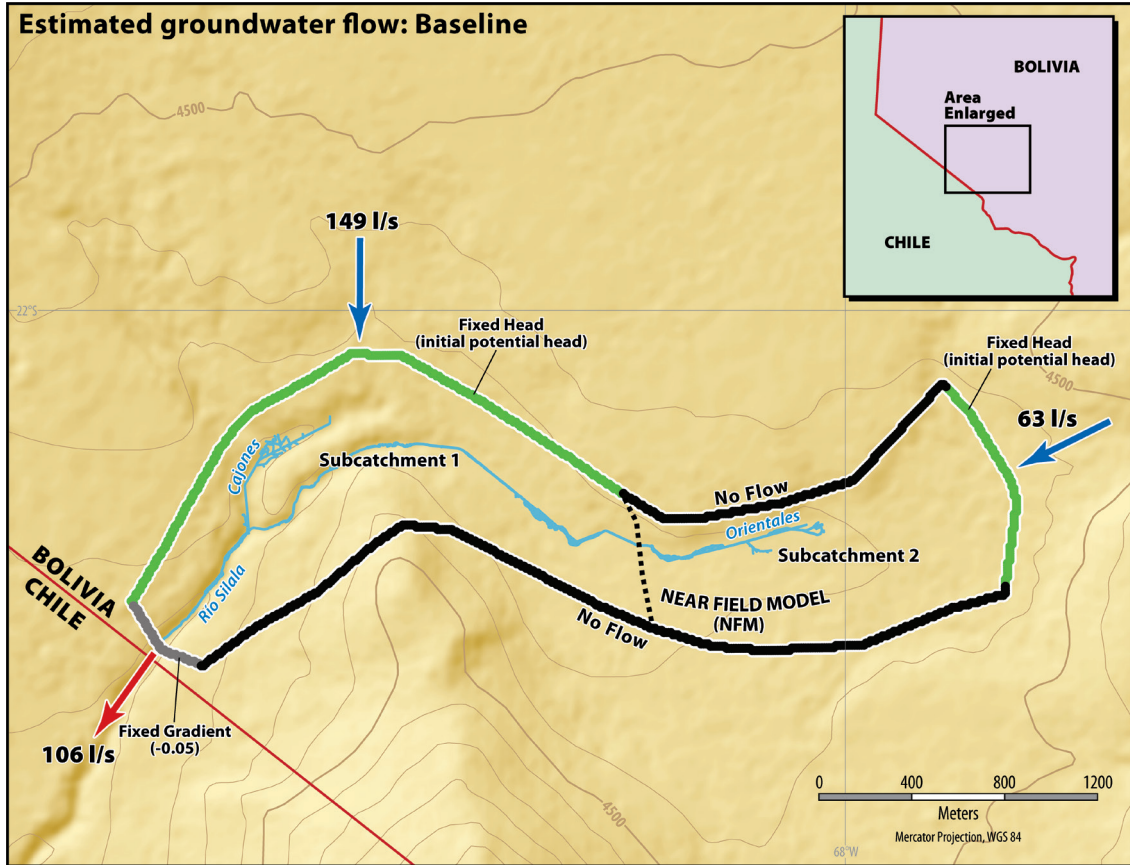


Figure 4-23. Sub-catchments (1 and 2) used to calculate the groundwater inflow from each boundary of the model.

4.2.8 Summary of unreported differences between the DHI scenarios

It can readily be seen from the above discussion that completely different modelling methodologies were used to simulate the scenarios for the evaluation of the impact of the channelization. This constitutes poor scientific practice, at the very least, and means that the results presented to the Court are highly misleading. Broadly speaking, the differences lie in the fact that (vastly) different topographic surfaces, different forms of calculating surface flows and different representations of the springs have been used for the different scenarios.

One of the most significant differences is in the topographies used in the Baseline, No Canal and Undisturbed scenarios. DHI (2018) only mentions changes made to the topography in the Undisturbed scenario, the implication being that there are no differences between the Baseline and the No Canal scenario topographies, other than the removal of the channels. However, examination of the requested model files reveals differences of up to 7 m between the MIKE-11 channel topographies used in the Baseline model and the MIKE-SHE overland flow surfaces used in the No Canal and

Undisturbed scenarios. These differences will have produced a large part of the supposed “impacts due to channelization” presented by DHI in the BCM.

Another incorrect and highly unrealistic aspect of the modelling approach is the addition of external fluxes to represent the springs (“spring recharge”), which should really be a result of groundwater interactions. Despite having an integrated surface-groundwater model, only the diffuse groundwater inflow is solely represented by surface-groundwater interaction: the spring inflows are additionally represented as external inputs to the model (spring recharge), with no justification of where this water actually comes from. In other words, instead of obtaining the spring water flows from groundwater through the hydrogeological model, artificial point flows are introduced.

In the baseline scenario a total of 42 l/s in the form of point injections is introduced into the channel system (distributed at 42 spring locations of 1 l/s each) while in the No Canal and Undisturbed scenarios 31 l/s are introduced via precipitation into the system. First, there is no explanation of where this spring water comes from (it is not from groundwater interaction as it should be). Second, the imposed flow is 11 l/s lower in the No Canal and Undisturbed scenarios than in the Baseline scenario, resulting in a lower outflow, and the reason to artificially impose a difference of 11 l/s is not explained by DHI (2018). Third, the addition of this water is not comparable even if the amounts were equivalent, since the way in which the water is added to the models is different in the different scenarios. There is no reason to assume that the natural springs would no longer discharge to surface if the artificial channelization was removed/restored.

The “spring recharge” flows in the Baseline model go directly into the surface water system, whereas in the No Canal and Undisturbed scenarios 31% of the precipitation representing the “spring recharge” enters directly into the groundwater system. Therefore, the way the different scenarios have been set up results in 9.7 l/s (31% of 31 l/s) being transferred directly from the surface water system to the groundwater system in the No Canal and Undisturbed scenarios. This transfer of water from the surface water to groundwater systems also produces an additional artificial “impact” or apparent increase in flow due to the artificial channels.

We conclude that the apparent impacts of the channelization presented in the BCM are largely a result of the unrealistic way in which the scenarios have been set up, with around 21 l/s of this apparent impact being due to the (unreported) differences in the ways the springs are represented in the scenarios, and the rest being due to the large (unreported) differences between the scenario topographies. Thus, very little of the supposed “impact” of the channelization presented in the BCM, and also in the BR, is actually due to the removal of the channels, and the conclusions of the BCM and BR must therefore be called into question.

We reiterate that the different ways that topographies and the “springs” have been represented in the different scenarios are not described in any way in the BCM. There is no mention of any differences to the topography between the Baseline and No Canal scenarios (only the Undisturbed scenario is supposed to have any topography changes according to DHI’s report), and the “spring” flows are presented in Table 1 of Annex H to the DHI Report (BCM, Vol. 5, p. 67) under the same heading labelled as “inflow”, with no distinction made at all between the two approaches, implying that this “inflow” is treated the same way in all scenarios. It has only been through detailed examination of the requested model files that these differences between the scenarios have been identified.

5. CONCLUSIONS

This report presents a critical analysis that demonstrates that the methodology used by DHI to estimate the “artificial flow” attributed to the channelization of the Bolivian wetlands is incorrect. The main emphasis of this study is the analysis of the NFM, since it is the main tool that supports Bolivia’s estimation of the “artificial flow”. Also, a brief analysis of the WBM, used to estimate the recharge of the hydrogeological system, is carried out. The main conclusions from this study are listed below:

Water Balance numerical model

- The southwestern no-flow boundary condition is not based on the geology of the studied area, but rather on a geopolitical boundary.
- The flow directions obtained from the initial groundwater levels do not represent a good approximation of reality since they are influenced by a boundary condition that is based on a geopolitical rather than a physical boundary.
- The no-flow boundary condition located in the western side of the WBM near the fixed head boundary influences the flow direction into the NFM, while it should be exiting the model from east to west.

Near Field conceptual model

- DHI’s hydrogeological understanding has been based on an incorrect interpretation of the geology including the stratigraphy and the age relationships of the various deposits, resulting in a flawed conceptual understanding of the groundwater flow regime. This has influenced aquifer delineation, selection of aquifer properties and boundary condition definition in their numerical models.
- DHI (2018) constructed the groundwater level contour map of the Silala Near Field using the levels measured in all the piezometers, making no distinction between piezometers that measure the shallow aquifer groundwater levels and

those that measure the deep aquifer groundwater levels, thus mixing the data from two aquifer systems.

- The groundwater flow directions interpreted from DHI's piezometric level contours do not correspond to DHI's own conceptual model in terms of the flow directions shown on their spring location maps.
- The groundwater level contours do not take into consideration the presence of a low permeability boundary at the south-west of the Orientales stream (Volcanic sequences from the Miocene).

Near Field numerical model

- There is a lack of consistency between the WBM and the NFM:
 - The WBM and NFM groundwater contour lines do not coincide.
 - There is an inconsistency between the boundary conditions and the groundwater flow direction of both models.
 - The 198 l/s that leaves the WBM model is not the same as the 212, 190 or 185 l/s that enter the NFM model scenarios as groundwater flow.
- The boundary conditions used in the NFM are inconsistent with the groundwater flow directions derived from the hydrogeological conceptual model, as well as with the flow directions from the WBM.
- The no-flow boundaries on the north-eastern and southern edges of the model have no physical or geological justification.
- The initial potential head used in the Baseline and No Canal scenarios is different to the one used in the Undisturbed scenario.
- Steady state is not reached after 91 days of simulation, so that there are cumulative systematic errors in the model water balances.
- The model topographies used in the three scenarios are not the same, differing from one another by up to 7 m. These unreported differences are likely to be one of the main reasons for the apparent differences in surface water flow between DHI's Baseline and No Canal and Undisturbed scenarios.
- The method used to calculate the surface flow through the international border in the Baseline scenario is different from that used in the No Canal and Undisturbed scenarios. Therefore, these flows are not directly comparable.
- In addition to the groundwater inflows to the Near Field that arise as a result of the boundary conditions, the springs have been modelled as localized surface water inflows in the Baseline scenario and as a local precipitation in the No Canal and Undisturbed scenarios (spring recharge). Neither of these representations is correct as the spring water should come entirely from interactions with the groundwater system. The amounts of extra spring recharge

added in the models have not been justified, no calculations are shown and no estimation methodology is described.

- The amount of water added as precipitation in the No Canal and Undisturbed scenarios is 11 l/s less than the amount added as surface water inflows in the baseline scenario, thereby artificially producing 11 l/s of apparent increase in flow due to the channels.
- The representations of the springs as surface water sources in the Baseline scenario but as precipitation sources in the No Canal and Undisturbed scenarios results in 31% of the precipitation being transferred directly from the surface water system to the groundwater system. This results in a further 9.7 l/s apparent increase in flow due to the channels.
- Presenting the flow values from the unstable MIKE-11 component of the Baseline scenario, rather than the surface water-groundwater interactions of the more stable MIKE-SHE component, the Baseline scenario results in a further 7 l/s over-estimate of the flows under current conditions. Neither this nor the previously mentioned 11 l/s or 9.7 l/s apparent increases are realistic.
- The differences between the ways the springs were represented in the different scenarios were not described in any way in the BCM and were presented under the same heading in their water balances, implying that they were represented in the same way.
- The downstream stage-discharge curve boundary condition in the Baseline scenario, that imposes critical flow, is not explained or justified in DHI's report.
- The slope between the two last cross sections (3560 and 3635) is zero, which is unrealistic and is not explained or justified in the DHI report.
- The Manning coefficient, n , was found to be representative of the highest values recommended for flood plains covered by dense trees ($n = 0.200$), which is not the case of the Silala River and is physically unrealistic.
- As a result of the high imposed value of the Manning coefficient, the normal depth of the channel is increased and the flow conditions are subcritical ($Fr < 1$) in almost all the cross sections, which does not coincide with what is observed in the field, i.e., supercritical flow conditions ($Fr > 1$). Hence, the results of DHI are unrealistic and conceptually inconsistent with the observed flow regime.
- At some of the cross sections water does not flow through the main channel and in other cross sections the channel is flooded.
- Errors were found in the hydraulic modelling of the DHI:
 - Abrupt changes in river flow were found at different points.
 - There are flow variations along the river that never stabilize.
- Different values for the upper bound effect of channelization on surface flows were reported in the BCM (40%) and the BR (33%) for the same simulations.

Final Conclusions

- The differences between the results obtained using the Near Field Model to represent the effects of channel removal and peat growth are largely due to unreported differences between the models used to represent the different scenarios. These differences were only discovered once the requested model files were examined in detail (and we recall that DHI originally refused to provide these files). The very large number of differences, and the fact that these were not reported, is disturbing, and at best represents very poor scientific practice. The Near Field modelling results presented to the Court in the BCM and BR written pleadings to demonstrate the effects of channelization and peat growth are grossly misleading.

6. REFERENCES

- ARCADIS, 2017. *Detailed Hydrogeological Study of the Silala River. (Chile's Memorial, Vol. 4, Annex II)*.
- Chow, V.T., 1959. *Open-Channel Hydraulics*. New York, McGraw-Hill.
- Chow, V.T., 2010. *Applied Hydrology*. Tata McGraw-Hill Education.
- Danish Hydraulic Institute (DHI), 2017a. *Provisional Report 3. Water balance of the basin and groundwater aquifer and update of measured surface water flow*.
- Danish Hydraulic Institute (DHI), 2017b. *MIKE 11. A Modelling system for Rivers and Channels*. User Guide.
- Danish Hydraulic Institute (DHI), 2018. *Study of the Flows in the Silala Wetlands and Springs System. (Bolivia's Counter-Memorial, Vol. 2-5, Annex 17)*.
- SERGEOMIN (National Service of Geology and Mining), 2003. *Study of the Geology, Hydrology, Hydrogeology and Environment of the Area of the Silala Springs. (Bolivia's Rejoinder, Vol. 3, Appendix a to Annex 23.5)*.
- SERNAGEOMIN (National Geology and Mining Service), 2017. *Geology of the Silala River Basin. (Chile's Memorial, Vol. 5, Annex VIII)*.
- SERNAGEOMIN (National Geology and Mining Service), 2019a. *Geology of the Silala River: an Updated Interpretation (Chile's Reply, Vol. 3, Annex XIV)*.
- SERNAGEOMIN (National Geology and Mining Service), 2019b. *A Brief Review of the Geology Presented in Annexes of the Rejoinder of the Plurinational State of Bolivia. (Chile's Additional Pleading, Vol. 2, Annex XVI)*
- Wheater, H., & Peach, D., 2019. *Impacts of Channelization of the Silala River in Bolivia on the Hydrology of the Silala River Basin (Chile's Reply, Vol. 1, Expert Report)*.

Annex XV

APPENDIX A.

DATA FILES PROVIDED BY DHI

A-1 MODEL FILES

In the DHI report, three models were used to analyze the hydrological behavior of the basin: Water Balance, Near Field and Near Border. Appendix A details the files provided by Bolivia which could be used to critically analyze these models. Each of these models has variations, marked as different versions, in which the boundary and/or initial conditions change. In particular, 12 configurations are presented for the Water Balance model for water balance and aquifer recharge (Table A-1), and two for the evaluation of groundwater travel times in aquifers (Table A-2).

Annex E Table 3, Line no	Parameter change	Model configuration file name	Directory
1	Baseline	Silala_model_200m_v24	WaterBalance
	Rainfall		
2	DGA Laguna Colorada	Silala_model_200m_v26	WaterBalance
3	DGA Linzor	Silala_model_200m_v27	WaterBalance
4	DGA Inacaliri - rainfall-altitude relation	Silala_model_200m_v5	WaterBalance
	Evaporation		
5	Et0 Laguna Colorada	Silala_model_200m_v33	WaterBalance
6	Et0 Sol de Manana	Silala_model_200m_v34	WaterBalance
	Soil parameters		
7	0-10 cm: Ks=9.7E-6 m/s, 10-20 cm: 4.5E-6 m/s	Silala_model_200m_v29	WaterBalance
8	0-10 cm: Ks=1.4E-5 m/s, 10-20 cm: 1.2E-5 m/s	Silala_model_200m_v28	WaterBalance
9	0-10 cm: n=1.619 (theta_FC=0.17), 10-50 cm: n=1.477 (theta_FC=0.19)	Silala_model_200m_v32	WaterBalance
10	0-10 cm: n=1.754 (theta_FC=0.12), 10-50 cm: n=1.699 (theta_FC=0.12)	Silala_model_200m_v35	WaterBalance
11	0-10 cm: theta_r=0.039, 10-50 cm: theta_r=0.042	Silala_model_200m_v36	WaterBalance
12	0-10 cm: theta_r=0.05, 10-50 cm: theta_r=0.132	Silala_model_200m_v37	WaterBalance

Table A-1. Configurations of the water balance and aquifer recharge model in the basin (DHI, 2018).

Task	Model configuration file name	Directory
Particle tracking in Saturated zone	Silala_model_gw_200m_v12_final.she	WaterBalance
WQ tracer in the unsaturated zone	Silala_model_gw_200m_v12_final_tracer.she	WaterBalance

Table A-2. Configurations of the evaluation of groundwater travel times (DHI, 2018).

The Near Field Model has three configurations (Table A-3): the (current) baseline scenario, the no channelization scenario, and the restored wetlands scenario (i.e., without human intervention).

Nº	Model setup name	Description
1	Silala_10m_withHydrogeologicalModel_DeepLowK_ModelArea_V18_OExplicit.she	An integrated hydrological model setup of the Silala Near Field area including canals.
2	Silala_10m_withHydrogeologicalModel_DeepLowK_ModelArea_V22_NoCanal_OExplicit.she	An integrated hydrological model setup of the Silala Near Field area without canals.
3	Silala_10m_withHydrogeologicalModel_DeepLowK_ModelArea_V22_NoCanal_OExplicit_undisturb.she	An integrated hydrological model setup of the Silala Near Field area with restored wetlands and without canals

Table A-3. Configurations of the water balance model in wetlands and springs (DHI, 2018).

The Near Border Model, for which the domain is delimited to study the flow at the international border, has six configurations considering channelization, and six configurations without channelization (Table A-4).

Baseline						Decrease in transborder surface flow		
Nº	Configuration file name with canal					I/sec	Pct	
1	Silala_NearBorder_grav_v4.she					2	Silala_NearBorder_grav_nat_v4.she	12 8
Sensitivity Analysis								
Nº	Configuration file name with canals	Parameters as in	Org baseline parameter	Scenario Parameters	Nº	Configuration file name without canals	I/sec Pct	
3	Silala_NearBorder_grav_v4_5m.she	Silala_NearBorder_grav_v4.she	10 m resolution	5 m resolution	8	Silala_NearBorder_grav_nat_v4_5m.she	14 8	
4	Silala_NearBorder_grav_v5.she	Silala_NearBorder_grav_v4.she	M2.5	M=15	9	Silala_NearBorder_grav_nat_v5.she	12 8	
5	Silala_NearBorder_grav_v6.she	Silala_NearBorder_grav_v4.she	Kh1=10-4, Kv2=5E-5	Kh1=10-3, Kv2=5E-4	10	Silala_NearBorder_grav_nat_v6.she	23 15	
6	Silala_NearBorder_grav_v7.she	Silala_NearBorder_grav_v6.she	Kuz, fine sand=2.74E-5	Kuz, fine sand=10-4	11	Silala_NearBorder_grav_nat_v7.she	24 15	
7	Silala_NearBorder_grav_v8.she	Silala_NearBorder_grav_v7.she	Kh2=3E-5	Kh2=10-4	12	Silala_NearBorder_grav_nat_v7.she	39 25	

Table A-4. Configurations of the water balance model near the border (DHI, 2018).

To carry out the analysis of the DHI simulations, we studied the model files presented in Table A-5. It was decided to study the WBM version “Silala_model_gw_200m_v12_final.she” because it simulates groundwater flow. The files from the NFM that were studied were the final version of each scenario.

Nº	Model	Comments	File name
1	WBM	-	Silala_model_gw_200m_v12_final.she
2	NFM	Baseline scenario	Silala_10m_withHydrogeologicalModel_DeepLowK_ModelArea_V18_OExplicit
3	NFM	No Canal scenario	Silala_10m_withHydrogeologicalModel_DeepLowK_ModelArea_V22_NoCanal_OExplicit
4	NFM	No Canal Undisturbed scenario	Silala_10m_withHydrogeologicalModel_DeepLowK_ModelArea_V22_NoCanal_OExplicit_undisturb

Table A-5. DHI model files analyzed in this study.

A-2 RESULT FILES

The results of the models developed by DHI, which are presented as text files, are presented in Tables A-6, A-7 and A-8.

Folder	Text File
Water Balance	1 Silala_model_200m_v5.she - Result Files Chart_wbl Silala_model_200m_v5_PreProcessed_SoilProf Wbl_Chile_sub_total
	2 Silala_model_200m_v24.she - Result Files Chart_Chile Chart_Chile_new Chart_Chile_new_v2 Chart_Chile_short Chart_Chile_sub_wbl Chart_long Chart_wbl Silala_model_200m_v24_PreProcessed_SoilProf
	3 Silala_model_200m_v26.she - Result Files Chart_wbl Silala_model_200m_v26_PreProcessed_SoilProf
	4 Silala_model_200m_v27.she - Result Files Chart_chile_wbl Chart_wbl Silala_model_200m_v27_PreProcessed_SoilProf Total_wbl
	5 Silala_model_200m_v28.she - Result Files Chart_wbl Silala_model_200m_v28_PreProcessed_SoilProf
	6 Silala_model_200m_v29.she - Result Files Chart_wbl Silala_model_200m_v29_PreProcessed_SoilProf
	7 Silala_model_200m_v32.she - Result Files Chart_wbl Silala_model_200m_v32_PreProcessed_SoilProf
	8 Silala_model_200m_v33.she - Result Files Chart_chile_wbl Chart_wbl Silala_model_200m_v33_PreProcessed_SoilProf
	9 Silala_model_200m_v34.she - Result Files Chart_chile_wbl Chart_wbl Silala_model_200m_v34_PreProcessed_SoilProf
	10 Silala_model_200m_v35.she - Result Files Chart_wbl Silala_model_200m_v35_PreProcessed_SoilProf
	11 Silala_model_200m_v36.she - Result Files Chart_wbl Silala_model_200m_v36_PreProcessed_SoilProf
	12 Silala_model_200m_v37.she - Result Files Chart_wbl Silala_model_200m_v37_PreProcessed_SoilProf
	13 Silala_model_gw_200m_v12_final.she - Result Files Silala_model_gw_200m_v12_final_PP_Print Silala_model_gw_200m_v12_final_PreProcessed_SoilProf Silala_model_gw_200m_v12_final_WM_Print Silala_model_gw_200m_v12_final_WQ_Print
	14 Silala_model_gw_200m_v12_final_tracer.she - Result Files Chart_wbl Silala_model_gw_200m_v12_final_tracer_PreProcessed_SoilProf

Table A-6. Results in the form of text files for Water Balance Models.

Annex XV Appendix A

Folder	Text File
	Silala_10m_withHydrogeologicalModel_DeepLowK_ModelArea_V18_OExplicit_PP_Print
	Silala_10m_withHydrogeologicalModel_DeepLowK_ModelArea_V18_OExplicit_PreProcessed_SoilProf1
	Silala_10m_withHydrogeologicalModel_DeepLowK_ModelArea_V18_OExplicit_PreProcessed_SoilProf4
1 Silala_10m_withHydrogeologicalModel_DeepLowK_ModelArea_V18_OExplicit.she - Result Files	Silala_10m_withHydrogeologicalModel_DeepLowK_ModelArea_V18_OExplicit_PreProcessed_SoilProf5
	Silala_10m_withHydrogeologicalModel_DeepLowK_ModelArea_V18_OExplicit_PreProcessed_SoilProf6
	Silala_10m_withHydrogeologicalModel_DeepLowK_ModelArea_V18_OExplicit_WM_Print
	wbl_va8_withcanal_OExp
	wbl_va8_withcanal_OExp_WBL_POST
Near Field	Silala_10m_withHydrogeologicalModel_DeepLowK_ModelArea_V22_NoCanal_OExp OL_TopoKor_PP_Print.rshe - Result Files
	Silala_10m_withHydrogeologicalModel_DeepLowK_ModelArea_V3_PP_Print
	Silala_10m_withHydrogeologicalModel_DeepLowK_ModelArea_V3_PreProcessed_SoilProf1
3 Hot_Silala_10m_withHydrogeologicalModel (MIKE 11)	Silala_10m_withHydrogeologicalModel_DeepLowK_ModelArea_V3_PreProcessed_SoilProf4
	Silala_10m_withHydrogeologicalModel_DeepLowK_ModelArea_V3_PreProcessed_SoilProf5
	Silala_10m_withHydrogeologicalModel_DeepLowK_ModelArea_V3_PreProcessed_SoilProf6

Table A-7. Results in the form of text files for Near Field Models.

Folder	Text File
Near Border	1 Silala_NearBorder_grav_nat_v4.she - Result Files Chart_wbl Silala_NearBorder_grav_nat_v4_PreProcessed_SoilProf1 Silala_NearBorder_grav_nat_v4_PreProcessed_SoilProf4
	2 Silala_NearBorder_grav_nat_v4_5m.she - Result Files Chart_wbl Silala_NearBorder_grav_nat_v4_5m_PreProcessed_SoilProf1 Silala_NearBorder_grav_nat_v4_5m_PreProcessed_SoilProf4
	3 Silala_NearBorder_grav_nat_v5.she - Result Files Chart_wbl Silala_NearBorder_grav_nat_v5_PreProcessed_SoilProf1 Silala_NearBorder_grav_nat_v5_PreProcessed_SoilProf4
	4 Silala_NearBorder_grav_nat_v6.she - Result Files Chart_wbl Silala_NearBorder_grav_nat_v6_PreProcessed_SoilProf1 Silala_NearBorder_grav_nat_v6_PreProcessed_SoilProf4
	5 Silala_NearBorder_grav_nat_v7.she - Result Files Chart_wbl Silala_NearBorder_grav_nat_v7_PreProcessed_SoilProf1 Silala_NearBorder_grav_nat_v7_PreProcessed_SoilProf4
	6 Silala_NearBorder_grav_nat_v8.she - Result Files Chart_wbl Silala_NearBorder_grav_nat_v8_PreProcessed_SoilProf1 Silala_NearBorder_grav_nat_v8_PreProcessed_SoilProf4
	7 Silala_NearBorder_grav_v4.she - Result Files Chart_wbl Silala_NearBorder_grav_v4_PreProcessed_SoilProf1 Silala_NearBorder_grav_v4_PreProcessed_SoilProf4
	8 Silala_NearBorder_grav_v4_5m.she - Result Files Chart_wbl Silala_NearBorder_grav_v4_5m_PreProcessed_SoilProf1 Silala_NearBorder_grav_v4_5m_PreProcessed_SoilProf4
	9 Silala_NearBorder_grav_v5.she - Result Files Chart_wbl Silala_NearBorder_grav_v5_PreProcessed_SoilProf1 Silala_NearBorder_grav_v5_PreProcessed_SoilProf4
	10 Silala_NearBorder_grav_v6.she - Result Files Chart_wbl Silala_NearBorder_grav_v6_PreProcessed_SoilProf1 Silala_NearBorder_grav_v6_PreProcessed_SoilProf4
	11 Silala_NearBorder_grav_v7.she - Result Files Chart_wbl Silala_NearBorder_grav_v7_PreProcessed_SoilProf1 Silala_NearBorder_grav_v7_PreProcessed_SoilProf4 Wbl_error
	12 Silala_NearBorder_grav_v8.she - Result Files Chart_wbl Cross_sections_main_canal Error_wbl Silala_NearBorder_grav_v8_PreProcessed_SoilProf1 Silala_NearBorder_grav_v8_PreProcessed_SoilProf4

Table A-8. Results in the form of text files for Near Border Models.

APPENDIX B.

VALUES OF THE ROUGHNESS MANNING COEFFICIENT

Type of channel and description	Minimum	Normal	Maximum
A. CLOSED CONDUITS FLOWING PARTLY FULL			
A-1. Metal			
a. Brass, smooth	0.009	0.010	0.013
b. Steel			
1. Lockbar and welded	0.010	0.012	0.014
2. Riveted and spiral	0.013	0.016	0.017
c. Cast iron			
1. Coated	0.010	0.013	0.014
2. Uncoated	0.011	0.014	0.016
d. Wrought iron			
1. Black	0.012	0.014	0.015
2. Galvanized	0.013	0.016	0.017
e. Corrugated metal			
1. Subdrain	0.017	0.019	0.021
2. Storm drain	0.021	0.024	0.030
A-2. Nonmetal			
a. Lucite	0.008	0.009	0.010
b. Glass	0.009	0.010	0.013
c. Cement			
1. Neat, surface	0.010	0.011	0.013
2. Mortar	0.011	0.013	0.015
d. Concrete			
1. Culvert, straight and free of debris	0.010	0.011	0.013
2. Culvert with bends, connections, and some debris	0.011	0.013	0.014
3. Finished	0.011	0.012	0.014
4. Sewer with manholes, inlet, etc., straight	0.013	0.015	0.017
5. Unfinished, steel form	0.012	0.013	0.014
6. Unfinished, smooth wood form	0.012	0.014	0.016
7. Unfinished, rough wood form	0.015	0.017	0.020
e. Wood			
1. Stave	0.010	0.012	0.014
2. Laminated, treated	0.015	0.017	0.020
f. Clay			
1. Common drainage tile	0.011	0.013	0.017
2. Vitrified sewer	0.011	0.014	0.017
3. Vitrified sewer with manholes, inlet, etc.	0.013	0.015	0.017
4. Vitrified subdrain with open joint	0.014	0.016	0.018
g. Brickwork			
1. Glazed	0.011	0.013	0.015
2. Lined with cement mortar	0.012	0.015	0.017
h. Sanitary sewers coated with sewage slimes, with bends and connections	0.012	0.013	0.016
i. Paved invert, sewer, smooth bottom	0.016	0.019	0.020
j. Rubble masonry cemented	0.018	0.025	0.030

Type of channel and description	Minimum	Normal	Maximum
B. LINED OR BUILT-UP CHANNELS			
B-1. Metal			
a. Smooth steel surface			
1. Unpainted	0.011	0.012	0.014
2. Painted	0.012	0.013	0.017
b. Corrugated	0.021	0.025	0.030
B-2. Nonmetal			
a. Cement			
1. Neat, surface	0.010	0.011	0.013
2. Mortar	0.011	0.013	0.015
b. Wood			
1. Planed, untreated	0.010	0.012	0.014
2. Planed, creosoted	0.011	0.012	0.015
3. Unplaned	0.011	0.013	0.015
4. Plank with battens	0.012	0.015	0.018
5. Lined with roofing paper	0.010	0.014	0.017
c. Concrete			
1. Trowel finish	0.011	0.013	0.015
2. Float finish	0.013	0.015	0.016
3. Finished, with gravel on bottom	0.015	0.017	0.020
4. Unfinished	0.014	0.017	0.020
5. Gunite, good section	0.016	0.019	0.023
6. Gunite, wavy section	0.018	0.022	0.025
7. On good excavated rock	0.017	0.020	
8. On irregular excavated rock	0.022	0.027	
d. Concrete bottom float finished with sides of			
1. Dressed stone in mortar	0.015	0.017	0.020
2. Random stone in mortar	0.017	0.020	0.024
3. Cement rubble masonry, plastered	0.016	0.020	0.024
4. Cement rubble masonry	0.020	0.025	0.030
5. Dry rubble or riprap	0.020	0.030	0.035
e. Gravel bottom with sides of			
1. Formed concrete	0.017	0.020	0.025
2. Random stone in mortar	0.020	0.023	0.026
3. Dry rubble or riprap	0.023	0.033	0.036
f. Brick			
1. Glazed	0.011	0.013	0.015
2. In cement mortar	0.012	0.015	0.018
g. Masonry			
1. Cemented rubble	0.017	0.025	0.030
2. Dry rubble	0.023	0.032	0.035
h. Dressed ashlar	0.013	0.015	0.017
i. Asphalt			
1. Smooth	0.013	0.013	
2. Rough	0.016	0.016	
j. Vegetal lining	0.030	0.500

Type of channel and description	Minimum	Normal	Maximum
C. EXCAVATED OR DREDGED			
a. Earth, straight and uniform			
1. Clean, recently completed	0.016	0.018	0.020
2. Clean, after weathering	0.018	0.022	0.025
3. Gravel, uniform section, clean	0.022	0.025	0.030
4. With short grass, few weeds	0.022	0.027	0.033
b. Earth, winding and sluggish			
1. No vegetation	0.023	0.025	0.030
2. Grass, some weeds	0.025	0.030	0.033
3. Dense weeds or aquatic plants in deep channels	0.030	0.035	0.040
4. Earth bottom and rubble sides	0.028	0.030	0.035
5. Stony bottom and weedy banks	0.025	0.035	0.040
6. Cobble bottom and clean sides	0.030	0.040	0.050
c. Dragline-excavated or dredged			
1. No vegetation	0.025	0.028	0.033
2. Light brush on banks	0.035	0.050	0.060
d. Rock cuts			
1. Smooth and uniform	0.025	0.035	0.040
2. Jagged and irregular	0.035	0.040	0.050
e. Channels not maintained, weeds and brush uncut			
1. Dense weeds, high as flow depth	0.050	0.080	0.120
2. Clean bottom, brush on sides	0.040	0.050	0.080
3. Same, highest stage of flow	0.045	0.070	0.110
4. Dense brush, high stage	0.080	0.100	0.140
D. NATURAL STREAMS			
D-1. Minor streams (top width at flood stage <100 ft)			
a. Streams on plain			
1. Clean, straight, full stage, no rifts or deep pools	0.025	0.030	0.033
2. Same as above, but more stones and weeds	0.030	0.035	0.040
3. Clean, winding, some pools and shoals	0.033	0.040	0.045
4. Same as above, but some weeds and stones	0.035	0.045	0.050
5. Same as above, lower stages, more ineffective slopes and sections	0.040	0.048	0.055
6. Same as 4, but more stones	0.045	0.050	0.060
7. Sluggish reaches, weedy, deep pools	0.050	0.070	0.080
8. Very weedy reaches, deep pools, or floodways with heavy stand of timber and underbrush	0.075	0.100	0.150

Type of channel and description	Minimum	Normal	Maximum
b. Mountain streams, no vegetation in channel, banks usually steep, trees and brush along banks submerged at high stages			
1. Bottom: gravels, cobbles, and few boulders	0.030	0.040	0.050
2. Bottom: cobbles with large boulders	0.040	0.050	0.070
D-2. Flood plains			
a. Pasture, no brush			
1. Short grass	0.025	0.030	0.035
2. High grass	0.030	0.035	0.050
b. Cultivated areas			
1. No crop	0.020	0.030	0.040
2. Mature row crops	0.025	0.035	0.045
3. Mature field crops	0.030	0.040	0.050
c. Brush			
1. Scattered brush, heavy weeds	0.035	0.050	0.070
2. Light brush and trees, in winter	0.035	0.050	0.060
3. Light brush and trees, in summer	0.040	0.060	0.080
4. Medium to dense brush, in winter	0.045	0.070	0.110
5. Medium to dense brush, in summer	0.070	0.100	0.160
d. Trees			
1. Dense willows, summer, straight	0.110	0.150	0.200
2. Cleared land with tree stumps, no sprouts	0.030	0.040	0.050
3. Same as above, but with heavy growth of sprouts	0.050	0.060	0.080
4. Heavy stand of timber, a few down trees, little undergrowth, flood stage below branches	0.080	0.100	0.120
5. Same as above, but with flood stage reaching branches	0.100	0.120	0.160
D-3. Major streams (top width at flood stage >100 ft). The <i>n</i> value is less than that for minor streams of similar description, because banks offer less effective resistance.			
a. Regular section with no boulders or brush	0.025	0.060
b. Irregular and rough section	0.035	0.100

Table B-1. Values of the roughness coefficient *n* (Boldface figures are values generally recommended in design). Source: Chow (1959).

APPENDIX C.

REJOINDER FILES PROVIDED BY BOLIVIA

Silala Sensitivityanalyses Data for Report

Inicio Compartir Vista

Este equipo > Escritorio > Silala Sensitivityanalyses Data for Report

Buscar en Silala Sensitivityana... ?

Nombre	Fecha de modificación	Tipo	Tamaño
G4_Baseline.she - Result Files	04-06-2019 11:23	Carpeta de archivos	
G4_NoCanal.she - Result Files	04-06-2019 11:35	Carpeta de archivos	
G4_Undisturbed.she - Result Files	04-06-2019 11:24	Carpeta de archivos	
G6_Baseline.she - Result Files	04-06-2019 11:36	Carpeta de archivos	
G6_NoCanal.she - Result Files	04-06-2019 11:24	Carpeta de archivos	
G6_Undisturbed.she - Result Files	04-06-2019 11:25	Carpeta de archivos	
GIS	04-06-2019 10:49	Carpeta de archivos	
H_Versions	04-06-2019 13:52	Carpeta de archivos	
HotStarts	04-06-2019 10:30	Carpeta de archivos	
Maps	04-06-2019 10:30	Carpeta de archivos	
MIKE11	04-06-2019 10:48	Carpeta de archivos	
NoCanal_plus_1.00_times_ADiff.she - Result Files	04-06-2019 13:28	Carpeta de archivos	
Silala_NoCanal.she - Result Files	04-06-2019 11:26	Carpeta de archivos	
Silala_Undisturbed.she - Result Files	04-06-2019 11:32	Carpeta de archivos	
Silala_WithCanal.she - Result Files	04-06-2019 11:28	Carpeta de archivos	
Undisturbed_A4.she - Result Files	12-06-2019 10:49	Carpeta de archivos	
UZ	04-06-2019 10:31	Carpeta de archivos	
G4_Baseline	10-04-2019 7:50	MIKE Zero Flow Model	422 KB
G4_NoCanal	10-04-2019 7:50	MIKE Zero Flow Model	424 KB
G4_Undisturbed	13-04-2019 7:59	MIKE Zero Flow Model	424 KB
G5_Baseline	05-04-2019 21:13	MIKE Zero Flow Model	422 KB
G5_NoCanal	02-04-2019 14:59	MIKE Zero Flow Model	424 KB
G6_Baseline	09-04-2019 10:47	MIKE Zero Flow Model	422 KB
G6_NoCanal	10-04-2019 7:46	MIKE Zero Flow Model	424 KB
G6_Undisturbed	12-04-2019 22:27	MIKE Zero Flow Model	424 KB
NoCanal_plus_1.00_times_ADiff	12-04-2019 10:31	MIKE Zero Flow Model	424 KB
ReadMe 1	12-06-2019 18:18	Microsoft Word Docum...	17 KB
Silala_NoCanal	02-04-2019 14:59	MIKE Zero Flow Model	424 KB
Silala_Undisturbed	18-03-2018 12:42	MIKE Zero Flow Model	423 KB
Silala_WithCanal	05-04-2019 21:13	MIKE Zero Flow Model	422 KB
Undisturbed_A4	13-04-2019 8:01	MIKE Zero Flow Model	424 KB
Water balance tables - Sensitivity Report	12-06-2019 18:16	Microsoft Excel 97-2003 ...	2,810 KB

Figure C-I. Rejoinder files submitted by Bolivia.

Annex XV

APPENDIX D



Contract CDP-I No 15/2017, Study of the Flows in the Silala Wetlands and Springs System

Product No. 3:

Provisional Report 3 – Water balance of the basin and groundwater aquifer and update of measured surface water flow



Pluri-national State of Bolivia, Ministry
of Foreign Affairs, Diremar

Report

The expert in **WATER ENVIRONMENTS**

November 15, 2017





This report has been prepared under the DHI Business Management System
certified by Bureau Veritas to comply with ISO 9001 (Quality Management)



Approved by
Oluf Zeilund Jessen, Head of
Projects Water Resources

A handwritten signature in blue ink, appearing to read "Oluf Zeilund Jessen".

Pluri-national State of Bolivia, Ministry
of Foreign Affairs, Diremar

Report

November 15, 2017

The expert in **WATER ENVIRONMENTS**



**Contract CDP-I No 15/2017 Study of the Flows in
the Silala Wetlands and Springs System.**

Product No. 3

**Provisional Report 3 – Water balance of the basin
and groundwater aquifer and update of measured
surface water flow**

Prepared for Pluri-national State of Bolivia, Ministry of Foreign Affairs, Diremar
Represented by Dr. Emerson Calderón



*Foto: SENAMHI 2017:
Weir C-2 Southern Wetland*

Project manager	Roar Askær Jensen
Quality supervisor	Michael Brian Butts

Project number	11820137
Approval date	November 15, 2017
Revision	0
Classification	Confidential





CONTENTS

1	Executive summary.....	1
2	Introduction	2
2.1	About this report and the following steps of the project	2
2.2	Project objective and areas of concern.....	2
2.3	Rationale and methodology of the analyses.....	4
2.3.1	Climate assessment.....	4
2.3.2	Water balances and ground water recharge.....	4
2.3.3	Analyses of surface flow measurements	4
3	Climate data.....	5
3.1	Precipitation data	5
3.1.1	Annual and seasonal variation.....	6
3.1.2	Spatial distribution of rainfall	7
3.2	Evapotranspiration	8
3.3	Temperature.....	9
3.4	Silala climate characteristics and conclusions.....	9
4	Water balance and groundwater recharge	10
4.1	Recharge estimation approach	10
4.2	Water balance assumptions.....	11
4.3	Water balance model setup	11
4.4	Water balance results and uncertainty	11
4.5	Groundwater flow and age.....	12
4.6	Water balance conclusions	15
5	Surface water flow measurements.....	16
5.1	Simultaneous canal flow data	17
5.2	Simultaneous spring flow data	18
5.3	Continuous flow data of installed flumes	20
5.4	Permanent Bolivian and Chilean flume flow records	20
5.5	Comparison and analysis of flow data	22
5.6	Data consistency and uncertainty.....	27
5.7	Conclusions on the measured flow data	27
6	Summary and conclusions	28
7	References.....	29

FIGURES

Figure 1	Approximate extent of the Silala Near Field. (Figure from Reference 1).....	3
Figure 2	Approximate extents and locations of the Silala Near Field, the Silala Far Field and the neighbouring Northern valley	3
Figure 3	Locations of weather stations with rainfall data in Bolivia and Chile (Senamhi stations in green).....	6
Figure 4	Annual precipitation at the Inacaliri and Silala gauges	7
Figure 5	Monthly average precipitation at the Inacaliri (1969-2016) and Silala gauges (2001-2016)	7



Figure 8	Regional annual average precipitation as a function of altitude based on CHIRPS data from 1981-2017 compared with station data at Silala, Linzor and Ollague and precipitation-elevation relationship derived by Muñoz et al., 2017	8
Figure 9	FAO reference E_t^* for Silala, Laguna Colorada and Sol de Manana (30 day moving averages) compared with the range (min to max daily values) of 7 nearby Stations from DGA Chile (Reference 10)	9
Figure 10	Daily rainfall, potential evapotranspiration and recharge for 2016 3 km north of the Silala wetlands	12
Figure 11	Geological model including cross-section from MIKE SHE model	13
Figure 12	Simulated potential head of the ignimbrite aquifer (above) and in cross section (below)	14
Figure 13	Simulated map of particle travel time and groundwater age	15
Figure 14	Particle age distribution	15
Figure 15	Overview of flow measurement locations (SENAMHI)	17
Figure 16	Longitudinal simultaneous flow profile (Southern Canal)	19
Figure 17	Long-term series of measured Silala Canal flows close to border, 2013-2017	21
Figure 18	Long-term series of measured Silala Canal flows close to border, May-September 2017	22
Figure 19	Southern canal profile (S-1 to C-5) showing canal elevation (m) on the Y-axis and canal chainage (m) on the X-axis	24
Figure 20	Northern canal profile (S-18 to C-6) showing canal elevation (m) on the Y-axis and canal chainage (m) on the X-axis	25
Figure 21	Mapping of flows and net inflows based on simultaneous mean canal flow measurements (in l/s)	26
Figure 22	Continuous (shown as lines) and simultaneous (shown as circles) flow measurement data, July-September 2017	27

TABLES

Table 1	Overview of rainfall gauges in Bolivia and Chile	5
Table 2	Canal flows by section, accumulated upstream spring inflows and derived diffuse inflows	19

APPENDICES

A	Climate data analysis
A.1	Precipitation
A.1.1	Annual and seasonal variation
A.1.2	Snow formation
A.1.3	Spatial distribution of rainfall
A.2	Evapotranspiration
A.3	Temperature
B	Water balances
B.1	Recharge estimation approach
B.2	Water balance assumptions
B.3	Water balance model setup
B.4	Water balance estimates and uncertainties
B.5	Groundwater flow model and age
C	Measured flows
C.1	The surface water flow measurement program
C.2	Simultaneous canal flow data
C.3	Continuous canal flow data



- C.3.1 The data collection campaign
- C.3.2 The rationale of the campaign
- C.3.3 Observations on the received data
- C.3.4 Conclusions on the continuous flow data
- C.4 Permanent flume flow data
- C.5 Long term flow series from Chile and Bolivia
- C.6 References



1 Executive summary

DHI (the Consultant) has been contracted by the Government of the Pluri-national State of Bolivia (Directorate: Diremar) to execute the technical study: Flow Analysis of the Silala Springs, Canal and Wetland System". The present report constitutes the third deliverable of the second part of the study." Product No. 3: Provisional Report 3 – Climate data, water balance and measured flows."

The report is divided into three main chapters covering 1) the climate data, 2) water balance and 3) measured flow. We begin with the evaluation of data sources and generation of climate datasets, these areas used subsequently in a model-based groundwater and catchment water balance analysis, which is then evaluated against canal flow measurements.

More specifically, the first chapter describes how climate data from local climate stations have been analysed, processed and combined with local data from satellites to derive long-term spatially distributed time series of precipitation, evapotranspiration and temperature for the Silala Catchment.

In the second chapter, climate data is used in a water balance model covering the delineated catchment to the Silala Springs System (Far Field area of 232 km²). Due to limitation in the subsurface geological data currently available, a generalised conceptual hydrogeological model has been used. A key output of the water balance model is a distributed estimate of groundwater recharge and the water age that can be compared with field data.

The third main chapter is devoted to Silala Canal flow measurements. Flow data from the two permanent flumes on the Bolivian and Chilean sides of the border, as well as flow data collected by SENAMHI during the May–September 2017 monitoring program have been plotted, analysed and compared. Therefore, the surface flow analyses presented here are based on more flow data than the previous analysis in the project's surface water report from July 2017.

The water balance calculations indicate that the groundwater recharge from the catchment is sufficient to maintain a discharge of 160–200 l/s to the Silala spring and canal system. From particle-tracking simulations, a water age of up to several thousand years from infiltration at the surface to discharge at the springs has been estimated. The results are, however, subject to considerable uncertainty, as demonstrated through a sensitivity analysis.

The flow observations show that the spatial distribution of inflows is approximately constant in time as expected from a groundwater fed stream. In addition to the springs in the Northern and Southern Wetlands, a limited reach of the main canal at the upper part of the ravine contributes to a relatively large inflow to the canal. The recorded fluctuations in flow are likely due to measurement inaccuracies rather than a response to climate events or surface runoff.

The various independently gauged flow series from locations close to the border (three locations in Bolivia and one downstream the border) would be expected to be almost identical. However, these series show significantly different flows ranging from 160 to 210 l/s.

The flow data analysis shows that the flows are approximately constant in time and dominated by groundwater discharge. The temporal variation observed in site-specific flow measurements cannot be explained by responses in neighbouring measurement locations or any climate or runoff events.

During the winter period July –Sept 2017, the large base flow component from groundwater is observed to be superimposed by smaller periodic daily flow variations. These cannot be explained by wetland evaporation but may be due to freezing/thawing of the water in the wetlands.



2 Introduction

Through Technical Report Diresilala/DDM N° 001/2017 of 6 February 2017, the Office for the Protection of Silala Springs, Diresilala, contracted DHI for the realisation of the first part of this technical study of the flows of the Silala Wetland and Springs System. The Silala Springs are located in an arid area of the Potosí Department of Bolivia, close to the border with Chile.

Diresilala was subsequently integrated into Diremar, the Strategic Office for the Maritime Vindication, Silala and International Water Resources. Diremar has signed a new contract with DHI (Contract No. CDP-I 15/2017) for the execution of the second part of the study. The present report constitutes the third deliverable under this second part of the technical study of the flows of the Silala Wetland and Springs System.

2.1 About this report and the following steps of the project

This report documents and analyses climate data, water balance and flow measurements for the Silala Catchment.

The report is organised as a relatively brief main report in which the rationale, analyses and results of each of these three main themes are broadly described in separate sections. The main report also summarises the conclusions on all the themes but does not include all technical details, arguments and references. These are described in the three appendices – one for each main theme - and organised so they may be read in isolation from the main report.

Diremar is in the process of conducting a field study program to supplement the existing information on geology, hydrology, hydrogeology and wetland characteristics. More details on the field survey activities are given in the Field Survey Specifications Report (see Reference 6).

The field survey activities on surface water flows started in May 2017 and are ongoing to capture as much hydrological information as possible. The hydrogeological drilling and testing program as well as the planned campaign for soil sampling and determination of soil hydraulic characteristics in the wetlands and uphill top soils were originally planned to end by August 2017. However, problems in finding and allocating the right teams and equipment have delayed the drilling and soil analysis programs. These programs are not yet finalised at the time of writing (November 2017). This report and the analyses it contains are therefore based on data received from DIREMAR up to October 15th, 2017.

The report forms parts of DHI's deliverable under this project. Further deliverables in the coming project stages are:

- Product 4 Provisional report 4, Subsurface flows
- Product 5 Provisional report 4, Integrated surface and subsurface flows and scenario analyses
- Product 6 Final Report, Summary of findings of the previous reports and project conclusions.

2.2 Project objective and areas of concern

The project objective is to carry out a technical study of the flows of the Silala Wetland and Spring System, quantifying the surface and subsurface flows in their current condition and in their natural state, i.e. the flows without the manmade canal and drainage network. The canalisation was introduced by the Antofagasta Railway Company in the early 20th century to control the flow from the Silala Springs and use it for supply to the steam locomotives on the



Antofagasta-Bolivia Railway. The objective concerns the 'Near Field' area in the Silala Valley from the international border to just upstream the Silala Northern and Southern wetlands (see Figure 1).

A robust assessment requires both data and information of sufficient quantity and quality. It has therefore been agreed between Diremar and DHI to confine the data collection and the flow assessment to the Silala Near Field, where data collection is possible within the time available, and not to extend the field survey to the whole upstream catchment (see Figure 2, the Far Field). The extent of the Far Field groundwater catchment and recharge area is not known in detail and its size and conditions can only be very roughly assessed within the time and resources available to this project. Considerable effort would be required to map the complete hydrogeology and piezometric surface systematically.

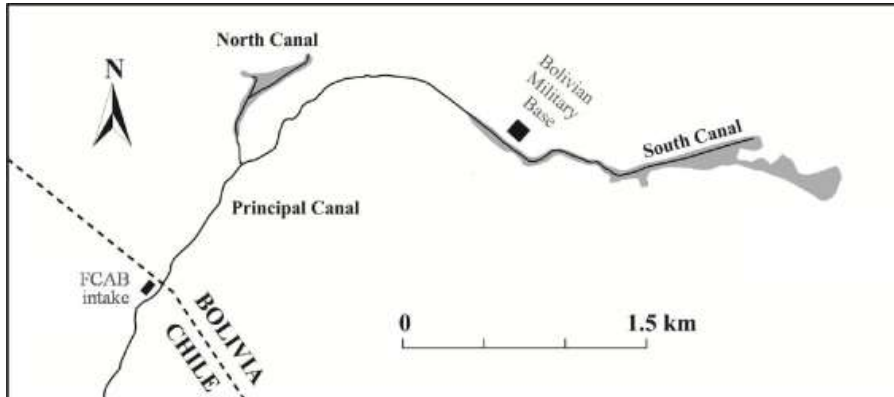


Figure 1 Approximate extent of the Silala Near Field. (Figure from Reference 1)

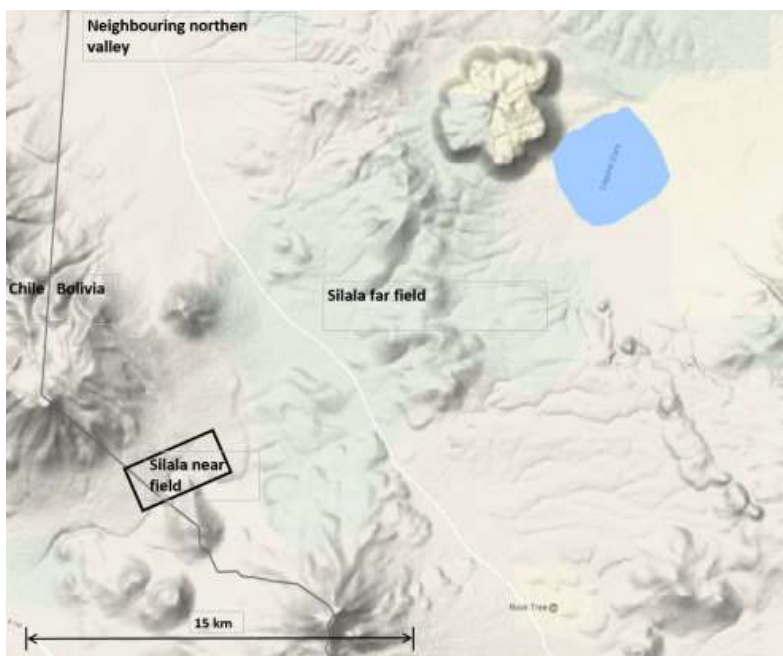


Figure 2 Approximate extents and locations of the Silala Near Field, the Silala Far Field and the neighbouring Northern valley



2.3 Rationale and methodology of the analyses

2.3.1 Climate assessment

Previous analyses (see Reference 10) have indicated large inter annual climate variations in the area and slow response of the Silala Springs System to climate variations. Long-term spatially distributed climate time series are required to understand the local hydrology, to analyse the recharge conditions of the system and the impacts of the manmade canals.

Such time series have been generated by combining daily and hourly climate observations from the ground stations within or close to the Silala Springs catchment with satellite data of the *local* area. This approach is deemed to be the best one to compensate for the sparse coverage of climate ground observations in the catchment area.

2.3.2 Water balances and ground water recharge

The Silala Springs System is fed by groundwater originating from the upstream groundwater catchment. Previous isotope analyses of the water in the Silala Springs have indicated water ages in the order of 1,000 -10,000 years. The present aquifer recharge analysis investigates whether the discharge through the Silala Springs System may be in balance with the present climate or the discharge is from slowly depleting aquifers holding fossil water, which has infiltrated during wetter pre-historic periods.

The spatial extent of the supplying groundwater catchment is unknown, but is for the purpose of a water balance analysis, approximated by the Catchment area to the Silala Springs System as delineated from a digital terrain model in our previous surface water report (Reference 10).

A water balance has been established. The main components include precipitation, evaporation, infiltration through the soil, recharge to a groundwater aquifer and groundwater flow. This water balance is then used to assess whether the order of magnitude of upstream recharge is sufficient to sustain groundwater discharge and flow rates at the downstream wetland and border area. Given the approximate groundwater flows, the groundwater travel time and groundwater age are estimated.

2.3.3 Analyses of surface flow measurements

Groundwater feeds the Silala Springs Systems through a number of seepage faces and springs along the edges and underneath the wetlands and canals. The spatial distribution of the groundwater contributions, as well as the magnitude and temporal variation of the canal flows, reveal information on the combined groundwater surface water system, which is important for the subsequent assessment of the flows in the system at present and under natural conditions without the canals.

Data from the project's flow observations campaign has been analysed and evaluated in combination with the longer records from DGA's weir in Chile, just downstream of the border. The flow observation campaign was launched in May 2017 and is still ongoing. Flows are measured at many strategic locations in the system, both as simultaneous spot measurements and in 7 strategic locations as continuous flow records. The analyses are presented in Section 5 of this report and constitute an update of the flow analyses previously presented in the surface water report from July 2017 (Reference 10).



3

Climate data

Climate data from Bolivia, Chile and satellites have been analysed in order to assess the Silala climate variables and produced what is considered to be the most representative climate time series for use in the analysis and models of the Silala Springs System and its catchment. The data sources are presented in this section, including how they were compiled and combined to derive a continuous dataset. The section gives an overall summary of the analyses and findings while further details are given in Appendix A.

3.1 Precipitation data

Daily records of precipitation are available for a number of stations in and around the Silala catchment. The stations are listed in Table 1 and the locations are shown in **Error! Reference source not found..**

As the stations in Bolivia generally only have a few years of rainfall and several gaps in the observed record, rain gauges at Inacaliri and Silala in Chile operated by Dirección General de Aguas (DGA) have been used to analyse the long-term daily rainfall series for the Silala Springs Catchment. The long-term average annual rainfall at DGA-Silala is 87 mm/year compared with 98 mm/year at Inacaliri for the corresponding period from 2001-2017. The rainfall varies considerably over time at both stations with high inter-annual variation. The average rainfall at Inacaliri for the full data period from 1969-2017 is, for example, higher at 122 mm/year due to the large climate variability in the data.

Table 1 Overview of rainfall gauges in Bolivia and Chile

Station	Source	Distance from Silala (km)	Altitude (m.a.s.l)	Period	Years
Silala	Senamhi	0	4402	12/6/2012-30/9/2017	4.5
Laguna Colorada*	Senamhi	28	4278	18/9/2010-25/9/2017	6
Sol de Manana	Senamhi	53	4916	1/1/2012-11/7/2017	5.5
Siloli	DGA	2	4000	25/10/2012-1/8/2017	4.5
Inacaliri**	DGA	6	4040	1/2/1969-28/2/2017	48
Silala**	DGA	2	4305	1/1/2001-28/2/2017	17
Ollague	DGA	90	3707	1/1/1971-28/2/2017	46
Linzor	DGA	25	4100	1/11/1973-28/2/2017	43

*) Very large values in 2016/17 indicate problems with station

**) The DGA gauges, Silala & Inacaliri have identical values for longer periods. - not raw data but it looks like one station may have been gap filled with values from the other station by DGA

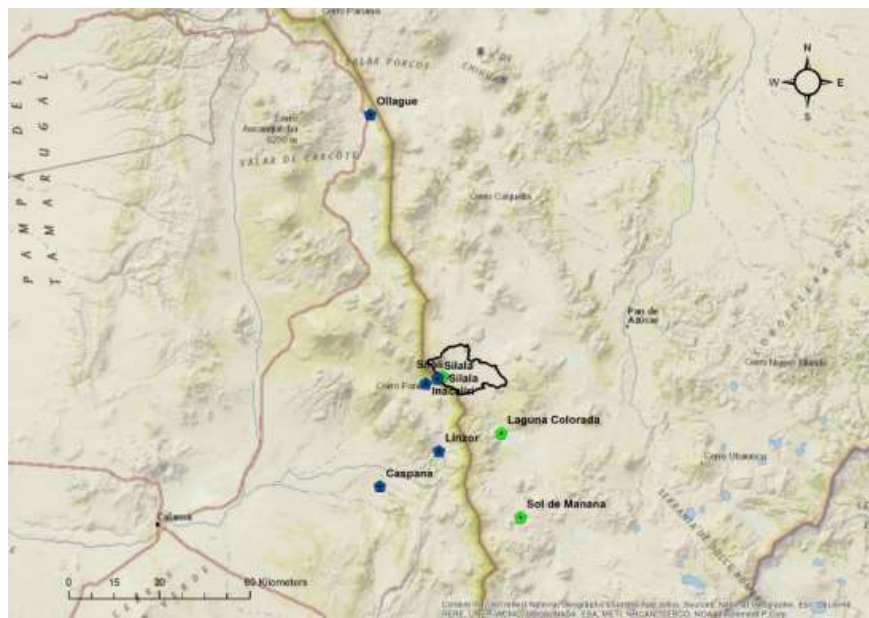


Figure 3 Locations of weather stations with rainfall data in Bolivia and Chile (Senamhi stations in green)

3.1.1 Annual and seasonal variation

The inter-annual variation in precipitation is very high. Figure 4 shows the annual rainfall at Inacaliri and Silala. Although the inter-annual variation may have some connection with large-scale atmospheric variations such as the El Niño, its correlation to this phenomenon does not seem to be very strong. It is noteworthy that, after 2001, the dry years seem to be drier and the annual average precipitation at Inacaliri lower than in the previous period. It has not been determined if this is an impact of a general global long-term change in climate or if it is a local decadal variation.

Most of the precipitation occurs during the austral summer months between December and March (see Figure 5). Very little precipitation is observed during the winter months from April to September. Snow has however been recorded and observed in the Silala catchment during the winter during site visits but this may not be captured adequately by the existing weather stations. The stations inspected for the analysis on the Bolivian territory are not equipped with instruments suitable for catching snow.

Daily MODIS satellite data of snow cover over the catchment from 2000 to 2017 confirm that some precipitation falls as snow during the winter months without being recorded at the precipitation gauges. While MODIS provides snow cover, it is not possible to reliably estimate snow depth or snow equivalent from these satellite data alone but they indicate that the gauged precipitation underestimates total precipitation. Further details are provided in Appendix A.

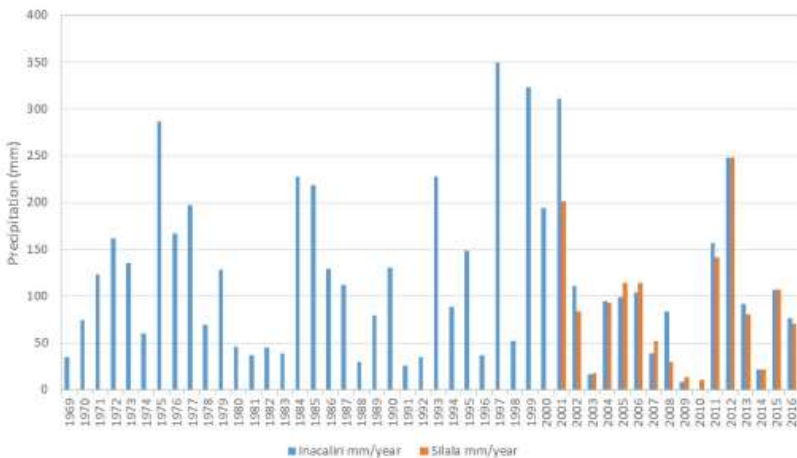


Figure 4 Annual precipitation at the Inacaliri and Silala gauges

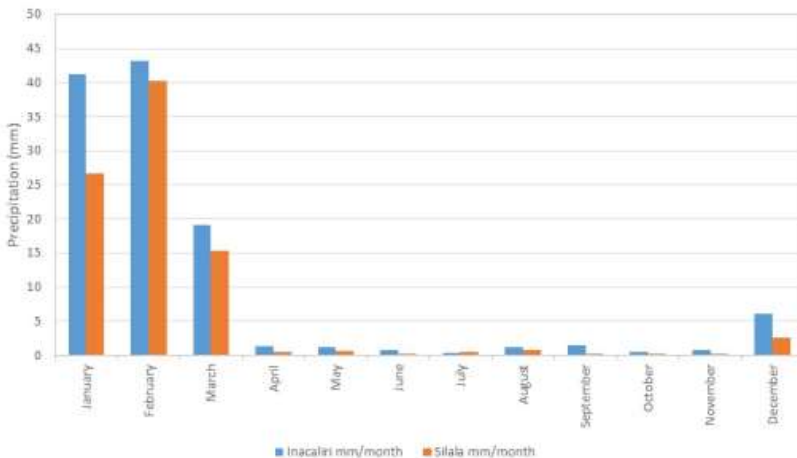


Figure 5 Monthly average precipitation at the Inacaliri (1969-2016) and Silala gauges (2001-2016)

3.1.2 Spatial distribution of rainfall

Rainfall in the area varies with altitude. To establish a reliable and longer data set of spatially distributed rainfall for the Silala catchment, this relationship was analysed using a combination of local ground stations and gridded long-term daily satellite precipitation data (CHIRPS) with a 5-kilometer resolution.

Based on the CHIRPS data within and close to the Silala catchment, a linear relation between precipitation and altitude has been established (see Figure 6). The established altitude relation was combined with the long-term precipitation series from the local weather station, Inacaliri, to estimate the spatial distribution of precipitation across the basin over time. This combination of local ground station data and the altitude variation from the local CHIRPS data provides the best estimate of the daily precipitation over the catchment. The data however does not capture snow events and may therefore underestimate rainfall in some years. The average annual



catchment rainfall obtained from the series is 137 mm/year. For comparison, the average annual precipitation, based directly on area weighed CHIRPS data for the Silala catchment, is 146 mm/year. These estimates are of the same order of magnitude as the value of 165 mm/year as derived by Muñoz et. al. (Reference 11) for a smaller Silala catchment but considerably higher than previous estimates around 60 mm/year, which were based on old data from Laguna Colorada.

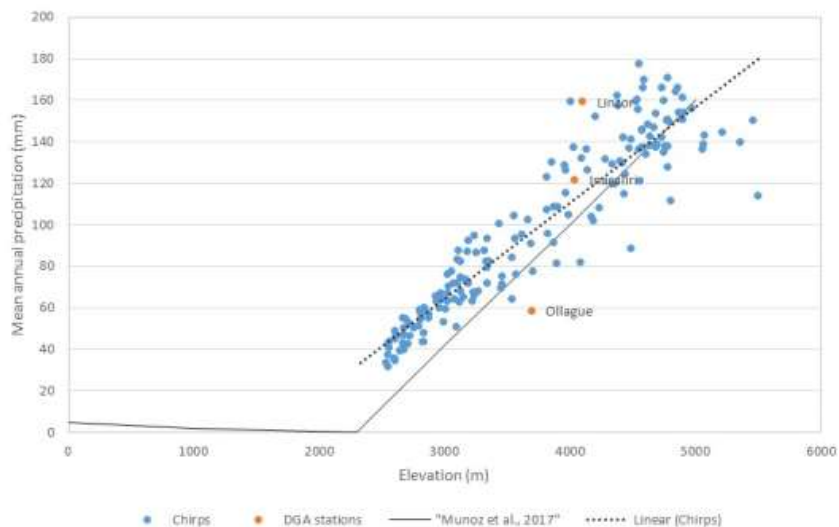


Figure 6 Regional annual average precipitation as a function of altitude based on CHIRPS data from 1981-2017 compared with station data at Silala, Linzor and Ollague and precipitation-elevation relationship derived by Muñoz et al., 2017

3.2 Evapotranspiration

Potential evapotranspiration (E_t) records have been estimated using the Penman-Monteith equation, at three weather stations close to the site: Silala, Laguna Colorada and Sol de Manana. The method is recognized worldwide for reliable approximations to E_t in a wide range of locations and climates.

Figure 7 shows the potential evapotranspiration estimates for the three locations. The average annual E_t ranges from 1268 mm/year at Sol de Manana to 1940 mm/year at Laguna Colorada with around 1472 mm/year at Silala. The derived series correspond well with the range of E_t from five nearby Chilean DGA stations also shown in the figure.

The altitude dependency of the potential evaporation in the area was found to be negligible. Therefore, the potential evaporation rate is assumed to be uniform over the Silala catchment area. The E_t record from the Silala station is assumed to best represent the E_t in the catchment and is therefore used in the water balance model. The uncertainty in E_t directly affects the range of simulated groundwater recharge. In order to take the large differences between the series from Laguna Colorada, Silala and Sol de Mañana into account, sensitivity analyses have been carried using data from each station as input for the model.

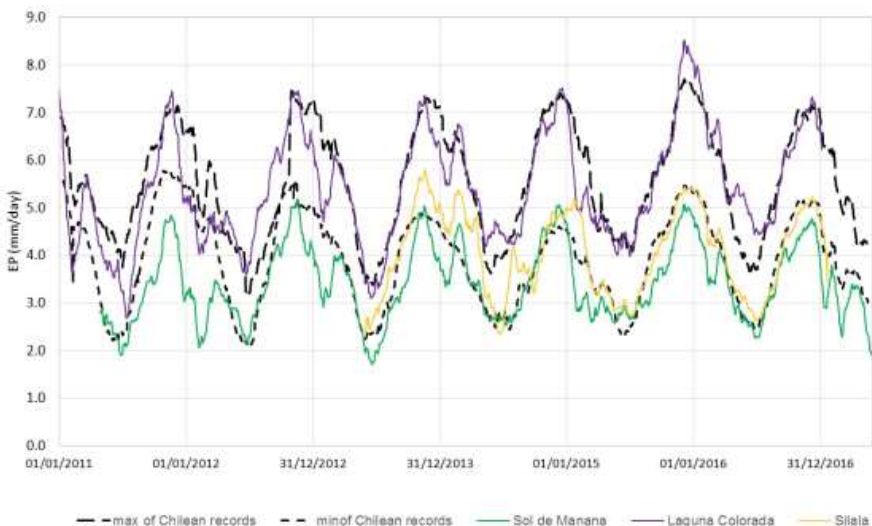


Figure 7 FAO reference E_{To} for Silala, Laguna Colorada and Sol de Manana (30 day moving averages) compared with the range (min to max daily values) of 7 nearby Stations from DGA Chile (Reference 10)

3.3 Temperature

Snowfall has been observed on higher grounds in the catchment also out of the austral winter season. To include the influence of snow on recharge, long-term spatially distributed temperature series with an hourly temporal resolution are required.

Based on the daily time series records from Inacaliri, Linzor, Silala and Laguna Colorada, a long-term time series of daily temperature for the period 1969-2017 has been constructed. A temperature lapse rate of $-7.1^{\circ}\text{C}/\text{km}$ has been derived from these stations, which are all located within or close to the catchment. Hourly variation in the long-term series has been generated from the hourly Silala records.

3.4 Silala climate characteristics and conclusions

Assessment of the recharge conditions in the Silala catchment as well as the detailed analyses of the impact of the manmade canals in the Silala Springs nearfield requires consistent and reliable climate data input, in the form of multi-year time series of precipitation, reference evapotranspiration (E_{To}) and temperature.

These time series have been determined specifically for the Silala catchment by combining *local* ground based observations, from within the catchment or very close to it, with the terrain information of the catchment. Where local ground based data have been insufficient to construct a reliable spatial variation satellite, observations of the *local* area have been used.

We find that this combination of ground based and remote sensing observations of the local area gives more reliable estimates for the Silala catchment than trying to correlate observations over long distances for other catchments with different characteristics as presented by Muñoz et al. (Reference 11).



Significant uncertainty in the climate series has been addressed in the water balance model in section 4 by sensitivity runs to assess the range of key model results.

A detailed description of climate data and the generation of the required model input is found in Appendix A.

4 Water balance and groundwater recharge

The Silala Springs and canal flow system is fed almost entirely by groundwater. Groundwater from the upstream catchment area (Far Field) is continuously discharging through the Silala Springs and canals in the Near Field and probably also as trans-border groundwater flow.

It is not clear if the discharge through the Silala Springs System is sustained by:

1. The upstream aquifers being recharged by infiltration of rainfall or melting snow reflecting current climatic conditions,
2. Solely by a gradual depletion of fossil aquifer storage or
3. A combination of 1. and 2.

Groundwater isotope analysis suggests that ancient, fossil water is part of the water discharged at the springs.

The purpose of the water balance analysis is to improve the understanding of the hydrological processes in the catchment and provide an independent estimate of groundwater age to backup this understanding and test if some of the above three explanations of the origin of the Silala flows may be eliminated.

4.1 Recharge estimation approach

A recharge and water balance assessment has been carried out for the approximate upstream catchment of the Silala wetlands. As the hydrogeological data in the area are limited, a conceptual approach has been adopted. It is not possible, with the data available, to determine the source of groundwater but based on generalised climate data, soil properties and overall geological features, the results may provide an indication of whether spring flows at Silala can be explained by a plausible range of recharge rates within the topographical catchment.

Groundwater recharge within the Silala area is driven by short-term precipitation events scattered in time and often separated by long dry periods. To estimate the sustainability of such desert recharge with high variability requires long-term dynamic simulation of the infiltration and evaporation processes, with a daily or finer temporal resolution in order to produce a reliable water balance. This approach constitutes a far better and more detailed analysis than previous simpler water balances for the area such as Reference 12, which compares only the average annual precipitation, potential evapotranspiration and surface water canal discharge from Silala.

The topography, soil types and depths, as well as representative precipitation, potential evaporation and temperature are used as input to a distributed hydrological model to produce a water balance for the contributing catchment under historic conditions. A first, rough assessment of travel times in the aquifers is made to ascertain to which extent these match the age of water determined from field measurements.

Dynamic rates of actual evaporation and groundwater recharge are estimated using the distributed integrated flow modelling system MIKE SHE (Reference 14). MIKE SHE is a dynamic flow modelling system, which couples advanced soil moisture and evapotranspiration



models with unsaturated zone and groundwater models for describing evaporation from both plants and soils, and recharge/infiltration to the underlying aquifers. The modelling system is described in detail in Appendix B.

4.2 Water balance assumptions

For the catchment upstream of the Silala Springs (the Far Field), the important processes for estimating groundwater recharge are soil evaporation, infiltration and snow processes. Overland processes may play a small role in parts of the catchment, for example on the volcanoes. However, since the areas that could generate overland flow are small as compared to the total catchment area and since the surface runoff seems to re-infiltrate in the foothills of the volcanoes, the overland flow component is expected to be of limited importance for recharge estimation. A number of generalized assumptions, listed below, have been made due to limited data availability and information in the topographic catchment. These assumptions are described in more detail in Appendix B.

- There are no significant surface water bodies or surface water flows within the catchment area.
- There is little or no vegetation to support any significant potential transpiration, i.e. evaporation losses are assumed to be in the form of soil evaporation and a small amount from sublimation from snow at high altitude
- The catchment area (232 km^2) is delineated from the NASA topographical model assuming that the surface water and groundwater catchments coincide
- The soils are generally coarse (sands or gravels), i.e. they are free draining with high permeability and a low capillary rise potential

4.3 Water balance model setup

For estimation of groundwater recharge and water balances for the Silala basin, a MIKE SHE unsaturated zone model was set up. The model has been set up using a grid size of 200 m resulting in a total of 5717 unsaturated zone columns for the catchment. Free drainage was assumed by fixing the water table at a constant depth of 3 m below ground.

Inputs consist of 48 years of daily and hourly climate time series for a period from 1969-2017 (described in section 3 and Appendix A) and estimates of soil properties were based on general literature values for sand and gravel, as no measurements of soil properties are available from the catchment at the time of producing this report. Details of the model setup can be found in Appendix B.

4.4 Water balance results and uncertainty

Based on the model results, the annual average actual evaporation over 48 years has been estimated at approximately 81 mm/year (6% of potential evapotranspiration) with a recharge rate of 56 mm/year corresponding to an outflow rate from the upper catchment of 412 l/s.

Some groundwater flow is expected to bypass the wetland, both below the sediments and in the deeper Ignimbrite aquifer. An old observation borehole in the Silala ravine, located 1.8 km downstream of the border in Chile (Reference 13), indicates artesian conditions and yields a constant rate of 90 l/s (without pumping). It seems plausible that the overall groundwater recharge is somewhat higher than the stream flow and borehole yields combined. Therefore, when compared to the recorded average stream flow at the Silala gauge of 160-210 l/s, our model-based estimate seems realistic.



In order to understand the importance of the model input parameters for the recharge estimates, a sensitivity analysis described in detail in Appendix B was undertaken. The sensitivity analysis looked at the effects of varying soil parameters and potential evapotranspiration rates, as they are associated with high uncertainty. It is clear from the analysis that both soil parameters and evapotranspiration rates have a significant impact on recharge rates. Using potential evapotranspiration from other stations at Laguna Colorado and Sol de Manana has an impact on total recharge in the order of +/- 20-30%. Soil hydraulic conductivity uncertainty could affect recharge by +/- 20%. Figure 8 shows daily rainfall, potential evapotranspiration, simulated actual evaporation and estimated recharge over time using the potential evapotranspiration rates from the Silala weather station. This illustrates how high intensity rainfall exceeds daily potential evapotranspiration leading to small amounts of occasional groundwater recharge in Silala. It also shows how actual evaporation and recharge are highly dependent on the variation of daily potential evapotranspiration during the year.

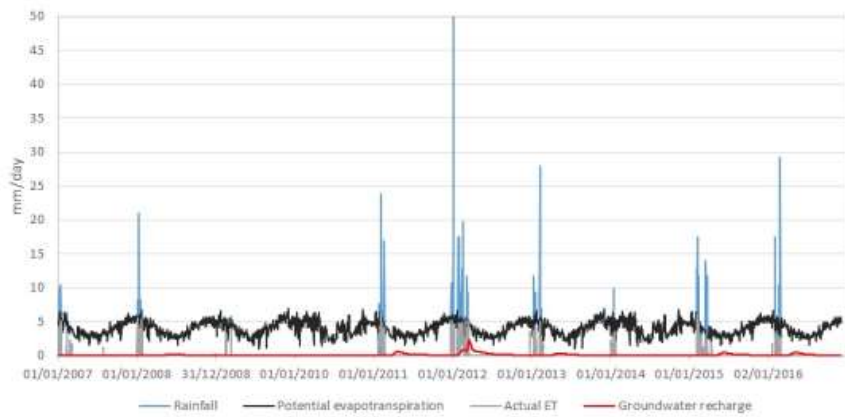


Figure 8 Daily rainfall, potential evapotranspiration and recharge for 2016 3 km north of the Silala wetlands

Based on the sensitivity analysis, the catchment recharge is estimated to be in the range 45-74 mm/year corresponding to 330-550 l/sec. This is consistent with measured flows in the Silala wetlands and the current knowledge of subsurface outflows into Chile. Actual recharge rates could potentially be higher as satellite maps of snow cover indicate that some snow events in the austral winter are not captured in the rainfall station data. Overall, the analysis indicates that it is plausible to assume that the current flows in the Silala Springs system may be sustained by groundwater recharge from the topographic catchment.

4.5 Groundwater flow and age

Groundwater age has been investigated using an extended version of the MIKE SHE integrated unsaturated zone groundwater model with particle tracking. The purpose of the particle tracking analysis was to estimate likely groundwater age of the water recharging the Silala canals and wetlands assuming inflows are from the topographic catchment. This will help ascertain whether the age of the water supports the findings from isotope analysis of water, which suggests that part of the spring water in Silala is fossil water.

The unsaturated model used for recharge estimation was modified for the analysis to include a relatively simple three-layer geological model comprising a lava layer at the top, overlying two Ignimbrite layers. Based on borehole information from the wetland area, the Ignimbrite aquifer was divided into a fractured high permeable top layer with a thickness of 20 m and a lower



less permeable layer with a thickness of 250 m. The geological model delineation is described in Appendix B and a geological profile is shown in Figure 9.

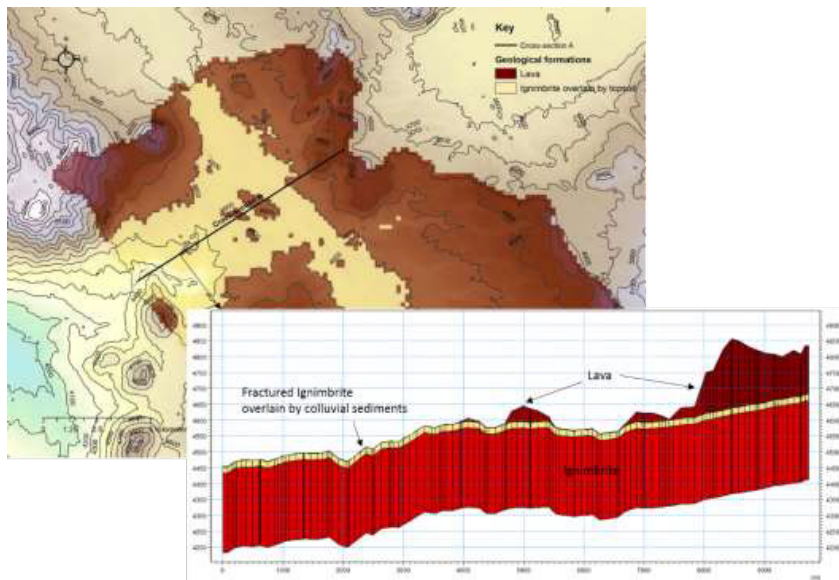


Figure 9 Geological model including cross-section from MIKE SHE model

The particle tracking analysis serves to estimate the origin and travel time of water recharging the Silala canal and springs system. Particles have been introduced at the upper groundwater layer, corresponding to infiltrating water recharging the aquifer. These particles are then displaced according to the simulated flow field until they reach the Silala Near Field area, where the groundwater discharges to the surface. Figure 10 shows the simulated potential head and groundwater flow vectors of the ignimbrite.

The origin, destination and travel time of each particle is registered. The simulated travel time is a proxy of groundwater age. In the Silala Far Field area, the depth to the groundwater table can be up to several hundred meters, especially at higher altitudes. A measure of water age from precipitation on the surface to discharge to the springs would thus have to consider both travel time through the unsaturated zone and through the groundwater aquifer.

Figure 11 shows groundwater age in the catchment based on the particle tracking model. The model results indicate an average groundwater age of approximately 900 years. The age varies with travel times from as little as 25 years in the vicinity of the wetland to up to 4,000 years for water coming from the far end of the catchment. The majority of the water is estimated to be between 400-1,000 years old (see Figure 12) based on groundwater flow transport time alone. Travel time in the unsaturated zone will add to the overall water age, particularly in the areas with volcanoes where the water table is assumed to be as deep as 1,000 m. The travel time in the unsaturated zone has been estimated based on a separate simple transport model run, with a tracer source with a constant concentration applied at the top of a number of unsaturated zone columns in the catchment. This provides a rough estimate of travel time through the unsaturated zone and using this approach, the travel time has been estimated to be between 0-50 years close to the wetland up to over 1,000 years below the volcanoes.

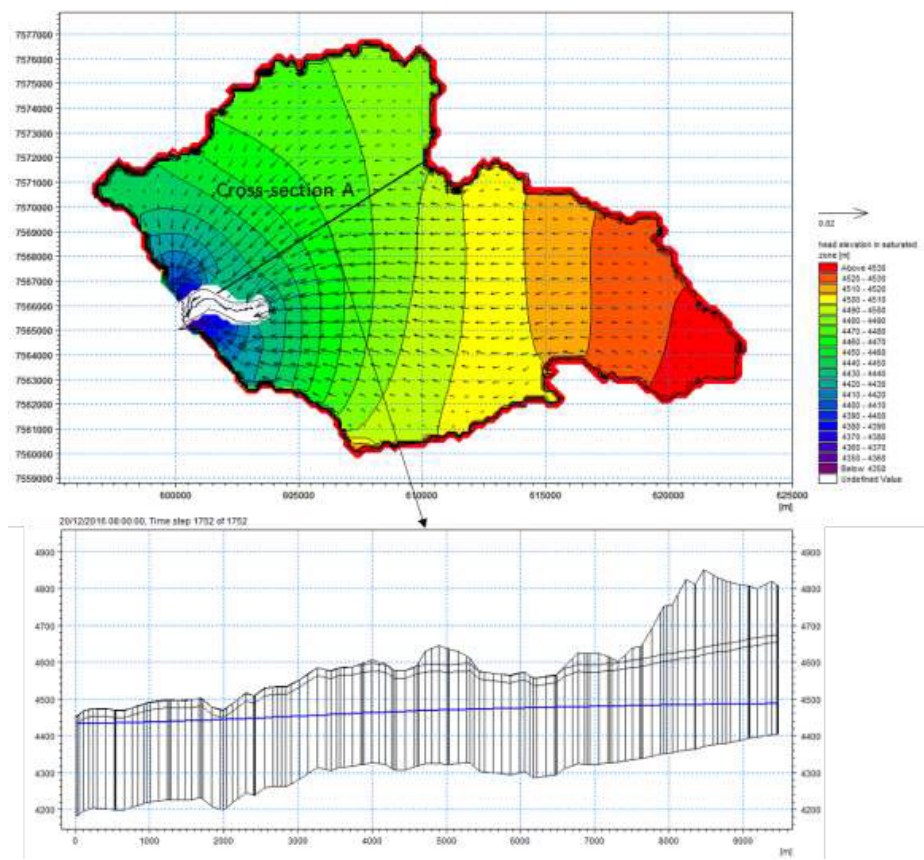


Figure 10 Simulated potential head of the ignimbrite aquifer (above) and in cross section (below)

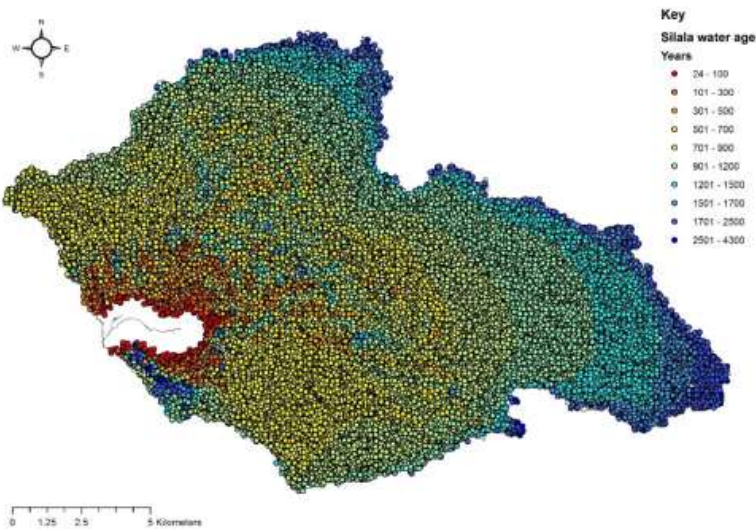


Figure 11 Simulated map of particle travel time and groundwater age

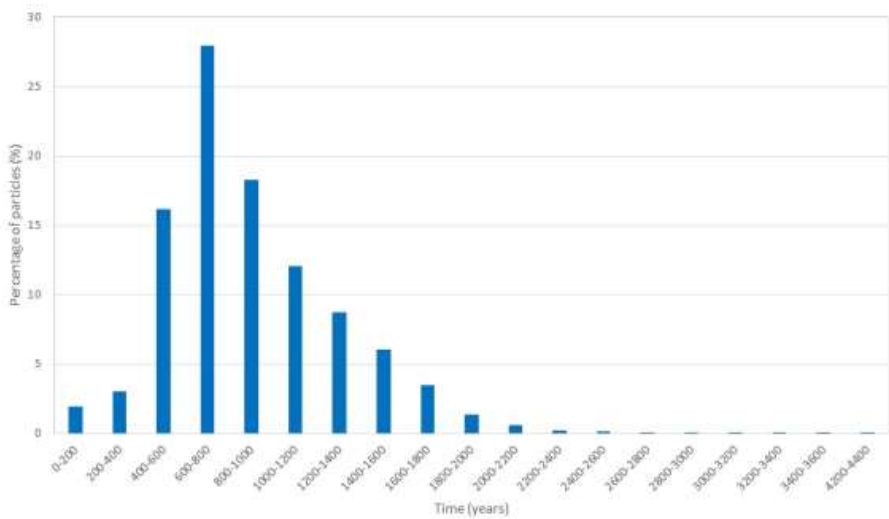


Figure 12 Particle age distribution

4.6 Water balance conclusions

Recharge estimates and water balances have been produced using the best available data for the Silala catchment. The results should be viewed as approximate and should not be interpreted as exact figures due to the scarcity of information on climate, soils and geology in the area. The main findings are summarized below:



- Average recharge for the period 1969-2017 has been estimated to 56 mm/year, which corresponds to a mean groundwater discharge to the Silala Near Field area of approximately 400 l/s. Compared to the recorded average stream flow at the Silala gauge of 160-210 l/s, this seems realistic as some groundwater flow is expected to bypass the wetland, both below the sediments and in the deeper Ignimbrite aquifer.
- Sensitivity runs considering key parameter and inputs indicate a range of recharge of 330-550 l/s. It shows that the recharge by infiltration of precipitation within the topographical catchment can provide sufficient groundwater flow to maintain discharges into the canal and springs system.
- The climate and recharge rate is highly variable with respect to both temporal and spatial distribution
- Overall, the analysis indicates that it is plausible to assume that the flows in the Silala Springs System may be sustained by groundwater recharge from the topographic catchment.
- A particle tracking analysis with the simulated groundwater flow field suggests variable groundwater travel times of up to 4,000 years, with a mean value of 900 years. The simulated travel time is a proxy of groundwater age.
- The age estimates do not include travel time of infiltrating water through the locally very deep unsaturated soil column. Based on average vertical travel time from a simple transport model run with a tracer and simulated depths to the groundwater table, the travel time has been estimated to range from 5-50 years where the groundwater table is closest to the surface by the wetland, to up to over a thousand years with the deepest groundwater table.
- Overall, the analysis confirms a high water age of over 1,000 years as compared to previous Isotope datings of 1,000-10,000 years.
- Given the lack of field data from the Silala Far Field area, the uncertainty and variability of climate data and the model sensitivity, these results should be viewed as indicative only.

A detailed description of the water balances and groundwater age calculations is found in Appendix B.

5 Surface water flow measurements

Groundwater continuously discharges in Silala as surface water through seepage faces and springs. In the present situation, the surface flow is collected by the artificial drainage and canal network and is conveyed through the manmade main canal across the border to Chile.

A key objective of the project is to quantify flows both under current conditions and under natural conditions assuming that the canals are closed and removed. A canal flow measurement campaign has been carried out during May-September 2017. Proven and reliable measurement methods have been applied in order to reduce uncertainties and provide a solid basis for analysing the current Silala surface water flows.

The surface flow measurements are analysed with the purpose of establishing:

- The canal flow rate at the permanent border site including mean rates and temporal variation
- The spatial distribution of canal flows and inflows from the wetlands to the border during the May-September field campaign



- The temporal variation of surface water flows during the May-September field campaign
- Flow measurement and water balance consistency checks
- Interpretation of flow measurement data in the context of a conceptual hydrological model of the Silala near field area

The distributed flow pattern contains information on sub-system contributions to canal flow, which is essential to the understanding, description and simulation of the surface hydrological processes. In later stages of the project, the surface water information will be combined with hydrogeological information collected as part of the groundwater field survey program to form an integrated surface water – groundwater model.

A surface flow measurement program planned by DIREMAR, SENAMHI and DHI was later adjusted during field inspections to pin down the best suitable locations (see Reference 6). SENAMHI has been contracted by DIREMAR to carry out the surface flow measurement program. The surface water flow measurement program was initiated in May 2017. The measurements include simultaneous canal and spring flow measurements, continuous flow records collected at flumes installed during 2017 and the permanent flume flows recorded close to the Bolivian-Chilean border.

Figure 13 shows the flow measurement locations including springs (Ojo de Agua), simultaneous flow measurement locations (S-1 – S-21) and continuous flume flow gauges (C-1 – C-7). Prior to the establishment of the flumes, simultaneous flow measurements have been carried out at both S-1 – S-21 locations and at the locations C-1 – C7 where six new flumes were later installed.

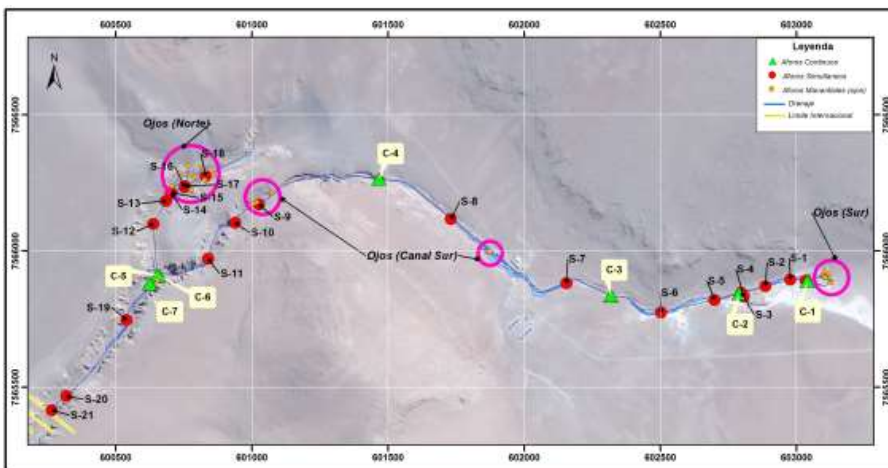


Figure 13 Overview of flow measurement locations (SENAMHI)

A preliminary assessment of measured flows was carried out as part of the Surface Water Report (see Reference 10). In the following sections, the flow data provided by the SENAMHI for the period May-September 2017 are updated, presented and analysed along with the permanent flumes flow records at the Bolivian and the Chilean side of the border.

5.1 Simultaneous canal flow data

The simultaneous flow measurement program is designed to provide a snapshot of flows in many points of the canal network. The measurements have been carried out ten times. Initially



at a bi-weekly and later at a monthly frequency, covering all locations within 2-3 days. Micro-propeller measurements in multiple points of the cross section provide a cross-sectional velocity profile, which is integrated to calculate the flow. The profile measurements have been carried out twice at each location to verify results and, if necessary, to take prompt on-site action to prevent errors.

5.2 Simultaneous spring flow data

The program of simultaneous spring-flow measurements was designed to assess flow rates at individual springs and the total spring flow contribution of sub-systems. By comparing measured spring flows and canal flows, a measure of diffuse canal inflows has been derived. Diffuse inflows describe non-point inflows, e.g. seepage faces or groundwater-canal flow exchange.

Spring flows have been measured at the discrete points of spring discharge (Ojo de Agua), which have been mapped across the entire Silala Near Field system. They include free flowing exposed springs, exposed springs with little or no flow and springs covered by soil and visible only by wet soil seepage faces. The first type is suitable for measurement of flow rates which has been carried out by collecting the spring discharge and deriving the flow rate from volume and time. In January 2017, flow rates were measured at the majority of springs while the data collected from May 2017 and onwards only includes 20 high-flow springs approximately. Unfortunately, the spring locations selected for measurement and the applied spring-naming convention are not consistent for all of the 10 measurement rounds during May-September 2017. This means that measured flow cannot be referred to the identical same locations.

Spring flow measurements were carried out for two days. In January 2017, flows at 64 springs were measured, with flow rates in the range of 0 – 11.9 l/s. In the Southern wetland upstream of station C3, 21 springs have been mapped and measured. The total spring flow adds up to approximately 40 l/s with an additional 15 l/s along the lower Southern Canal reach. On the Northern Canal, spring flows adding up to 46 l/s have been recorded. For the entire Silala Near Field area, the sum of spring flows is approximately 100 l/s compared to downstream canal flow measurements in the range of 160-200 l/s, meaning that 60 -100 l/s enters the canal, not as spring point sources, but as diffuse sources.

The canal and springs flow measurements indicate that the Silala canal system receives considerable lateral inflows, which are not accounted for by the spring flow measurements. The canal system gains water from both diffuse sources and spring point discharges, while potentially losing water due to diversion to wetlands, seepage and evapotranspiration. It is not possible to close the canal water balance from the flow measurements but the difference between measured canal flow and measured spring flows indicates a magnitude of diffuse inflows

A total of ten simultaneous flow measurements in 26 locations were carried during May-September 2017. Figure 16 is a longitudinal flow profile along the Southern Canal with measurements from 10 different dates. The flow increases from approximately 20 l/s at the Southern wetland to C-5 at the confluence between the Northern and Southern Canal. The measured simultaneous flow rates are approximately constant in time. Simultaneous flow data are also presented in Figure 17 to Figure 19 and in Appendix C.

Table 2 shows approximate diffuse net inflows by section of the Silala Canal estimated as the difference between measured mean canal flows and springs flows. At the upstream reaches of the Southern Canal (C-1 – C-3), the measured spring flows are almost equal to the measured canal flow, which implies limited diffuse inflows. However, on the lower section (C4 – C5) where only a few springs have been mapped, a large diffuse inflow indicates significant groundwater discharge to the Silala Canal in the upper canyon/ravine section.

On the Northern Canal, the sum of spring flows accounts for 75-80 % of the canal flow, leaving 20-25 % for diffuse lateral net inflow. Similarly, derived total diffuse net inflows for the Southern Canal are expected to be in the order of 35-45 %



The measurements of simultaneous canal flow and spring flow are associated with uncertainty. The spring flow measurement method is coarse and relies on capturing all of the spring flow within a given time interval, preventing any bypass flow. Measurements of canal flows suggest that the groundwater discharge is approximately constant. Consequently, spring flows should accordingly be approximately constant. However, for the most frequently measured spring, the flows vary between $\pm 40\%$ of the average value. The highest relative deviations are found for springs with low flow rates. The variation in measured flow is not consistent across the springs, suggesting that the variations are caused by measurement uncertainty and not hydrological temporal variations driven by, for example, climate.

Section	Measured spring flow (l/s)	Measured Canal Flow (l/s)	Difference, canal-springs (l/s)
C1, springs 1-12 (Zone 2)	23.8	27.8	4.0
C2, springs 1-20 (Zone 2)	41.2	36.7	-4.5
C3, springs 1-21 (Zone 2)	41.2	38.0	-3.2
C4, springs 1-22 (Zone 3)	45.2	59.5	14.3
C5, springs 1-32 (Zone 4)	56.9	97.0	40.1
C6, springs 33-64 (Zone 1)	46.1	56.9	10.8
C5+C6, springs 1-64	103.0	154.0	51.0

Table 2 Canal flows by section, accumulated upstream spring inflows and derived diffuse inflows

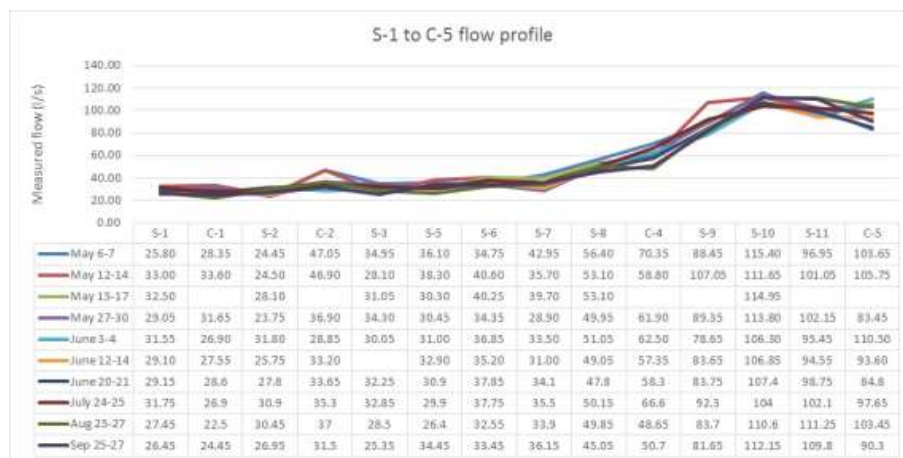


Figure 14 Longitudinal simultaneous flow profile (Southern Canal)



5.3 Continuous flow data of installed flumes

During May-June 2017, SENAMHI installed six new flumes and V-notch weirs, in accordance with the Final Field Survey Specifications (Reference 6). Once installed, the weirs were calibrated in the field to derive rating curves which describe the relation between water level and flow. Calibration was performed by controlling upstream flows. A number of corresponding values of flow and water level were measured, covering the low to normal flow range at each site. For the low flow ranges, the flow was calculated by collecting the volume in a container for a period of time. For the higher flow ranges, micro propeller measurements were used. The rating curves were approximated by curve fitting to the set of water level and flow data.

All of the weirs are equipped with continuous, automated pressure sensors, which provide continuous records of high temporal resolution

The purpose of this part of the flow observation campaign is to determine the flow rate at strategic locations in the canals of the Silala Springs System as exactly as possible, and therefore:

1. Reveal the temporal variation of the flow rate
2. Evaluate the daily flow variations and detect possible short-term impact of precipitation event. The daily variations are important to evaluate the simultaneous observation taken at more locations and may also open for an independent, although not isolated, evaluation of the evaporation rates
3. Ease the observation of possible surface water impacts from the planned borehole pump tests.

The resulting time series cover the period July – Sept 2017. All series shows a high base flow level superimposed with a smaller periodic daily variation peaking around midday.

Unfortunately, the base flow in all series exhibits abrupt jumps at certain dates and sometimes trends in the intermediate periods. None of these variations can be assigned to climatic events and must therefore be due to malfunctions of the equipment.

Although the daily flow variations may play a role in the uncertainty of the simultaneous observations, they are too small to explain the spread in the simultaneous measurements at the locations. The flows peaks at midday at all stations and daily variations can therefore not be due to evaporation losses that peaks at the same time. Hence, the daily variation is assigned to freezing and thawing of the water in the wetlands.

The results from the two two-week periods, during which the data are most consistent, confirm contributions from the Southern and Northern wetlands to be in approximately 60% and 40% of the confluence flow, respectively and that the flow contribution in the ravine between C4 and C5 is a significant part of the flow at the confluence.

5.4 Permanent Bolivian and Chilean flume flow records

Long-term time series of the flows in the Silala primary canal are available at two locations, one at the old siltation chambers in Bolivia around 700m upstream of the border and the other from Chile's Dirección General Del Agua (DGA), just downstream of the border on the Chilean side. Given the locations and proximity (less than 1 km) of the permanent flumes, no significant differences in canal flows are expected and the same level of flow should be found in both of the two flow time series.

At the Bolivian gauging site, a flume is constructed in a rectangular concrete trench constructed along the old siltation chambers and equipped with a V-notch and automatic (electronic) water level registration by floater with resolution around one mm. Hence, the station should be almost ideal for measuring the narrow flow range of the canal. Water levels



are measured both manually (two times a day) by the military personnel and automatically (hourly). Each of the two water level series has been converted to flows by a formula relating specific water level observations to flows. Particularly for V-notch weirs, the standard formula is considered accurate within 3-5 %.

Both manual and automatic water level readings and corresponding flow records exist. A comparison of measured flow time series covering the period August 2013- August 2017 is shown in Figure 15. The series is characterised by a constant base flow of 150-200 l/s, which clearly indicates that the canal is fed almost entirely by groundwater. However, frequent abrupt changes in the calculated flows, sometimes from one time step to the next, are also observed. The rapid fluctuations in flow originate from similar changes in the water level observations. It is, in general, not been possible to relate them to climatic conditions, runoff events or seasonality. It seems likely that these fluctuations must be attributed to uncertainty in water level observations, due to e.g. jamming of the float or sediment deposition in the stilling canal. The automatically gauged water levels include sudden jumps of 0.5 cm or 1 cm although the resolution of the instrument is 1 mm. This also points out to possible errors in the automated sensor registration. In spite of the near ideal flow gauge conditions provided by the weir, the uncertainty is therefore substantial, in the order of 25-30 % of the flow rate.

The Chilean flow time series also includes abrupt changes in flow. The Chilean flow series are generally approximately 15-25 l/s lower than the Bolivian series. A difference in flow of 40-50 l/s is seen in the most recent data from September 2017 (Figure 16). It seems unlikely that local canal losses along a generally gaining canal could explain the recorded differences in flow. Although both series shows significant variations over time, 125-225 l/s for the Chilean series and 160-210 l/s for the shorter Bolivian series, neither shows clear sign of seasonality or a direct correlation with local rainfall. Hence, the variation must be assigned to uncertainty in the measurements.

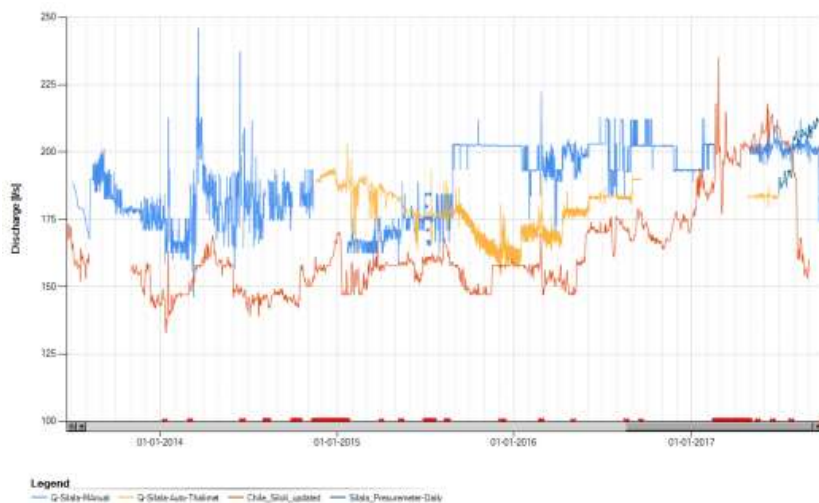


Figure 15 Long-term series of measured Silala Canal flows close to border, 2013-2017 Blue curve: manual readings C7, yellow curve: automatic floater instrument C7, turquoise curve: daily average from the new pressure sensor C7; red curve daily data from DGA's Siloli station just downstream of the border.



Figure 16 Long-term series of measured Silala Canal flows close to border, May–September 2017.
 Blue curve: manual readings C7, yellow curve: automatic floater instrument C7, turquoise curve: daily average from the new pressure sensor C7; red curve daily data from DGA's Siloli station just downstream of the border.

5.5 Comparison and analysis of flow data

Figure 17 and Figure 18 show simultaneous flow measurement plotted respectively for the Southern and Northern canal elevation profile. The left axis shows elevations (m) of the canal and the right axis shows flow rates (l/s). In addition, the elevations of springs adjacent to the canal have been marked.

On the Southern canal branch (Figure 17), the mean flow in the Southern wetland increases from 30 l/s upstream at S-1 to 36 l/s downstream at S-6. On the upper canal reaches, the slope is almost constant and from S-6 to C-4, the canal flow increases at an approximately steady rate reaching 60 l/s at C-4. However, from C-4 to S-10, in the upper reach of the ravine, the surface elevation drops and the canal bed slope increases. According to the measurements, a significant inflow to the canal, in the order of 50 l/s, occurs along this section. Since only a few springs have been recorded, the majority of the canal flow increase is due to groundwater discharges through seepage entering the deepest section of the ravine as diffuse discharge to the canal. The spring water level elevations have been plotted as an indication of the groundwater table elevation along the canal. Between S-9 and S-10, the spring elevations are significantly above the canal level. This is indicative of a relatively high water level gradient from the groundwater towards the canal and consistent with the high inflow rates recorded.

The results suggest that the topography is a main controlling factor of groundwater discharges to the canal. As the surface elevations drop, the groundwater table is forced closer to the surface, where it exchanges flow with springs, typically aligned with fractures, or directly to the canal. Larger scale hydrogeological features, such as faults, may play a role with respect to canal discharge patterns. On the steep canal section from S-10 to C-5, the mean flow decreases by approximately 10 l/s, which is attributed to either canal losses or measurement errors.

On the Northern Canal branch (Figure 18), the slope is less variable. The increase in mean flow is relatively high from S-18 to S-13, 5 l/s to 45 l/s. This section is characterized by a dense drainage network distributed across the width of the wetland. This is also the section where the vast majority of the springs of the Northern wetland discharge into the drainage



network. From S-13 to C-6, close to the confluence between the Southern and the Northern canals, the wetland is narrowly constrained by the ravine, with an approximately uniform canal bed slope. In this section, only a few springs have been mapped and the mean flow rate increases from 45 l/s to 57 l/s along a distance of approximately 300 m.

Figure 19 shows a map of canal flows and canal net inflows in the Silala Near Field area based on mean simultaneous flow measurements. This figure shows the flow at the continuous measurements stations (C1 – C7), the inflow between the stations and the percentage of flow relative to the downstream measurements, assuming that C7 flow equals the sum of C5 and C6 flows. Approximately 63 % of C-7 flows originate from the Southern canal and wetlands. Most of it enters the canal on the C-3 – C-5 reach. The reach has relatively few mapped springs and the gaining canal flow must thus be attributed to either diffuse seepage sources or groundwater discharging directly through the base of the canal in the deepest section of the canyon. Although not explicitly shown in the map, losses occur on each reach, e.g. by evapotranspiration or canal seepage to the adjacent riparian area.

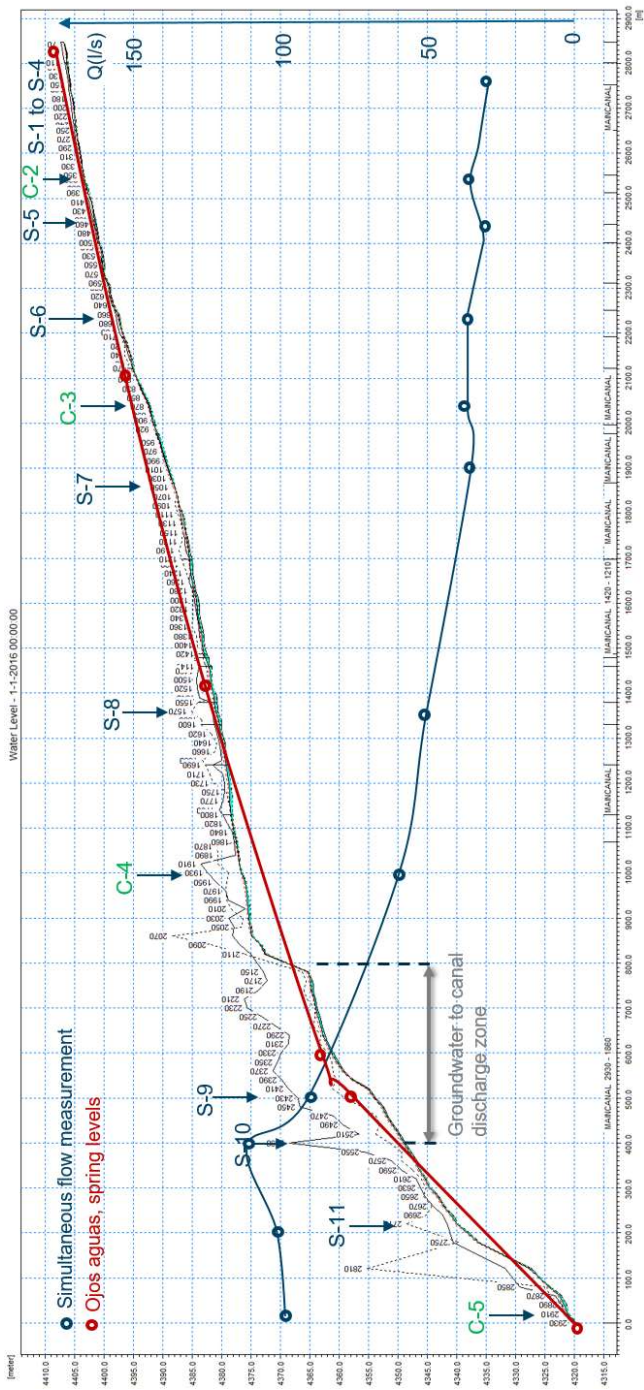


Figure 17

Southern canal profile (S-1 to C-5) showing canal elevation (m) on the Y-axis and canal chainage (m) on the X-axis

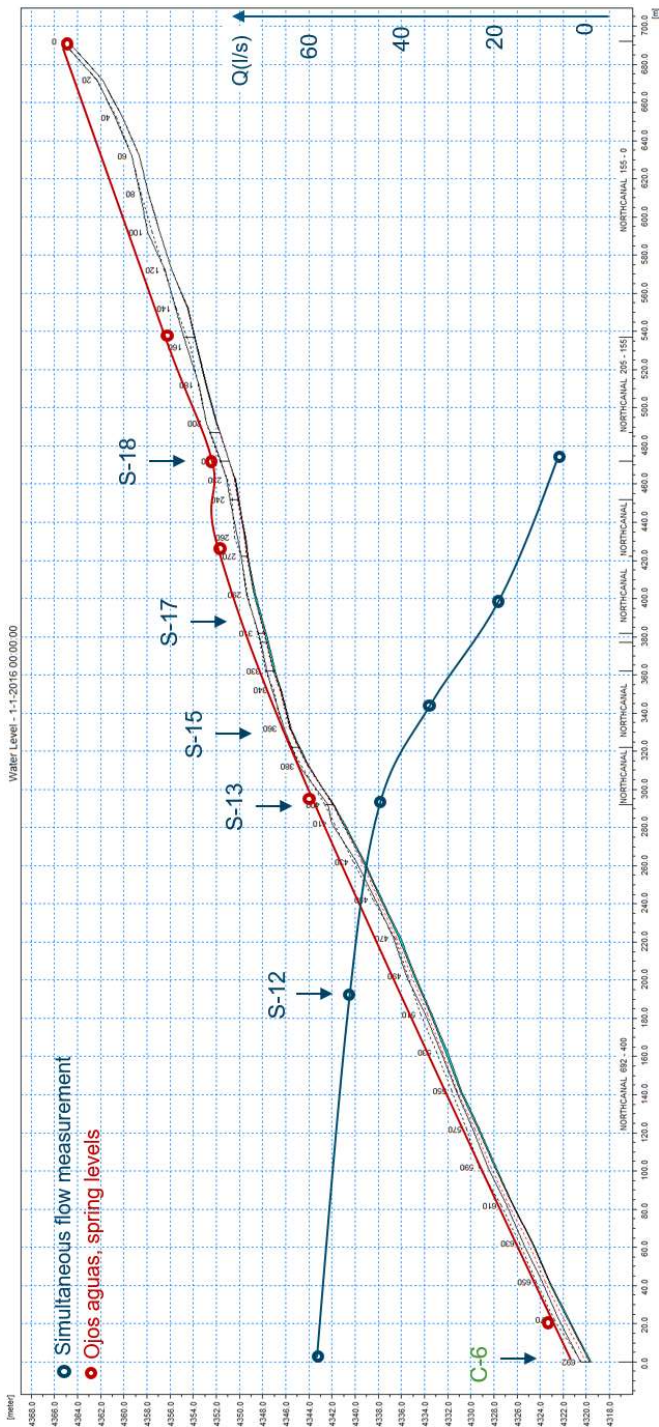


Figure 18 Northern canal profile (S-18 to C-6) showing canal elevation (m) on the Y-axis and canal chainage (m) on the X-axis

The expert in WATER ENVIRONMENTS

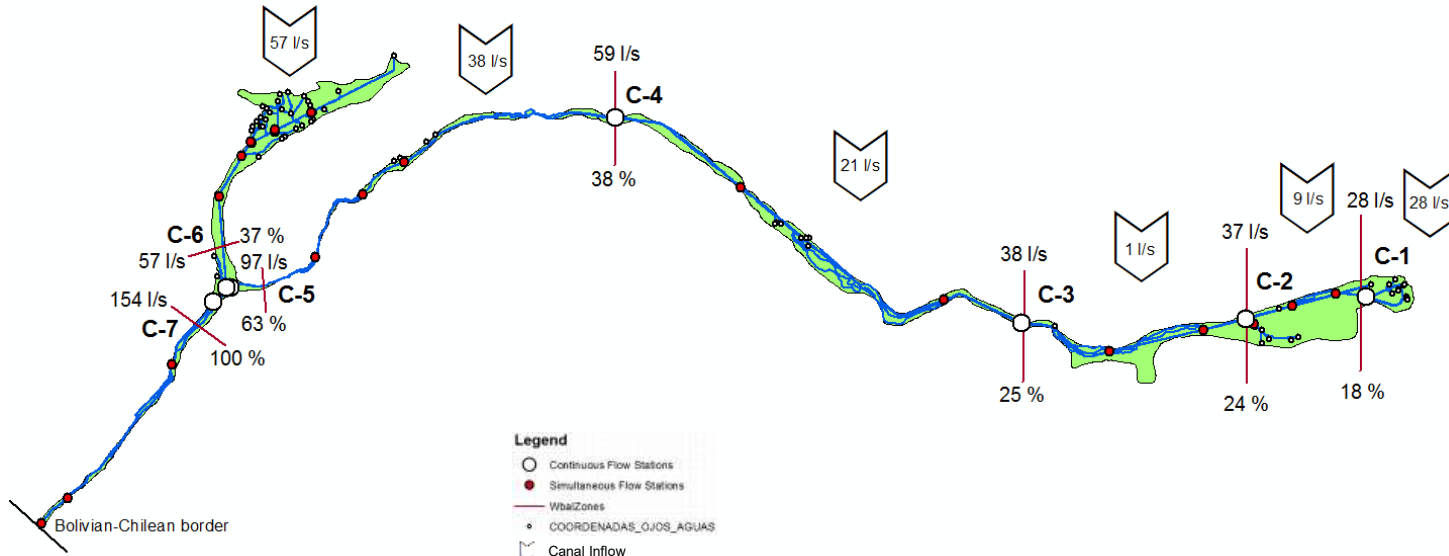


Figure 19 Mapping of flows and net inflows based on simultaneous mean canal flow measurements (in l/s)

5.6 Data consistency and uncertainty

The canal flows have been measured for different periods, at different locations and by different methods. Comparison of the long-term flow records from the permanent flumes in Bolivia and Chile respectively show significant differences in both the mean flow levels and temporal variation.

The shorter term continuous and simultaneous flow measurements carried out in January–September 2017 exhibit inconsistencies both at the individual gauging points but also when cross comparing the data. Figure 20 shows C-5, C-6 and C-7 flow measurements in July–September 2017. The measured continuous flows are significantly higher than the simultaneous flow measurements for all three locations and there are unexplained, but significant differences between the sum of C5 and C6 versus C-7 flows.



Figure 20 Continuous (shown as lines) and simultaneous (shown as circles) flow measurement data, July–September 2017

5.7 Conclusions on the measured flow data

- The long-term time series from the Bolivian and Chilean permanent flumes show mean flow rates around 160 l/s – 210 l/s with differences between the locations of 15–25 l/s. The temporal variations in flow at both locations are generally not mutually correlated or correlated with seasons, climate or runoff events.



- The flow data collected by SENAMHI during May-September 2017, including both simultaneous and continuous flow measurements, show approximately constant flow rates.
- The measured flows have been used to calculate the spatial distribution of inflows. The spring inflows to the Northern and Southern wetland account for roughly 60 % of the total canal flow at C-7. Diffuse inflows, in particular along the upper ravine reach (C-4 – C-5) of the Southern Canal, account for the remaining 40 %.
- The comparison of flow measurements show significant differences and deviations, under what would be expected to be well-controlled flume measurements. The additional measurements carried out in January-September 2017 have not narrowed the flow range in the downstream reach between C-7 and the border. Despite independent continuous and simultaneous flow measurements on the Chilean and Bolivian side of the border, the actual canal flow remains uncertain (160 -210 l/s).
- Smaller periodic daily flow variations have been detected at all of the seven continuous gauging sites during July-Sept 2017 (winter period). They cannot be caused by wetland evaporation but are likely the effect of freezing/melting of the water in the wetlands.

A more detailed description of flow data and the flow data analyses is found in Appendix C.

6 Summary and conclusions

The hydrology and hydrogeology for Silala is linked with the climate. Flow and water balance estimates thus require reliable distributed climate datasets. These were not available but have been estimated for this project. By combining *local* ground based observations with satellite data and the topography of the catchment, precipitation, potential evapotranspiration and temperature, time series have been established specifically for the Silala catchment. Considering the large spatial climate variability in the Andes This method is deemed to provide better climate datasets than correlating observations over long distances as suggested by Muñoz et al. (Reference 11).

Given the climate variability of the area and the quantity and quality of data, uncertainty must be recognised. Significant uncertainty in the climate series has been addressed in the water balance model by sensitivity simulations and the range of key model results assessed.

A water balance, recharge and flow-tracking model have been set up for the delineated catchment upstream the Silala springs and canal system. It is based on available data, e.g. precipitation and potential evapotranspiration time series and on a number of general assumptions concerning the characteristics and properties of the area.

Results show recharge rates of approximately 56 mm/year in the upstream catchment (232 km²) corresponding to a total long-term catchment discharge (groundwater *and* surface water) of roughly 400 l/s.

The results indicate that recharge generated inside the topographical catchment under current climate is sufficient to sustain the spring and canal discharges of 160-210 l/s and potentially a cross-border groundwater flow.

The simulated groundwater flow field has been used in a particle tracking analysis in order to map the possible origin and age of water discharging the Silala springs and canal system. The highest age of up to 4,000 years is found for the remote, higher altitude areas with an age of 900 years on average across the catchment. The age estimates do not include travel time of infiltrating water through the locally very deep unsaturated soil column. Based on averaged vertical flow velocities in the unsaturated zone and the simulated depths to the groundwater



table, the travel time range from 0-200 years, where the groundwater table is closest to the surface (3-4 m below surface at the downstream boundary) and up to several thousand years with the deepest groundwater table.

Overall, the analysis indicates a water age within the range of previous Isotope datings of 1,000-10,000 years.

Given the lack of field data from the Silala Far Field area, the uncertainty and variability of climate data and the model sensitivity, the results should be viewed as indicative only.

The continuous Silala canal flow measurements at the two permanent gauging stations on Bolivian and Chilean territory immediately upstream and downstream of the border have been supplemented by new measurements carried out by SENAMHI during January-September 2017. SENAMHIs field program includes simultaneous micro-propeller flow measurements (21 locations), spring flow measurements (20-33 Ojos De Agua) and six continuous flume water level recorders converted to flows.

The flow data analysis shows that the flows are dominated by groundwater discharges and approximately constant in time. The temporal variation observed in site-specific flow measurements cannot be explained by responses in neighbouring measurement locations or any climate or runoff events.

The flow measurements have provided valuable information regarding the spatial distribution of inflows and allowed a breakdown of water balances by reach. Although considerable flows (approximately 95 l/s) enter through the springs at the Northern and Southern wetlands, a large groundwater inflow contribution has been identified along the Southern Canal between C3-C5, especially along the upper reaches of the ravine, coinciding with a locally steep drop in topography and canal levels.

The different flow measurements around C5-C7 just upstream the border revealed inconsistencies between the flow records and have not contributed to narrowing the canal flow range.

Smaller periodic daily flow variations have been detected at all of the seven continuous gauging sites during July-Sept 2017 (winter period). They cannot be caused by wetland evaporation but are more likely due to freezing/melting of the water in the wetlands.

The continuous flow measurements have confirmed that the Northern and Southern wetlands contribute to respectively around 40% and 60% of the confluence flow and that a significant part of the flow in the Southern canal enters along the ravine upstream of the confluence. The uncertainties for assumingly well controlled flume measurements appear high and the data available up to the deadline of this report do not further constrain the wide flow range of 160-210 l/s measured at the border.

7 References

Reference 1

B.M. Mulligan and G.E. Eckstein, 2011: The Silala/Siloli Watershed: Dispute over the Vulnerable Basin in South America. Water Resources Development Vol 27, no 3.

Reference 2

Christian Neumann-Redlin, Juan Torres, after 2004: Hydrological Hydro-chemical and Isotopic Investigations in the Area of the Silala Wetlands.

Reference 3



G.Skrzypek, Z. Engel, T.Chuman, L. Šefrna, 2011: Distichia peat — A new stable isotope paleoclimate proxy for the Andes, Earth and Planetary Science Letters vol 307, 298-308

Reference 4

A. F Squeo, G. B. Warner, R. Aravena, D. Espinoza, 2006 : Bofedales: high altitude peatlands of the central Andes, Revista Chilena de Historia Natural, 79: 245-255.

Reference 5

DHI Feb 2017: Contract CDP-I N° 01/2017 Study of the Flows in the Silala Wetlands and Springs System, Phase I: Product no. 1, Inception Brief.

Reference 6

DHI Feb 2017: Contract CDP-I N° 01/2017 Study of the Flows in the Silala Wetlands and Springs System, Phase II Product 1 Final Field Survey Specifications

Reference 7

NASA 2017: Shuttle Radar Topography Mission. <https://www2.jpl.nasa.gov/srtm/statistics.html>

Reference 8

Robert H Fox, (1922): The Water works Department of the Antofagasta (Chili) and Bolivia Railway Company.

Reference 9

Servicio Nacional de Geología y Minería (2001): Estudio de la Geología, Hidrología, Hidrogeología y Medio Ambiente de Área de los Manantiales de Silala

Reference 10

DHI July 2017: Contract CDP-I No 15/2017, Study of the Flows in the Silala Wetlands and Springs System – Second Part Product No. 1: Provisional Report 1, Surface Flows

Reference 11

Muñoz J.F., Suárez, F., Fernández, b., Maas T.,2017 Hydrology of the Silala River Basin International Court of Justice Dispute over the status and use of the waters of Silala (Chile vs.Bolivia), Memorial of the Republic of Chile Volume 5 annex VII.

Reference 12

Graham, D.N. and M. B. Butts (2006) Flexible, integrated watershed modelling with MIKE SHE. In Watershed Models, (Eds. V.P. Singh & D.K. Frevert) CRC Press. Pages 245-272, ISBN: 0849336090.

Reference 13

Arcadis, 2017. International Court of Justice Dispute over the status and use of the waters of Silala (Chile vs.Bolivia), Memorial of the Republic of Chile, Volume 4, Annex 2. Detailed Hydrogeological Study of the Silala River

Reference 14

DHI, 2012, MIKE SHE User Manual Volume 2: Reference Guide, MIKE by DHI



Reference 15

<https://trmm.gsfc.nasa.gov>

Reference 16

<https://pmm.nasa.gov/GPM>

Reference 17

Home page of Food and Agricultural Organisation of the United Nations:

<http://www.fao.org/land-water/databases-and-software/Et0-calculator/en/>

Reference 18

De Wit, C.T., Gooudriaan, J. and van Laar, H.H., 1978. Simulation of Simulation, Respiration and Transpiration of Crops, Pudoc. Wageningen, The Netherlands, 148 pp. 1978

Reference 19

Xiao, X., R.Horton, T.Sauer, J. L.Heitman, and T.Ren (2011), Cumulative soil water evaporation as a function of depth and time, Vadose Zone J., 10, 1016–1022

Reference 20

Kasenov, 2001. Applied Ground-Water Hydrology and Well Hydraulics by Michael Kasenov, 2nd Ed., ISBN: 9781887201629, pp. 214

Reference 21

Freeze, R. A. and J. A. Cherry, 1979. Groundwater, ISBN: 0-13-365312-9





APPENDICES



Climate data analysis



APPENDIX A

Climate data



A Climate data analysis

This appendix documents a climate and hydrological analysis of the Silala Springs system in Bolivia close to the Chilean border. The purpose of the analysis was to develop an understanding of the hydrological processes in the spring catchment, with the aim to produce a water balance for the upper part of the catchment.

The appendix presents the available climate data for the area including precipitation, evapotranspiration and temperature, and our analyses of their spatial and temporal variations. It gives our best estimates of long-term distributed climate series, to be used in the catchment water balance studies in this report and in the detailed integrated groundwater –surface water studies of the Silala Nearfield to be established later in the project.

A.1 Precipitation

Daily records of precipitation are available for a number of stations in and around the Silala catchment in both Bolivia and Chile. Senamhi has provided data for three stations in Bolivia and station data has been extracted for six stations operated by Dirección General de Aguas (DGA) in Chile. The stations are listed in Table A-1 and the locations are shown in Figure A-1. Historical data for Laguna Colorada is also available for a period from 1980-2000. However, this data set looks erroneous, with repeating patterns of rainfall for longer periods. It has therefore not been used in the analysis.

Table A-1 Overview of rainfall gauges in Bolivia and Chile

Station	Source	Distance from Silala (km)	Altitude (m.a.s.l)	Period	Years
Silala	Senamhi	0	4402	12/6/2012-30/9/2017	4.5
Laguna Colorada*	Senamhi	28	4278	18/9/2010-25/9/2017	6
Sol de Manana	Senamhi	53	4916	1/1/2012-11/7/2017	5.5
Siloli	DGA	2	4000	25/10/2012-1/8/2017	4.5
Inacaliri**	DGA	6	4040	1/2/1969-28/2/2017	48
Silala**	DGA	2	4305	1/1/2001-28/2/2017	17
Ollague	DGA	90	3707	1/1/1971-28/2/2017	46
Linzor	DGA	25	4100	1/11/1973-28/2/2017	43
Caspiana	DGA	40	3246	12/6/2012-30/9/2017	4

*) Very large values in 2016/17 - problems with station

**) Identical values for longer periods - not raw data but it looks like one station may have been gap filled with values from the other station by DGA

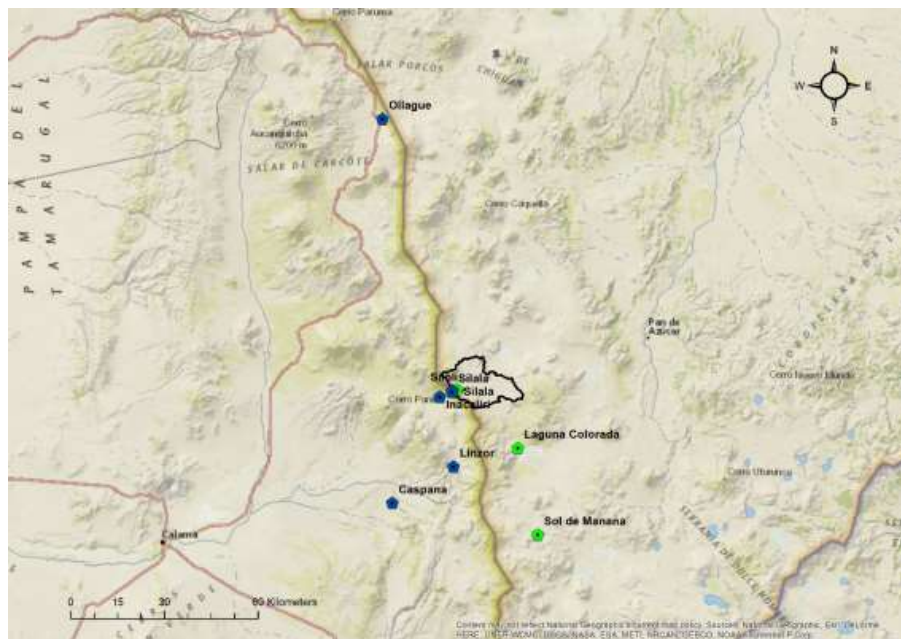


Figure A-1 Locations of weather stations with rainfall data in Bolivia and Chile (Senamhi stations in green)

As the stations in Bolivia generally only have a few years of rainfall and also have several gaps in the records, some of the stations from Chile have been used for analysing the long-term variations in rainfall and for looking at long-term annual average rainfall for the Silala catchment. The DGA rain gauges at Inacaliri and Silala (hereafter named DGA-Silala) are located closest to the study area and both have long records. However, it was noted that, for some years after 2010, the rainfall is identical at the stations, which could indicate that one of the stations may not have been operating properly and some gap filling was undertaken. The long-term average annual rainfall at DGA-Silala is 87 mm/year compared to 98 mm/year at Inacaliri for the period from 2001-2017. The average rainfall at Inacaliri for the full data period from 1969-2017 is 122 mm/year.

A.1.1 Annual and seasonal variation

The inter-annual variation in precipitation is very high, as illustrated in Figure A-2, which shows the annual rainfall at Inacaliri and Silala. The calendar years 2003, 2009 and 2010 were particularly dry years. Although the inter-annual variation may partly be explained by large scale atmospheric variations such as the El Niño effect, all three years are only moderate El Niño years. On the other hand, 2015 was very strong but was not particularly dry in the records. Hence, the inter-annual variation in precipitation does not seem to have a very strong El Niño correlation. A similar inter-annual pattern is observed at the other DGA stations. It is also interesting to note that the dry years seem to be drier after 2001 than for the previous period. Whether this and the detected generally lower average precipitation at Inacaliri is due to a general global long-term change in climate or whether it is a local decadal variation cannot be determined from the available data.

Climate data analysis

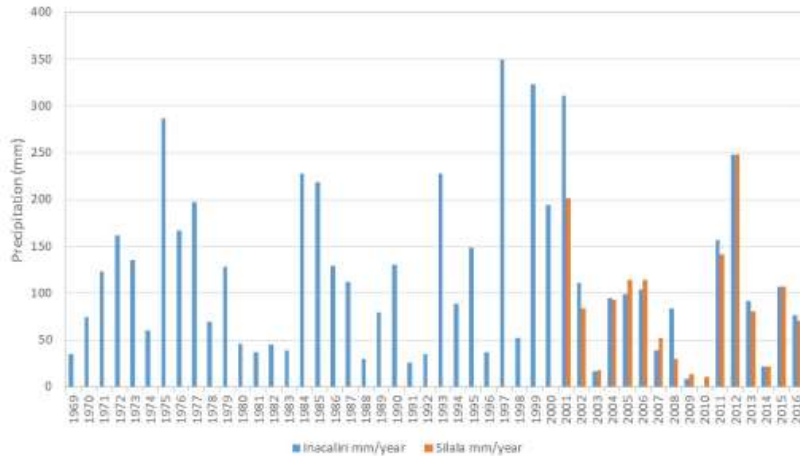


Figure A-2 Annual precipitation at the Inacaliri and Silala gauges

Most of the precipitation in the Silala catchment occurs during the austral summer months between December and March (Figure A-3). Very little precipitation is observed during the winter months from April until September. Snow has been recorded and observed in the Silala catchment during the winter but this may not be captured adequately by the weather stations. In fact, the stations inspected on the Bolivian territory were not equipped with instruments suitable for catching snow. The station data from Inacaliri and DGA-Silala has some minor precipitation events during the winter month for some years but no precipitation has been observed at the two stations after 2005.

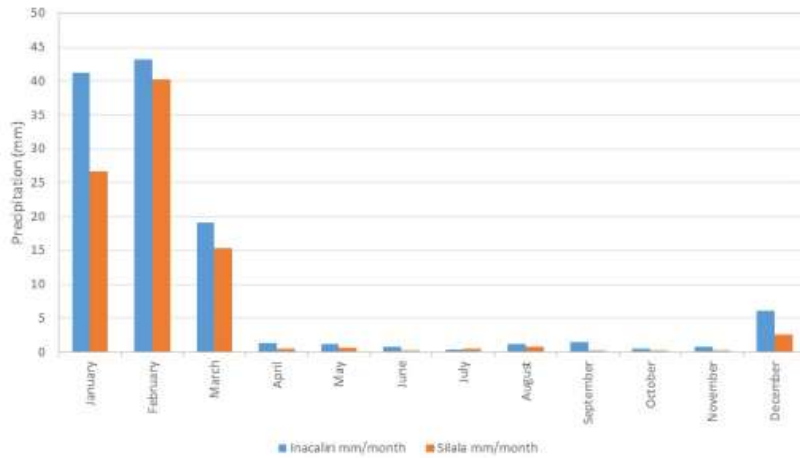


Figure A-3 Monthly average precipitation at the Inacaliri (1969-2016) and Silala gauges (2001-2016)

A.1.2 Snow formation

In order to investigate the importance of snow events in more details, MODIS satellite data was acquired, with a spatial resolution of 500 m showing the snow cover of the catchment on a daily basis from 2000-2017. Percentage snow cover in the Silala topographic catchment area



indicates that some precipitation falls as snow during the winter months. Particularly large snow (wet) events were observed in July 2002, August 2011 and June 2013 (see Figure A-4 and Figure A-5). However, this was not observed in any of the rain gauge data. Only a small amount of precipitation was recorded at the Inacaliri station in 2002 and none during the other periods. While MODIS provides snow cover, it is not possible to reliably estimate snow depth or snow equivalent from the data alone but they indicate that the gauged precipitation underestimates total precipitation.

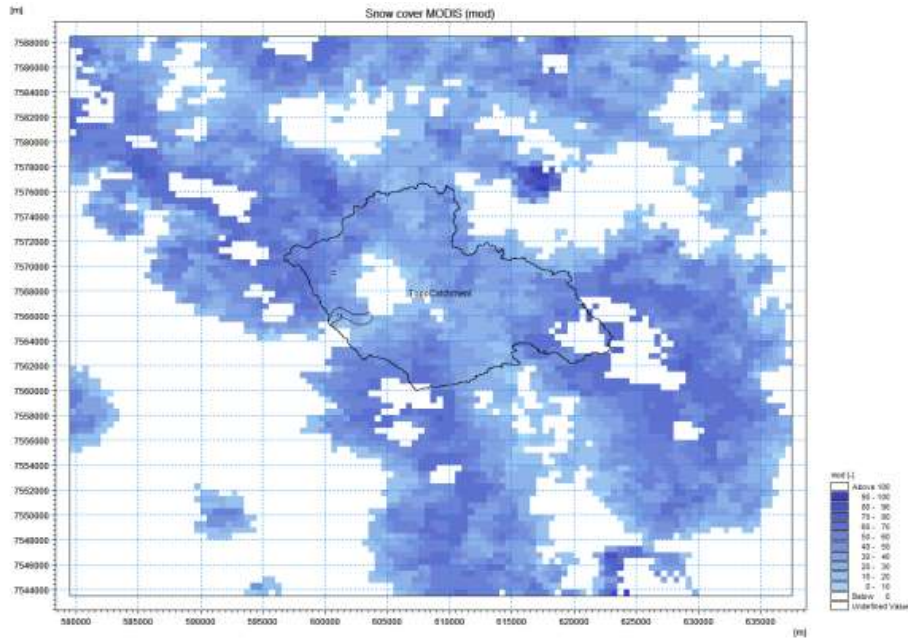


Figure A-4 MODIS satellite snow cover in the Silala catchment in June 2013

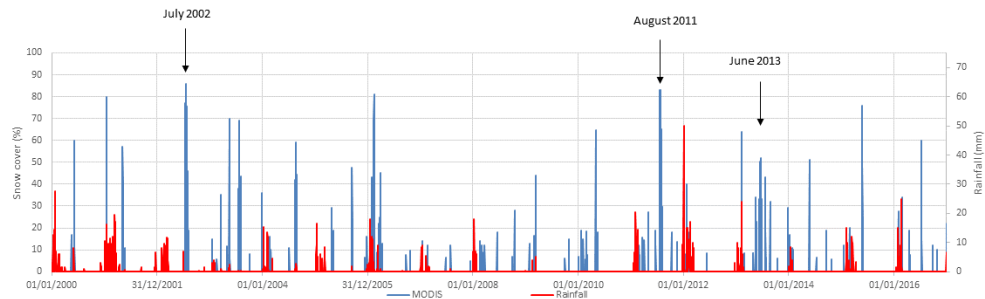


Figure A-5 Comparison of satellite snow cover (blue) to the north of the wetland on the ridge with rainfall daily recorded at Inacaliri (red).

A.1.3 Spatial distribution of rainfall

Due to the limited number of rainfall station with longer-term rainfall records in the Silala catchment area, it is difficult to make a reliable assessment of the spatial distribution of rainfall. Muñoz et al., 2017 (Reference 11) has, based on long-term rainfall records at a large number of DGA stations in Chile, developed a simple rainfall-altitude relationship and used it, combined with local elevation data, to make an assessment of the annual average rainfall for the catchment delineated by them. However, there is a large spread in the rainfall data at heights above 3,500 meters. It was therefore decided to look at satellite data to see if a more reliable relationship could be established from local data.

Climate Hazards Group Infrared Precipitation with Station data (CHIRPS) was used for the analysis. The data consists of daily gridded values with a resolution of 0.05 degrees or approximately 5 km, covering a 30-year period starting in 1981. Other gridded remote sensing rainfall series were also considered for the analysis but since these (TRMM and GPM, Reference 15 and 16) have a much lower spatial resolution (0.25° and 0.1° compared with 0.05°), the CHIRPS is considered the best source of distributed precipitation available for the Silala catchment. Furthermore, GPM data is only available for 2015-2017.

Like the ground station records in the area, the CHIRPS data does not show precipitation outside the austral summer months. Hence, CHIRPS does not capture any snow events in the winter months. The spatial variation of long-term annual average rainfall indicates that the highest amount of rainfall is seen in the North-Eastern part of the Silala catchment, reducing towards the South-West. This is consistent with the fact that precipitation in the basin is mainly caused by convective activity in a North-East South-West direction. More than 90% of the precipitation in the basin occurs between January and March, as a result of the significant atmospheric pressure coming from the East. During the rest of the year, the atmospheric moisture in the air decreases due to dry winds from the West.

Based on the CHIRPS data within and nearby the Silala catchment, a linear relation between precipitation and altitude has been established (Figure A-6 below). There is some scatter at the higher elevations and in general the curve is not as steep as the one derived by Muñoz et al., 2017.

As input to the water balance modelling, local gridded elevation data has been combined with the derived altitude/precipitation relation and long-term station data from the Inacaliri weather station to generate spatial precipitation distribution estimates across the basin over time. This combination of local ground station data and the altitude variation from the local CHIRPS data is deemed to give the best estimate of the daily precipitation over the catchment.

The average annual rainfall obtained from the series is 137 mm/year. This is lower than the value derived by Muñoz et al., 2017 of 165 mm/year, which was based on Chilean data from a larger area. It is also assumed that the Silala catchment area was smaller than the area used in this study. For comparison, the average annual precipitation based directly on area weighed CHIRPS data for the Silala catchment is 146 mm/year, less than 7% higher than what we consider the best estimate. The three estimates are within the same order of magnitude and considerably higher than previous estimates of around 60 mm/year, which were based on data from Laguna Colorada.

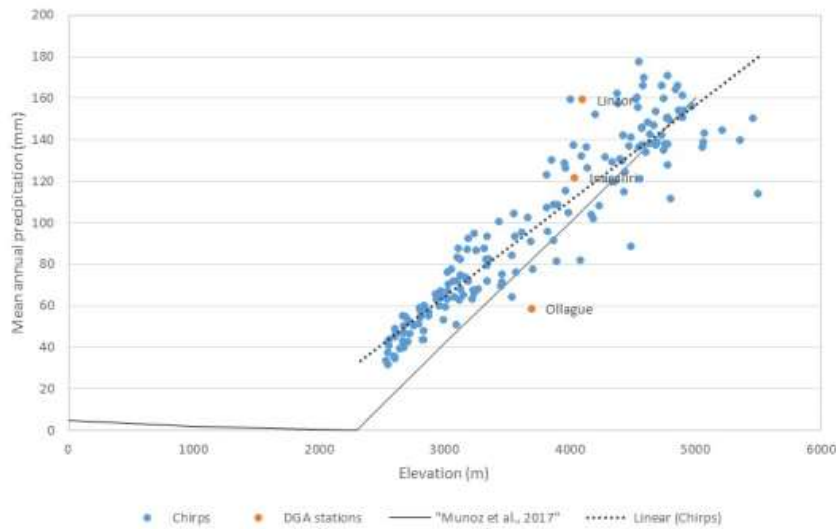


Figure A-6 Regional annual average precipitation as a function of altitude based on CHIRPS data from 1981-2017 compared with station data at Silala, Linzor and Ollague and precipitation-elevation relationship derived by Munoz et al., 2017

A.2 Evapotranspiration

Potential evapotranspiration records have been calculated for three weather stations: Silala, Laguna Colorada and Sol de Manana. Estimates have been derived using the E_t^* calculator, a software tool developed by the Land and Water Division of FAO (Reference 17), which calculates reference evapotranspiration (E_t^*) according to FAO standards based on temperatures, solar radiation and wind speed using the Penman-Monteith equation. The method is recognized worldwide for reliable approximations of E_t^* over a wide range of locations with different climates. It is physically based and explicitly incorporates both physiological and aerodynamic parameters.

Figure A-7 shows the potential evapotranspiration estimates for the three locations. For Silala, the evapotranspiration is higher in 2013/14 than later years, which is due to an abrupt change in average wind speeds in 2014, from around 12 m/s to less than 5 m/s. This indicates some problems with the station. Unfortunately, it has not been possible to establish what has caused the change. For Laguna Colorada, reference evapotranspiration is generally higher than for the other two stations, which is mainly due to high average wind speeds of 15 m/s. At Sol de Manana, the average wind speed is less than half (7 m/s). This indicates that the potential evapotranspiration is highly sensitive to wind speeds in this region. The average annual E_t^* ranges from 1268 mm/year at Sol de Manana to 1940 mm/year at Laguna Colorada with around 1472 mm/year at Silala. Compared to the range of E_t^* from seven nearby Chilean DGA stations (Figure A-7), these values seem reasonable.

The relationship between elevation and average annual evapotranspiration rates for the three Bolivian stations and five DGA stations is shown in Figure A-8. Although a downward trend in evapotranspiration with elevation is detected, it is small (-100mm/1000m) corresponding to less than 7% change in EP rate of the Silala station, over the whole altitude range of the Silala catchment. Furthermore, the slope of the trend line is uncertain due to the large spread in the data.

Climate data analysis



Consequently, the potential evaporation has been assumed to be uniformly distributed over the catchment. Since the Silala station is located inside the catchment, the series from this station are deemed to be the most representative for the catchment conditions. This series has been repeated to form a long multiyear time series. To account for the uncertainty illustrated by the rather big difference in EP levels between the three Bolivian stations, sensitivity analyses of the impact on the modelled groundwater recharge from the EP rates has been made. This was done by substituting the Silala series with the series from respectively Sol de Mañana and Laguna Colorada.

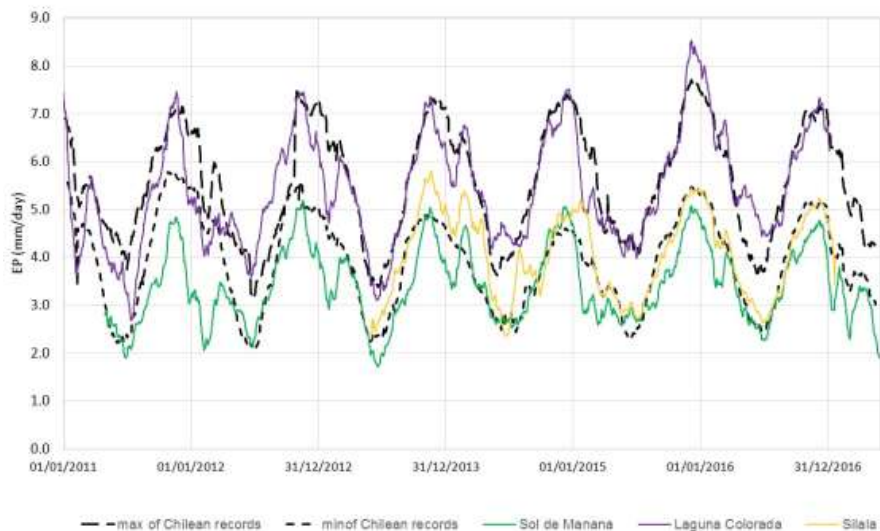


Figure A-7 FAO reference E_t^0 for Silala, Laguna Colorada and Sol de Mañana (30 day moving averages) compared with the range (min to max daily values) of 7 nearby Stations from DGA Chile (Reference 10)

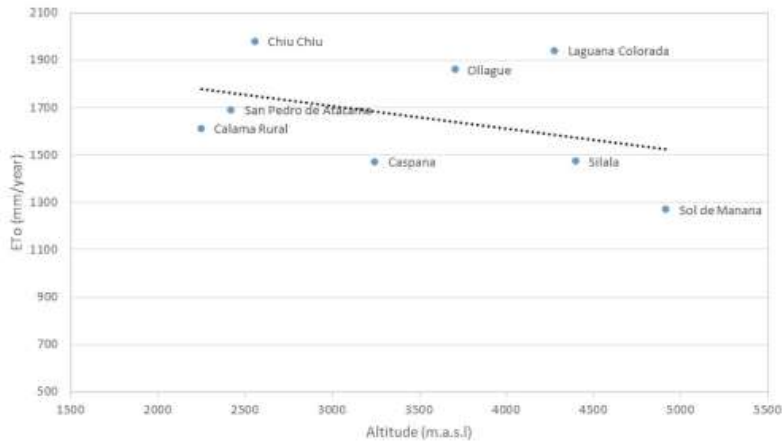


Figure A-8 Regional annual reference E_t^0 as a function of altitude

A.3 Temperature

Daily temperature records are available for three Bolivian weather stations in Table A-1 and longer-term records have also been collected from two Chilean DGA stations: Inacaliri and Linzor. The annual average temperature varies considerably between stations, with an average temperature at Inacaliri of 5.71°C compared with 1.49 °C at Silala. The temperature gradient based on this dataset as a function of elevation is illustrated in Figure A-9. It should be noted that the average temperature was calculated for different time periods. However, the gradient is still quite clear from the graph. At an altitude between 4 and 5 kilometers, this corresponds to a reduction in temperature of 7.1 °C/km compared to 4.6 °C derived by Muñoz et al., 2017 who used station data for a larger region. 7.1 °C/km is also high compared to general global numbers of 4-6 °C/km but the regression of the nearby stations in Figure A-9 seems to strongly support this lapse rate.

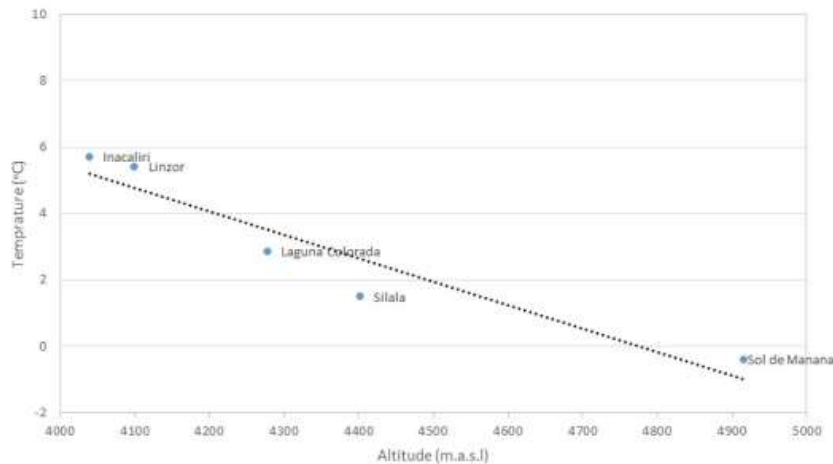


Figure A-9 Annual mean temperature gradient as a function of altitude

Based on the daily time series records from Inacaliri, Linzor, Silala and Laguna Colorado, a long-term time series of daily temperature for the period 1969-2017 has been constructed. However, data for the period 1986-2010 is not available and has therefore been gap-filled with data from Laguna Colorado and Silala from 2011-2016.

In order to be able to model snow formation and melting as accurately as possible, hourly temperature data was also acquired. Hourly data for Laguna Colorado for the period 2011-2016 was used for testing a diurnal model developed by De Wit et al. (1978) (Reference 18). Based on average, minimum and maximum daily temperature can be used for generating hourly data. This method was then used for converting daily data at Silala for 2016 into hourly data. As minimum and maximum values were not readily available for the Chilean stations, the hourly data from 2011-2016 based on Laguna Colorado and Silala data have been used for long-term water balance calculations.

An analysis of the temperature data shows that the annual average temperature is 2.2 °C with a minimum annual average temperature of 1.9 °C and maximum of 3 °C. Maximum daily temperatures are in the range 17.3-21.5 °C with an average of 19.6 °C. Minimum temperatures vary more between -24 °C to -16 °C with an average of -19.6 °C. Overall, the inter-annual temperature pattern is fairly similar. It was therefore assessed reasonable to repeat the data for the period from 1969-2010 in order to generate a long-term temperature time series. Some variation in temperatures for specific years will not be captured and this could have some impact

Climate data analysis



on snow formation for the earlier period. However, as some of the snow events in the austral winter months are not captured in the rainfall data, this is more of an issue and may mean that infiltration rates using the rainfall data may be slightly underestimated for some years..



Climate data analysis



APPENDIX B

Water balance



B Water balances

Appendix B describes a water balance analysis undertaken for the Silala River basin located in Bolivia. The purpose of the analysis was to develop an understanding of the hydrological processes in the catchment, with the aim to produce a water balance for the upper part of the catchment feeding the Silala wetlands.

The Silala springs and canal flow system is fed almost entirely by groundwater. Groundwater from the upstream catchment area for the wetlands is continuously discharging the springs and canal of the Silala wetlands. In order to sustain the groundwater flow, the groundwater aquifer must be either:

1. Recharged by infiltration of rainfall or melting snow reflecting current climatic conditions,
2. Associated with a gradual depletion of groundwater storage or
3. A combination of 1. and 2.

Groundwater isotope analysis suggest that ancient fossil water is part of the water discharged at the springs.

B.1 Recharge estimation approach

As the hydrogeological data from the area is limited, a conceptual approach has been adopted for estimating recharge and water balances. With the data available, it is not possible to determine the source of groundwater. However, based on generalized climate data, soil properties and overall geological features, the water balance estimates as presented in this appendix confirm that flows at Silala *may* be sustained by plausible infiltration and groundwater recharge rates occurring within the topographic catchment.

Groundwater recharge in the Silala area is driven by short-term precipitation events scattered in time and often separated by long dry periods. Correct reproduction of such desert recharge requires long-term dynamic simulation of the infiltration and evaporation processes with a daily or finer temporal resolution. This simulation approach has been adopted in the analyses and constitutes a far better and more detailed approach than previous simpler water balances for the area such as Arcadis (2017) (Reference 13), which compares only the average annual precipitation and surface water canal discharge from Silala.

The MIKE SHE hydrological modelling system (DHI, 2012) (Reference 14) has been selected for this analysis. The rationale behind this selection is that this modelling system is one of the most advanced and well-proven spatially distributed modelling systems available. It incorporates and dynamically links all the relevant hydrological processes for the analyses. The process representations are all physically based, which makes it possible to fill in information not measured in the field with generally accepted estimates, without sacrificing the transparency of the analysis.

MIKE SHE includes a soil moisture model by Kristensen and Jensen (Graham and Butts, 2006) (Reference 12) combined with an unsaturated zone flow model (Richard's equation) for describing evaporation from plants and soils and recharge/infiltration to the underlying aquifers. The model has a snow module, which accounts for the formation of snow based on diurnal variations in temperature and snow melt, including sublimation from dry snow. The evapotranspiration module accounts for evaporation from plant interception, ponded water, soil evaporation as well as transpiration from plants. Surface runoff processes are also included



using a simple diffusive wave model. Finally, the model includes a 3D-groundwater flow model coupled with the surface water and unsaturated flow modules.

A schematic of the MIKE SHE flow modelling system illustrating the different flow processes included in the system is presented in Figure B-1. Detailed descriptions of the different modules and equations can be found in the MIKE SHE documentation.

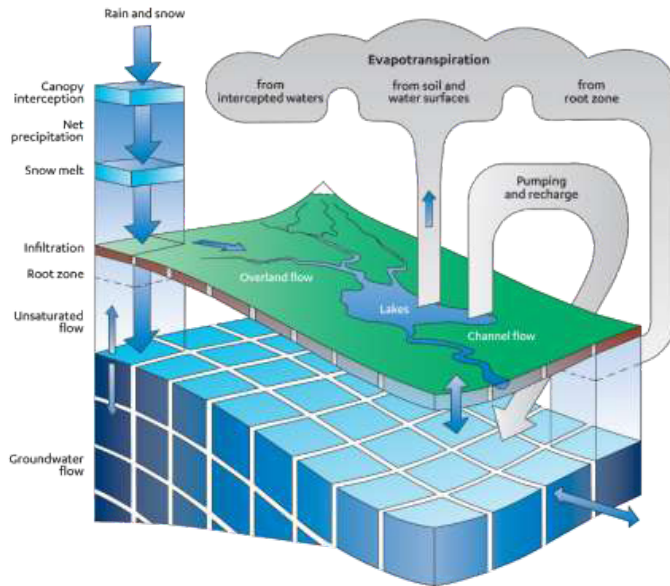


Figure B-1 MIKE SHE flow and transport modelling system

B.2 Water balance assumptions

For the Silala catchment, the important processes for estimating groundwater recharge are soil evaporation, infiltration and snow processes. Overland processes may play a small role in parts of the catchment, for example on the volcanoes. However, since the areas that could generate overland flow are small compared to the total catchment area and since the surface runoff seems to re-infiltrate in the foothills of the volcanoes, the overland flow component is expected to be of limited importance for recharge estimation. The topographic catchment area has been delineated based on a NASA digital elevation model (DEM) and covers an area of 231.5 km² excluding the wetlands. The catchment area contributing to recharge is uncertain due to limited information on the underlying geological aquifers. However, it is reasonable to assume, as a first assumption, that the groundwater divide coincides with the topographic divide.

The catchment is characterized by being very dry with very limited vegetation outside the wetland areas. Soils consist of sandy gravels with very little evidence of surface runoff or ponding near the surface. Soil evaporation is therefore the main process for removing water. Some evaporation also takes place from snow through sublimation but, as little information is available on rates and literature is sparse on this subject, this is assumed to be limited. A small sublimation factor of 5% of the potential evapotranspiration rate has been assumed reasonable.

Soil evaporation typically takes place from the upper 2 cm of soil (Xiao et al., 2011) (Reference 19) and will depend on soil properties such as hydraulic conductivity and capillary effects as well as the location of the water table. The recent drilling of boreholes by SERGEOMIN indicate

depths to the water table of approximately 4 meters immediately upstream of the wetland, with a likely increasing depth of several hundred meters moving away from the wetland into the lavas. For recharge estimation, it is therefore assessed reasonable to assume that outside of the wetland areas all soils across the catchment have free drainage conditions.

Limited information is currently available on soil properties in the basin. However, based on observations during site visits, top soils consist of mainly coarse sand and gravels with no indication of surface runoff or water ponding. On some of the volcanoes, there is some evidence of old flow pathways but runoff has not been observed in recent time. Investigations by Arcadis (2017) (Reference 13) in Chile indicate fairly sandy gravelly soils with hydraulic conductivities in the order of 0.1-2 m/day. However, this may not apply inside the Silala catchment and requires further investigations. Capillary effects are also of importance and will depend on grain size distribution, with limited capillary rises of 15 cm for coarse sands and up to 0.5 m for finer sands (Kasenov, 2001) (Reference 20). For soils with lower hydraulic conductivities, capillary forces will tend to be higher.

B.3 Water balance model setup

For an initial estimate of groundwater recharge and water balances for the Silala basin, a MIKE SHE unsaturated zone model was set up. The model has been set up using a grid size of 200 m resulting in a total of 5717 individual unsaturated zone columns for the catchment. Free drainage was assumed by fixing the water table at a constant depth of 3 m below ground.

Long-term daily and hourly climate time series for a period from 1969-2017 (described in Appendix A) was used as input for the model. Daily station rainfall from Inacaliri was used as input in the model along with a precipitation lapse rate to account for variations in rainfall with altitude. A daily potential evapotranspiration time series at Silala was constructed based on 4 years of data from 2013-2016 and assumed to apply for the whole the catchment. Some variation will occur with altitude and varying wind speeds but no clear correlation could be found in the data. In terms of temperature, an hourly record of temperature generated from hourly values at Laguna Colorado (2011-2015) and daily values at Silala (2016) was used as input for the model, combined with a temperature lapse factor of -0.71 °C/100 m derived from station data. Snow formation has been included using a standard melting threshold temperature of 0 °C and a sublimation factor of 0.05.

Soils were assumed to be homogeneous with a saturated hydraulic conductivity of 1.4×10^{-5} m/s (~ 1.2 m/day) corresponding to sand (Freeze and Cherry, 1979) (Reference 21) and capillary parameters were set using standard empirical Van Genuchten parameters of $\alpha = 0.05$ and $n = 3$ corresponding to well graded sand. The unsaturated zone model input parameters are summarized in Table B-1 below.

Table B-1 Overview of unsaturated model parameters

Model component	Parameters	Values
Unsaturated zone	Saturated conductivity K_s	1.4×10^{-5} m/s
	Saturated water content Θ_s	0.37
	Residual water content Θ_r	0.03
	Water content at wilting Θ_{wp}	0.03
	Water content at field cap. Θ_{fc}	0.044
	Van Genuchten α	0.05
	Van Genuchten n	3



B.4 Water balance estimates and uncertainties

Based on the model results, the annual average evaporation over 48 years was estimated to 81 mm/year with a recharge rate of 56 mm/year corresponding to an outflow rate from the upper catchment of 412 l/s. The recharge varies considerably in space as illustrated in Figure B-2 below. Compared to the recorded average stream flow at the Silala gauge of 160-210 l/s, this seems realistic. Some groundwater flow is expected to bypass the wetland both below the sediments and in the deeper Ignimbrite aquifer. An observation borehole downstream of Silala located in Chile (Arcadis, 2017) (Reference 13) indicates partly confined conditions and currently yields a constant rate of 90 l/s. It seems plausible that the overall groundwater recharge is somewhat higher than the stream flow and borehole yields combined.

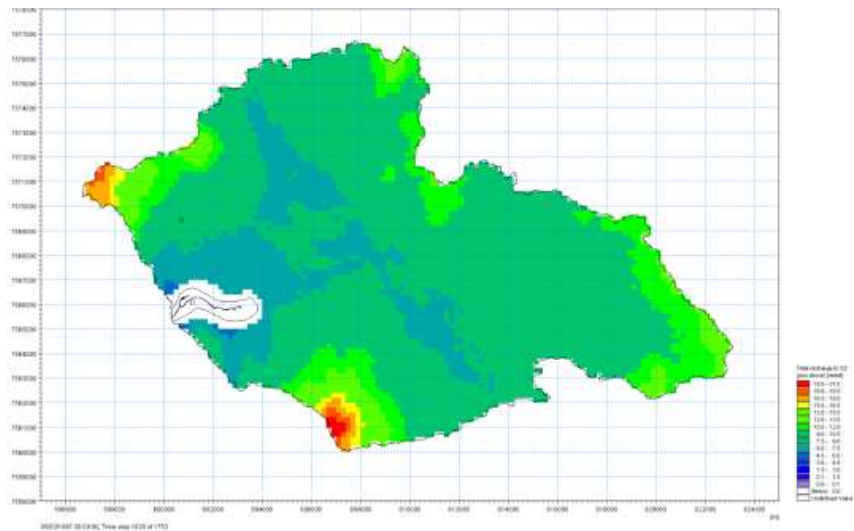


Figure B-2 Estimated groundwater recharge across the catchment on 5/3/1997

In order to understand the importance of the soil properties and potential evapotranspiration estimates for the recharge estimates, a sensitivity analysis was undertaken. Due to large run times, a representative unsaturated zone column located 3 km north of the wetland was selected for the analysis. Model runs were undertaken for a shorter period from 1998-2017 (~19 years). The column was selected as it has approximately the same precipitation as the catchment being located at an altitude of 4660 m close to the average for the catchment of around 4,700 m. Precipitation for the shorter period is slightly lower with an average of 131 mm/year. Evaporation is higher than for the full catchment. Baseline recharge from the column is therefore lower, 48 mm/year compared with 56 mm/year for the full catchment. The results of the sensitivity analysis are summarized in Table B-2.

It is clear from the analysis that both soil parameters and evapotranspiration rates have a significant impact on recharge rates. The potential evapotranspiration has a particular impact on total recharge. Interestingly, the annual average potential evapotranspiration at Sol de Mana is only 15% below the annual average at Silala but this results in a 33% increase in recharge. Conversely, the average potential evapotranspiration at Laguna Colorada is 32% higher than at Silala but only results in a reduction in recharge of 8%. An analysis of the daily potential evapotranspiration records at the three stations show considerable variations during the periods of rainfall, which explains the differences in impact on recharge. The graph in Figure B-3 below shows daily rainfall, potential evapotranspiration and estimated recharge over time. It

Water balances



illustrates how high intensity rainfall exceeds potential evapotranspiration rates leading to small amounts of groundwater recharge in Silala. Soil parameters also have an impact on soil evaporation. Particularly saturated hydraulic conductivities affect evaporation with an increased evaporative loss for less permeable soils.

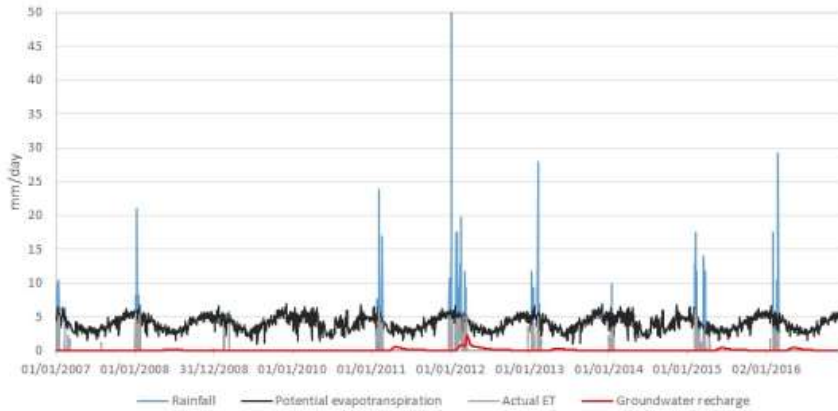


Figure B-3 Daily rainfall, potential evapotranspiration and recharge for 2016 3 km north of the Silala wetlands

Based on the sensitivity analysis of groundwater recharge, taking into account the fact that the column model has lower recharge than the full catchment, the catchment recharge is estimated to be in the range of 45-74 mm/year corresponding to 330-550 l/sec. This is consistent with measured flows in the Silala wetlands and current knowledge of subsurface outflows into Chile. Actual recharge rates could potentially be higher as satellite maps of snow cover indicate that some snow events in the austral winter are not captured in the rainfall station data. It may be possible to reduce the uncertainty of the recharge estimates if more information on soil properties become available but potential evapotranspiration rates remain uncertain. Overall, the analysis indicates that it is plausible to assume that the wetland is fed by groundwater recharge from the topographic catchment.

Table B-2 Sensitivity analysis of recharge estimates to soil parameters and potential evapotranspiration

Sensitivity run	Parameter	Rain	Evaporation	Recharge	Recharge	Change from baseline
		mm/year	mm/year	(mm/year)	(l/sec)	(%)
Baseline	See Table 1	131.2	83.8	47.4	348.1	-
1	Ks=1.4E-4 m/s	131.2	75.5	55.7	409.1	17.5
2	Ks=1.4E-6 m/s	131.2	92.8	38.4	281.6	-19.1
4	Van Genuchten $\alpha = 0.2$	131.2	74.5	56.7	416.1	19.5
5	Van Genuchten $\alpha = 0.1$	131.2	78.9	52.3	384.0	10.3
6	Epot -	131.2	87.6	43.6	319.9	-8.1



	Laguna Colorado					
7	Epot - Sol de Manana	131.2	67.8	63.4	465.5	33.7

B.5 Groundwater flow model and age

Groundwater age has been investigated using an extended version of the MIKE SHE integrated unsaturated zone groundwater model with particle tracking. The purpose of the particle tracking analysis was to estimate likely groundwater age of the water recharging the Silala canals and wetlands assuming inflows are from the topographic catchment. This will help ascertain whether the age of the water supports the findings from isotope analysis of water suggesting that part of the spring water in Silala is fossil water.

The unsaturated model used for recharge estimation was modified for the analysis to include a relatively simple three-layer geological model comprising a lava layer at the top, overlying two Ignimbrite layers. Based on borehole information from the wetland area, the Ignimbrite aquifer was divided into a fractured high permeable top layer with a thickness of 20 m and a lower less permeable layer with a thickness of 250 m. The extent of the lava deposits was delineated based on both a geological map provided by SERGEOMIN reproduced in Figure B-4 below and another updated map: SEARGEOMIN: PROYECTO MAPEO GEOLÓGICO ESTRUCTURAL ÁREAS CIRCUNDANTES AL MANANTIAL SILALA, La Paz, 2017 in Figure B-5. The applied delineation is fairly simple and does not represent the lava deposits very precisely, particularly in the Eastern part of the catchment. Outside the areas covered by lava, the Ignimbrite aquifer is assumed to be covered by colluvial/glacial topsoil of 1 m thickness. A geological profile of the model layers is presented in Figure B-6.

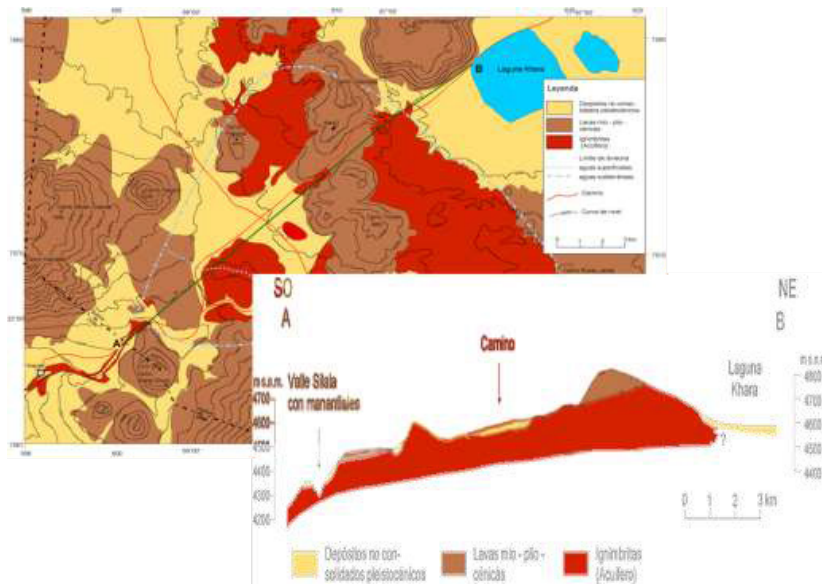


Figure B-4 Geological interpretations provided by SERGEOMIN (from Powerpoint)

Water balances

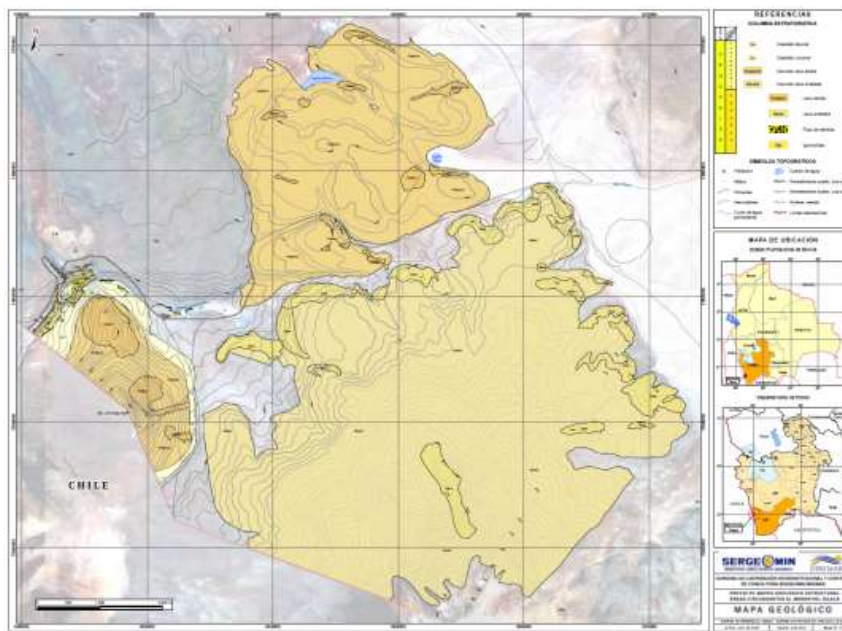


Figure B-5 Updated geological map provided by SERGEOMIN, 2017

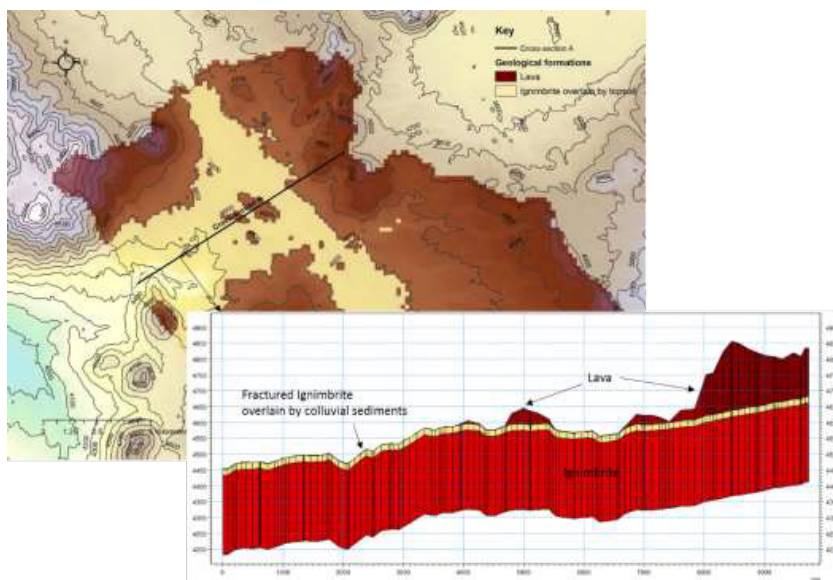


Figure B-6 Geological model including cross-section from MIKE SHE model



In terms of aquifer properties, the Ignimbrite aquifer has been assumed to have fairly high horizontal hydraulic conductivities in the order of 10^{-5} - 10^{-4} m/s. The lava deposits have been assumed to have lower saturated conductivities than the underlying Ignimbrite. Currently, there is no borehole information on aquifer properties in the catchment but pumping tests across the border in Chile (Arcadis, 2017)¹ indicate values for Ignimbrite in this range. One borehole also indicates partly confined conditions in the lower Ignimbrite but this has not been possible to confirm in the Silala catchment. It is likely that parts of the aquifer could be semi-confined but for the purposes of this analysis the aquifer has been assumed to be unconfined in the topographic catchment.

In the particle tracking model the unsaturated zone parameters were modified slightly compared to the values in Table B-1 using a higher α value of 0.15 to reduce the capillary effects. Currently, there is very limited information on soil parameters but the nature of the deposits do seem to indicate sandy gravel with low capillary effects. Using the modified parameters, the modelled recharge increases to 63.6 mm/year compared with the previous 56 mm/year, which is at the higher end of the range of recharge from the sensitivity analysis above. Table B-3 provides a summary of the saturated zone model input parameters.

Table B-3 Overview of geological units and parameters

Soil name	Horizontal K (m/s)	Vertical K (m/s)	Specific yield (-)	Specific storage (-)	Porosity (-)
Weathered Ignimbrite	0.0001	1.00E-05	0.15	0.0001	0.2
Ignimbrite	2.50E-05	2.50E-06	0.15	0.0001	0.2
Lava	1.00E-06	1.00E-07	0.15	0.0001	0.2
Colluvial/Glacial top soil	1.40E-05	1.40E-06	0.3	0.0001	0.2

Modelled groundwater levels at the end of 2016 are shown in Figure B-7 both as contours with flow vectors and along a cross-section. The results are presented at the end of the simulation in December 2016. Since recharge rates are small and the unsaturated is very deep, in some places between 500-800 m, limited annual fluctuations in the groundwater table are observed. The location of the water table in the middle of the catchment is approximately between 20-50 m below ground. This seems reasonable, as the area is very dry with no indication of a shallow groundwater table. There are three small dry lakes in this area, which indicates that locally the groundwater table may occasionally be higher but, with the regional model using a 200 m grid, it has not been possible to capture it in the model.

¹ Arcadis, 2017. Memoria, Volume 4, Annex 2. Detailed Hydrogeological Study of the Silala River

Water balances

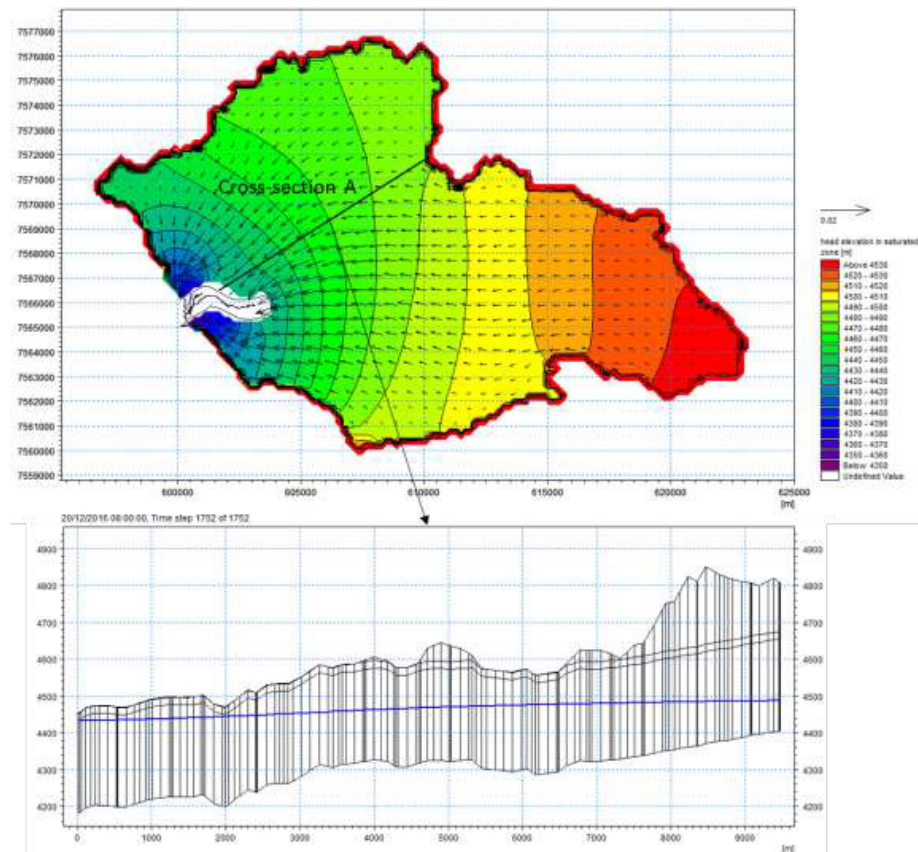


Figure B-7 Simulated potential head in the Ignimbrite aquifer including flow vectors (layer 3) and profile of water table on 20/12/2016

The combined unsaturated zone and saturated zone flow model has been used for a particle tracking analysis. The particle tracking analysis serves to estimate the origin and travel time of water recharging the Silala canal and springs system. Particles have been introduced in the upper groundwater layer, corresponding to infiltrating water recharging the aquifer and subsequently displaced step by step according to the simulated flow field until reaching the Silala wetland area, corresponding to groundwater discharging into the surface water system or leaving the area as sub-surface flows.

The origin, destination and travel time of each particle are registered. The simulated travel time is a proxy of groundwater age. In the Silala Far Field area, the unsaturated zone, i.e. the depth to the groundwater table, can be up to several hundred meters, especially at higher altitudes. A measure of water age from precipitation on the surface to discharge to the springs would thus have to consider both travel time in the unsaturated zone and groundwater.

Figure B-8 shows groundwater age in the catchment based on the particle-tracking model. The model results indicate an average groundwater age of approximately 900 years. The age varies with travel times from as little as 25 years in the vicinity of the wetland to up to 4,000 years for water coming from the far end of the catchment. The majority of the water is estimated to be between 400-1,000 years old (Figure B-9) based on groundwater flow transport time alone.

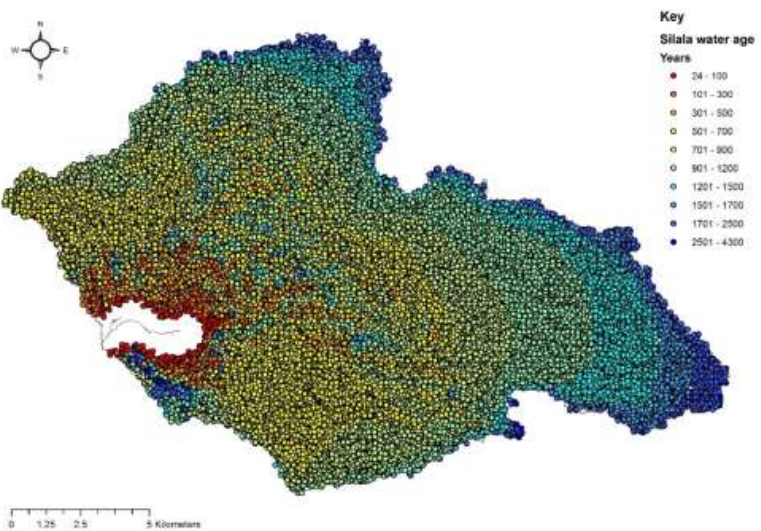


Figure B-8 Simulated map of particle travel time in the saturated zone

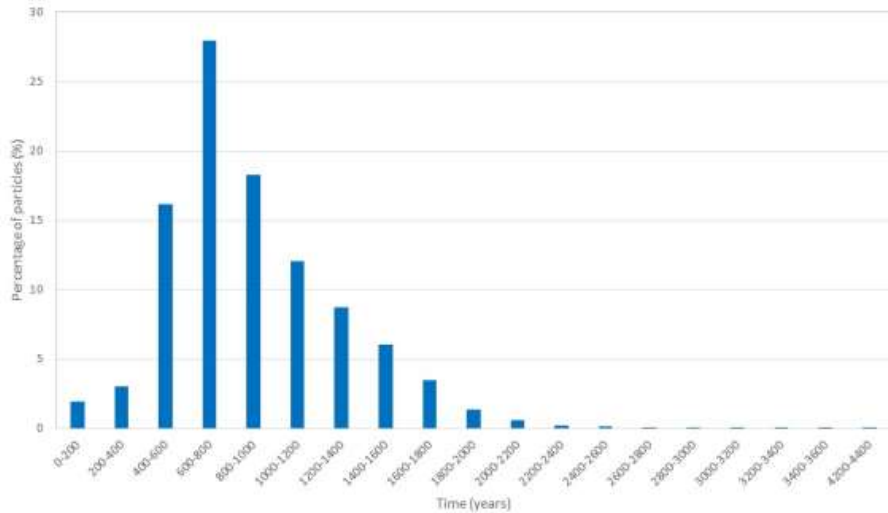


Figure B-9 Particle age distribution

Travel time in the unsaturated zone will add to the overall water age, particularly in the areas with volcanoes where the water table tends to be very deep, down to 1,000 m. The travel time in the unsaturated zone has been estimated based on a separate simple transport model run with a tracer source with a constant concentration applied at the top of a number of unsaturated zone columns scattered across the catchment. Four columns with different depths to the groundwater table were selected and travel times were found to be approximately 1 m/year. Combined with the modelled depth to the water table, this provides a very rough estimate of travel time through the unsaturated zone presented in Figure B-10. In the model, it has been assumed that the flow through the unsaturated zone takes place as matrix flow through a highly porous medium. Flow is more likely to be a combination of fracture and low permeable matrix flow at depth but as no information is available on the unsaturated zone properties, this could not be modelled at this time. The travel time in the unsaturated zone using this approach has been estimated to be between 5-50 years close to the wetland up to over 1,000 years below the volcanoes.

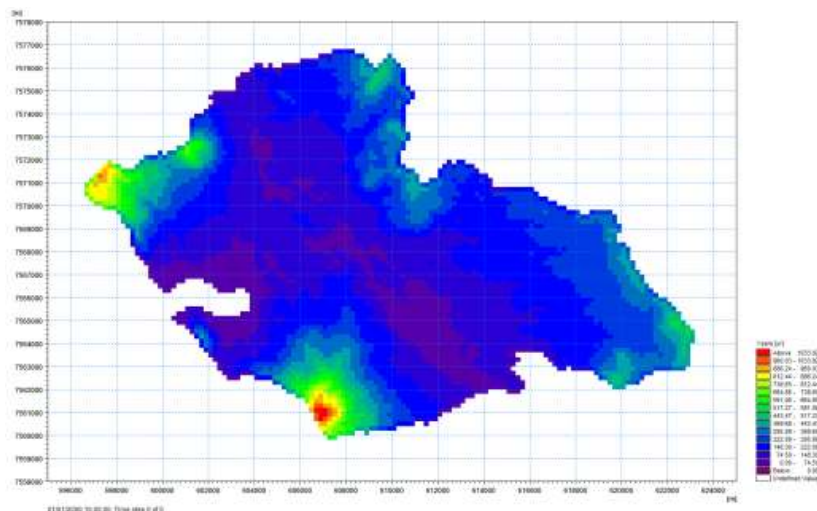


Figure B-10 Unsaturated travel time in years for the catchment based on simple transport model runs

Overall the total travel time from the analysis confirms fairly old water, over 1,000 years old on average. The thickness of the ignimbrite aquifer is unknown and could be more than the 250 m assumed in this assessment. A larger thickness of this main water-bearing layer would lead to a proportionally larger water age (assuming the unchanged groundwater gradients). However, even with a significant increase of the thickness of this layer, the model assessment would not be as large as 10,000 years, as indicated by the isotope analysis of the water from the wetland. Isotope dating is however uncertain and it is possible that some of the water feeding the wetlands is younger.





APPENDIX C

Measured surface water flows





C Measured flows

C.1 The surface water flow measurement program

Until the initiation of the surface water monitoring program under the present project, time series of flows in the Silala canals were only available at two locations, one at the old siltation chambers in Bolivia around 700m upstream of the border and another close to the border on the Chilean side.

These two continuous flow time series are of paramount importance for the assessment of the surface water discharge of the spring system at the border. However, the initial flow assessment (Reference 10) found that they contained significant uncertainty as to the magnitude of the flows in the Silala main canal.

Furthermore, the two series do not contain sufficient information to understand and quantify the processes in the various parts of the system. Such understanding is important to quantify how the canalisation and drainage of wetlands may have affected the natural flows at the border and to assess water requirements of a healthy natural wetland.

A consistent and mutually accepted flow assessment at the border will also be important if an agreement on fair sharing of the water resource between Bolivia and Chile.

To improve the accuracy of the existing series and to gain knowledge on the distributed flow contribution in the Silala Springs System, a surface flow measurement program¹⁸ (Reference 5) has been planned by DIREMAR, SENAMHI and DHI. The surface flow measurement program is based on field inspections to pin down the best suitable gauging locations. SENAMHI was contracted by DIREMAR to carry out the program, which was initiated in May 2017. The measurements include simultaneous canal and spring flow measurements, continuous flow records collected at weirs installed during 2017 at six new strategic locations (C1-C6) and at the existing permanent flume at the de-siltation chambers close to the Bolivian-Chilean border. At the latter location, the old automatic floater-based water level instrument has been supplemented with a new automatic pressure sensor similar to the ones used at the weirs (C1-C6).

This appendix describes the observations and findings derived from the data collected through this measurement program, as obtained up to October 15th, 2017. It is divided in three parts: "Simultaneous canal flow measurements", "Continuous canal flow measurements" from the new weirs and "Long term flow series" from the two permanent flumes.

Figure C-1 shows the flow measurement locations including springs (Ojo de Agua), simultaneous flow measurement locations (S-1 – S-21) and continuous flume flow gauges (C-1 – C-7). Prior to establishment of the flumes, simultaneous flow measurements have been carried out at both S-1 – S-21 locations and at the locations C-1 – C7 where the flumes were later installed or already existed (C7).

A preliminary assessment of measured flows was carried out as part of the Surface water report¹⁸. In the following sections the flow data provided by the SENAMHI for the period May–September 2017 and the permanent flumes flow records at the Bolivian and the Chilean side of the border are updated, presented and analysed.

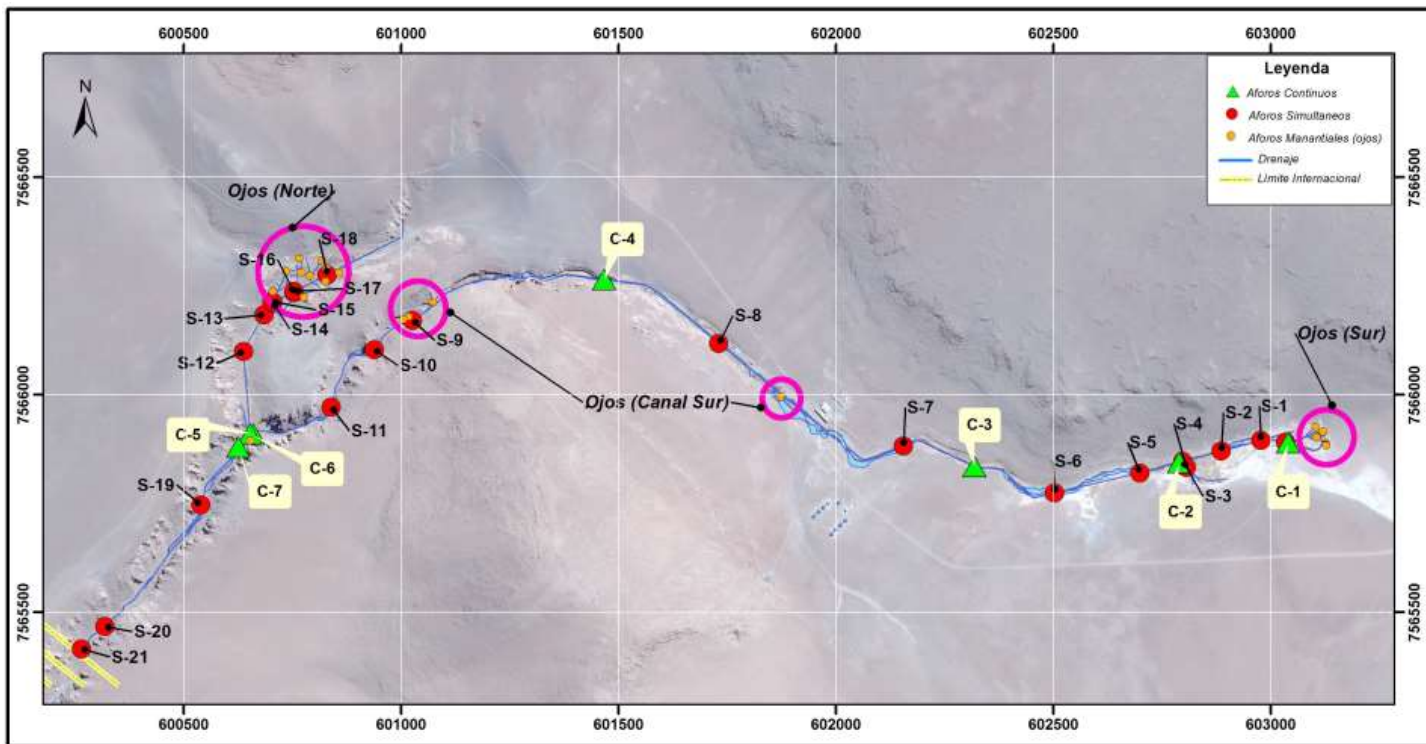


Figure C-1 Overview of flow measurement locations (SENAMHI)

C-4



C.2 Simultaneous canal flow data

The simultaneous flow measurement program is designed to provide a snapshot of flows in many points of the canal network. The measurements have been carried out, initially at a bi-weekly and later at a monthly frequency covering all locations within 2-3 days. Micro-propeller measurements in multiple points of the cross section provide a cross-sectional velocity profile, which is integrated to calculate the flow. The profile measurements have been carried out twice at each location to verify results and, if necessary, to take prompt on site action to prevent errors.

Figure C-1 shows the flow measured each location at ten different dates from May to September 2017. The average, minimum and maximum values have been calculated.

Figure C-2 shows minimum, maximum and mean simultaneous flow rates measured between May and September 2017.

Figure C-3 shows time series of simultaneous flows measured, i.e. ten values between May and September 2017. The C-7 flow ranging from 115 to 170 l/s is highlighted by a thicker line.

Figure C-4 to Figure C-6 show longitudinal flow profiles along the Southern Canal, the Northern Canal and the reach from C-7 to the border, respectively, for the ten dates measured.



Puntos de Aforo		May 6-7	May 12-14	May 15-17	May 27-30	June 3-4	June 12-14	June 20-22	July 24-25	Aug 25-27	Sep 25-27	Average	Min	Max	Std.dev
S-1, canal sur	S-1	25.80	33.00	32.50	29.05	31.55	29.10	29.15	31.75	27.45	26.45	29.58	25.80	33.00	2.41
C-1, canal sur	C-1	28.35	33.60	31.65	26.90	27.55	28.6	26.9	22.5	24.45	27.83	22.50	33.60	33.17	
S-2, canal sur	S-2	24.45	24.50	28.10	23.75	31.80	25.75	27.8	30.9	30.45	26.95	27.45	23.75	31.80	2.74
C-2, canal sur	C-2	47.05	46.90	36.90	28.85	33.20	33.65	35.3	37	31.5	36.71	28.85	47.05	6.00	
S-3, canal sur	S-3	34.95	28.10	31.05	34.30	30.05	32.25	32.85	28.5	25.35	30.82	25.35	34.95	2.96	
S-5, canal sur	S-5	36.10	38.30	30.30	30.45	31.00	32.90	30.9	29.9	26.4	34.45	32.07	26.40	38.30	3.26
S-6, canal sur	S-6	34.75	40.60	40.25	34.35	36.85	35.20	37.85	37.75	32.55	33.45	36.36	32.55	40.60	2.62
S-7, canal sur	S-7	42.95	35.70	39.70	28.90	33.50	31.00	34.1	35.5	33.9	36.15	35.14	28.90	42.95	3.80
S-8, canal sur	S-8	56.40	53.10	53.10	49.95	51.05	49.05	47.8	50.15	49.85	45.05	50.55	45.05	56.40	2.98
C-4, canal sur	C-4	70.35	58.80	61.90	62.50	57.35	58.3	66.6	48.65	50.7	59.46	48.65	70.35	65.4	
S-9, canal sur	S-9	88.45	107.05	89.35	78.65	83.65	83.75	92.3	83.7	81.65	87.62	78.85	107.05	7.93	
S-10, canal sur	S-10	115.40	111.65	114.95	113.80	106.30	106.85	107.4	104	110.6	112.15	110.31	104.00	115.40	3.76
S-11, canal sur	S-11	96.95	101.05	102.15	95.45	94.55	98.75	102.1	111.25	109.8	101.34	94.25	111.25	5.56	
C-5, canal sur	C-5	103.65	105.75	83.45	110.50	93.60	84.8	97.65	103.45	90.3	97.02	83.45	110.50	9.03	
C-7, canal principal	C-7	169.70	126.90	126.10	126.45	130.40	112.90	128.6	128.45	130.95	138.25	131.83	112.90	169.70	13.95
S-19, canal principal	S-19	214.85	209.15	163.85	143.90	149.95	156.1	148.35	152.05	155.05	165.92	143.90	214.85	25.22	
S-20, canal principal	S-20	167.80	194.15	149.70	157.55	141.55	157.1	175.4	152.95	157.1	161.48	141.55	194.15	14.77	
S-21, canal principal	S-21	179.45	169.30	147.15	156.60	148.45	155.55	173.25	141.55	141.43	156.96	141.30	179.45	13.24	
S-18, canal norte	S-18	6.15	6.20	7.05	4.85	5.60	3.95	4.55	3.8	4.9	5.23	3.80	7.05	1.03	
S-17, canal norte	S-17	23.40	28.40	27.10	25.65	24.10	25.75	22.4	23.8	25.2	25.09	22.40	28.40	1.78	
S-16, canal norte	S-16	15.75	14.85	10.30	11.40	13.25	12.2	12.05	9.85	10.6	12.25	9.85	15.75	1.92	
S-15, canal norte	S-15	49.15	54.80	39.70	34.25	30.35	30.5	41.5	33.3	33.3	38.58	30.35	54.80	8.09	
S-14, canal norte	S-14	11.00	11.10		8.90	10.90	10.7	9.9	11.15	12.85	10.81	8.90	12.85	1.05	
S-13, canal norte	S-13	38.95	46.75	41.35	37.90	51.90	46.9	57.85	34.55	45.4	44.62	34.55	57.85	6.89	
S-12, canal norte	S-12	53.40	58.15	51.35	46.60	52.30	52.45	53.35	51.05	50.45	52.12	46.80	58.15	2.88	
C-6, canal norte	C-6	62.65	63.85	60.40	55.15	53.85	56.65	65.35	42.5	52	56.93	42.50	65.35	6.74	

Table C-1 Table of simultaneous mean canal flow measurements (in l/s)

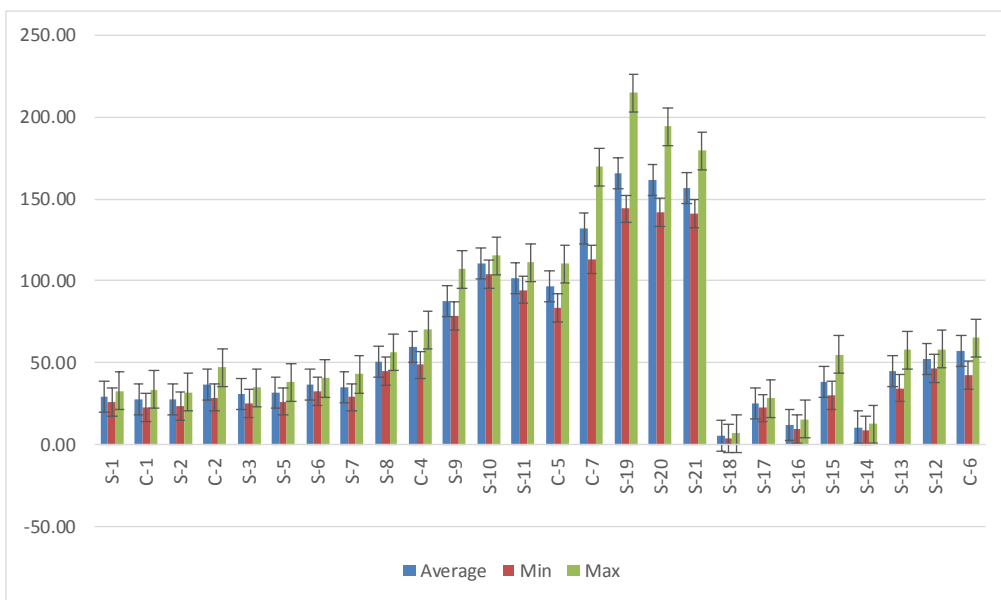


Figure C-2 Simultaneous flow measurements (Qmean, Qmin and Qmax in l/s)

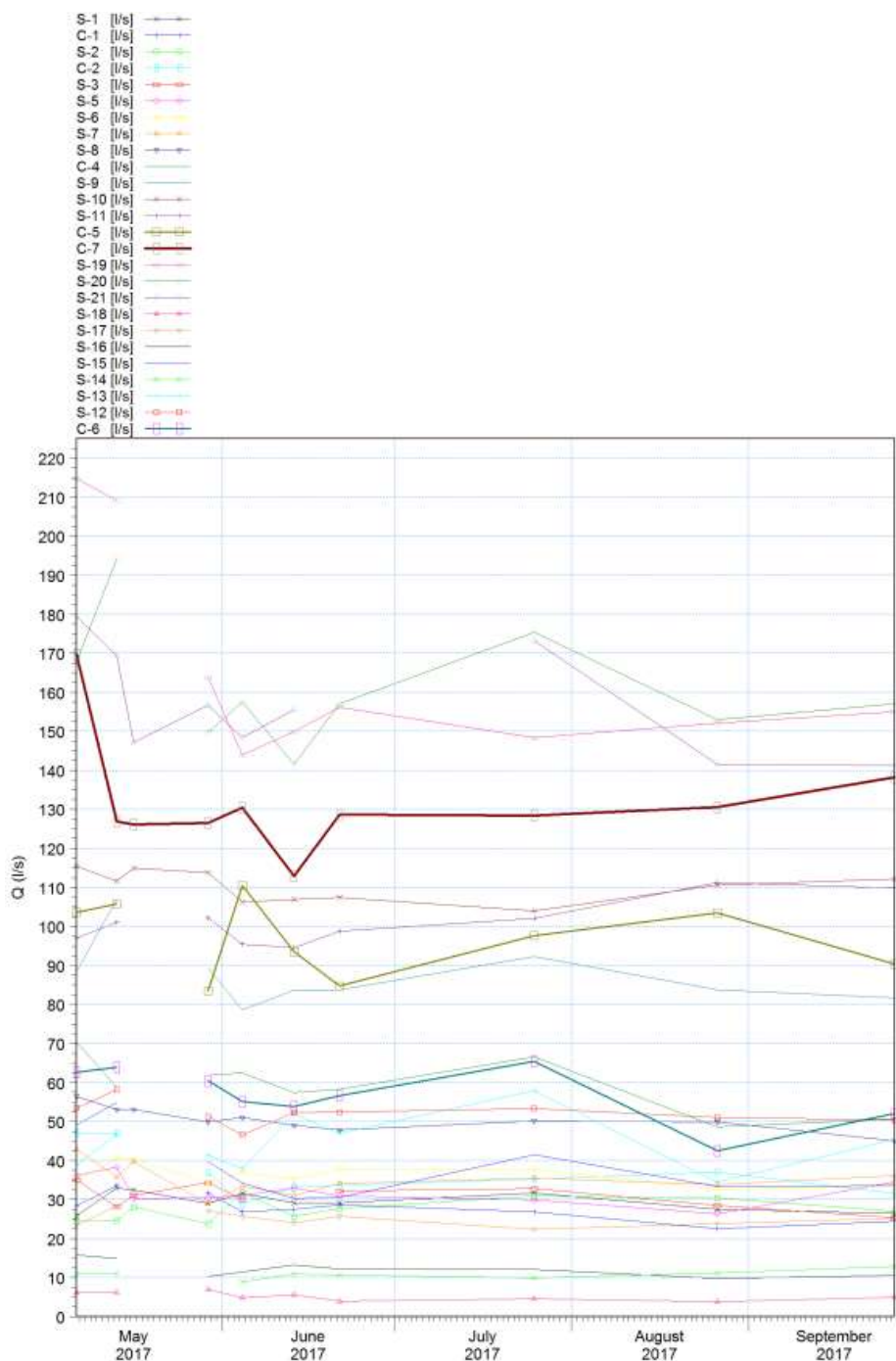


Figure C-3 Time series of flows (l/s)

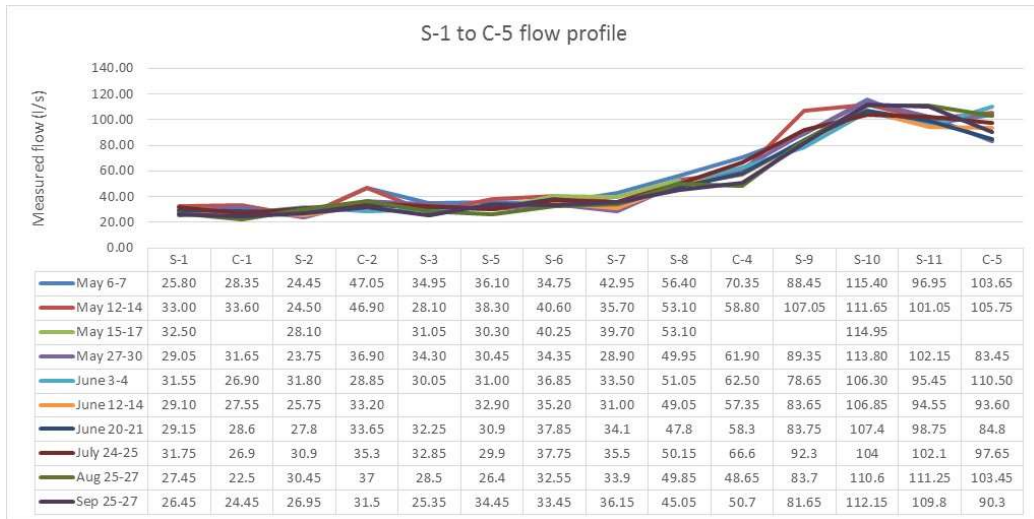


Figure C-4 Simultaneous flow profiles, Southern Canal (S-1 to C-5)



Figure C-5 Simultaneous flow profiles, Northern Canal (S-18 to C-6)

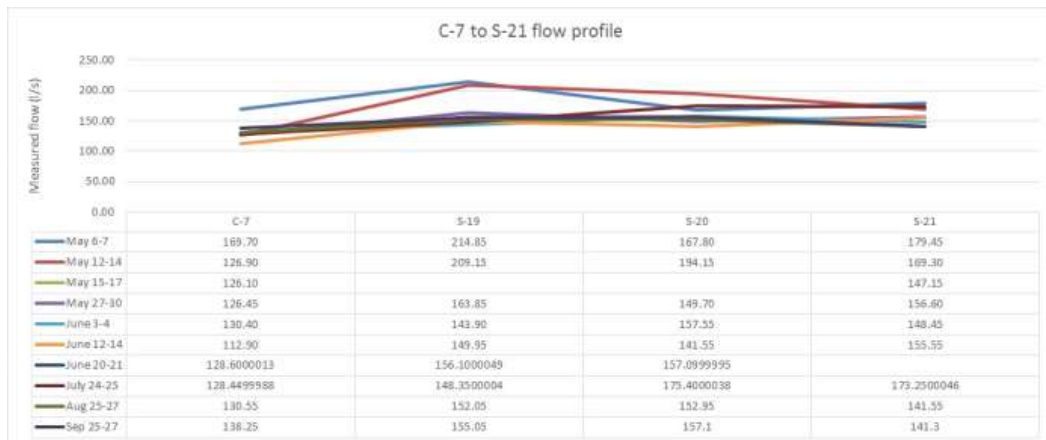


Figure C-6 Simultaneous flow profiles, permanent flume to border (C-7 to S-21)

Measured flows



Puntos de Aforo	May 9	May 14	May 27	May 31	June 5	June 16	June 22	June 27	aug-28	sep-28	Average	Min	Max	Std.dev.
OJO 1 SUR	3.9	4.2		4.0	3.9	3.7	4.1	5.6	4.1	4.5	4.2	3.7	5.6	0.5
OJO 2 SUR	3.0	2.4			2.8	3.2	2.0	2.7	2.0	1.2	2.4	1.2	3.2	0.6
OJO 3 SUR	3.5	3.5		3.1	3.0	2.8	2.8	3.8	2.9	3.3	3.2	2.8	3.8	0.3
OJO 4 SUR	2.5	2.1			2.2	2.5	2.4	2.4	2.2	2.2	2.3	2.1	2.5	0.1
OJO 5 SUR	1.3	1.7			0.9	0.6	0.6	0.8	0.6	0.4	0.9	0.4	1.7	0.4
OJO 6 SUR	8.0	5.0				4.6		4.4	5.3	4.8	5.4	4.4	8.0	1.2
OJO 22 SUR	4.6							2.8	2.0	2.3	2.9	2.0	4.6	1.0
OJO 22 SUR	4.5										4.5	4.5	4.5	0.0
OJO UNION 9-10-11 SUR	1.9	2.0		1.5	1.2	1.5	1.1	1.2	1.1	0.8	1.4	0.8	2.0	0.4
OJO UNION 9-10-11 SUR	1.6	1.6									1.6	1.6	1.6	0.0
OJO - 30 - 84 SUR	6.3	3.9						4.0	3.2	3.2	4.1	3.2	6.3	1.1
OJO - 30 - 84 SUR	6.4	3.9									5.1	3.9	6.4	1.2
OJO 31 SUR	3.5	3.8			3.5	3.8	3.2	1.8	4.4	2.7	3.3	1.8	4.4	0.7
OJO - 32 - A SUR	2.5	1.0									1.7	1.0	2.5	0.7
OJO - 32 - A SUR	2.4	1.0									1.7	1.0	2.4	0.7
OJO 32 SUR	6.2	3.6			3.0	3.9	3.7	2.0	3.8	1.9	3.5	1.9	6.2	1.3
OJO - 35 NORTE	1.6	2.6			1.4	1.5	1.4	1.4	1.9	1.5	1.7	1.4	2.6	0.4
OJO - 35 NORTE	2.3	2.7									2.5	2.3	2.7	0.2
OJO 37-38 NORTE	3.2	3.1			2.9	2.3	3.0	3.2	3.0	3.6	3.0	2.3	3.6	0.3
OJO - 41 NORTE	3.6	4.1		3.4		4.1					3.8	3.4	4.1	0.3
OJO 41 NORTE	3.6	4.1				4.1					3.9	3.6	4.1	0.2
OJO 46 NORTE	3.0	2.3		4.1	1.8	2.4	2.4	2.3	2.6	2.3	2.6	1.8	4.1	0.6
OJO 48 NORTE	1.3	1.2			0.9	1.2	1.2	0.7		1.0	1.1	0.7	1.3	0.2
OJO - 44 NORTE	8.1	8.6		9.0	9.2	9.6	9.8	9.7	9.9	9.3	9.2	8.1	9.9	0.6
OJO - 44 NORTE	9.1	8.7									8.9	8.7	9.1	0.2
OJO 49 SUR	2.0	1.8			2.1	1.8	1.8				1.9	1.8	2.1	0.1
OJO - 50	2.1	2.7									2.4	2.1	2.7	0.3
OJO 50	1.9	2.7			1.4						2.0	1.4	2.7	0.5
OJO 54, NORTE	4.5	5.2									4.8	4.5	5.2	0.4
OJO 59 NORTE	2.5	1.8		2.3	2.0	2.6	1.3	2.1	2.5	2.9	2.2	1.3	2.9	0.5
OJO - S7	1.4	1.8									1.6	1.4	1.8	0.2
OJO-S7	1.4	1.8									1.6	1.4	1.8	0.2
OJO 64 - SUR	3.7	4.3			5.3	5.0	3.4	3.5	6.1		4.5	3.4	6.1	1.0
Sum (l/s)	80.4	69.7	0.0	30.4	42.9	51.7	41.8	54.2	49.0	44.0	70.9			

Table C-2 Table of simultaneous spring flow measurements (in l/s)



C.3 Continuous canal flow data

C.3.1 The data collection campaign

Six new V-notch weirs were installed at strategic locations in the system and equipped with water level sensors (pressure transducers). Subsequently, discharge – water level relations were established during June- August 2017 by comparing different water levels with corresponding flows measured by propeller measurement in reliable cross sections downstream of each weirs.

Calibration was performed by controlling upstream flows and a number of corresponding values of flow and water level were measured covering the low to normal flow range at each site. For the low flow ranges, the flow was calculated by collecting the volume in a container for a period of time. For the higher flow ranges, micro propeller measurements were used. The rating curves were approximated by curve fitting to the set of water level and flow data.

The same type of water level sensor as used in the new weirs was installed at the existing flume at the old desilting chamber (station C7). Measurement of water levels at 15 minutes intervals were taken during the period late June to end of September 2017 and corresponding discharges calculated by SENAMHI who has been in charge of the measurement campaign.

C.3.2 The rationale of the campaign

The rationale of the collection of continuous flows at strategic locations are:

4. To determine the flow rate as exact as possible at strategic locations in the canals of the Silala Springs System.
5. To reveal the temporal variation of the flow rate
6. To evaluate the daily flow variations and to detect possible short-term impact of precipitation event. The daily variations are important to evaluate the simultaneous observation taken at more locations and may also open for an independent, although not isolated, evaluation of the evaporation rates
7. To ease the observation of possible surface water impacts from the planned borehole pump tests.

C.3.3 Observations on the received data

A time series of the received data are shown in Figure C-8 for the stations C1 to C4 representing the conditions in the southern wetland in Figure C-10 for the stations C4-C7 illustrating the flow contributions in the ravine and from the Northern wetland

The water levels have been registered every 15 minutes and the raw discharges calculated with the same frequency.

A rather constant pattern of daily flow variations, with the highest flows after midday and lowest flows during nights, are visible in all the flow series. Although the amplitudes of the flow variations vary from series to series and sometimes also significantly with time, all series shows a general pattern of rather small and periodic daily variations, superimposing a much larger and relatively constant base flow component.

Measured flows



Abrupt changes in the base flow values as well as the daily variations are also noted. To further illustrate these base flow changes, the series have been averaged on a daily basis and the most obvious measurement errors substituted with missing values as shown in Figure C-9.

Abrupt changes in the base flow levels occurs at several weirs at the end of June, around July 29th and August 24th. While the base flows during the period (from the start of records to the first abrupt change) seem to be relatively stable, it is decreasing and sometimes reaching a new constant level in most of the stations, before exerting a new upwards abrupt jump. No explanation or comments on this behavior have been given by SENAMHI.

The abrupt changes in base flow only allow to analyse the series in the two periods: 1 July – 28 July and 29 July – 23 Aug. In these two periods, the individual series are rather constant and the sum of the flows from the two main branches are within 4% of the observed confluence flow at the de-siltation chambers (C7). After August 23rd, the flows both in C6 (Northern Branch) expels spurious variations which are not observed in the neighboring weirs. The confluence flows are on average 18% higher than the observations at the de-siltation chambers.

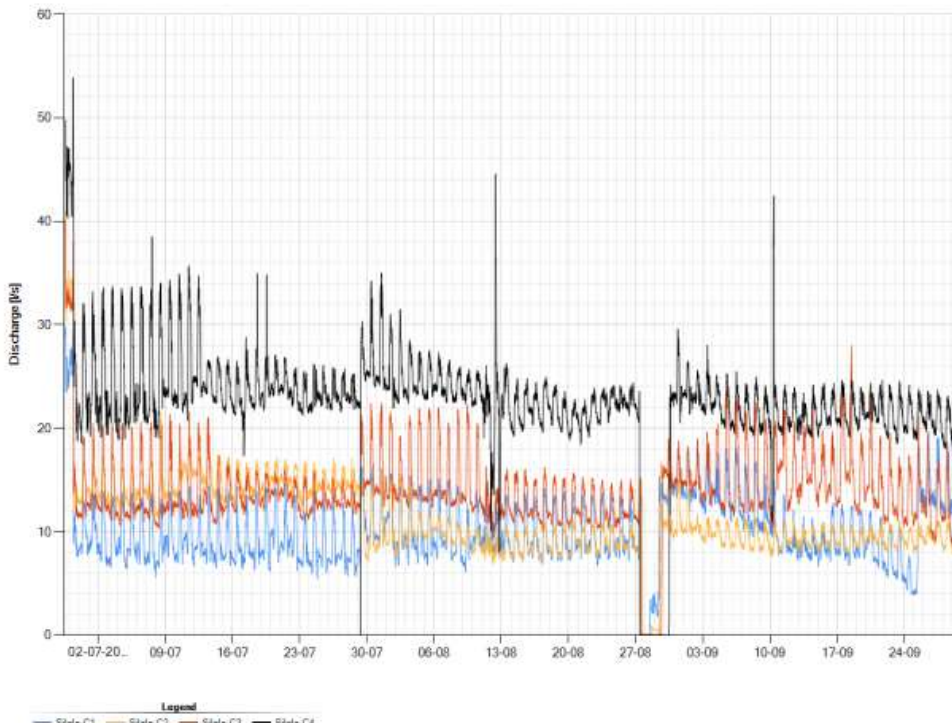


Figure C-7 Measured continuous flows in weirs C1-C4 located in the Southern wetland

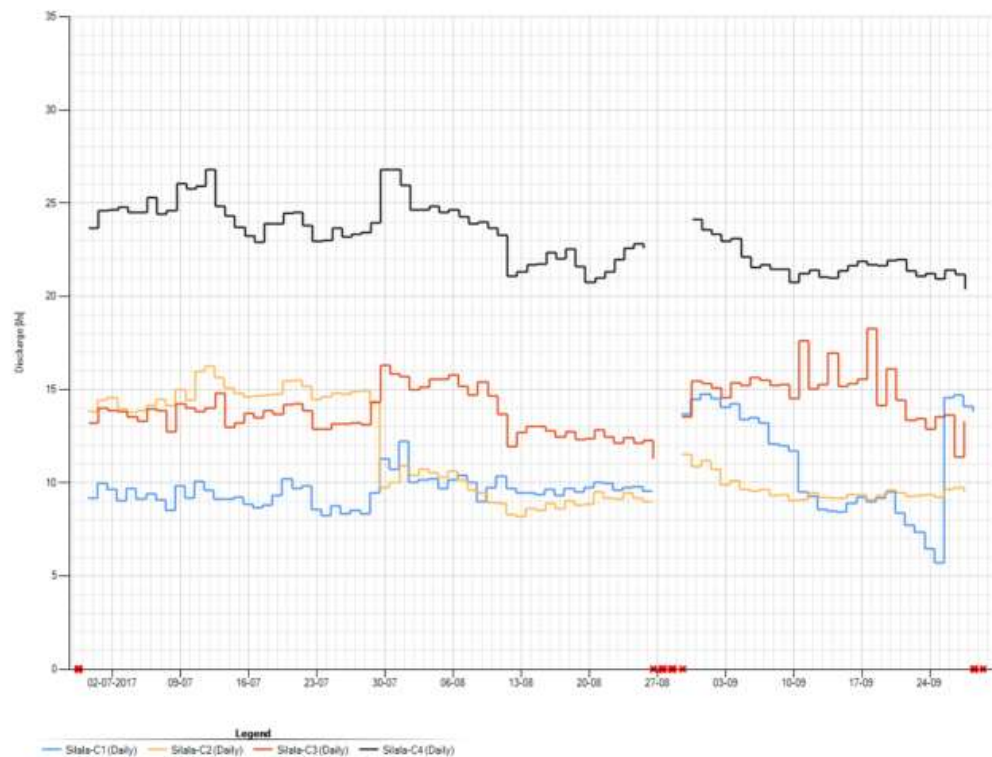


Figure C-8 Measured flows in weirs C1-C4 located in the Southern wetland averaged to daily values and with obviously spurious data replaced by missing values (red crosses)

Measured flows

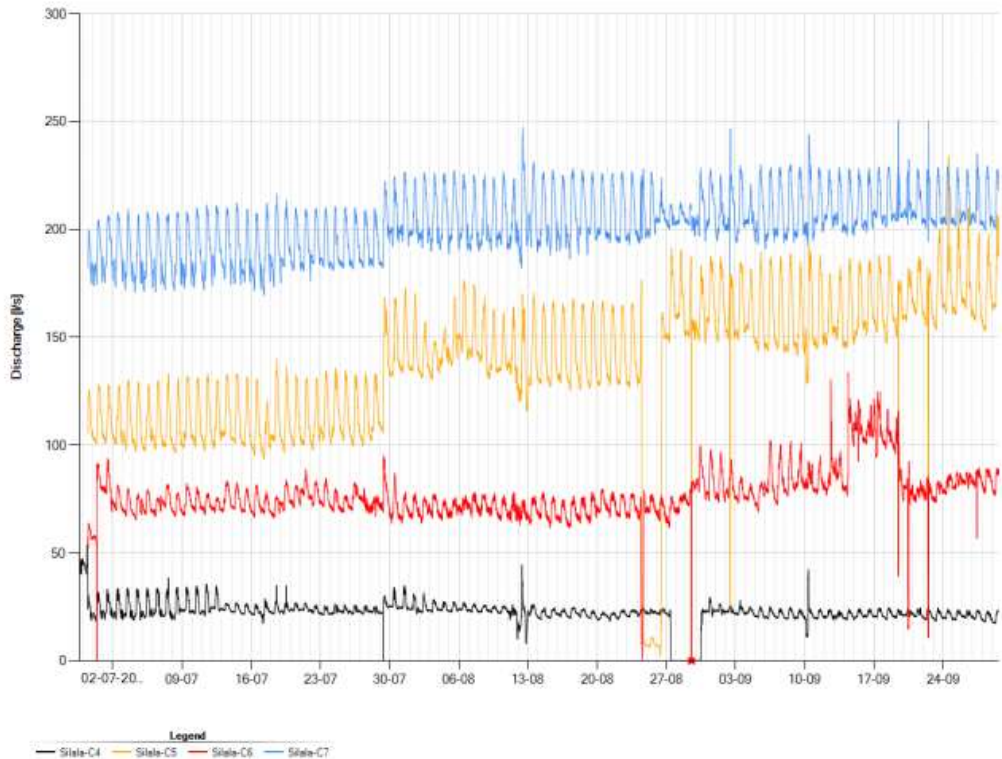


Figure C-9 Measured continuous flows in the weirs C4-C7 illustrating the flow contributions in through the ravine and from the Northern wetland.

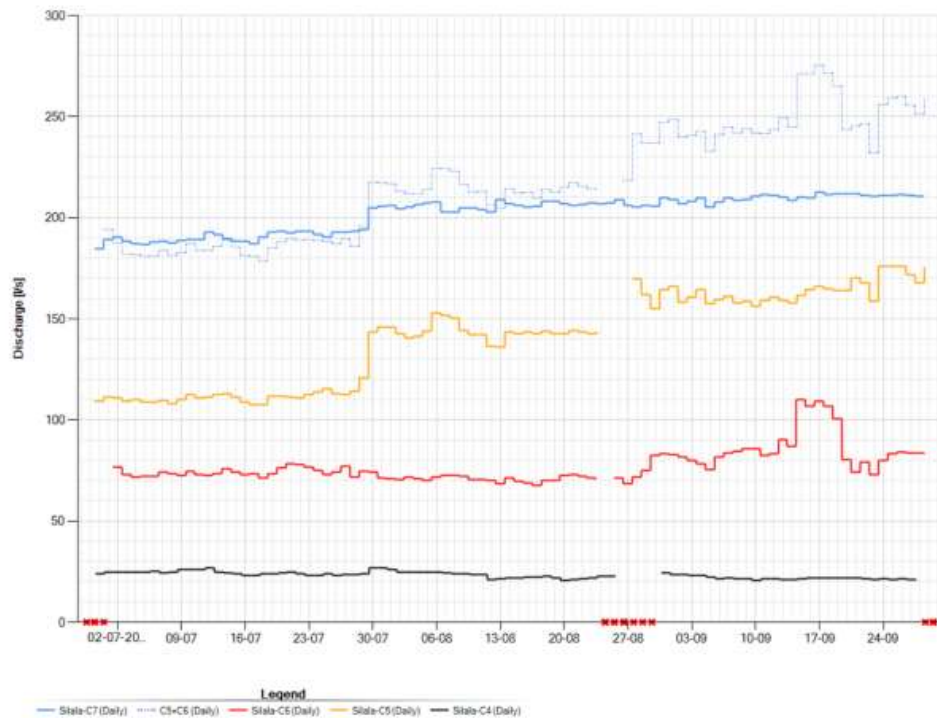


Figure C-10 Measured continuous flows in the weirs C4-C7 illustrating the flow contributions in through the ravine and from the Northern wetland averaged to daily values and with obviously spurious data replaced by missing values (red crosses)

C.3.4 Conclusions on the continuous flow data

All series shows a high base flow level, superimposed with a smaller periodic daily variation peaking around midday. In all the series, the base flow exhibits abrupt jumps at certain dates and sometimes trends in the intermediate periods. None of which can be assigned to climatic events and must therefore be due to the equipment.

The daily variations vary slightly in amplitude for C7, the permanent weir, where the variation over the day is 25-35 l/s. The daily variations cannot explain the spread in flows at the simultaneous measurements, which at C7 approximate 65 l/s. The flows peaks at midday at all stations and can therefore not be due to evaporation losses which peak at the same time. Hence, the daily variation must be assigned to freezing and thawing of the water in the wetlands.

For C5-C7, base flows seems rather consistent from 1-28 July and 29 July-23 Aug. The last period (24 Aug – 29 Sept) seems inconsistent with combined flows from C5 and C6, being 18% higher than the flows in C7. In the first two periods, this combined flow is within 4% of C7.

Measured flows



The data from the two periods confirms contributions from the Southern and Northern wetlands to be respectively ca. 60% and 40% of the confluence flow and that the flow contribution in the ravine between C4 and C5 is significant.

The most trustworthy period is deemed to be the one from 1 to 28 July 2017 where the records have the smallest trends and variations.

Location		C4	c5-c4	c5	c6	c5+c6	c7
Simultaneous	Average Flow (l/s)	60.6	38.1	98.7	57.6	156.3	131.8
Simultaneous	Fraction of (C5+C6)	0.39	0.24	0.63	0.37	1.00	0.84
Continuous Weirs	Average Flow (l/s) 01 Jul -> 28 Jul	24.3	87.0	111.3	74.1	185.4	190.4
Continuous Weirs	Fraction of (C5+C6) 01 Jul -> 28 Jul	0.13	0.47	0.60	0.40	1.00	1.03
Continuous Weirs	Average Flow (l/s) 29 Jul -> 23 Aug	23.2	120.4	143.6	70.9	214.5	205.8
Continuous Weirs	Fraction of (C5+C6) 29 Jul -> 23 Aug	0.11	0.56	0.67	0.33	1.00	0.96

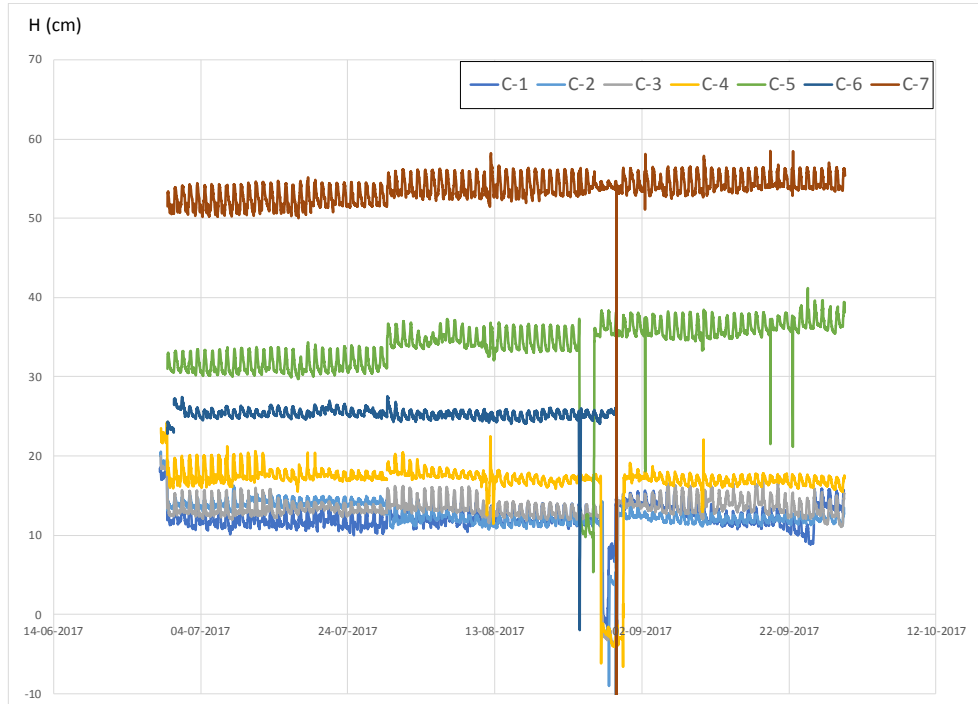


Figure C-11 Recorded water levels at the C-1 – C-7 flumes, July-September 2017 (SENAMHI)

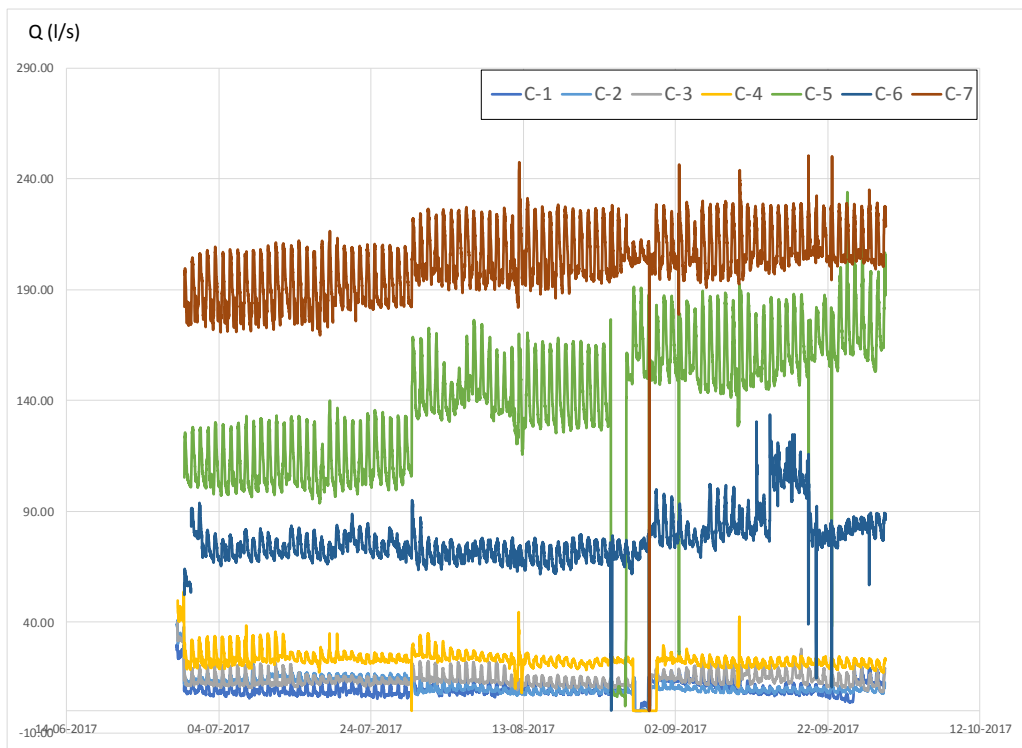


Figure C-12 Recorded flows at the C-1 – C-7 flumes, July-September 2017 (SENAMHI)

C.4 Permanent flume flow data

While qualitative descriptions of historical flows in the system are available from various sources (Reference 1, Reference 2, Reference 8, Reference 9 of the main report), long-term quantitative flow time series are only available at two locations, one at the old siltation chambers in Bolivia around 700m upstream of the border and another close to the border on the Chilean side.

While these continuous flow time series are of paramount importance for the study as information on the total outflow of the spring system as a whole, they do not contain sufficient information to understand and quantify the processes in the various parts of the system. Such understanding is important to quantify how the canalisation and drainage of wetlands may have affected the natural flows at the border and to assess water requirements of a healthy natural wetland.

The continuous flow series have therefore been supplemented by a number simultaneous propeller measurements of the canal flows at various locations and dates in the canal system upstream the border. This campaign has been intensified and streamlined during May and June 2017 to improve the basis for this flow assessment.

Measured flows



C.5 Long term flow series from Chile and Bolivia

Previous to the initiation of the intensive flow monitoring program, time series of the flows in the Silala primary canal were only available at two locations, one at the old siltation chambers in Bolivia around 700m upstream of the border and the other from Chile's Dirección General Del Agua (DGA), close to the border on the Chilean side. An initial assessment of the flows from the two series was made in the surface water report (Reference 10) based on the data available by mid-June 2017. The present section gives an update of the analyses accounting for the additional data available by October 15th, 2017.

The two series would be expected to measure almost the same flow rates. Even though some flow losses between the two stations have been detected by the simultaneous flow observations, as described in the previous section, the two series would be expected – as a minimum – to show the same long-term variation and to react in the same way to hydrological events.

Flow records for the flume at the siltation chambers (Bolivian Territory)

The gauging site is a flume in a rectangular concrete trench constructed along the old siltation chambers and equipped with a V-notch and automatic (electronic) water level registration by floater with resolution around one millimetre.



The canal is not expected to carry substantial peak flows from sudden runoff events and the station should therefore be almost ideal for measuring the flows in the canal. Water levels are measured both manually (two times a day) by the military personnel and automatically (hourly).

Each of the two water level series has been converted to flows by a formula relating specific water level observations to flows and are shown with different temporal resolution in Figure C-14, Figure C-15 and Figure C-16. Particularly for V-notch weirs, such as the one installed here, standard formulae are regarded to be quite precise with uncertainties as low as 3-5 %.

It is noted that the two series (shown as blue and yellow lines in the figures) are characterised by a large constant base flow of 160-200 l/s, which clearly indicates that the canal is fed almost entirely by groundwater springs. However, many abrupt jumps in the calculated flows, sometimes from one time step to the next, are also observed. These jumps originate from similar jumps in the water level observations and it has, in general, not been possible to relate them to hydrological events or seasonality.

Figure C-13 The existing flow-gauging flume at the old de-siltation chambers

Consequently, the uncertainty they introduce must be assigned to uncertainty in the observations, maybe due to jamming of the float or sediment deposition in the stilling canal. The uncertainty in the two series is substantial, in the order of 25-30 % of the flow rate. This might also point out to possible faults in the electronic registration.



It was therefore decided to double the water level sensor in the weir with a pressure sensor of the same type as those installed in the new continuous weirs and that temporally overlapping data from both sensors should be collected during 2017. Unfortunately, the old sensor has not been reporting since start of June 2017 so no overlapping period can be analysed.

Data from the new sensor is shown on the figures in dark green on the above-mentioned figures. Although the observations from the new pressure sensor start at the same level as the old automatic floater-based device (of mark: Thalimedes), the pressure sensor increases with time and has an abrupt jump around June 29th (at the same time as the other pressure sensors). The increasing trend continues after the jump resulting in flow values around 210 l/s by the end of September. This is still less than the sum of the two upstream weirs (C5 and C6) that should represent the same flow as the permanent flume in question (C7) and in the end of the period higher than measured manually (200l/s rather constantly after May 2017)

It is noteworthy that the upward trend in the observations from the new sensor is in contradiction with the observations from the DGA gauge in Chile, which shows an abrupt fall from around 200 l/s to less than 106 l/s in the same period.

So even the new sensors still leaves the flow assessment at the border with a significant uncertainty.

Flow records from Dirección General de Agua (DGA), Chile

The DGA records cover the period from 2001 to 2017, a much longer period than the Bolivian series.

The data is illustrated as red lines in Figure C-14, Figure C-15 and Figure C-16. This series also includes abrupt jumps and does not resolve the problem of uncertainty. The DGA series indicate flow values around 15-25 l/s lower than the Bolivian series in large parts of the observation period but from January to end July 2017, it measures the same flow levels in the order of 200 l/s. During August, the flow level decreases rapidly to a level in the order of 160 l/s contradicting the observations in Bolivia.

As described in the foregoing section, since the simultaneous measurements indicate flow to be slightly increasing from around 150 l/s at the siltation chambers to around 160l/s at the border, it seems unlikely that the generally lower values of the DGA series are due to flow losses between the two gauging sites.

Although both series shows significant variations over time, 125-225 l/s for the Chilean series and 160-210 for the shorter Bolivian series, neither shows clear sign of seasonality or a direct correlation with local rainfall.

Measured flows

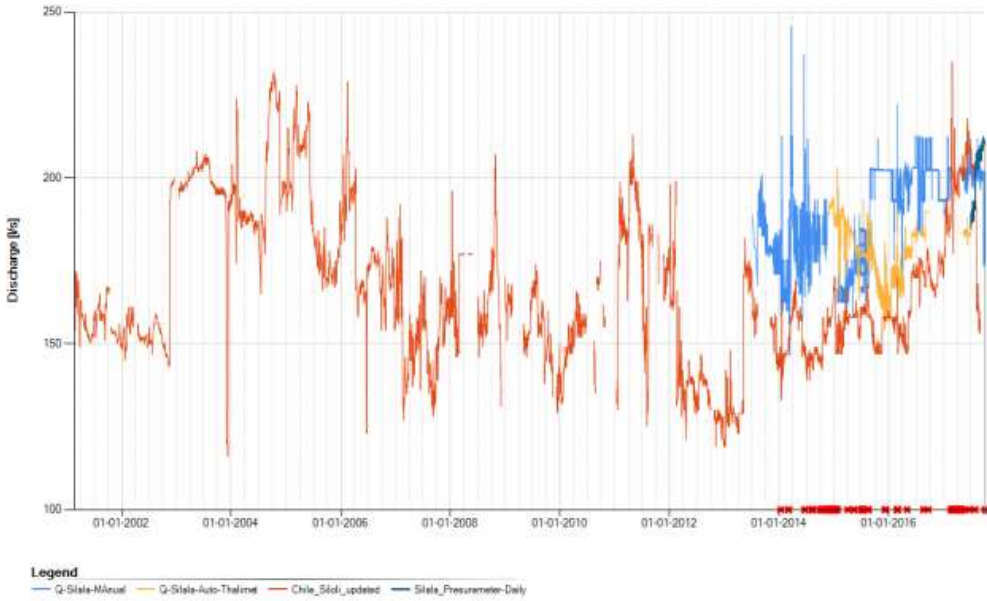


Figure C-14 Long-term series of Silala flows close to border In Chile and at the desiltingation chambers and at DGA's Siloli Station in Chile close to the border upstream of the Fcab offtake

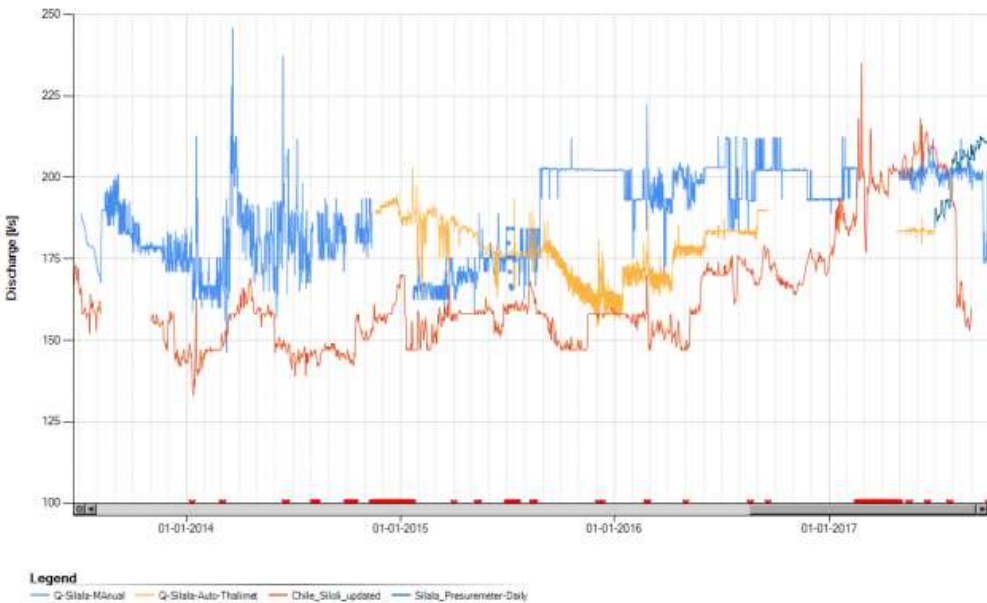


Figure C-15 Long-term series of Silala flows close to border In Chile and at the desiltingation chambers and DGA's Siloli Station in Chile close to the border upstream of the Fcab offtake. Data after 2013



Figure C-16

Long-term series of Silala flows close to border In Chile and at the desiltation chambers and at DGA's Siloli Station in Chile Close to the border upstream of the Fcab offtake. Data from 2017.

Annex XVI

SERNAGEOMIN (National Geology and Mining Service), 2019.
*A Brief Review of the Geology presented in Annexes of the
Rejoinder of the Plurinational State of Bolivia*



A BRIEF REVIEW OF THE GEOLOGY PRESENTED IN ANNEXES OF THE REJOINDER OF THE PLURINATIONAL STATE OF BOLIVIA

Nicolás Blanco P. (MSc)

Geologist Project Manager of the Regional Geology Unit of the Department of Basic
Geology

Edmundo Polanco V. (DSc)

Project Geologist of the Regional Geology Unit of the Department of Basic
Geology

Jorge Vivallos C. (MSc)

Geophysical Unit Manager of the Geophysic Unit of the Department of Basic
Geology

August 2019

GLOSSARY

This glossary of geologic terms is based on the glossary in Earth: An Introduction to Geologic Change, by S. Judson and S.M. Richardson (Englewood Cliffs, NJ, Prentice Hall, 1995). Where possible, definitions conform generally, and in some cases specifically, to definitions given in Robert L. Bates and Julia A. Jackson (editors), Glossary of Geology, 3rd ed., American Geological Institute, Alexandria, Virginia, 1987. Additionally, used the bibliography of Le Maitre (2002) and Bull and McPhie (2007) for the specific terms.

$^{39}\text{Ar}/^{40}\text{Ar}$ method: A different method that was invented to supersede K/Ar method, to be more accurate.

Amphibole: Any of a group of dark green to black mineral often found in igneous rocks that contain calcium, sodium, magnesium, aluminum, or iron ions or a combination of them.

Andesite: A fine-grained volcanic rock of intermediate composition, consisting largely of plagioclase and one or more mafic minerals.

Assemblage: The collection of minerals that characterize a rock or a facies.

Basalt: A dark colored extrusive igneous rock composed chiefly of calcium plagioclase and pyroxene. Extrusive equivalent of gabbro, underlies the ocean basins and comprises oceanic crust.

Biotite: A generally black or dark green form of mica that is a constituent of crystalline rocks and consists of a silicate of iron, magnesium, potassium, and aluminium with excellent cleavage.

Caldera: A large, basin-shaped volcanic depression, more or less circular in form. Typically steep-sided, found at the summit of a shield volcano.

Cenozoic: Geological Era that meaning "new life", is the current and most recent of the three Phanerozoic geological eras, following the Mesozoic Era and extending from 66 million years ago to the present day.

Conformable: Lying parallel to, rather than cutting across surrounding strata.

Crystal: The multi-sided form of a mineral, bounded by planar growth surfaces, that is the outward expression of the ordered arrangement of atoms within it.

Debris flow: Fast-moving, turbulent mass movement with a high content of both water and rock debris. The more rapid debris flows rival the speed of rock slides.

Devonian: A geologic period and system of the Paleozoic, spanning 60 million years from the end of the Silurian, 419.2 million years ago (Mya), to the beginning of the Carboniferous, 358.9 Ma.

Dextral fault (right lateral-fault): The sense of displacement in strike-slip fault zones where one block is displaced to the right of the block from which the observation is made.

Diaclase: Planar discontinuities involving no relative displacement of the adjacent blocks.

Dome: An uplift or anticlinal structure, roughly circular in its outcrop exposure, in which beds dip gently away from the center in all directions.

Eutaxitic texture: Bedding-parallel alignment of fiamme in welded ignimbrite (see Bull and McPhie, 2007).

Extrusive: Pertaining to igneous rocks or features formed from lava released on the Earth's surface.

Fault: The fracture or surface along which rock units break apart or rupture, and along which there has clearly been movement of the rock on either side. A fault plane can be paper-thin or it can be a zone, metres wide.

Fiamme: Aligned, "flame-like" lenses found in welded ignimbrite (see Bull and McPhie, 2007).

Hanging wall block: The body of rock that lies above an inclined fault plane.

Hercynian: A geologic mountain-building event caused by Late Paleozoic continental collision between Euramerica (Laurussia) and Gondwana to form the supercontinent of Pangaea.

Igneous rock: A rock that has crystallized from a molten state.

Joint: A surface of fracture in a rock, without displacement parallel to the fracture.

Lava: Molten rock that flows at the Earth's surface.

Magma: Molten rock, containing dissolved gases and suspended solid particles. At the Earth's surface, magma is known as lava.

Mesozoic: An interval of geological time from about 252 to 66 million years ago. It is also called the Age of Reptiles and the Age of Conifers.

Mineral: A naturally occurring inorganic solid that has a well-defined chemical composition and in which atoms are arranged in an ordered fashion.

nanoTesla (nT): Unit of measurement of magnetic field strength; $T = \text{Tesla}$ ($\text{Maxwell} / \text{cm}^2$), and $nT = 10^{-9}\text{T}$).

Normal fault: A geological fault where the hanging wall block has moved downwards relative to the foot wall block.

Oligocene: A geologic epoch of the Paleogene Period and extends from about 33.9 million to 23 million years before the present (33.9 ± 0.1 to 23.03 ± 0.05 Ma).

Olivine: A group of high temperature, dark magnesium iron silicate mineral.

Onlap: The termination of shallowly dipping, younger strata against more steeply dipping, older strata.

Ordovician: A geologic period and system, the second of six periods of the Paleozoic Era. The Ordovician spans 41.2 million years from the end of the Cambrian Period 485.4 Ma to the start of the Silurian Period 443.8 Ma.

Petrography: A branch of petrology that focuses on detailed descriptions of rocks.

Pyroclastic: Pertaining to clastic material formed by volcanic explosion or aerial expulsion from a volcanic vent.

Pyroclastic flow: A dense, hot (sometimes incandescent) cloud of volcanic ash and gas produced in a Pelean eruption.

Pyroxene: Any of a group of igneous-rock-forming silicate minerals of black color, that contain calcium, sodium, magnesium, iron, or aluminum.

Reverse fault: A dip-slip fault on which the hanging wall block is offset upward relative to the foot wall block.

Rock: An aggregate of one or more minerals in varying proportions.

Salt diapir: Type of geologic intrusion in which a more mobile and ductily deformable material (salt) is forced into brittle overlying rocks.

Silica: Silicon dioxide (SiO_2) as a pure crystalline substance makes up quartz and related forms such as flint and chalcedony. More generally, silica is the basic chemical constituent common to all silicate minerals and magmas.

Silurian: A spanning 24.6 million years from the end of the Period, at 443.8 Ma, to the beginning of the Period, 419.2 Ma.

Structural domain: A portion of land, a geographically delimited volume with a longitude, latitude and height, a set of lithologies, kinematically related and delimited by a set of major structures (faults) with similar structural characteristics.

Sinistral fault (left lateral-fault): The sense of displacement in strike-slip fault zones where one block is displaced to the left of the block from which the observation is made.

Structural Geology: Structural Geology aims to characterise deformation structures (geometry), to characterize flow paths followed by particles during deformation (kinematics), and to infer the direction and magnitude of the forces involved in driving deformation (dynamics).

Structural model: A self-consistent framework providing a coherent explanation for the observed facts and allows to make verifiable predictions. A model is proven wrong if key predictions are not verified.

Synsedimentary: That forms or grows within a sediment during sedimentation.

TAS: A binary diagram (“Total Alkali versus Silica”) of the content of silica (axis X) and content of total alkali (oxides of sodium and potassium) (axis Y) recommended for the classification of the volcanic rocks.

Tectonics: A general term that refers to the large-scale movements and deformation of the Earth’s crust.

Tertiary: Geological Period widely used, but obsolete term for the geologic period from 66 to 2.6 Ma.

Texture: The general appearance of a rock as shown by the size, shape, and arrangement of the materials composing it.

Tuff: A general term for all consolidated pyroclastic rock. Not to be confused with tufa.

Unconformity: Cutting across surrounding strata.

Vitrophyre: A term for variety of porphyry in which the groundmass is glassy. Also applied to the basal portions of many welded ignimbrites (see Le Maitre, 2002).

Vesicular: A textural term applied to an igneous rock containing abundant vesicles, formed by the expansion of gases initially dissolved in the lava.

Volcanic ash: The dust-sized, sharp-edged, glassy particles resulting from an explosive volcanic eruption.

Volcano: A vent in the surface of the Earth, from which lava, ash, and gases erupt, forming a structure that is roughly conical.

Welded tuff: A pyroclastic rock in which glassy clasts have been fused by the combination of the heat retained by the clasts, the weight of overlying material, and hot gases.

σ_1 : The state of major or main tension acting on a material point.

TABLE OF CONTENTS

1.	INTRODUCTION	1
2.	STRATIGRAPHY AND GEOLOGICAL MAPPING OF BOLIVIA	2
2.1	Bolivian stratigraphy.....	3
2.1.1	Observations	4
2.2	Bolivian Petrography	11
2.2.1	Observations	13
3.	STRUCTURAL GEOLOGY	16
3.1	Bolivian Structural Interpretation	16
3.2	Analysis of Bolivian structural data.....	17
3.2.1	The “Silala Fault”	18
3.2.2	The “Silala-Llancor Lineament”	25
3.2.3	Conclusions	30
3.3	Chile’s interpretation of the geological deformation in the Silala River area	33
3.3.1	The Uyuni-Khenayani Fault System	35
3.3.2	Ratio of deformation and crustal depth	38
4.	CONCLUSIONS.....	40
5.	ACKNOWLEDGEMENTS	43
6.	REFERENCES.....	44

APPENDIX A

APPENDIX B

Annex XVI

1. INTRODUCTION

On 15 May 2019 Bolivia submitted to the International Court of Justice (ICJ) the Rejoinder of the Plurinational State of Bolivia (BR) in the Dispute over the Status and Use of the Waters of the Silala (Chile v. Bolivia). In this context, the National Director of the Dirección Nacional de Fronteras y Límites del Estado (DIFROL) of the Ministry of Foreign Affairs of Chile, Mrs. Ximena Fuentes, asked SERNAGEOMIN for its technical opinion of the geological content of the Rejoinder of Bolivia.

A major problem for the analysis of the several documents annexed to the BR that concern the geology of the Silala River area is that the quality of the Bolivian geological information is in many cases poor, inconsistent and confusing and is not adequate, in our opinion, to support the geological conclusions determined by Bolivian geologists.

This report discusses the validity of some of the geological statements, radiometric dates and assumptions made by Bolivian geologists in their reports, which caused them to arrive at their interpretations of the stratigraphy, rock petrography and structural geology. The geological understanding of the Silala Basin is fundamental to understanding the hydrogeology of the region and developing a conceptual model of groundwater flow to the Bolivian wetland springs and unseen groundwater flow across the international border into Chile.

This report is based on study and review of the following documents that were presented with the BR:

1. Annex 23.5: F. Urquidi, “Technical analysis of geological, hydrological, hydrogeological and hydrochemical surveys completed for the Silala water system”, June 2018. (BR, Vol. 3, pp. 233-332).
2. Annex 23.5, Appendix a: SERGEOMIN (National Service of Geology and Mining), Study of the Geology, Hydrology, Hydrogeology and Environment of the Area of the Silala Springs, June 2000-2001, Final Edition 2003. (BR, Vol. 3, pp. 333-401).

3. Annex 23.5, Appendix b: SERGEOMIN, “Structural Geological Mapping of the Area Surrounding the Silala Springs”, September 2017. (BR, Vol. 4, pp. 5-136).¹
4. Annex 23.5, Appendix c: Tomás Frías Autonomous University, (TFAU), “Hydrogeological Characterization of the Silala Springs”, 2018. (BR, Vol. 4, pp. 137-462).
5. Annex 24: DHI, “Analysis and assessment of Chile’s reply to Bolivia’s counter-claims on the Silala Case”, March 2019. (BR, Vol. 5, pp. 5-46).

The main aims of the review were to establish the underpinning geological science behind the Bolivian experts’ interpretation of the stratigraphy of the geological succession and the ages of the deposits in the area of the Silala River and ravine in Bolivia as well as the geological structure, including the evidence for the geological faults that have been interpreted as existing in the area. The stratigraphy and geological structure have been used to underpin an interpretation of the hydrogeology of the area, develop a conceptual understanding of groundwater flow and hence construct a numerical model of the hydrology and hydrogeology of the Silala wetlands and springs, referred to later as Bofedales Norte (Cajones) and Bofedales Sur (Orientales).

2. STRATIGRAPHY AND GEOLOGICAL MAPPING OF BOLIVIA

The stratigraphy presented by Bolivia in the technical geological annexes, either in maps or in stratigraphic columns, is inconsistent with the geological units defined in Chile by Chilean geologists and contains internal inconsistencies with Bolivia’s own data and maps presented in the annexes of the Bolivian Rejoinder.

¹ The SERGEOMIN, 2017 report, including annexes C and D, was submitted by Bolivia on 22 November 2018, in response to Chile’s data request dated 5 November 2018. Bolivia resubmitted the SERGEOMIN, 2017 report with its Rejoinder, but this time only the first two (out of 95) pages of Annex C were included and Annex D was excluded entirely. Hence, the references contained in the present report to Annex C and Annex D to SERGEOMIN, 2017, refer to annexes C and D as filed on 22 November 2018. For the convenience of the Court, Annex C to SERGEOMIN, 2017 is resubmitted as Appendix A and Annex D to SERGEOMIN, 2017 is resubmitted as Appendix B of the present report.

The following provides a series of observations on the Bolivian stratigraphy, followed by a series of observations on Bolivian petrography:

2.1 Bolivian stratigraphy

The unit “Silala Ignimbrite” (Bolivian name, hereinafter “Bol”), of dacitic-andesitic composition, is assigned to the Upper Miocene (7.8-6.6 Ma) (BR, Vol. 3, p. 248; BR, Vol. 4, pp. 39, 43 and 46) and Bolivian geologists affirm that it constitutes the regional basement (BR, Vol. 4, pp. 39, 125 and 148). According to the geological maps presented by Bolivia (BR, Vol. 3, p. 245; BR, Vol. 4, pp. 113-115) for the Silala Ignimbrites (Bol) there is an age of 7.8 ± 0.3 Ma obtained from a sample located south of Bofedales Norte (Cajones) (BR, Vol. 4, pp. 113-115).

Table 1 summarizes the stratigraphy of the Silala Ignimbrites (Bol) unit, with the ages indicated for each subunit and the differences between the descriptions among the different studies conducted by Bolivia.

References	SERGEOMIN (2017)	TFAU (2018)	Observations
Annex	23.5b	23.5c	
Silala Ignimbrites (Bol)	Silala Ignimbrite 3 (Nis-3)	Dacitic Ignimbrites with Na-Plagioclase	6.6 ± 0.5 Ma
	Debris flow (Nfd2)		
	Silala Ignimbrite 2 (Nis-2)	Dacitic Ignimbrite with Andesitic Clast	
	Crystal vitreous tuff (Ntcv)		
	Silala Ignimbrites 1	Hypocrystalline Dacitic Ignimbrites	correlation with 7.8 ± 0.3 Ma
	Debris flow 1 (Nfd1)		

Table 1. Summary of the stratigraphy of the Silala Ignimbrites (Bol) of Annex 23.5b (BR, Vol. 4, pp. 44-51) and Annex 23.5c (BR, Vol. 4, pp. 157-159) documents.

2.1.1 Observations

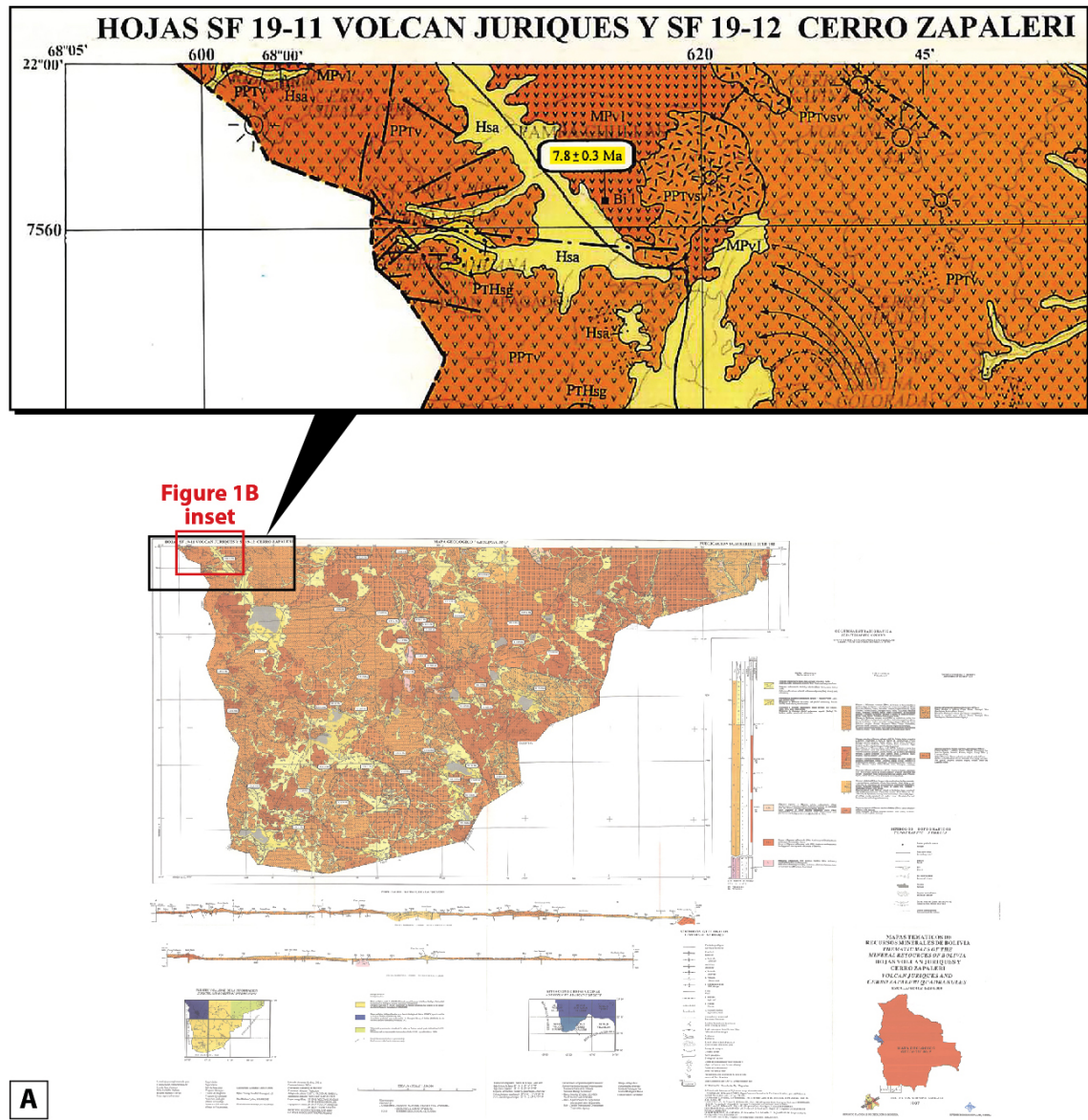
The so-called Silala Ignimbrites (Bol) correspond to several pyroclastic flows of contrasting chemical composition, radiometric age and stratigraphic position. In Annex 23.5c (BR, Vol. 4, pp. 157-160) the Silala Ignimbrites (Bol) succession is reported to have three units (Table 1), from the oldest to youngest: Dacitic-Hypocrystalline Ignimbrite, Dacitic ignimbrite with andesitic clasts and Dacitic Ignimbrites (with Na plagioclase). The Dacitic ignimbrite with andesitic clasts is important because they “[...] pertain to the first Inacaliri volcanic event” (BR, Vol. 4, p. 158) and are the source of the andesitic composition. However, since the age of the Inacaliri volcano lavas is 5.84 ± 0.09 Ma (Almendras et al., 2002) the Dacitic Ignimbrite with andesitic clasts must be younger, indicating that Bolivia’s age of the overlying Dacitic Ignimbrite with Na Plagioclase (6.6 ± 0.5 Ma) must be incorrect.

On the basis of our field observations in Chile, photointerpretation of satellite images and observation of photographs in annexes of Bolivian Rejoinder, it is clearly observed that the unit of the pyroclastic flow that crops out along the course of the Silala River in Chile, corresponding to the Silala Ignimbrite (Chilean name, herein after Chi) can be traced with complete confidence in the continuity of outcrop beyond the international border and to the Bofedales Sur (Orientales) in Bolivia. This deposit corresponds to several flow units, of andesitic composition, which as a whole constitutes a single cooling unit. In addition, it includes several slag fluxes, with centimetre to decimetre sized fragments of vesicular andesitic slag, which according to the Bolivian geology corresponds to the Debris Flows 1 and 2 units (BR, Vol. 3, pp. 250-251; BR, Vol. 4, pp. 44 and 49). The Silala Ignimbrite (Chi) is from the Lower Pleistocene and was dated at 1.61 ± 0.068 Ma ($^{40}\text{Ar}/^{39}\text{Ar}$ in plagioclase; Blanco and Polanco, 2018). This is significantly younger than the ages of 7.8 ± 0.3 Ma and 6.6 ± 0.5 Ma assigned by Bolivia to the so-called Silala Ignimbrites (Bol).

The age of 7.8 Ma for the Silala Ignimbrites (Bol) comes from a regional context and has been extrapolated to this location (BR, Vol. 4, p. 149), near the “confluencia” (confluence in English) area of the Cajones and Orientales ravines.

In fact, in the regional geological map of the Volcán Juriques and Cerro Zapaleri area, scale 1:250,000 (Ríos et al., 1997) an age of 7.8 ± 0.3 Ma (K-Ar in biotite) is attributed to Baker and Francis (1978), and located on that map 16.5 km SE of Bofedales Norte (Cajones), in an ignimbrite field (Figure 1A). However, according to the original work of Baker and Francis (1978), this age corresponds to andesitic lavas located 8 km E of the hill Silala Grande (sample B51). On the 2017 map found in BR, Vol. 4. p. 115, this age is correctly located in the lava of the La Apacheta-Cerro Chico hills (Figure 1B, Age 1). According to this last map, a large part of this field of ignimbrites corresponds to the unit “Tobas Pastos Grandes” (Ntpg), dated at 3.2 ± 0.4 Ma (biotite) (Figure 1B Age 2). From this discussion it is clear that there is considerable inconsistency between the maps presented in the Bolivian Rejoinder and an erroneous interpretation of the date for the Silala Ignimbrites (Bol) has been made.

On the other hand, 6.5 km E of Bofedales Sur (Orientales), an age of 6.6 ± 0.5 Ma is presented for the unit “Silala Ignimbrite 3” (Nis-3) (biotite, BR, Vol. 4, p. 115) (Figure 1B Age 3). However, to the ENE of Bofedales Sur (Orientales), it can be seen in Figure 2 (prepared by the authors of this report using satellite imagery) that the Silala Ignimbrite (Chi) lies under the 1.48 Ma andesitic lava (Figure 1B, Age 4) flow and this deposit is in unconformable contact (*onlap*) with the Silala Ignimbrite 3 (Nis-3) (Bol), which is the uppermost ignimbrite unit described by the Bolivian geologists. This is quite clearly not the youngest ignimbrite in the sequence because the Silala Ignimbrite (Chi) overlies this sub-unit, and as already shown (see above) the age of 6.6 Ma must be incorrect. The Silala Ignimbrite (Chi) is not recognised in any Bolivian maps or SERGEOMIN reports.



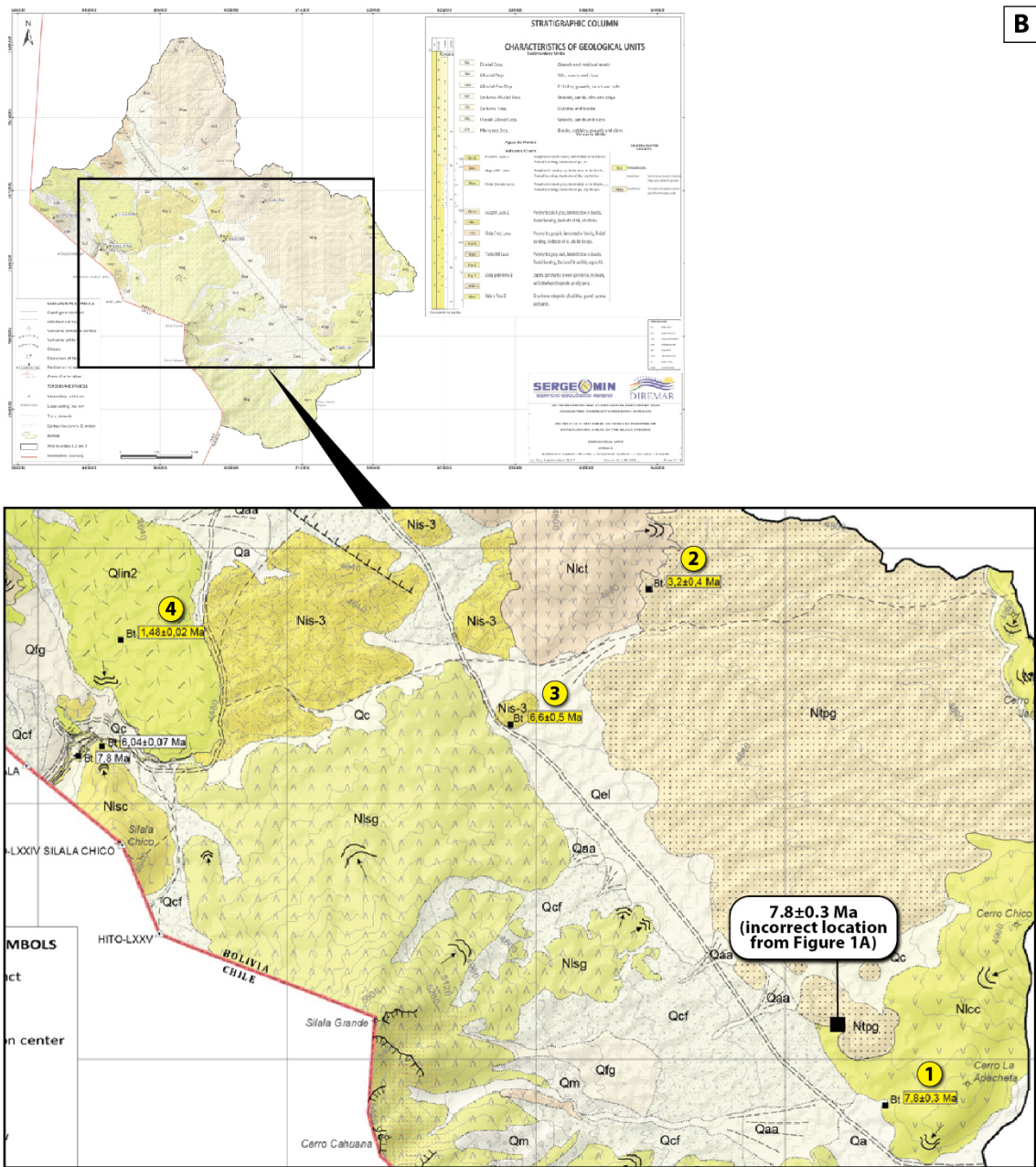


Figure 1. Source of ages for the Silala Ignimbrites (Bol). The origin of the age of 7.8 Ma of Baker and Francis (1978) extrapolated to this unit in the area of the Silala River, has been erroneously mapped in Volcán. Juriques Cerro Zapaleri map (A), but rectified on the 2017 map of Annex 23.5b (BR, Vol. 4, p. 115) (Figure 1B, Age 1). Part of what was mapped as Silala Ignimbrites corresponds to the 'Toba Pasos Grande', age 3.2 Ma (Figure 1B, Age 2). The age of 6.6 Ma (Figure 1B, Age 3) corresponds to the Silala Ignimbrite 3 (Bol) unit (Nis-3).

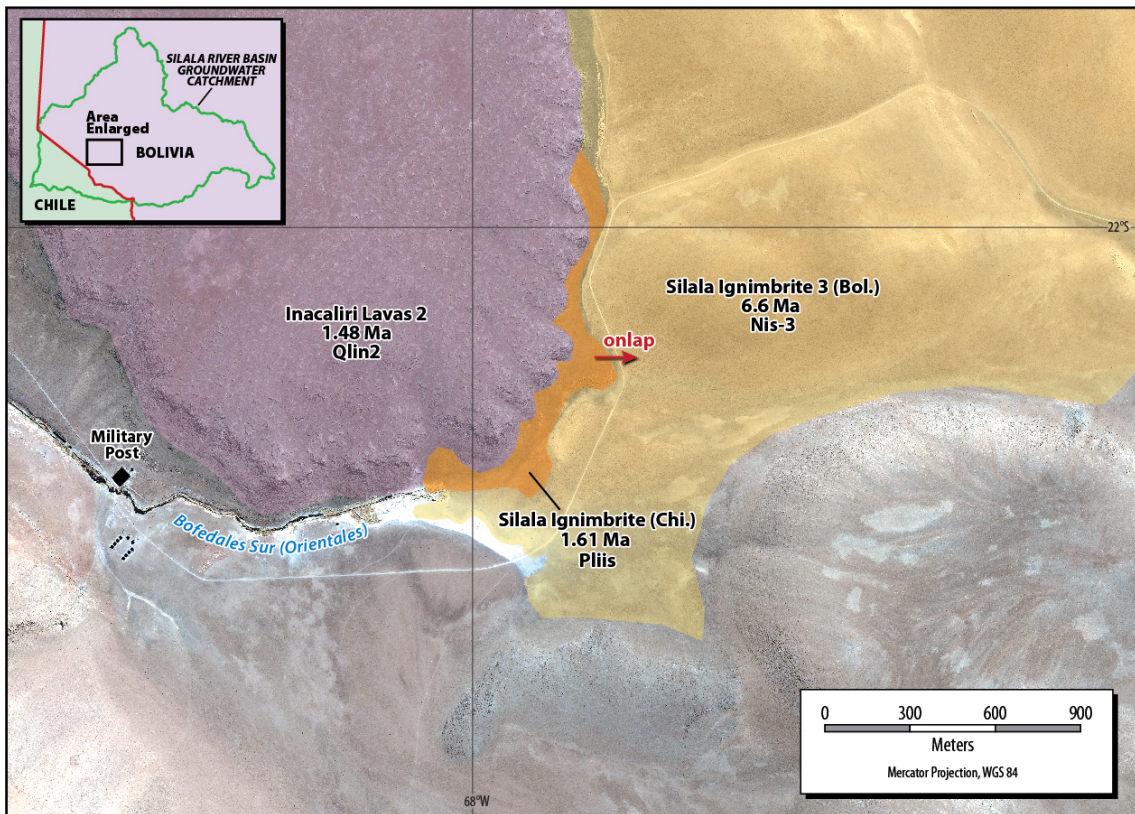


Figure 2. Unconformity or onlap relationship between the Silala Ignimbrite (Chi) and the Silala Ignimbrite 3 (Bol), located east of Bofedales Sur (Orientales).

It is also mentioned that the Silala Chico (Bolivian name, Cerrito de Silala in Chile) volcanic dome intrudes the Silala Ignimbrites (Bol) (BR, Vol. 4, pp. 125 and 149). That statement is based on an age of 6.6 Ma obtained for the Silala Ignimbrites (Bol) (BR, Vol. 4, p. 115), subunit Silala Ignimbrite 3 (Nis-3), which is the youngest or uppermost ignimbrite subunit recognised by Bolivia, located 8.5 km to the ENE of the summit of the Silala Chico hill. As shown above this age is incorrect. According to the geological cartography carried out by Chile (CM, Vol. 5, Annex VIII) the geological units that are in contact with the Silala Chico dome are the Silala Ignimbrite (Chi), dated at 1.6 Ma and the lavas that descend from the Silala Grande (Bol) (Volcán Apagado in Chile) dated at 1.74 Ma (BR, Complete Copies of Certain Annexes, Vol. 2, Annex 23.5 Appendix a, p. 69); both units cover in *onlap* (unconformably overlying) the deposits of this volcanic dome at its base. So, the Bolivian statement above is wrong, because a

volcanic dome dated in 6.04 ± 0.07 Ma (biotite) (BR, Vol. 4, pp. 113-115) cannot intrude and settle on younger rocks that are dated 1.74 to 1.6 Ma.

Further confusion arises from Bolivia's depiction of the relationship between the Silala Chico Dome unit (Nevsch on Bolivia's geological map at Figure 3), with the age 6.04 ± 0.07 Ma, and the Silala Grande volcano deposits (Nevs on Bolivia's geological map at Figure 3), with the younger age of 1.74 ± 0.02 Ma. Bolivia's Generalized Geologic Section (BR, Vol. 4, p. 125), is inconsistent with these dates (see Figure 4). It shows the older Silala Chico Dome unit overlying the younger Silala Grande volcano deposits. The correct stratigraphic relationship is therefore the opposite, namely, the lava flows of Silala Grande volcano overlie the older volcanic rocks of the Silala Chico Dome unit.

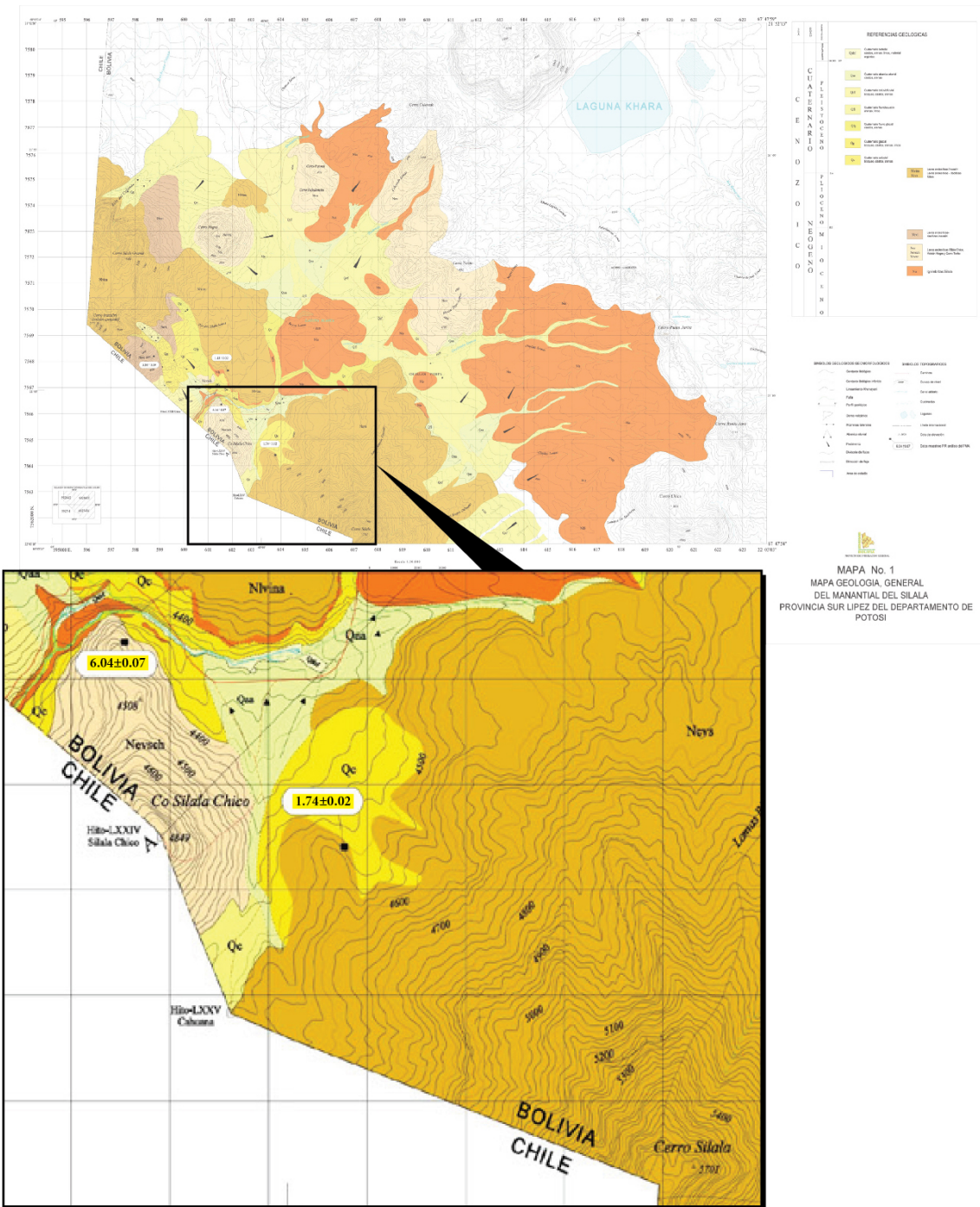


Figure 3. Zoom of the part of Geological Map (BR, Complete Copies of Certain Annexes, Vol. 2, Annex 23.5 Appendix a, p. 69), showing the location of an age of 1.74 ± 0.02 Ma in a lava flow of the Silala Grande (Bol) volcano and the location age of 6.04 ± 0.07 Ma of the volcanics of the Silala Chico (Bol) dome.

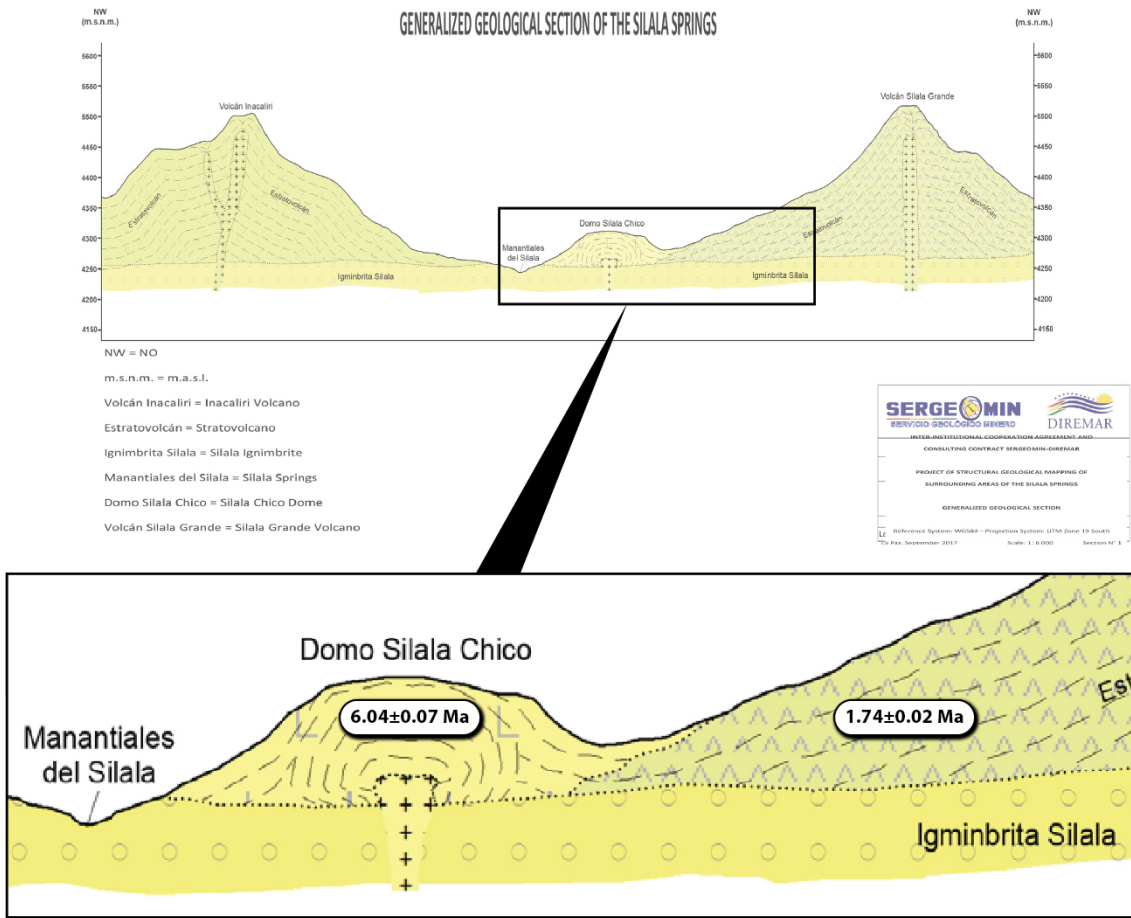


Figure 4. Generalized Geologic Section that shows that the ages (added for clarity) cited in Figure 3 do not support the stratigraphic relationship determined by Bolivian geologists. The section also shows the ignimbrites underlying the lavas of the Silala Chico dome, which is also incorrect, since they are younger than the lavas of the dome (BR, Vol. 4, p. 125).

2.2 Bolivian Petrography

Table 2 summarizes the petrographic characteristics of the Silala Ignimbrites (Bol) unit, and the differences between the descriptions among the different studies conducted by Bolivia. There are several difficulties with the information contained therein.

SERGEOMIN (2017)				TFAU (2018)		
Unit	Description	Assemblage	Petrography	TAS	% SiO ₂	Petrography
Silala Ignimbrite 3 (Nis-3)	Moderate welded tuff of 12 m of thickness with lithics (dacite and andesite) and pumice (BR, Vol. 4, pp. 50-51)	Pl- K feld-qz-bt (BR, Vol. 4, p. 51)	Pl-qz-bt±amph±K feld-Fe oxides (pp.7-8,23-24, 27-28; SERGEOMIN, 2017)	Andesite	55-60	Pl Na-qz-K feld (BR, Vol. 4, p. 50 and pp. 158-159)
Debris flow 2 (Nfd2)	Massive and chaotic unit with igneous clast subangular to subrounded (< 40 cm) in sandy-claytly and 50-180 cm of thickness with vesicular texture in some sectors (BR, Vol. 4, pp. 49-50)					
Silala Ignimbrite 2 (Nis-2)	Ignimbrites (or flow tuffs) welded, banded to massive texture of 10 m of thickness with lithics (andesites) and pumice (<10 cm) (BR, Vol. 4, pp. 48-49)	Pl-qz-px-amph (BR, Vol. 4, p. 49)	Pl-amph±px-Fe oxides (pp.55-56; SERGEOMIN, 2017)	Dacite	> 66	Pl-qz-K feld (BR, Vol. 4, p. 158)
Crystal-vitreous tuff (Ntcv)	Fine ash fall tuff (andesitic ignimbrite) of 15 cm of thickness average, vesicular texture in some sectors and an alternation of lenses of bands of different colors (banded and fluidal texture) (BR, Vol. 4, pp. 47-48)	K feld-bt-pl±px (BR, Vol. 4, p. 47)	Pl-px±qz±Fe oxides (pp.1-4; SERGEOMIN, 2017)			
Silala Ignimbrite 1 (Nis-1)	3-8 m of thickness with vertical fractures parallel and subparallel to lithics (igneous) and pumice. Fluidal or banded microtexture (BR, Vol. 4, pp. 46-47)	K feld-qz-bt±px (BR, Vol. 4, p. 46)	Pl-qz-bt-Fe oxides	Dacite	63-66	Pl-qz-bt (BR, Vol. 4, p. 157)
Debris flow 1 (Nfd1)	Massive and chaotic unit with igneous clast subangular to subrounded (< 40 cm) in sandy-claytly matrix and 60-140 cm of thickness (BR, Vol. 4, p. 44)					

Table 2. Descriptions of the Silala Ignimbrites of TFAU and SERGEOMIN documents. TAS is a diagram of classification of the volcanic rock (Total Alcalis versus Silica, Le Maitre, 2002).

Petrography corresponds to petrographic descriptions of the samples in both documents.

2.2.1 Observations

The Debris flow 1 (Nfd1) (Tables 1 and 2) is in reality a “scoria blocks tuff” (or tuff with scoria blocks) with rounded and subrounded fragments of vesicular scoria with plagioclase and pyroxene and is a flow unit or cooling unit of the ignimbrite of age 1.61 Ma, the Silala Ignimbrite (Chi). This kind of ignimbrite is well studied in other places (for example, Lohmar et al., 2007).

The Bolivian samples 7702, 7706, 7807 and 7808 are from Ntcv unit, Crystal-vitreous tuff (“Toba Cristalo Vítreo” in Spanish) (Tables 1 and 2), (BR, Vol. 4, p. 47). This is named “Andesitic ignimbrite” too (BR, Vol. 4, pp. 134-135) but the name of the sample 7807 has been changed to Andesite of pyroxene lava (Annex C to SERGEOMIN, 2017, p. 13²). In reality this level of “Silala Ignimbrites” is a vitrophyre, a highly welded tuff with fiammes and eutaxitic texture and normally is located at the base of ignimbrite (for example, Gimeno et al., 2003).

The Silala Ignimbrite 2 unit (Nis-2) (Bol) (BR, Vol. 4 p. 116) is the same deposit as the Chilean Silala Ignimbrite (RSP-52t), which can be traced crossing the border into Bolivia. A pumice sample collected in the Silala ravine in Chile, within approximately 5 metres of the border, of Chilean Silala Ignimbrite (RSP-52t), corresponds to a fragment that under the petrographic microscope appears as a vesicular pyroxene andesite (see Figure 5). It is possible to recognize an accumulation of pyroxene crystals, which is a very common texture. This rock, as found in Chile, at the border, is an andesitic ignimbrite, not a dacitic ignimbrite. Nevertheless, in all descriptions in the Bolivian documents, they refer to Nis-2 as a dacitic ignimbrite (see Table 2), which is incorrect.

² Resubmitted as Appendix A to this report.

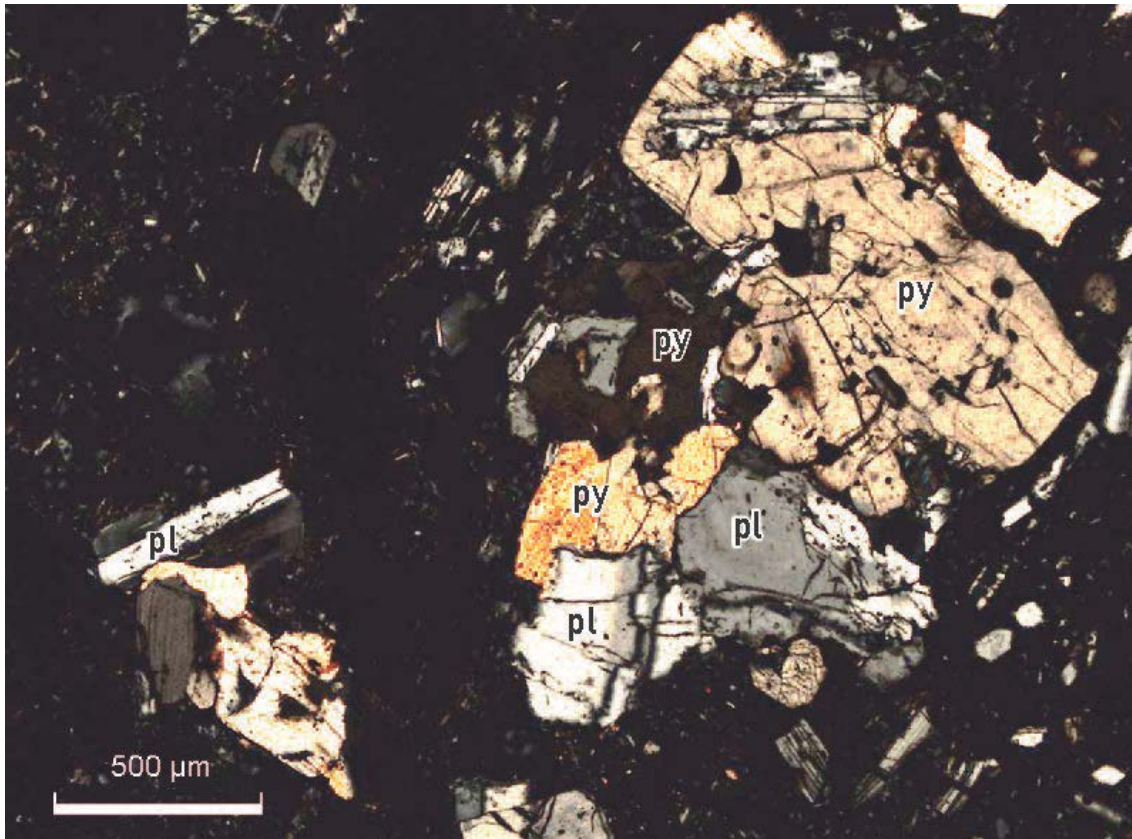


Figure 5. Photograph of the thin section of RSP-52t sample (Silala Ignimbrite (Chi)) showing pyroxene and plagioclase crystals. This sample was collected on 7 November, 2018, within approximately 5 metres of the international border in the south wall of the Silala River ravine.

Another issue with the descriptions of the different units of Silala Ignimbrites (Bol) is that the mineral assemblage in the main text and the petrographic descriptions are different and inconsistent. Also these descriptions differ from those of TFAU. For example, the Silala Ignimbrite 2 (Bol) (Nis-2), is described as having a quartz-like mineral assemblage in the main text (BR, Vol. 4, p. 158) but quartz does not appear in the petrographic descriptions of the thin sections (Table 2). The same inconsistency occurs between the mineral assemblage and petrographic description of Silala Ignimbrite 3 Nis-3 (Bol) (Table 2). No amphibole appears in the mineral assemblage but is found in the petrographic description (Table 2).

In addition, our examination provides evidence of a lack of systematic nomenclature by Bolivian geologists for the naming of the rocks in the various units. Normally, the nomenclature of a volcanic rock is a function of the relative abundance of the mafic minerals present (olivine, pyroxene, amphibole and biotite) as determined by its petrography. Table 3, prepared with data from Annex C to SERGEOMIN (2017) (Annex C to SERGEOMIN, 2017, pp. 49-50 and 53-54), shows two samples with the minerals and relative content (% in volume). These very similar rocks have been given different rock names, for example, if samples 7810 and 7811 are compared, it can be seen they have very similar mineral contents but different petrographic names (basalt and andesite; Table 3 below).

Sample	7810	7811
Quartz		
Plagioclase	31-33%	25-27%
Biotite		
K-Feldspate		
Hornblende		
Clinopyroxene	2-3%	3-5%
Groundmass	58-60%	56-58%
Fe-oxides	1-2%	
Calcite		
Pumice		
Other	1-2% (very high mafic oxide)	8-10% (lithoclast)
Name	Pyroxenic basalt	Pyroxenic andesite
Systematic rock	Pyroxene andesite	Pyroxene andesite

Table 3. Percentage of minerals (crystals content) of two “andesite” samples in Annex C to SERGEOMIN (2017). Systematic rock names should correspond to the rock name based on the mineralogy recognized in the rock sample.

Rock samples of the Silala Chico Lava (Cerrito de Silala) unit correspond to a dacitic dome, but in Table 4, prepared with data from Annex C to SERGEOMIN (2017) (Annex C to SERGEOMIN, 2017, pp. 5-6, 15-16 and 47-48), three different names are recognized by Bolivia for the same geological unit, however the systematic name that can be deduced is simply: biotite and amphibole dacite. There seems no reason for the three rock names for this same unit. This confusion and inconsistency does not give any confidence in the Bolivian geological expertise.

Sample	7809	7712	7713
Quartz	1-2%	6-8%	1-2%
Plagioclase	25-27%	23-25%	25-28%
Biotite	4-6%	3-5%	3-5%
K-Feldespat			
Hornblende	2-3%	2-3%	2-3%
Clinopyroxene	1-2%	1-2%	1-2%
Groundmass	53-55%	50-52%	55-57%
Fe-oxides	2-3%	2-3%	2-3%
Calcite	1-2%	1-2%	
Pumice			
Rock name	Biotitic andesite	Biotitic dacite	Biotitic andesite (quartzily)
Systematic rock	Biotite and amphibole dacite	Biotite and amphibole dacite	Biotite and amphibole dacite

Table 4. Relative percentage of minerals (crystals content) of selected samples of Silala Chico Lava unit in the Annex C to SERGEOMIN (2017). Systematic rock correspond to the rock name based in the mineralogy recognized in the rock sample.

3. STRUCTURAL GEOLOGY

3.1 Bolivian Structural Interpretation

Two main structural systems have been defined by Bolivia in the area of the wetland springs of the Silala River in Bolivia, which are assigned great importance by Bolivia as providing high permeability pathways for groundwater and controlling the locations of the springs in Bolivia (BR, Vol. 3, p. 249), in particular the Bofedales Norte (Cajones) and Bofedales Sur (Orientales). For the Bofedales Norte (Cajones), a fault called the “Silala Fault” (BR, Vol. 3, pp. 254 and 283), of NE-SW orientation, has been interpreted by Bolivia, as part of the Uyuni-Khenayani Fault System (UKFS) (Sempere et al., 1990; Martínez et al., 1994; Elger et al., 2005). For the Bofedales Sur (Orientales), a structure linked to the Silala-Llancor lineament (BR, Vol. 4, p. 73), of ENE-WSW (70°) orientation has been invoked. According to its authors, both structural systems are due to regional compressive stress (σ_1), in general, of East-West orientation (BR, Vol. 4, p. 66). The structures were determined on the basis of numerous measurements of fractures and, subordinately, faults. Also, a regional aeromagnetic map

was used to define the main magnetic lineaments, some of which, in our opinion, were forced to coincide with these structures (see discussion in relation to the structures below).

3.2 Analysis of Bolivian structural data

In geological science a fault is a planar or gently curved fracture in the rocks of the Earth's crust, where compressional or tensional forces cause relative displacement of the rocks on the opposite sides of the fracture. There are three types of fault, normal, reverse (or inverse) and transcurrent (or strike-slip). The relative displacement of transcurrent faults can be sinistral or dextral (left or right to the observer). SERGEOMIN (2017) reports 2754 geographically located structural data items (Annex D to SERGEOMIN, 2017³) (Table 5). Of these, only 487 (dextral, inverse, normal, sinistral faults) can be used in structural analysis and an attempt to formulate a structural model of the structural stresses that produced the faults. However, it is clear that some of the items included are fractures caused by primary cooling of lava flows or ignimbrite primary cooling (prismatic) joints. These are not indicative of faults. Indeed in the description of Silala Ignimbrite 1 (Bol) (Table 2) the presence of parallel and subparallel vertical fractures (columnar jointed) are noted but again, these do not indicate faults.

Additionally, the data in Table 5 are not ascribed to rock units of particular ages, i.e., there is mixing of faults of different ages which make their interpretation uncertain, unreliable or meaningless.

³ Resubmitted as Appendix B to this report.

STRUCTURES	QUANTITY
Diaclase	1955
Fault	179
Dextral fault	23
Inverse fault	87
Normal fault	331
Sinistral fault	12
Strike lip fault	6
inverse fault	34
Pseudostratification	127
Structures total	2754

Table 5. Quantitative statistics of the structural data (Annex C to SERGEOMIN, 2017).

179 of these structural data are listed as faults, but none of these in Table 5 above, show relative movement (by defining the movement, i.e. sinistral, dextral, inverse, normal), so that one can reasonably think that they correspond to diaclases (fractures or joints). Also, 127 of the data points correspond to pseudo-stratification, i.e., indicating the flow direction or spatial disposition of the lava flow or ignimbrite, so the incorporation of this type of data in a structural model is also incorrect. In other words, many of these data are not structural and so are not useful to understand local or regional stress regimes.

3.2.1 The “Silala Fault”

From their structural analysis the Bolivian geologists from TFAU concluded “that the maximum stress axis has a preferred E-W direction, which gave rise to four structural domains, each with particular characteristics” (BR, Vol. 3, pp. 257-258).

The Bolivian-described “Falla Silala” is a NE-SW oriented structure, which runs along the Silala River ravine, from Bofedales Norte (Cajones) following the course of the river to the SW, crossing the border into Chile (BR, Vol. 3, pp. 254 and 283). The measurement of fractures by Bolivia in this sector (Domain 4) they indicate is dominated by a NW-SE pattern (125-305°), corresponding to normal faults, and coinciding with the orientation of Inacaliri Graben (BR, Vol. 3, p. 267). However,

according to the deformation model proposed by Bolivia (BR, Vol. 3, p. 263), with a main stress vector σ_1 WNW-ESE ($\sim N85^\circ W$) such normal faults should have a WNW-ESE orientation ($\sim 275-95$), which does not coincide with the preferential or most frequent fractures measurements (NW-SE) (BR, Vol. 3, p. 267, Figure 13a) or with orientation of the Graben Inacaliri.

Also, a fault oriented $N45^\circ E$ and inclined 48° towards the SE, with fault stria or slickenlines forming an angle of 11° to the SW (BR, Vol. 4, p. 322) with respect to the strike of the fault was measured. The Bolivian authors indicate that this fault plane coincides with the current direction of the Silala ravine in that area and that the vertical and almost vertical walls of the ravine are “strong evidence of the formation of the ravines by tectonism and movement of glacial ice and fluvioglacial waters” (BR, Vol 3, p. 323). This assertion is inconsistent, because they define a fault with an inclined plane at 48° to the SE, so that the vertical walls of the ravine must have another origin, not from one influenced by a structure, or by the action of glacial ice. This has previously been demonstrated by Chile as has the fluvial origins of the ravine (SERNAGEOMIN, 2017; Latorre and Frugone, 2017).

In relation to the structure that supposedly controls the Silala River ravine ($N45^\circ E/48^\circ SE$), it has stria or slickenlines that form an angle of 11° with respect to the strike of the fault ($rake = 11^\circ SW$) (Figure 6), which indicates that it would be a fault of lateral displacement or heading, with very little vertical displacement. In the deformation model for Domain 4, the NE-SW orientation faults correspond to right lateral faults, with which the south-eastern block of the fault drops slightly with respect to the north-western block (Figure 6). This situation contrasts with the assertion that the units that are located on the eastern side of the river, south of Bofedales Norte (Cajones), are raised 5 metres from the western side (BR, Vol. 5, p. 24), implying that the Silala Fault is responsible for that upward displacement (BR, Vol. 5, p. 24; BR, Vol. 4, p. 48). In fact such a fault would result in the opposite displacement, as shown in Figure 6; the south eastern block would be displaced downwards.

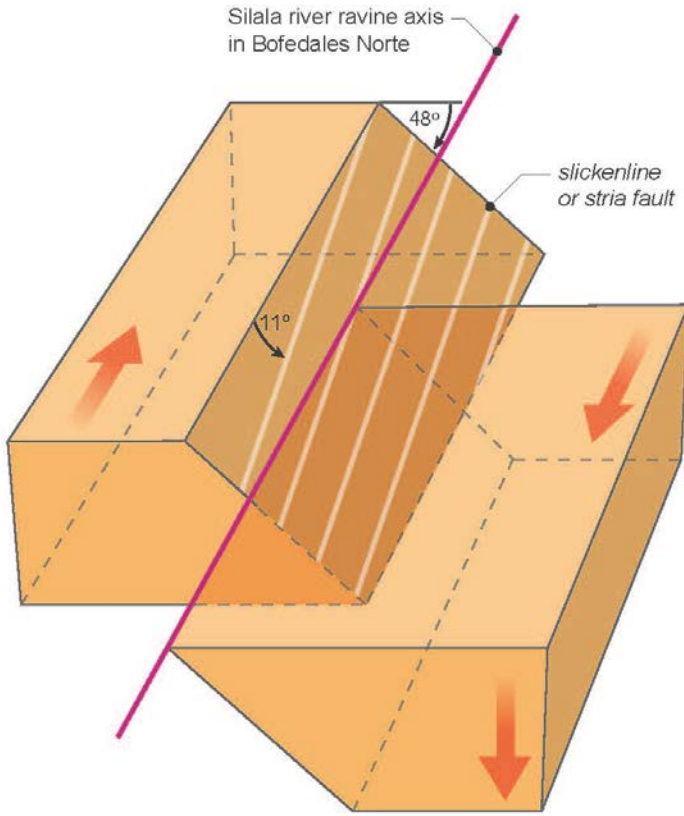


Figure 6. Block diagram for the structural model of the Silala Fault, of orientation N45°E/48°SE, with dextral displacement and southeast block slightly displaced downwards with respect to the northwestern block according to rake= 11°SW.

In their analysis of fractures in the structural domains (BR, Vol. 3, pp. 260-263; BR, Vol. 4, pp. 306-325) it is mentioned that in Domains 2 and 3 the orientation of the predominant fractures coincide with compressive and shear fractures, which are closed fractures, and that therefore, in those sectors, there are no springs, because there are no open fractures to facilitate the emergence of groundwater (BR, Vol. 3, pp. 258-259). This assertion and structural interpretation is clearly in contradiction with what they interpreted for the Bofedales Norte (Cajones), in which it is asserted that the upwelling of water is controlled by NE-SW shear structure that coincides with the orientation of the Silala ravine (BR, Vol. 3, p. 258), also aligned NE-SW. There, a dextral shear structure is mapped by Bolivia and matches their proposed structural model. But according to this the Bolivian geologists would postulate that shear fractures or shear

faults are closed and unlikely to support the emergence of springs and, therefore, at Bofedales Norte (Cajones) spring arisings would not be expected to be favorably influenced by a NE-SW structure shear structure because it would be closed. There is clearly another control for water upwelling in that sector but it would not be by a NE-SW shear fault.

A possible control for the emergence of groundwater in Bofedales Norte (Cajones) could be related to its location being on the trace of a regional structure, of N-S orientation, determined by the alignment of dacitic volcanic domes, which we will call the Silala Chico-Cerro Negro Lineament. For this reason and, possibly like the Quebrada Negra spring located in Chilean territory, the emergence of underground water in Bofedales Norte (Cajones) could be determined by the existence of this regional structure (Figure 7).

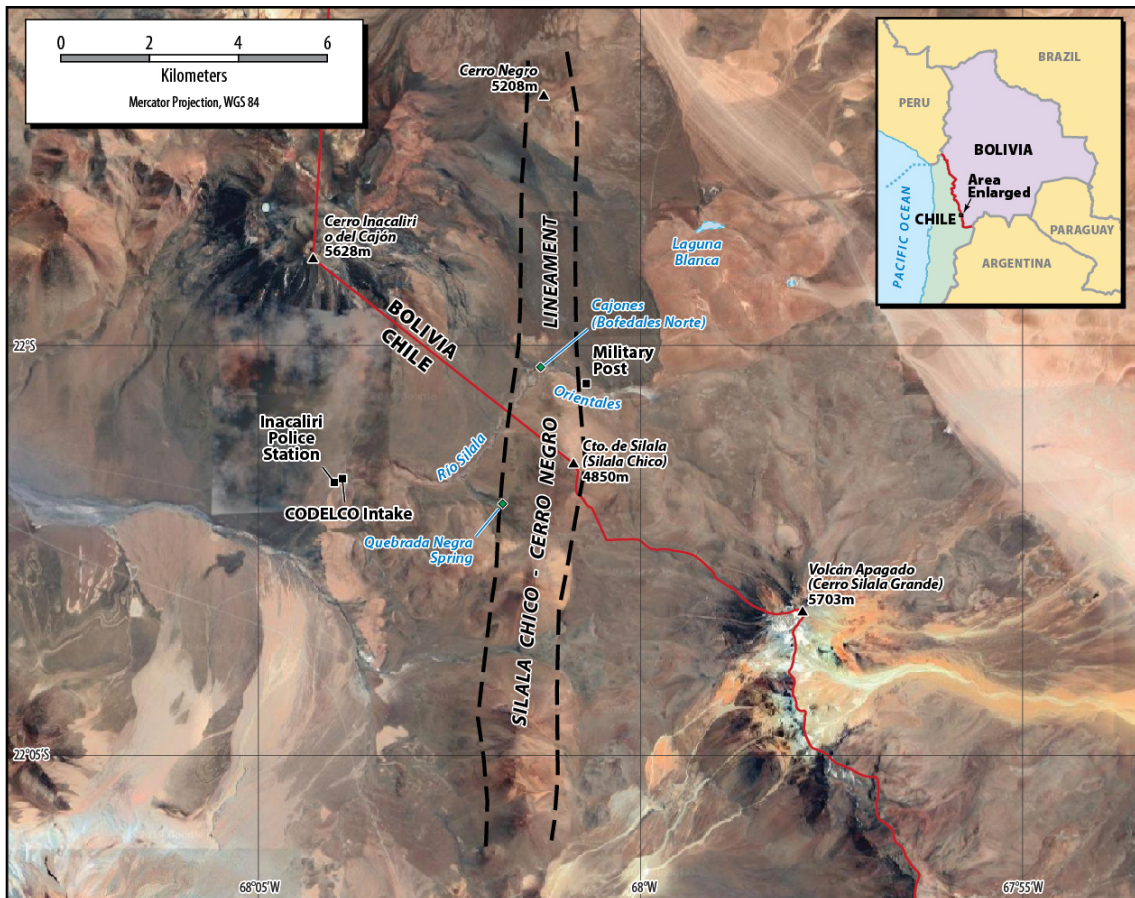


Figure 7. Spatial relationship of the emergence of underground water springs possibly associated with the Silala Chico-Cerro Negro structural lineament, in particular for the Quebrada Negra springs in Chile and Bofedales Norte (Cajones) in Bolivia.

For the Bolivian cross section of the Silala River ravine located SW of Bofedales Norte (Cajones), with a NW-SE orientation, it is indicated that there is a displacement of approximately 5 metres of the rock units located on the southeast side of the river (Figure 8) (BR, Vol. 5, p. 24). Moreover, this is explicitly said with the phrase “subdividing the Silala Ignimbrite in two members (Nis1 and Nis2) and it is also an indicator of possible vertical displacements produced by the faulting” (BR, Vol. 4, p. 48). This indicator appears to be intended, in our opinion, to reinforce the idea of the existence of a fault in that sector that is the cause of this displacement. However, if the hypothesis of the existence of this fault is accepted, as indicated for the Silala Fault (Figure 6), the movement of the south-eastern block of the fault should be displaced

downwards according to the dextral shear movement and the orientation of the stria or slickenlines associated with the fault, that is, the opposite of what is indicated by Bolivian geologists. On the other hand, a slightly higher position of the SE block can also be explained because the Silala Ignimbrites (Bol) unit is tilted to the west as indicated by the Bolivian geologists (BR, Vol. 4, p.149).

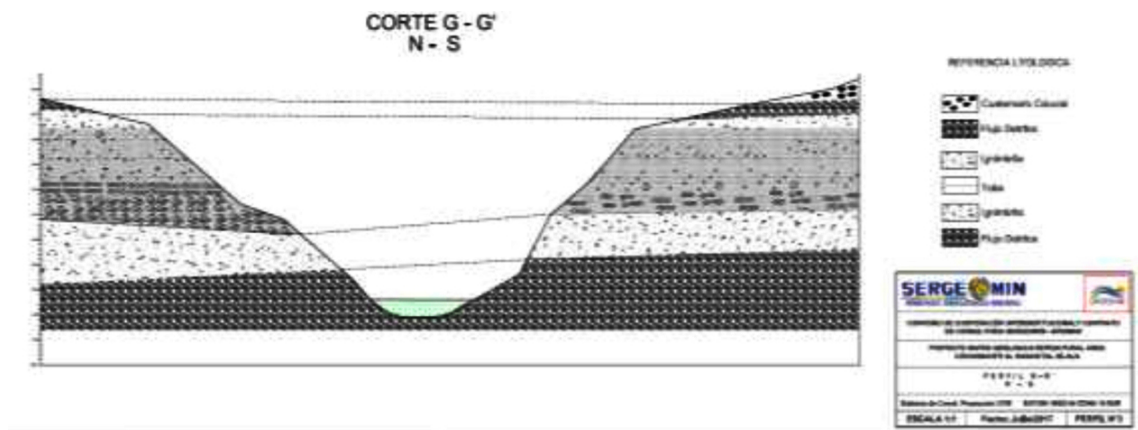


Figure 8. Profiles GG' located SW of Bofedales Norte (Cajones), that indicate there is displacement of ~ 5 m of the rock units located on righthand side of the river in this figure. (BR, Vol. 5, p. 24).

In the Bofedales Norte (Cajones) area it is not possible to see or photo-interpret any NE-SW lineament or structure. The dominant structural fabric has a NW-SE trend (Figure 9), as indicated by the fracture rose diagram (BR, Vol. 3, p. 263). The association of vertical walls with the supposed structure NE-SW is erroneous, and it is possible to see that the verticality of the slopes of the ravine corresponds to an erosional form that follows the course of the river (Figure 9).

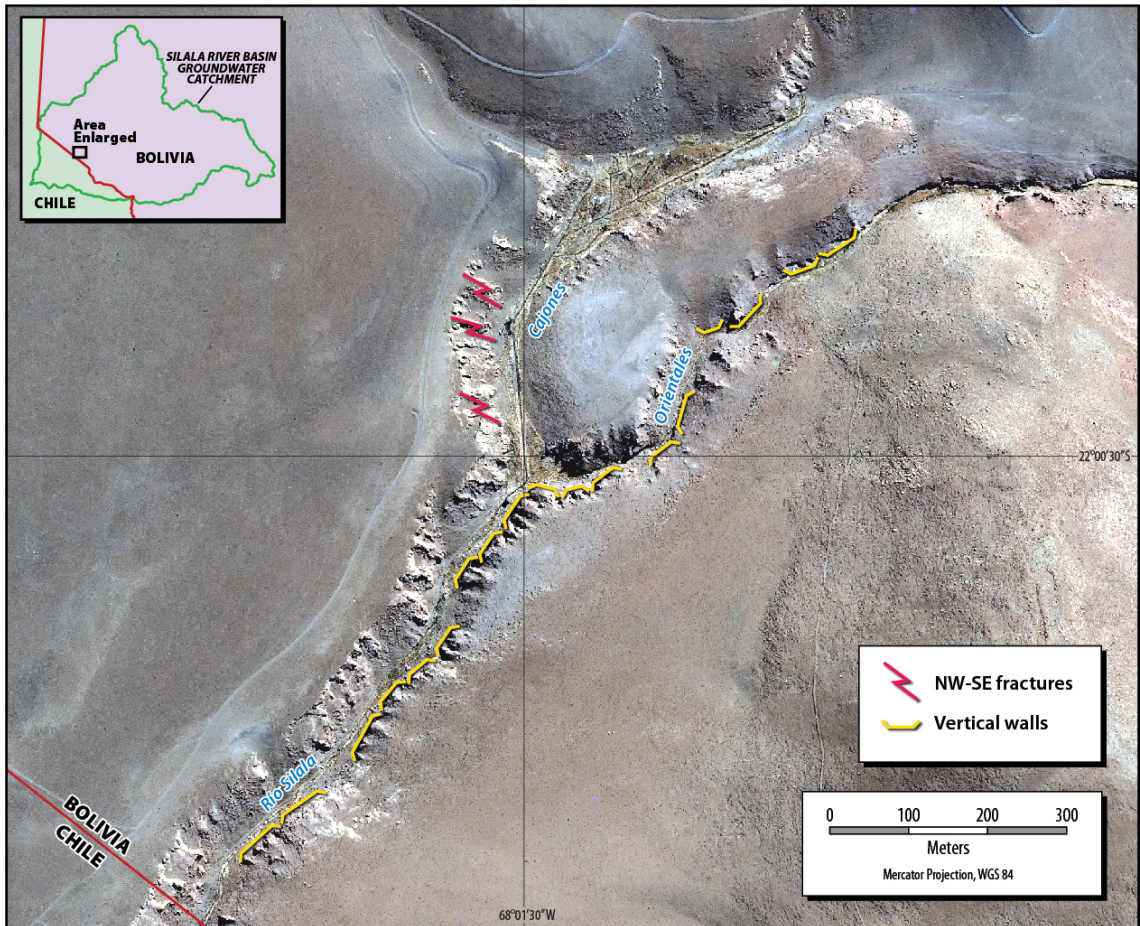


Figure 9. This shows the main orientation of NW-SE fractures, transverse to the course of the Silala ravine. The orientation of vertical walls in the ravine follows the course of the river, indicating that they are formed by erosion.

In our opinion, the change of direction of the course of the Silala River, starting from Bofedales Sur (Orientales), is due to a lithological control, that is to say, to the resistance that the rocks present to the fluvial erosion. Indeed, where the course of the river intersects the dacitic lavas, both at the northern end of Cerrito de Silala (Chi) hill and NE of the Inacaliri police station, the course is modified significantly and then it is restored its general direction to the SW from Bofedales Norte (Cajones) (Figure 10).

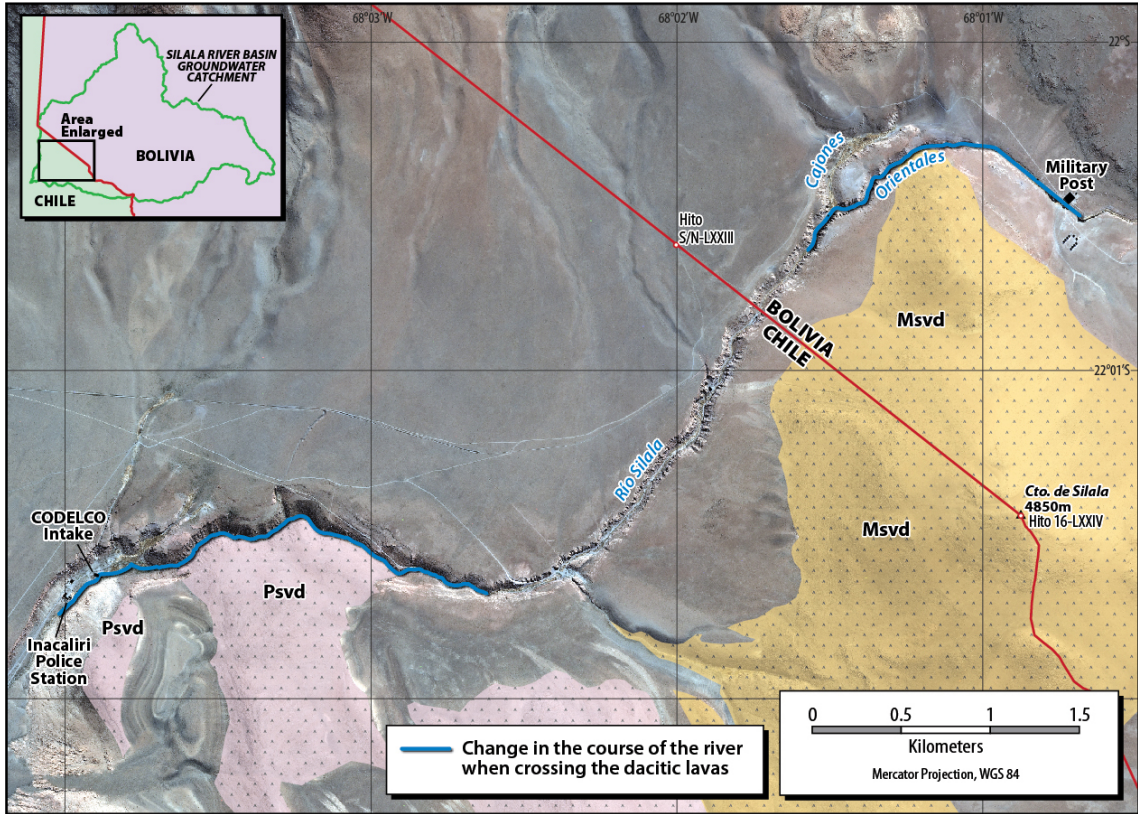


Figure. 10. Effects of competent lithology (dacitic lavas) on the Silala River course. Light brown (Msvd code) and light pink (Psvd code) colors represents the envelope of dacitic lavas.

3.2.2 The “Silala-Llancor Lineament”

Bolivia asserts: “The Silala-Llancor lineament – which has an ENE-WSW (75°) orientation, that coincides pro parte with the South Canal of the Silala springs – is modeled in the middle of the Silala Ignimbrite [Bol] and the Silala Grande (Bol) hill lava” (BR, Vol. 4, p. 106). Its trace towards the East is dextrally displaced by another system or transversal lineament of NW (300°) direction at the level of the lavas of Cerro Torito, (Figure 11A). For the Silala-Llancor lineament, a sinistral displacement was determined (BR, Vol. 4, p. 106), in part, using satellite images and aeromagnetic geophysics. They indicate this lineament may have some influence on the upwelling of water in Bofedales Sur (Orientales) (BR, Vol. 4, p. 106).

We have the following comments:

1.- In our opinion, this lineament does not correspond to the rectilinear alignment of any geological element (eg. volcanic emission centers, water drainage systems, escarpments, etc.) (Figure 11 A). Its layout appears to have been chosen to coincide with and hence justify the groundwater springs of Bofedales Sur (Orientales). Its “trace”, which would pass between the lavas of the Silala Grande (Volcán Apagado) and Silala Ignimbrites (Bol), is not a tectonic feature, and there is not a structural escarpment inclined 45° to the North (BR, Vol. 4, p. 102). In this area, there is a contact between the ignimbrites and the front of an andesitic lava with a lobed face (Figure 11 B). The escarpment corresponds to the end of the andesitic lava flow, whose morphology is sinuous or lobed, far from being rectilinear as would be expected by the presence of a fault (Figure 11 B). In addition, it is mentioned that this lineament is displaced, in the dextral sense, by a NW fault. That is based on the supposed displacement between the Cerro Torito lavas and the lavas of the Silala Grande (Volcán Apagado). However such a displacement is not real, because the lavas of these hills have very different ages: 5.8 Ma in Cerro Torito lavas (Almendras et al., 2002) and 1.7 Ma for Silala Grande (Volcán Apagado) lava flows. Thus, this displacement caused by this supposed structure, is incorrect. The structure does not exist so there can be no displacement.

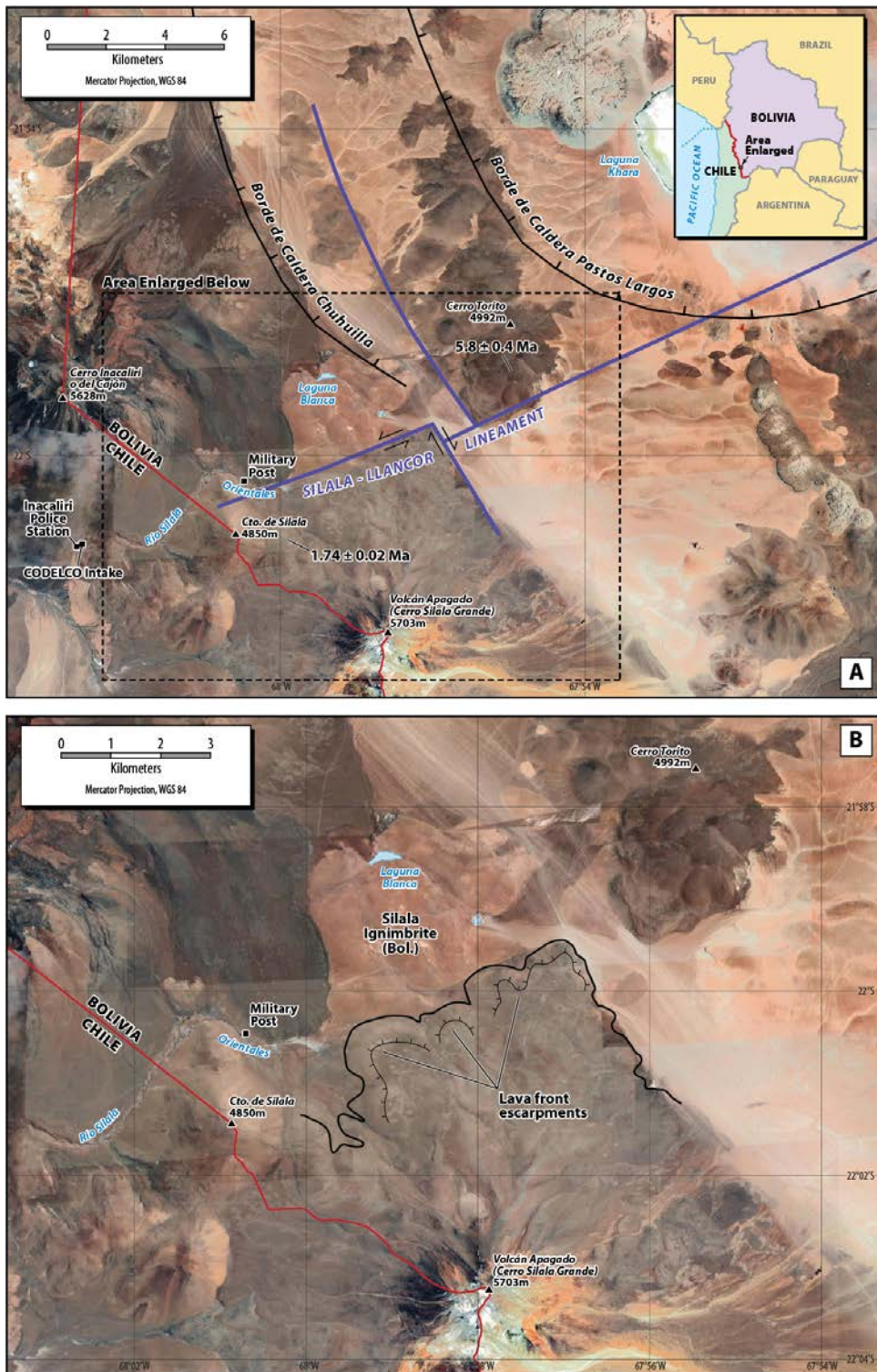


Figure 11. Layout of the Silala-Llancor lineament (A) and its supposed control over Bofedales Sur (Orientales), displaced dextrally by the NW-SE structure, which uses very different ages of rocks as displacement reference. The lobed end of Pleistocene lava flows (B) that is interpreted as an escarpment fault by Bolivian geologists.

2. - On a local scale, the Bolivian geologists suggest that the sinistral movement of the “Silala-Llancor fault” is supported by fractures in the Cerro Torito and Silala Grande (Volcán Apagado) lava flows. The Bolivian geologists established that in the Cerro Torito lavas there are tension fractures of NE-SW trend (15 to 35 degrees) arranged obliquely to the Silala-Llancor lineament forming an angle inferior to 35 degrees (BR, Vol. 4, p. 103). In the Silala Grande (Volcán Apagado) lava flows, tension fractures have a similar orientation (BR, Vol. 4, p. 103). The orientation of these tension fractures involves a tectonic maximum principal stress σ_1 - oriented NE-SW. However, it is described that in Silala Grande (Volcán Apagado) lavas there are reverse faults (only 6 inverse faults and 23 unidentified faults) of general orientation $\sim N36-38^\circ E / \sim 75-80^\circ SE$ (BR, Vol. 4, p. 95). For this average plane of reverse faulting a maximum principal stress σ_1 oriented NW-SE is required, which would generate tensional fractures or tensional fault(s) in the NW-SE direction, almost 90° from the tension fractures observed in Silala Grande (Volcán Apagado) and Cerro Torito lava flows, which supposedly justify a sinistral movement along Silala-Llancor lineament.

Furthermore, for structural Domain 1 (BR, Vol. 3, p. 260) the maximum principal stress σ_1 determined for the Bofedales Sur (Orientales) area is oriented ENE-WSW, generating a dextral fault in a NE-SW direction. As determined by the Bolivian geologists this would be a non-extensional fault. The information provided for the interpretation of the kinematics of the Silala-Llancor lineament is contradictory and is not compatible with a sinistral movement for this proposed structure.

3.- To define the trace of the Silala-Llancor lineament at regional scale, a map of total magnetic intensity reduced to the local pole, first derivative, is used (BR, Vol. 4, p. 118) (Figure 12). This magnetic map is questionable for the following reasons:

- (i) It is indicated that it is a magnetic map processed with the first derivative, but in the scale of intensities it has magnetic field units in (nT). If it were the correct scale the units should be nT /m or nT /km.
- (ii) The Bolivian report (BR, Vol. 4, p. 118) does not present information about the spacing, height and orientation of main flight lines. This information is

fundamental, since the patterns of anomalies can be caused by the effect of the direction of flight and not necessarily indicate a real geophysical anomaly. The flight height is also important to know in order to establish the depth range of the anomalies (> flight height > depth of the anomaly, and vice-versa). Due to the attenuation of magnetic field anomalies with altitude, it may not be possible to provide information to the required scale for recognition of important structures.

(iii)The map presents a marked trend E-W to ENE-WSW, which could reflect a flight direction and not a real anomaly. (Note that the magnetic anomalies cross the international boundary in an approximate EW to WNW direction, which suggests that the direction of the flight line could have the same path and not a path, for example, in a N-S direction.)

The magnetic anomaly used to define the trace of the Silala-Llancor lineament is more consistent with the clearer definition of the southern segment of the Pastos Largos caldera boundary, because this lineament is not clearly traceable beyond the limits of this caldera (Figure 12). The magnetic anomalies in the area of the springs of the Silala River could be explained, alternatively, by the presence of lavas and andesitic volcanic edifices of the Pleistocene age and not a structure. For this it is essential to know the flight height of the data collection, in order to know if these anomalies are deep or shallow, however this information was not presented.

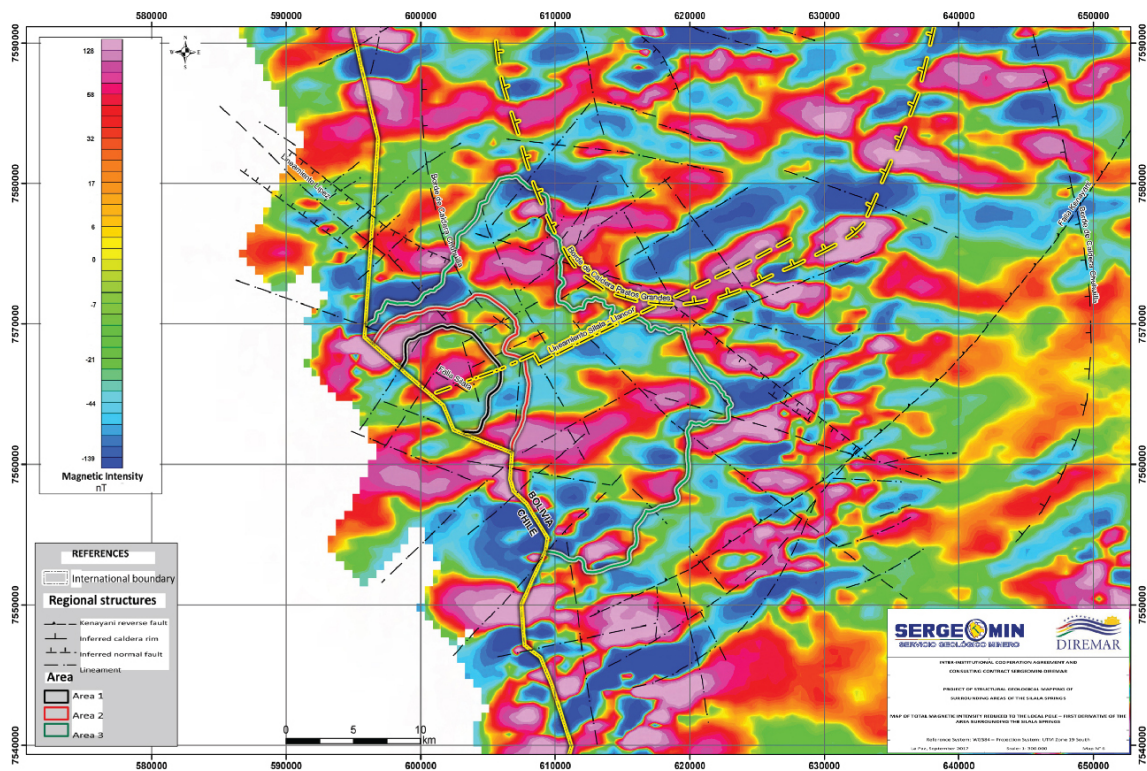


Figure 12. Total magnetic intensity map local pole reduced, first derivative (BR, Vol. 4, p. 118). Note that the magnetic information traverses the international border (solid yellow line), which infers a possible E-W to ENE-WSW flight direction (uninformed data), thus favorably conditioning the anomaly trend of this map. For clarity, yellow highlighting has been applied to the international border, Silala-Llancor Lineament, and edge of the Pastos Largos Caldera. Grey highlighting has been applied to the borders of Area 1, Area 2, and Area 3, where Area 3 is equivalent to the hydrological catchment area and Area 1 encompasses the Orientales and Cajones wetlands.

3.2.3 Conclusions

The main lineaments in the near Silala River area are markedly oriented to the NW-SE, followed by a secondary NE-SW trend and, subordinately a N-S trend (Figure 13). The main and objective geological elements to define these lineaments are the dispositions of eruptive centers (Sellés and Gardeweg, 2017; Tibaldi et al., 2017), and none of these agree with the orientation of the regional structures proposed in the Bolivian technical reports (Figures 13 and 14).

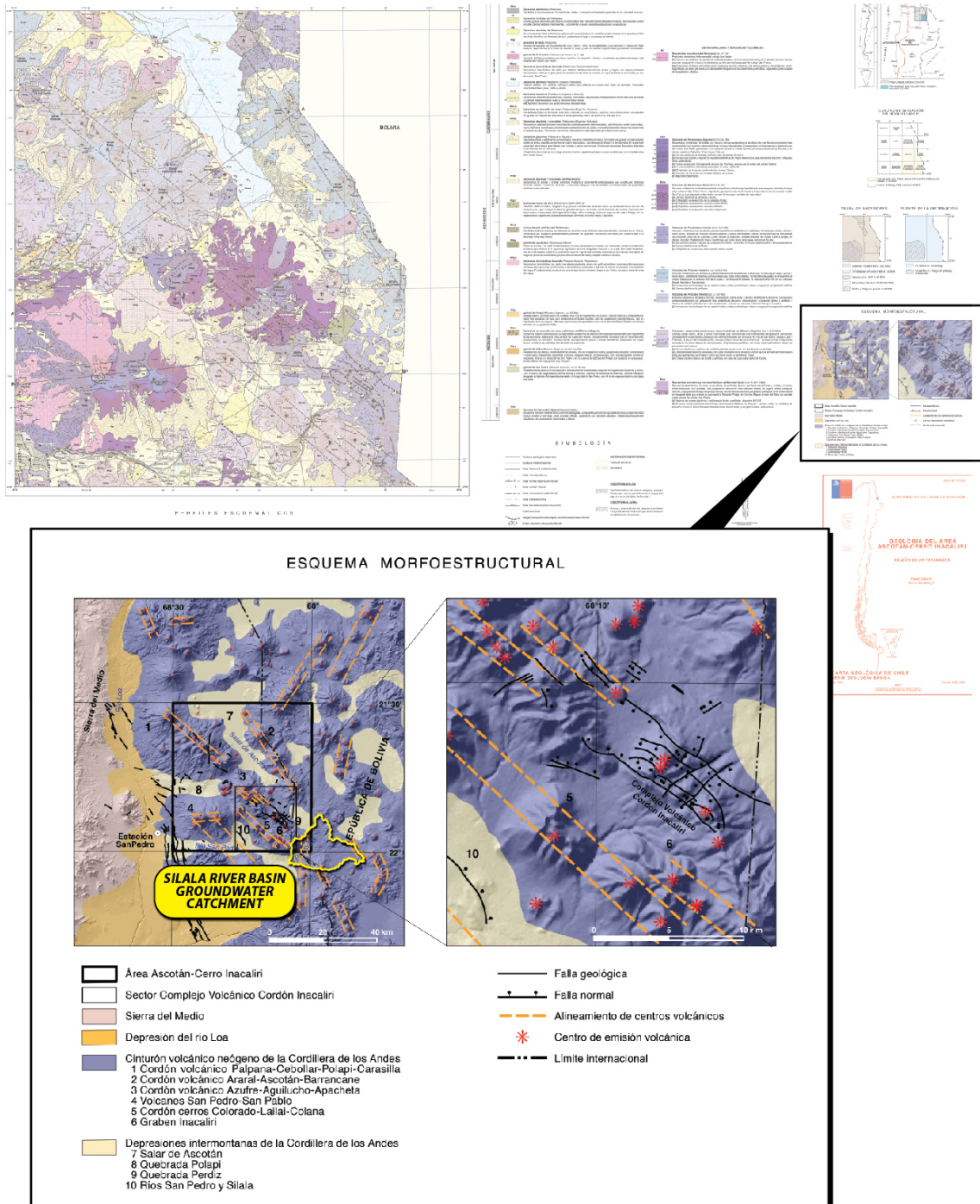


Figure 13. Regional lineaments located in the vicinity of the Silala River. Yellow label added. Those are objectively supported, by lineament of eruptive centers (Sellés and Gardeweg, 2017).

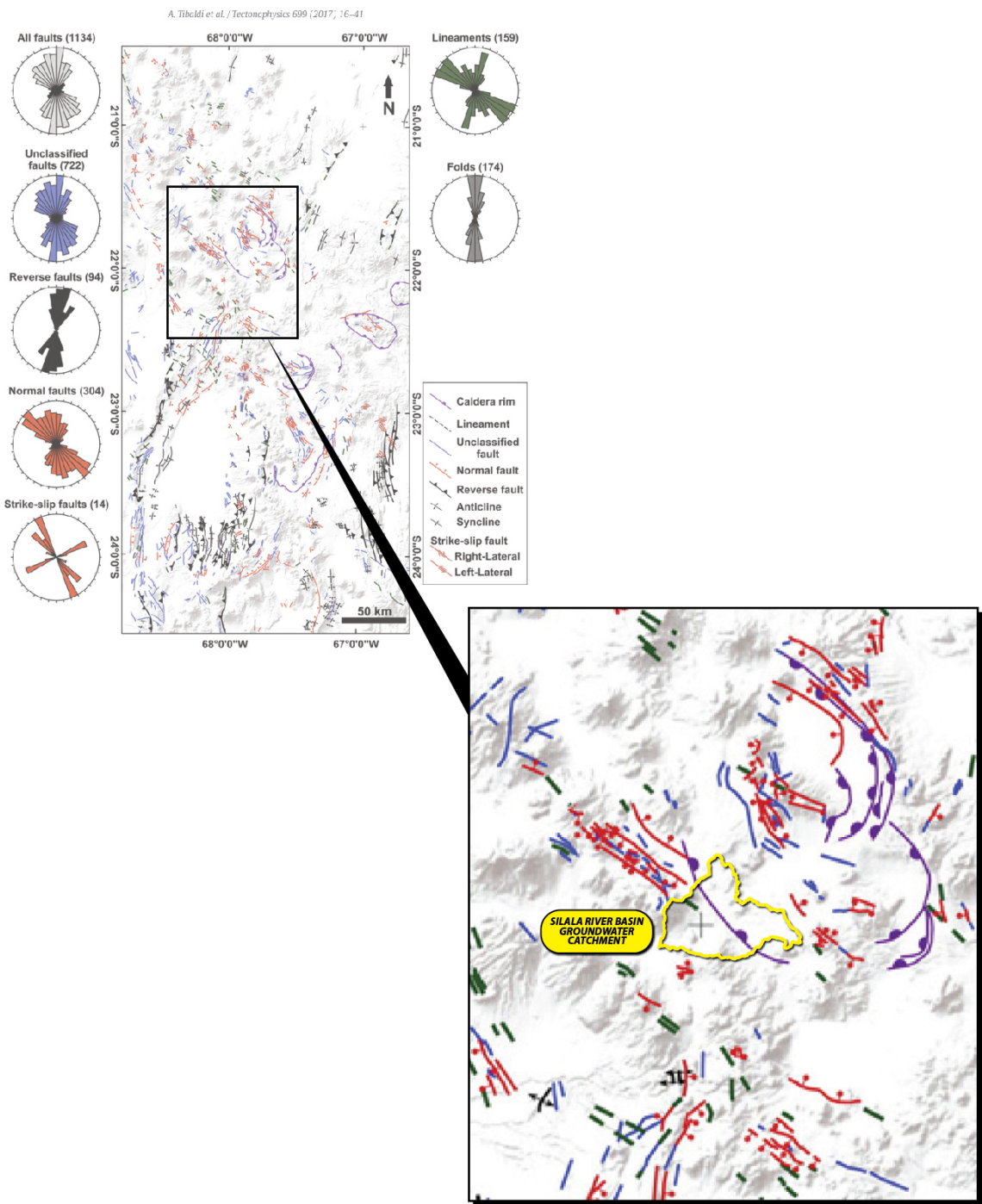


Figure 14. Structural map around Silala River area with main Neogene-Quaternary faults and folds (Tibaldi et al., 2017). Yellow label added.

3.3 Chile's interpretation of the geological deformation in the Silala River area

In order to better understand the errors in Bolivian Structural geological interpretations it is necessary to understand Chile's knowledge and interpretations from recent geological mapping in the Silala River area in Chile.

The most specific deformation history recorded in the Silala River area corresponds to the activity of the Cabana reverse fault, located in Chilean territory. This structure, from N-S to NNW-SSE orientation, is not exposed, but is inferred by the alignment of water drainages and by the deformation of adjacent units, tilting to the East (11°) in both the Cabana Ignimbrite (Chi) (4.1 Ma) as well as the dacitic lavas of 2.6 Ma (SERNAGEOMIN, 2017) that overlie it. This deformation does not affect the Silala Ignimbrite (Chi), which seals or covers its trace and fills depressions formed by subsidiary normal faults that accommodate the rise and rotation in the deformation front (Figure 15). This deformation is located in the time period between 2.6 and 1.6 Ma (Lower Pleistocene).

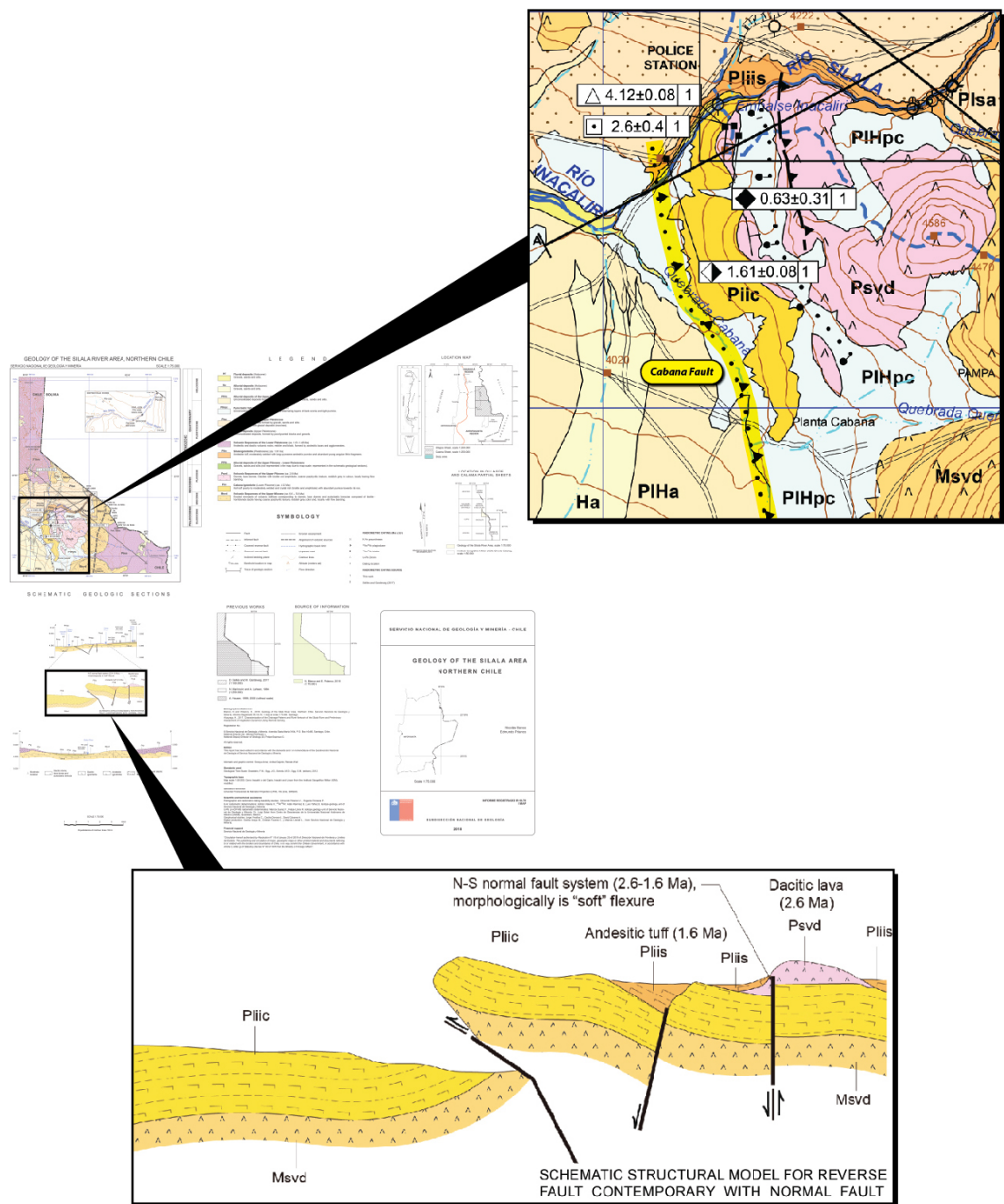


Figure 15. Pleistocene deformation in the Silala River area, represented by Cabana reverse fault activity (Blanco and Polanco, 2018).

3.3.1 The Uyuni-Khenayani Fault System

This system “corresponds to an east vergent thrust zone, which separates the western sector of the southern Altiplano from the Lipez Basin, a Cenozoic intramontane basin located between that area of thrusts and the converging eastern system, Falla San Vicente [SVFZ on Figure 16]. The upper block of the Uyuni-Khenayani thrust system involves an Ordovician and Silurian-Devonian basement; which folded, fractured and elevated, supports some Mesozoic remnants and an incomplete coverage of Cenozoic” (Martínez et al., 1994).

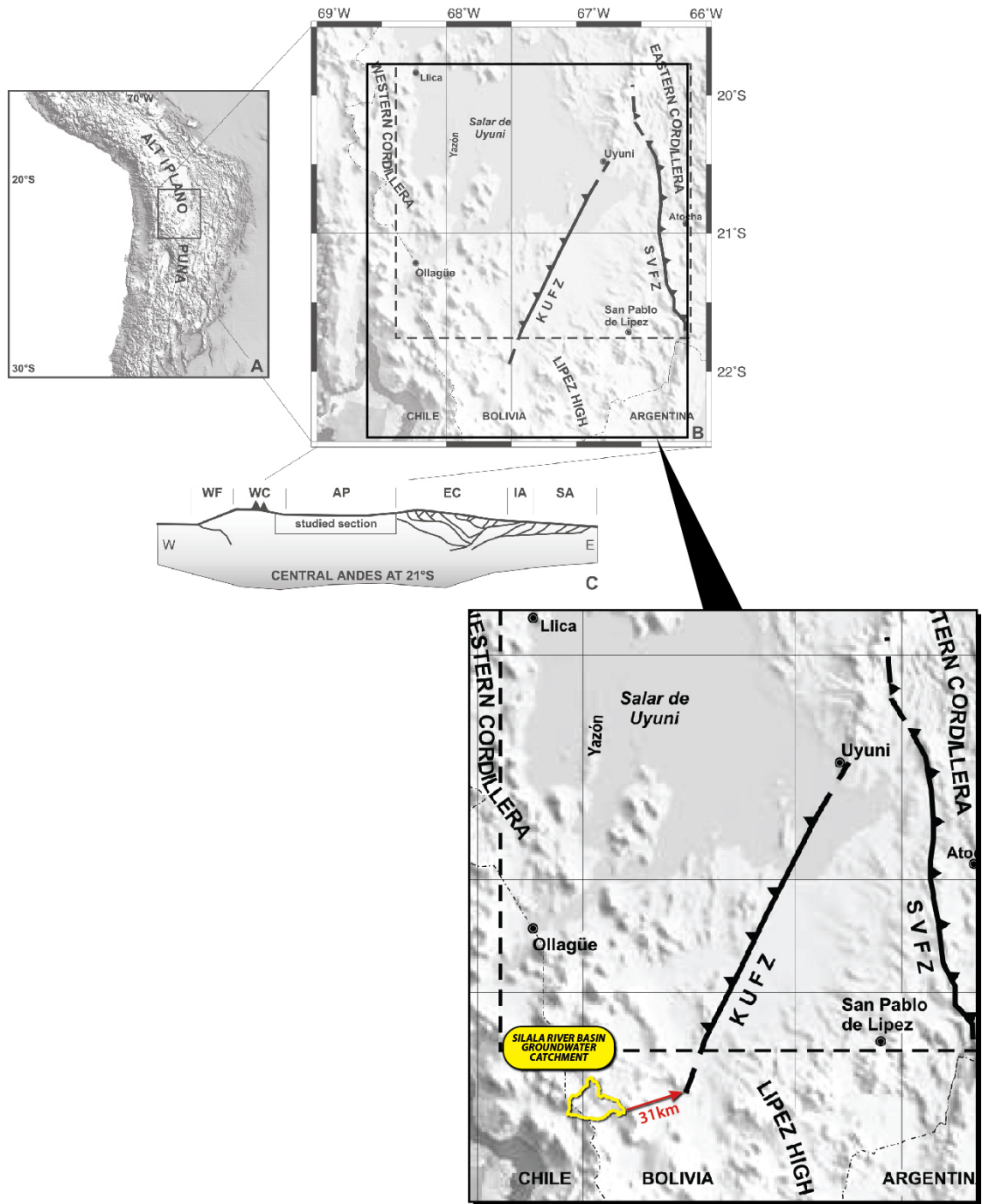


Figure 16. Uyuni-Khenayani fault system, located 31 km to ENE of the Silala River basin groundwater catchment (Elger, 2003). The abbreviation KUFZ refers to the Uyuni-Khenayani Fault System used in this report.

“The structural complexity of the upper hanging wall of the Uyuni-Khenayani crustal thrust system (UKFS) results from the arrangement of Andean deformation to a substratum previously deformed by Hercynian tectonics and then subdivided into smaller, scaled and eroded blocks during the Upper Cretaceous. The successive deformations, synsedimentary in the Tertiary, reactivated the paleo-structures and caused the propagation, to the east, of a system of thrusts and associated folds, accompanied by superficial landslides” (Martínez et al., 1994).

In several studies it has been documented that the UKFS was active between the Oligocene and Middle Miocene (27-10 Ma) (Sempere et al., 1990; Martínez et al., 1994; Elger, 2003; Elger et al., 2005). This deformation would have finished between 11 and 10 Ma when its trace was sealed by subhorizontal tuffs and dacitic lavas dated at 10 ± 0.3 Ma and 11 ± 0.5 Ma, respectively. (Silva-González, 2004 in Elger et al., 2005). The Upper Miocene, sinistral faults, of NW-SE orientation, tear the UKFS (Martínez et al., 1994).

On the other hand, some authors indicate that the UKFS extends beyond Bolivia and into Chile and is related to the system of thrusts of the Cordillera de Domeyko - Salar de Atacama in Chile, with similar structural characteristics (Buddin et al., 1993; Martínez et al., 1994). In the Cordillera de Domeyko - Salar de Atacama area, tectonic activity has been documented in the Upper Oligocene with normal faults and a system of reverse faults in the Upper Miocene, including salt diapirism during Quaternary (Mpodozis et al., 2000; Henríquez et al., 2014). Such an extension of the fault system would not pass through the Silala River groundwater catchment (Figure 16).

At item 9.1 “Regional Geology of Bolivia, chapter 9, Conclusions and recommendations” (BR, Vol. 3, p. 397), the Bolivian authors write the following:

“The area of the Silala Springs was geologically formed during the Upper Miocene (7.5 to 8 Myr), when the Silala Ignimbrites were deposited. The latter were strongly fractured and jointed by tectonic movements caused by the Khenayani Faulting system.”

There is clearly a mistake in this official translation because there are two very important omissions that change the sense of exposed ideas. The omissions are: the age “of 27-17 Ma” of the Khenayani Fault System and the phrase “"that is, before the ignimbrite deposition”.

A literal translation of the original Spanish document (SERGEOMIN, 2003) is:

“The Silala Ignimbrites are deposited during the Upper Miocene (between 8 to 7.5 Ma) (A).

These rocks are strongly fractured and diaclasized by the tectonic movements caused by the Khenayani Fault System *of 27-17 Ma, that is, before the ignimbrite deposition (B.)*.”

We have the following comments:

- (1) The oldest age obtained in the Silala Ignimbrites (Bol), by Bolivia is 6.6 ± 0.5 Ma (K-Ar in biotite; BR, Vol. 4, p. 115), so the Bolivian statement (A), above, is incorrect.
- (2) The assertion (B) is a contradiction. It is not possible that an older tectonic process (27-17 Ma) can affect younger rocks. The fracturing in the Silala Ignimbrites (Bol) must have been caused by an event after the deposition of these ignimbrites, i.e., younger than 6.6 Ma.
- (3) It would appear that the incorrect age of 7.8 ± 0.3 Ma attributed to the Silala Ignimbrites (Bol) has been used to justify the proposed faults as active structures of the Uyuni-Khenayani Fault System, even though this fault system had ceased to be active more recently than 10-8 Ma.

3.3.2 Ratio of deformation and crustal depth

In relation to fracturing found in the Silala Ignimbrite (Chi), it is most probable that these structures have been formed by cooling or gravitational adjustments rather than by tectonic effects. Indeed, much experimental data in rocks show that in the upper crust the differential stress due to the tectonic forces increases linearly from the surface,

where it has a zero value, with depth (Brace and Kohlstedt, 1980; Kohlstedt et al., 1995; Townend, 2006; Scholz, 2019) (Figure 17).

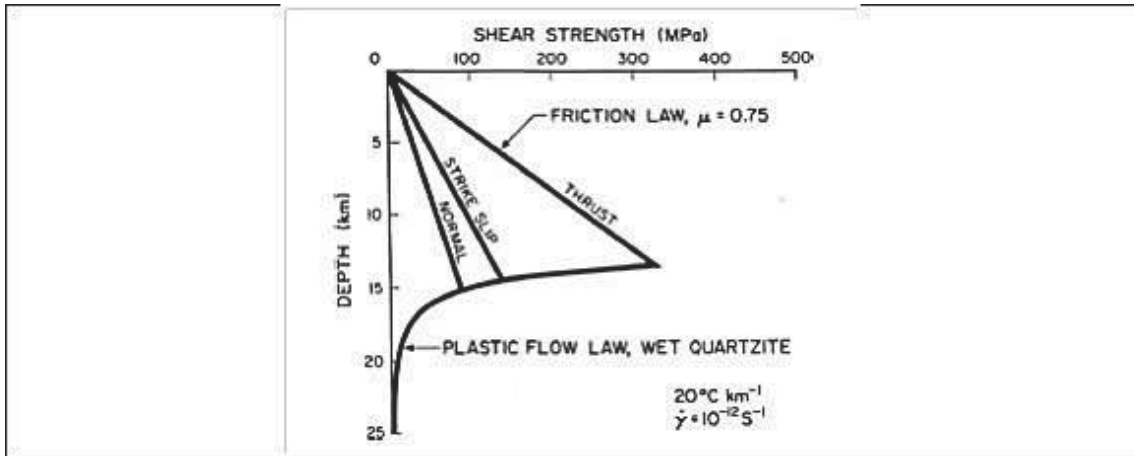


Figure. 17. Graph showing the linear increase of the deformation stress with the depth in the crust, with a value of zero at the earth's surface (Scholz, 2019).

Since the Silala Ignimbrite (Chi) constitutes a thin sheet on the surface of the land, with a free face (the alluvial cover is not considered because it is very thin), it is very unlikely that it is affected by tectonic stresses and, therefore, the family of fractures that affect it are most likely to be cooling and/or gravitational fractures, and cannot be attributed to a regional structural system such as the UKFS, which also was most active over the Oligo-Miocene period, well before the dated Silala Ignimbrite (Chi) or the Cabana Ignimbrite (Chi) was deposited, or the Silala Ignimbrites (Bol).

4. CONCLUSIONS

1. The so-called Silala Ignimbrites (Bol), correspond to several pyroclastic flows of contrasting chemical composition, radiometric age and stratigraphic position. This Bolivian unit is composed of three pyroclastic flows, two of them of dacitic-rhyolitic composition, of 6.6 Ma, although we suspect that this date is incorrect (see section 2.1.1) and 3.2 Ma, and a third of andesitic composition, of 1.6 Ma (Chilean date). The latter corresponds to the Silala Ignimbrite (Chi) that overlaps unconformably onto the ignimbrite of 6.6 Ma. found in Bofedales Sur (Orientales) and that in Chilean territory is deposited on top of the Cabana Ignimbrite of 4.12 Ma. (SERNAGEOMIN, 2017). Bolivian ignimbrites of 6.6 and 3.2 Ma have not been recognized in the area of the Silala River basin in Chilean territory.
2. The Bolivian affirmation that Silala Chico (Cerrito de Silala) volcanic dome intrudes the Silala Ignimbrites (Bol), which was dated at 6.04 ± 0.07 Ma (biotite), is not correct. The Silala Ignimbrite (Chi), dated 1.6 Ma covers in onlap the deposits of this volcanic dome at its base.
3. As a general conclusion, the unit Silala Ignimbrites (Bol) is assigned, erroneously, to the Upper Miocene (7.8 Ma). The supposed structures that affect it and that control the upwelling of groundwater in the springs of Silala River (e.g. the proposed Silala Fault) are attributed to the activity of the Uyuni-Khenayani Fault System, a structural system which was active until ca. 10 Ma and, furthermore, is 31 kilometres to ENE away from the Silala River area. We know that the ignimbrite units that are exposed in the Silala River ravine correspond to Silala Ignimbrite (Chi) unit, dated at 1.6 Ma. It would appear that the incorrect age attributed to these rocks has been used to justify the proposed faults as active structures of the Uyuni-Khenayani Fault System, even though this fault system had ceased to be active more recently than 10-8 Ma.
4. The incorrectly interpreted regional faults in the area of the Bofedales Sur (Orientales) and Bofedales Norte (Cajones) springs that feed the Silala River, are

conveniently located where the groundwater sources are located. The interpreted data for these proposed faults are found in four structural domains. Structural domains 2 and 3 are of a different nature to domains 1 and 4. That is, domains 2 and 3 are shear or compression fractures, which do not conduct water because these types of fractures are closed. However, this criterion has not been considered for the Bofedales Norte (Cajones) springs, where Bolivian geologists interpret the existence of a NE-SW dextral fault through which groundwater is conducted and emerges. This structure corresponds to a shear fracture or closed fracture, therefore there should be no groundwater springs there. This is a clear contradiction.

5. The family of fractures that affect the Silala Ignimbrite (Chi), 1.6 Ma, which is considered as a thin exposed sheet on the surface of the land, correspond to cooling fractures and/or gravitational adjustments during and soon after deposition, and they cannot be attributed to the effects of crustal tectonics, nor to the regional structural system such as the Uyuni-Khenayani Fault System, which was active between the Oligocene and the Upper Miocene, ending its activity ca. 10-8 Ma.
6. The normal faults of the principal structural trend in the Silala River area are of NW-SE orientation (125 to 305 degrees) and these have been related by Bolivia to the Inacaliri Graben. However, according to the determined stress model, particularly for Domain 4, normal faults should have a WNW-ESE orientation (275 to 95 degrees). This suggests that the Graben Inacaliri is a structure linked to the magmatic chambers of the effusive centres and not to a result of deep and ancient regional faults.
7. The Silala-Llancor lineament has been used by Bolivia as a geological artefact related to the upwelling of water in the Bofedales Sur (Orientales) area. The presented data contradict the kinematics deduced for this structure and the Bolivian model of the orientation of the regional stress field. The fault escarpments supposedly associated with it correspond to fronts of lobate lava flows.
8. The magnetic data presented by Bolivia to justify the regional lineaments are not valid, since the basic information is not presented (height of flight, direction of flight

lines, spacing of flight lines), which would allow correction for geophysical artefacts conditioned by the direction of the flight lines and depth of investigation.

9. The only evidence of compressive deformation registered in the area is documented between 2.6-1.6 Ma (Lower Pleistocene), and is linked to the activity of the Cabana Fault, in Chilean territory, and is not linked to an Oligo-Miocene deformation as proposed by the Bolivian geologists.

10. It is stated that the Silala River ravine was carved by erosive activity of the glacial ice through a Silala fault trace, which is attributed to the Uyuni-Khenayani Fault System activity. It has been clearly established that the origin of the Silala River ravine has been excavated by river action during the Upper Pleistocene and 8,400 cal. year BP, and that the ice action had no part in the formation of the ravine (SERNAGEOMIN, 2017; Latorre and Frugone, 2017). It should be noted that glacial activity never generates valleys as narrow as 80 meters (the ravine of the Silala River to SW of Bofedales Norte (Cajones)). In the Silala River area, where vestiges of glacial activity are found, the valleys formed by the action of the ice and that descend from the volcanic edifices have dimensions of 480 to 740 metres wide, far greater than the channel of fluvial origin of the Silala River.

11. This review of several Bolivian technical documents has identified many errors in the mapping of the ignimbrite units in Bolivia. It demonstrates that the contact relationships and stratigraphic position proposed by Bolivia have been mistaken, data have been ignored, and the Bolivian mineralogical description of the ignimbrites is confused and contradictory. They have been grouped into a single age-bounded unit, yet there are published age dates that indicate they can be separated into at least two separate units of distinctly different ages.

5. ACKNOWLEDGEMENTS

The authors thanks to colleague Andrew J. Tomlinson, PhD in structural geology, SERNAGEOMIN geologist, for his contributions to the discussion of faults and structures in general as well as providing specialized literature in the area of crustal deformation. We also thank the librarian of SERNAGEOMIN, Mrs. María Teresa Cortés, who provided us with access to the technical bibliography.

6. REFERENCES

- Almendras, A.O., Balderrama, Z.B., Menacho, L.M., and Quezada, C.G., 2002. Mapa geológico hoja Volcán Ollagüe, escala 1:250.000. *Mapas Temáticos de Recursos Minerales de Bolivia*. SERGEOMIN, Bolivia.
- Baker, M.C.W. and Francis, P.W., 1978. Upper Cenozoic volcanism in the central Andes - ages and volumes. *Earth and Planetary Science Letters*, 41 (2), 175–187.
- Blanco, N. and Polanco, E., 2018. *Geology of the Silala River Basin, Northern Chile*. Servicio Nacional de Geología y Minería (SERNAGEOMIN) (**Chile's Reply, Vol. 3, Appendix C to Annex XIV**).
- Brace, W.F. and Kohlstedt, D.L., 1980. Limits on lithospheric stress imposed by laboratory experiments. *Journal of Geophysical Research: Solid Earth*, 85 (B11), 6248-6252.
- Buddin, T., Stimpson, I. and Williams, G., 1993. North Chilean forearc tectonics and Cenozoic plate kinematics. *Tectonophysics*, 220, 193-203.
- Danish Hydraulic Institute (DHI), 2019. *Analysis and assessment of Chile's reply to Bolivia's counter-claims on the Silala Case. (Bolivia's Rejoinder, Vol. 5, Annex 24)*.
- Elger, K., 2003. Analysis of deformation and tectonic history of the Southern Altiplano Plateau (Bolivia) and their importance for plateau formation, Phd Thesis. *Scientific Technical Report STR; 03/05, Potsdam: Deutsches GeoForschungsZentrum GFZ*.
- Elger, K., Onccken, O. and Glodny, J., 2005. Plateau-style accumulation of deformation: Southern Altiplano. *Tectonics*, 24 (4), TC4020.
- Gimeno, D., Díaz, N., García-Vellés, M. and Martínez-Manent, S., 2003. Genesis of bottom vitrophyre facies in rhyolitic pyroclastic flow: a case study of syneruptive glass weldind (nuraxu unit, Sulcis, SW Sardinia, Italy). *Journal of Non-Crystalline Solids*, 323, 91-96.
- Henríquez, S., Becerra, J. and Arriagada, C., 2014. *Geología del Área San Pedro de Atacama Geológica, Región de Antofagasta*. Servicio Nacional de Geología y Minería, Carta Geológica de Chile, Serie Geología Básica 171, 1 mapa, escala 1:100.000. Santiago.
- Kohlstedt, D.L., Evans, B. and Mackwell, S.J., 1995. Strength of the lithosphere: Constraints imposed by laboratory experiments. *Journal of Geophysical Research: Solid Earth*, 100 (B9), 17587-17602.

- Latorre, C. and Frugone, M., 2017. *Holocene sedimentary history of the Río Silala (Antofagasta Region, Chile)*. (**Chile's Memorial, Vol. 5, Annex IV**).
- Le Maitre, R.W., 2002. *Igneous Rocks. A Classification and Glossary of Terms. Recommendations of the International Union of Geological Sciences Subcommission on the Systematics of Igneous Rocks*, Cambridge University Press, Cambridge, England.
- Lohmar, S., Robin, C., Gourgaud, A., Clavero, J., Parada, M.A., Moreno, H., Ersoy, O., López-Escobar, L. and Naranjo, J.A., 2007. Evidence of magma-water interaction during the 13,800 years BP explosive cycle of the Licán Ignimbrite, Villarrica volcano (southern Chile). *Revista Geológica de Chile*, 34 (2), 233-247.
- Martínez, C., Soria, E., Uribe, H., Escobar, A. and Hinojosa, A., 1994. Estructura y evolución del altiplano suroccidental: el sistema de cabalgamientos de Uyuni-Khenayani y su relación con la sedimentación terciaria. *Revista Técnica de Yacimientos Petrolíferos Fiscales Bolivianos*, 15 (3-4), 245-264.
- Mpodozis, C., Blanco, N., Jordan, T. and Gardeweg, M.C., 2000. *Estratigrafía y deformación del Cenozoico Tardío en la región norte de la Cuenca del Salar de Atacama: la zona de Vilama-Pampa Vizcachitas*, IX Congreso Geológico de Chile, Puerto Varas.
- Ríos, H., Baldellón, E., Mobarec, R. and Aparicio, H., 1997. Mapa Geológico Hojas Volcán Inacaliri y Cerro Zapaleri, escala 1:250.000. *Mapas Temáticos de Recursos Minerales de Bolivia*, SGM Serie II-MTB-15B. SERGEOMIN.
- Scholz, C.H., 2019. *The mechanics of earthquakes and faulting*. Cambridge University Press, Cambridge, England.
- Sellés, D. and Gardeweg, M., 2017. *Geología del área Ascotán-Cerro Inacaliri, Región de Antofagasta*. Servicio Nacional de Geología y Minería, Carta Geológica de Chile, Serie Geología Básica 190, 1 mapa escala 1:100.000. Santiago. (**Chile's Memorial, Vol. 6, Appendix G**).
- Sempere, T., Herail, G., Oller, J. and Bonhomme, M., 1990. Late Oligocene-early Miocene major tectonic crisis and related basins in Bolivia. *Geology*, 18, 946-949.
- SERGEOMIN (National Service of Geology and Mining), 2003. *Study of the Geology, Hydrology, Hydrogeology and Environment of the Area of the Silala Springs*. (**Bolivia's Rejoinder, Vol. 3, Annex 23.5, Appendix a**).
- SERGEOMIN (National Service of Geology and Mining), 2017. *Structural Geological Mapping of the Area Surrounding the Silala Springs*. (**Bolivia's Rejoinder, Vol. 4, Annex 23.5, Appendix b**). NB: Annex C is submitted as **Appendix A** to the present report. Annex D is submitted as **Appendix B** to the present report.

SERNAGEOMIN (National Geology and Mining Service), 2017. *Geology of the Silala River Basin. (Chile's Memorial, Vol. 5, Annex VIII)*.

Silva-González, P. (2004), *Der südliche Altiplano im Tertiär: Sedimentäre Entwicklung und tektonische Implikationen*, Ph.D. thesis, Freie Univ., Berlin, Germany.

Tibaldi A., Bonali, F. and Corazzato, C., 2017. Structural control on volcanoes and magma paths from local- to orogen-scale: The central Andes case. *Tectonophysics*, 699, 16–41.

Tomás Frías Autonomous University (TFAU), 2018. *Hydrogeological Characterization of the Silala Springs. (Bolivia's Rejoinder, Vol. 4, Annex 23.5, Appendix c)*.

Townend, J., 2006. What do faults feel? Observational constraints on the stresses acting on seismogenic faults. *Washington DC American Geophysical Union Geophysical Monograph Series*, 170, 313-327.

Urquidi, F., 2018. *Technical analysis of geological, hydrological, hydrogeological and hydrochemical surveys completed for the Silala water system. (Bolivia's Rejoinder, Vol. 3, Annex 23.5)*.

APPENDIX A

CONVENIO DE COOPERACIÓN INTERINSTITUCIONAL Y
CONTRATO DE CONSULTORIA DIREMAR - SERGEOMIN



ANEXO C

RESULTADOS DE ANÁLISIS DE LABORATORIO

Calle Federico Suazo N° 1673 Esquina Reyes Ortiz – La Paz - Bolivia
Telf. (591 – 2) 2330981 – 2331236 – Fax 2391725 – 2318295
www.sergeomin.gob.bo



SERVICIO GEOLOGICO MINERO

DIRECCION ESTRATEGICA DE REINVINDICACION MARITIMA, SILALA Y RECURSOS

HIDRICOS INTERNACIONALES MAPEO GEOLOGICO DEL AREA CIRCUNDANTE AL MANANTIAL DEL SILALA

TABLA RESUMINDA DE RESULTADOS DE LABORATORIO



Nº	ESTE (UTM)	NORTE (UTM)	ELEVACION (m.s.n.m)	CODIGO MUESTRA	ENVIADOS LABORATORIO	NOMBRE DE LA ROCA	RESULTADO PETROGRÁFICO	RESULTADO MINERAGRAFICO (Asociaciones Minerales)
1	601181	7565996	4457	7801	SERGEOMIN	LAVA INTERMEDIA	ANDESITA BIOTITICA	
2	604895	7567297	4541	7802	SERGEOMIN	TOBA VITRO CRISTALINA	DACITA BIOTITICA	
3	605449	7566078	4602	7803	SERGEOMIN	LAVA INTERMEDIA	ANDESITA PIROXENICA	
4	608499	7567690	4595	7804	SERGEOMIN	LAVA INTERMEDIA	ANDESITA BIOTITICA	
5	609737	7568016	4597	7805	SERGEOMIN	LAVA ACIDA	DACITA BIOTITICA	
6	606789	7561214	5649	7806	SERGEOMIN	LAVA INTERMEDIA	ANDESITA PIROXENICA	
7	606758	7562878	5041	7807	SERGEOMIN	TOBA CRISTALO VITREA	IGNIMBRITA ANDESITICA	Magnetita-Hematita-Limonita
8	607192	7567230	4601	7808	SERGEOMIN	TOBA CRISTALO VITREA	IGNINBRITA ANDESITICA	Magnetita-Hematita-Limonita
9	600816	7566953	4485	7809	SERGEOMIN	LAVA INTERMEDIA	ANDESITA BIOTITICA	
10	600661	7567938	4547	7810	SERGEOMIN	LAVA BASICA	BASALTO PIROXENICO	
11	600166	7569312	4671	7811	SERGEOMIN	TOBA LITICA INTERMEDIA	ANDESITA PIROXENICA	
12	599317	7568831	4759	7813	SERGEOMIN	TOBA SOLDADA INTERMEDIA	IGNIMBRITA ANDESITICA	
13	603126	7565890	4422	7814	SERGEOMIN	TOBA INTERMEDIA	ANDESITA HORNBLENDICA	
14	603483	7564079	4558	7816	SERGEOMIN	LAVA INTERMEDIA	ANDESITA PIROXENICA	
15	606447	7562228	5165	7817	SERGEOMIN	LAVA INTERMEDIA	ANDESITA PIROXENICA	
16	606447	7562228	5165	7818	SERGEOMIN	LAVA INTERMEDIA	ANDESITA PIROXENICA	
17	607792	7564663	4802	7820	SERGEOMIN	LAVA INTERMEDIA	ANDESITA PIROXENICA	
18	601256	7572117	5181	7821	SERGEOMIN	LAVA INTERMEDIA	ANDESITA HORNBLENDICA	
19	601256	7572117	5181	7822	SERGEOMIN	LAVA INTERMEDIA	ANDESITA HORNBLENDICA	
20	606578	7568225	4555	7824	SERGEOMIN	VOLCANO SEDIMENTARIA	ARCILLITA	
21	600813	7566226	4367	7702	SERGEOMIN	TOBA CRISTALO VITREA	IGNINBRITA ANDESITICA	Hematita-Magnetita-Calcopirita Limonita
22	600973	7566397	4395	7706	SERGEOMIN	TOBA CRISTALO VITREA	IGNINBRITA ANDESITICA	Hematita-Magnetita-Calcopirita Limonita
23	604396	7576010	4522	7708	SERGEOMIN	TOBA	IGNIMBRITA ANDESITICA	
24	601942	7564641	4606	7712	SERGEOMIN	LAVA ACIDA	DACITA BIOTITICA	
25	602052	7564099	4756	7713	SERGEOMIN	LAVA INTERMEDIA	ANDESITA BIOTITICA CUARZOSA	
26	606242	7568071	4593	7716	SERGEOMIN	TOBA VITRO CRISTALINA	DACITA BIOTITICA	
27	600879	7566738	4437	7717	SERGEOMIN	TOBA VITRO CRISTALINA	DACITA BIOTITICA	
28	603557	7567635	4500	7720	SERGEOMIN	LAVA INTERMEDIA	ANDESITA CUARZOSA	
29	605051	7569399	4580	7721	SERGEOMIN	TOBA VITRO CRISTALINA	DACITA BIOTITICA	
Nº	ESTE (UTM)	NORTE (UTM)	ELEVACION (m.s.n.m)	CODIGO MUESTRA	ENVIADOS LABORATORIO	NOMBRE DE LA ROCA	RESULTADO PETROGRÁFICO	RESULTADO MINERAGRAFICO (Asociaciones Minerales)
30	611232	7567663	4626	7722	SERGEOMIN	TOBA VITRO CRISTALINA	DACITA BIOTITICA	

31	611225	7567577	4640	7723	SERGEOMIN	TOBA VITRO CRISTALINA	DACTITA BIOTITICA
32	609442	7569033	4630	7726	SERGEOMIN	LAVA ACIDA	DACTITA DE BIOTITA Y HORNBLENDA
33	601557	7573260	4834	7727	SERGEOMIN	LAVA INTERMEDIA	ANDESITA BIOTITICA OXIDADA
34	605330	7574972	4741	7729	SERGEOMIN	LAVA INTERMEDIA	ANDESITA BIOTITICA OXIDADA
35	602573	7575219	4607	7732	SERGEOMIN	LAVA INTERMEDIA	ANDESITA BIOTITICA OXIDADA
36	610800	7562642	4647	7825	SERGEOMIN	LAVA INTERMEDIA	ANDESITA PIROXENICA
37	619857	7562113	5107	7827	SERGEOMIN	LAVA ACIDA	DACTITA PIROXENICA
38	608546	7556911	5420	7830	SERGEOMIN	LAVA INTERMEDIA	ANDESITA HORNBLENDICA
39	598653	7567307	4609	7833	SERGEOMIN	LAVA INTERMEDIA	ANDESITA HORNBLENDICA
40	620023	7566597	4864	7737	SERGEOMIN	LAVA INTERMEDIA	ANDESITA PIROXENICA
41	595872	7569264	5631	7743	SERGEOMIN	LAVA INTERMEDIA	ANDESITA HORNBLENDICA

CONVENIO DE COOPERACIÓN INTERINSTITUCIONAL Y
CONTRATO DE CONSULTORÍA DIREMAR - SERGEOMIN



RESULTADOS ANÁLISIS DE PETROGRAFÍA

Calle Federico Suazo N° 1673 Esquina Reyes Ortiz – La Paz - Bolivia
Telf. (591 – 2) 2330981 – 2331236 - Fax 2391725 – 2318295
www.sergeomin.gob.bo

INTERESADO:

Ing. Adolfo Orsolini Campana

UBICACIÓN:

Proyecto Mapeo Geológico del Área del Manantial del Silala

FECHA:

22 de Junio de 2016

Nº LAB: SGM-087/17

Muestra 7702.

ANÁLISIS PETROGRÁFICO**Descripción Macroscópica.-**

Fragmento de una roca de origen piroclástico (toba ignimbótica) de composición intermedia, muestra estructura bandeadada o fluidal y textura porfídica de grano medio (>1 mm), donde se observa una intercalación entre bandas lenticulares de color marrón y bandas de tono negruzco, ambas muestran cristales de feldespatos blanquecinos, escaso cuarzo, piroxenos, pómex alargadas y óxidos de hierro diseminados, rodeados por una pasta ferruginosa y vítreo, con mayor presencia de hierro en las bandas negruzcas. La toba cristalo-vítreo presenta alto grado de soldadura (ignimbrita), por lo que muestra elevada dureza y compactación, y también es llamada toba soldada.

Descripción Microscópica.-**Mineralogía.-**

Cuarzo.- Es un componente muy reducido de la toba, presente en forma de cristales anhédrales con bordes sub-angulosos, de hasta 0,5 mm de largo, muestran fracturas y engolfamientos, también se presentan como fragmentos de bordes angulosos (Fig. 1).

Plagioclasas.- Se presentan en abundante porcentaje, en forma de fenocristales subhédrales tabulares y prismáticos, de hasta 2 mm de largo, muestran maclas polisintéticas tipo Albita, y combinada Albita-Carlsbad, con inclusiones de la pasta vítreo, corresponden a la variedad Oligoclasa (An: 25), se hallan fracturadas y ligeramente orientadas (Fig. 1).

Clinopiroxenos.- Se observan en moderado porcentaje, fenocristales subhédrales de hábito prismático y tabular de clinopiroxenos de tono pardo pálido, algunos con maclas polisintéticas, alcanzan hasta 0,7 mm de largo y probablemente se tratan del tipo augita (Fig. 1).

Pasta.- La pasta de la toba es abundante y está conformada principalmente por óxidos de hierro de tono marrón-rojizo del tipo limonita (ferruginosa), más abundante en las bandas oscuras, junto a vidrio volcánico de tonalidad parda oscura que muestra textura masiva, y en menor porcentaje por microlitos de plagioclasas, rodeando a los fenocristales (Fig. 1).

Pómex.- Se observan en reducido porcentaje, pómex blanquecinos de formas ovaladas y alargadas con bordes irregulares, formados por esquirlas de vidrio volcánico, que alcanzan hasta 3 mm de largo, contienen cristales de plagioclasas y minerales máficos muy oxidados.

Óxidos de Hierro.- Se presentan en reducido porcentaje, como pequeños minerales opacos de hábito subhedral, diseminados en la pasta también ferruginosa, que corresponderían a las variedades hematita y magnetita.

Composición porcentual observada.-

Cuarzo (SiO_2).....	2-3 %
Plagioclasas (Oligoclasa) $\text{NaCaAl}(\text{Si}_3\text{O}_8)$	28-30 %
Clinopiroxenos (Augita) ($\text{Mg}, \text{Fe}(\text{SiO}_3)$).....	3-5 %
Pasta (Óxidos de hierro y Vidrio volcánico).....	53-55 %
Pómez (Vidrio volcánico).....	3-4 %
Óxidos de Hierro (Hematita y magnetita).....	2-3 %
Total.....	100 %

Textura y estructura.- La toba presenta una estructura bandeada o fluidal y textura porfídica de grano medio (>1 mm), con pasta ferruginosa y vítreo de textura masiva, pómez y diseminación de óxidos de hierro (Fig. 1).

Nombre de la roca.- De acuerdo al análisis petrográfico, es una roca piroclástica (toba cristalo-vítreo soldada) de composición intermedia, que corresponde a una **Ignimbrita ANDESÍTICA**.

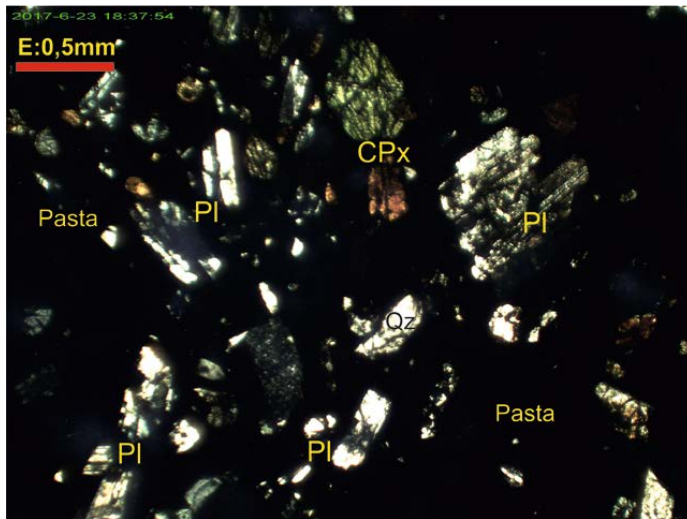


Fig. 1. Muestra 7702, aumento 4x, polarizadores X. Toba Ignimbritica Andesítica, con fenocristales de plagioclasas (PI), poco cuarzo (Qz), clinopiroxenos (CPx), pómez, y una pasta ferruginosa-vítreo.

Analizado por: Ing. José Luis Argandoña C.
ENCARGADO DEL LABORATORIO

INTERESADO:

Ing. Adolfo Orsolini Campana

UBICACIÓN:

Proyecto Mapeo Geológico del Área del Manantial del Silala

FECHA:

23 de Junio de 2016

Nº LAB: SGM-088/17

Muestra 7706.

ANÁLISIS PETROGRÁFICO

Descripción Macroscópica.-

Fragmento de una roca de origen piroclástico (toba ignimbótica) de composición intermedia, muestra estructura bandeadada o fluidal y textura porfídica de grano medio (>1 mm), donde se observa una intercalación entre bandas lenticulares de color marrón y otras bandas de tono negruzco, ambas muestran cristales de feldespatos blanquecinos, muy escaso cuarzo, piroxenos, pómex alargadas y abundantes óxidos de hierro diseminados, rodeados por una pasta ferruginosa y vítreo, con mayor contenido de hierro en las bandas negruzcas. La toba cristalo-vítreo presenta alto grado de soldadura (ignimbrita), por lo que muestra elevada dureza y compactación, y también es llamada toba soldada.

Descripción Microscópica.-

Mineralogía.-

Cuarzo.- Es un componente escaso de la toba, presente en forma de cristales anhedrales con bordes sub-angulosos, de tamaño inferior a 0,5 mm de largo, muestran fracturas y engolfamientos, también se observan como fragmentos de bordes angulosos (Fig. 2).

Plagioclasas.- Se presentan en muy abundante porcentaje, en forma de fenocristales subhédrales tabulares y prismáticos, de hasta 1,5 mm de largo, muestran maclas polisintéticas tipo Albita, y combinada Albita-Carlsbad, con inclusiones de la pasta vítreo, corresponden al límite entre los tipos Oligoclásica-Andesina (An: 30), se hallan fracturadas y orientadas (Fig. 2).

Clinopiroxenos.- Se observan en reducido porcentaje, fenocristales subhédrales de hábito prismático y tabular de clinopiroxenos de tono pardo pálido, algunos con maclas polisintéticas, alcanzan hasta 0,6 mm de largo y probablemente se tratan del tipo augita (Fig. 2).

Pasta.- La pasta de la toba es abundante y está conformada principalmente por óxidos de hierro de tono marrón-rojizo del tipo limonita (ferruginosa), que es más abundante en las bandas oscuras, junto a vidrio volcánico de tono pardo oscuro que muestra textura masiva, y en menor porcentaje por microlitos de plagioclasas, rodeando a los fenocristales (Fig. 2).

Pómex.- Se observan en reducido porcentaje, pómex blanquecinos de formas ovaladas y alargadas con bordes irregulares, formados por esquirlas de vidrio volcánico, que alcanzan hasta 2,5 mm de largo, contienen micro-cristales de plagioclasas.

Óxidos de Hierro.- Se presentan en reducido porcentaje, como pequeños minerales opacos de hábito subhedral, diseminados en la pasta también ferruginosa, que corresponderían a las variedades hematita y magnetita.

Composición porcentual observada.-

Cuarzo (SiO_2).....	1-2 %
Plagioclasas (Oligoclasa-Andesina) $\text{NaCaAl}(\text{Si}_3\text{O}_8)$	31-33 %
Clinopiroxenos (Augita) $(\text{Mg}, \text{Fe})(\text{SiO}_3)$	3-4 %
Pasta (Óxidos de hierro y Vidrio volcánico).....	53-55 %
Pómez (Vidrio volcánico).....	2-3 %
Óxidos de Hierro (Hematita y magnetita).....	2-3 %
Total.....	100 %

Textura y estructura.- La toba presenta estructura bandeada o fluidal y textura porfídica de grano medio (>1 mm), con pasta ferruginosa y vítreas de textura masiva, pómez y diseminación de óxidos de hierro (Fig. 2).

Nombre de la roca.- De acuerdo al análisis petrográfico, es una roca piroclástica (toba cristalo-vítreas soldadas) de composición intermedia, que corresponde a una **Ignimbrita ANDESÍTICA**.

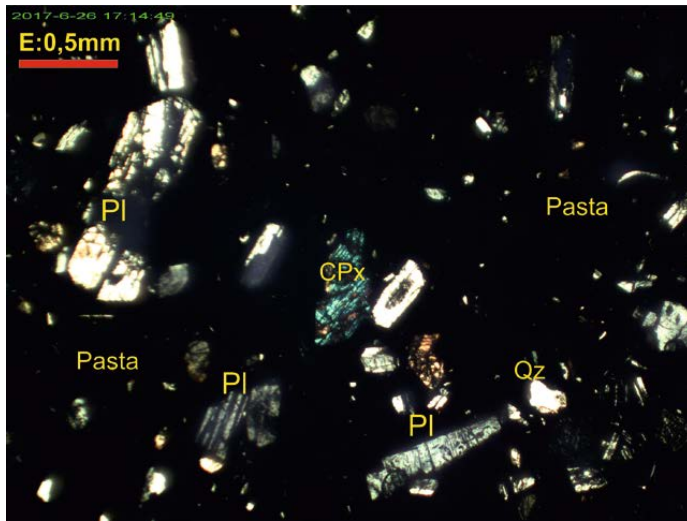


Fig. 2. Muestra 7706, aumento 4x, polarizadores X. Toba Ignimbritica Andesitica, con fenocristales de plagioclasas (PI), escaso cuarzo (Qz), clinopiroxenos (CPx), pómez, y una pasta ferruginosa-vítreas.

Analizado por: Ing. José Luis Argandoña C.
ENCARGADO DEL LABORATORIO

INTERESADO:

Ing. Adolfo Orsolini Campana

UBICACIÓN:

Proyecto Mapeo Geológico del Área del Manantial del Silala

FECHA:

04 de Julio de 2017

Nº LAB: SGM-115/17

Muestra 7712.

ANÁLISIS PETROGRÁFICO**Descripción Macroscópica.-**

Fragmento de una roca de origen volcánico (lava), de color gris con superficies de meteorización, composición ácida, muestra estructura holocristalina y textura porfídica de grano medio (>2 mm), donde se observan cristales de feldespatos blanquecinos, escaso cuarzo, biotita, anfíboles, piroxenos y óxidos de hierro diseminados, rodeados por una pasta de grano muy fino, contiene agregados de calcita llenando pequeñas cavidades de la roca, la cual muestra elevada dureza y compactación.

Descripción Microscópica.-**Mineralogía.-**

Cuarzo.- Es un componente moderado de la lava, presente en forma de fenocristales anhedrales con bordes sub-redondeados de hasta 2,5 mm de largo, muestran fracturas y engolfamientos, también se presentan como fragmentos de bordes sub-angulosos (Fig. 3).

Plagioclasas.- Se presentan en muy abundante porcentaje, en forma de fenocristales subhédrales tabulares y prismáticos, de hasta 5 mm de largo, muestran zonación, maclas polisintéticas tipo Albita y combinadas Albita-Carlsbad, con bordes de reacción, corresponden a la variedad Andesina (An: 35), se hallan fracturadas y ligeramente orientadas (Fig. 3).

Biotita.- Se presenta en moderada proporción, en forma de fenocristales subhédrales tabulares y euhédrales poligonales que alcanzan hasta 4 mm de largo, de color marrón oscuro por la oxidación de sus bordes y planos de exfoliación, con inclusiones de plagioclasas.

Clinopiroxenos.- Se observan en reducido porcentaje, fenocristales subhédrales de hábito prismático y de tono verdoso pálido, de hasta 1 mm de largo, se trata del tipo augita (Fig. 3).

Hornblenda.- Se observan en reducido porcentaje fenocristales euhédrales poligonales de color marrón, se hallan reemplazados parcialmente por limonita, alcanzan hasta 3 mm de largo.

Pasta.- La pasta de la lava es abundante y está formada principalmente por microlitos de plagioclasas ligeramente orientados con textura afieltrada, y en menor porcentaje por óxidos de hierro diseminados de tono marrón oscuro del tipo limonita y hematita (Fig. 3); también se observan en escaso porcentaje micro-cristales de apatito de hábito prismático.

Óxidos de Hierro.- Se presentan en reducido porcentaje, como pequeños minerales opacos de hábito anhedral, diseminados en la pasta y sobre todo alterando a cristales de biotita y hornblenda, que corresponderían a las variedades hematita y limonita.

Calcita.- Se observan agregados anhedrales de calcita secundaria de grano fino y de color blanquecino, llenando pequeñas cavidades, mejor observables en la muestra de mano.

Composición porcentual observada.-

Cuarzo (SiO_2).....	6-8 %
Plagioclasas (Andesina) $\text{NaCaAl}(\text{Si}_3\text{O}_8)$	23-25 %
Biotita ($\text{K}_2(\text{Mg},\text{Fe})_2(\text{OH})_2(\text{AlSiO}_{10})$).....	3-5 %
Clinopiroxenos (Augita) ($\text{Mg},\text{Fe})(\text{SiO}_3)$	2-3 %
Hornblenda $\text{Ca}_2(\text{Mg},\text{Fe},\text{Al})_5(\text{OH})_2[(\text{Si},\text{Al})_4\text{O}_{11}]_2$	1-2 %
Pasta (microlitos de plagioclasas).....	50-52 %
Óxidos de Hierro (Hematita y limonita).....	2-3 %
Calcita (CaCO_3).....	1-2 %
Total.....	100 %

Textura y estructura.- Presenta estructura holocrystalina y textura porfídica de grano medio (>2 mm), con pasta microlítica de textura afieltrada y disseminación de óxidos de hierro (Fig. 3).

Nombre de la roca.- De acuerdo al análisis petrográfico, es una lava de composición ácida, que corresponde a una **DACITA BIOTÍTICA**, ligeramente oxidada, contiene cavidades con calcita.

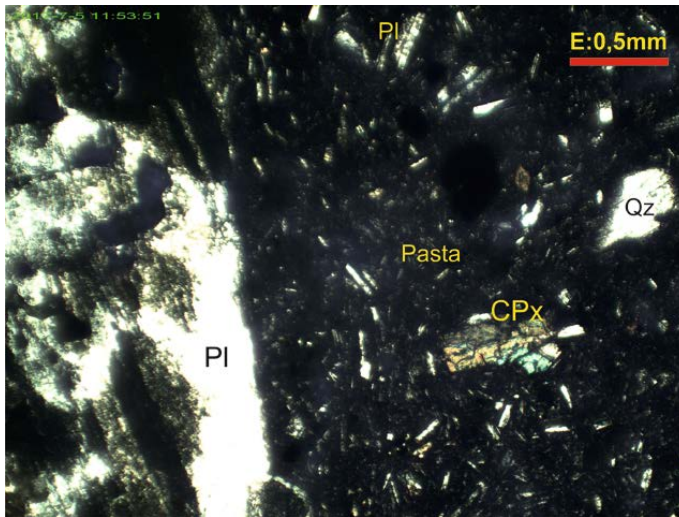


Fig. 3. Muestra 7712, aumento 4x, polarizadores X. Lava Dacítica, con fenocristales de plagioclasas (PI), cuarzo (Qz), clinopiroxenos (CPx) y pasta con microlitos de plagioclasas.

Analizado por: Ing. José Luis Argandoña C.
ENCARGADO DEL LABORATORIO

INTERESADO:

Ing. Adolfo Orsolini Campana

UBICACIÓN:

Proyecto Mapeo Geológico del Área del Manantial del Silala

FECHA:

04 de Julio de 2017

Nº LAB: SGM-116/17

Muestra 7716.

ANÁLISIS PETROGRÁFICO**Descripción Macroscópica.-**

Fragmento de una roca de origen piroclástico (toba vitro-cristalina), de color gris-rosáceo con superficies de meteorización, de composición ácida, muestra estructura hipocristalina y textura porfídica de grano medio (>1 mm), donde se observan cristales de feldespatos, cuarzo, biotita con orientación, pómex blanquecinas y óxidos de hierro diseminados, rodeados por una pasta vítreos, muestra moderado grado de soldadura y de dureza.

Descripción Microscópica.-**Mineralogía.-**

Cuarzo.- Es un componente moderado de la toba, presente en forma de fenocristales anhédrales con bordes sub-angulosos de hasta 2 mm de largo, muestran fracturas y engolfamientos, también se presentan como fragmentos de bordes angulosos (Fig. 4).

Plagioclásas.- Se presentan en abundante porcentaje, en forma de fenocristales subhédrales tabulares y prismáticos, de hasta 2,5 mm de largo, muestran zonación, maclas polisintéticas tipo Albita y combinadas Albita-Carlsbad, con bordes de reacción, corresponden a la variedad Oligoclasa (An: 25), se hallan también como fragmentos angulosos (Fig. 4).

Feldespato potásico.- Se observan en reducido porcentaje, fenocristales anhédrales y subhédrales de feldespatos potásicos, sin maclas, de hasta 1,5 mm de largo (sanidina).

Biotita.- Se presenta en moderada proporción, como fenocristales subhédrales prismáticos y euhédrales poligonales que alcanzan hasta 2 mm de largo, de color marrón oscuro por la oxidación de sus bordes y planos de exfoliación, con inclusiones de plagioclásas (Fig. 4).

Pasta.- La pasta de la toba es abundante y está formada principalmente por esquirlas de vidrio volcánico de tono pardo oscuro con textura masiva, junto a óxidos de hierro del tipo limonita (Fig. 2); también se observan en muy escaso porcentaje micro-cristales prismáticos de circón.

Óxidos de Hierro.- Se presentan en reducido porcentaje, como pequeños minerales opacos de hábito anhedral, diseminados en la pasta y sobre todo alterando a cristales de biotita, que corresponderían a las variedades hematita y limonita.

Pómex.- Se observan en moderado porcentaje, pómex blanquecinas de forma ovalada, constituidas por esquirlas de vidrio volcánico de tono pardo y textura masiva que contienen cristales de plagioclásas, cuarzo y biotita, que alcanzan hasta 1 mm de largo en la sección delgada y hasta 2,5 cm en la muestra de mano.

Composición porcentual observada.-

Cuarzo (SiO_2).....	13-15 %
Plagioclasas (Oligoclasa) $\text{NaCaAl}(\text{Si}_3\text{O}_8)$	23-25 %
Biotita ($\text{K}_2(\text{Mg},\text{Fe})_2(\text{OH})_2(\text{AlSiO}_{10})$).....	4-5 %
Feldespato Potásico ($\text{K}\text{AlSi}_3\text{O}_8$).....	2-3 %
Pasta (Vidrio volcánico).....	45-47 %
Óxidos de Hierro (Hematita y limonita).....	2-3 %
Pómez (vidrio volcánico).....	1-2 %
Total.....	100 %

Textura y estructura.- Presenta estructura hipocristalina y textura porfídica de grano medio (>1 mm), con pasta vítreos de textura masiva, pómez y diseminación de óxidos de hierro (Fig.4).

Nombre de la roca.- De acuerdo al análisis petrográfico, es una toba vitro-cristalina de composición ácida, que corresponde a una **DACITA Biotítica**, con contenido de pómez.

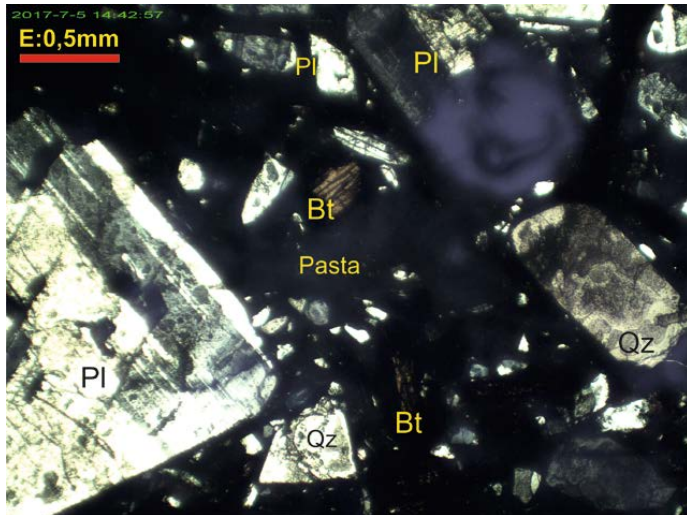


Fig. 4. Muestra 7716, aumento 4x, polarizadores X. Toba Dacítica, con fenocristales de plagioclasas (PI), cuarzo (Qz), biotita oxidada (Bt), pómez y pasta vítreos de textura masiva.

Analizado por: Ing. José Luis Argandoña C.
ENCARGADO DEL LABORATORIO

INTERESADO:

Ing. Adolfo Orsolini Campana

UBICACIÓN:

Proyecto Mapeo Geológico del Área del Manantial del Silala

FECHA:

05 de Julio de 2017

Nº LAB: SGM-117/17

Muestra 7804.

ANÁLISIS PETROGRÁFICO**Descripción Macroscópica.-**

Fragmento de una roca de origen volcánico (lava), de color gris oscuro con superficies de meteorización, de composición intermedia, muestra estructura holocrystalina y textura porfídica de grano medio (>1 mm), donde se observan abundantes cristales de feldespatos blanquecinos, biotita oxidada, piroxenos y óxidos de hierro diseminados, rodeados por una pasta de grano muy fino. La lava muestra elevada dureza y compactación.

Descripción Microscópica.-**Mineralogía.-**

Plagioclasas.- Se presentan en muy abundante porcentaje, en forma de fenocristales subhédrales tabulares y prismáticos, de hasta 2 mm de largo, muestran zonación, maclas polisintéticas tipo Albita y combinadas Albita-Carlsbad, con bordes de reacción, corresponden a la variedad Andesina (An: 35), se hallan fracturadas y marcadamente orientadas (Fig. 5).

Biotita.- Se presenta en reducida proporción, en forma de fenocristales subhédrales y tabulares que alcanzan hasta 0,5 mm de largo, de color marrón oscuro por la oxidación de sus bordes y planos de exfoliación.

Clinopiroxenos.- Se observan en reducido porcentaje, en forma de fenocristales subhédrales de hábito prismático y de tono verdoso pálido, de hasta 0,5 mm de largo, se hallan fracturados y se trata del tipo augita (Fig. 5).

Pasta.- La pasta de la lava es abundante y está formada principalmente por microlitos de plagioclasas marcadamente orientados de acuerdo al flujo de la lava, con textura afieltrada, rodeando a fenocristales, y en menor porcentaje por óxidos de hierro diseminados de tono marrón oscuro del tipo limonita, hematita y magnetita (Fig. 5).

Óxidos de Hierro.- Se presentan en reducido porcentaje, como pequeños minerales opacos de hábito anhedral y cúbico, diseminados en la pasta y alterando a fenocristales de biotita, que corresponderían a las variedades hematita, limonita y probablemente magnetita.

Composición porcentual observada.-

Plagioclasas (Andesina) $\text{NaCaAl}(\text{Si}_3\text{O}_8)$	28-30 %
Biotita $(\text{K}_2(\text{Mg},\text{Fe})_2(\text{OH})_2(\text{AlSiO}_{10}))$	3-5 %
Clinopiroxenos (Augita) $(\text{Mg},\text{Fe})(\text{SiO}_3)$	1-2 %

Pasta (microlitos de plagioclasas).....	58-60 %
Óxidos de Hierro (Hematita, limonita, magnetita).....	2-3 %
Total.....	100 %

Textura y estructura.- Presenta una estructura holocrystalina y textura porfídica de grano medio (>1 mm), con pasta microlítica de textura afieltrada y disseminación de óxidos de hierro (Fig. 5).

Nombre de la roca.- De acuerdo al análisis petrográfico, es una lava de composición intermedia, que corresponde a una **ANDESITA Biotítica**, ligeramente oxidada.

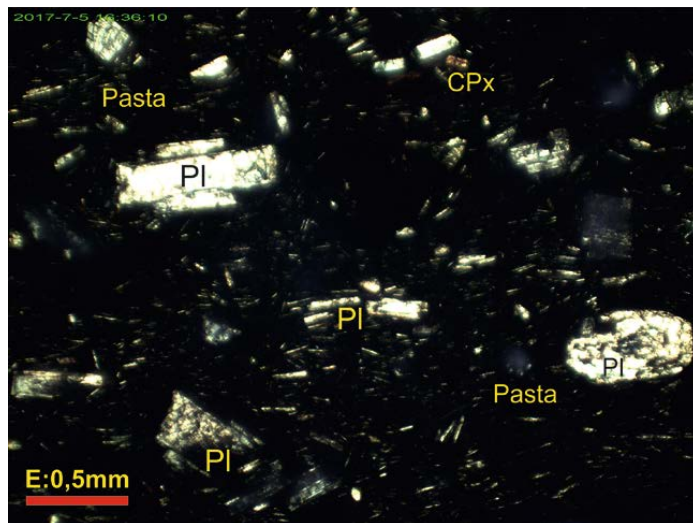


Fig. 5. Muestra 7804, aumento 4x, polarizadores X. Lava Andesítica, con fenocristales de plagioclasas (PI), escasos clinopiroxenos (CPx) y pasta con microlitos de plagioclasas orientadas.

Analizado por: Ing. José Luis Argandoña C.
ENCARGADO DEL LABORATORIO

INTERESADO:

Ing. Adolfo Orsolini Campana

UBICACIÓN:

Proyecto Mapeo Geológico del Área del Manantial del Silala

FECHA:

05 de Julio de 2017

Nº LAB: SGM-118/17

Muestra 7805.

ANÁLISIS PETROGRÁFICO**Descripción Macroscópica.-**

Fragmento de una roca de origen volcánico (lava), de color gris con superficies de meteorización, de composición ácida, muestra estructura holocristalina y textura porfídica de grano medio (>3 mm), donde se observan grandes cristales de feldespatos blanquecinos, cuarzo, biotita, anfíboles, piroxenos y óxidos de hierro diseminados, rodeados por una pasta de grano muy fino. La lava muestra elevada dureza y compactación.

Descripción Microscópica.-**Mineralogía.-**

Cuarzo.- Es un componente moderado de la lava, presente como fenocristales anhedrales y subhedrales con bordes sub-redondeados de hasta 2 mm de largo, muestran fracturas y engolfamientos, también se presentan como fragmentos de bordes sub-angulosos (Fig. 6).

Plagioclasas.- Se presentan en muy abundante porcentaje, en forma de fenocristales subhedrales tabulares y prismáticos de hasta 7 mm de largo, muestran zonación, maclas polisintéticas tipo Albite y combinadas Albite-Carlsbad, con bordes de reacción e inclusiones de la pasta, corresponden a la variedad Oligoclasa (An: 25), se hallan fracturadas (Fig. 6).

Biotita.- Se presenta en moderada proporción, en forma de fenocristales subhedrales tabulares que alcanzan hasta 1,5 mm de largo, de color marrón oscuro por la oxidación de sus bordes y planos de exfoliación, con inclusiones de plagioclasas.

Clinopiroxenos.- Se observan en reducido porcentaje, fenocristales subhedrales de hábito prismático y euhedrales poligonales de tono verdoso pálido, de hasta 1 mm de largo, se trata de la variedad augita (Fig. 6).

Hornblenda.- Se observan en reducido porcentaje fenocristales euhedrales romboédricos de color marrón oscuro, que se hallan reemplazados parcialmente en sus bordes por limonita, alcanzan hasta 1 mm de largo (Fig. 6).

Pasta.- La pasta de la lava es abundante y está formada principalmente por microlitos de plagioclasas ligeramente orientados con textura afiltrada, y en menor porcentaje por óxidos de hierro diseminados de tono marrón oscuro del tipo limonita y hematita (Fig. 6).

Óxidos de Hierro.- Se presentan en reducido porcentaje, como pequeños minerales opacos de hábito anhedral, diseminados en la pasta y sobre todo alterando a cristales de biotita y hornblenda, que corresponderían a las variedades limonita, hematita y magnetita.

Composición porcentual observada.-

Cuarzo (SiO_2).....	10-12 %
Plagioclasas (Oligoclasa) $\text{NaCaAl}(\text{Si}_3\text{O}_8)$	23-25 %
Biotita ($\text{K}_2(\text{Mg},\text{Fe})_2(\text{OH})_2(\text{AlSiO}_{10})$).....	4-5 %
Clinopiroxenos (Augita) ($\text{Mg},\text{Fe})(\text{SiO}_3)$	2-3 %
Hornblenda $\text{Ca}_2(\text{Mg},\text{Fe},\text{Al})_5(\text{OH})_2[(\text{Si},\text{Al})_4\text{O}_{11}]_2$	1-2 %
Pasta (microlitos de plagioclasas).....	48-50 %
Óxidos de Hierro (Hematita, limonita, magnetita).	2-3 %
Total.....	100 %

Textura y estructura.- Presenta estructura holocristalina y textura porfídica de grano medio (>3 mm), con pasta microlítica de textura afieltrada y disseminación de óxidos de hierro (Fig. 6).

Nombre de la roca.- De acuerdo al análisis petrográfico, es una lava dacítica, que corresponde a una **DACITA BIOTÍTICA**, ligeramente oxidada.

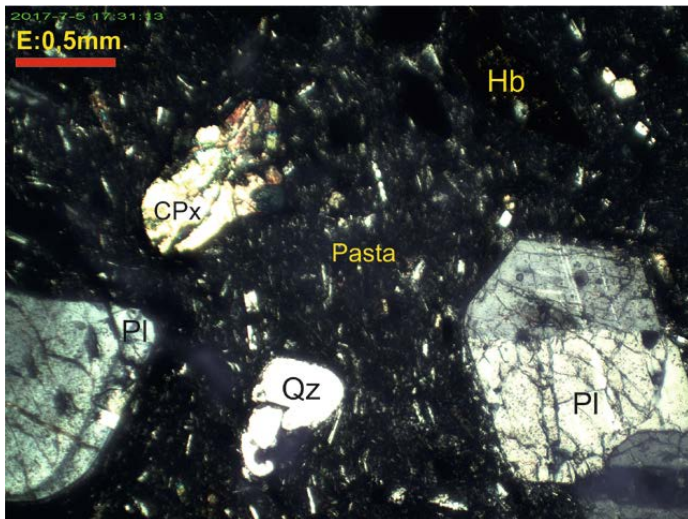


Fig. 6. Muestra 7805, aumento 4x, polarizadores X. Lava Dacítica, con fenocristales de plagioclasas (PI), cuarzo (Qz), clinopiroxenos (CPx), hornblenda oxidada, y pasta con microlitos de plagioclasas.

Analizado por: Ing. José Luis Argandoña C.
ENCARGADO DEL LABORATORIO

INTERESADO:

Ing. Adolfo Orsolini Campana

UBICACIÓN:

Proyecto Mapeo Geológico del Área del Manantial del Silala

FECHA:

05 de Julio de 2017

Nº LAB: SGM-119/17

Muestra 7807.

ANÁLISIS PETROGRÁFICO**Descripción Macroscópica.-**

Fragmento de una roca de origen volcánico (flujo de lava) de composición intermedia, muestra estructura ligeramente bandeada y textura porfídica de grano medio (>1 mm), donde se observa una intercalación entre bandas lenticulares de color marrón-rojizo y bandas de tono gris oscuro, ambas muestran cristales de feldespatos blanquecinos, biotita, piroxenos y óxidos de hierro diseminados, rodeados por una pasta ferruginosa y vítreas, con más presencia de hierro en las bandas grises. La toba presenta coloración gris-verdusca, por lo que muestra elevada dureza y compactación.

Descripción Microscópica.-**Mineralogía.-**

Plagioclasas.- Se presentan en muy abundante porcentaje, en forma de fenocristales subhédrales tabulares y prismáticos de hasta 2,5 mm de largo, muestran zonación, macras polisintéticas tipo Albite y combinadas Albite-Carlsbad, con bordes de reacción e inclusiones de la pasta, corresponden a la variedad Andesina (An: 35), se hallan como fragmentos (Fig. 7).

Biotita.- Se presenta en reducida proporción, en forma de fenocristales subhédrales tabulares que alcanzan hasta 1 mm de largo, de color marrón oscuro por la oxidación de sus bordes y planos de exfoliación, con inclusiones de plagioclasas (Fig. 7).

Clinopiroxenos.- Se observan en moderado porcentaje, fenocristales subhédrales de hábito prismático y euhédrales poligonales de tono verdoso pálido con macras de dos individuos, alcanzan hasta 1 mm de largo, se trata de la variedad augita (Fig. 7).

Hornblenda.- Se observan en reducido porcentaje fenocristales euhédrales romboédricos de color marrón-rojizo, que se hallan reemplazados parcialmente en sus bordes por limonita, alcanzan hasta 0,5 mm de largo (Fig. 7).

Pasta.- La pasta de la toba es abundante y está formada principalmente por esquirlas de vidrio volcánico de tono pardo oscuro de textura masiva, junto a óxidos de hierro diseminados de tono marrón del tipo limonita y en menor porcentaje por microlitos de plagioclasas ligeramente orientados (Fig. 7).

Óxidos de Hierro.- Se presentan en moderado porcentaje, como pequeños minerales opacos de hábito anhedral, diseminados en la pasta y sobre todo alterando a cristales de biotita y hornblenda, que corresponderían a las variedades limonita, hematita y magnetita.

Composición porcentual observada.-

Plagioclasas (Andesina) $\text{NaCaAl}(\text{Si}_3\text{O}_8)$	30-32 %
Biotita ($\text{K}_2(\text{Mg},\text{Fe})_2(\text{OH})_2(\text{AlSiO}_{10})$).....	3-4 %
Clinopiroxenos (Augita) ($\text{Mg},\text{Fe})(\text{SiO}_3)$	3-5 %
Hornblenda $\text{Ca}_2(\text{Mg},\text{Fe},\text{Al})_5(\text{OH})_2\{(\text{Si},\text{Al})_4\text{O}_{11}\}_2$	2-3 %
Pasta (vidrio, limonita y microlitos).....	50-53 %
Óxidos de Hierro (Hematita, limonita, magnetita).	2-3 %
Total.....	100 %

Textura y estructura.- Presenta estructura bandeada y lenticular, y textura porfídica de grano medio (>1 mm), con pasta vítreo masiva, ferruginosa y en menor grado microlítica. La roca se presenta compacta y dura (Fig. 7).

Nombre de la roca.- De acuerdo al análisis petrográfico, es una roca volcánica (cristalo-vítreo) de composición intermedia, que corresponde a una **ANDESÍTICA piroxenica**.

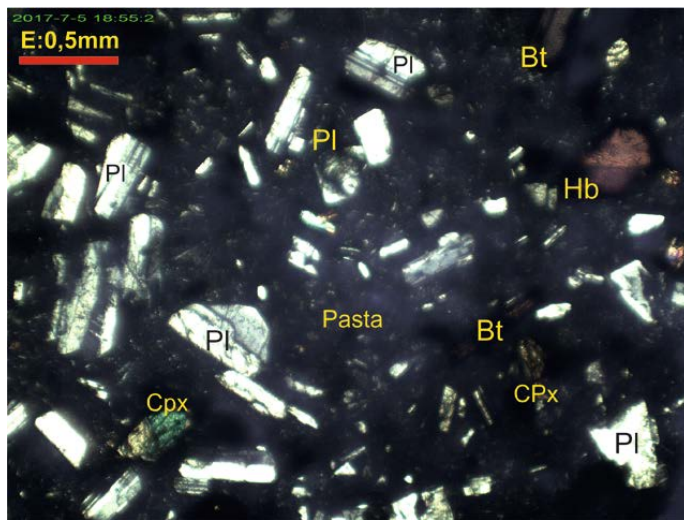


Fig. 7. Muestra 7807, aumento 4x, polarizadores X. Ignimbrita Andesítica, con fenocristales de plagioclasas (PI), clinopiroxenos (CPx), biotita (Bt), hornblenda (Hb) y pasta vítreo-ferruginosa con microlitos de plagioclasas.

Analizado por: Ing. José Luis Argandoña C.
ENCARGADO DEL LABORATORIO

INTERESADO:

Ing. Adolfo Orsolini Campana

UBICACIÓN:

Proyecto Mapeo Geológico del Área del Manantial del Silala

FECHA:

06 de Julio de 2017

Nº LAB: SGM-120/17

Muestra 7713.

ANÁLISIS PETROGRÁFICO**Descripción Macroscópica.-**

Fragmento de una roca de origen volcánico (lava), de color gris con tono rosáceo, presenta superficies de meteorización, de composición intermedia, muestra estructura holocrystalina y textura porfídica de grano medio (>2 mm), donde se observan grandes cristales de feldespatos blanquecinos, escaso cuarzo, biotita, anfíboles, piroxenos y óxidos de hierro diseminados, rodeados por una pasta de grano muy fino. La lava muestra elevada dureza y compactación.

Descripción Microscópica.-**Mineralogía.-**

Cuarzo.- Es un componente presente en escaso porcentaje, en forma de fenocristales anhedrales con bordes sub-redondeados, de hasta 0,5 mm de largo, muestran fracturas y engolfamientos (Fig. 8).

Plagioclásas.- Se presentan en muy abundante porcentaje, en forma de fenocristales subhédrales tabulares y prismáticos de hasta 3 mm de largo, muestran zonación, maclas polisintéticas tipo Albita y combinadas Albita-Carlsbad, con bordes de reacción e inclusiones de la pasta, corresponden al límite entre las variedades Oligoclasa-Andesina (An: 30) (Fig. 8).

Biotita.- Se presenta en moderada proporción, en forma de fenocristales subhédrales tabulares que alcanzan hasta 2 mm de largo, de color marrón oscuro por la oxidación de sus bordes y planos de exfoliación, contienen pequeñas inclusiones de plagioclásas.

Clinopiroxenos.- Se observan en reducido porcentaje, fenocristales subhédrales de hábito prismático y tabular, de tono verdoso pálido, de hasta 0,4 mm de largo, se trata de la variedad augita (Fig. 8).

Hornblenda.- Se observan en reducido porcentaje fenocristales euhédrales romboédricos de color marrón oscuro, que se hallan reemplazados parcialmente por limonita, alcanzan hasta 2,5 mm de largo (Fig. 8).

Pasta.- La pasta de la lava es abundante y está formada principalmente por vidrio volcánico de textura masiva, y en menor porcentaje por microlitos de plagioclásas sin orientación, y óxidos de hierro diseminados de tono marrón oscuro del tipo limonita y hematita (Fig. 8).

Óxidos de Hierro.- Se presentan en reducido porcentaje, como pequeños minerales opacos de hábito anhedral, diseminados en la pasta y sobre todo alterando a cristales de biotita y hornblenda, que corresponderían a las variedades limonita y hematita.

Composición porcentual observada.-

Cuarzo (SiO_2).....	1-2 %
Plagioclasas (Oligoclasa-Andesina) $\text{NaCaAl}(\text{Si}_3\text{O}_8)$	25-28 %
Biotita ($\text{K}_2(\text{Mg},\text{Fe})_2(\text{OH})_2(\text{AlSiO}_{10})$).....	3-5 %
Clinopiroxenos (Augita) ($\text{Mg},\text{Fe})(\text{SiO}_3)$	1-2 %
Hornblenda $\text{Ca}_2(\text{Mg},\text{Fe},\text{Al})_5(\text{OH})_2\{(\text{Si},\text{Al})_4\text{O}_{11}\}_2$	2-3 %
Pasta (Vidrio volcánico, microlitos de plagioclasas)	55-57 %
Óxidos de Hierro (Hematita, limonita).	2-3 %
Total.....	100 %

Textura y estructura.- Presenta una estructura holocrystalina y textura porfídica de grano medio (>1 mm), con pasta vítreo y microlítica, junto a óxidos de hierro (Fig. 8).

Nombre de la roca.- De acuerdo al análisis petrográfico, es una lava de composición intermedia, que corresponde a una **ANDESITA Biotítica (cuarzosa)**, ligeramente oxidada.

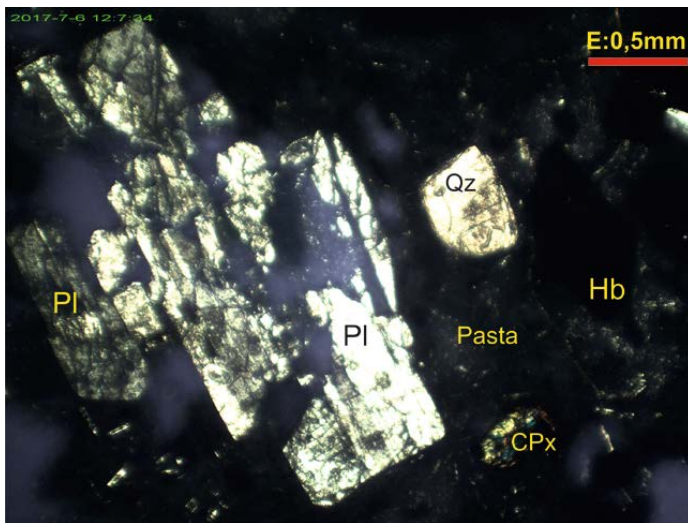


Fig. 8. Muestra 7713, aumento 4x, polarizadores X. Lava Andesítica, con fenocristales de plagioclasas (PI), escaso cuarzo (Qz), clinopiroxenos (CPx), hornblenda oxidada y pasta vítreo con microlitos de plagioclasas.

Analizado por: Ing. José Luis Argandoña C.
ENCARGADO DEL LABORATORIO

INTERESADO:

Ing. Adolfo Orsolini Campana

UBICACIÓN:

Proyecto Mapeo Geológico del Área del Manantial del Silala

FECHA:

19 de Julio de 2017

Nº LAB: SGM-121/17

Muestra 7708.

ANÁLISIS PETROGRÁFICO

Descripción Macroscópica.-

Fragmento de una roca de origen volcánico (lava) de composición acida, muestra estructura bandeadas y textura porfídica de grano medio (>1 mm), donde se observa una intercalación entre delgadas bandas lenticulares de color marrón-negruzco y bandas de tono gris claro, ambas muestran cristales de feldespatos blanquecinos, biotita, piroxenos y óxidos de hierro diseminados, rodeados por una pasta vítreos, con más presencia de hierro en las bandas oscuras. La roca se presenta masiva, compacta, por lo que muestra elevada dureza y compactación.

Descripción Microscópica.-

Mineralogía.-

Plagioclasas.- Se presentan en muy abundante porcentaje, en forma de fenocristales subhédrales tabulares y prismáticos de hasta 2,5 mm de largo, muestran zonación, macras polisintéticas tipo Albite y combinadas Albite-Carlsbad, con bordes de reacción e inclusiones de la pasta y de piroxenos, corresponden a la variedad Andesina (An: 40) (Fig. 9).

Biotita.- Se presenta en moderada proporción, en forma de fenocristales subhédrales tabulares que alcanzan hasta 0,7 mm de largo, de color marrón oscuro por la oxidación de sus bordes y planos de exfoliación, con inclusiones de plagioclasas.

Clinopiroxenos.- Se observan en moderado porcentaje, fenocristales subhédrales de hábito prismático y euhédrales poligonales de tono verdoso pálido con macras de dos individuos, alcanzan hasta 1 mm de largo, se trata de la variedad augita (Fig. 9).

Pasta.- La pasta de la toba es abundante y está formada principalmente por esquirlas de vidrio volcánico de tono pardo oscuro de textura masiva y localmente esferulítica, junto a óxidos de hierro diseminados de tono marrón del tipo limonita (Fig. 9).

Óxidos de Hierro.- Se presentan en moderado porcentaje, como pequeños minerales opacos de hábito anhedral, diseminados en la pasta y sobre todo alterando a cristales de biotita, que corresponderían a las variedades limonita (Fig. 9), hematita y magnetita (magnética).

Composición porcentual observada.-

Plagioclasas (Andesina) $\text{NaCaAl}(\text{Si}_3\text{O}_8)$	30-32 %
Biotita $(\text{K}_2(\text{Mg},\text{Fe})_2(\text{OH})_2(\text{AlSiO}_{10}))$	5-7 %
Clinopiroxenos (Augita) $(\text{Mg},\text{Fe})(\text{SiO}_3)$	<1 %

Pasta (vidrio, limonita y microlitos).....	51-55 %
Óxidos de Hierro (Hematita, limonita, magnetita).....	<1 %
Total.....	100 %

Textura y estructura.- Presenta estructura bandeada y textura porfídica de grano medio (>1 mm), con pasta vítreo masiva y esferulítica. La roca es masiva, compacta y presenta elevada dureza (Fig. 9).

Nombre de la roca.- De acuerdo al análisis petrográfico, es una roca volcánica (cristalo-vítreo) de composición intermedia, que corresponde a una **DACITICA biotítica**.

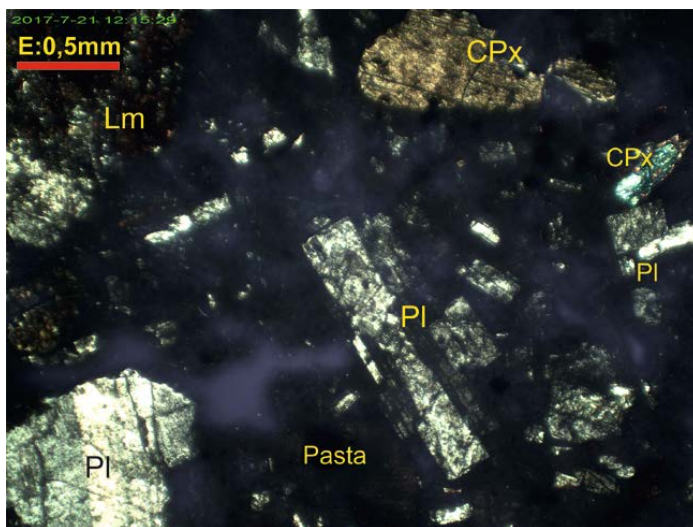


Fig. 9. Muestra 7708, aumento 4x, polarizadores X. Ignimbrita Andesítica, con fenocristales de plagioclásas (Pl), clinopiroxenos (CPx), limonita diseminada (Lm) y pasta vítreo masiva.

Analizado por: Ing. José Luis Argandoña C.
ENCARGADO DEL LABORATORIO

INTERESADO:

Ing. Adolfo Orsolini Campana

UBICACIÓN:

Proyecto Mapeo Geológico del Área del Manantial del Silala

FECHA:

24 de Julio de 2017

Nº LAB: SGM-123/17

Muestra 7717.

ANÁLISIS PETROGRÁFICO**Descripción Macroscópica.-**

Fragmento de una roca de origen volcánico, de color gris oscuro con superficies de meteorización, de composición ácida, muestra estructura vitro-cristalina y textura porfídica de grano medio (>3 mm), donde se observan grandes cristales de feldespatos blanquecinos, cuarzo, biotita, anfíboles, escasos piroxenos, pómex alargadas de tono rosáceo y óxidos de hierro diseminados, rodeados por una pasta vítreo, muestra moderada dureza y compactación.

Descripción Microscópica.-**Mineralogía.-**

Cuarzo.- Es un componente moderado de la lava, presente como fenocristales anhedrales y subhedrales con bordes sub-redondeados de hasta 2 mm de largo, muestran fracturas y engolfamientos, también se presentan como fragmentos de bordes sub-angulosos (Fig. 10).

Plagioclásas.- Se presentan en abundante porcentaje, en forma de fenocristales subhedrales tabulares y prismáticos de hasta 5 mm de largo, muestran zonación, maclas polisintéticas tipo Albita y combinadas Albita-Carlsbad, con bordes de reacción e inclusiones de la pasta, corresponden a la variedad Oligoclasa (An: 25), se hallan fracturadas (Fig. 10).

Biotita.- Se presenta en moderada proporción, en forma de fenocristales subhedrales tabulares que alcanzan hasta 3,5 mm de largo, de color marrón oscuro por la intensa oxidación de sus bordes y planos de exfoliación, con inclusiones de plagioclásas y muestran orientación (Fig.10).

Clinopiroxenos.- Se observan en muy reducido porcentaje, como fenocristales subhedrales de hábito prismático y anhedral, de tono verdoso pálido, de hasta 0,5 mm de largo, corresponden a la variedad augita.

Hornblenda.- Se observan en reducido porcentaje fenocristales euhedrales romboédricos de color marrón-rojizo, que se hallan reemplazados parcialmente en sus bordes por limonita, alcanzan hasta 1 mm de largo (Fig. 10).

Pasta.- La pasta de la toba es abundante y está formada principalmente por vidrio volcánico de textura masiva y en menor porcentaje por microlitos de plagioclásas y óxidos de hierro diseminados de tono marrón oscuro del tipo limonita (Fig. 10).

Óxidos de Hierro.- Se presentan en reducido porcentaje, como pequeños minerales opacos de hábito anhedral, diseminados en la pasta y alterando a cristales de biotita y hornblenda, que corresponderían a las variedades limonita, hematita y magnetita.

Pómez.- Se observan ocasionalmente, clastos de pómez de forma sub-redondeada y otra alargada formadas por esquirlas de vidrio volcánico y micro-cristales de plagioclasas, biotita y hornblenda (Fig. 10).

Composición porcentual observada.-

Cuarzo (SiO_2).....	8-10 %
Plagioclasas (Oligoclasa) $\text{NaCaAl}(\text{Si}_3\text{O}_8)$	20-22 %
Biotita ($\text{K}_2(\text{Mg},\text{Fe})_2(\text{OH})_2(\text{AlSiO}_{10})$).....	4-5 %
Clinopiroxenos (Augita) ($\text{Mg},\text{Fe})(\text{SiO}_3)$	< 1 %
Hornblenda $\text{Ca}_2(\text{Mg},\text{Fe},\text{Al})_5(\text{OH})_2\{(\text{Si},\text{Al})_4\text{O}_{11}\}_2$	2-3 %
Pasta (vidrio volcánico y microlitos).....	48-50 %
Óxidos de Hierro (Hematita, limonita, magnetita).	2-3 %
Pómez (vidrio y micro-cristales).....	< 1%
Total.....	100 %

Textura y estructura.- Presenta estructura vitro-cristalina y textura porfídica de grano medio (>3 mm), con pasta vítreo y microlítica, y pómez alargadas (Fig. 10).

Nombre de la roca.- De acuerdo al análisis petrográfico, es una roca vitro-cristalina de composición ácida, que corresponde a una **DACITA Biotítica**, débilmente oxidada.

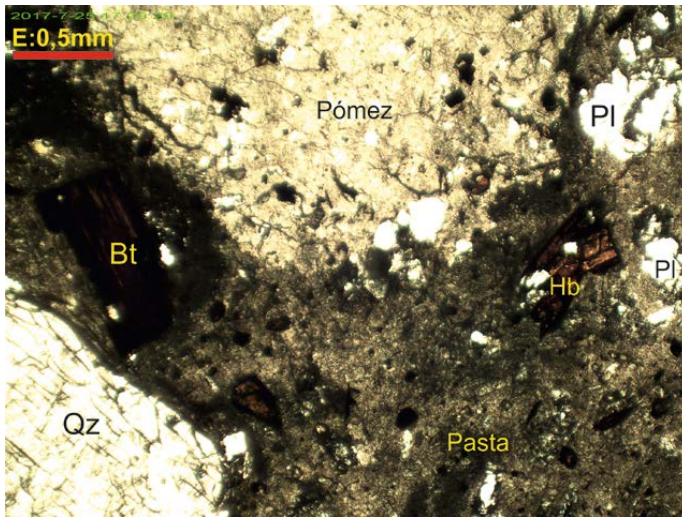


Fig. 10. Muestra 7717, aumento 4x, polarizadores II. Toba Dacítica, con fenocristales de plagioclasas (Pl), cuarzo (Qz), biotita (Bt), hornblenda (Hb), pómez y pasta vítreo masiva.

Analizado por: Ing. José Luis Argandoña C.
ENCARGADO DEL LABORATORIO

INTERESADO:

Ing. Adolfo Orsolini Campana

UBICACIÓN:

Proyecto Mapeo Geológico del Área del Manantial del Silala

FECHA:

24 de Julio de 2017

Nº LAB: SGM-124/17

Muestra 7720.

ANÁLISIS PETROGRÁFICO**Descripción Macroscópica.-**

Fragmento de una roca de origen volcánico (lava), de color gris, presenta superficies de meteorización, de composición intermedia, muestra estructura cavernosa o vesicular y textura porfídica de grano medio (>2 mm), donde se observan cristales de feldespatos blanquecinos, escaso cuarzo, piroxenos y óxidos de hierro diseminados, rodeados por una pasta de grano muy fino. La lava muestra moderada dureza y compactación, y cavidades llenas por cuarzo.

Descripción Microscópica.-**Mineralogía.-**

Cuarzo.- Es un componente presente en escaso porcentaje, en forma de fenocristales anhedrales y subhendrales con bordes sub-redondeados, de hasta 0,5 mm de largo, muestran fracturas y engolfamientos.

Plagioclásas.- Se presentan en abundante porcentaje, en forma de fenocristales subhendrales tabulares y prismáticos de hasta 4 mm de largo, muestran zonación, maclas polisintéticas tipo Albita y combinadas Albita-Carlsbad, con bordes de reacción e inclusiones de la pasta, corresponden a la variedad Andesina (An: 45) (Fig. 11).

Clinopiroxenos.- Se observan en reducido porcentaje, fenocristales subhendrales de hábito prismático, de tono verdoso pálido, de hasta 0,5 mm de largo, se trata de la variedad augita.

Pasta.- La pasta es abundante y está formada principalmente por microlitos de plagioclásas con textura afieltrada (sin orientación), y en menor porcentaje por vidrio volcánico de textura masiva y óxidos de hierro de tono marrón oscuro del tipo limonita y hematita (Fig. 11).

Óxidos de Hierro.- Se presentan en reducido porcentaje, como pequeños minerales opacos de hábito anhedral, diseminados en la pasta y sobre todo alterando a cristales de biotita y hornblenda, que corresponderían a las variedades limonita y hematita.

Composición porcentual observada.-

Cuarzo (SiO_2).....	1-2 %
Plagioclásas (Andesina) $\text{NaCaAl}(\text{Si}_3\text{O}_8)$	30-32 %
Clinopiroxenos (Augita) $(\text{Mg}, \text{Fe})(\text{SiO}_3)$	1-2 %
Pasta (Microlitos de plagioclásas).....	58-60 %
Óxidos de Hierro (Hematita, limonita)	3-4 %
Total.....	100 %

Textura y estructura.- Presenta una estructura cavernosa o vesicular y textura porfídica de grano medio (>2 mm), con pasta microlítica, junto a óxidos de hierro (Fig. 11).

Nombre de la roca.- De acuerdo al análisis petrográfico, es una lava de composición intermedia, que corresponde a una **ANDESITA (cuarzosa)**, ligeramente oxidada.

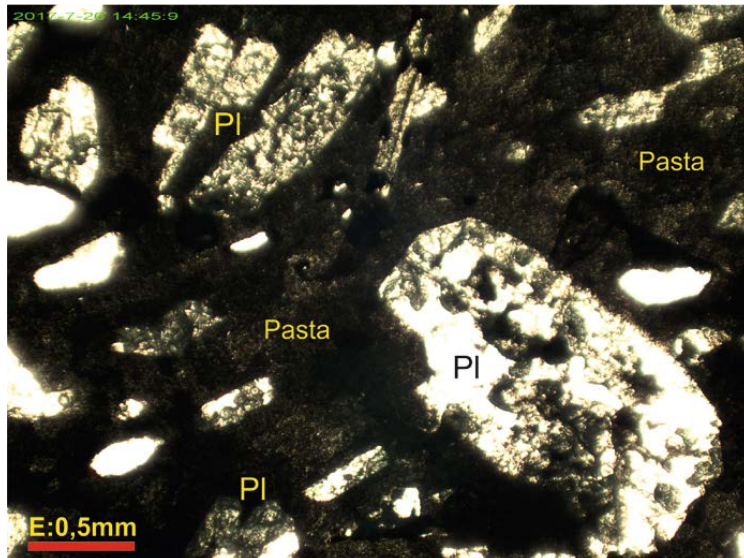


Fig. 11. Muestra 7720, aumento 4x, polarizadores II. Lava Andesítica, con fenocristales de plagioclasas (PI), óxidos de hierro, y pasta con microlitos de plagioclasas y vidrio volcánico.

Analizado por: Ing. José Luis Argandoña C.
ENCARGADO DEL LABORATORIO

INTERESADO:

Ing. Adolfo Orsolini Campana

UBICACIÓN:

Proyecto Mapeo Geológico del Área del Manantial del Silala

FECHA:

24 de Julio de 2017

Nº LAB: SGM-125/17

Muestra 7721.

ANÁLISIS PETROGRÁFICO

Descripción Macroscópica.-

Fragmento de una roca de origen volcánico (toba), de color marrón con tono grisáceo, tiene superficies de meteorización, de composición ácida, muestra estructura vitro-cristalina y textura porfídica de grano medio (>2 mm), donde se observan cristales de feldespatos blanquecinos, cuarzo, biotita oxidada, litoclastos y óxidos de hierro diseminados, rodeados por una pasta vítreo, muestra moderada dureza y grado de soldadura.

Descripción Microscópica.-

Mineralogía.-

Plagioclasas.- Se presentan en abundante porcentaje, en forma de fenocristales subhédrales tabulares y prismáticos de hasta 2 mm de largo, muestran fracturas, zonación, maclas polisintéticas tipo Albita y combinadas Albita-Carlsbad, con bordes de reacción e inclusiones de la pasta, corresponden a la variedad Oligoclásica (An: 25) (Fig. 12).

Feldespato potásico.- Se observan en reducido porcentaje, fenocristales anhédrales y subhédrales tabulares de feldespatos potásicos, con maclas tipo Carlsbad, de hasta 1,5 mm de largo (posiblemente de la variedad sanidina).

Biotita.- Se presenta en moderada proporción, en forma de fenocristales subhédrales tabulares y prismáticos que alcanzan hasta 3 mm de largo, de color marrón-rojizo por la oxidación de sus bordes y planos de exfoliación, con inclusiones de plagioclasas (Fig. 12).

Pasta.- La pasta de la toba es abundante, está formada principalmente por vidrio volcánico de textura masiva y localmente esferulítica y en menor porcentaje por óxidos de hierro diseminados de tono marrón oscuro del tipo limonita (Fig. 12).

Óxidos de Hierro.- Se presentan en reducido porcentaje, como pequeños minerales opacos de hábito anhedral, diseminados en la pasta y alterando a cristales de biotita, que corresponderían a las variedades limonita y hematita.

Litoclastos.- Se observan algunos litoclastos formados por rocas volcánicas con cristales de plagioclasas y óxidos de hierro, así como de rocas ferruginosas de tono rojizo, alcanzan hasta 2 mm de largo.

Composición porcentual observada.-

Cuarzo (SiO_2).....	13-15 %
Plagioclasas (Oligoclasa) $\text{NaCaAl}(\text{Si}_3\text{O}_8)$	23-25 %
Feldespato Potásico (KAlSi_3O_8).....	2-3 %
Biotita ($\text{K}_2(\text{Mg},\text{Fe})_2(\text{OH})_2(\text{AlSiO}_{10})$).....	4-5 %
Pasta (vidrio volcánico).....	45-47 %
Óxidos de Hierro (limonita, hematita,.).....	2-3 %
Litoclastos (volcánicos y ferruginosos).....	1-2 %
Total.....	100 %

Textura y estructura.- Presenta estructura vitro-cristalina y textura porfídica de grano medio (>2 mm), con pasta vítreo y litoclastos (Fig. 12).

Nombre de la roca.- De acuerdo al análisis petrográfico, es una toba vitro-cristalina de composición ácida, que corresponde a una **DACITA Biotítica**, débilmente oxidada.

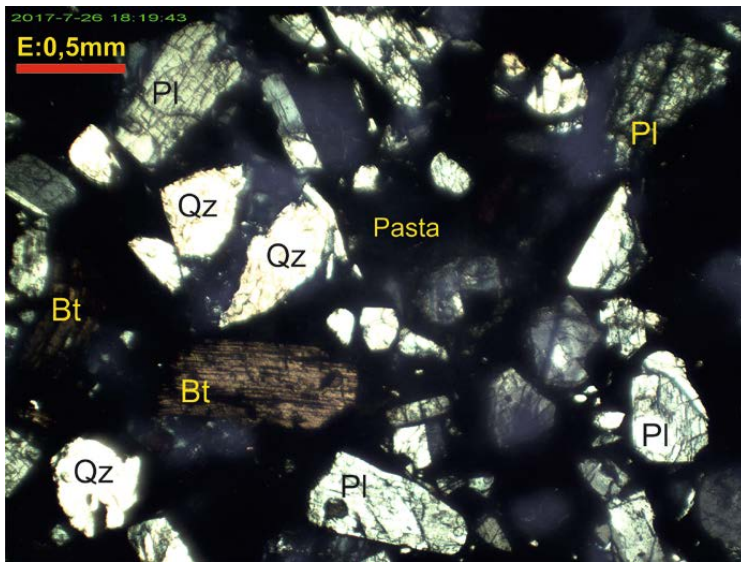


Fig. 12. Muestra , aumento 4x, polarizadores X. Toba Dacítica, con fenocristales de plagioclasas (Pl), cuarzo (Qz), biotita oxidada (Bt), y pasta vítreo de textura masiva.

Analizado por: Ing. José Luis Argandoña C.
ENCARGADO DEL LABORATORIO

INTERESADO:

Ing. Adolfo Orsolini Campana

UBICACIÓN:

Proyecto Mapeo Geológico del Área del Manantial del Silala

FECHA:

25 de Julio de 2017

Nº LAB: SGM-126/17

Muestra 7801.

ANÁLISIS PETROGRÁFICO**Descripción Macroscópica.-**

Fragmento de una roca de origen volcánico (lava), de color gris, presenta superficies de meteorización, de composición intermedia, muestra estructura holocrystalina y textura porfídica de grano medio (>2 mm), donde se observan cristales de feldespatos blanquecinos, biotita y anfíboles muy oxidados, piroxenos y óxidos de hierro diseminados, rodeados por una pasta de grano muy fino. La lava muestra moderada dureza y compactación.

Descripción Microscópica.-**Mineralogía.-**

Plagioclasas.- Se presentan en abundante porcentaje, en forma de fenocristales subhedrales tabulares y prismáticos de hasta 2,5 mm de largo, muestran zonación, maclas polisintéticas tipo Albita y combinadas Albita-Carlsbad, con bordes de reacción e inclusiones de la pasta, se hallan ligeramente argilizadas y corresponden a la variedad Andesina (An: 40) (Fig. 13).

Biotita.- Se presenta en moderada proporción, en forma de fenocristales subhedrales tabulares y prismáticos que alcanzan hasta 2 mm de largo, de color marrón-rojizo por la intensa oxidación de sus bordes y planos de exfoliación (Fig. 13).

Hornblenda.- Se observan en reducido porcentaje fenocristales euhedrales romboédricos de color marrón-rojizo reemplazados parcialmente por limonita, de hasta 1,5 mm de largo (Fig. 13).

Clinopiroxenos.- Se observan en reducido porcentaje, fenocristales subhedrales y prismáticos, de tono verdoso pálido de hasta 0,5 mm de largo, se trata de la variedad augita (Fig. 13).

Pasta.- La pasta es abundante y está formada principalmente por microlitos de plagioclasas con textura afiltrada que muestran orientación, y en menor porcentaje por vidrio volcánico de textura masiva (Fig. 13).

Óxidos de Hierro.- Se presentan en reducido porcentaje, como pequeños minerales opacos de hábito anhedral, diseminados en la pasta y sobre todo alterando a cristales de biotita y hornblenda, que corresponderían a las variedades limonita, hematita y magnetita.

Composición porcentual observada.-

Plagioclasas (Andesina) $\text{NaCaAl}(\text{Si}_3\text{O}_8)$	23-25 %
Biotita $(\text{K}_2(\text{Mg},\text{Fe})_2(\text{OH})_2(\text{AlSiO}_{10}))$	4-6 %
Hornblenda $\text{Ca}_2(\text{Mg},\text{Fe},\text{Al})_5(\text{OH})_2\{(\text{Si},\text{Al})_4\text{O}_{11}\}_2$	2-3 %

Clinopiroxenos (Augita) ($Mg,Fe)(SiO_3$).....	2-3 %
Pasta (Microlitos de plagioclasas).....	58-60 %
Óxidos de Hierro (Hematita, limonita, magnetita).....	2-3 %
Total.....	100 %

Textura y estructura.- Presenta una estructura holocristalina y textura porfídica de grano medio (>2 mm), con pasta microlítica y vítreo (Fig. 13).

Nombre de la roca.- De acuerdo al análisis petrográfico, es una lava de composición intermedia, que corresponde a una **ANDESITA Biotítica**, débilmente oxidada.

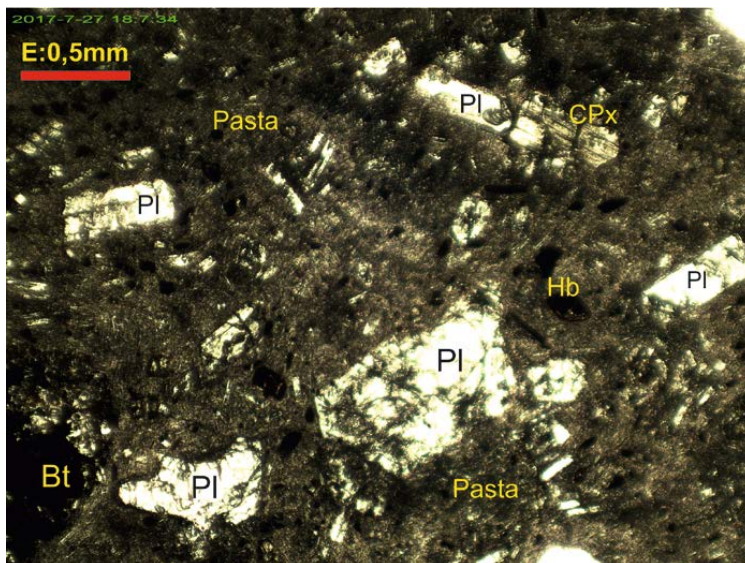


Fig. 13. Muestra 7801, aumento 4x, polarizadores II. Lava Andesítica, con fenocristales de plagioclasas (Pl), biotita (Bt), hornblenda (Hb), clinopiroxenos (CPx) y pasta con microlitos de plagioclasas y vidrio volcánico.

Analizado por: Ing. José Luis Argandoña C.
ENCARGADO DEL LABORATORIO

INTERESADO:

Ing. Adolfo Orsolini Campana

UBICACIÓN:

Proyecto Mapeo Geológico del Área del Manantial del Silala

FECHA:

25 de Julio de 2017

Nº LAB: SGM-127/17

Muestra 7802.

ANÁLISIS PETROGRÁFICO**Descripción Macroscópica.-**

Fragmento de una roca de origen volcánico (toba), de color marrón con tono rosáceo, tiene superficies de meteorización, de composición ácida, muestra estructura vitro-cristalina y textura porfídica de grano medio (>2 mm), donde se observan cristales de feldespatos blanquecinos, biotita muy oxidada, anfíboles, pómex alargadas de tono blanquecino y óxidos de hierro, rodeados por una pasta vítreo y ferruginosa, muestra moderada dureza y grado de soldadura.

Descripción Microscópica.-**Mineralogía.-**

Cuarzo.- Es un componente reducido de la toba, presente como fenocristales anhedrales y subhedrales con bordes sub-redondeados, de hasta 1 mm de largo, muestran fracturas.

Plagioclasas.- Se presentan en abundante porcentaje como fenocristales subhedrales y prismáticos de tamaño muy variable, entre 0,5 a 4 mm de largo, predominando los de grano fino, muestran zonación, maclas polisintéticas tipo Albita y combinadas Albita-Carlsbad, con bordes de reacción e inclusiones de la pasta, corresponden a la variedad Oligoclase (An: 20), se hallan fracturadas y orientadas (Fig. 14).

Biotita.- Se presenta en moderada proporción, en forma de fenocristales subhedrales tabulares que alcanzan hasta 2,5 mm de largo, de color marrón oscuro por la intensa oxidación de sus bordes y planos de exfoliación, muestran cierta orientación (Fig. 14).

Hornblenda.- Se observan en reducido porcentaje fenocristales subhedrales y euhedrales romboédricos de color marrón-rojizo, que se hallan reemplazados parcialmente en sus bordes por limonita, alcanzan hasta 1 mm de largo (Fig. 14).

Pasta.- La pasta de la toba es abundante y está formada principalmente por vidrio volcánico de textura masiva y en menor porcentaje por óxidos de hierro diseminados (ferruginosa) de tono marrón oscuro del tipo limonita (Fig. 14).

Óxidos de Hierro.- Se presentan en moderado porcentaje, como pequeños minerales opacos de hábito anhedral, diseminados en la pasta y alterando a cristales de biotita y hornblenda, que corresponden a las variedades limonita y hematita.

Pómex.- Se observan pómex blanquecinos y deformadas (alargadas), formadas por esquirlas de vidrio volcánico y micro-cristales de plagioclasas y biotita oxidada, que se observan mejor en la muestra de mano, alcanzando varios cm de largo.

Composición porcentual observada.-

Cuarzo (SiO_2).....	3-5 %
Plagioclasas (Oligoclasa) $\text{NaCaAl}(\text{Si}_3\text{O}_8)$	30-32 %
Biotita ($\text{K}_2(\text{Mg},\text{Fe})_2(\text{OH})_2(\text{AlSiO}_{10})$).....	4-5 %
Hornblenda $\text{Ca}_2(\text{Mg},\text{Fe},\text{Al})_5(\text{OH})_2\{(\text{Si},\text{Al})_4\text{O}_{11}\}_2$	2-3 %
Pasta (vidrio volcánico y limonita).....	45-47 %
Óxidos de Hierro (Limonita y hematita).....	2-3 %
Pómez (vidrio y micro-cristales).....	3-5 %
Total.....	100 %

Textura y estructura.- Presenta estructura vitro-cristalina y textura porfídica de grano medio (>2 mm), con pasta vítreo-ferruginosa y pómez alargadas (Fig. 14).

Nombre de la roca.- De acuerdo al análisis petrográfico, es una toba vitro-cristalina de composición ácida, que corresponde a una **DACITA Biotítica**, moderadamente oxidada.

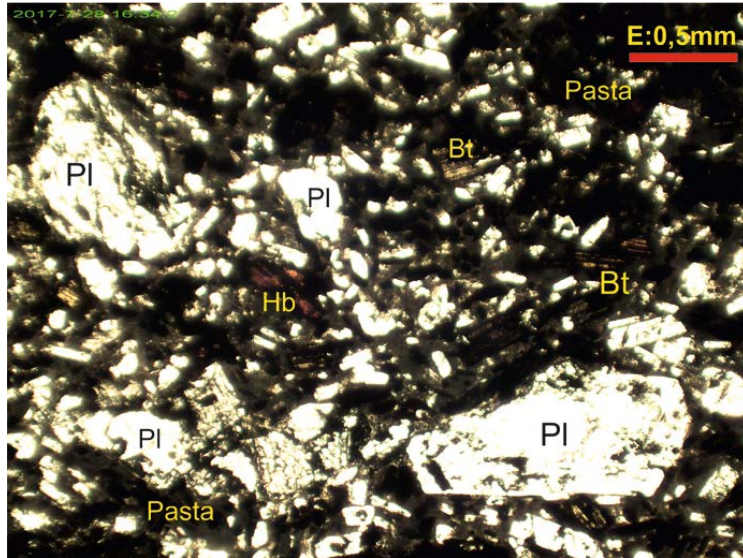


Fig. 14. Muestra 7802, aumento 4x, polarizadores II. Toba Dacítica, con fenocristales de plagioclasas (PI), biotita (Bt) y hornblenda (Hb) oxidadas, y una pasta vítreo-ferruginosa.

Analizado por: Ing. José Luis Argandoña C.
ENCARGADO DEL LABORATORIO

INTERESADO:

Ing. Adolfo Orsolini Campana

UBICACIÓN:

Proyecto Mapeo Geológico del Área del Manantial del Silala

FECHA:

26 de Julio de 2017

Nº LAB: SGM-128/17

Muestra 7803.

ANÁLISIS PETROGRÁFICO**Descripción Macroscópica.-**

Fragmento de una roca de origen volcánico (lava), de color gris oscuro con superficies de meteorización, de composición intermedia, muestra estructura holocrystalina y textura porfídica de grano medio (>1 mm), donde se observan abundantes cristales de feldespatos blanquecinos orientados, biotita oxidada, piroxenos y óxidos de hierro diseminados, rodeados por una pasta de grano fino. La lava muestra elevada dureza y compactación.

Descripción Microscópica.-**Mineralogía.-**

Plagioclasas.- Se presentan en muy abundante porcentaje, en forma de fenocristales subhendrales tabulares y prismáticos, de hasta 2,5 mm de largo, muestran zonación, maclas polisintéticas tipo Albita y combinadas Albita-Carlsbad, con bordes de reacción, corresponden a la variedad Andesina (An: 35), se hallan fracturadas y orientadas (Fig. 15).

Biotita.- Se presenta en moderada proporción, en forma de fenocristales subhendrales y tabulares que alcanzan hasta 2 mm de largo, de color marrón oscuro por la oxidación de sus bordes y planos de exfoliación, con inclusiones de plagioclasas (Fig. 15).

Hornblenda.- Se observan en reducido porcentaje fenocristales subhendrales y anhendrales de color marrón-rojizo, que se hallan reemplazados parcialmente en sus bordes por limonita, alcanzan hasta 1 mm de largo.

Clinopiroxenos.- Se observan en moderado porcentaje, en forma de fenocristales subhendrales de hábito prismático y de tono verdoso pálido, de hasta 1,5 mm de largo, se hallan fracturados, con maclas de dos individuos, se trata del tipo augita (Fig. 15).

Pasta.- La pasta de la lava es abundante y está formada principalmente por micro-cristales y microlitos de plagioclasas marcadamente orientados de acuerdo al flujo de la lava, con textura afieltrada, rodeando a los fenocristales, y en menor porcentaje por óxidos de hierro diseminados de tono marrón oscuro del tipo limonita, hematita y magnetita (Fig. 15).

Óxidos de Hierro.- Se presentan en moderado porcentaje, como pequeños minerales opacos de hábito anhedral y cúbico, diseminados en la pasta y alterando a fenocristales de biotita, que corresponderían a las variedades hematita, limonita y probablemente magnetita.

Composición porcentual observada.-

Plagioclasas (Andesina) $\text{NaCaAl}(\text{Si}_3\text{O}_8)$	28-30 %
Biotita $(\text{K}_2(\text{Mg},\text{Fe})_2(\text{OH})_2(\text{AlSiO}_{10}))$	2-3 %
Hornblenda $\text{Ca}_2(\text{Mg},\text{Fe},\text{Al})_5(\text{OH})_2\{(\text{Si},\text{Al})_4\text{O}_{11}\}_2$	1-2 %
Clinopiroxenos (Augita) $(\text{Mg},\text{Fe})(\text{SiO}_3)$	4-5 %
Pasta (microlitos de plagioclasas).....	55-57 %
Óxidos de Hierro (Hematita, limonita, magnetita).....	2-3 %
Total.....	100 %

Textura y estructura.- Presenta una estructura holocrystalina y textura porfídica de grano medio ($>1 \text{ mm}$), con pasta microlítica de textura afieltrada y disseminación de óxidos de hierro (Fig. 15).

Nombre de la roca.- De acuerdo al análisis petrográfico, es una lava de composición intermedia, que corresponde a una **ANDESITA Piroxénica**, ligeramente oxidada.

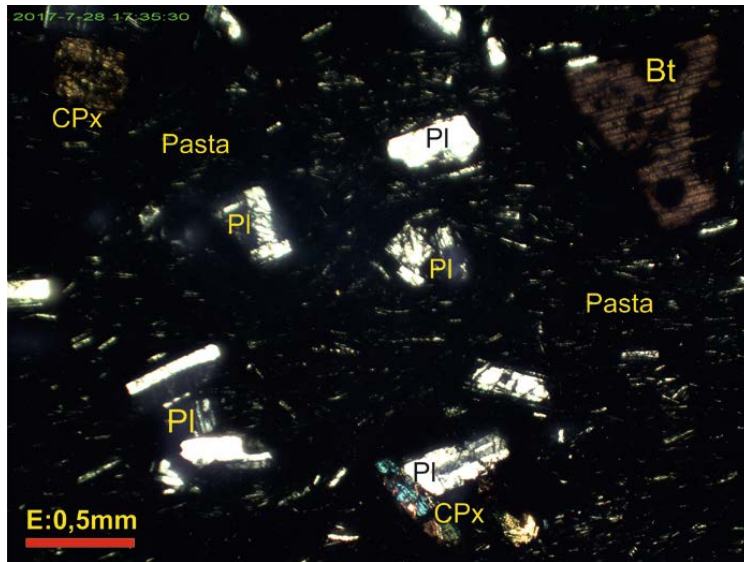


Fig. 15. Muestra 7803, aumento 4x, polarizadores X. Lava Andesítica, con fenocristales de plagioclasas (PI), clinopiroxenos (CPX), biotita (Bt) y pasta con microlitos de plagioclasas orientadas.

Analizado por: Ing. José Luis Argandoña C.
ENCARGADO DEL LABORATORIO

INTERESADO:

Ing. Adolfo Orsolini Campana

UBICACIÓN:

Proyecto Mapeo Geológico del Área del Manantial del Silala

FECHA:

26 de Julio de 2017

Nº LAB: SGM-129/17

Muestra 7806.

ANÁLISIS PETROGRÁFICO**Descripción Macroscópica.-**

Fragmento de una roca de origen volcánico (lava), de color gris oscuro, tiene superficies de meteorización, de composición intermedia, muestra estructura holocrystalina y textura porfídica de grano medio (>1 mm), donde se observan abundantes cristales de feldespatos blanquecinos orientados, biotita oxidada, piroxenos y óxidos de hierro diseminados, rodeados por una pasta de grano muy fino. La lava muestra elevada dureza y compactación.

Descripción Microscópica.-**Mineralogía.-**

Plagioclasas.- Se presentan en muy abundante porcentaje, en forma de fenocristales subhédrales tabulares y prismáticos, de tamaño variable, entre 0,3 hasta 2 mm de largo, muestran zonación, maclas polisintéticas tipo Albita y combinadas Albita-Carlsbad, con bordes de reacción, corresponden a la variedad Oligoclasa (An: 25), se hallan fracturadas y orientadas (Fig. 16).

Biotita.- Se presenta en reducida proporción, en forma de fenocristales subhédrales y tabulares que alcanzan hasta 1 mm de largo, de color marrón oscuro por la oxidación de sus bordes y planos de exfoliación (Fig. 16).

Hornblenda.- Se observan en muy reducido porcentaje fenocristales subhédrales y anhédrales de color marrón-rojizo por la oxidación de sus bordes, alcanzan hasta 0,5 mm de largo.

Clinopiroxenos.- Se observan en moderado porcentaje, en forma de fenocristales subhédrales de hábito prismático y euhédrales poligonales de tono verdoso pálido, de hasta 1 mm de largo, se hallan fracturados, de la variedad augita (Fig. 16).

Pasta.- La pasta de la lava es abundante y está formada principalmente por micro-cristales y microlitos de plagioclasas marcadamente orientados de acuerdo al flujo de la lava, con textura afieltrada, y en menor porcentaje por óxidos de hierro diseminados de tono marrón oscuro del tipo limonita, hematita y magnetita (Fig. 16).

Óxidos de Hierro.- Se presentan en moderado porcentaje, como pequeños minerales opacos de hábito anhedral y cúbico, diseminados en la pasta y alterando a fenocristales de biotita, que corresponderían a las variedades hematita, limonita y magnetita.

Composición porcentual observada.-

Plagioclasas (Oligoclásica) $\text{NaCaAl}(\text{Si}_3\text{O}_8)$	25-27 %
Biotita $(\text{K}_2(\text{Mg},\text{Fe})_2(\text{OH})_2(\text{AlSiO}_{10}))$	2-3 %
Hornblenda $\text{Ca}_2(\text{Mg},\text{Fe},\text{Al})_5(\text{OH})_2\{(\text{Si},\text{Al})_4\text{O}_{11}\}_2$	1-2 %
Clinopiroxenos (Augita) $(\text{Mg},\text{Fe})(\text{SiO}_3)$	3-5 %
Pasta (microlitos de plagioclasas).....	58-60 %
Óxidos de Hierro (Hematita, limonita, magnetita).....	2-3 %
Total.....	100 %

Textura y estructura.- Presenta una estructura holocrystalina y textura porfídica de grano medio ($>1 \text{ mm}$), con pasta microlítica de textura afieltrada y disseminación de óxidos de hierro (Fig. 16).

Nombre de la roca.- De acuerdo al análisis petrográfico, es una lava de composición intermedia, que corresponde a una **ANDESITA Piroxénica**, ligeramente oxidada.

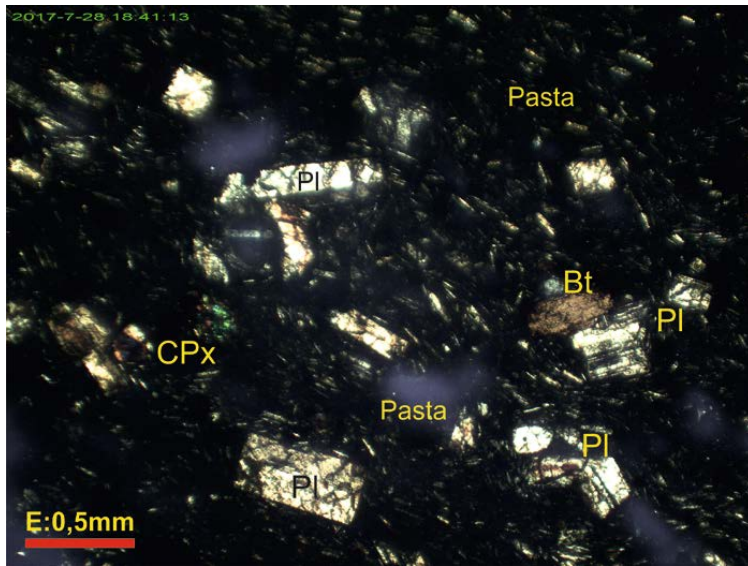


Fig. 16. Muestra 7806, aumento 4x, polarizadores X. Lava Andesítica, con fenocristales de plagioclasas (PI), clinopiroxenos (CPx), biotita (Bt) y pasta con microlitos de plagioclasas orientadas.

Analizado por: Ing. José Luis Argandoña C.
ENCARGADO DEL LABORATORIO

INTERESADO:

Ing. Adolfo Orsolini Campana

UBICACIÓN:

Proyecto Mapeo Geológico del Área del Manantial del Silala

FECHA:

26 de Julio de 2017

Nº LAB: SGM-130/17

Muestra 7808.

ANÁLISIS PETROGRÁFICO**Descripción Macroscópica.-**

Fragmento de una roca de origen piroclástico (toba ignimbótica) de composición intermedia, muestra estructura bandeadada y textura porfídica de grano medio (>1 mm), donde se observa una intercalación entre bandas lenticulares de tono gris oscuro y bandas de color marrón-rojizo, ambas muestran cristales de feldespatos blanquecinos, biotita, piroxenos y óxidos de hierro diseminados, rodeados por una pasta ferruginosa y vítreo, con más presencia de hierro en las bandas grises. La toba presenta alto grado de soldadura (ignimbrita), por lo que muestra elevada dureza y compactación, también es llamada toba soldada.

Descripción Microscópica.-**Mineralogía.-**

Plagioclasas.- Se presentan en abundante porcentaje, en forma de fenocristales subhédrales tabulares y prismáticos de hasta 1,5 mm de largo, muestran zonación, maclas polisintéticas tipo Albita y combinadas Albita-Carlsbad, con bordes de reacción e inclusiones de la pasta, corresponden a la variedad Oligoclásica (An: 25) (Fig. 17).

Biotita.- Se presenta en reducida proporción, en forma de fenocristales subhédrales tabulares que alcanzan hasta 0,5 mm de largo, de color marrón oscuro por la oxidación de sus bordes y planos de exfoliación (Fig. 17).

Clinopiroxenos.- Se observan en moderado porcentaje, fenocristales subhédrales de hábito prismático y euédrales poligonales de tono verdoso pálido con maclas de dos individuos, alcanzan hasta 0,8 mm de largo, se trata de la variedad augita (Fig. 17).

Hornblenda.- Se observan en reducido porcentaje fenocristales euédrales romboédricos y subhédrales prismáticos de color marrón-rojizo, que se hallan reemplazados parcialmente en sus bordes por limonita, alcanzan hasta 0,5 mm de largo.

Pasta.- La pasta de la toba es abundante, está formada principalmente por microlitos de plagioclasas ligeramente orientados y en menor porcentaje por esquirlas de vidrio volcánico de tono pardo oscuro y de textura masiva, junto a óxidos de hierro diseminados de tono marrón del tipo limonita y hematita (Fig. 17).

Óxidos de Hierro.- Se presentan en moderado porcentaje, como pequeños minerales opacos de hábito anhedral y subhedral, diseminados en la pasta y alterando a cristales de biotita y hornblenda, que corresponderían a las variedades limonita, hematita y magnetita.

Composición porcentual observada.-

Plagioclasas (Oligoclásica) $\text{NaCaAl}(\text{Si}_3\text{O}_8)$	30-32 %
Biotita ($\text{K}_2(\text{Mg},\text{Fe})_2(\text{OH})_2(\text{AlSiO}_{10})$).....	2-3 %
Clinopiroxenos (Augita) ($\text{Mg},\text{Fe})(\text{SiO}_3)$	3-5 %
Hornblenda $\text{Ca}_2(\text{Mg},\text{Fe},\text{Al})_5(\text{OH})_2\{(\text{Si},\text{Al})_4\text{O}_{11}\}_2$	1-2 %
Pasta (Microlitos y vidrio volcánico).....	53-55 %
Óxidos de Hierro (Hematita, limonita y magnetita).....	2-3 %
Total.....	100 %

Textura y estructura.- Presenta estructura bandeadada y lenticular, y textura porfídica de grano medio (>1 mm), con pasta microlítica y vítreos masivos, y en menor grado ferruginosa. La toba muestra elevado grado de soldadura y dureza (Fig. 17).

Nombre de la roca.- De acuerdo al análisis petrográfico, es una roca piroclástica (toba cristalovítreos soldados) de composición intermedia, que corresponde a una **Ignimbrita ANDESÍTICA**.

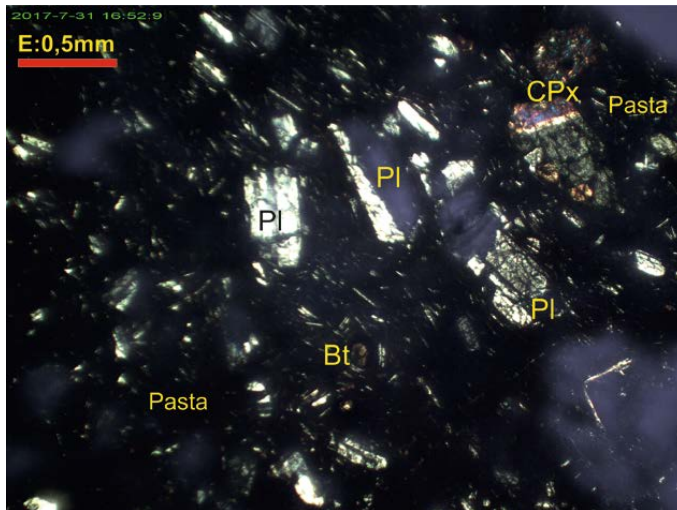


Fig. 17. Muestra 7808, aumento 4x, polarizadores X. Ignimbrita Andesítica, con fenocristales de plagioclasas (PI), clinopiroxenos (CPx), biotita (Bt) y pasta con microlitos de plagioclasas, vidrio y óxidos de hierro.

Analizado por: Ing. José Luis Argandoña C.
ENCARGADO DEL LABORATORIO

INTERESADO:

Ing. Adolfo Orsolini Campana

UBICACIÓN:

Proyecto Mapeo Geológico del Área del Manantial del Silala

FECHA:

21 de Agosto de 2017

Nº LAB: SGM-142/17

Muestra 7722.

ANÁLISIS PETROGRÁFICO**Descripción Macroscópica.-**

Fragmento de una roca de origen piroclástico (toba vitro-cristalina), de color gris-blanquecino con superficies de meteorización, de composición ácida, muestra estructura hipocristalina y textura porfídica de grano medio (>1 mm), donde se observan cristales de feldespatos, cuarzo, biotita con orientación, litoclastos de rocas volcánicas y óxidos de hierro diseminados, rodeados por una pasta vítreos, muestra reducido grado de dureza y soldadura, por lo que es deleznable.

Descripción Microscópica.-**Mineralogía.-**

Cuarzo.- Es un componente abundante de la toba, presente en forma de fenocristales anhedrales con bordes sub-angulosos de hasta 1,5 mm de largo, muestran fracturas y engolfamientos, también se presentan como fragmentos de bordes angulosos (Fig. 18).

Plagioclasas.- Se presentan en abundante porcentaje, en forma de fenocristales subhédrales tabulares y prismáticos, de hasta 2 mm de largo, con zonación, maclas polisintéticas tipo Albita y combinadas Albita-Carlsbad, con bordes de reacción, corresponden a la variedad Oligoclasa (An: 25), se hallan también como fragmentos angulosos, y muestran meteorización (Fig. 18).

Biotita.- Se presenta en moderada proporción, como fenocristales subhédrales prismáticos y tabulares que alcanzan hasta 1 mm de largo, de color marrón oscuro por la oxidación de sus bordes y planos de exfoliación, con pequeñas inclusiones de apatito y muestran orientación preferencial (Fig. 18).

Pasta.- La pasta de la toba es muy abundante y está formada principalmente por esquirlas de vidrio volcánico de tono pardo oscuro que muestran textura masiva, junto a pequeños fragmentos de cuarzo y feldespatos (Fig. 18).

Óxidos de Hierro.- Se presentan en reducido porcentaje, como pequeños minerales opacos de hábito anhedral, diseminados en la pasta y sobre todo alterando a cristales de biotita, que corresponderían a la variedad limonita.

Litoclastos.- Se observan en reducido porcentaje, litoclastos de bordes sub-redondeados formados por rocas volcánicas de grano fino, con cristales de cuarzo, plagioclasas y biotita, alcanzan hasta 2,5 mm de largo.

Composición porcentual observada.-

Cuarzo (SiO_2).....	13-15 %
Plagioclasas (Oligoclasa) $\text{NaCaAl}(\text{Si}_3\text{O}_8)$	18-20 %
Biotita ($\text{K}_2(\text{Mg},\text{Fe})_2(\text{OH})_2(\text{AlSiO}_{10})$).....	4-6 %
Pasta (Vidrio volcánico).....	53-55 %
Óxidos de Hierro (Limonita).....	1-2 %
Litoclastos (rocas volcánicas).....	1-2 %
Total.....	100 %

Textura y estructura.- Presenta una estructura hipocrystalina y textura porfídica de grano medio (>1 mm), con pasta vítreos de textura masiva y algunos litoclastos (Fig. 18).

Nombre de la roca.- De acuerdo al análisis petrográfico, es una toba vitro-cristalina de composición ácida, que corresponde a una **DACITA Biotítica**, con pasta vítreos.

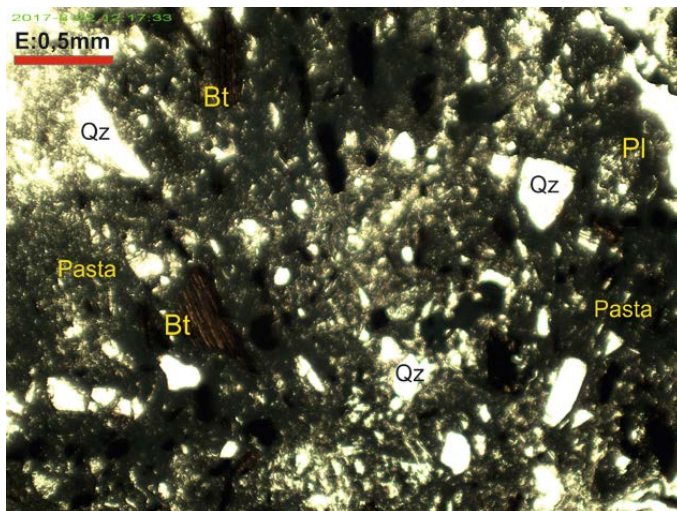


Fig. 18. Muestra 7722, aumento 4x, polarizadores X. Toba Dacítica, con fenocristales de plagioclasas (PI), cuarzo (Qz), biotita oxidada (Bt), y pasta vítreos de textura masiva.

Analizado por: Ing. José Luis Argandoña C.
ENCARGADO DEL LABORATORIO

INTERESADO:

Ing. Adolfo Orsolini Campana

UBICACIÓN:

Proyecto Mapeo Geológico del Área del Manantial del Silala

FECHA:

21 de Agosto de 2017

Nº LAB: SGM-143/17

Muestra 7723.

ANÁLISIS PETROGRÁFICO

Descripción Macroscópica.-

Fragmento de una roca de origen piroclástico (toba vitro-cristalina), de color gris-blanquecino con superficies de meteorización, de composición ácida, muestra estructura hipocristalina y textura porfídica de grano medio (>1 mm), donde se observan cristales de feldespatos, cuarzo, biotita con orientación y óxidos de hierro diseminados, rodeados por una pasta vítreo, muestra moderado grado de dureza y soldadura.

Descripción Microscópica.-

Mineralogía.-

Cuarzo.- Es un componente muy abundante de la toba, presente en forma de fenocristales anhedrales con bordes sub-angulosos de hasta 2 mm de largo, muestran fracturas, engolfamientos e inclusiones de la pasta vítreo, también se presentan como fragmentos de bordes angulosos (Fig. 19).

Plagioclasas.- Se presentan en abundante porcentaje, en forma de fenocristales subhedrales tabulares y prismáticos, de hasta 2,5 mm de largo, con zonación, macetas polisintéticas tipo Albita y combinadas Albita-Carlsbad, con bordes de reacción, corresponden a la variedad Oligoclasa (An: 25-30), se hallan también como pequeños fragmentos angulosos (Fig. 19).

Biotita.- Se presenta en moderada proporción, como fenocristales subhedrales prismáticos y tabulares que alcanzan hasta 1,5 mm de largo, de color marrón oscuro por la oxidación de sus bordes y planos de exfoliación, con pequeñas inclusiones de apatito y muestran orientación preferencial (Fig. 19).

Hornblenda.- Se observan en reducido porcentaje fenocristales anhedrales y subhedrales de color marrón-verdoso, se hallan ligeramente oxidados, alcanzan hasta 1 mm de largo.

Pasta.- La pasta de la toba es abundante y está formada principalmente por esquirlas de vidrio volcánico de tono pardo oscuro que muestran una textura masiva, junto a pequeños fragmentos de cuarzo, feldespatos y circón (Fig. 19).

Óxidos de Hierro.- Se presentan en reducido porcentaje, como pequeños minerales opacos de hábito anhedral, diseminados en la pasta y alterando a cristales de biotita y hornblenda, que corresponden a la variedad limonita.

Composición porcentual observada.-

Cuarzo (SiO_2).....	20-22 %
Plagioclasas (Oligoclasa) $\text{NaCaAl}(\text{Si}_3\text{O}_8)$	18-20 %
Biotita ($\text{K}_2(\text{Mg},\text{Fe})_2(\text{OH})_2(\text{AlSiO}_{10})$).....	4-6 %
Hornblenda $\text{Ca}_2(\text{Mg},\text{Fe},\text{Al})_5(\text{OH})_2\{(\text{Si},\text{Al})_4\text{O}_{11}\}_2$	1-2 %
Pasta (Vidrio volcánico).....	46-48 %
Óxidos de Hierro (Limonita).....	1-2 %
Total.....	100 %

Textura y estructura.- Presenta una estructura hipocrystalina y textura porfídica de grano medio (>1 mm), con pasta vítreos de textura masiva (Fig. 19).

Nombre de la roca.- De acuerdo al análisis petrográfico, es una toba vitro-cristalina de composición ácida, que corresponde a una **DACITA Biotítica**, con pasta vítreos.

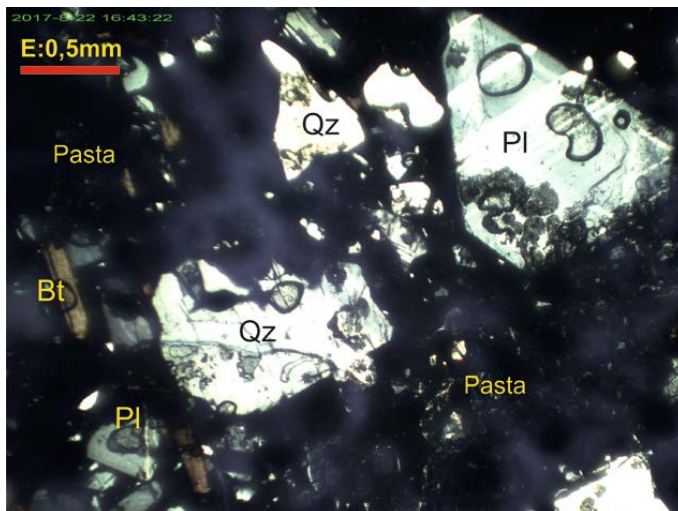


Fig. 19. Muestra 7723, aumento 4x, polarizadores X. Toba Dacítica, con fenocristales de plagioclasas (Pl), cuarzo (Qz), biotita oxidada (Bt), y pasta vítreos de textura masiva.

Analizado por: Ing. José Luis Argandoña C.
ENCARGADO DEL LABORATORIO

INTERESADO:

Ing. Adolfo Orsolini Campana

UBICACIÓN:

Proyecto Mapeo Geológico del Área del Manantial del Silala

FECHA:

21 de Agosto de 2017

Nº LAB: SGM-144/17

Muestra 7726.

ANÁLISIS PETROGRÁFICO**Descripción Macroscópica.-**

Fragmento de una roca de origen volcánico (lava), de color gris con superficies de meteorización, composición relativamente ácida, muestra estructura holocristalina y textura porfídica de grano medio (>2 mm), donde se observan grandes cristales de feldespatos blanquecinos, escaso cuarzo, biotita, anfíboles, piroxenos y óxidos de hierro diseminados, rodeados por una pasta de grano muy fino, contiene agregados de calcita llenando pequeñas cavidades, la roca muestra elevada dureza y compactación.

Descripción Microscópica.-**Mineralogía.-**

Cuarzo.- Es un componente reducido de la lava, presente en forma de fenocristales anhedrales con bordes sub-redondeados de hasta 1 mm de largo, muestran fracturas y engolfamientos, también se presentan como fragmentos de bordes sub-angulosos.

Plagioclasas.- Se presentan en abundante porcentaje, en forma de fenocristales subhédrales tabulares y prismáticos, de hasta 5 mm de largo, muestran zonación, maclas polisintéticas tipo Albita y combinadas Albita-Carlsbad, con bordes de reacción y fracturas, corresponden a la variedad Oligoclasa (An: 25-30) (Fig. 20).

Biotita.- Se presenta en moderada proporción, en forma de fenocristales subhédrales tabulares que alcanzan hasta 2 mm de largo, de color marrón oscuro por la intensa oxidación de sus bordes y planos de exfoliación, con inclusiones de plagioclásas (Fig.20).

Clinopiroxenos.- Se observan en moderado porcentaje fenocristales euhédrales poligonales y subhédrales prismáticos de tono verdoso pálido, que alcanzan hasta 2 mm de largo, se trata del tipo augita. En escaso porcentaje se observan ortopiroxenos de hábito prismático (Fig. 20).

Hornblenda.- Se observan en reducido porcentaje fenocristales euhédrales poligonales de color marrón, se hallan reemplazados parcialmente por limonita, alcanzan hasta 3 mm de largo.

Pasta.- La pasta de la lava es abundante y está formada principalmente por microlitos de plagioclásas sin orientación y con textura afieltrada, y en menor porcentaje por vidrio volcánico de tono pardo y textura masiva (Fig. 20).

Óxidos de Hierro.- Se presentan en reducido porcentaje, como pequeños minerales opacos de hábito anhedral, diseminados en la pasta y sobre todo alterando a cristales de biotita y hornblenda, corresponderían a las variedades limonita, hematita y magnetita.

Calcita.- Se observan en escaso porcentaje, agregados anhedrales de calcita secundaria de grano fino y de color blanquecino, llenando pequeñas cavidades de la lava.

Composición porcentual observada.-

Cuarzo (SiO_2).....	4-5 %
Plagioclasas (Oligoclasa) $\text{NaCaAl}(\text{Si}_3\text{O}_8)$	25-27 %
Biotita ($\text{K}_2(\text{Mg},\text{Fe})_2(\text{OH})_2(\text{AlSiO}_{10})$).....	4-5 %
Clinopiroxenos (Augita) ($\text{Mg},\text{Fe})(\text{SiO}_3)$	3-4 %
Hornblenda $\text{Ca}_2(\text{Mg},\text{Fe},\text{Al})_5(\text{OH})_2\{(\text{Si},\text{Al})_4\text{O}_{11}\}_2$	1-2 %
Pasta (microlitos de plagioclasas).....	50-52 %
Óxidos de Hierro (Limonita, hematita y magnetita).....	2-3 %
Calcita (CaCO_3).....	1-2 %
Total.....	100 %

Textura y estructura.- Presenta estructura holocristalina y textura porfídica de grano medio (>2 mm), con pasta vítrea y microlítica de textura afieltrada (Fig. 20).

Nombre de la roca.- De acuerdo al análisis petrográfico, es una lava de composición ácida, que corresponde a una **DACITA de Biotita y Hornblenda**, cercana a una Andesita cuarzosa, ligeramente oxidada, con cavidades de calcita.

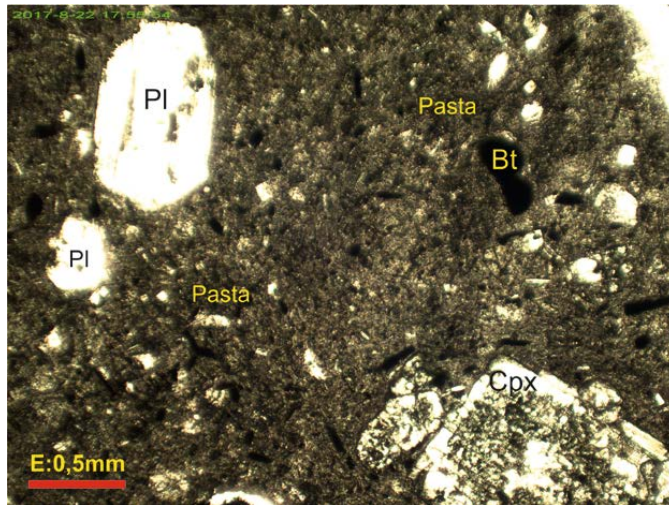


Fig. 20. Muestra 7726, aumento 4x, polarizadores II. Lava Dacítica, con fenocristales de plagioclasas (PL), clinopiroxeno (CPx), biotita (Bt) y pasta con microlitos de plagioclasas.

Analizado por: Ing. José Luis Argandoña C.
ENCARGADO DEL LABORATORIO

INTERESADO:

Ing. Adolfo Orsolini Campana

UBICACIÓN:

Proyecto Mapeo Geológico del Área del Manantial del Silala

FECHA:

22 de Agosto de 2017

Nº LAB: SGM-145/17

Muestra 7727.

ANÁLISIS PETROGRÁFICO**Descripción Macroscópica.-**

Fragmento de una roca de origen volcánico (lava), de color gris con tono oscuro y superficies de meteorización, composición intermedia, muestra estructura holocrystalina y textura porfídica de grano medio (>2 mm), donde se observan cristales de feldespatos blanquecinos, muy escaso cuarzo, biotita y anfíboles oxidados, piroxenos y óxidos de hierro diseminados, rodeados por una pasta de grano muy fino, la lava muestra elevada dureza y compactación.

Descripción Microscópica.-**Mineralogía.-**

Cuarzo.- Es un componente muy reducido de la lava, presente en forma de fenocristales anhédrales con bordes sub-redondeados de hasta 0,5 mm de largo, muestran fracturas y engolfamientos.

Plagioclasas.- Se presentan en abundante porcentaje, en forma de fenocristales subhedrales tabulares y prismáticos, de hasta 3 mm de largo, muestran zonación, maclas polisintéticas tipo Albita y combinadas Albita-Carlsbad, con bordes de reacción, fracturas e inclusiones de la pasta, corresponden a la variedad Andesina (An: 35) (Fig. 21).

Biotita.- Se presenta en moderada proporción, en forma de fenocristales subhedrales tabulares que alcanzan hasta 1,5 mm de largo, de color marrón oscuro por la oxidación de sus bordes y planos de exfoliación (Fig. 21).

Clinopiroxenos.- Se observan en reducido porcentaje fenocristales subhedrales prismáticos de tono verdoso pálido, que alcanzan hasta 0,5 mm de largo, se trata del tipo augita.

Hornblenda.- Se observan en reducido porcentaje fenocristales euhedrales poligonales de color marrón, están reemplazados parcialmente por limonita, alcanzan hasta 0,5 mm de largo.

Pasta.- La pasta de la lava es abundante y está formada principalmente por microlitos de plagioclasas con cierta orientación y textura afieltrada, y en menor porcentaje por vidrio volcánico de tono pardo y textura masiva (Fig. 21).

Óxidos de Hierro.- Se presentan en reducido porcentaje, como pequeños minerales opacos de hábito anhedral, diseminados en la pasta y alterando a cristales de biotita y hornblenda, corresponderían a las variedades limonita, hematita y magnetita.

Composición porcentual observada.-

Cuarzo (SiO_2).....	1-2 %
Plagioclasas (Andesina) $\text{NaCaAl}(\text{Si}_3\text{O}_8)$	23-25 %
Biotita ($\text{K}_2(\text{Mg},\text{Fe})_2(\text{OH})_2(\text{AlSiO}_{10})$).....	4-5 %
Clinopiroxenos (Augita) ($\text{Mg},\text{Fe})(\text{SiO}_3)$	2-3 %
Hornblenda $\text{Ca}_2(\text{Mg},\text{Fe},\text{Al})_5(\text{OH})_2\{(\text{Si},\text{Al})_4\text{O}_{11}\}_2$	1-2 %
Pasta (microlitos de plagioclasas).....	58-60 %
Óxidos de Hierro (Limonita, hematita y magnetita).....	2-3 %
Total.....	100 %

Textura y estructura.- Presenta estructura holocrystalina y textura porfídica de grano medio (>2 mm), con pasta vítrea y microlítica de textura afieltrada (Fig. 21).

Nombre de la roca.- De acuerdo al análisis petrográfico, es una lava de composición intermedia que corresponde a una **ANDESITA BIOTÍTICA**, ligeramente oxidada.

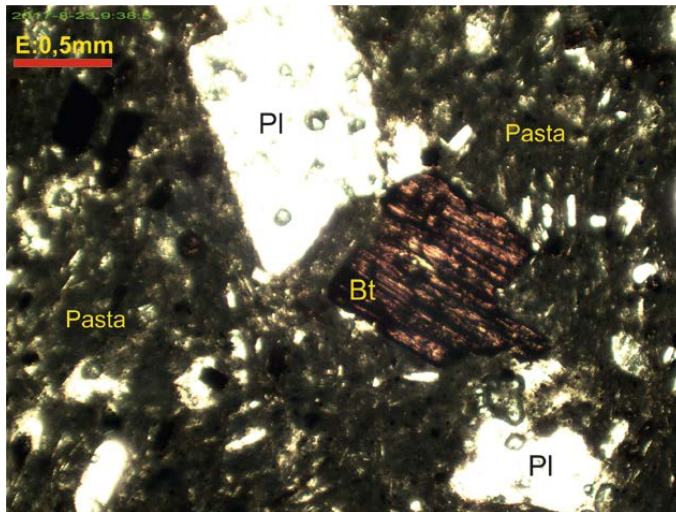


Fig. 21. Muestra 7727, aumento 4x, polarizadores II. Lava Andesítica, con fenocristales de plagioclasas (PI), biotita oxidada (Bt), y una pasta con microlitos de plagioclasas y vidrio.

Analizado por: Ing. José Luis Argandoña C.
ENCARGADO DEL LABORATORIO

INTERESADO:

Ing. Adolfo Orsolini Campana

UBICACIÓN:

Proyecto Mapeo Geológico del Área del Manantial del Silala

FECHA:

22 de Agosto de 2017

Nº LAB: SGM-146/17

Muestra 7729.

ANÁLISIS PETROGRÁFICO

Descripción Macroscópica.-

Fragmento de una roca de origen volcánico (lava), de color gris con tono rosáceo, presenta superficies de intensa meteorización, composición intermedia, muestra estructura holocristalina y textura porfídica de grano medio (>2 mm), donde se observan cristales de feldespatos blanquecinos, muy escaso cuarzo, biotita oxidada y óxidos de hierro diseminados, rodeados por una pasta de grano muy fino, la lava muestra moderada dureza y compactación, por lo que es ligeramente deleznable.

Descripción Microscópica.-

Mineralogía.-

Cuarzo.- Es un componente escaso de la lava, presente en forma de fenocristales anhedrales con bordes sub-redondeados de hasta 1 mm de largo, muestran fracturas y engolfamientos.

Plagioclasas.- Se presentan en abundante porcentaje, en forma de fenocristales subhedrales tabulares y prismáticos, de hasta 4 mm de largo, muestran zonación, maclas polisintéticas tipo Albita y combinadas Albita-Carlsbad, con bordes de reacción, muchas fracturas e inclusiones de la pasta, corresponden al límite entre las variedades Andesina-Oligoclase (An: 30) (Fig. 22).

Biotita.- Se presenta en moderada proporción, en forma de fenocristales subhedrales tabulares que alcanzan hasta 2 mm de largo, de color marrón oscuro por la fuerte oxidación de sus bordes y planos de exfoliación; es posible que algunos cristales correspondan a hornblenda, los que no pueden ser diferenciados de la biotita por su intensa oxidación (Fig. 22).

Clinopiroxenos.- Se observan en escaso porcentaje fenocristales subhedrales prismáticos de tono verdoso pálido, que alcanzan menos de 0,5 mm de largo, se trata del tipo augita (Fig. 22).

Pasta.- La pasta de la lava es abundante y está formada principalmente por microlitos de plagioclasas sin orientación y con textura afieltrada, y en menor porcentaje por vidrio volcánico de tono pardo y textura masiva (Fig. 22).

Óxidos de Hierro.- Se presentan en reducido porcentaje, como pequeños minerales opacos de hábito anhedral, diseminados en la pasta y alterando a cristales de biotita, corresponderían a las variedades limonita y hematita (Fig. 22).

Composición porcentual observada.-

Cuarzo (SiO_2).....	1-2 %
Plagioclasas (Andesina-Oligoclasa) $\text{NaCaAl}(\text{Si}_3\text{O}_8)$	24-26 %
Biotita ($\text{K}_2(\text{Mg},\text{Fe})_2(\text{OH})_2(\text{AlSiO}_{10})$).....	4-6 %
Clinopiroxenos (Augita) ($\text{Mg},\text{Fe})(\text{SiO}_3)$).....	1-2 %
Pasta (microlitos de plagioclasas y vidrio).....	58-60 %
Óxidos de Hierro (Limonita y hematita).....	3-4 %
Total.....	100 %

Textura y estructura.- Presenta una estructura holocrystalina y textura porfídica de grano medio (>2 mm), con pasta microlítica de textura afieltrada y vidrio volcánico (Fig. 22).

Nombre de la roca.- De acuerdo al análisis petrográfico, es una lava de composición intermedia que corresponde a una **ANDESITA Biotítica**, moderadamente oxidada.

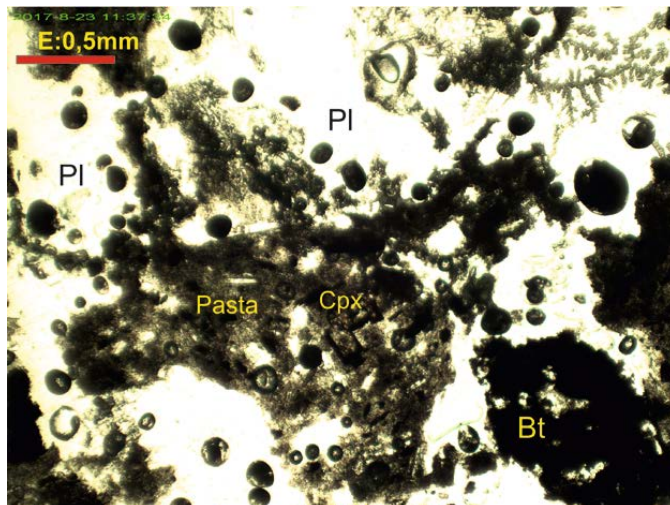


Fig.22. Muestra 7729, aumento 4x, polarizadores II. Lava Andesítica, con fenocristales de plagioclasas (PI), clinopiroxeno (CPx), biotita oxidada (Bt) y pasta con microlitos de plagioclasas.

Analizado por: Ing. José Luis Argandoña C.
 ENCARGADO DEL LABORATORIO

INTERESADO:

Ing. Adolfo Orsolini Campana

UBICACIÓN:

Proyecto Mapeo Geológico del Área del Manantial del Silala

FECHA:

22 de Agosto de 2017

Nº LAB: SGM-147/17

Muestra 7732.

ANÁLISIS PETROGRÁFICO

Descripción Macroscópica.-

Fragmento de una roca de origen volcánico (lava), de color gris oscuro, presenta superficies de meteorización, composición intermedia, muestra estructura holocrystalina y textura porfídica de grano medio (>2 mm), donde se observan cristales de feldespatos blanquecinos, muy escaso cuarzo, biotita y anfíboles oxidados y óxidos de hierro diseminados, rodeados por una pasta de grano muy fino, la lava muestra elevada dureza y compactación.

Descripción Microscópica.-

Mineralogía.-

Cuarzo.- Es un componente escaso de la lava, presente en forma de fenocristales anhedrales con bordes sub-redondeados de hasta 0,5 mm de largo, muestran fracturas y engolfamientos.

Plagioclasas.- Se presentan en abundante porcentaje, en forma de fenocristales subhedrales tabulares y prismáticos, de hasta 3 mm de largo, muestran zonación, maclas polisintéticas tipo Albita y combinadas Albita-Carlsbad, con bordes de reacción, muchas fracturas e inclusiones de la pasta, corresponden a la variedad Oligoclase (An: 25) (Fig. 23).

Biotita.- Se presenta en moderada proporción, en forma de fenocristales subhedrales tabulares que alcanzan hasta 1,5 mm de largo, de color marrón oscuro por la fuerte oxidación de sus bordes y planos de exfoliación, muestran cierta orientación preferencial (Fig. 23).

Hornblenda.- Se observan en reducido porcentaje fenocristales euhedrales poligonales y subhedrales prismáticos de color marrón-rojizo, están reemplazados parcialmente por limonita, y alcanzan hasta 0,5 mm de largo (Fig. 23).

Clinopiroxenos.- Se observan en escaso porcentaje fenocristales anhedrales de tono pardo pálido, que alcanzan hasta 0,5 mm de largo, se trata del tipo augita, y se encuentran rodeados por micro-cristales de hornblenda formando aureolas de alteración (Fig. 23).

Pasta.- La pasta de la lava es abundante y está formada principalmente por vidrio volcánico de tono pardo y textura fluidal, junto a pequeños fragmentos de plagioclasas (Fig. 23).

Óxidos de Hierro.- Se presentan en reducido porcentaje, como pequeños minerales opacos de hábito anhedral, diseminados en la pasta y alterando a cristales de biotita y hornblenda, corresponderían a las variedades limonita, hematita y magnetita.

Composición porcentual observada.-

Cuarzo (SiO_2).....	1-2 %
Plagioclasas (Oligoclasa) $\text{NaCaAl}(\text{Si}_3\text{O}_8)$	23-25 %
Biotita ($\text{K}_2(\text{Mg},\text{Fe})_2(\text{OH})_2(\text{AlSiO}_{10})$).....	4-5 %
Hornblenda $\text{Ca}_2(\text{Mg},\text{Fe},\text{Al})_5(\text{OH})_2\{(\text{Si},\text{Al})_4\text{O}_{11}\}_2$	1-2 %
Clinopiroxenos (Augita) $(\text{Mg},\text{Fe})(\text{SiO}_3)$	1-2 %
Pasta (vidrio volcánico).....	58-60 %
Óxidos de Hierro (Limonita, hematita y magnetita).....	3-4 %
Total.....	100 %

Textura y estructura.- Presenta una estructura holocrystalina y textura porfídica de grano medio (>2 mm), con pasta vítreos de textura fluidal (Fig. 23).

Nombre de la roca.- De acuerdo al análisis petrográfico, es una lava de composición intermedia que corresponde a una **ANDESITA BIOTÍTICA**, moderadamente oxidada.

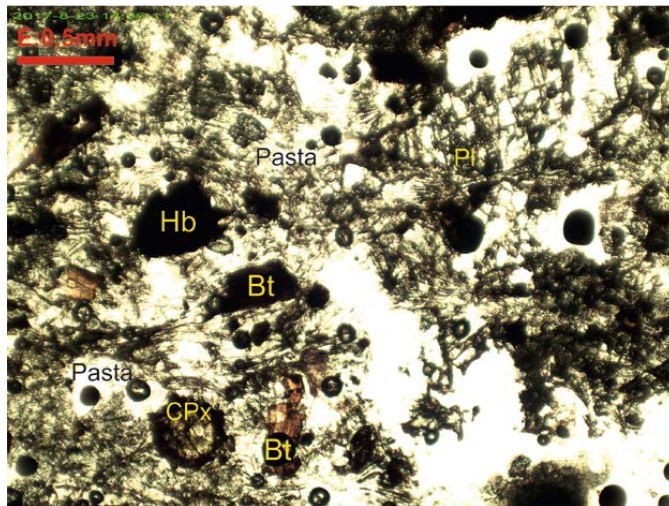


Fig. 23. Muestra 7732, aumento 4x, polarizadores II. Lava Andesítica, con fenocristales de plagioclasas (Pl), biotita (Bt) y hornblenda (Hb) oxidadas, clinopiroxeno (CPx) y pasta vítreos.

Analizado por: Ing. José Luis Argandoña C.
ENCARGADO DEL LABORATORIO

INTERESADO:

Ing. Adolfo Orsolini Campana

UBICACIÓN:

Proyecto Mapeo Geológico del Área del Manantial del Silala

FECHA:

23 de Agosto de 2017

Nº LAB: SGM-148/17

Muestra 7809.

ANÁLISIS PETROGRÁFICO**Descripción Macroscópica.-**

Fragmento de una roca de origen volcánico (lava), de color gris, presenta superficies de intensa meteorización, composición intermedia, muestra estructura holocrystalina y textura porfídica de grano medio (>2 mm), donde se observan cristales de feldespatos blanquecinos, muy escaso cuarzo, biotita y anfíboles oxidados, piroxenos y óxidos de hierro diseminados, rodeados por una pasta de grano muy fino, la lava muestra elevada dureza y compactación.

Descripción Microscópica.-**Mineralogía.-**

Cuarzo.- Es un componente escaso de la lava, presente en forma de fenocristales anhedrales con bordes sub-redondeados inferiores a 0,5 mm de largo, muestran fracturas y engolfamientos.

Plagioclasas.- Se presentan en abundante porcentaje, en forma de fenocristales subhedrales tabulares y prismáticos, de hasta 3 mm de largo, muestran zonación, maclas polisintéticas tipo Albita y combinadas Albita-Carlsbad, con bordes de reacción, fracturas e inclusiones de la pasta, corresponden a la variedad Andesina (An: 30-35) (Fig. 24).

Biotita.- Se presenta en moderada proporción, en forma de fenocristales subhedrales tabulares que alcanzan hasta 2 mm de largo, de color marrón oscuro por la fuerte oxidación de sus bordes y planos de exfoliación, muestran cierta orientación preferencial (Fig.24).

Hornblenda.- Se observan en reducido porcentaje fenocristales euhedrales poligonales y subhedrales prismáticos de color marrón-rojizo, están reemplazados parcialmente por limonita, y alcanzan hasta 0,5 mm de largo (Fig. 7).

Clinopiroxenos.- Se observan en escaso porcentaje, fenocristales subhedrales y prismáticos de tono pardo pálido, que alcanzan hasta 0,5 mm de largo, se trata del tipo augita.

Pasta.- La pasta de la lava es abundante y está formada principalmente por microlitos de plagioclasas, junto a vidrio volcánico de tono pardo y textura masiva (Fig. 24).

Óxidos de Hierro.- Se presentan en reducido porcentaje, como minerales opacos de hábito anhedral, diseminados en la pasta y alterando a cristales de biotita y hornblenda, corresponderían a las variedades limonita, hematita y magnetita.

Calcita.- Se observan en reducido porcentaje, agregados anhedrales de calcita secundaria de grano muy fino y de color blanquecino, llenando pequeñas cavidades de la lava.

Composición porcentual observada.-

Cuarzo (SiO_2).....	1-2 %
Plagioclasas (Andesina) $\text{NaCaAl}(\text{Si}_3\text{O}_8)$	25-27 %
Biotita ($\text{K}_2(\text{Mg},\text{Fe})_2(\text{OH})_2(\text{AlSiO}_{10})$).....	4-6 %
Hornblenda $\text{Ca}_2(\text{Mg},\text{Fe},\text{Al})_5(\text{OH})_2\{(\text{Si},\text{Al})_4\text{O}_{11}\}_2$	2-3 %
Clinopiroxenos (Augita) $(\text{Mg},\text{Fe})(\text{SiO}_3)$	1-2 %
Pasta (Microlitos de plagioclasas y vidrio).....	53-55 %
Óxidos de Hierro (Limonita, hematita y magnetita).....	2-3 %
Calcita (CaCO_3).....	1-2 %
Total.....	100 %

Textura y estructura.- Presenta una estructura holocristalina y textura porfídica de grano medio (>2 mm), con pasta de microlitos de plagioclasas y vidrio de textura masiva (Fig. 24).

Nombre de la roca.- De acuerdo al análisis petrográfico, es una lava de composición intermedia que corresponde a una **ANDESITA Biotítica**, meteorizada.

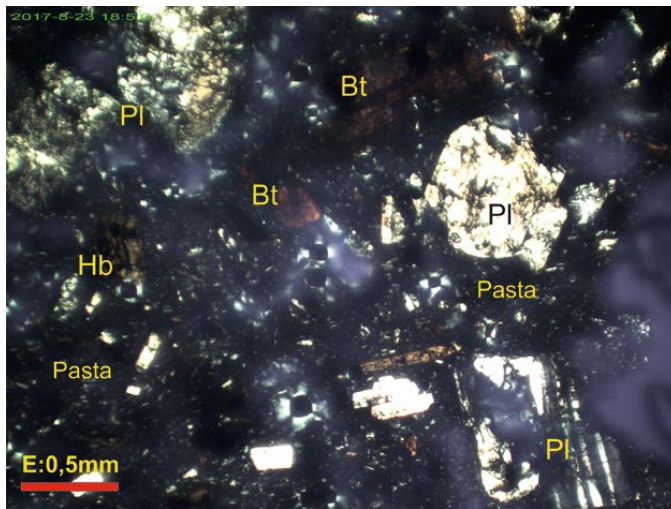


Fig. 24. Muestra 7809, aumento 4x, polarizadores X. Lava Andesítica, con fenocristales de plagioclasas (Pl), biotita (Bt), hornblenda (Hb), y pasta con microlitos de plagioclasas y vidrio.

Analizado por: Ing. José Luis Argandoña C.
ENCARGADO DEL LABORATORIO

INTERESADO:

Ing. Adolfo Orsolini Campana

UBICACIÓN:

Proyecto Mapeo Geológico del Área del Manantial del Silala

FECHA:

23 de Agosto de 2017

Nº LAB: SGM-149/17

Muestra 7810.

ANÁLISIS PETROGRÁFICO**Descripción Macroscópica.-**

Fragmento de una roca de origen volcánico (lava), de color gris con tono negruzco, presenta superficies de meteorización y composición básica, muestra estructura holocrystalina y textura porfídica de grano medio a fino (>1 mm), donde se observan cristales de feldespatos blanquecinos con orientación, minerales maficos muy oxidados, piroxenos y óxidos de hierro diseminados, rodeados por una pasta de grano muy fino, la lava muestra elevada dureza y compactación, así como numerosas cavidades o amígdalas vacías.

Descripción Microscópica.-**Mineralogía.-**

Plagioclasas.- Son los principales componentes de la lava, se presentan en forma de fenocristales subhédrales de hábito tabular y prismático, alcanzan hasta 2 mm de largo, muestran zonación, maclas polisintéticas tipo Albita y combinadas Albita-Carlsbad, con orientación preferencial que sigue el flujo de la lava, bordes de reacción, e inclusiones de la pasta, corresponden a la variedad Andesina (An: 40) (Fig. 25).

Minerales Máficos oxidados.- Se presenta en reducida proporción, en forma de pseudomorfos de fenocristales subhédrales de hasta 0,5 mm de largo, tienen color marrón oscuro por la completa oxidación de los cristales, probablemente correspondían a hornblendas originales.

Clinopiroxenos.- Se observan en escaso porcentaje, fenocristales anhédrales y subhédrales de hábito prismático y de tono pardo pálido, que alcanzan menos de 0,5 mm de largo, se trata de la variedad augita (Fig. 25).

Pasta.- La pasta de la lava es abundante y está formada principalmente por microlitos muy finos de plagioclasas, junto a vidrio volcánico de tono pardo y textura masiva (Fig. 25).

Óxidos de Hierro.- Se presentan en reducido porcentaje, como minerales opacos de hábito anhedral, diseminados en la pasta y reemplazando a cristales de minerales maficos, corresponderían a las variedades limonita, hematita y magnetita.

Composición porcentual observada.-

Plagioclasas (Andesina) $\text{NaCaAl}(\text{Si}_3\text{O}_8)$	31-33 %
Minerales Máficos muy oxidados.....	1-2 %
Clinopiroxenos (Augita) $(\text{Mg}, \text{Fe})(\text{SiO}_3)$	2-3 %
Pasta (Microlitos de plagioclasas y vidrio).....	58-60 %

Óxidos de Hierro (Limonita, hematita y magnetita).....	1-2 %
Total.....	100 %

Textura y estructura.- Presenta una estructura holocristalina y cavernosa con textura porfídica de grano medio a fino (>1 mm), con pasta de microlitos de plagioclasas y vidrio de textura masiva (Fig. 25).

Nombre de la roca.- De acuerdo al análisis petrográfico, es una lava de composición básica que corresponde a un **BASALTO Piroxénico**.

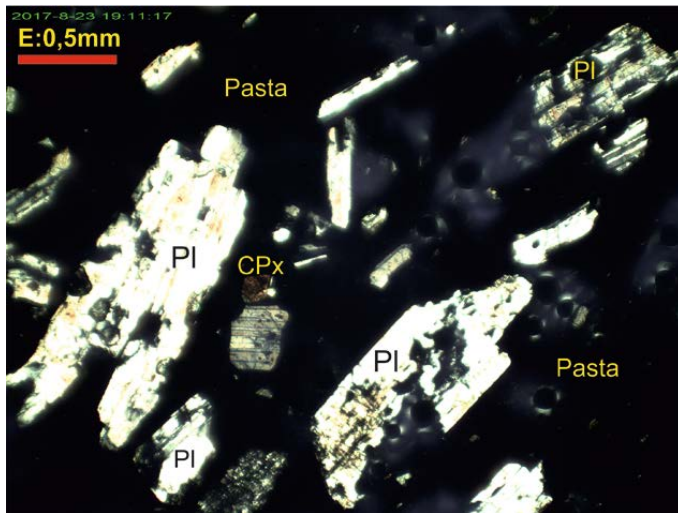


Fig. 25. Muestra 7810, aumento 4x, polarizadores X. Lava Basáltica, con fenocristales de plagioclasas (PI), clinopiroxenos (CPx) y una pasta con microlitos de plagioclasas y vidrio.

Analizado por: Ing. José Luis Argandoña C.
ENCARGADO DEL LABORATORIO

INTERESADO:

Ing. Adolfo Orsolini Campana

UBICACIÓN:

Proyecto Mapeo Geológico del Área del Manantial del Silala

FECHA:

24 de Agosto de 2017

Nº LAB: SGM-151/17

Muestra 7813.

ANÁLISIS PETROGRÁFICO

Descripción Macroscópica.-

Fragmento de una roca de origen volcánico (lava andesítica) de composición intermedia, muestra estructura bandeadas o fluidal y textura porfídica de grano medio (>1 mm), donde se observa una intercalación entre bandas lenticulares de color marrón-rojizo y bandas de tono negruzco, ambas muestran cristales de feldespatos blanquecinos, muy escaso cuarzo, piroxenos, rodeados por una pasta ferruginosa y vítreos, con mayor presencia de hierro en las bandas negruzcas. La roca presenta coloración verdusca oscura y elevada dureza y compactación.

Descripción Microscópica.-

Mineralogía.-

Plagioclasas.- Se presentan en abundante porcentaje, en forma de fenocristales subhédrales tabulares y prismáticos, de hasta 2,5 mm de largo, muestran zonación, macras polisintéticas tipo Albite y combinada Albite-Carlsbad, con inclusiones de la pasta, corresponden al tipo Andesina (An: 35-40), se hallan muy fracturadas y también como fragmentos angulosos (Fig. 26).

Clinopiroxenos.- Se observan en moderado porcentaje, como fenocristales anhédrales y subhédrales de hábito prismático y tabular de clinopiroxenos de tono pardo pálido, algunos con macras polisintéticas, alcanzan hasta 0,7 mm de largo y se tratan del tipo augita (Fig. 26).

Cuarzo.- Es un componente muy escaso, presente en forma de cristales anhédrales con bordes sub-angulosos, inferiores a 0,5 mm de largo, muestran fracturas y engolfamientos.

Pasta.- La pasta es abundante y está conformada principalmente por óxidos de hierro de tono marrón-rojizo del tipo limonita-goethita (ferruginosa), que es más abundante en las bandas lenticulares oscuras, junto a vidrio volcánico de tono pardo oscuro que muestra textura masiva con esquirlas aplanas por el alto grado de soldadura de la roca, y en escaso porcentaje por microlitos de plagioclasas (Fig. 26).

Litoclastos.- Se observan litoclastos de bordes angulosos, formados por rocas volcánicas de similar composición que la roca hospedante, con mayor contenido de plagioclasas, pocos piroxenos y óxidos de hierro diseminados, alcanzan hasta 1 cm de largo.

Composición porcentual observada.-

Cuarzo (SiO_2).....	0,5-1 %
Plagioclasas (Andesina) $\text{NaCaAl}(\text{Si}_3\text{O}_8)$	28-30 %

Clinopiroxenos (Augita) (Mg,Fe)(SiO ₃).....	3-5 %
Pasta (Óxidos de hierro y Vidrio volcánico).....	58-60 %
Litoclastos (rocas volcánicas).....	3-4 %
Total.....	100 %

Textura y estructura.- La roca presenta estructura bandeada (lenticular) o fluidal y textura porfídica de grano medio (>1 mm), con abundante pasta ferruginosa y vítreas de textura masiva (Fig. 26).

Nombre de la roca.- De acuerdo al análisis petrográfico, se trataría de un flujo de lava de composición intermedia, que correspondería a una **roca ANDESÍTICA**. Si bien es muy similar a una lava, por las esquirlas de vidrio deformadas y aplastadas, junto a la textura bandeada lenticular puede constituirse en parte de una brecha basal de flujo volcánico.

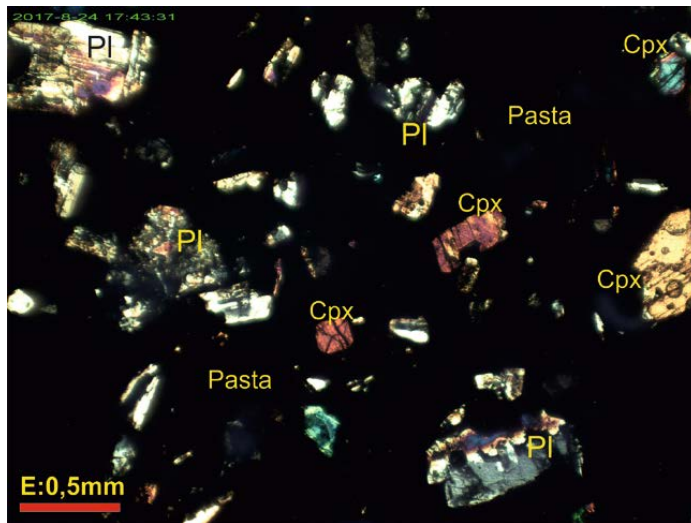


Fig. 26. Muestra 7813, aumento 4x, polarizadores X. Toba Ignimbótica Andesítica, con fenocristales de plagioclasas (PI), clinopiroxenos (CPx), y abundante pasta ferruginosa (limonita-goethita) y vítreas.

Analizado por: Ing. José Luis Argandoña C.
ENCARGADO DEL LABORATORIO

INTERESADO:

Ing. Adolfo Orsolini Campana

UBICACIÓN:

Proyecto Mapeo Geológico del Área del Manantial del Silala

FECHA:

24 de Agosto de 2017

Nº LAB: SGM-150/17

Muestra 7811.

ANÁLISIS PETROGRÁFICO

Descripción Macroscópica.-

Fragmento de una roca de origen volcánico de composición intermedia y color violáceo oscuro, muestra estructura aglomerada y textura porfídica de grano medio (>2 mm), donde se observan abundantes cristales de feldespatos blanquecinos, piroxenos y grandes litoclastos de rocas volcánicas de tono gris, rodeados por una pasta ferruginosa de tono violáceo. La roca presenta moderado grado de dureza y compactación.

Descripción Microscópica.-

Mineralogía.-

Plagioclasas.- Se presentan en abundante porcentaje, en forma de fenocristales subhendrales tabulares y prismáticos, de hasta 2,5 mm de largo, muestran zonación, maclas polisintéticas tipo Albita y combinada Albita-Carlsbad, con inclusiones de la pasta, corresponden a la variedad Andesina (An: 35), se hallan fracturadas y también como fragmentos angulosos (Fig. 27).

Clinopiroxenos.- Se observan en moderado porcentaje, como fenocristales anhendrales y subhendrales de hábito prismático y tabular de clinopiroxenos de tono pardo pálido, algunos con maclas polisintéticas, alcanzan hasta 1,5 mm de largo y se tratan del tipo augita.

Pasta.- La pasta es abundante y está conformada fundamentalmente por óxidos de hierro de tono marrón-rojizo y hábito terroso del tipo limonita-goethita (ferruginosa), probablemente junto a pequeños contenidos de vidrio volcánico de textura masiva, enmascarado por los óxidos de hierro que se observan como minerales opacos (Fig. 27).

Litoclastos.- Se observan grandes litoclastos de bordes angulosos, formados por rocas volcánicas de tono gris y similar composición que la roca hospedante, con mayor contenido de plagioclasas, pocos piroxenos y óxidos de hierro diseminados de hábito anhedral y cúbico que corresponderían a hematita, magnetita y limonita, alcanzan hasta 2 cm de largo en la sección delgada y hasta 4 cm en la muestra de mano (Fig. 27).

Composición porcentual observada.-

Plagioclasas (Andesina) $\text{NaCaAl}(\text{Si}_3\text{O}_8)$	25-27 %
Clinopiroxenos (Augita) $(\text{Mg}, \text{Fe})(\text{SiO}_3)$	3-5 %
Pasta (Óxidos de hierro).....	56-58 %
Litoclastos (rocas volcánicas).....	8-10 %
Total.....	100 %

Textura y estructura.- La roca presenta estructura aglomerada y textura porfídica de grano medio (>2 mm), con abundante pasta ferruginosa de limonita-goethita (Fig. 27).

Nombre de la roca.- De acuerdo al análisis petrográfico, se trataría probablemente de una roca de composición intermedia, que correspondería a una **ANDESITA Piroxénica** con pasta muy ferruginosa. y por los contenidos de litoclastos de una brecha basal de un flujo de lava andesítico.

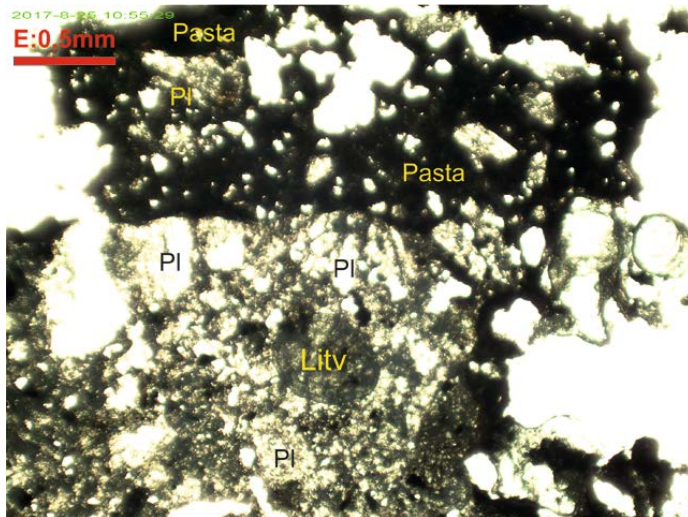


Fig. 27. Muestra 7811, aumento 4x, polarizadores II. Toba Lítica Andesítica, con fenocristales de plagioclasas (PI), litoclasto volcánico (Litv) y abundante pasta ferruginosa (limonita-goethita).

Analizado por: Ing. José Luis Argandoña C.
ENCARGADO DEL LABORATORIO

INTERESADO:

Ing. Adolfo Orsolini Campana

UBICACIÓN:

Proyecto Mapeo Geológico del Área del Manantial del Silala

FECHA:

24 de Agosto de 2017

Nº LAB: SGM-152/17

Muestra 7814.

ANÁLISIS PETROGRÁFICO

Descripción Macroscópica.-

Fragmento de una roca de origen piroclástico (toba), de color gris con tono rosáceo, muestra superficies de meteorización, composición acida, con estructura masiva y textura porfídica de grano medio (>1 mm), donde se observan cristales de feldespatos blanquecinos, anfíboles, piroxenos y óxidos de hierro diseminados, rodeados por una pasta de grano muy fino, la roca muestra moderada dureza y compactación, y presenta costras delgadas de malaquita.

Descripción Microscópica.-

Mineralogía.-

Plagioclasas.- Se presentan en abundante porcentaje, en forma de fenocristales subhédrales tabulares y prismáticos, de hasta 1,5 mm de largo, muestran zonación, maclas polisintéticas tipo Albita y combinadas Albita-Carlsbad, con bordes de reacción y fracturas, corresponden a la variedad Andesina (An: 35) (Fig. 28).

Clinopiroxenos.- Se observan en reducido porcentaje pequeños fenocristales anhédrales y subhédrales prismáticos de tono verdoso pálido, que alcanzan hasta 0,5 mm de largo, se trata del tipo augita (Fig. 28).

Hornblenda.- Se observan en moderado porcentaje fenocristales euhédrales poligonales de color marrón, se hallan reemplazados parcialmente por limonita en los bordes, alcanzan hasta 1 mm de largo (Fig. 28).

Pasta.- La pasta es abundante y está formada principalmente por microlitos de plagioclasas sin orientación, en menor porcentaje por vidrio volcánico de tono pardo y textura masiva, y óxidos de hierro de grano muy fino (Fig. 28).

Óxidos de Hierro.- Se presentan en reducido porcentaje, como minerales opacos anhédrales, diseminados en la pasta y alterando cristales de hornblenda, corresponden al tipo limonita.

Composición porcentual observada.-

Plagioclasas (Andesina) $\text{NaCaAl}(\text{Si}_3\text{O}_8)$	23-25 %
Clinopiroxenos (Augita) $(\text{Mg}, \text{Fe})(\text{SiO}_3)$	<1 %
Hornblenda $\text{Ca}_2(\text{Mg}, \text{Fe}, \text{Al})_5(\text{OH})_2\{\text{Si}, \text{Al}\}_4\text{O}_{11}{}_2$	3-5 %
Pasta (microlitos de plagioclasas y vidrio).....	63-65 %
Óxidos de Hierro (Limonita).....	2-3 %
Total.....	100 %

Textura y estructura.- Presenta estructura masiva y textura porfídica de grano medio (>1 mm), con pasta vítreo y microlitos de plagioclasas, presenta delgadas costras superficiales de malaquita verdosa (Fig. 28).

Nombre de la roca.- De acuerdo al análisis petrográfico, es una toba de composición acida, que corresponde a una **DACITA Hornbléndica**, ligeramente oxidada.

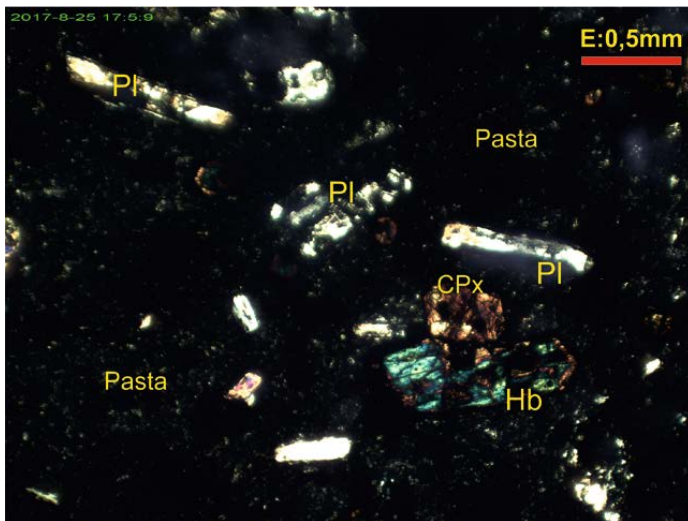


Fig. 28. Muestra 7814, aumento 4x, polarizadores X. Toba Andesítica, con fenocristales de plagioclasas (PI), hornblenda (Hb), clinopiroxeno (CPx), y una pasta con microlitos y vidrio.

Analizado por: Ing. José Luis Argandoña C.
ENCARGADO DEL LABORATORIO

INTERESADO:

Ing. Adolfo Orsolini Campana

UBICACIÓN:

Proyecto Mapeo Geológico del Área del Manantial del Silala

FECHA:

25 de Agosto de 2017

Nº LAB: SGM-153/17

Muestra 7816.

ANÁLISIS PETROGRÁFICO

Descripción Macroscópica.-

Fragmento de una roca de origen volcánico (lava), de color gris oscuro con superficies de meteorización, composición intermedia, muestra estructura holocrystalina y textura porfídica de grano medio (>1 mm), donde se observan cristales de feldespatos blanquecinos, biotita, piroxenos y óxidos de hierro diseminados, rodeados por una pasta de grano fino, contiene agregados de calcita llenando pequeñas cavidades, la roca muestra elevada dureza y compactación, y contiene algunos litoclastos de rocas volcánicas.

Descripción Microscópica.-

Mineralogía.-

Plagioclasas.- Se presentan en abundante porcentaje, en forma de fenocristales subhédrales tabulares y prismáticos, de hasta 2 mm de largo, muestran zonación, maclas polisintéticas tipo Albita y combinadas Albita-Carlsbad, con bordes de reacción y fracturas, corresponden a la variedad Andesina (An: 35), se hallan débilmente alterados a calcita (Fig. 29).

Biotita.- Se presenta en moderada proporción, en forma de fenocristales subhédrales tabulares que alcanzan hasta 1 mm de largo, de color marrón oscuro por la oxidación de sus bordes y planos de exfoliación, con inclusiones de plagioclasas.

Clinopiroxenos.- Se observan en moderado porcentaje fenocristales euhédrales poligonales y subhédrales prismáticos de tono verdoso pálido, que alcanzan hasta 1 mm de largo, se trata del tipo augita, algunos presentan maclas polisintéticas (Fig. 29).

Pasta.- La pasta de la lava es abundante y está formada principalmente por microlitos de plagioclasas con marcada orientación y textura traquílica, y en menor porcentaje por vidrio volcánico de tono pardo y textura masiva (Fig. 29).

Óxidos de Hierro.- Se presentan en reducido porcentaje, como pequeños minerales opacos de hábito anhedral y subhedral, diseminados en la pasta y alterando a cristales de biotita, corresponderían a las variedades limonita, hematita y magnetita.

Calcita.- Se observan en escaso porcentaje, agregados anhédrales de calcita secundaria de grano fino y de color blanquecino, llenando pequeñas cavidades de la lava.

Composición porcentual observada.-

Plagioclasas (Andesina) NaCaAl(Si ₃ O ₈).....	28-30 %
Biotita (K ₂ (Mg,Fe) ₂ (OH) ₂ (AlSiO ₁₀)).....	2-3 %

Clinopiroxenos (Augita) ($Mg,Fe)(SiO_3$).....	5-7 %
Pasta (microlitos de plagioclasas).....	53-55 %
Óxidos de Hierro (Limonita, hematita y magnetita).....	2-3 %
Calcita ($CaCO_3$).....	1-2 %
Total.....	100 %

Textura y estructura.- Presenta una estructura holocrystalina y textura porfídica de grano medio (>1 mm), con pasta microlítica de textura traquítica (Fig. 29).

Nombre de la roca.- De acuerdo al análisis petrográfico, es una lava de composición intermedia, que corresponde a una **ANDESITA Piroxénica**, débilmente carbonatada.

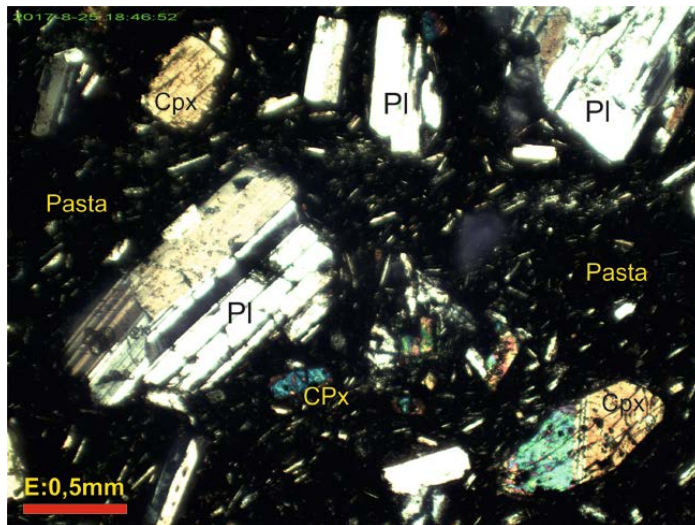


Fig. 29 Muestra 7816, aumento 4x, polarizadores X. Lava Andesítica, con fenocristales de plagioclasas (Pl), clinopiroxeno (Cpx), y pasta con microlitos de plagioclasas y vidrio.

Analizado por: Ing. José Luis Argandoña C.
ENCARGADO DEL LABORATORIO

INTERESADO:

Ing. Adolfo Orsolini Campana

UBICACIÓN:

Proyecto Mapeo Geológico del Área del Manantial del Silala

FECHA:

25 de Agosto de 2017

Nº LAB: SGM-154/17

Muestra 7817.

ANÁLISIS PETROGRÁFICO

Descripción Macroscópica.-

Fragmento de una roca de origen volcánico (lava), de color gris oscuro con superficies de intensa meteorización, composición intermedia, muestra estructura holocristalina y textura porfídica de grano medio (>1 mm), donde se observan cristales de feldespatos blanquecinos, biotita y anfíboles muy oxidados, piroxenos y óxidos de hierro diseminados, rodeados por una pasta de grano fino, la roca muestra moderada dureza y compactación.

Descripción Microscópica.-

Mineralogía.-

Plagioclasas.- Se presentan en abundante porcentaje, en forma de fenocristales subhédrales tabulares y prismáticos, de hasta 4 mm de largo, muestran zonación, maclas polisintéticas tipo Albita y combinadas Albita-Carlsbad, con bordes de reacción y fracturas, corresponden a la variedad Oligoclasa (An: 25-30), muestran ligera orientación preferencial (Fig. 30).

Biotita.- Se presenta en reducida proporción, en forma de fenocristales subhédrales tabulares que alcanzan hasta 0,7 mm de largo, de color marrón oscuro por la intensa oxidación de sus bordes y planos de exfoliación (Fig. 30).

Clinopiroxenos.- Se observan en moderado porcentaje fenocristales euhédrales poligonales y subhédrales prismáticos de tono verdoso pálido, que alcanzan hasta 2 mm de largo, se trata del tipo augita, algunos cristales muestran cierta oxidación de los bordes (Fig. 30).

Hornblenda.- Se observan en moderado porcentaje como fenocristales euhédrales poligonales y subhédrales de color marrón, se hallan intensamente oxidados en los bordes, alcanzan hasta 1 mm de largo (Fig. 30).

Pasta.- La pasta de la lava es abundante y está formada principalmente por microlitos de plagioclasas con marcada orientación y textura traquílica, y en menor porcentaje por vidrio volcánico de tono pardo y textura masiva (Fig. 30).

Óxidos de Hierro.- Se presentan en reducido porcentaje, como pequeños minerales opacos de hábito anhedral y subhedral, diseminados en la pasta y alterando a cristales de biotita, corresponderían a las variedades limonita, hematita y escasa magnetita.

Composición porcentual observada.-

Plagioclasas (Oligoclasa) $\text{NaCaAl}(\text{Si}_3\text{O}_8)$	30-32 %
Biotita $(\text{K}_2(\text{Mg},\text{Fe})_2(\text{OH})_2(\text{AlSiO}_{10}))$	1-2 %

Clinopiroxenos (Augita) ($Mg,Fe)(SiO_3$).....	4-5 %
Hornblenda $Ca_2(Mg,Fe,Al)_5(OH)_2[(Si,Al)_4O_{11}]_2$	2-3 %
Pasta (microlitos de plagioclasas).....	53-55 %
Óxidos de Hierro (Limonita, hematita y magnetita).....	2-3 %
Total.....	100 %

Textura y estructura.- Presenta una estructura holocrystalina y textura porfídica de grano medio (>1 mm), con pasta microlítica de textura traquítica (Fig. 30).

Nombre de la roca.- De acuerdo al análisis petrográfico, es una lava de composición intermedia, que corresponde a una **ANDESITA Piroxénica**, débilmente oxidada.

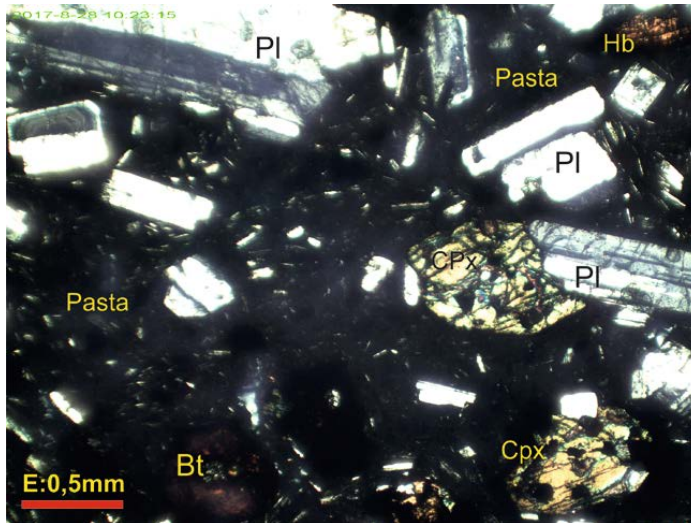


Fig. 30. Muestra 7817, aumento 4x, polarizadores X. Lava Andesítica, con fenocristales de plagioclasas (PI), clinopiroxeno (CPx), hornblenda (Hb), biotita (Bt) y pasta con microlitos.

Analizado por: Ing. José Luis Argandoña C.
ENCARGADO DEL LABORATORIO

INTERESADO:

Ing. Adolfo Orsolini Campana

UBICACIÓN:

Proyecto Mapeo Geológico del Área del Manantial del Silala

FECHA:

28 de Agosto de 2017

Nº LAB: SGM-155/17

Muestra 7818.

ANÁLISIS PETROGRÁFICO**Descripción Macroscópica.-**

Fragmento de una roca de origen volcánico (lava), de color gris con superficies de intensa meteorización, composición intermedia, muestra estructura holocrystalina y cavernosa, con textura porfídica de grano medio (>1 mm), donde se observan abundantes cristales de feldespatos blanquecinos, biotita oxidada, piroxenos y óxidos de hierro diseminados, rodeados por una pasta de grano fino, la roca muestra elevada dureza y compactación.

Descripción Microscópica.-**Mineralogía.-**

Plagioclasas.- Se presentan en abundante porcentaje, en forma de fenocristales subhédrales tabulares y prismáticos, de hasta 3 mm de largo, muestran zonación, maclas polisintéticas tipo Albita y combinadas Albita-Carlsbad, con bordes de reacción y fracturas, corresponden a la variedad Andesina (An: 35), muestran ligera orientación preferencial (Fig. 31).

Biotita.- Se presenta en reducida proporción, como fenocristales subhédrales tabulares que alcanzan hasta 1 mm de largo, de color marrón oscuro por la oxidación de sus bordes (Fig. 31).

Clinopiroxenos.- Se observan en moderado porcentaje fenocristales subhédrales prismáticos y anhédrales de tono verdoso pálido, que alcanzan hasta 2 mm de largo, se trata del tipo augita, algunos cristales muestran fracturas y oxidación de los bordes (Fig. 31).

Pasta.- La pasta de la lava es abundante y está formada principalmente por micro-cristales y microlitos de plagioclasas sin orientación, y en menor porcentaje por vidrio volcánico de tono pardo y textura fluidal (Fig. 31).

Óxidos de Hierro.- Se presentan en reducido porcentaje, como pequeños minerales opacos de hábito anhedral y subhedral, diseminados en la pasta y alterando a cristales de biotita, corresponderían a las variedades limonita, hematita y magnetita.

Composición porcentual observada.-

Plagioclasas (Andesina) $\text{NaCaAl}(\text{Si}_3\text{O}_8)$	30-32 %
Biotita $(\text{K}_2(\text{Mg},\text{Fe})_2(\text{OH})_2(\text{AlSiO}_{10}))$	3-4 %
Clinopiroxenos (Augita) $(\text{Mg},\text{Fe})(\text{SiO}_3)$	4-6 %
Pasta (microlitos de plagioclasas y vidrio).....	53-55 %
Óxidos de Hierro (Limonita, hematita y magnetita).....	2-3 %
Total.....	100 %

Textura y estructura.- Presenta una estructura holocrystalina y cavernosa, con textura porfídica de grano medio (>1 mm), la pasta es microlítica y vítreo (Fig. 31).

Nombre de la roca.- De acuerdo al análisis petrográfico, es una lava de composición intermedia, que corresponde a una **ANDESITA Piroxénica**.

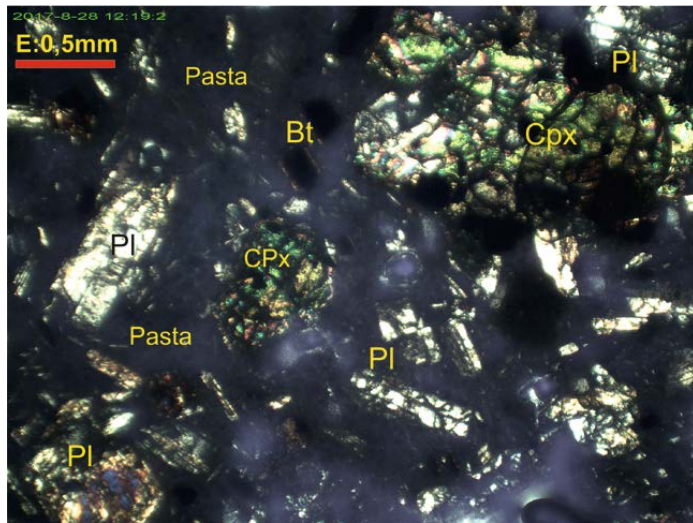


Fig. 31. Muestra 7818, aumento 4x, polarizadores X. Lava Andesítica, con fenocristales de plagioclasas (PI), clinopiroxeno (CPx), biotita oxidada (Bt) y pasta con microlitos y vidrio fluidal.

Analizado por: Ing. José Luis Argandoña C.
ENCARGADO DEL LABORATORIO

INTERESADO:

Ing. Adolfo Orsolini Campana

UBICACIÓN:

Proyecto Mapeo Geológico del Área del Manantial del Silala

FECHA:

28 de Agosto de 2017

Nº LAB: SGM-156/17

Muestra 7820.

ANÁLISIS PETROGRÁFICO

Descripción Macroscópica.-

Fragmento de una roca de origen volcánico (lava), de color gris con tono rosáceo, tiene superficies de meteorización, composición intermedia, muestra estructura holocristalina y textura porfídica de grano medio (>2 mm), donde se observan abundantes cristales de feldespatos blanquecinos, biotita y anfíboles oxidados, piroxenos, óxidos de hierro diseminados y pequeños litoclastos de rocas volcánicas, rodeados por una pasta de grano fino, la roca muestra elevada dureza y compactación.

Descripción Microscópica.-

Mineralogía.-

Plagioclasas.- Se presentan en abundante porcentaje, en forma de fenocristales subhédrales tabulares y prismáticos, de hasta 3 mm de largo, muestran zonación, maclas polisintéticas tipo Albita y combinadas Albita-Carlsbad, con bordes de reacción y fracturas, corresponden al límite entre Oligoclasa-Andesina (An: 30), muestran ligera orientación preferencial (Fig. 32).

Biotita.- Se presenta en reducida proporción, en forma de fenocristales subhédrales y tabulares que alcanzan hasta 0,5 mm de largo, de color marrón oscuro por una débil oxidación de sus bordes.

Clinopiroxenos.- Se observan en moderado porcentaje fenocristales subhédrales prismáticos y anhédrales de tono verdoso pálido, que alcanzan hasta 1 mm de largo del tipo augita, algunos cristales muestran fracturas y oxidación de los bordes (Fig. 32).

Hornblenda.- Se observan en reducido porcentaje como fenocristales euhédrales poligonales y subhédrales prismáticos de color marrón, se hallan oxidados en los bordes, alcanzan hasta 0,5 mm de largo (Fig. 32).

Pasta.- La pasta de la lava es abundante y está formada principalmente por microlitos de plagioclasas sin orientación, y en menor porcentaje por óxidos de hierro de grano fino (Fig. 32).

Óxidos de Hierro.- Se presentan en reducido porcentaje, como pequeños minerales opacos de hábito anhedral y subhedral, diseminados en la pasta y alterando a cristales de biotita y hornblenda, corresponderían a las variedades limonita, hematita y poca magnetita.

Litoclastos.- Se observan pequeños litoclastos de bordes sub-angulosos, formados por rocas volcánicas de tono gris y similar composición que la roca hospedante, contienen plagioclasas, piroxenos y anfíboles oxidados, alcanzan hasta 2 mm de largo.

Composición porcentual observada.-

Plagioclasas (Andesina) $\text{NaCaAl}(\text{Si}_3\text{O}_8)$	30-32 %
Biotita $(\text{K}_2(\text{Mg},\text{Fe})_2(\text{OH})_2(\text{AlSiO}_{10}))$	1-2 %
Clinopiroxenos (Augita) $(\text{Mg},\text{Fe})(\text{SiO}_3)$	3-5 %
Hornblenda $\text{Ca}_2(\text{Mg},\text{Fe},\text{Al})_5(\text{OH})_2\{(\text{Si},\text{Al})_4\text{O}_{11}\}_2$	2-3 %
Pasta (microlitos de plagioclasas).....	51-53 %
Óxidos de Hierro (Limonita, hematita y magnetita).....	2-3 %
Litoclastos (rocas volcánicas).....	1-2 %
Total.....	100 %

Textura y estructura.- Presenta una estructura holocristalina y textura porfídica de grano medio (>2 mm), la pasta es microlítica (Fig. 32).

Nombre de la roca.- De acuerdo al análisis petrográfico, es una lava de composición intermedia, que corresponde a una **ANDESITA Piroxénica**, débilmente oxidada.

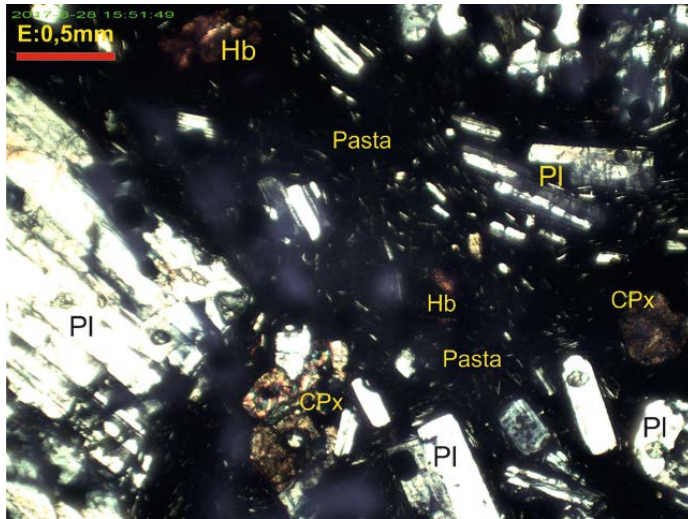


Fig. 32. Muestra 7820, aumento 4x, polarizadores X. Lava Andesítica, con fenocristales de plagioclasas (PI), clinopiroxeno (CPx), hornblenda (Hb) y pasta con microlitos de plagioclasas.

Analizado por: Ing. José Luis Argandoña C.
ENCARGADO DEL LABORATORIO

INTERESADO:

Ing. Adolfo Orsolini Campana

UBICACIÓN:

Proyecto Mapeo Geológico del Área del Manantial del Silala

FECHA:

28 de Agosto de 2017

Nº LAB: SGM-157/17

Muestra 7821.

ANÁLISIS PETROGRÁFICO**Descripción Macroscópica.-**

Fragmento de una roca de origen volcánico (lava), de color gris oscuro, composición intermedia, muestra estructura holocristalina y textura porfídica de grano medio (>2 mm), donde se observan abundantes cristales de feldespatos blanquecinos, biotita y anfíboles oxidados, escaso cuarzo y piroxenos, y óxidos de hierro diseminados, rodeados por una pasta de grano fino, la roca muestra elevada dureza y compactación, en general se halla fresca.

Descripción Microscópica.-**Mineralogía.-**

Cuarzo.- Es un componente escaso, presente en forma de fenocristales anhedrales con bordes sub-angulosos, de hasta 1 mm de largo, muestran fracturas y engolfamientos.

Plagioclasas.- Se presentan en abundante porcentaje, en forma de fenocristales subhédrales tabulares y prismáticos, de hasta 4 mm de largo, muestran zonación, maclas polisintéticas tipo Albita y combinadas Albita-Carlsbad, con bordes de reacción y fracturas, corresponden al tipo Oligoclásica (An: 25-30) (Fig. 33).

Biotita.- Se presenta en reducida proporción, en forma de fenocristales subhédrales y tabulares que alcanzan hasta 2,5 mm de largo, de color marrón oscuro por una débil oxidación de sus bordes, contienen pequeñas inclusiones de plagioclasas.

Clinopiroxenos.- Se observan en reducido porcentaje como fenocristales anhedrales de tono verdoso pálido, que alcanzan hasta 0,5 mm de largo del tipo augita, algunos cristales muestran fracturas y oxidación de los bordes (Fig. 33).

Hornblenda.- Se observan en moderado porcentaje como fenocristales euhédrales poligonales y subhédrales prismáticos de color marrón, se hallan oxidados en los bordes, alcanzan hasta 1,5 mm de largo (Fig. 33).

Pasta.- La pasta de la lava es abundante y está formada principalmente por microlitos de plagioclasas sin orientación, y en menor porcentaje por vidrio volcánico de textura masiva y óxidos de hierro de grano muy fino (Fig. 33).

Óxidos de Hierro.- Se presentan en reducido porcentaje, como pequeños minerales opacos de hábito anhedral y subhedral, diseminados en la pasta y alterando a cristales de biotita y hornblenda, corresponderían a las variedades limonita, hematita y magnetita.

Composición porcentual observada.-

Cuarzo (SiO_2).....	1-2 %
Plagioclasas (Oligoclasa) $\text{NaCaAl}(\text{Si}_3\text{O}_8)$	20-22 %
Biotita ($\text{K}_2(\text{Mg},\text{Fe})_2(\text{OH})_2(\text{AlSiO}_{10})$).....	2-3 %
Clinopiroxenos (Augita) ($\text{Mg},\text{Fe})(\text{SiO}_3)$	2-3 %
Hornblenda $\text{Ca}_2(\text{Mg},\text{Fe},\text{Al})_5(\text{OH})_2[(\text{Si},\text{Al})_4\text{O}_{11}]_2$	4-5 %
Pasta (microlitos de plagioclasas).....	60-62 %
Óxidos de Hierro (Limonita, hematita y magnetita).....	2-3 %
Total.....	100 %

Textura y estructura.- Presenta una estructura holocrystalina y textura porfídica de grano medio (>2 mm), la pasta es principalmente microlítica (Fig. 33).

Nombre de la roca.- De acuerdo al análisis petrográfico, es una lava de composición intermedia, que corresponde a una **ANDESITA Hornbléndica**.

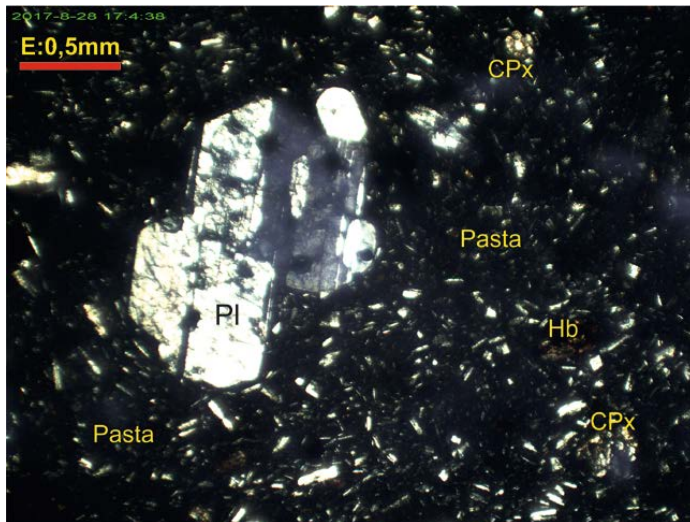


Fig. 33. Muestra 7821, aumento 4x, polarizadores X. Lava Andesítica, con fenocristales de plagioclasas (PI), clinopiroxeno (CPx), hornblenda (Hb) y pasta con microlitos de plagioclasas.

Analizado por: Ing. José Luis Argandoña C.
ENCARGADO DEL LABORATORIO

INTERESADO:

Ing. Adolfo Orsolini Campana

UBICACIÓN:

Proyecto Mapeo Geológico del Área del Manantial del Silala

FECHA:

28 de Agosto de 2017

Nº LAB: SGM-158/17

Muestra 7822.

ANÁLISIS PETROGRÁFICO**Descripción Macroscópica.-**

Fragmento de una roca de origen volcánico (lava), de color gris con tono rosáceo, composición intermedia, muestra estructura holocristalina y textura porfídica de grano medio (>2 mm), donde se observan abundantes cristales de feldespatos blanquecinos, biotita y anfíboles oxidados, escaso cuarzo y óxidos de hierro diseminados, rodeados por una pasta de grano fino, la roca muestra moderada dureza y compactación, en general se halla meteorizada.

Descripción Microscópica.-**Mineralogía.-**

Cuarzo.- Es un componente reducido, presente en forma de fenocristales anhedrales con bordes sub-redondeados, de hasta 1,5 mm de largo, muestran fracturas y bordes de reacción.

Plagioclasas.- Se presentan en abundante porcentaje, en forma de fenocristales subhédrales tabulares y prismáticos, de hasta 3 mm de largo, muestran zonación, maclas polisintéticas tipo Albita y combinadas Albita-Carlsbad, con bordes de reacción y muchas fracturas, corresponden al tipo Oligoclasa (An: 25-30) (Fig. 34).

Biotita.- Se presenta en moderada proporción, en forma de fenocristales subhédrales y tabulares que alcanzan hasta 1,5 mm de largo, de color marrón oscuro por una débil oxidación de sus bordes, contienen pequeñas inclusiones de plagioclasas (Fig. 34).

Hornblenda.- Se observan en reducido porcentaje como fenocristales euédrales poligonales y subhédrales prismáticos de color marrón, se hallan oxidados en los bordes y alcanzan hasta 1 mm de largo (Fig. 34).

Pasta.- La pasta de la lava es abundante y está formada principalmente por microlitos de plagioclasas sin orientación, y en menor porcentaje por vidrio volcánico de textura masiva y óxidos de hierro de grano muy fino (Fig. 34).

Óxidos de Hierro.- Se presentan en reducido porcentaje, como pequeños minerales opacos de hábito anhedral y subhedral, diseminados en la pasta y alterando a cristales de biotita y hornblenda, corresponderían a las variedades limonita, hematita y escasa magnetita.

Composición porcentual observada.-

Cuarzo (SiO_2).....	2-3 %
Plagioclasas (Oligoclasa) $\text{NaCaAl}(\text{Si}_3\text{O}_8)$	25-27 %
Biotita ($\text{K}_2(\text{Mg},\text{Fe})_2(\text{OH})_2(\text{AlSiO}_{10})$).	5-7 %

Hornblenda $\text{Ca}_2(\text{Mg},\text{Fe},\text{Al})_5(\text{OH})_2\{\text{(Si},\text{Al})_4\text{O}_{11}\}_2$	2-3 %
Pasta (microlitos de plagioclasas).....	55-57 %
Óxidos de Hierro (Limonita, hematita y magnetita).....	2-3 %
Total.....	100 %

Textura y estructura.- Presenta una estructura holocristalina y textura porfídica de grano medio (>2 mm), la pasta es principalmente microlítica (Fig. 34).

Nombre de la roca.- De acuerdo al análisis petrográfico, es una lava de composición intermedia, que corresponde a una **ANDESITA BIOTÍTICA** (con escaso Cuarzo).

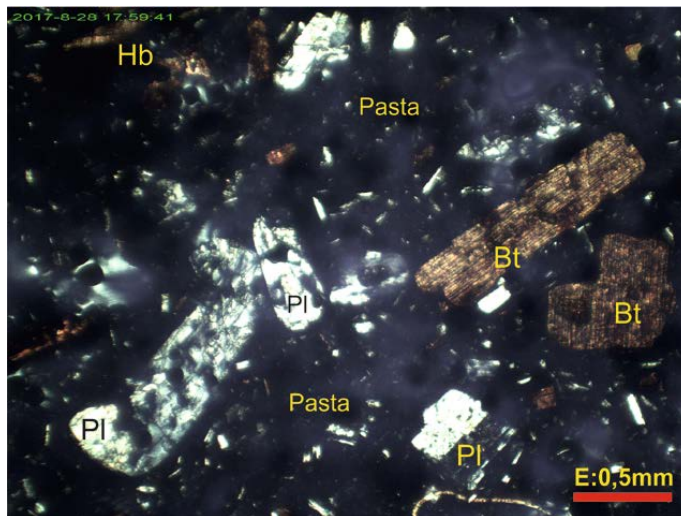


Fig. 34. Muestra 7822, aumento 4x, polarizadores X. Lava Andesítica, con fenocristales de plagioclasas (Pl), biotita (Bt), hornblenda (Hb), y una pasta con microlitos de plagioclasas.

Analizado por: Ing. José Luis Argandoña C.
ENCARGADO DEL LABORATORIO

INTERESADO:

Ing. Adolfo Orsolini Campana

UBICACIÓN:

Proyecto Mapeo Geológico del Área del Manantial del Silala

FECHA:

28 de Agosto de 2017

Nº LAB: SGM-159/17

Muestra 7824.

ANÁLISIS PETROGRÁFICO**Descripción Macroscópica.-**

Fragmento de una roca sedimentaria pelítica (probablemente una arcillita) y color marrón-grisáceo, presenta una estructura masiva y terrosa con indicios de estratificación y textura clástica de grano muy fino (<0,5 mm), donde se observan bandas formadas por abundantes limos y arcillas, junto a óxidos de hierro y probablemente polvo de vidrio volcánico, por lo que la roca es muy suave, con reducida compactación y es deleznable.

Descripción Microscópica.-**Mineralogía.-**

Plagioclasas.- Se presentan en escaso porcentaje, en forma de micro-clastos anhedrales de bordes angulosos, con tamaño variable de 0,1 a 0,5 mm de largo, muestran zonación y maclas polisintéticas tipo Albita, diseminados dentro de un abundante material arcilloso-limoso (Fig. 35).

Cuarzo.- Se presenta en muy escaso porcentaje, como micro-clastos anhedrales con bordes angulosos de grano muy fino, entre 0,1 a 0,4 mm de largo, diseminados dentro del abundante material arcilloso-limoso (Fig. 35).

Piroxenos.- Se observan diseminados en muy escaso porcentaje, como micro-clastos subhedrales de tono verdoso pálido, que alcanzan hasta 0,5 mm de largo, del tipo augita.

Arcillas y Limos.- Son los principales componentes de la roca argilácea, se observan en forma de agregados de grano muy fino (<0,1 mm) y de tono marrón-rojizo, estrechamente asociados con micro-cristales de limonita y probablemente de polvo de vidrio volcánico pardo (Fig. 18).

Óxidos de Hierro.- Ocurren como pequeños minerales opacos diseminados en moderado porcentaje dentro del material arcillosos-limoso, muestran hábito terroso, tono marrón-rojizo y corresponderían a la variedad limonita (Fig. 35).

Composición porcentual observada.-

Plagioclasas NaCaAl(Si ₃ O ₈).....	1-2 %
Cuarzo (SiO ₂).....	<1 %
Piroxenos (Augita) (Mg,Fe)(SiO ₃).....	<1 %
Arcillas y Limos	92-94 %
Óxidos de Hierro (Limonita).....	4-5 %
Total.....	100 %

Textura y estructura.- La roca argilácea presenta estructura masiva y terrosa con textura clástica de grano muy fino (<0,1 mm), con escasos micro-clastos de plagioclasas cuarzo y piroxenos. Es deleznable y muestra escasa dureza y cohesión por el abundante contenido de arcillas y limos (Fig. 35).

Nombre de la roca.- De acuerdo al análisis petrográfico, corresponde a una roca sedimentaria o volcán-sedimentaria de composición pelítica (argilácea), clasificada como una **ARCILLITA**, cuyos escasos micro-clastos corresponden a minerales originales que fueron erosionados de rocas volcánicas; probablemente se trata de una roca de edad cuaternaria.

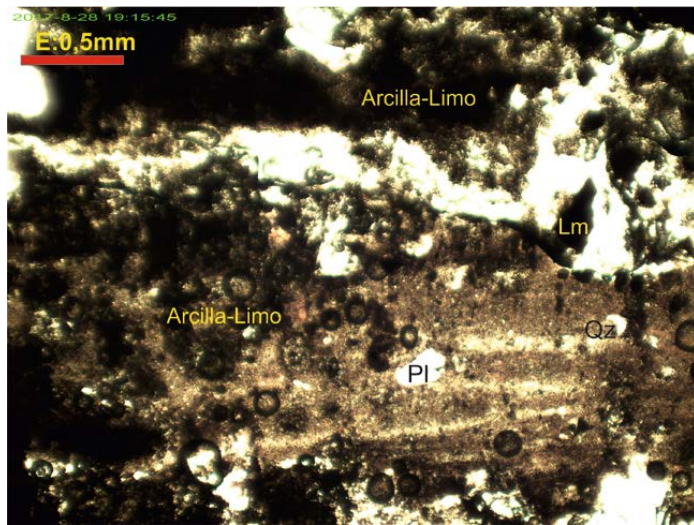


Fig. 35. Muestra 7824, aumento 4x, polarizadores II. Arcillita, formada fundamentalmente por arcillas y limos de tono marrón, con escasos micro-clastos de plagioclasas (Pl), cuarzo (Qz) y limonita (Lm).

Analizado por: Ing. José Luis Argandoña C.
ENCARGADO DEL LABORATORIO

INTERESADO:

Ing. Adolfo Orsolini Campana

UBICACIÓN:

Proyecto Mapeo Geológico del Área del Manantial del Silala

FECHA:

28 de Agosto de 2017

Nº LAB: SGM-160/17

Muestra 7825.

ANÁLISIS PETROGRÁFICO

Descripción Macroscópica.-

Fragmento de una roca de origen volcánico (lava), de color gris con tono oscuro, tiene superficies de meteorización, composición intermedia, muestra estructura cavernosa con cavidades vacías y textura porfídica de grano medio (>2 mm), donde se observan abundantes cristales de feldespatos blanquecinos, biotita muy oxidada, piroxenos y óxidos de hierro diseminados, rodeados por una pasta de grano muy fino, la roca muestra moderada dureza y compactación y un aspecto escoriáceo por sus numerosas cavidades.

Descripción Microscópica.-

Mineralogía.-

Plagioclasas.- Se presentan en abundante porcentaje, en forma de fenocristales subhédrales tabulares y prismáticos, de hasta 3,5 mm de largo, muestran zonación, maclas polisintéticas tipo Albita y combinadas Albita-Carlsbad, con bordes de reacción y fracturas, corresponden a la variedad Andesina (An: 30-35), muestran ligera orientación preferencial (Fig. 36).

Biotita.- Se presenta en reducida proporción, en forma de fenocristales anhédrales y subhédrales tabulares que alcanzan hasta 1 mm de largo, de color marrón oscuro por la intensa oxidación de gran parte de sus cristales.

Clinopiroxenos.- Se observan en moderado porcentaje fenocristales subhédrales prismáticos y anhédrales de tono verdoso pálido, que alcanzan hasta 0,7 mm de largo del tipo augita, algunos cristales muestran fracturas y oxidación de los bordes (Fig. 36).

Pasta.- La pasta de la lava es abundante y está formada principalmente por micro-cristales y microlitos de plagioclasas con cierta orientación, y en menor porcentaje por vidrio volcánico masivo y óxidos de hierro de grano fino (Fig. 36).

Óxidos de Hierro.- Se presentan en reducido porcentaje, como pequeños minerales opacos de hábito anhedral y subhedral (cúbico), diseminados en la pasta y alterando a cristales de biotita, corresponderían a las variedades limonita, hematita y poca magnetita.

Composición porcentual observada.-

Plagioclasas (Andesina) $\text{NaCaAl}(\text{Si}_3\text{O}_8)$	32-34 %
Biotita $(\text{K}_2(\text{Mg},\text{Fe})_2(\text{OH})_2(\text{AlSiO}_{10}))$	2-3 %
Clinopiroxenos (Augita) $(\text{Mg},\text{Fe})(\text{SiO}_3)$	4-5 %
Pasta (microlitos de plagioclasas).....	53-55 %

Óxidos de Hierro (Limonita, hematita y magnetita).....	2-3 %
Total.....	100 %

Textura y estructura.- Presenta una estructura cavernosa y textura porfídica de grano medio (>2 mm), la pasta es microlítica y vítreo (Fig. 36).

Nombre de la roca.- De acuerdo al análisis petrográfico, es una lava de composición intermedia, que corresponde a una **ANDESITA Piroxénica**, débilmente oxidada.

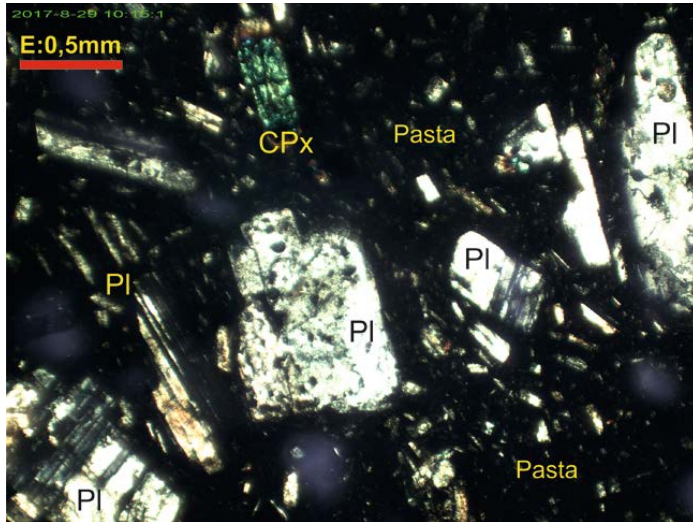


Fig. 36. Muestra 7825, aumento 4x, polarizadores X. Lava Andesítica, con fenocristales de plagioclasas (PI), clinopiroxeno (CPx), y pasta con microlitos de plagioclasas y vidrio.

Analizado por: Ing. José Luis Argandoña C.
ENCARGADO DEL LABORATORIO

INTERESADO:

Ing. Adolfo Orsolini Campana

UBICACIÓN:

Proyecto Mapeo Geológico del Área del Manantial del Silala

FECHA:

29 de Agosto de 2017

Nº LAB: SGM-161/17

Muestra 7827.

ANÁLISIS PETROGRÁFICO**Descripción Macroscópica.-**

Fragmento de una roca de origen volcánico (lava), de color gris, muestra superficies de meteorización, composición relativamente ácida, muestra estructura holocristalina y textura porfídica de grano medio (>2 mm), donde se observan abundantes cristales de feldespatos blanquecinos, cuarzo, biotita muy oxidada, piroxenos y óxidos de hierro diseminados, rodeados por una pasta de grano muy fino, la roca muestra elevada dureza y compactación.

Descripción Microscópica.-**Mineralogía.-**

Cuarzo.- Es un componente presente en moderado porcentaje forma de cristales anhedrales y subhedrales con bordes sub-angulosos, que alcanzan hasta 2 mm de largo, muestran fracturas, engolfamientos e inclusiones de la pasta (Fig. 37).

Plagioclasas.- Se presentan en abundante porcentaje, en forma de fenocristales subhedrales tabulares y prismáticos, de hasta 2,5 mm de largo, muestran zonación, maclas polisintéticas tipo Albita y combinadas Albita-Carlsbad, con bordes de reacción y fracturas, corresponden a la variedad Oligoclasa (An: 25-30) (Fig. 37).

Biotita.- Se presenta en moderada proporción en forma de fenocristales euherdales poligonales y subhedrales tabulares que alcanzan hasta 2 mm de largo, de color marrón oscuro por la intensa oxidación de gran parte de sus cristales.

Clinopiroxenos.- Se observan en moderado porcentaje fenocristales subhedrales prismáticos y euherdales poligonales de tono verdoso pálido, que alcanzan hasta 1,5 mm de largo del tipo augita, algunos muestran fracturas y maclas polisintéticas (Fig. 37).

Pasta.- La pasta es abundante y está formada principalmente por microlitos de plagioclasas con cierta orientación, y en menor porcentaje por óxidos de hierro de grano muy fino (Fig. 37).

Óxidos de Hierro.- Se presentan en reducido porcentaje, como pequeños minerales opacos de hábito anhedral y subhedral (trapezoidal), diseminados en la pasta y alterando a cristales de biotita, corresponderían a las variedades limonita, hematita y magnetita.

Composición porcentual observada.-

Cuarzo (SiO_2).....	5-7 %
Plagioclasas (Oligoclasa) $\text{NaCaAl}(\text{Si}_3\text{O}_8)$	20-22 %
Biotita ($\text{K}_2(\text{Mg},\text{Fe})_2(\text{OH})_2(\text{AlSiO}_{10})$).	3-4 %

Clinopiroxenos (Augita) ($Mg,Fe)(SiO_3$).....	4-6 %
Pasta (microlitos de plagioclasas).....	56-58 %
Óxidos de Hierro (Limonita, hematita y magnetita).....	2-3 %
Total.....	100 %

Textura y estructura.- Presenta una estructura holocristalina y textura porfídica de grano medio (>2 mm), la pasta es microlítica (Fig. 37).

Nombre de la roca.- De acuerdo al análisis petrográfico, es una lava de composición ácida, que corresponde a una **DACITA Piroxénica**, débilmente oxidada.

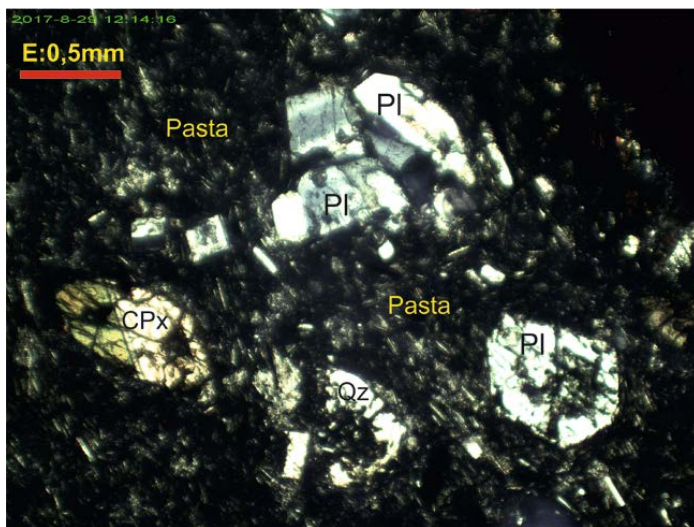


Fig. 37. Muestra 7827, aumento 4x, polarizadores X. Lava Dacítica, con fenocristales de plagioclasas (PI), clinopiroxeno (CPx), cuarzo (Qz) y pasta con microlitos de plagioclasas.

Analizado por: Ing. José Luis Argandoña C.
ENCARGADO DEL LABORATORIO

INTERESADO:

Ing. Adolfo Orsolini Campana

UBICACIÓN:

Proyecto Mapeo Geológico del Área del Manantial del Silala

FECHA:

29 de Agosto de 2017

Nº LAB: SGM-162/17

Muestra 7830.

ANÁLISIS PETROGRÁFICO

Descripción Macroscópica.-

Fragmento de una roca de origen volcánico (lava), de color gris con tono oscuro, tiene superficies de meteorización, composición intermedia, muestra estructura holocrystalina y textura porfídica de grano medio (>2 mm), donde se observan abundantes cristales de feldespatos blanquecinos, anfíboles, biotita, piroxenos y óxidos de hierro diseminados, rodeados por una pasta de grano muy fino, la roca muestra elevada dureza y compactación.

Descripción Microscópica.-

Mineralogía.-

Plagioclasas.- Se presentan en abundante porcentaje, en forma de fenocristales subhédrales tabulares y prismáticos, de hasta 3,5 mm de largo, muestran zonación, maclas polisintéticas tipo Albita y combinadas Albita-Carlsbad, con bordes de reacción y fracturas, corresponden a la variedad Oligoclasa (An: 25), muestran ligera orientación preferencial (Fig. 38).

Biotita.- Se presenta en reducida proporción, en forma de fenocristales anhédrales y subhédrales tabulares que alcanzan hasta 1 mm de largo, de color marrón (Fig. 38).

Hornblenda.- Se observan en moderado porcentaje fenocristales euhédrales poligonales y subhédrales prismáticos de color marrón, con maclas y se hallan reemplazados parcialmente por limonita en los bordes, alcanzan hasta 1,5 mm de largo (Fig. 38).

Clinopiroxenos.- Se observan en reducido porcentaje fenocristales subhédrales prismáticos y anhédrales de tono verdoso pálido, que alcanzan hasta 1 mm de largo del tipo augita, algunos cristales muestran oxidación de los bordes (Fig. 38).

Pasta.- La pasta de la lava es abundante y está formada principalmente por microlitos de plagioclasas con cierta orientación, y en menor porcentaje por vidrio volcánico masivo y óxidos de hierro de grano fino (Fig. 38).

Óxidos de Hierro.- Se presentan en reducido porcentaje, como pequeños minerales opacos de hábito anhedral y subhedral, diseminados en la pasta, corresponderían a las variedades limonita, hematita y magnetita.

Composición porcentual observada.-

Plagioclasas (Oligoclasa) $\text{NaCaAl}(\text{Si}_3\text{O}_8)$	28-30 %
Biotita $(\text{K}_2(\text{Mg},\text{Fe})_2(\text{OH})_2(\text{AlSiO}_{10}))$	2-3 %
Hornblenda $\text{Ca}_2(\text{Mg},\text{Fe},\text{Al})_5(\text{OH})_2\{(\text{Si},\text{Al})_4\text{O}_{11}\}_2$	3-5 %

Clinopiroxenos (Augita) ($Mg,Fe)(SiO_3$).....	2-3 %
Pasta (microlitos de plagioclasas).....	54-56 %
Óxidos de Hierro (Limonita, hematita y magnetita).....	2-3 %
Total.....	100 %

Textura y estructura.- Presenta una estructura holocrystalina y textura porfídica de grano medio (>2 mm), la pasta es microlítica y vítreo (Fig. 38).

Nombre de la roca.- De acuerdo al análisis petrográfico, es una lava de composición intermedia, que corresponde a una **ANDESITA Hornbléndica**.

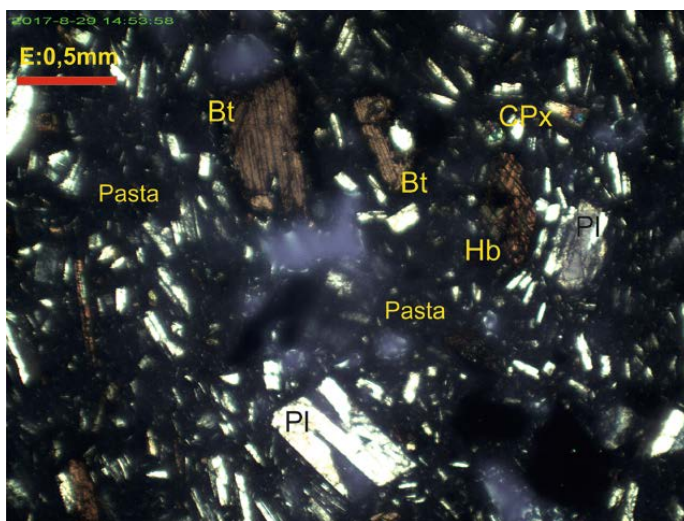


Fig. 38. Muestra 7830, aumento 4x, polarizadores X. Lava Andesítica, con fenocristales de plagioclasas (PI), clinopiroxeno (CPX), hornblenda (Hb), biotita (Bt) y pasta con microlitos de plagioclasas y poco vidrio.

Analizado por: Ing. José Luis Argandoña C.
ENCARGADO DEL LABORATORIO

INTERESADO:

Ing. Adolfo Orsolini Campana

UBICACIÓN:

Proyecto Mapeo Geológico del Área del Manantial del Silala

FECHA:

29 de Agosto de 2017

Nº LAB: SGM-163/17

Muestra 7833.

ANÁLISIS PETROGRÁFICO**Descripción Macroscópica.-**

Fragmento de una roca de origen volcánico (lava), de color gris con tono oscuro, tiene superficies de intensa meteorización, composición intermedia, muestra estructura holocristalina y textura porfídica de grano medio (>2 mm), donde se observan abundantes cristales de feldespatos, anfíboles, biotita, piroxenos, poco cuarzo y óxidos de hierro diseminados, rodeados por una pasta de grano muy fino, la roca muestra moderada dureza y compactación.

Descripción Microscópica.-**Mineralogía.-**

Cuarzo.- Es un componente presente en reducido porcentaje forma de cristales anhédrales y subhédrales con bordes sub-angulosos, que alcanzan hasta 0,5 mm de largo, muestran fracturas, engolfamientos e inclusiones de la pasta.

Plagioclasas.- Se presentan en abundante porcentaje, en forma de fenocristales subhédrales tabulares y prismáticos, de hasta 2,5 mm de largo, muestran zonación, maclas polisintéticas tipo Albita y combinadas Albita-Carlsbad, con bordes de reacción y fracturas, corresponden a la variedad Oligoclasa (An: 25), muestran ligera orientación preferencial (Fig. 39).

Biotita.- Se presenta en reducida proporción, en forma de fenocristales euhédrales poligonales y subhédrales tabulares que alcanzan hasta 2 mm de largo, de color marrón, contienen pequeñas inclusiones de plagioclasas (Fig. 39).

Hornblenda.- Se observan en moderado porcentaje fenocristales euhédrales poligonales y subhédrales prismáticos de color marrón, se hallan reemplazados parcialmente por limonita en los bordes, alcanzan hasta 2,5 mm de largo.

Clinopiroxenos.- Se observan en reducido porcentaje fenocristales subhédrales prismáticos y anhédrales de tono verdoso pálido, que alcanzan hasta 1,5 mm de largo del tipo augita, algunos cristales muestran oxidación de los bordes y maclas (Fig. 4).

Pasta.- La pasta es abundante y está formada principalmente por microlitos de plagioclasas con cierta orientación, y en menor porcentaje por vidrio volcánico masivo y óxidos de hierro de grano fino (Fig. 39).

Óxidos de Hierro.- Se presentan en reducido porcentaje, como pequeños minerales opacos de hábito anhedral y subhedral, diseminados en la pasta y como alteración de hornblendas y biotitas, corresponderían a las variedades limonita, hematita y magnetita.

Composición porcentual observada.-

Cuarzo (SiO_2).....	1-2 %
Plagioclasas (Oligoclasa) $\text{NaCaAl}(\text{Si}_3\text{O}_8)$	26-28 %
Biotita ($\text{K}_2(\text{Mg},\text{Fe})_2(\text{OH})_2(\text{AlSiO}_{10})$).....	2-3 %
Hornblenda $\text{Ca}_2(\text{Mg},\text{Fe},\text{Al})_5(\text{OH})_2\{(\text{Si},\text{Al})_4\text{O}_{11}\}_2$	4-5 %
Clinopiroxenos (Augita) ($\text{Mg},\text{Fe})(\text{SiO}_3)$	2-3 %
Pasta (microlitos de plagioclasas).....	53-55 %
Óxidos de Hierro (Limonita, hematita y magnetita).....	3-4 %
Total.....	100 %

Textura y estructura.- Presenta una estructura holocrystalina y textura porfídica de grano medio (>2 mm), la pasta es mayoritariamente microlítica (Fig. 39).

Nombre de la roca.- De acuerdo al análisis petrográfico, es una lava de composición intermedia, que corresponde a una **ANDESITA Hornbléndica**, débilmente oxidada.

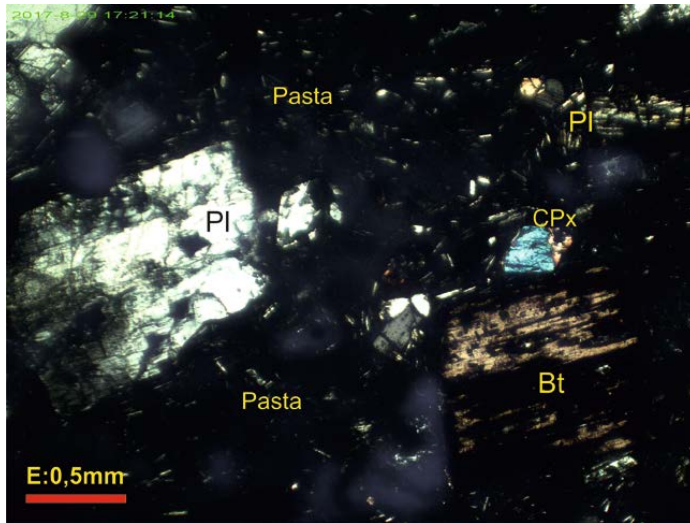


Fig. 39. Muestra 7833, aumento 4x, polarizadores X. Lava Andesítica, con fenocristales de plagioclasas (PI), clinopiroxeno (CPx), biotita (Bt) y pasta con microlitos de plagioclasas.

Analizado por: Ing. José Luis Argandoña C.
ENCARGADO DEL LABORATORIO

INTERESADO:

Ing. Adolfo Orsolini Campana

UBICACIÓN:

Proyecto Mapeo Geológico del Área del Manantial del Silala

FECHA:

29 de Agosto de 2017

Nº LAB: SGM-164/17

Muestra 7737.

ANÁLISIS PETROGRÁFICO**Descripción Macroscópica.-**

Fragmento de una roca de origen volcánico (lava), de color gris oscuro, tiene superficies de meteorización, composición acida, muestra estructura holocristalina y textura porfídica de grano medio (>2 mm), donde se observan abundantes y grandes cristales de feldespatos, anfíboles, biotita, escasos piroxenos y óxidos de hierro diseminados, rodeados por una pasta de grano muy fino, la roca muestra elevada dureza y compactación.

Descripción Microscópica.-**Mineralogía.-**

Plagioclasas.- Se presentan en abundante porcentaje, en forma de fenocristales subhedrales tabulares y prismáticos, de hasta 2,5 mm de largo, muestran zonación, maclas polisintéticas tipo Albita y combinadas Albita-Carlsbad, con bordes de reacción y fracturas, corresponden a la variedad Oligoclasa (An: 25-30) (Fig. 40).

Biotita.- Se presenta en reducida proporción, en forma de fenocristales subhedrales tabulares que alcanzan hasta 1 mm de largo, de color marrón, contienen pequeñas inclusiones de plagioclasas, están ligeramente oxidados (Fig. 40).

Hornblenda.- Se observan en reducido porcentaje fenocristales euhedrales poligonales y subhedrales prismáticos de color marrón, se hallan reemplazados parcialmente por limonita en los bordes, alcanzan hasta 1 mm de largo.

Clinopiroxenos.- Se observan en escaso porcentaje fenocristales subhedrales prismáticos y anhedrales de tono verdoso pálido, que alcanzan hasta 2 mm de largo del tipo augita, algunos cristales muestran oxidación de los bordes y se hallan aglomerados en grupos (Fig. 5).

Pasta.- La pasta es muy abundante y está formada principalmente por vidrio volcánico de textura masiva y perlítica, y en menor porcentaje por microlitos de plagioclasas y óxidos de hierro de grano muy fino (Fig. 40).

Óxidos de Hierro.- Se presentan en reducido porcentaje, como pequeños minerales opacos de hábito anhedral y subhedral (cúbico), diseminados en la pasta y como alteración de hornblendas y biotitas, corresponderían a las variedades limonita, hematita y magnetita.

Composición porcentual observada.-

Plagioclasas (Oligoclásica) $\text{NaCaAl}(\text{Si}_3\text{O}_8)$	23-25 %
Biotita $(\text{K}_2(\text{Mg},\text{Fe})_2(\text{OH})_2(\text{AlSiO}_{10}))$	4-5 %
Hornblenda $\text{Ca}_2(\text{Mg},\text{Fe},\text{Al})_5(\text{OH})_2\{(\text{Si},\text{Al})_4\text{O}_{11}\}_2$	1-2 %
Clinopiroxenos (Augita) $(\text{Mg},\text{Fe})(\text{SiO}_3)$	<1%
Pasta (vidrio volcánico).....	58-60 %
Óxidos de Hierro (Limonita, hematita y magnetita).....	2-3 %
Total.....	100 %

Textura y estructura.- Presenta una estructura holocrystalina y textura porfídica de grano medio (>2 mm), la pasta es vítreo con textura perlítica (Fig. 40).

Nombre de la roca.- De acuerdo al análisis petrográfico, es una lava de composición acida, que corresponde a una **DACITA Biotítica**.

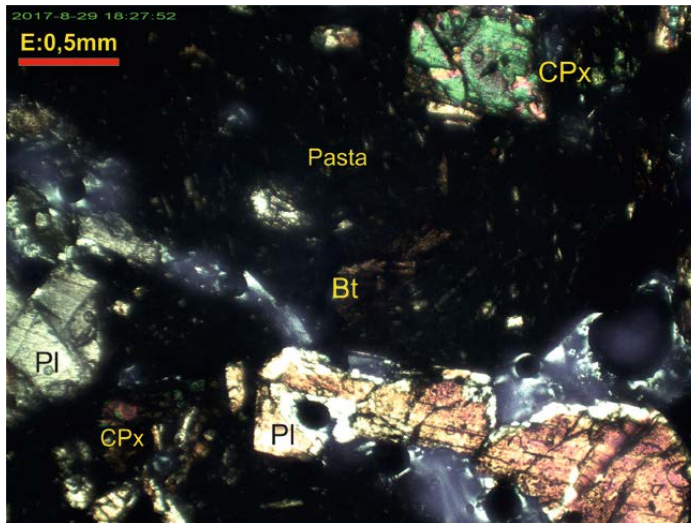


Fig. 40. Muestra 7737, aumento 4x, polarizadores X. Lava Andesítica, con fenocristales de plagioclasas (PI), clinopiroxeno (CPx), biotita (Bt) y pasta vítreo con textura perlítica.

Analizado por: Ing. José Luis Argandoña C.
ENCARGADO DEL LABORATORIO

INTERESADO:

Ing. Adolfo Orsolini Campana

UBICACIÓN:

Proyecto Mapeo Geológico del Área del Manantial del Silala

FECHA:

29 de Agosto de 2017

Nº LAB: SGM-165/17

Muestra 7743.

ANÁLISIS PETROGRÁFICO**Descripción Macroscópica.-**

Fragmento de una roca de origen volcánico (lava), de color gris oscuro, tiene superficies de meteorización, composición intermedia, muestra estructura bandeada o fluidal y textura porfídica de grano medio a fino (>1 mm), donde se observan abundantes cristales de feldespatos, anfíboles, biotita, piroxenos y óxidos de hierro diseminados, rodeados por una pasta de grano muy fino, la roca muestra elevada dureza y compactación.

Descripción Microscópica.-**Mineralogía.-**

Plagioclasas.- Se presentan en abundante porcentaje, en forma de fenocristales subhédrales tabulares y prismáticos, de hasta 1,5 mm de largo, muestran zonación, macras polisintéticas tipo Albita y combinadas Albita-Carlsbad, con bordes de reacción, fracturas y tienen orientación preferencial, corresponden al límite entre las variedades Oligoclásica-Andesina (An: 30) (Fig. 41).

Biotita.- Se presenta en reducida proporción, en forma de fenocristales subhédrales tabulares que alcanzan hasta 0,8 mm de largo, de color marrón, están ligeramente oxidados en los bordes.

Hornblenda.- Se observan en moderado porcentaje fenocristales euhédrales poligonales y subhédrales prismáticos de color marrón, se hallan reemplazados parcialmente por limonita en los bordes, alcanzan hasta 1 mm de largo (Fig. 41).

Clinopiroxenos.- Se observan en reducido porcentaje fenocristales subhédrales prismáticos y anhédrales de tono verdoso pálido, que alcanzan hasta 0,5 mm de largo del tipo augita, algunos cristales muestran oxidación de los bordes (Fig. 41).

Pasta.- La pasta es abundante y está formada principalmente por microlitos de plagioclasas con orientación preferencial siguiendo la dirección de flujo de la lava (textura eutáctica), y en menor porcentaje por vidrio volcánico de textura masiva, junto a óxidos de hierro de grano muy fino (Fig. 41).

Óxidos de Hierro.- Se presentan en reducido porcentaje, como pequeños minerales opacos de hábito anhedral y subhedral (cúbico), diseminados en la pasta y como alteración de hornblendas y biotitas, corresponderían a las variedades limonita, hematita y poca magnetita.

Composición porcentual observada.-

Plagioclasas (Oligoclasa-Andesina) NaCaAl(Si ₃ O ₈).....	25-27 %
Biotita (K ₂ (Mg,Fe) ₂ (OH) ₂ (AlSiO ₁₀)).....	1-2 %
Hornblenda Ca ₂ (Mg,Fe,Al) ₅ (OH) ₂ {(Si,Al) ₄ O ₁₁ } ₂	4-5 %
Clinopiroxenos (Augita) (Mg,Fe)(SiO ₃).....	2-3 %
Pasta (microlitos de plagioclasas).....	58-60 %
Óxidos de Hierro (Limonita, hematita y magnetita).....	2-3 %
Total.....	100 %

Textura y estructura.- Presenta una estructura bandeada o fluidal y textura porfídica de grano medio a fino (>1 mm), la pasta es microlítica de textura pilotáxica (Fig. 41).

Nombre de la roca.- De acuerdo al análisis petrográfico, es una lava de composición intermedia, que corresponde a una **ANDESITA Hornbléndica**.

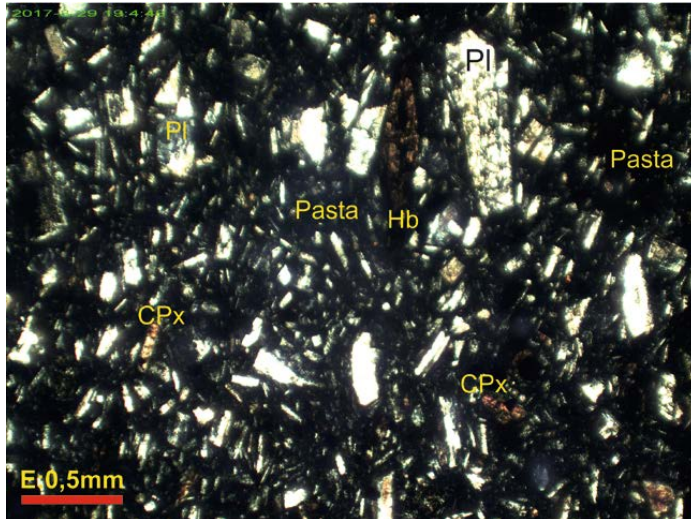


Fig. 41. Muestra 7743, aumento 4x, polarizadores X. Lava Andesítica, con fenocristales de plagioclasas (PI), clinopiroxeno (CPx), hornblenda (Hb), y pasta microlítica de plagioclasas.

Analizado por: Ing. José Luis Argandoña C.
ENCARGADO DEL LABORATORIO

CONVENIO DE COOPERACIÓN INTERINSTITUCIONAL Y
CONTRATO DE CONSULTORÍA DIREMAR - SERGEOMIN



RESULTADOS ANÁLISIS DE MINERAGRAFÍA

Calle Federico Suazo N° 1673 Esquina Reyes Ortiz – La Paz - Bolivia
Telf. (591 – 2) 2330981 – 2331236 - Fax 2391725 – 2318295
www.sergeomin.gob.bo

INTERESADO:

Ing. Adolfo Orsolini Campana

UBICACIÓN:

Proyecto Mapeo Geológico del Área del Manantial del Silala

FECHA:

27 de Julio de 2016

Nº LAB: SGM-131/17

Muestra 7807.

ANÁLISIS MINERAGRÁFICO

DESCRIPCIÓN MACROSCÓPICA

Fragmento de una roca piroclástica (toba ignimbólica) de composición intermedia, muestra estructura bandeada y textura porfídica de grano medio (>1 mm), donde se observa una intercalación entre bandas lenticulares de color marrón-rojizo y bandas de tono gris oscuro, ambas muestran cristales de feldespatos, biotita, piroxenos y óxidos de hierro del tipo hematita y magnetita diseminados, rodeados por una pasta ferruginosa y vítreo, con más presencia de hierro en las bandas grises. La toba presenta alto grado de soldadura (ignimbrita), muestra elevada dureza y compactación, y también es llamada toba soldada.

MINERALES OBSERVADOS EN SECCIÓN PULIDA

En la muestra se observan los siguientes minerales y sus porcentajes aproximados (Fig. 1).

Minerales Observados	Porcentaje
Hematita (Fe_2O_3)	2-3 %
Magnetita (Fe_3O_4)	<1 %
Limonita (FeOOH) (pasta de la toba)	1-2 %
Feldespatos de la toba soldada	93-95 %
Total	100 %

DESCRIPCIÓN DE MINERALES

Hematita

Está presente en reducido porcentaje como cristales anhedrales de grano muy fino ($<0,1$ a $0,5$ mm), diseminados en la toba soldada y asociados con magnetita y limonita. Este óxido de hierro cristaliza en el sistema hexagonal, de color gris en la muestra de mano y gris-blancuecino en sección pulida, con brillo metálico, reflectancia media a alta, débil pleocroísmo, moderada anisotropía y dureza alta al pulido, muestra texturas de reemplazamiento de magnetita (Fig. 1).

Magnetita

La magnetita está presente en escaso porcentaje, muestra texturas de reemplazamiento por cristales de hematita, llenando sus planos de clivaje. Este óxido de hierro es magnético, muestra color gris opaco en la muestra de mano, y gris con tinte marrón pálido en sección pulida, tiene brillo metálico, reflectancia media, es isotrópico, con dureza alta al pulido (Fig. 1).

Limonita

La limonita es un óxido de hierro presente en la pasta de la toba soldada, muestra hábito masivo, color marrón-rojizo en la muestra de mano y gris-oscuro en sección pulida, brillo opaco, reflectancia baja, moderada anisotropía, reflejos internos rojos y dureza media al pulido.

ASOCIACIONES MINERALES

Se observan asociaciones minerales entre: Hematita-Magnetita-Limonita.

SECUENCIA PARAGENETICA

Primera Fase: Magnetita- Hematita.

Segunda Fase: Limonita.

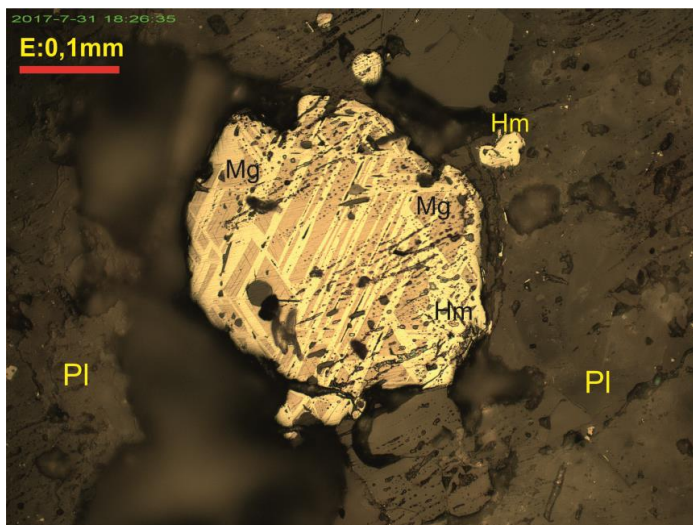


Fig. 1. Muestra 7807. Aumento 20X, Polarizadores II. Toba Ignimbrítica, con plagioclasas (PI) y diseminación de micro-cristales de magnetita (Mg) reemplazados parcialmente por hematita (Hm).

Analizado por: Ing. José Luis Argandoña C.
ENCARGADO DEL LABORATORIO

INTERESADO:

Ing. Adolfo Orsolini Campana

UBICACIÓN:

Proyecto Mapeo Geológico del Área del Manantial del Silala

FECHA:

27 de Julio de 2016

Nº LAB: SGM-132/17

Muestra 7808.

ANÁLISIS MINERAGRÁFICO**DESCRIPCIÓN MACROSCÓPICA**

Fragmento de una roca piroclástica (toba ignimbótica) de composición intermedia, muestra estructura bandeadada y textura porfídica de grano medio (>1 mm), donde se observa una intercalación entre bandas lenticulares de tono gris oscuro y bandas de color marrón-rojizo, ambas muestran cristales de feldespato, biotita, piroxenos y óxidos de hierro diseminados de la variedad hematita y magnetita, rodeados por una pasta microlítica y vítreos, con más presencia de hierro en las bandas oscuras. La toba presenta alto grado de soldadura (ignimbrita), muestra elevada dureza y compactación, también es llamada toba soldada.

MINERALES OBSERVADOS EN SECCIÓN PULIDA

En la muestra se observan los siguientes minerales y sus porcentajes aproximados (Fig. 2).

Minerales Observados	Porcentaje
Hematita (Fe_2O_3)	2-3 %
Magnetita (Fe_3O_4)	<1 %
Limonita (FeOOH) (pasta de la toba)	2-3 %
Feldespato de la toba soldada	92-94 %
Total	100 %

DESCRIPCIÓN DE MINERALES***Hematita***

Está presente en reducido porcentaje como cristales anhedrales de grano muy fino ($<0,1$ a $0,5$ mm), diseminados en la toba soldada y asociados con magnetita y limonita. Este óxido de hierro cristaliza en el sistema hexagonal, de color gris en la muestra de mano y gris-blancuzco en sección pulida, con brillo metálico, reflectancia media a alta, débil pleocroísmo, moderada anisotropía y alta dureza al pulido, muestra texturas de reemplazamiento de magnetita (Fig. 2).

Magnetita

La magnetita está presente en escaso porcentaje, muestra texturas de reemplazamiento por cristales de hematita, llenando sus planos de clivaje. Este óxido de hierro es magnético, muestra color gris opaco en la muestra de mano, y gris con tinte marrón pálido en sección pulida, tiene brillo metálico, reflectancia media, es isotrópico, con dureza alta al pulido (Fig. 2).

Limonita

La limonita es un óxido de hierro presente sobre todo en la pasta de la toba, muestra hábito masivo, color marrón-rojizo en la muestra de mano y gris-oscuro en sección pulida, brillo opaco, reflectancia baja, moderada anisotropía, reflejos internos rojos y dureza media al pulido (Fig. 2).

ASOCIACIONES MINERALES

Se observan asociaciones minerales entre: Hematita-Magnetita-Limonita.

SECUENCIA PARAGENETICA

Primera Fase: Magnetita- Hematita.

Segunda Fase: Limonita.

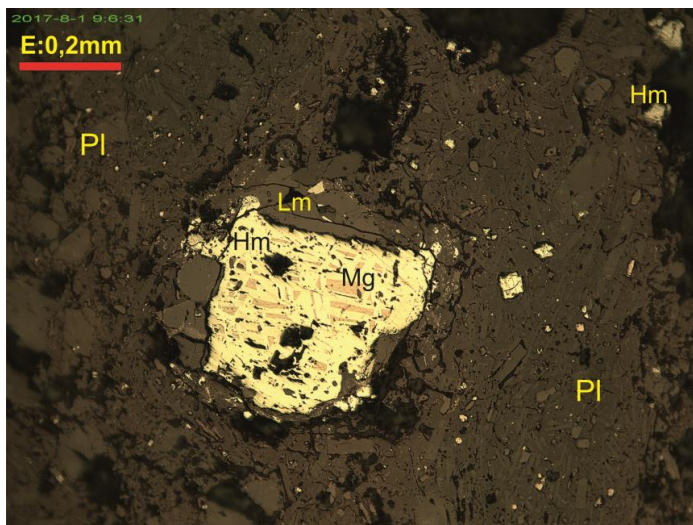


Fig. 2. Muestra 7808. Aumento 10X, Polarizadores II. Toba Ignimbética, con plagioclasas (PI) y micro-cristales de magnetita (Mg) reemplazados en gran parte por hematita (Hm) y limonita (Lm).

Analizado por: Ing. José Luis Argandoña C.
ENCARGADO DEL LABORATORIO

INTERESADO:

Ing. Adolfo Orsolini Campana

UBICACIÓN:

Proyecto Mapeo Geológico del Área del Manantial del Silala

FECHA:

27 de Julio de 2016

Nº LAB: SGM-131/17

Muestra 7807.

ANÁLISIS MINERAGRÁFICO

DESCRIPCIÓN MACROSCÓPICA

Fragmento de una roca piroclástica (toba ignimbólica) de composición intermedia, muestra estructura bandeadada y textura porfídica de grano medio (>1 mm), donde se observa una intercalación entre bandas lenticulares de color marrón-rojizo y bandas de tono gris oscuro, ambas muestran cristales de feldespatos, biotita, piroxenos y óxidos de hierro del tipo hematita y magnetita diseminados, rodeados por una pasta ferruginosa y vítreas, con más presencia de hierro en las bandas grises. La toba presenta alto grado de soldadura (ignimbrita), muestra elevada dureza y compactación, y también es llamada toba soldada.

MINERALES OBSERVADOS EN SECCIÓN PULIDA

En la muestra se observan los siguientes minerales y sus porcentajes aproximados (Fig. 3).

Minerales Observados	Porcentaje
Hematita (Fe_2O_3)	2-3 %
Magnetita (Fe_3O_4)	<1 %
Limonita (FeOOH) (pasta de la toba)	1-2 %
Feldespatos de la toba soldada	93-95 %
Total	100 %

DESCRIPCIÓN DE MINERALES

Hematita

Está presente en reducido porcentaje como cristales anhedrales de grano muy fino ($<0,1$ a $0,5$ mm), diseminados en la toba soldada y asociados con magnetita y limonita. Este óxido de hierro cristaliza en el sistema hexagonal, de color gris en la muestra de mano y gris-blancuzco en sección pulida, con brillo metálico, reflectancia media a alta, débil pleocroísmo, moderada anisotropía y dureza alta al pulido, muestra texturas de reemplazamiento de magnetita (Fig. 3).

Magnetita

La magnetita está presente en escaso porcentaje, muestra texturas de reemplazamiento por cristales de hematita, llenando sus planos de clivaje. Este óxido de hierro es magnético, muestra color gris opaco en la muestra de mano, y gris con tinte marrón pálido en sección pulida, tiene brillo metálico, reflectancia media, es isótropo, con dureza alta al pulido (Fig. 3).

Limonita

La limonita es un óxido de hierro presente en la pasta de la toba soldada, muestra hábito masivo, color marrón-rojizo en la muestra de mano y gris-oscuro en sección pulida, brillo opaco, reflectancia baja, moderada anisotropía, reflejos internos rojos y dureza media al pulido.

ASOCIACIONES MINERALES

Se observan asociaciones minerales entre: Hematita-Magnetita-Limonita.

SECUENCIA PARAGENETICA

Primera Fase: Magnetita- Hematita.

Segunda Fase: Limonita.

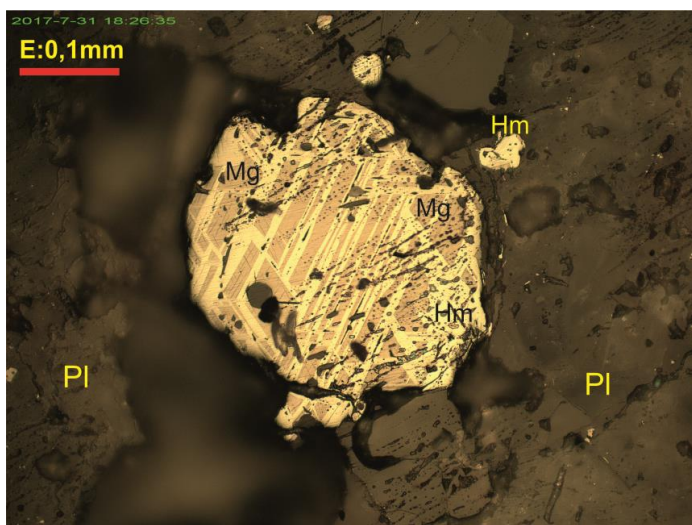


Fig. 3. Muestra 7807. Aumento 20X, Polarizadores II. Toba Ignimbótica, con plagioclasas (PI) y diseminación de micro-cristales de magnetita (Mg) reemplazados parcialmente por hematita (Hm).

Analizado por: Ing. José Luis Argandoña C.
ENCARGADO DEL LABORATORIO

INTERESADO:

Ing. Adolfo Orsolini Campana

UBICACIÓN:

Proyecto Mapeo Geológico del Área del Manantial del Silala

FECHA:

27 de Julio de 2016

Nº LAB: SGM-132/17

Muestra 7808.

ANÁLISIS MINERAGRÁFICO

DESCRIPCIÓN MACROSCÓPICA

Fragmento de una roca piroclástica (toba ignimbólica) de composición intermedia, muestra estructura bandeadada y textura porfídica de grano medio (>1 mm), donde se observa una intercalación entre bandas lenticulares de tono gris oscuro y bandas de color marrón-rojizo, ambas muestran cristales de feldespatos, biotita, piroxenos y óxidos de hierro diseminados de la variedad hematita y magnetita, rodeados por una pasta microlítica y vítreo, con más presencia de hierro en las bandas oscuras. La toba presenta alto grado de soldadura (ignimbrita), muestra elevada dureza y compactación, también es llamada toba soldada.

MINERALES OBSERVADOS EN SECCIÓN PULIDA

En la muestra se observan los siguientes minerales y sus porcentajes aproximados (Fig. 4).

Minerales Observados	Porcentaje
Hematita (Fe_2O_3)	2-3 %
Magnetita (Fe_3O_4)	<1 %
Limonita (FeOOH) (pasta de la toba)	2-3 %
Feldespatos de la toba soldada	92-94 %
Total	100 %

DESCRIPCIÓN DE MINERALES

Hematita

Está presente en reducido porcentaje como cristales anhedrales de grano muy fino ($<0,1$ a $0,5$ mm), diseminados en la toba soldada y asociados con magnetita y limonita. Este óxido de hierro cristaliza en el sistema hexagonal, de color gris en la muestra de mano y gris-blancuzco en sección pulida, con brillo metálico, reflectancia media a alta, débil pleocroísmo, moderada anisotropía y alta dureza al pulido, muestra texturas de reemplazamiento de magnetita (Fig. 4).

Magnetita

La magnetita está presente en escaso porcentaje, muestra texturas de reemplazamiento por cristales de hematita, llenando sus planos de clivaje. Este óxido de hierro es magnético, muestra color gris opaco en la muestra de mano, y gris con tinte marrón pálido en sección pulida, tiene brillo metálico, reflectancia media, es isótropo, con dureza alta al pulido (Fig. 4).

Limonita

La limonita es un óxido de hierro presente sobre todo en la pasta de la toba, muestra hábito masivo, color marrón-rojizo en la muestra de mano y gris-oscuro en sección pulida, brillo opaco, reflectancia baja, moderada anisotropía, reflejos internos rojos y dureza media al pulido (Fig. 4).

ASOCIACIONES MINERALES

Se observan asociaciones minerales entre: Hematita-Magnetita-Limonita.

SECUENCIA PARAGENETICA

Primera Fase: Magnetita- Hematita.

Segunda Fase: Limonita.

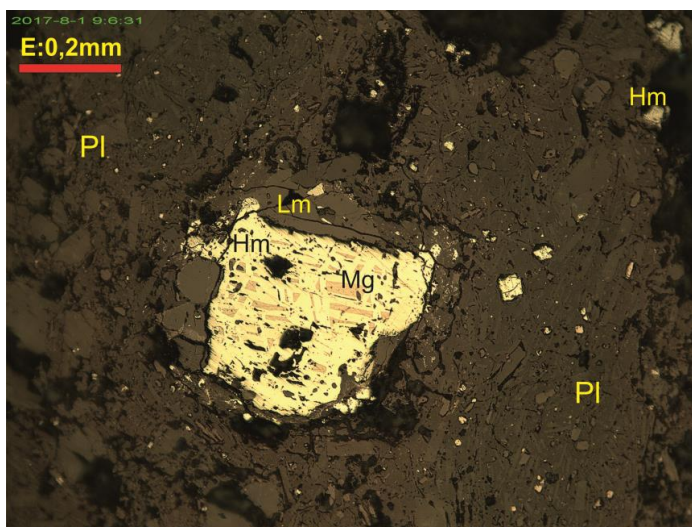


Fig. 4. Muestra 7808. Aumento 10X, Polarizadores II. Toba Ignimbritica, con plagioclasas (Pl) y micro-cristales de magnetita (Mg) reemplazados en gran parte por hematita (Hm) y limonita (Lm).

Analizado por: Ing. José Luis Argandoña C.
ENCARGADO DEL LABORATORIO

Annex XVI

APPENDIX B

CONVENIO DE COOPERACIÓN INTERINSTITUCIONAL Y
CONTRATO DE CONSULTORIA DIREMAR - SERGEOMIN



ANEXO D

BASE DE DATOS

Calle Federico Suazo N° 1673 Esquina Reyes Ortiz – La Paz - Bolivia
Telf. (591 – 2) 2330981 – 2331236 - Fax 2391725 – 2318295
www.sergeomin.gob.bo

CONVENIO DE COOPERACIÓN INTERINSTITUCIONAL Y
CONTRATO DE CONSULTORIA DIREMAR - SERGEOMIN



BASE DE DATOS GEOLÓGICOS

Calle Federico Suazo N° 1673 Esquina Reyes Ortiz – La Paz - Bolivia
Telf. (591 – 2) 2330981 – 2331236 - Fax 2391725 – 2318295
www.sergeomin.gob.bo

Nº	ESTE (UTM)	NORTE (UTM)	ALTURA (m.s.n.m.)	DIRECCIÓN DE FLUJO	CODIGO MUESTRA	LITOLOGIA	DESCRIPCION MACROSCOPICA	FECHA
S1	600773	7566342	4382	250/11NW		Ignimbrita	Se puede ver ignimbritas de grano fino, de una matrix ferruginosa.Nis-2	22/05/2017
S2	600813	7566226	4383	50/6SE	7702	Toba	Toba ignimbritica de composicion intermedia de grano medio donde se observa una intercalacion entre bandas lenticulares de color marron y bandas de tono negruco, ambas muestras cristales de feldespatos blanquecinos, escasos cuarzo, piroxenos, pomez alargadas y oxicodos de hierro diseminados, rodeados por una pasta ferruginosa y vitrea, con mayor presencia de hierro en las bandas negruzcas, la toba presenta alto nivel de soldadura, por lo que muestra elevada dureza y compactacion y tambien es llamada toba soldada.	22/05/2017
S3	600956	7566439	4411	250/15SE		Flujo de detritos	Clastos angulosos a subredondeados monoliticos, diametro de los clastos (1mm-30cm),matrix ferruginosa terrosa. Nfd2	22/05/2017
S4	600972	7566398	4399	250/20SE		Ignimbrita	Se puede ver ignimbritas de grano fino, de una matrix ferruginosa.Nis-2	22/05/2017
S5	600973	7566397	4395	250/10SE	7706	Ignimbrita	Toba ignimbritica de composicion intermedia, de una estructura bandeada de grano medio(>1 mm), donde se observa una intercalacion entre bandas lenticulares de color marron, muestran cristales de feldespatos blanquecinos y muy escasos cuarzos, piroxenos, pomez alargadas y abundantes oxicodos de hierro diseminados rodeados por una pasta ferruginosa y vitrea, con mayor presencia de hierro en las bandas negruzcas, la toba presenta alto nivel de soldadura, por lo que muestra elevada dureza y compactacion y tambien es llamada toba soldada. Nis-2	22/05/2017
S6	600982	7566368	4378	245/8SE		Ignimbrita	Clastos angulosos a subredondeados monoliticos en matriz ferruginosa silicificada. Nis-1	22/05/2017
S7	600998	7566324	4376	245/20SE		Ignimbrita	Clastos angulosos a subredondeados monoliticos en matriz ferruginosa silicificada. Nis-1	22/05/2017
S8	601012	7566321	4386	240/8SE		Ignimbrita	Clastos angulosos a subredondeados monoliticos en matriz ferruginosa silicificada. Nis-1	22/05/2017
S9	601011	7566289	4399	240/6SE		Flujo de detritos	Clastos angulosos a subredondeados monoliticos, diametro de los clastos (1mm-10 cm),matrix ferruginosa terrosa. Nfd2	22/05/2017
S10	601030	7566237	4401	245/8SE		Flujo de detritos	Clastos angulosos a subredondeados monoliticos, diametro de los clastos (1mm -10 cm),matrix ferruginosa terrosa. Nfd2	22/05/2017
S11	601031	7566226	4398	243/10SE		Toba	Tamaño de grano medio,texture bandeada compuesta de hematita y magnetita en matriz ferruginosa, y un espesor de 5 cm aproximadamente.	22/05/2017
S12	600875	7566672	4356	220/42SE		Lava	Flujos de lavas de grano medio a grueso en sectores se observa horizontes con bandeamiento, los cristales se encuentran fragmentados muy raras biotitas idiomorfas. Nls2	23/05/2017
S13	600508	7565835	4363	210/10SE		Flujo de detritos	Clastos angulosos a subredondeados monoliticos, diametro de los clastos (1mm-10cm),matrix ferruginosa terrosa. Nfd2	23/05/2017
S14	600533	7565836	4352	207/8SE		Ignimbrita	Tamaño de grano medio,texture bandeada compuesta de hematita en matriz ferruginosa. Nis-2	23/05/2017
S15	600540	7565820	4347	204/5SE		Toba	Tamaño de grano medio,texture bandeada compuesta de hematita y magnetita en matriz ferruginosa, espesor = 8 cm.	23/05/2017



SERVICIO GEOLOGICO MINERO
DIRECCION ESTRATEGICA DE REINVINDICACION MARITIMA, SILALA Y RECURSOS HIDRICOS INTERNACIONALES
MAPEO GEOLOGICO DEL AREA CIRCUNDANTE AL MANANTIAL DEL SILALA
BASE DE DATOS



Nº	ESTE (UTM)	NORTE (UTM)	ALTURA (m.s.n.m.)	DIRECCIÓN DE FLUJO	CODIGO MUESTRA	LITOLOGIA	DESCRIPCION MACROSCOPICA	FECHA
S16	600540	7565819	4345	205/8SE		Toba	Tamaño de grano medio, textura bandeda compuesta de hematita y magnetita en matriz ferruginosa, espesor = 10 cm.	23/05/2017
S17	600547	7565806	4332	203/10SE		Ignimbrita	Clastos monolíticos, matriz en proceso de alteración argilica supergenica, diámetro (1mm-2 cm). Nis-1	23/05/2017
S18	600568	7565773	4333	202/8SE		Ignimbrita	Clastos monolíticos, matriz en proceso de alteración argilica supergenica, diámetro (1mm-2 cm). Nis-1	23/05/2017
S19	600587	7565776	4339	200/5SE		Ignimbrita	Clastos monolíticos, matriz en proceso de alteración argilica supergenica, diámetro (1mm-2 cm). Nis-1	23/05/2017
S20	600592	7565774	4339	199/15SE		Ignimbrita	Clastos monolíticos, matriz en proceso de alteración argilica supergenica, diámetro (1mm-2 cm). Nis-1	23/05/2017
S21	600616	7565776	4357	215/10SE		Flujo de detritos	Se puede ver ignimbritas de grano fino, de una matrix ferruginosa. Nis-2	23/05/2017
S22	600942	7566168	4395	230/8SE		Toba	Tamaño de grano medio, textura bandeda compuesta de hematita en matriz ferruginosa, y un espesor de 10 cm aproximadamente.	23/05/2017
S23	600831	7566233	4376	215/5SE		Toba	Tamaño de grano medio, textura bandeda compuesta de hematita y magnetita en matriz ferruginosa, y un espesor de 15 cm aproximadamente.	23/05/2017
S24	600822	7566241	4365	220/10SE		Ignimbrita	Clastos monolíticos, matriz en proceso de alteración argilica supergenica, diámetro (1mm -4cm). Nis-1	23/05/2017
S25	600704	7566320	4398	235/8SE		Ignimbrita	Clastos monolíticos, matriz en proceso de alteración argilica supergenica, diámetro (1mm -4cm). Nis-1	23/05/2017
S26	600647	7566317	4389	220/5SE		Ignimbrita	Clastos monolíticos, matriz en proceso de alteración argilica supergenica, diámetro (1mm -6cm). Nis-1	23/05/2017
S27	601181	7565996	4457	220/10SE	7801	Lava	Fragmento de una roca de origen volcánico (lava), de color gris, presenta superficies de meteorización, de composición intermedia, muestra estructura holocristalina y textura porfídica de grano medio (>2 mm), donde se observan cristales de feldespatos blanquecinos, biotita y anfíboles muy oxidados, piroxenos y óxidos de hierro diseminados, rodeados por una pasta de grano muy fino. La lava muestra moderada dureza y compactación. Nls-2	23/05/2017
S28	604895	7567297	4541	240/15SE		Ignimbrita	Afloramiento de ignimbrita, de tamaño de grano medio, cuarzo lechoso y cristalino subredondeados, biotitas frescas y alteradas. Nls-3	23/05/2017
S29	600564	7566022	4369	195/10SE		Ignimbrita	Ignimbrita color gris claro leve tono rosaceo con fragmentos de cuarzo con bordes sub redondeados y engolfamientos, biotita en fragmentos rodeados de una pasta ferruginosa polilítica clastos con aureolas de recalentamiento soldamiento moderado. Ns2	26/05/2017
S30	600216	7565447	4326	210/6NW		Ignimbrita	Ignimbrita color gris claro leve tono rosaceo con fragmentos de cuarzo con bordes sub redondeados y engolfamientos, biotita en fragmentos rodeados de una pasta ferruginosa polilítica clastos con aureolas de recalentamiento soldamiento moderado textura vesicular en sectores gradacion normal en la base se tiene un horizonte de ceniza volcánica de 8 cm de espesor. Ns1	26/05/2017

Nº	ESTE (UTM)	NORTE (UTM)	ALTURA (m.s.n.m.)	DIRECCIÓN DE FLUJO	CODIGO MUESTRA	LITOLOGIA	DESCRIPCION MACROSCOPICA	FECHA
S31	600247	7565411	4303	215/9NW		Flujo de detritos	Contacto aglomerado volcánico y aluvial matrix soportado color marrón rojizo con clastos en su matriz que varian de 10 cm a 40 cm, sub redondeados de grano medio a grueso débil soldamiento matrix con alto contenido de fragmetos de, cuarzo, biotita bloques polilíticos mal clasificados, aluvial material suelto y con cubierta de vegetacion	26/05/2017
S32	604898	7567298	4543	60/5Nw	7802	Ignimbrita	Fragmento de una roca de origen volcánico (toba), de color marrón con tono rosáceo, tiene superficies de meteorización, de composición ácida, muestra estructura vitro-crystalina y textura porfídica de grano medio (>2 mm), donde se observan cristales de feldespatos blanquecinos, biotita muy oxidada, anfiboles, pómex alargadas de tono blanquecino y óxidos de hierro, rodeados por una pasta vitrea y ferruginosa, muestra moderada dureza y grado de soldadura. Nls-3	15/06/2017
S33	605450	7566080	4602	60/39NW	7803	Lava	Fragmento de una roca de origen volcánico (lava), de color gris oscuro con superficies de meteorización, de composición intermedia, muestra estructura holocrystalina y textura porfídica de grano medio (>1 mm), donde se observan abundantes cristales de feldespatos blanquecinos orientados, biotita oxidada, piroxenos y óxidos de hierro diseminados, rodeados por una pasta de grano fino. La lava muestra elevada dureza y compactación. Nlsg	15/06/2017
S34	605074	7567088	4547	45/64NW		Ignimbrita	Plagioclasas alteradas y frescas, predominancia de biotita, cuarzo lechosos y cristalino subredondeados, presencia de pomez en la matriz en forma alineada. Nls-3	15/06/2017
S35	601828	7565534	4426	344/9SW		Lava	Flujos de lavas textura porfídica biotítica grano medio a grueso en sectores se observa horizontes con bandeoamiento, los cristales se encuentran fragmentados muy raras biotitas idiomorfias. Nlsc	15/06/2017
S36	601728	7565604	4437	314/12SW		Lava	Flujos de lavas textura porfídica biotítica grano medio a grueso en sectores se observa horizontes con bandeoamiento, los cristales se encuentran fragmentados muy raras biotitas idiomorfias. Nlsc	15/06/2017
S37	601630	7565591	4474	239/62SE		Lava	Flujos de lavas textura porfídica biotítica grano medio a grueso en sectores se observa horizontes con bandeoamiento, los cristales se encuentran fragmentados muy raras biotitas idiomorfias dirección de flujo sub vertical. Nlsc	15/06/2017
S38	601362	7565777	4518	316/22SW		Lava	Flujos de lavas textura porfídica biotítica grano medio a grueso en sectores con bandeoamiento, los cristales se encuentran fragmentados muy raras biotitas idiomorfias superficialmente con una patina de oxidación. Nlsc	15/06/2017
S39	604803	7567280	4542	258/23NW		Ignimbrita	Se observa toba en su mayor parte distorsionadas, de color violaceo claro, de un adiametro de 3 cm, de forma angulosa y grano medio, presentan cuarzos subangulosos en su matriz, poca presencia de biotita, el espesor aproximado de la colada de lava es de 1 m, de textura afanitica. Nls-3	15/06/2017
S40	604132	7566944	4496	255/7SE		Ignimbrita	Se observa toba de color violaceo claro, tamaño de grano medio, en su mayor parte distorsionadas, presentan cuarzos angulosos en su matrix, poca presencia de biotita, de textura afanitica. Nls-3	15/06/2017
S41	604018	7566910	4489	251/18SE		Ignimbrita	Se observa toba de color violaceo y marron, de diametro de los clastos de 0.3 cm, angulosos y de grano medio, en su mayor parte distorsionadas, presentan cuarzosangulosos en su matrix, poca presencia de biotita,, el espesor aproximado de la colada de lava es de 1.5 m, de textura afanitica. Nls-3	15/06/2017



SERVICIO GEOLOGICO MINERO
DIRECCION ESTRATEGICA DE REINVINDICACION MARITIMA, SILALA Y RECURSOS HIDRICOS INTERNACIONALES
MAPEO GEOLICO DEL AREA CIRCUNDANTE AL MANANTIAL DEL SILALA
BASE DE DATOS



Nº	ESTE (UTM)	NORTE (UTM)	ALTURA (m.s.n.m.)	DIRECCIÓN DE FLUJO	CODIGO MUESTRA	LITOLOGIA	DESCRIPCION MACROSCOPICA	FECHA
S42	603641	7566505	4446	153/24SW		Flujo de detritos	Se observa flujo de detritos con de color marron claro con clastos en su matriz que varian de 0.5cm a 25 cm, angulosos y de grano medio en su matrix con alto contenido de vidrio, cuarzo y biotita. Su espesor aproximado es de 0.6cm, de textura terrosa. Ndf2	15/06/2017
S43	608497	7567689	4583		7804	Lava	Fragmento de una roca de origen volcánico (lava), de color gris oscuro con superficies de meteorización, de composición intermedia, muestra estructura holocristalina y textura porfídica de grano medio (>1 mm), donde se observan abundantes cristales de feldespatos blanquecinos, biotita oxidada, piroxenos y óxidos de hierro diseminados, rodeados por una pasta de grano muy fino. La lava muestra elevada dureza y compactación. Nlsg	16/06/2017
S44	609739	7568018	4596		7805	Lava	Fragmento de una roca de origen volcánico (lava), de color gris con superficies de meteorización, de composición ácida, muestra estructura holocristalina y textura porfídica de grano medio (>3 mm), donde se observan grandes cristales de feldespatos blanquecinos, cuarzo, biotita, anfiboles, piroxenos y óxidos de hierro diseminados, rodeados por una pasta de grano muy fino. La lava muestra elevada dureza y compactación. Nlet	16/06/2017
S45	605988	75653322	4653	28/62SE		Lava	Pseudo estratificación (pseudo plegamiento) de lavas dacíticas silicificadas, tamaño de grano medio, esporádicas biotitas. Nlsg	16/06/2017
S46	604393	7566010	4523	215/27NW		Lavas	Flujos de lavas andesíticas de color gris con tonos marrones con clastos que varian de 0.2 mm a 25 cm, subangulosos y de grano medio en su matrix, con contenido de cuarzo, biotita y feldespatos. El espesor total de la colada de lava es de 1.9 m aproximadamente, de textura bandead. Nlsg	16/06/2017
S47	604897	7564887	4606	284/11SW		Lava	Se observa flujos de lavas de contenido andesítico de color marron violaceo, con clastos en su matrix que vaian de 1cm a 1 m, angulosos y de grano medio en su matrix, que presentan bandeadimiento, cuarzo biotita muy silificado. El espesor aproximado de la colada de lava es de 3 m, de textura bandead. Nlsg	16/06/2017
S48	600959	7566047	4395	221/6SE		Ignimbrita	Ignimbrita color gris claro leve tono rosaceo polílitico clastos de 1 a 3 cm con fragmentos de cuarzo con bordes sub redondeados y engolfamientos, biotita en fragmentos rodeados de una pasta ferruginosa polílitica clastos con aureolas de recalentamiento soldamiento moderado, aglomerado polílitico matrix soportado. Nis-2	16/06/2017
S49	601377	7565285	4538	245/4SE		Lava	Color gris claro grano fino a medio textura porfídica biotítica muestra pseudo estratificación muy raras biotitas idiomorfias. Nlsc	16/06/2017
S50	604787	7576158	4522		7708	Toba	Fragmento de una roca de origen piroclástico (toba ignimbritica) de composición intermedia, muestra estructura bandead y textura porfídica de grano medio (>1 mm), donde se observa una intercalación entre delgadas bandas lenticulares de color marrón-negruco y bandas de tono gris claro, ambas muestran cristales de feldespatos blanquecinos, biotita, piroxenos y óxidos de hierro diseminados, rodeados por una pasta vitrea, con más presencia de hierro en las bandas oscuras. La toba presenta un grado de soldadura moderado a alto (ignimbrita), por lo que muestra elevada dureza y compactación, también es llamada toba soldada. Ntpg	17/06/2017
S51	601942	7564641	4606		7712	Lava	Fragmento de una roca de origen volcánico (lava), de color gris con superficies de meteorización, composición ácida, muestra estructura holocristalina y textura porfídica de grano medio (>2 mm), donde se observan cristales de feldespatos blanquecinos, escaso cuarzo, biotita, anfiboles, piroxenos y óxidos de hierro diseminados, rodeados por una pasta de grano muy fino, contiene agregados de calcita llenando pequeñas cavidades de la roca, la cual muestra elevada dureza y compactación. Nlsc	17/06/2017

Nº	ESTE (UTM)	NORTE (UTM)	ALTURA (m.s.n.m.)	DIRECCIÓN DE FLUJO	CÓDIGO MUESTRA	LITOLOGIA	DESCRIPCION MACROSCOPICA	FECHA
S52	606624	7563670	4939	240/50NW		Lava	Pseudo estratificación de lavas dacíticas silicificadas, con clastos monolíticos subredondeados a redondeados en la matriz, tamaño de grano medio, esporádicas biotitas. Nlsg	17/06/2017
S53	606660	7563630	4951	235/75NW		Lava	Pseudo estratificación de lavas dacíticas silicificadas, con clastos monolíticos subredondeados a redondeados en la matriz, tamaño de grano medio, esporádicas biotitas. Nlsg	17/06/2017
S54	606688	7563466	4973	250/60NW		Lava	Dacita silicificada, con clastos monolíticos subredondeados a redondeados en la matriz, diámetro de los clastos (1 mm - 8 cm), tamaño de grano medio, esporádicas biotitas, textura bandeadada constituida por mineral de Fe. Nlsg	17/06/2017
S55	606752	7563334	4999	235/65NW		Lava	Dacita silicificada, con clastos monolíticos subredondeados a redondeados en la matriz, diámetro de los clastos (1 mm-8 cm), tamaño de grano medio, esporádicas biotitas, textura bandeadada constituida por mineral de Fe. Nlsg	17/06/2017
S56	606911	7563173	5037	230/65NW		Lava	Flujo de lava dacítica de coloración grisaceo de grano medio. Nlsg	17/06/2017
S59	606789	7561214	5649	35/50NW	7806	Lava	Fragmento de una roca de origen volcánico (lava), de color gris oscuro, tiene superficies de meteorización, de composición intermedia, muestra estructura holocristalina y textura porfídica de grano medio (>1 mm), donde se observan abundantes cristales de feldespatos blanquecinos orientados, biotita oxidada, piroxenos y óxidos de hierro diseminados, rodeados por una pasta de grano muy fino. La lava muestra elevada dureza y compactación. Nlsg	17/06/2017
S60	606758	7562878	5041	240/70SE	7807	Lava	Fragmento de una roca de origen volcánico (lava), de color gris oscuro, tiene superficies de meteorización, de composición intermedia, muestra estructura holocristalina y textura porfídica de grano medio (>1 mm), donde se observan abundantes cristales de feldespatos blanquecinos orientados, biotita oxidada, piroxenos y óxidos de hierro diseminados, rodeados por una pasta de grano muy fino. La lava muestra elevada dureza y compactación. Nlsg	17/06/2017
S61	601966	7564742	4560	262/80NW		Lava	Color gris blanquecino porfido feldespático biotítico grano medio a grueso las biotitas son idiomorfas muestra pseudo estratificación. Nlsc	17/06/2017
S62	601972	7564714	4574	288/8SW		Lava	Lava color gris claro grano fino a medio textura porfido feldespático biotítico cuarzo fragmentado sub redondeado con engolfamientos, en sectores muestra dirección de flujo. Nlsc	17/06/2017
S63	602053	7564203	4721	316/61SW		Lava	Afloramiento lavas color gris oscuro grano medio a fino disposición de cristales fragmentados textura porfídica silicificado. Nlsc	17/06/2017
S64	602044	7564108	4760	173/41SW		Lava	Afloramiento lava color gris claro con xenolitos con aureolas de recalentamiento textura porfido feldespático biotítico grano medio a fino. Nlsc	17/06/2017
S65	601966	7564718	4573	85/23NW		Lava	Presenta flujos de lavas andesíticas de coloración marrón blanquesino, granos de medio a grueso en su matriz, cristales de biotita sub redondeados. Clastos < 10 cm. Nlsc	17/06/2017



SERVICIO GEOLOGICO MINERO
DIRECCION ESTRATEGICA DE REINVINDICACION MARITIMA, SILALA Y RECURSOS HIDRICOS INTERNACIONALES
MAPEO GEOLICO DEL AREA CIRCUNDANTE AL MANANTIAL DEL SILALA
BASE DE DATOS



Nº	ESTE (UTM)	NORTE (UTM)	ALTURA (m.s.n.m.)	DIRECCIÓN DE FLUJO	CODIGO MUESTRA	LITOLOGIA	DESCRIPCION MACROSCOPICA	FECHA
S66	601941	7564642	4609	135/37SW		Lava	Presenta flujos de lavas andesiticos de coloracion marron blanquesino, de granos de medio a grueso en su matrix, cristales de biotita sub redondeados. Nlsc	17/06/2017
S67	602053	7564206	4719	85/30NW		Lava	Presenta flujos de lavas andesiticos de coloracion gris, de grano grueso en su matrix, cristales de biotita sub redondeados. Nlsc	17/06/2017
S68	602052	7564099	4766	178/66SW	7713	Lava	Fragmento de una roca de origen volcánico (lava), de color gris con tono rosáceo, presenta superficies de meteorización, de composición intermedia, muestra estructura holocristalina y textura porfídica de grano medio (>2 mm), donde se observan grandes cristales de feldespatos blanquecinos, escaso cuarzo, biotita, anfiboles, piroxenos y óxidos de hierro diseminados, rodeados por una pasta de grano muy fino. La lava muestra elevada dureza y compactación. Nlsc	17/06/2017
S69	607807	7567446	4604	31/61NW		Lava	Coladas de lava andesitica ,plagioclasicas frescas y alteradas, biotitas frescas y alteradas.Nlsg	18/06/2017
S70	608466	7567135	4664	120/25NE		Lava	Coladas de lava andesitica, tamaño de grano medio, plagioclasicas frescas, esporadicas biotitas. Nlsg	18/06/2017
S71	608487	7566245	4650	30/60SE		Lava	Roca dacitica de color gris con matriz silicificada, textura bandeda, tamaño de grano fino , posible vidrio volcanico como patina.Nlsg	18/06/2017
S72	605556	7566660	4558	331/8SW		Ignimbrita	Toba de color gris claro porfido feldespatico de grano, sub redondeados y aureolas de recalentamiento cristales fragmentados. Nls-3	18/06/2017
S74	606154	7566472	4596	74/17SE		Lava	Lava color gris oscuro textura afanitica con fragmentos de cuarzo, biotita muestra direccion de flujo y bandedamiento. Nlsg	18/06/2017
S75	606397	7566315	4625	160/9SW		Lava	Lava color gris oscuro textura afanitica con fragmentos de cuarzo, biotita muestra direccion de flujo y bandedamiento muy silicificado. Nlsg	18/06/2017
S76	605180	7566103	4593	3/26NW		Lavas	Presenta flujos de lavas andesiticos de coloracion gris blanquecino, de grano medio a grueso en su matrix, con menor contenido de cristales de biotita angulosos. Nlsg	18/06/2017
S77	606156	7566475	4595	280/32NE		Lavas	Presenta flujos de lavas andesiticos de coloracion gris blanquecino, de grano medio a grueso en su matrix, con menor contenido de cristales de cuarzo angulosos y menor contenido biotita angulosos. Con clastos < 12 cm. Nlsg	18/06/2017
S78	607188	7567230	4596		7808	Lava	Fragmento de una roca de origen volcánico (lava), de color gris oscuro, tiene superficies de meteorización, de composición intermedia, muestra estructura holocristalina y textura porfídica de grano medio (>1 mm), donde se observan abundantes cristales de feldespatos blanquecinos orientados, biotita oxidada, piroxenos y óxidos de hierro diseminados, rodeados por una pasta de grano muy fino. La lava muestra elevada dureza y compactación. Nlsg	19/06/2017
S79	607192	7567230	4601	N-S/30E		Lava	Lava de color gris oscuro, con algunos fragmentos de cuarzo. Nlsg	19/06/2017

Nº	ESTE (UTM)	NORTE (UTM)	ALTURA (m.s.n.m.)	DIRECCION DE FLUJO	CODIGO MUESTRA	LITOLOGIA	DESCRIPCION MACROSCOPICA	FECHA
S80	607216	7567216	4599	130/67SW		Lava	Lava de color gris oscuro, con algunos fragmetos de cuarzo. Nlsg	19/06/2017
S81	604876	7567156	4555	326/3SW		Ignimbrita	Toba con pseudo estratificacion color gris claro porfido feldespatico con fragmentos de biotita en algunos casos idiomorfos. Nls-3	19/06/2017
S82	604877	7566773	4568	311/4SW		Ignimbrita	Afloramiento de toba de color gris claro textura porfidica cion biotita idiomorfa en algunos sectores mas cuarzo fragmentado. Nls-3	19/06/2017
S83	605150	7566818	4561	305/3SW		Ignimbrita	Toba color gris blanquecino matrix ferruginosa muestra pseudo estratificación. Nls-3	19/06/2017
S84	606290	7568048	4594	285/5SW		Ignimbrita	Toba color gris blanquecino matrix ferruginosa muestra pseudo estratificación. Nls-3	19/06/2017
S85	606425	7567952	4588	321/77NE		Ignimbrita	Toba color gris blanquecino matrix ferruginosa muestra pseudo estratificación. Nls-3	19/06/2017
S86	606242	7568071	4596	348/12NE	7716	Toba	Fragmento de una roca de origen volcánico (toba), de color marrón con tono grisáceo, tiene superficies de meteorización, de composición ácida, muestra estructura vitro-cristalina y textura porfidica de grano medio (>2 mm), donde se observan cristales de feldespatos blanquecinos, cuarzo, biotita oxidad, litoclastos y óxidos de hierro diseminados, rodeados por una pasta vítreo, muestra moderada dureza y grado de soldadura. Nls-3	19/06/2018
S87	608847	7566066	4661	340/35SW		Lava	Flujo de lava , de color grisaceo rosado, de grano medio a grueso. Nlsg	21/06/2017
S88	609452	7565671	4647	150/70NE		Lava	Flujo de lava , de color grisaceo rosado, de grano medio a grueso. Nlsg	21/06/2017
S89	600871	7566783	4437	317/19SW	7717	Lava	Fragmento de una roca de origen volcánico (lava), de color gris, presenta superficies de intensa meteorización, composición intermedia, muestra estructura holocristalina y textura porfidica de grano medio (>2 mm), donde se observan cristales de feldespatos blanquecinos, muy escaso cuarzo, biotita y anfiboles oxidados, piroxenos y óxidos de hierro diseminados, rodeados por una pasta de grano muy fino, la lava muestra elevada dureza y compactación. Nlsc	21/06/2017
S90	603511	7567642	4500	175/12NE	7720	Lava	Fragmento de una roca de origen volcánico (lava), de color gris, presenta superficies de meteorización, de composición intermedia, muestra estructura cavernosa o vesicular y textura porfidica de grano medio (>2 mm), donde se observan cristales de feldespatos blanquecinos, escaso cuarzo, piroxenos y óxidos de hierro diseminados, rodeados por una pasta de grano muy fino. La lava muestra moderada dureza y compactación, y cavidades llenadas por cuarzo. Nlin1	21/06/2017



SERVICIO GEOLOGICO MINERO
DIRECCION ESTRATEGICA DE REINVINDICACION MARITIMA, SILALA Y RECURSOS HIDRICOS INTERNACIONALES
MAPEO GEOLOGICO DEL AREA CIRCUNDANTE AL MANANTIAL DEL SILALA
BASE DE DATOS



Nº	ESTE (UTM)	NORTE (UTM)	ALTURA (m.s.n.m.)	DIRECCIÓN DE FLUJO	CODIGO MUESTRA	LITOLOGIA	DESCRIPCION MACROSCOPICA	FECHA
S92	605051	7569399	4580		7721	Ignimbrita	Fragmento de una roca de origen volcánico (toba), de color marrón con tono grisáceo, tiene superficies de meteorización, de composición ácida, muestra estructura vitro-cristalina y textura porfídica de grano medio (>2 mm), donde se observan cristales de feldespatos blanquecinos, cuarzo, biotita oxidada, litoclastos y óxidos de hierro diseminados, rodeados por una pasta vítreas, muestra moderada dureza y grado de soldadura. Nls-3	21/06/2017
S93	609644	7564821	4652	E - W/68S		Lava	Presenta flujos de lavas andesíticos de coloración gris blanquecino, de grano medio fino en su matrix, con menor contenido de cristales de biotita angulosos. Nlsg	22/06/2017
S94	610068	7564182	4677	195/70SE		Lava	Presenta flujos de lavas andesíticos de coloración gris blanquecino, de grano medio fino en su matrix, con menor contenido de cristales de biotita angulosos. Nlsg	22/06/2017
S95	610088	7564531	4627	240/53SE		Lava	Presenta flujos de lavas andesíticos de coloración gris blanquecino, de grano medio fino en su matrix, con menor contenido de cristales de biotita angulosos. Nlsg	22/06/2017
S96	600816	7566953	4485	335/70SW	7809	Lava	Fragmento de una roca de origen volcánico (lava), de color gris, presenta superficies de intensa meteorización, composición intermedia, muestra estructura holocristalina y textura porfídica de grano medio (>2 mm), donde se observan cristales de feldespatos blanquecinos, muy escaso cuarzo, biotita y anfíboles oxidados, piroxenos y óxidos de hierro diseminados, rodeados por una pasta de grano muy fino, la lava muestra elevada dureza y compactación. Nlsc	12/07/2017
S97	600661	7567938	4547		7810	Lava	Fragmento de una roca de origen volcánico (lava), de color gris con tono negruzco, presenta superficies de meteorización y composición básica, muestra estructura holocristalina y textura porfídica de grano medio a fino (>1 mm), donde se observan cristales de feldespatos blanquecinos con orientación, minerales máficos muy oxidados, piroxenos y óxidos de hierro diseminados, rodeados por una pasta de grano muy fino, la lava muestra elevada dureza y compactación, así como numerosas cavidades o amigdalas vacías. Nlin1	12/07/2020
S98	600166	7569312	4671	280/Sub.Hz.	7811	Brecha basal	Muy localizado, monolítico clastos angulosos matrix ferruginosa de composición similar a la lava posiblemente sea una auto brecha.	12/07/2017
S99	600666	7567935	4544	210/80NW		Lava	Coladas de lava dacítica porfirícas de color gris oscura, con fenocristales de sanidina, hornblendita, Qz, Bio, con pseudoestratificación laminadas. Nlin1	12/07/2017
S100	600240	7565400	4292	229/4NW		Flujo de detritos	Flujo detritos matrix soportado color marrón rojizo con clastos en su matrix que varían de 5 cm a 25 cm, sub redondeados de grano medio a grueso débil soldamiento matrix con alto contenido de fragmentos de, cuarzo, biotita, textura terrosa.	12/07/2017
S101	600563	7565784	4320	209/9SE		Ignimbrita	Ignimbrita color gris claro leve tono rosaceo con fragmentos de cuarzo con bordes sub redondeados y engolfamientos, biotita en fragmentos rodeados de una pasta ferruginosa polilítica clastos con aureolas de recalentamiento soldamiento moderado.	12/07/2017

Nº	ESTE (UTM)	NORTE (UTM)	ALTURA (m.s.n.m.)	DIRECCIÓN DE FLUJO	CODIGO MUESTRA	LITOLOGIA	DESCRIPCION MACROSCOPICA	FECHA
S103	603136	7569882	4610	193/4SE		Lavas	Color gris con estructura holocristalina y textura porfídica de grano medio, donde se observan cristales de feldespatos blanquecinos, escaso cuarzo, biotita, anfiboles, piroxenos y óxidos de hierro diseminados, rodeados por una pasta de grano muy fino. la roca, muestra elevada dureza y compactación. Nlin 1	13/07/2017
S104	599317	7568831	4759	30/30SE	7813	Brecha basal	Muy localizado, monolítico clastos angulosos matrix ferruginosa de composición similar a la lava posiblemente sea una auto brecha.	13/07/2017
S105	599174	7571415	5019	270/74SW		Lava	Color gris con textura porfídica de grano medio, donde se observan cristales de feldespatos blanquecinos, escaso cuarzo, biotita, rodeados por una pasta de grano muy fino. la roca, muestra elevada dureza y compactación. Nlin 1	14/07/2017
S106	602960	7568618	4561	188/7SE		Lava	Color gris con textura porfídica de grano medio, donde se observan cristales de feldespatos blanquecinos, escaso biotita, rodeados por una pasta de grano muy fino. Nlin 1	14/07/2017
S107	603440	7565926	4422		7814	Toba	Fragmento de una roca de origen piroclástico (toba), de color gris con tono rosáceo, muestra superficies de meteorización, composición intermedia, con estructura masiva y textura porfídica de grano medio (>1 mm), donde se observan cristales de feldespatos blanquecinos, anfiboles, piroxenos y óxidos de hierro diseminados, rodeados por una pasta de grano muy fino, la roca muestra moderada dureza y compactación, y presenta costras delgadas de malaquita.	14/07/2017
S108	602468	7565749	4415	273/20SW		Flujo de detritos	Clastos angulosos a subredondeados monolíticos, diámetro de los clastos (1mm-30cm), matriz ferruginosa terrosa. Nfd2	14/07/2017
S109	602431	7565759	4420	60/16SE		Flujo de detritos	Clastos angulosos a subredondeados monolíticos, diámetro de los clastos (1mm-30cm), matriz ferruginosa terrosa. Nfd2	14/07/2017
S110	603483	7564079	4558	160/55SW	7816	Lava	Fragmento de una roca de origen volcánico (lava), de color gris oscuro con superficies de meteorización, composición intermedia, muestra estructura holocristalina y textura porfídica de grano medio (>1 mm), donde se observan cristales de feldespatos blanquecinos, biotita, anfiboles muy oxidados, piroxenos y óxidos de hierro diseminados, rodeados por una pasta de grano fino, contiene agregados de calcita rellenando pequeñas cavidades, la roca muestra elevada dureza y compactación, y contiene algunos litoclastos de rocas volcánicas. Nlsg	15/07/2017
S111	606447	7562228	5165	290/25SW	7817	Lava	Fragmento de una roca de origen volcánico (lava), de color gris oscuro con superficies de intensa meteorización, composición intermedia, muestra estructura holocristalina y textura porfídica de grano medio (>1 mm), donde se observan cristales de feldespatos blanquecinos, biotita y anfiboles muy oxidados, piroxenos y óxidos de hierro diseminados, rodeados por una pasta de grano fino, la roca muestra moderada dureza y compactación. Nlsg	15/07/2017
S112	606447	7562228	5165	290/25NW	7818	Lava	Fragmento de una roca de origen volcánico (lava), de color gris con superficies de intensa meteorización, composición intermedia, muestra estructura holocristalina y cavernosa, con textura porfídica de grano medio (>1 mm), donde se observan abundantes cristales de feldespatos blanquecinos, biotita oxidada, piroxenos y óxidos de hierro diseminados, rodeados por una pasta de grano fino, la roca muestra elevada dureza y compactación. Nlsg	15/07/2017



SERVICIO GEOLOGICO MINERO
DIRECCION ESTRATEGICA DE REINVINDICACION MARITIMA, SILALA Y RECURSOS HIDRICOS INTERNACIONALES
MAPEO GEOLOGICO DEL AREA CIRCUNDANTE AL MANANTIAL DEL SILALA
BASE DE DATOS



Nº	ESTE (UTM)	NORTE (UTM)	ALTURA (m.s.n.m.)	DIRECCIÓN DE FLUJO	CÓDIGO MUESTRA	LITOLOGIA	DESCRIPCION MACROSCOPICA	FECHA
S113	607734	7564099	4868	290/13SW		Lava	Lava dacitica porfiritica laminadas y en bloques del Cerro Silala Grande de color gris negruzco. Nlsg	16/07/2017
S114	611232	7567663	4626		7722	Toba	Fragmento de una roca de origen piroclástico (toba vitro-cristalina), de color gris-blanquecino con superficies de meteorización, de composición ácida, muestra estructura hipocristalina y textura porfídica de grano medio (>1 mm), donde se observan cristales de feldespatos, cuarzo, biotita con orientación, litoclastos de rocas volcánicas y óxidos de hierro diseminados, rodeados por una pasta vítreo, muestra reducido grado de dureza y soldadura, por lo que es deleznable. Ntpg	16/07/2017
S115	607925	7564449	4820	278/5SW		Lava	Lava dacitica porfiríticas laminares y en bloques del Cerro Silala Grande de color gris negruzco. Nlsg	16/07/2017
S116	607734	7564099	4868	290/13SW		Lava	Colada de lava volcánica posible dacita de textura bandeada, fenocristales de cuarzo, plagioclasa, biotita y ortoclasa. Nlsg	16/07/2017
S117	607792	7564663	4802	145/55SW	7820	Lava	Fragmento de una roca de origen volcánico (lava), de color gris con tono rosáceo, tiene superficies de meteorización, composición intermedia, muestra estructura holocristalina y textura porfídica de grano medio (>2 mm), donde se observan abundantes cristales de feldespatos blanquecinos, biotita y anfiboles oxidados, piroxenos, óxidos de hierro diseminados y pequeños litoclastos de rocas volcánicas, rodeados por una pasta de grano fino, la roca muestra elevada dureza y compactación. Nlsg	16/07/2017
S118	607069	7564443	4770	100/20NE		Lava	De color gris claro en superficie fresca y gris con patinas marron rojizas en superficie alterada. el afloramiento presenta textura afanítica con elastos líticos de ignimbritas de formas subredondeadas, de 0.5 a 2.5 cm. de diámetro en una matriz de vidrio volcánico con presencia aislada de cristales de plagioclasas biotitas y feldespatos. Nlsg	16/07/2017
S119	611225	7567577	4640		7723	Toba	Fragmento de una roca de origen piroclástico (toba vitro-cristalina), de color gris-blanquecino con superficies de meteorización, de composición ácida, muestra estructura hipocristalina y textura porfídica de grano medio (>1 mm), donde se observan cristales de feldespatos, cuarzo, biotita con orientación y óxidos de hierro diseminados, rodeados por una pasta vítreo, muestra moderado grado de dureza y soldadura. Ntpg	16/07/2017
S120	609442	7569033	4653	37/64SE	7726	Lava	Fragmento de una roca de origen volcánico (lava), de color gris con superficies de meteorización, composición relativamente ácida, muestra estructura holocristalina y textura porfídica de grano medio (>2 mm), donde se observan grandes cristales de feldespatos blanquecinos, escaso cuarzo, biotita, anfiboles, piroxenos y óxidos de hierro diseminados, rodeados por una pasta de grano muy fino, contiene agregados de calcita relleno de pequeñas cavidades, la roca muestra elevada dureza y compactación. Nlc	16/07/2017
S121	610029	7568343	4652	90/75NE		Lava	Color gris claro textura profídica feldespática el porcentaje de biotita es de 1-2% en algunos casos idiomorfo, el cuarzo es fragmentado con engolfamientos. Nlc	16/07/2017
S122	601256	7572117	5181	266/67S	7821	Lava	Fragmento de una roca de origen volcánico (lava), de color gris oscuro, composición intermedia, muestra estructura holocristalina y textura porfídica de grano medio (>2 mm), donde se observan abundantes cristales de feldespatos blanquecinos, biotita y anfiboles oxidados, escaso cuarzo y piroxenos, y óxidos de hierro diseminados, rodeados por una pasta de grano fino, la roca muestra elevada dureza y compactación, en general se halla fresca. Nlc	18/07/2017

Nº	ESTE (UTM)	NORTE (UTM)	ALTURA (m.s.n.m.)	DIRECCIÓN DE FLUJO	CODIGO MUESTRA	LITOLOGIA	DESCRIPCION MACROSCOPICA	FECHA
S123	601256	7572117	5181	266/67S	7822	Lava	Fragmento de una roca de origen volcánico (lava), de color gris con tono rosáceo, composición intermedia, muestra estructura holocristalina y textura porfídica de grano medio (>2 mm), donde se observan abundantes cristales de feldespatos blanquecinos, biotita y anfíboles oxidados, escaso cuarzo y óxidos de hierro diseminados, rodeados por una pasta de grano fino, la roca muestra moderada dureza y compactación, en general se halla meteorizada. Nlcn	18/07/2017
S125	606484	7567980	4581	240/22NW		Ignimbrita	Roca de origen piroclástico (toba vitro-cristalina), de color gris-rosáceo con superficies de meteorización, de composición ácida, muestra estructura hipocristalina y textura porfídica de grano medio (>1 mm). Nls-3	18/07/2017
S126	602762	7574297	4604	251/31NW		Lava	Color gris oscuro, muestra estructura holocristalina y textura porfídica de grano medio a grueso, se observan abundantes cristales de feldespatos blanquecinos, biotita oxidada, rodeados por una pasta de grano muy fino. Nlcn	18/07/2017
S127	602419	7574426	4632	234/8NW		Lava	Color gris oscuro de composición intermedia, muestra estructura holocristalina y textura porfídica de grano grueso, donde se observan abundantes cristales de feldespatos blanquecinos, biotita oxidada, piroxenos y óxidos de hierro diseminados, rodeados por una pasta de grano muy fino. Nlcn	18/07/2017
S128	601860	7574652	4636	95/17NE		Lava	Color gris oscuro de textura porfídica feldespática de grano grueso - medio, donde se observan abundantes cristales de feldespatos, superficialmente se observa una patina color café rojizo.	18/07/2017
S129	601481	7574425	4674	48/10SE		Brecha basal	Muy localizado, monolítico clastos angulosos matrix ferruginosa de composición similar a la lava posiblemente sea una auto brecha.	18/07/2017
S130	601174	7573895	4738	48/9SE		Lava	Color gris oscuro de textura porfídica feldespática de grano grueso - medio, donde se observan abundantes cristales de feldespatos, superficialmente se observa una patina color café rojizo	18/07/2017
S131	601912	7573842	4731	84/6SE		Lava	Color gris oscuro, muestra estructura holocristalina y textura porfídica de grano medio a grueso, se observan abundantes cristales de feldespatos blanquecinos, escasa biotita oxidada, rodeados por una pasta de grano muy fino. Nlcn	18/07/2017
S132	601757	7573261	4833	32/6SW	7727	Lava	Fragmento de una roca de origen volcánico (lava), de color gris con tono oscuro y superficies de meteorización, composición intermedia, muestra estructura holocristalina y textura porfídica de grano medio (>2 mm), donde se observan cristales de feldespatos blanquecinos, muy escaso cuarzo, biotita y anfíboles oxidados, piroxenos y óxidos de hierro diseminados, rodeados por una pasta de grano muy fino, la lava muestra elevada dureza y compactación. Nlcn	18/07/2017
S133	602531	7573450	4708	222/80SE		Lava	Color gris oscuro, muestra estructura holocristalina y textura porfídica de grano grueso, donde se observan grandes cristales de feldespatos blanquecinos, cuarzo, biotita, y óxidos de hierro diseminados, rodeados por una pasta de grano muy fino. La lava muestra elevada dureza y compactación. Nlcn	18/07/2017
S134	602604	7575147	4607		7732	Lava	Fragmento de una roca de origen volcánico (lava), de color gris oscuro, presenta superficies de meteorización, composición intermedia, muestra estructura holocristalina y textura porfídica de grano medio (>2 mm), donde se observan cristales de feldespatos blanquecinos, muy escaso cuarzo, biotita y anfíboles oxidados y óxidos de hierro diseminados, rodeados por una pasta de grano muy fino, la lava muestra elevada dureza y compactación. Nlcn	18/07/2017



SERVICIO GEOLOGICO MINERO
DIRECCION ESTRATEGICA DE REINVINDICACION MARITIMA, SILALA Y RECURSOS HIDRICOS INTERNACIONALES
MAPEO GEOLICO DEL AREA CIRCUNDANTE AL MANANTIAL DEL SILALA
BASE DE DATOS



Nº	ESTE (UTM)	NORTE (UTM)	ALTURA (m.s.n.m.)	DIRECCIÓN DE FLUJO	CODIGO MUESTRA	LITOLOGIA	DESCRIPCION MACROSCOPICA	FECHA
S135	605330	7574972	4741	118/48NE	7729	Lava	Fragmento de una roca de origen volcánico (lava), de color gris con tono rosáceo, presenta superficies de intensa meteorización, composición intermedia, muestra estructura holocristalina y textura porfídica de grano medio (>2 mm), donde se observan cristales de feldespatos blanquecinos, muy escaso cuarzo, biotita oxidada y óxidos de hierro diseminados, rodeados por una pasta de grano muy fino, la lava muestra moderada dureza y compactación, por lo que es ligeramente deleznable. Nlc	19/07/2017
S136	606578	7568225	4555		7824	Arcillita	Fragmento de una roca sedimentaria pélitica (probablemente una arcillita) y color marrón-grisáceo, presenta una estructura masiva y terrosa con indicios de estratificación y textura clástica de grano muy fino (<0,5 mm), donde se observan bandas formadas por abundantes limos y arcillas, junto a óxidos de hierro y probablemente polvo de vidrio volcánico, por lo que la roca es muy suave, con reducida compactación y es deleznable.	19/07/2017
S137	606903	7568405	4558	275/15SW		Ignimbrita	Roca de origen piroclástico (toba vitro-crystalina), de color gris-rosáceo con superficies de meteorización, de composición ácida, muestra estructura hipocrystalina y textura porfídica de grano medio (>1 mm). Nls-3	19/07/2017
S138	606472	7568766	4614	290/14SW		Ignimbrita	Roca de origen piroclástico (toba vitro-crystalina), de color gris-rosáceo con superficies de meteorización, de composición ácida, muestra estructura hipocrystalina y textura porfídica de grano medio (>1 mm). Nls-3	19/07/2017
S139	606215	7568969	4637	310/20SW		Ignimbrita	Roca de origen piroclástico (toba vitro-crystalina), de color gris-rosáceo con superficies de meteorización, de composición ácida, muestra estructura hipocrystalina y textura porfídica de grano medio (>1 mm). Nls-3	19/07/2017
S140	605826	7569255	4618	305/16SW		Ignimbrita	Roca de origen piroclástico (toba vitro-crystalina), de color gris-rosáceo con superficies de meteorización, de composición ácida, muestra estructura hipocrystalina y textura porfídica de grano medio (>1 mm). Nls-3	19/07/2017
S141	605460	7570190	4573	220/16NW		Ignimbrita	Roca de origen piroclástico (toba vitro-crystalina), de color gris-rosáceo con superficies de meteorización, de composición ácida, muestra estructura hipocrystalina y textura porfídica de grano medio (>1 mm). Nls-3	19/07/2017
S142	606379	7569804	4581	105/30NE		Ignimbrita	Roca de origen piroclástico (toba vitro-crystalina), de color gris-rosáceo con superficies de meteorización, de composición ácida, muestra estructura hipocrystalina y textura porfídica de grano medio (>1 mm). Nls-3	19/07/2017
S143	606469	7569775	4581	120/26NE		Ignimbrita	Roca de origen piroclástico (toba vitro-crystalina), de color gris-rosáceo con superficies de meteorización, de composición ácida, muestra estructura hipocrystalina y textura porfídica de grano medio (>1 mm). Nls-3	19/07/2017
S144	606610	7569749	4585	125/30NE		Ignimbrita	Roca de origen piroclástico (toba vitro-crystalina), de color gris-rosáceo con superficies de meteorización, de composición ácida, muestra estructura hipocrystalina y textura porfídica de grano medio (>1 mm). Nls-3	19/07/2017
S145	607112	7569352	4591	140/28NE		Ignimbrita	Roca de origen piroclástico (toba vitro-crystalina), de color gris-rosáceo con superficies de meteorización, de composición ácida, muestra estructura hipocrystalina y textura porfídica de grano medio (>1 mm). Nls-3	19/07/2017
S146	604894	7574836	4685	60/45NW		Lava	Color gris oscuro, grano grueso, textura porfídica donde se observan grandes cristales de feldespatos blanquecinos, no se observan afloramiento bien definidos. Nlc	19/07/2017
S147	605332	7574970	4729	118/48NW		Lava	Flujo de lava, feldespático color griz rozaceo debido a la presencia de óxidos de hierro diseminados, en algunos casos las biotitas presentan cristales idiomorfos y el cuarzo con engolfamientos. Nlc	19/07/2017

Nº	ESTE (UTM)	NORTE (UTM)	ALTURA (m.s.n.m.)	DIRECCIÓN DE FLUJO	CODIGO MUESTRA	LITOLOGIA	DESCRIPCION MACROSCOPICA	FECHA
S148	605391	7574041	4673	153/20NW		Lava	Flujo de lava, feldespatico color griz rozaeo debido a la presencia de oxicos de hierro diseminados, en algunos casos las biotitas presentan cristales idiomorfos y el cuarzo con engolfamientos.Nlct	19/07/2017
S149	609620	7561040	4881	261/12SE		Lava	Presenta flujos de lavas andesiticos de coloracion gris blanquecino, de grano medio a grueso en su matrix, con menor contenido de cristales de cuarzo angulosos y menor contenido biotita angulosos. Nlsg	06/08/2017
S150	609749	7561333	4885	253/10SE		Lava	Presenta flujos de lavas andesiticos de coloracion gris blanquecino, de grano medio a grueso en su matrix, con menor contenido de cristales de cuarzo angulosos y menor contenido biotita angulosos. Nlsg	06/08/2017
S151	608832	7561019	5033	13/30NW		Lava	Presenta flujos de lavas andesiticos de coloracion gris blanquecino, de grano medio a grueso en su matrix, con menor contenido de cristales de cuarzo angulosos y menor contenido biotita angulosos. Nlsg	06/08/2017
S152	608686	7560971	5090	275/43SW		Lava	Presenta flujos de lavas andesiticos de coloracion gris blanquecino, de grano medio a grueso en su matrix, con menor contenido de cristales de cuarzo angulosos y menor contenido biotita angulosos. Nlsg	06/08/2017
S153	608560	7560971	5113	314/18NE		Lava	Presenta flujos de lavas andesiticos de coloracion gris blanquecino, de grano medio a grueso en su matrix, con menor contenido de cristales de cuarzo angulosos y menor contenido biotita angulosos. Nlsg	06/08/2017
S154	612126	7562928	4582	140/45NE		Lava	Presenta flujos de lavas andesiticos de coloracion gris blanquecino, de grano medio a grueso en su matrix, con menor contenido de cristales de cuarzo angulosos y menor contenido biotita angulosos. Nlsg	06/08/2017
S155	611768	7562919	4620	260/38NW		Lava	Presenta flujos de lavas andesiticos de coloracion gris blanquecino, de grano medio a grueso en su matrix, con menor contenido de cristales de cuarzo angulosos y menor contenido biotita angulosos. Nlsg	06/08/2017
S156	611481	7562814	4613	30/30NW		Lava	Presenta flujos de lavas andesiticos de coloracion gris blanquecino, de grano medio a grueso en su matrix, con menor contenido de cristales de cuarzo angulosos y menor contenido biotita angulosos. Nlsg	06/08/2017
S157	610800	7562642	4647	205/83NW	7825	Lava	Fragmento de una roca de origen volcánico (lava), de color gris con tono oscuro, tiene superficies de meteorización, composición intermedia, muestra estructura cavernosa con cavidades vacías y textura porfídica de grano medio (>2 mm), donde se observan abundantes cristales de feldespatos blanquecinos, biotita muy oxidada, piroxenos y óxidos de hierro diseminados, rodeados por una pasta de grano muy fino, la roca muestra moderada dureza y compactación y un aspecto escoriáceo por sus numerosas cavidades. Nlsg	06/08/2017
S158	612434	7561644	4648	240/39NW		Lava	Presenta flujos de lavas andesiticos de coloracion gris blanquecino, de grano medio a grueso en su matrix, con menor contenido de cristales de cuarzo angulosos y menor contenido biotita angulosos. Nlsg	06/08/2017
S159	611835	7562022	4642	245/70NW		Lava	Presenta flujos de lavas andesiticos de coloracion gris blanquecino, de grano medio a grueso en su matrix, con menor contenido de cristales de cuarzo angulosos y menor contenido biotita angulosos. Nlsg	06/08/2017
S160	612206	7562500	4618	290/60NE		Lava	Presenta flujos de lavas andesiticos de coloracion gris blanquecino, de grano medio a grueso en su matrix, con menor contenido de cristales de cuarzo angulosos y menor contenido biotita angulosos. Nlsg	06/08/2017



SERVICIO GEOLOGICO MINERO
DIRECCION ESTRATEGICA DE REINVINDICACION MARITIMA, SILALA Y RECURSOS HIDRICOS INTERNACIONALES
MAPEO GEOLOGICO DEL AREA CIRCUNDANTE AL MANANTIAL DEL SILALA
BASE DE DATOS



Nº	ESTE (UTM)	NORTE (UTM)	ALTURA (m.s.n.m.)	DIRECCIÓN DE FLUJO	CÓDIGO MUESTRA	LITOLOGIA	DESCRIPCION MACROSCOPICA	FECHA
S161	609147	7560225	4989	260/12SE		Lava	Presenta flujos de lavas andesíticos de coloración gris blanquecino, de grano medio a grueso en su matrix, con menor contenido de cristales de cuarzo angulosos y menor contenido biotita angulosos. Nlsg	06/08/2017
S162	608925	7560251	5026	282/12SW		Lava	Presenta flujos de lavas andesíticos de coloración gris blanquecino, de grano medio a grueso en su matrix, con menor contenido de cristales de cuarzo angulosos y menor contenido biotita angulosos. Nlsg	06/08/2017
S163	620510	7566218	4910	352/64NE		Lava	Presenta flujos de lavas andesíticos de coloración gris blanquecino, de grano medio a grueso en su matrix, con menor contenido de cristales de cuarzo angulosos y mayor contenido biotita angulosos. Nlrj	07/08/2017
S164	620023	7566597	4864	8/86NW	7737	Lava	Fragmento de una roca de origen volcánico (lava), de color gris oscuro, tiene superficies de meteorización, composición intermedia, muestra estructura holocristalina y textura porfídica de grano medio (>2 mm), donde se observan abundantes y grandes cristales de feldespatos, anfiboles, biotita, piroxenos y óxidos de hierro diseminados, rodeados por una pasta de grano muy fino, la roca muestra elevada dureza y compactación. Nlrj	07/08/2017
S165	619280	7564248	4776	220/17NW		Lava	Coladas de lavas andesíticos de coloración rojizo blanquecino, de grano medio en su matrix, con menor contenido de cristales de cuarzo angulosos y mayor contenido biotita, presencia de turmalina con pseudoestratificación casi sub horizontal . Nlcc	07/08/2017
S166	619257	7568501	4918	210/60NW		Lava	Presenta flujos de lavas andesíticos de coloración gris blanquecino, de grano medio a grueso en su matrix, con menor contenido de cristales de cuarzo angulosos y mayor contenido biotita angulosos. Nlrj	07/08/2017
S167	620924	7566120	4921	218/56NW		Lava	Presenta flujos de lavas andesíticos de coloración gris blanquecino, de grano medio a grueso en su matrix, con menor contenido de cristales de cuarzo angulosos y mayor contenido biotita angulosos. Nlrj	07/08/2017
S168	620759	7566225	4934	330/80NE		Lava	Presenta flujos de lavas andesíticos de coloración gris blanquecino, de grano medio a grueso en su matrix, con menor contenido de cristales de cuarzo angulosos y mayor contenido biotita angulosos. Nlrj	07/08/2017
S169	620545	7566244	4928	230/60NW		Lava	Presenta flujos de lavas andesíticos de coloración gris blanquecino, de grano medio a grueso en su matrix, con menor contenido de cristales de cuarzo angulosos y mayor contenido biotita angulosos. Nlrj	07/08/2017
S170	621867	7564722	4951	20/30NW		Lava	Presenta flujos de lavas andesíticos de coloración gris blanquecino, de grano medio a grueso en su matrix, con menor contenido de cristales de cuarzo angulosos y mayor contenido biotita angulosos. Nlrj	07/08/2017
S171	622291	7564992	5142	25/83NW		Lava	Presenta flujos de lavas andesíticos de coloración gris blanquecino, de grano medio a grueso en su matrix, con menor contenido de cristales de cuarzo angulosos y mayor contenido biotita angulosos. Nlrj	07/08/2017
S172	620821	7566719	4973	263/10SE		Lava	Presenta flujos de lavas andesíticos de coloración gris blanquecino, de grano medio a grueso en su matrix, con menor contenido de cristales de cuarzo angulosos y mayor contenido biotita angulosos. Nlrj	07/08/2017
S173	618904	7564384	4763	278/18SW		Lava	Coladas de lavas andesíticos de coloración rojizo blanquecino, de grano medio en su matrix, con menor contenido de cristales de cuarzo angulosos y mayor contenido biotita,con pseudoestratificación casi sub horizontal . Nlcc	07/08/2017

Nº	ESTE (UTM)	NORTE (UTM)	ALTURA (m.s.n.m.)	DIRECCIÓN DE FLUJO	CODIGO MUESTRA	LITOLOGIA	DESCRIPCION MACROSCOPICA	FECHA
S174	618817	7564254	4768	132/5SE		Lava	Coladas de lavas andesiticos de coloracion rojiso blanquecino, de grano medio en su matrix, con menor contenido de cristales de cuarzo angulosos y mayor contenido biotita,con pseudoestratificacion casi sub horizontal . Nlcc	07/08/2017
S175	617482	7561112	4655	300/8NE		Lava	Coladas de lavas andesiticos de coloracion rojiso blanquecino, de grano medio en su matrix, con menor contenido de cristales de cuarzo angulosos y mayor contenido biotita,con pseudoestratificacion casi sub horizontal . Nlcc	08/08/2017
S176	617615	7560949	4657	177/20NE		Lava	Coladas de lavas andesiticos de coloracion rojiso blanquecino, de grano medio en su matrix, con menor contenido de cristales de cuarzo angulosos y mayor contenido biotita,con pseudoestratificacion casi sub horizontal . Nlcc	08/08/2017
S177	618822	7561429	4775	187/18SE		Lava	Coladas de lavas andesiticos de coloracion rojiso blanquecino, de grano medio en su matrix, con menor contenido de cristales de cuarzo angulosos y mayor contenido biotita,con pseudoestratificacion casi sub horizontal . Nlcc	08/08/2017
S178	618730	7560378	4635	175/15SW		Lava	Coladas de lavas andesiticos de coloracion rojiso blanquecino, de grano medio en su matrix, con menor contenido de cristales de cuarzo angulosos y mayor contenido biotita,con pseudoestratificacion casi sub horizontal . Nlcc	08/08/2017
S179	618713	7559993	4743	210/11NW		Lava	Coladas de lavas andesiticos de coloracion rojiso blanquecino, de grano medio en su matrix, con menor contenido de cristales de cuarzo angulosos y mayor contenido biotita,con pseudoestratificacion casi sub horizontal . Nlcc	08/08/2017
S180	618587	7559454	4793	105/40SW		Lava	Coladas de lavas andesiticos de coloracion rojiso blanquecino, de grano medio en su matrix, con menor contenido de cristales de cuarzo angulosos y mayor contenido biotita,con pseudoestratificacion casi sub horizontal . Nlcc	08/08/2017
S181	618584	7559481	4783	350/22SW		Lava	Coladas de lavas andesiticos de coloracion rojiso blanquecino, de grano medio en su matrix, con menor contenido de cristales de cuarzo angulosos y mayor contenido biotita,con pseudoestratificacion casi sub horizontal . Nlcc	08/08/2017
S182	618526	7559441	4799	200/11NW		Lava	Coladas de lavas andesiticos de coloracion rojiso blanquecino, de grano medio en su matrix, con menor contenido de cristales de cuarzo angulosos y mayor contenido biotita,con pseudoestratificacion casi sub horizontal . Nlcc	08/08/2017
S183	618333	7559089	4723	168/26NE		Lava	Coladas de lavas andesiticos de coloracion rojiso blanquecino, de grano medio en su matrix, con menor contenido de cristales de cuarzo angulosos y mayor contenido biotita,con pseudoestratificacion casi sub horizontal . Nlcc	08/08/2017
S184	618217	7558961	4723	295/63SW		Lava	Coladas de lavas andesiticos de coloracion rojiso blanquecino, de grano medio en su matrix, con menor contenido de cristales de cuarzo angulosos y mayor contenido biotita,con pseudoestratificacion casi sub horizontal . Nlcc	08/08/2017
S185	618034	7561259	4713	305/15SW		Lava	Coladas de lavas andesiticos de coloracion rojiso blanquecino, de grano medio en su matrix, con menor contenido de cristales de cuarzo angulosos y mayor contenido biotita,con pseudoestratificacion casi sub horizontal . Nlcc	08/08/2017
S186	617174	7560894	4622	130/2SW		Toba	Toba color gris blanquecino con presencia de vidrio volcanico y fragmentos de biotita, cuarzo fracturado, se observan cristales de feldespato y biotita con orientacion, pomez y liticos menor a 2 cm. Ntpg	08/08/2017



SERVICIO GEOLOGICO MINERO
DIRECCION ESTRATEGICA DE REINVINDICACION MARITIMA, SILALA Y RECURSOS HIDRICOS INTERNACIONALES
MAPEO GEOLOGICO DEL AREA CIRCUNDANTE AL MANANTIAL DEL SILALA
BASE DE DATOS



Nº	ESTE (UTM)	NORTE (UTM)	ALTURA (m.s.n.m.)	DIRECCIÓN DE FLUJO	CODIGO MUESTRA	LITOLOGIA	DESCRIPCION MACROSCOPICA	FECHA
S187	619703	756092	5107	102/60NE	7827	Lava	Fragmento de una roca de origen volcánico (lava), de color gris, muestra superficies de meteorización, composición relativamente ácida, muestra estructura holocristalina y textura porfídica de grano medio (>2 mm), donde se observan abundantes cristales de feldespatos blanquecinos, cuarzo, biotita muy oxidada, piroxenos y óxidos de hierro diseminados, rodeados por una pasta de grano muy fino, la roca muestra elevada dureza y compactación. Nlc	08/08/2017
S188	619421	7562642		100/56NE		Lava	Coladas de lavas andesíticos de coloración rojizo blanquecino, de grano medio en su matrix, con menor contenido de cristales de cuarzo angulosos y mayor contenido biotita, con pseudoestratificación casi sub horizontal . Nlc	08/08/2017
S189	618360	7561365	4717	310/75NE		Lava	Coladas de lavas andesíticos de coloración rojizo blanquecino, de grano medio en su matrix, con menor contenido de cristales de cuarzo angulosos y mayor contenido biotita, con pseudoestratificación casi sub horizontal . Nlc	08/08/2017
S190	612064	7558181	4728	240/10NE		Lava	Presenta flujos de lavas andesíticos de coloración gris blanquecino, de grano medio a grueso en su matrix, con menor contenido de cristales de cuarzo angulosos y menor contenido biotita angulosos. Nls	09/08/2017
S191	612332	7558220	4694	140/35SW		Lava	Presenta flujos de lavas andesíticos de coloración gris blanquecino, de grano medio a grueso en su matrix, con menor contenido de cristales de cuarzo angulosos y menor contenido biotita angulosos. Nls	09/08/2017
S192	612754	7557905	4682	215/75SE		Lava	Presenta flujos de lavas andesíticos de coloración gris blanquecino, de grano medio a grueso en su matrix, con menor contenido de cristales de cuarzo angulosos y menor contenido biotita angulosos. Nls	09/08/2017
S193	612979	7558120	4671	210/70SE		Lava	Presenta flujos de lavas andesíticos de coloración gris blanquecino, de grano medio a grueso en su matrix, con menor contenido de cristales de cuarzo angulosos y menor contenido biotita angulosos. Nls	09/08/2017
S194	613267	7557851	4662	190/60SE		Lava	Presenta flujos de lavas andesíticos de coloración gris blanquecino, de grano medio a grueso en su matrix, con menor contenido de cristales de cuarzo angulosos y menor contenido biotita angulosos. Nls	09/08/2017
S195	613602	7557947	4637	140/85SW		Lava	Presenta flujos de lavas andesíticos de coloración gris blanquecino, de grano medio a grueso en su matrix, con menor contenido de cristales de cuarzo angulosos y menor contenido biotita angulosos. Nls	09/08/2017
S196	611802	7556921	4803	307/27SE		Lava	Presenta flujos de lavas andesíticos de coloración gris blanquecino, de grano medio a grueso en su matrix, con menor contenido de cristales de cuarzo angulosos y menor contenido biotita angulosos. Nls	09/08/2017
S197	611298	7556999	4899	315/40SW		Lava	Presenta flujos de lavas de coloración gris blanquecino, de grano medio a grueso en su matrix, con menor contenido de cristales de cuarzo angulosos y menor contenido biotita angulosos. Nls	09/08/2017
S198	611597	7556827	4823	244/19NW		Lava	Presenta flujos de lavas andesíticos de coloración gris blanquecino, de grano medio a grueso en su matrix, con menor contenido de cristales de cuarzo angulosos y menor contenido biotita angulosos. Nls	09/08/2017
S199	612357	7557311	4752	278/50SW		Lava	Presenta flujos de lavas andesíticos de coloración gris blanquecino, de grano medio a grueso en su matrix, con menor contenido de cristales de cuarzo angulosos y menor contenido biotita angulosos. Nls	09/08/2017

Nº	ESTE (UTM)	NORTE (UTM)	ALTURA (m.s.n.m.)	DIRECCIÓN DE FLUJO	CODIGO MUESTRA	LITOLOGIA	DESCRIPCION MACROSCOPICA	FECHA
S200	608527	7575347	4839	105/23SW		Lava	Coladas de lavas de coloracion rojizo blanquecino, de grano grueso en su matrix, con mayor contenido de cristales de cuarzo angulosos y mayor contenido biotita, presenta una pseudoestratificacion. Nlt	09/08/2017
S201	608386	7574825	4793	170/10SW		Lava	Coladas de lavas de coloracion rojizo blanquecino, de grano grueso en su matrix, con mayor contenido de cristales de cuarzo angulosos y mayor contenido biotita, presenta una pseudoestratificacion. Nlt	09/08/2017
S202	596557	7583978	4504	278/12SW		Lava	Coladas de lavas andesiticos de coloracion rojizo blanquecino, de grano grueso en su matrix, con mayor contenido de cristales de cuarzo angulosos y mayor contenido biotita, presenta una seudoestratificacion.	09/08/2017
S203	608386	7574825	4793	170/10SW		Lava	Coladas de lavas de coloracion rojizo blanquecino, de grano grueso en su matrix, con mayor contenido de cristales de cuarzo angulosos y mayor contenido biotita, presenta una pseudoestratificacion. Nlt	09/08/2017
S204	612000	7563000	5189	175/40NE		Lava	Presenta flujos de lavas de coloracion gris blanquecino, de grano medio a grueso en su matrix, con menor contenido de cristales de cuarzo angulosos y menor contenido biotita angulosos. Nlsq	09/08/2017
S205	609524	7556683	5145	325/60SW		Lava	Presenta flujos de lavas de coloracion gris blanquecino, de grano medio a grueso en su matrix, con menor contenido de cristales de cuarzo angulosos y menor contenido biotita angulosos. Nlsq	09/08/2017
S206	607927	7571754	4656	214/35NW		Lava	Coladas de lavas de coloracion rojizo blanquecino, de grano grueso en su matrix, con mayor contenido de cristales de cuarzo angulosos y mayor contenido biotita, presenta una pseudoestratificacion. Nlt	09/08/2017
S207	607923	7571638	4670	348/33NW		Lava	Coladas de lavas de coloracion rojizo blanquecino, de grano grueso en su matrix, con mayor contenido de cristales de cuarzo angulosos y mayor contenido biotita, presenta una pseudoestratificacion. Nlt	09/08/2017
S208	608212	7572823	4656	272/5SE		Toba	Color gris-claro politica rosáceo con superficies de meteorización, con vidrio volcanico en sectores pomez con direccion de flujo. Ntpg	09/08/2017
S209	608546	7556911	5420	220/62NW	7830	Lava	Fragmento de una roca de origen volcánico (lava), de color gris con tono oscuro, tiene superficies de meteorización, composición intermedia, muestra estructura holocristalina y textura porfídica de grano medio (>2 mm), donde se observan abundantes cristales de feldespatos blanquecinos, anfíboles, biotita, piroxenos y óxidos de hierro diseminados, rodeados por una pasta de grano muy fino, la roca muestra elevada dureza y compactación. Nlsq	09/08/2017
S210	596988	7583971	4504	35/9NW		Lava	Color gris-oscuro textura porfídica de grano medio-fino, donde se observan grandes cristales de feldespatos blanquecinos, cuarzo, biotita, en fragmentosdiseminados, rodeados por una pasta de grano muy fino. La lava muestra elevada dureza y compactación.	11/08/2017
S211	596557	7583978	4504	278/12SW		Lava	Presenta flujos de lavas andesiticos de coloracion gris blanquecino, de grano medio a fino en su matrix, con menor contenido de cristales de biotita angulosos.	11/08/2017
S212	612647	7576961	4693	314/3SW		Toba	Coladas de lava con pseudo estratificacion (estrato volcan).	13/08/2017
S213	614063	7578118	4885	75/60NW		Lava	Coladas de lava con pseudo estratificacion (estrato volcan).	13/08/2017



SERVICIO GEOLOGICO MINERO
DIRECCION ESTRATEGICA DE REINVINDICACION MARITIMA, SILALA Y RECURSOS HIDRICOS INTERNACIONALES
MAPEO GEOLOGICO DEL AREA CIRCUNDANTE AL MANANTIAL DEL SILALA
BASE DE DATOS



Nº	ESTE (UTM)	NORTE (UTM)	ALTURA (m.s.n.m.)	DIRECCIÓN DE FLUJO	CODIGO MUESTRA	LITOLOGIA	DESCRIPCION MACROSCOPICA	FECHA
S214	614027	7578154	4917	310/50SW		Lava	Coladas de lava con pseudo estratificacion (estrato volcan).	13/08/2017
S215	613978	7578222	4960	50/25NW		Lava	Coladas de lava con pseudo estratificacion (estrato volcan).	13/08/2017
S216	614081	7578187	4922	350/45SW		Lava	Coladas de lava con pseudo estratificacion (estrato volcan).	13/08/2017
S217	614113	7578135	4865	60/58SE		Lava	Coladas de lava con pseudo estratificacion (estrato volcan).	13/08/2017
S218	612702	7577120	4608	60/54NW		Toba	Toba volcánica de consistencia porosa, formada por la acumulación de cenizas volcánicos muy pequeños, menor concentración en cristales su consistencia es media, de color va desde blanco - amarillento.	13/08/2017
S219	613149	7577836	4987	153/42NE		Lava	Coladas de lavas andesíticas de coloracion gris, de grano grueso en su matrix, cristales de biotita sub redondeados, presenta una pseudoestratificación casi sub horizontal..	13/08/2017
S220	613774	7578211	5005	230/60SE		Lava	Lavas de textura porfirítica de color gris blanquesino con presencia de cristales de plagioclasas, feldespatos y turmalina. Se observan una pseudoestratificación sub vertical de espesores entre 0.20 a 0.90 m.	13/08/2017
S221	613706	7578166	5053	290/50SW		Lava	Lavas de textura porfirítica de color gris blanquesino con presencia de cristales de plagioclasas, feldespatos y turmalina. Se observan una pseudoestratificación sub vertical de espesores entre 0.20 a 0.90 m.	13/08/2017
S222	598256	7570240	5176	188/4NW		Lava	Color gris-oscuro estructura holocrystalina y textura porfidia de grano medio-fino, donde se observan cristales de feldespatos elevada dureza y compactación. Nlin1	14/08/2017
S223	596049	7568972	5622	260/45SE		Lava	Color gris oscuro estructura holocrystalina elevada dureza y compactacion textura bandeadas con dirección de flujo. Nlin1 , Zona de Alteración.	14/08/2017
S224	598689	7570632	5039	145/25NE		Lava	Color gris oscuro estructura holocrystalina elevada dureza y compactacion textura bandeadas con dirección de flujo. Nlin1 , Zona de Alteración.	14/08/2017
S225	599394	7568611	4696	303/17SW		Lava	Color gris-oscuro estructura holocrystalina y textura porfidia de grano medio-fino, donde se observan cristales de feldespatos elevada dureza y compactación. Nlin1	14/08/2017
S226	595872	7569264	5631	145/25NE	7743	Lava	Fragmento de una roca de origen volcánico (lava), de color gris oscuro, tiene superficies de meteorización, composición intermedia, muestra estructura bandeadas o fluidas y textura porfidia de grano medio a fino (>1 mm), donde se observan abundantes cristales de feldespatos, anfíboles, biotita, piroxenos y óxidos de hierro diseminados, rodeados por una pasta de grano muy fino, la roca muestra elevada dureza y compactación. Nlin1	14/08/2017
S227	598532	7567548	4609	160/67SW	7833	Lava	Fragmento de una roca de origen volcánico (lava), de color gris con tono oscuro, tiene superficies de intensa meteorización, composición intermedia, muestra estructura holocrystalina y textura porfidia de grano medio (>2 mm), donde se observan abundantes cristales de feldespatos, anfíboles, biotita, piroxenos, poco cuarzo y óxidos de hierro diseminados, rodeados por una pasta de grano muy fino, la roca muestra moderada dureza y compactación. Nlin2	14/08/2017

CONVENIO DE COOPERACIÓN INTERINSTITUCIONAL Y
CONTRATO DE CONSULTORIA DIREMAR - SERGEOMIN



BASE DE DATOS ESTRUCTURALES

Calle Federico Suazo N° 1673 Esquina Reyes Ortiz – La Paz - Bolivia
Telf. (591 – 2) 2330981 – 2331236 - Fax 2391725 – 2318295
www.sergeomin.gob.bo

DIRECCIÓN TÉCNICA DE PROSPECCIÓN Y EXPLORACIÓN
 "ESTUDIO GEOLÓGICO-ESTRUCTURAL DEL AREA
 CIRCUNDANTE DEL MANANTIAL DEL SISAL"

PTO.	ESTE	NORTE	ELEV.	Az	Bz	DipDir	Pitch	CONTINUADO	PERSISTENCIA (10m)	ABERTURA (cm)	RELLENO	FORMA	JRC	AGUA	TIPO ROCA	ALTERACION	DUREZA	FECHA	OBSERVACIONES
E1	600516	7565580	4339	Diáclisis	97	89	30	D	1	0	SR	Plana	8	Saco	Igumintitas	R2	21-may-		
J1	601277	7566098	4447	Diáclisis	85	285		C	1	2	SR	Plana	8	Saco	Arribadas	R4	21-may-		
J2	601277	7566098	4447	Diáclisis	74	205		D	1	2	SR	Plana	8	Saco	Arribadas	R4	21-may-		
J3	601277	7566098	4447	Diáclisis	324			D	1	3	SR	Plana	8	Saco	Arribadas	R4	21-may-		
L1	600453	7566473	4344	Diáclisis	67	185		C	1	0	SR	Esclerótica	6	Saco	Igumintitas	R2	21-may-		
L2	600453	7566473	4344	Diáclisis	48	104		C	1	11	Acilia	Esclerótica	6	Saco	Igumintitas	R2	21-may-		
L3	600453	7566473	4344	Diáclisis	73	74		C	1	1	Acilia	Esclerótica	6	Saco	Igumintitas	R2	21-may-		
L4	601154	7566061	4434	Diáclisis	87	185		D	3	0	SR	Plana	8	Saco	Arribadas	R4	21-may-		
L5	601154	7566061	4434	Diáclisis	152			D	1	0	SR	Plana	8	Saco	Arribadas	R4	21-may-		
L7	601154	7566061	4434	Diáclisis	67	281		D	1	0	SR	Plana	8	Saco	Arribadas	R4	21-may-		
M1	601159	7566005	4448	Diáclisis	71	6		D	1	10	Acilia	Curva-Escalónada	2	Saco	Arribadas	R4	21-may-		
M4	601282	7566072	4440	Diáclisis	67	195		D	1	10	Acilia	Plana	4	Saco	Arribadas	R4	21-may-		
M5	601280	7566394	4452	Diáclisis	78	235		C	4	5	Acilia	Plana	4	Saco	Arribadas	R4	21-may-		
N2	600516	7565580	4339	Diáclisis	130	56	30	D	1	0	SR	Plana	6	Saco	Igumintitas	R2	21-may-		
N3	600516	7565580	4339	Diáclisis	116	80	26	C	2	5	SR	Plana	8	Saco	Igumintitas	R2	21-may-		
N4	600516	7565580	4339	Falla	120	60	20	D	1	3	SR	Plana	6	Saco	Igumintitas	R2	21-may-		
M3	601242	7565990	4464	Falla Central	83	263		C	2	0	Acilia	Plana	4	Saco	Arribadas	R4	21-may-		
L5	601154	7566061	4434	Poerturística-Frac	285			D						Saco	Igumintitas	R4	21-may-		
L9	601444	7566094	4415	Poerturística-Frac	2	10		C						Saco	Arribadas	R4	21-may-		
M4	601292	7566072	4440	Poerturística-Frac	245			C						Saco	Arribadas	R4	21-may-		
L1.1	600390	7565536	4313	Diáclisis	84	65		C	4	2	SR	Plana	6	Saco	Igumintitas	R3	22-may-		
L1.2	600390	7565536	4313	Diáclisis	67	65		C	4	0	SR	Plana	6	Saco	Igumintitas	R3	22-may-		
L1.3	600390	7565536	4313	Diáclisis	83	54		C	4	0	SR	Plana	6	Saco	Igumintitas	R3	22-may-		
L1.4	600390	7565536	4313	Diáclisis	78	56		C	4	0	SR	Plana	6	Saco	Igumintitas	R3	22-may-		
L1.5	600390	7565536	4313	Diáclisis	80	75		C	3	0	SR	Plana	6	Saco	Igumintitas	R3	22-may-		
L1.6	600390	7565536	4313	Diáclisis	87	40		C	3	0	SR	Plana	6	Saco	Igumintitas	R3	22-may-		
L1.7	600390	7565536	4313	Diáclisis	9	318		C	2	4	SR	Plana	6	Saco	Igumintitas	R3	22-may-		
L1.8	600390	7565536	4313	Diáclisis	85	36		C	11	0	SR	Plana	6	Saco	Igumintitas	R3	22-may-		
L1.9	600405	7565561	4305	Diáclisis	80	59		D	1	0	SR	Plana	6	Saco	Igumintitas	R3	22-may-		
L2.0	600405	7565561	4305	Diáclisis	84	51		C	2	0	SR	Plana	11	Saco	Igumintitas	R3	22-may-		
L2.1	600405	7565561	4305	Diáclisis	87	49		C	2	0	SR	Plana	3	Saco	Igumintitas	R3	22-may-		
L2.2	600405	7565561	4305	Diáclisis	88	210		C	3	0	SR	Plana	7	Saco	Igumintitas	R3	22-may-		
C3	600447	756516	4311	Diáclisis	86	220		C	3	0	SR	Plana	7	Saco	Igumintitas	R3	22-may-		
C4	600527	7565719	4316	Diáclisis	89	35		C	5	0	SR	Plana	7	Saco	Igumintitas	R3	22-may-		
C5	600527	7565719	4316	Diáclisis	76	34		C	6	0	SR	Plana	9	Saco	Igumintitas	R3	22-may-		
C6	600527	7565719	4316	Diáclisis	87	215		C	6	0	SR	Plana	9	Saco	Igumintitas	R3	22-may-		
C7	600527	7565761	4327	Diáclisis	12	225		C	2	0	SR	Plana	9	Saco	Igumintitas	R3	22-may-		
C8	600526	7565761	4327	Diáclisis	82	20		C	1	50	SR	Plana	9	Saco	Igumintitas	R3	22-may-		
C9	600526	7565761	4327	Diáclisis	89	357		D	1	2	SR	Plana	9	Saco	Igumintitas	R3	22-may-		
C10	600526	7565761	4327	Diáclisis	85	20		D	10	1	SR	Plana	9	Saco	Igumintitas	R3	22-may-		
C11	600526	7565761	4327	Diáclisis	82	16		D	1	0	SR	Plana	9	Saco	Igumintitas	R3	22-may-		
C12	600526	7565761	4327	Diáclisis	89	25		C	3	0	SR	Plana	9	Saco	Igumintitas	R3	22-may-		
C13	600526	7565761	4327	Diáclisis	15	255		C	2	0	SR	Plana	9	Saco	Igumintitas	R3	22-may-		
C14	600526	7565761	4327	Diáclisis	88	10		C	3	0	SR	Plana	9	Saco	Igumintitas	R3	22-may-		
C15	600526	7565761	4324	Diáclisis	85	35		D	10	0	SR	Plana	9	Saco	Igumintitas	R3	22-may-		
C16	600526	7565761	4324	Diáclisis	80	50		D	3	0	SR	Plana	9	Saco	Igumintitas	R3	22-may-		
C18	600525	7565761	4324	Diáclisis	74	30		C	1	0	SR	Plana	9	Saco	Igumintitas	R3	22-may-		
C19	600525	7565761	4324	Diáclisis	89	20		C	2	0	SR	Plana	9	Saco	Igumintitas	R3	22-may-		
C20	600525	7565761	4324	Diáclisis	83	16		C	1	0	SR	Plana	9	Saco	Igumintitas	R3	22-may-		
C21	600525	7565761	4324	Diáclisis	80	20		C	2	0	SR	Plana	9	Saco	Igumintitas	R3	22-may-		
C22	600525	7565761	4324	Diáclisis	85	30		C	3	0	SR	Plana	9	Saco	Igumintitas	R3	22-may-		
C23	600525	7565761	4324	Diáclisis	86	28		C	3	0	SR	Plana	9	Saco	Igumintitas	R3	22-may-		
C24	600525	7565761	4324	Diáclisis	85	30		C	2	0	SR	Plana	9	Saco	Igumintitas	R3	22-may-		
C25	600525	7565761	4324	Diáclisis	85	30		C	3	0	SR	Plana	9	Saco	Igumintitas	R3	22-may-		
C26	600525	7565761	4324	Diáclisis	86	31		C	1	0	SR	Plana	9	Saco	Igumintitas	R3	22-may-		
C27	600525	7565761	4324	Diáclisis	80	18		C	2	0	SR	Plana	9	Saco	Igumintitas	R3	22-may-		
C28	600525	7565761	4324	Diáclisis	84	12		C	1	0	SR	Plana	9	Saco	Igumintitas	R3	22-may-		
C29	600525	7565761	4324	Diáclisis	84	12		C	6	0	SR	Plana	9	Saco	Igumintitas	R3	22-may-		
C30	600525	7565761	4324	Diáclisis	86	28		C	3	0	SR	Plana	9	Saco	Igumintitas	R3	22-may-		
C31	600525	7565761	4324	Diáclisis	85	30		C	2	0	SR	Plana	9	Saco	Igumintitas	R3	22-may-		
C32	600525	7565761	4324	Diáclisis	85	30		C	3	0	SR	Plana	9	Saco	Igumintitas	R3	22-may-		
C33	600525	7565761	4324	Diáclisis	85	30		C	2	0	SR	Plana	9	Saco	Igumintitas	R3	22-may-		
C34	600525	7565761	4324	Diáclisis	85	30		C	3	0	SR	Plana	9	Saco	Igumintitas	R3	22-may-		
C35	600525	7565761	4324	Diáclisis	85	30		C	2	0	SR	Plana	9	Saco	Igumintitas	R3	22-may-		
C36	600525	7565761	4324	Diáclisis	85	30		C	3	0	SR	Plana	9	Saco	Igumintitas	R3	22-may-		
C37	600525	7565761	4324	Diáclisis	85	30		C	2	0	SR	Plana	9	Saco	Igumintitas	R3	22-may-		
C38	600525	7565761	4324	Diáclisis	85	30		C	3	0	SR	Plana	9	Saco	Igumintitas	R3	22-may-		
C39	600525	7565761	4324	Diáclisis	85	30		C	2	0	SR	Plana	9	Saco	Igumintitas	R3	22-may-		
C40	600525	7565761	4324	Diáclisis	85	30		C	3	0	SR	Plana	9	Saco	Igumintitas	R3	22-may-		
C41	600525	7565761	4324	Diáclisis	85	30		C	2	0	SR	Plana	9	Saco	Igumintitas	R3	22-may-		
C42	600525	7565761	4324	Diáclisis	85	30		C	3	0	SR	Plana	9	Saco	Igumintitas	R3	22-may-		
C43	600525	7565761	4324	Diáclisis	85	30		C	2	0	SR	Plana	9	Saco	Igumintitas	R3	22-may-		
C44	600525	7565761	4324	Diáclisis	85	30		C	3	0	SR	Plana	9	Saco	Igumintitas	R3	22-may-		
C45	600525	7565761	4324	Diáclisis	85	30		C	2	0	SR	Plana	9	Saco	Igumintitas	R3	22-may-		
C46	600525	7565761	4324	Diáclisis	85	30		C	3	0	SR	Plana	9	Saco	Igumintitas	R3	22-may-		
C47	600525	7565761	4324	Diáclisis	85	30		C	2	0	SR	Plana	9	Saco	Igumintitas	R3	22-may-		
C48	600525	7565761	4324	Diáclisis	85	30		C	3	0	SR	Plana	9	Saco	Igumintitas	R3	22-may-		
C49	600525	7565761	4324	Diáclisis	85	30		C	2	0	SR	Plana	9	Saco	Igumintitas	R3	22-may-		
C50	600525	7565761	4324	Diáclisis	85	30		C	3	0	SR	Plana	9	Saco	Igumintitas	R3	22-may-		
C51	600525	7565761	4324	Diáclisis	85	30		C	2	0	SR	Plana	9	Saco	Igumintitas	R3	22-may-		
C52	600525	7565761	4324	Diáclisis	85	30		C	3	0	SR	Plana	9	Saco	Igumintitas	R3	22-may-		
C53	600525	7565761	4324	Diáclisis	85	30		C	2	0	SR	Plana	9	Saco	Igum				

**DIRECCIÓN TÉCNICA DE PROSPECCIÓN Y EXPLORACIÓN
ESTUDIO GEOLÓGICO-ESTRUCTURAL DEL ÁREA
CIRCUNDANTE DEL MANANTIAL DEL SISALÁ***



PTO.	ESTE	NORTE	ELEV.	TIPO	Az	Bz	DipDir	Pitch	CONTINUO	PERSISTENCIA (10m)	ABERTURA (10m)	FORMA	RELLENO	JRC	AGUA	TIPO ROCA	ALTERACION	DUREZA	FECHA	OBSERVACIONES
L52	6000636	7365943	7342	Diciplsa	88	11.0	C	1	SR	0	SR	Plana	9	Saco	Iginitritas		R3	22-may-		
L53	6000636	7365943	7342	Diciplsa	83	18	C	2	SR	20	SR	Plana	9	Saco	Iginitritas		R3	22-may-		
L54	6000636	7365943	7342	Diciplsa	68	29	C	2	SR	10	SR	Plana	9	Saco	Iginitritas		R3	22-may-		
L55	6000631	73660042	4338	Diciplsa	82	15	D	2	SR	0	SR	Plana	9	Saco	Iginitritas		R3	22-may-		
L56	6000631	73660042	4338	Diciplsa	61	26	D	2	SR	0	SR	Plana	9	Saco	Iginitritas		R3	22-may-		
L57	6000631	73660042	4338	Diciplsa	89	12.0	C	1	SR	0	SR	Plana	9	Saco	Iginitritas		R3	22-may-		
L58	6000631	73660042	4338	Diciplsa	86	50	C	1	SR	0	SR	Plana	9	Saco	Iginitritas		R3	22-may-		
L59	6000631	73660042	4338	Diciplsa	85	30	C	1	SR	0	SR	Plana	9	Saco	Iginitritas		R3	22-may-		
L60	6000634	73660042	4349	Diciplsa	82	33	C	3	SR	0	SR	Plana	9	Saco	Iginitritas		R3	22-may-		
L61	6000634	73660042	4349	Diciplsa	84	12	C	1	SR	0	SR	Plana	9	Saco	Iginitritas		R3	22-may-		
L62	6000634	73660042	4349	Diciplsa	80	27	C	7	SR	0	SR	Plana	6	Saco	Iginitritas		R3	22-may-		
L63	6000634	73660042	4349	Diciplsa	70	20	C	2	SR	0	SR	Plana	6	Saco	Iginitritas		R3	22-may-		
L64	6000634	73660042	4349	Diciplsa	78	22	C	2	SR	0	SR	Plana	6	Saco	Iginitritas		R3	22-may-		
L65	6000634	73660042	4349	Diciplsa	80	28	C	1	SR	0	SR	Plana	6	Saco	Iginitritas		R3	22-may-		
L66	6000634	73660042	4349	Diciplsa	60	25	C	3	SR	0	SR	Plana	6	Saco	Iginitritas		R3	22-may-		
L67	6000634	73660042	4349	Diciplsa	79	30	C	1	SR	0	SR	Plana	6	Saco	Iginitritas		R3	22-may-		
L68	6000634	73660042	4349	Diciplsa	81	25	C	1	SR	0	SR	Plana	6	Saco	Iginitritas		R3	22-may-		
L69	6000745	73660220	4335	Diciplsa	89	21.2	C	5	SR	0	SR	Plana	6	Saco	Iginitritas		R3	22-may-		
L70	6000745	73660220	4335	Diciplsa	52	18.0	D	2	SR	0	SR	Plana	6	Saco	Iginitritas		R3	22-may-		
L71	6000745	73660220	4335	Diciplsa	71	18.2	D	1	SR	0	SR	Plana	6	Saco	Iginitritas		R3	22-may-		
L72	6000745	73660220	4335	Diciplsa	79	18.5	C	1	SR	0	SR	Plana	6	Saco	Iginitritas		R3	22-may-		
L73	6000745	73660220	4335	Diciplsa	80	19.0	C	2	SR	0	SR	Plana	6	Saco	Iginitritas		R3	22-may-		
L74	6000745	73660220	4335	Diciplsa	45	95	D	2	SR	0	SR	Plana	6	Saco	Iginitritas		R3	22-may-		
L75	6000870	73662278	4336	Diciplsa	88	65	C	5	SR	0	SR	Plana	6	Saco	Iginitritas		R3	22-may-		
L76	6000870	73662278	4336	Diciplsa	87	71	C	2	SR	0	SR	Plana	6	Saco	Iginitritas		R3	22-may-		
L77	6000870	73662278	4336	Diciplsa	89	70	C	2	SR	0	SR	Plana	6	Saco	Iginitritas		R3	22-may-		
L78	6000870	73662278	4336	Diciplsa	89	68	C	1	SR	0	SR	Plana	6	Saco	Iginitritas		R3	22-may-		
L79	6000870	73662278	4336	Diciplsa	90	70	C	1	SR	0	SR	Plana	6	Saco	Iginitritas		R3	22-may-		
L80	6000870	73662278	4336	Diciplsa	78	10	D	5	SR	0	SR	Plana	6	Saco	Iginitritas		R3	22-may-		
L81	6000870	73662278	4336	Diciplsa	88	8	D	5	SR	0	SR	Plana	6	Saco	Iginitritas		R3	22-may-		
L82	6000870	73662278	4336	Diciplsa	87	2	D	5	SR	0	SR	Plana	6	Saco	Iginitritas		R3	22-may-		
L83	6000870	73662278	4336	Diciplsa	85	5	D	4	SR	0	SR	Plana	6	Saco	Iginitritas		R3	22-may-		
L84	6000870	73662278	4336	Diciplsa	83	6	D	3	SR	0	SR	Plana	6	Saco	Iginitritas		R3	22-may-		
L85	6000870	73662278	4336	Diciplsa	80	85	C	4	SR	0	SR	Plana	6	Saco	Iginitritas		R3	22-may-		
L86	6000870	73662278	4336	Diciplsa	88	96	C	3	SR	0	SR	Plana	6	Saco	Iginitritas		R3	22-may-		
L87	6000870	73662278	4336	Diciplsa	89	92	C	5	SR	0	SR	Plana	6	Saco	Iginitritas		R3	22-may-		
L88	6000887	7366343	4339	Diciplsa	82	84	D	3	SR	0	SR	Plana	6	Saco	Iginitritas		R3	22-may-		
L89	6000887	7366343	4339	Diciplsa	80	85	D	2	SR	0	SR	Plana	6	Saco	Iginitritas		R3	22-may-		
L90	6000924	7366343	4339	Diciplsa	320	87	D	3	SR	0	SR	Plana	4	Saco	Iginitritas		R3	22-may-		
L91	6000987	7366343	4339	Diciplsa	85	87	D	3	SR	0	SR	Plana	6	Saco	Iginitritas		R3	22-may-		
L92	6000987	7366343	4339	Diciplsa	85	15	C	3	SR	0	SR	Plana	6	Saco	Iginitritas		R3	22-may-		
L93	6000987	7366343	4339	Diciplsa	82	11	C	2	SR	0	SR	Plana	6	Saco	Iginitritas		R3	22-may-		
L94	6001034	7366411	4336	Diciplsa	87	60	D	3	SR	0	SR	Plana	6	Saco	Iginitritas		R3	22-may-		
L95	6001034	7366411	4336	Diciplsa	80	54	C	4	SR	0	SR	Plana	6	Saco	Iginitritas		R3	22-may-		
L96	6001034	7366411	4336	Diciplsa	78	46	C	4	SR	0	SR	Plana	6	Saco	Iginitritas		R3	22-may-		
M11	6000549	7366711	4324	Diciplsa	82	50	C	3	SR	0	SR	Escalafón-Rugosa	6	Saco	Iginitritas		R3	22-may-		
M12	6000591	7366818	4323	Diciplsa	80	25	C	2	SR	0	SR	Plana-Rugosa	7	Saco	Iginitritas		R2	22-may-		
M12	6000591	7366818	4323	Diciplsa	88	28	C	2	SR	0	SR	Plana-Rugosa	7	Saco	Iginitritas		R2	22-may-		
M12	6000591	7366818	4323	Diciplsa	85	30	C	2	SR	0	SR	Plana-Rugosa	10	Saco	Iginitritas		R2	22-may-		
M12	6000591	7366818	4323	Diciplsa	23	55	C	5	SR	0	SR	Plana-Rugosa	10	Saco	Iginitritas		R2	22-may-		
M12	6000591	7366818	4323	Diciplsa	82	38	C	4	SR	0	SR	Plana-Rugosa	12	Saco	Iginitritas		R2	22-may-		
M12	6000591	7366818	4323	Diciplsa	89	301	C	4	SR	0	SR	Plana-Rugosa	12	Saco	Iginitritas		R2	22-may-		
M12	6000591	7366818	4323	Diciplsa	78	268	C	4	SR	0	SR	Plana-Rugosa	13	Saco	Iginitritas		R2	22-may-		
M13	6000632	7365589	4330	Diciplsa	72	260	C	4	SR	0	SR	Plana-Rugosa	8	Saco	Iginitritas		R2	22-may-		
M13	6000632	7365589	4330	Diciplsa	75	120	C	2	SR	0	SR	Plana-Rugosa	10	Saco	Iginitritas		R2	22-may-		
M13	6000632	7365589	4330	Diciplsa	80	95	C	2	SR	0	SR	Plana-Rugosa	3	Saco	Iginitritas		R2	22-may-		
M13	6000632	7365589	4330	Diciplsa	87	188	D	3	SR	0	SR	Plana-Rugosa	6	Saco	Iginitritas		R2	22-may-		
M13	6000632	7365589	4330	Diciplsa	67	216	D	1	SR	0.5	SR	Plana-Rugosa	8	Saco	Iginitritas		R2	22-may-		
M13	6000632	7365589	4330	Diciplsa	90	20	D	3	SR	0	SR	Plana-Rugosa	1	Saco	Iginitritas		R2	22-may-		

Base de datos

Página 2

Annex XVI Appendix B



DIRECCIÓN TÉCNICA DE PROSPECCIÓN Y EXPLORACIÓN
ESTUDIO GEOLÓGICO-ESTRUCTURAL DEL ÁREA
CIRCUNDANTE DEL MANANTIAL DEL SINALOA*

PTO.	ESTE	NORTE	ELEV.	TIPO	Az.	Bz.	DipDir	Pitch	CONTINUAD.	PERSISTENCIA (10m)	ABERTURA (cm)	FORMA	RELLENO	JRC	AGUA	TIPO ROCA	ALTERACION	DUREZA	FECHA	OBSERVACIONES
M7	600293	7365437	4315	Diciplsa	72	150	C		3	SR	Escalonada	3	Saco	Igumintitas	Oxidacion	R2	22-may-			
M7	600293	7365437	4315	Diciplsa	10	146	C		2	SR	Cueva-Escalonada	8	Saco	Igumintitas	Oxidacion	R2	22-may-			
M7	600293	7365437	4315	Diciplsa	75	226	D		2	SR	Plana	6	Saco	Igumintitas	Oxidacion	R2	22-may-			
M8	600346	7365516	4298	Diciplsa	70	240	D		3	SR	Buena	8	Saco	Igumintitas	Oxidacion	R2	22-may-			
M8	600346	7365516	4298	Diciplsa	82	260	C		3	SR	Plana	4	Saco	Igumintitas	Oxidacion	R2	22-may-			
M8	600346	7365516	4298	Diciplsa	86	264	C		3	SR	Plana	4	Saco	Igumintitas	Oxidacion	R2	22-may-			
M8	600346	7365516	4298	Diciplsa	82	92	C		1	SR	Plana	3	Saco	Igumintitas	Oxidacion	R2	22-may-			
M8	600347	7365592	4334	Falla inversa	82	34	C		1	5	Milofita	9	Saco	Igumintitas	Oxidacion	R3	22-may-			
M13	600632	7365597	4330	Falla inversa	21	95	C		1	2	SR	Rugosa	8	Saco	Igumintitas	Oxidacion	R2	22-may-		
M13	600632	7365597	4330	Falla inversa	12	120	D		1	0.2	Acelia	3	Saco	Igumintitas	Oxidacion	R2	22-may-	Desplazamiento de 10 cm		
M6	600293	7365356	4298	Falla inversa	82	52	C		3	SR	Escalonada	6	Saco	Igumintitas	Oxidacion	R2	22-may-			
M8	600346	7365356	4298	Falla inversa	81	60	C		5	SR	Rugosa	5	Saco	Igumintitas	Oxidacion	R2	22-may-			
M10	600531	7365686	4315	Falla Normal	80	41	C		5	SR	Rugosa	8	Saco	Igumintitas	Oxidacion	R2	22-may-			
M13	600632	7365689	4330	Falla Normal	78	192	C		2	SR	Curva	12	Saco	Igumintitas	Oxidacion	R2	22-may-			
M7	600293	7365437	4315	Falla Normal	79	248	C		1	SR	Escalonada	10	Saco	Igumintitas	Oxidacion	R2	22-may-	Desplazamiento de 25 cm		
M8	600346	7365516	4298	Falla Normal	74	268	C		1	5	SR	Buena	10	Humedo	Igumintitas	Oxidacion	R2	22-may-		
M8	600346	7365516	4298	Falla Normal	84	96	C		1	1	SR	Escalonada-Rugosa	10	Saco	Igumintitas	Oxidacion	R2	22-may-		
M9	600347	7365548	4298	Falla Normal	146	77	D		5	SR	Rugosa	5	Saco	Igumintitas	Oxidacion	R2	22-may-			
M11	600632	7365548	4298	Falla Normal	79	379	C		3	SR	Plana	6	Saco	Igumintitas	Oxidacion	R3	22-may-			
M10	600632	7365548	4315	Falla inversa	47	100	C		1	0	SR	Plana	6	Saco	Igumintitas	Oxidacion	R3	22-may-		
M11	600632	7365548	4315	Falla inversa	68	270	C		1	0	SR	Plana	6	Saco	Igumintitas	Oxidacion	R3	22-may-		
M12	600632	7365548	4315	Falla inversa	78	345	C		1	0	SR	Plana	6	Saco	Igumintitas	Oxidacion	R3	22-may-		
M13	600632	7365548	4315	Falla inversa	70	366	C		1	0	SR	Plana	6	Saco	Igumintitas	Oxidacion	R3	22-may-		
M14	600632	7365548	4315	Falla inversa	70	36	C		1	0	SR	Plana	6	Saco	Igumintitas	Oxidacion	R3	22-may-		
M15	600632	7365548	4315	Falla inversa	81	50	C		1	0	SR	Plana	6	Saco	Igumintitas	Oxidacion	R3	22-may-		
M16	600632	7365548	4315	Falla inversa	83	138	C		1	3	SR	Plana	6	Saco	Igumintitas	Oxidacion	R3	22-may-		
M17	600632	7365548	4315	Falla inversa	88	40	C		4	1	SR	Plana	6	Saco	Igumintitas	Oxidacion	R3	22-may-		
M18	600632	7365548	4315	Falla inversa	72	332	C		3	0	SR	Plana	6	Saco	Igumintitas	Oxidacion	R3	22-may-		
M19	600632	7365548	4315	Falla inversa	80	342	C		2	3	SR	Plana	6	Saco	Igumintitas	Oxidacion	R3	22-may-		
M20	600632	7365548	4315	Falla inversa	70	34	C		3	0	SR	Plana	6	Saco	Igumintitas	Oxidacion	R3	22-may-		
M21	600632	7365548	4315	Falla inversa	25	53	C		1	0	SR	Plana	6	Saco	Igumintitas	Oxidacion	R3	22-may-		
M22	600632	7365548	4315	Falla inversa	56	315	D		2	3	SR	Plana	6	Saco	Igumintitas	Oxidacion	R3	22-may-		
M23	600632	7365548	4315	Falla inversa	80	335	C		3	5	SR	Plana	6	Saco	Igumintitas	Oxidacion	R3	22-may-		
M24	600632	7365548	4315	Falla inversa	72	33	C		3	10	SR	Plana	6	Saco	Igumintitas	Oxidacion	R4	23-may-		
M25	600632	7365548	4315	Falla inversa	34	55	D		1	5	SR	Plana	2	Saco	Arboladas	Oxidacion	R4	23-may-		
M26	600632	7365548	4315	Falla inversa	60	210	C		1	0	SR	Plana	2	Saco	Arboladas	Oxidacion	R4	23-may-		
M27	600632	7365548	4315	Falla inversa	63	237	D		1	0	SR	Plana-Rugosa	2	Saco	Arboladas	Oxidacion	R4	23-may-		
M28	600632	7365548	4315	Falla inversa	82	315	D		1	0	SR	Plana	2	Saco	Arboladas	Oxidacion	R4	23-may-		
M29	600632	7365548	4315	Falla inversa	12	155	C		2	1	SR	Plana	6	Saco	Arboladas	Oxidacion	R4	23-may-		
M30	600632	7365548	4315	Falla inversa	14	62	C		3	3	SR	Plana	6	Saco	Arboladas	Oxidacion	R4	23-may-		
M31	600632	7365548	4315	Falla inversa	65	125	C		1	0	SR	Plana	6	Saco	Arboladas	Oxidacion	R4	23-may-		
M32	600632	7365548	4315	Falla inversa	74	160	C		2	0.5	SR	Escalonada	2	Humedo	Igumintitas	Oxidacion	R2	23-may-		
M33	600632	7365548	4315	Falla inversa	74	160	C		4	0	SR	Escalonada	15	Saco	Igumintitas	Oxidacion	R2	23-may-		
M-1.5	600747	7365629	4387	Diciplsa	130	18	C		25	SR	Escalonada-Rugosa	8	Saco	Igumintitas	Oxidacion	R2	23-may-			
M-1.6	600747	7365629	4387	Diciplsa	64	216	C		3	0.5	SR	Escalonada	16	Saco	Flujo de dientes	Oxidacion	R3	23-may-		
M-1.7	600747	7365629	4387	Diciplsa	75	215	C		4	2	SR	Plana-Rugosa	10	Saco	Flujo de dientes	Oxidacion	R3	23-may-		
M-1.8	600747	7365629	4387	Diciplsa	82	240	C		0.5	SR	Escalonada-Rugosa	8	Saco	Flujo de dientes	Oxidacion	R3	23-may-			
M-1.9	600747	7365629	4387	Diciplsa	25	195	D		0.5	SR	Escalonada	16	Saco	Flujo de dientes	Oxidacion	R3	23-may-			
M-20	600747	7365629	4387	Diciplsa	72	60	C		1	1	SR	Escalonada	2	Humedo	Igumintitas	Oxidacion	R2	23-may-		
M-21	600747	7365629	4387	Diciplsa	74	160	C		2	0.5	SR	Escalonada	2	Humedo	Igumintitas	Oxidacion	R2	23-may-		
M-22	600747	7365629	4387	Diciplsa	82	230	C		5	0.5	SR	Escalonada	6	Humedo	Igumintitas	Oxidacion	R2	23-may-		
M-23	600747	7365629	4387	Diciplsa	70	222	D		5	0.8	SR	Escalonada	6	Humedo	Igumintitas	Oxidacion	R2	23-may-		
M-24	600747	7365629	4387	Diciplsa	84	221	C		3	1	SR	Escalonada	6	Humedo	Igumintitas	Oxidacion	R2	23-may-		
M-25	600747	7365629	4387	Diciplsa	80	256	C		5	5	SR	Plana-Rugosa	8	Saco	Igumintitas	Oxidacion	R2	23-may-		

Base de datos

Página 3

DIRECCIÓN TÉCNICA DE PROSPECCIÓN Y EXPLORACIÓN
 "ESTUDIO GEOLÓGICO-ESTRUCTURAL DEL ÁREA
 CIRCUNDANTE DEL MANANTIAL DEL SISALÁ"

PTO.	ESTE	NORTE	ELEV.	TIPO	Az.	Bz.	DipDir	Ptch	CONTINUADO	PERSISTENCIA (10m)	ABERTURA (10m)	RELLENO	FORMA	JRC	AGUA	TIPO ROCA	ALTERACION	DUREZA	FECHA	OBSERVACIONES
M.21	60.1177	7566251	43.79	Diciélsa	59	95	C	2	SR	Plana-Rugosa	8	Seco	Igumintitas	Oxidación	R2	23-may-				
M.21	60.1177	7566252	43.79	Diciélsa	24	25	C	1	SR	Plana-Rugosa	8	Seco	Igumintitas	Oxidación	R2	23-may-				
M.22	60.1263	7566256	43.72	Diciélsa	85	15	C	2	20	SR	Escalonada	12	Seco	Igumintitas	Oxidación	R2	23-may-			
M.23	60.1325	7566256	43.90	Diciélsa	81	280	C	1	3	SR	Escalonada	12	Seco	Igumintitas	Oxidación	R2	23-may-			
M.23	60.1325	7566256	43.90	Diciélsa	65	115	C	1	2	SR	Escalonada	12	Seco	Igumintitas	Oxidación	R2	23-may-			
M.23	60.1325	7566256	43.90	Diciélsa	65	115	C	1	1	SR	Escalonada	12	Seco	Igumintitas	Oxidación	R2	23-may-			
M.23	60.1325	7566256	43.90	Diciélsa	76	215	D	1	1	SR	Es calonada	12	Seco	Igumintitas	Oxidación	R2	23-may-			
M.23	60.1325	7566257	43.98	Diciélsa	80	45	C	3	0	SR	Plana	6	Humedo	Igumintitas	Oxidación	R2	23-may-			
M.23	60.1326	7566271	43.98	Diciélsa	61	52	C	4	0	SR	Plana	7	Humedo	Igumintitas	Oxidación	R2	23-may-			
M.23	60.1326	7566271	43.98	Diciélsa	72	49	C	2	0	SR	Plana	6	Humedo	Igumintitas	Oxidación	R2	23-may-			
M.23	60.1326	7566271	43.98	Diciélsa	40	190	D	5	0	Acilia	Plana	6	Humedo	Igumintitas	Oxidación	R2	23-may-			
M.23	60.1326	7566271	43.98	Falla	88	84	C	2	5	SR	Plana-Rugosa	12	Seco	Igumintitas	Oxidación	R2	23-may-			
M.15	60.0775	7565936	43.56	Falla de Rumbo	8	150	C	3	1	SR	Escalonada-Rugosa	10	Seco	Igumintitas	Oxidación	R2	23-may-			
M.15	60.0775	7565936	43.56	Falla de Rumbo	77	148	D	1	2	SR	Clive-Escalonada	8	Seco	Igumintitas	Oxidación	R2	23-may-			
M.14	60.0732	7565903	43.49	Falla Normal	7	32	C	5	1	SR	Escalonada-Rugosa	18	Humedo	Igumintitas	Oxidación	R2	23-may-			
M.14	60.0732	7565903	43.49	Falla Normal	68	75	C	2	5	SR	Plana	4	Seco	Igumintitas	Oxidación	R2	23-may-			
M.15	60.0775	7565936	43.56	Falla Normal	84	122	C	4	2	SR	Plana	4	Seco	Igumintitas	Oxidación	R2	23-may-			
M.15	60.0775	7565936	43.56	Falla Normal	86	132	C	2	2.5	SR	Plana	4	Seco	Igumintitas	Oxidación	R2	23-may-			
M.15	60.0775	7565936	43.56	Falla Normal	80	120	C	2	2.5	SR	Plana	4	Seco	Igumintitas	Oxidación	R2	23-may-			
M.15	60.0775	7565936	43.56	Falla Normal	82	124	C	1	2.5	SR	Es calonada	10	Seco	Igumintitas	Oxidación	R2	23-may-			
M.15	60.0775	7565936	43.56	Falla Normal	37	230	C	2	2	SR	Es calonada-Rugosa	5	Seco	Igumintitas	Oxidación	R2	23-may-			
M.19	60.0969	7566209	43.65	Falla Normal	302	85	C	5	1	SR	Clive-Escalonada	8	Seco	Igumintitas	Oxidación	R2	23-may-			
M.20	60.1079	7566209	43.67	Falla Normal	80	210	C	2	5	SR	Escalonada	5	Humedo	Igumintitas	Oxidación	R2	23-may-			
M.20	60.1079	7566209	43.67	Falla Normal	88	218	C	1	3	SR	Plana	3	Humedo	Igumintitas	Oxidación	R2	23-may-			
M.20	60.1079	7566209	43.67	Falla Normal	86	218	C	2	1	SR	Plana	6	Humedo	Igumintitas	Oxidación	R2	23-may-			
M.20	60.1079	7566209	43.67	Falla Normal	86	220	C	2	1	SR	Escalonada	6	Seco	Igumintitas	Oxidación	R2	23-may-			
M.17	60.09817	7566049	43.61	Pseudotratificación	34	180	C	2	3	SR	Plana	8	Seco	Dientes	Oxidación	R2	23-may-			
E2	60.0984	7566159	45.63	Diciélsa	70	85	D	2	3	SR	Plana	8	Seco	Dientes	Oxidación	R4	15-jun-			
E3	60.09447	7566138	45.63	Diciélsa	81	100	C	6	1	SR	Escalonada	6	Seco	Dientes	Oxidación	R4	15-jun-			
E4	60.09105	7566048	46.18	Diciélsa	196	286	D	1	2	SR	Ortogonal	12	Seco	Dientes	Oxidación	R4	15-jun-			
L.00	60.09404	7567284	45.44	Diciélsa	74	334	D	2	2	SR	Plana	8	Seco	Igumintitas	Oxidación	R3	15-jun-			
L.01	60.09404	7567284	45.44	Diciélsa	70	335	D	2	2	SR	Plana	8	Seco	Igumintitas	Oxidación	R3	15-jun-			
L.02	60.09404	7567284	45.44	Diciélsa	80	220	C	3	3	SR	Plana	8	Seco	Igumintitas	Oxidación	R3	15-jun-			
L.03	60.09404	7567284	45.44	Diciélsa	78	205	C	2	3	SR	Plana	8	Seco	Igumintitas	Oxidación	R3	15-jun-			
L.04	60.09404	7567284	45.44	Diciélsa	80	323	D	2	1	SR	Plana	8	Seco	Igumintitas	Oxidación	R3	15-jun-			
L.05	60.09705	7567074	45.45	Diciélsa	78	134	D	2	0	SR	Plana	8	Seco	Igumintitas	Oxidación	R3	15-jun-			
L.06	60.09705	7567074	45.45	Diciélsa	80	160	D	2	0	SR	Plana	6	Seco	Dientes	Oxidación	R3	15-jun-			
L.07	60.09705	7567074	45.45	Diciélsa	70	160	D	3	0	SR	Plana	6	Seco	Dientes	Oxidación	R3	15-jun-			
L.08	60.09474	7566741	45.51	Diciélsa	88	95	C	7	8	SR	Plana	6	Seco	Dientes	Oxidación	R4	15-jun-			
L.09	60.09474	7566741	45.51	Diciélsa	84	81	C	7	2	SR	Plana	6	Seco	Dientes	Oxidación	R4	15-jun-			
L.10	60.09474	7566741	45.51	Diciélsa	80	86	C	7	3	SR	Plana	6	Seco	Dientes	Oxidación	R4	15-jun-			
L.11	60.09474	7566741	45.51	Diciélsa	84	75	C	7	0	SR	Plana	6	Seco	Dientes	Oxidación	R4	15-jun-			
L.12	60.09474	7566741	45.51	Diciélsa	88	82	C	8	0	SR	Plana	6	Seco	Dientes	Oxidación	R4	15-jun-			
L.13	60.09474	7566741	45.51	Diciélsa	87	94	C	8	0	SR	Plana	6	Seco	Dientes	Oxidación	R4	15-jun-			
L.14	60.09474	7566741	45.51	Diciélsa	81	85	C	4	0	SR	Plana	6	Seco	Dientes	Oxidación	R4	15-jun-			
L.15	60.09474	7566741	45.51	Diciélsa	89	175	D	3	5	SR	Plana	6	Seco	Dientes	Oxidación	R4	15-jun-			
L.16	60.09474	7566741	45.51	Diciélsa	85	160	D	3	0	SR	Plana	8	Seco	Dientes	Oxidación	R4	15-jun-			
L.17	60.09474	7566741	45.51	Diciélsa	87	80	D	1	0	SR	Plana	8	Seco	Dientes	Oxidación	R4	15-jun-			
L.18	60.09647	7565833	46.70	Diciélsa	74	105	D	1	0	SR	Plana	8	Seco	Dientes	Oxidación	R4	15-jun-			
L.19	60.09359	7565778	46.70	Diciélsa	80	200	D	1	0	SR	Plana	8	Seco	Dientes	Oxidación	R4	15-jun-			
L.20	60.09373	7565924	46.60	Diciélsa	75	348	C	15	0	SR	Plana	8	Seco	Dientes	Oxidación	R4	15-jun-			
L.22	60.09373	7565924	46.60	Diciélsa	79	35	C	2	0	SR	Plana	8	Seco	Dientes	Oxidación	R4	15-jun-			
L.23	60.09373	7565924	46.60	Diciélsa	89	85	C	10	0	SR	Plana	8	Seco	Dientes	Oxidación	R4	15-jun-			
L.24	60.09460	7566441	45.51	Diciélsa	74	230	D	3	0	SR	Plana	8	Seco	Dientes	Oxidación	R4	15-jun-			
L.25	60.09460	7566441	45.51	Diciélsa	82	300	D	1	1	SR	Plana	8	Seco	Dientes	Oxidación	R4	15-jun-			
L.26	60.09326	7565154	45.53	Diciélsa	75	235	D	2	0	SR	Plana	8	Seco	Dientes	Oxidación	R4	15-jun-			
L.27	60.09326	7565154	45.53	Diciélsa	84	368	C	5	3	SR	Plana	8	Seco	Dientes	Oxidación	R3	15-jun-			
L.28	60.09326	7565154	45.53	Diciélsa	78	365	D	3	2	SR	Plana	8	Seco	Dientes	Oxidación	R3	15-jun-			
L.29	60.09326	7565154	45.53	Diciélsa	72	320	C	2	2	SR	Plana	8	Seco	Dientes	Oxidación	R4	15-jun-			
M1	60.0921	7566167	45.71	Diciélsa	75	70	C	2	5	SR	Escalonada	14	Seco	Dientes	Oxidación	R4	15-jun-			

Base de datos

Annex XVI Appendix B



DIRECCIÓN TÉCNICA DE PROSPECCIÓN Y EXPLORACIÓN
"ESTUDIO GEOLÓGICO-ESTRUCTURAL DEL ÁREA
CIRCUNDANTE DEL MANANTIAL DEL SISALÁ"

PTO.	ESTE	NORTE	ELEV.	TIPO	Az.	Bz.	DipDir	Pitch	CONTINUADO	PERSISTENCIA (km)	ABERTURA (km)	RELLENO	FORMA	JRC	AGUA	TIPO ROCA	ALTERACION	DUREZA	FECHA	OBSERVACIONES
M10	6060009	75641550	4756	Dicielsa	46	52	D		1	15	SR	Escalonada	12	Seco	Dicielsa		R4	15jun.		
M11	6060003	75641525	4756	Dicielsa	59	201	D		7	10	SR	Escalonada	12	Seco	Dicielsa		R4	15jun.		
M11	6060003	75641525	4756	Dicielsa	75	20	C		1	8	SR	Escalonada	14	Seco	Dicielsa		R4	15jun.		
M2	60601925	75661612	4558	Dicielsa	340	84	D		1	1	SR	Cañonada	8	Seco	Dicielsa		R4	15jun.		
M3	60601920	75661613	4550	Dicielsa	77	68	D		2	10	SR	Cañonada	12	Seco	Dicielsa		R4	15jun.		
M4	60601938	75661614	4555	Dicielsa	43	212	D		1	<1	SR	Cañonada	12	Seco	Dicielsa		R4	15jun.		
M4	60601938	75661614	4555	Dicielsa	15	205	D		1	2	SR	Cañonada	14	Seco	Dicielsa		R4	15jun.		
M4	60601938	75661614	4555	Dicielsa	80	245	D		4	10	SR	Cañonada	12	Seco	Dicielsa		R4	15jun.		
M4	60601938	75661614	4555	Dicielsa	42	6	D		3	3	SR	Cañonada	12	Seco	Dicielsa		R4	15jun.		
M4	60601938	75661614	4555	Dicielsa	82	106	D		1	<1	SR	Plana	10	Seco	Dicielsa		R4	15jun.		
M5	60601947	75661550	4554	Dicielsa	51	241	D		3	3	SR	Plana	8	Seco	Dicielsa		R4	15jun.		
M5	60601947	75661550	4554	Dicielsa	60	92	C		1	5	SR	Ornillada	8	Seco	Dicielsa		R4	15jun.		
M6	6060032	75661136	4537	Dicielsa	85	337	D		3	20	SR	Plana	4	Seco	Dicielsa		R4	15jun.		
M6	6060032	75661136	4537	Dicielsa	72	260	D		3	20	SR	Plana	4	Seco	Dicielsa		R4	15jun.		
M6	6060032	75661136	4537	Dicielsa	42	177	D		3	15	SR	Plana	8	Seco	Dicielsa		R4	15jun.		
M6	6060032	75661136	4537	Dicielsa	81	130	D		2	2	SR	Plana	4	Seco	Dicielsa		R4	15jun.		
M6	6060032	75661136	4537	Dicielsa	65	172	D		2	2	SR	Plana	8	Seco	Dicielsa		R4	15jun.		
M6	6060032	75661136	4537	Dicielsa	62	40	D		3	<1	SR	Plana	8	Seco	Dicielsa		R4	15jun.		
M6	6060032	75661136	4537	Dicielsa	78	215	D		2	<1	SR	Plana	8	Seco	Dicielsa		R4	15jun.		
M7	60600113	75660777	4613	Dicielsa	72	345	C		1	5	SR	Plana	4	Seco	Dicielsa		R4	15jun.		
M7	60600113	75660777	4613	Dicielsa	49	286	D		2	10	SR	Plana	10	Seco	Dicielsa		R4	15jun.		
M8	6060574	75641904	4643	Dicielsa	34	204	C		2	10	SR	Plana	10	Seco	Dicielsa		R4	15jun.		
M8	6060574	75641904	4643	Dicielsa	50	71	D		3	5	SR	Plana	16	Seco	Dicielsa		R4	15jun.		
M8	6060574	75641904	4643	Dicielsa	49	335	D		2	<1	SR	Plana	6	Seco	Dicielsa		R4	15jun.		
M8	6060574	75641904	4643	Dicielsa	160	90	D		1	SR	Plana	10	Seco	Dicielsa		R4	15jun.			
M9	6060574	75641904	4643	Dicielsa	54	135	D		1	<1	SR	Ornillada	6	Seco	Dicielsa		R4	15jun.		
M9	6060574	75641904	4643	Dicielsa	65	81	D		1	8	SR	Plana	8	Seco	Dicielsa		R4	15jun.		
M9	60605914	75641756	4713	Dicielsa	83	15	D		1	8	SR	Plana	8	Seco	Dicielsa		R4	15jun.		
M9	60605914	75641756	4713	Dicielsa	42	162	C		1	1	SR	Plana	12	Seco	Dicielsa		R4	15jun.		
E1	60601967	75661618	4558	Falla Herivel	58	165	C		1	10	SR	Plana	8	Seco	Dicielsa		R4	15jun.		
E3	60601447	75661318	4553	Pastodestratificación	57	257	C		2	2	SR	Plana	2	Seco	Dicielsa		R4	15jun.		
E4	60601015	75661318	4516	Pastodestratificación	210	90	120		0	0	SR	Plana	2	Seco	Dicielsa		R4	15jun.		
M1	60601921	75661547	4752	Pastodestratificación	36	145	C		3	10	SR	Plana	4	Seco	Dicielsa		R4	15jun.		
E11	6060784	75651481	4935	Dicielsa	76	250	C		4	4	SR	Plana	10	Seco	Dicielsa		R4	16jun.		
E11	6060784	75651481	4935	Dicielsa	69	39	D		3	2	SR	Ornillada	6	Seco	Dicielsa		R4	16jun.		
E11	6060784	75651481	4935	Dicielsa	77	35	C		2	25	SR	Plana	12	Seco	Dicielsa		R4	16jun.		
E12	6060909	75631710	5029	Dicielsa	81	70	C		4	2	SR	Plana	14	Seco	Arenisca		R4	16jun.		
E12	6060909	75631710	5029	Dicielsa	78	294	C		4	4	SR	Escalonada	12	Seco	Arenisca		R4	16jun.		
E12	6060909	75631710	5029	Dicielsa	66	310	D		2	2	SR	Escalonada	12	Seco	Arenisca		R4	16jun.		
E12	6060909	75631710	5029	Dicielsa	74	279	D		3	0	SR	Plana	2	Seco	Arenisca		R4	16jun.		
E13	6060624	75621299	5253	Dicielsa	74	144	C		6	20	SR	Escalonada	12	Seco	Arenisca		R4	16jun.		
E3	6060624	75621299	5253	Dicielsa	82	122	D		5	15	SR	Plana	2	Seco	Arenisca		R4	16jun.		
E9	6060748	7565106	4704	Dicielsa	82	50	D		1	0	SR	Plana	4	Seco	Dicielsa		R4	16jun.		
J1	6060628	75651234	5238	Dicielsa	81	55	C		3	5	SR	Plana	8	Seco	Dicielsa		R4	16jun.		
J1	6060628	75651234	5238	Dicielsa	83	215	C		3	15	SR	Escalonada	14	Seco	Dicielsa		R4	16jun.		
J1	6060628	75651234	5238	Dicielsa	54	84	C		6	3	SR	Escalonada	14	Seco	Dicielsa		R4	16jun.		
J1	6060628	75651234	5238	Dicielsa	65	265	D		6	6	SR	Plana	6	Seco	Dicielsa		R4	16jun.		
J1	6060628	75651234	5238	Dicielsa	65	105	C		3	7	SR	Ornillada	6	Seco	Dicielsa		R4	16jun.		
M14	6060544	75651302	4652	Dicielsa	85	303	D		6	5	SR	Ornillada	8	Seco	Dicielsa		R4	16jun.		
M14	6060544	75651302	4652	Dicielsa	78	96	C		2	<1	SR	Plana	10	Humedo	Dicielsa		R4	16jun.		
M14	6060444	75651302	4652	Dicielsa	77	96	C		2	6	SR	Plana	14	Seco	Dicielsa		R4	16jun.		

Base de datos

**DIRECCIÓN TÉCNICA DE PROSPECCIÓN Y EXPLORACIÓN
ESTUDIO GEOLÓGICO-ESTRUCTURAL DEL ÁREA
CIRCUNDANTE DEL MANANTIAL DEL SISALÁ***



PTO.	ESTE	NORTE	ELEV.	Az.	Bz.	DipDir	Pthn	CONTINUADO	PERSISTENCIA (10m)	ABERTURA (cm)	RELLENO	FORMA	JRC	AGUA	TIPO ROCA	ALTERACION	DUREZA	FECHA	OBSERVACIONES
M.14*	6060152	73651203	4677	Diclessa	77	105	C	2	4	SR	Plana	12	Seco	Diclessa		R4	15jun.		
M.15	60601264	73651180	4686	Diclessa	75	82	C	4	2	SR	Plana	14	Seco	Diclessa		R4	15jun.		
M.15	60601264	73651180	4686	Diclessa	77	130	C	2	4	SR	Plana	8	Seco	Diclessa		R4	15jun.		
M.15	60601264	73651180	4686	Diclessa	56	136	D	3	<1	SR	Plana	12	Seco	Diclessa		R4	15jun.		
M.16	60601249	73651173	4687	Diclessa	72	168	C	4	4	SR	Brena	13	Seco	Diclessa		R4	15jun.		
M.16	60601249	73651173	4687	Diclessa	85	10	D	1	2	SR	Orificada	12	Seco	Diclessa		R4	15jun.		
M.16	60601249	73651173	4687	Diclessa	76	94	C	3	<1	SR	Orificada	12	Seco	Diclessa		R4	15jun.		
M.16	60601249	73651173	4687	Diclessa	55	165	D	2	<1	SR	Orificada	10	Seco	Diclessa		R4	15jun.		
M.16	60601249	73651173	4687	Diclessa	70	94	D	2	<1	SR	Plana	10	Seco	Diclessa		R4	15jun.		
M.17	6060331	73641278	4831	Diclessa	77	322	C	3	2	SR	Plana	2	Seco	Arribitales		R4	15jun.		
M.17	6060331	73641278	4831	Diclessa	84	326	D	5	1	SR	Plana	2	Seco	Arribitales		R4	15jun.		
M.18	6060638	73631652	4945	Diclessa	66	156	C	5	2	SR	Escalonada	18	Seco	Arribitales		R4	15jun.		
M.18	6060638	73631652	4945	Diclessa	145	78	C	2	10	SR	Escalonada	18	Seco	Arribitales		R4	15jun.		
M.18	6060638	73631652	4945	Diclessa	88	248	D	1	2	SR	Plana	6	Seco	Arribitales		R4	15jun.		
M.19	6060718	73631593	4941	Diclessa	74	258	C	2	10	SR	Plana	18	Seco	Arribitales		R4	15jun.		
M.19	6060718	73631593	4941	Diclessa	66	87	C	2	3	SR	Plana	12	Seco	Arribitales		R4	15jun.		
M.19	6060718	73631593	4941	Diclessa	71	235	C	3	5	SR	Plana	12	Seco	Arribitales		R4	15jun.		
M.19	6060718	73631593	4941	Diclessa	81	230	D	3	0	SR	Plana	9	Seco	Arribitales		R4	15jun.		
M.19	6060718	73631593	4941	Diclessa	65	322	C	1	6	SR	Escalonada	18	Seco	Arribitales		R4	15jun.		
M.20	6060732	73631443	4970	Diclessa	74	119	C	3	2	SR	Plana	4	Seco	Arribitales		R4	15jun.		
M.20	6060732	73631443	4970	Diclessa	74	35	D	2	0	SR	Plana	14	Seco	Arribitales		R4	15jun.		
M.20	6060732	73631443	4970	Diclessa	64	272	D	2	<1	SR	Plana	8	Seco	Arribitales		R4	15jun.		
M.21	6060519	73621224	5263	Diclessa	85	102	C	5	3	SR	Plana	14	Seco	Arribitales		R4	15jun.		
M.21	6060519	73621224	5263	Diclessa	156	83	246	C	6	2	SR	Plana	14	Seco	Arribitales		R4	15jun.	
M.21	6060519	73621224	5263	Diclessa	155	87	245	C	3	10	SR	Escalonada	14	Seco	Arribitales		R4	15jun.	
M.21	6060519	73621224	5263	Diclessa	86	48	D	4	<1	SR	Plana	14	Seco	Arribitales		R4	15jun.		
M.21	6060519	73621224	5263	Diclessa	10	75	C	1	20	SR	Escalonada	14	Seco	Arribitales		R4	15jun.		
M.21	6060519	73621224	5263	Diclessa	67	222	D	4	4	SR	Plana	2	Seco	Arribitales		R4	15jun.		
M.21	6060519	73621224	5263	Diclessa	84	222	C	3	10	SR	Plana	2	Seco	Arribitales		R4	15jun.		
E.11	6060764	73621481	4995	Pseudotrastratificación	56	140	C	3	5	SR	Plana	5	Seco	Arribitales		R3	15jun.		
E.12	6060839	73631110	5029	Pseudotrastratificación	48	160	C	3	5	SR	Plana	5	Seco	Arribitales		R3	15jun.		
E.13	60607383	73631158	4707	Pseudotrastratificación	38	200	D	2	0	SR	Plana	10	Seco	Arribitales		R4	15jun.		
M.14	60605044	73631302	4852	Pseudotrastratificación	45	204	C	2	0	SR	Plana	10	Seco	Arribitales		R4	15jun.		
M.17	6060331	73621278	4831	Pseudotrastratificación	42	200	C	30	0	SR	Plana	10	Seco	Arribitales		R4	15jun.		
M.18	6060638	73631652	4945	Pseudotrastratificación	42	30	C	2	0	SR	Plana	10	Seco	Arribitales		R4	15jun.		
M.18	6060638	73631652	4945	Pseudotrastratificación	77	158	C	4	2	SR	Plana	14	Seco	Arribitales		R4	15jun.		
M.18	6060638	73631652	4945	Pseudotrastratificación	222	132	D	132	2	SR	Plana	8	Seco	Arribitales		R4	15jun.		
M.19	6060718	73631593	4941	Pseudotrastratificación	49	175	C	30	5	SR	Plana	15	Seco	Arribitales		R4	15jun.		
M.19	6060718	73631593	4941	Pseudotrastratificación	53	30	C	3	5	SR	Plana	10	Seco	Arribitales		R4	15jun.		
M.20	6060718	73631593	4941	Pseudotrastratificación	52	162	C	240	0	SR	Plana	10	Seco	Arribitales		R4	15jun.		
M.21	6060519	73621224	5263	Diclessa	68	5	C	6	7	SR	Brena	12	Seco	Diclessa		R4	15jun.		
M.21	6060519	73621224	5263	Diclessa	49	15	D	1	0	SR	Plana	2	Seco	Diclessa		R4	15jun.		
M.21	6060519	73621224	5263	Diclessa	70	365	D	3	2	SR	Plana	5	Seco	Diclessa		R3	17jun.		
M.21	6060519	73621224	5263	Diclessa	65	235	C	3	5	SR	Plana	10	Seco	Diclessa		R3	17jun.		
M.21	6060519	73621224	5263	Diclessa	88	110	D	5	0	SR	Plana	10	Seco	Diclessa		R3	17jun.		
M.21	6060519	73621224	5263	Diclessa	87	265	D	2	0	SR	Plana	10	Seco	Diclessa		R3	17jun.		
M.21	6060704	73631369	4945	Diclessa	82	271	D	2	0	SR	Plana	10	Seco	Diclessa		R3	17jun.		
M.21	6060704	73631369	4945	Diclessa	65	280	D	1	0	SR	Plana	10	Seco	Diclessa		R3	17jun.		
M.21	6060704	73631369	4945	Diclessa	80	310	D	1	0	SR	Plana	10	Seco	Diclessa		R3	17jun.		
M.21	6060704	73631369	4945	Diclessa	60	295	C	4	3	SR	Plana	10	Seco	Diclessa		R3	17jun.		
M.21	6060704	73631369	4945	Diclessa	62	290	C	2	0	SR	Plana	10	Seco	Diclessa		R3	17jun.		
M.21	6060704	73631369	4945	Diclessa	59	275	C	1	0	SR	Plana	10	Seco	Diclessa		R3	17jun.		
M.21	6060704	73631369	4945	Diclessa	52	260	C	1	0	SR	Plana	10	Seco	Diclessa		R3	17jun.		
M.21	6060704	73631369	4945	Diclessa	60	235	C	1	0	SR	Plana	10	Seco	Diclessa		R3	17jun.		
M.21	6060704	73631369	4945	Diclessa	59	188	D	3	0	SR	Plana	10	Seco	Diclessa		R4	17jun.		
M.21	6060704	73631369	4945	Diclessa	48	245	D	1	0	SR	Plana	10	Seco	Diclessa		R4	17jun.		
M.21	6060704	73631369	4945	Diclessa	60	330	D	3	0	SR	Plana	10	Seco	Diclessa		R4	17jun.		
M.21	6060704	73631369	4945	Diclessa	82	263	D	2	0	SR	Plana	10	Seco	Diclessa		R4	17jun.		

Base de datos

Annex XVI Appendix B



DIRECCIÓN TÉCNICA DE PROSPECCIÓN Y EXPLORACIÓN
"ESTUDIO GEOLÓGICO-ESTRUCTURAL DEL ÁREA
CIRCUNDANTE DEL MANANTIAL DEL SISALÁ"

PTO.	ESTE	NORTE	ELEV.	TIPO	Az.	Bz.	DipDir	Pitch	CONTINUADO	PERSISTENCIA (10m)	ABERTURA (10m)	RELLENO	FORMA	JRC	AGUA	TIPO ROCA	ALTERACION	DUREZA	FECHA	OBSERVACIONES
L1.82	6091569	7365775	4550	Dicielsa	70	82	D	2	SR	SR	0	Plana	10	Seco	Dicielsa-Ardeñita	R4	17/jun.			
L1.84	6091569	7365775	4550	Dicielsa	68	76	D	1	0	SR	0	Plana	10	Seco	Dicielsa-Ardeñita	R4	17/jun.			
L1.85	6091576	7365729	4558	Dicielsa	70	76	D	0	SR	0	0	Plana	10	Seco	Dicielsa-Ardeñita	R4	17/jun.			
L1.86	6091576	7365729	4558	Dicielsa	80	145	D	3	0	SR	0	Plana	10	Seco	Dicielsa-Ardeñita	R4	17/jun.			
L1.87	6091576	7365729	4558	Dicielsa	70	140	D	2	0	SR	0	Plana	10	Seco	Dicielsa-Ardeñita	R4	17/jun.			
L1.88	6091578	7365729	4558	Dicielsa	45	235	D	1	0	SR	0	Plana	10	Seco	Dicielsa-Ardeñita	R4	17/jun.			
L1.89	6091578	7365729	4558	Dicielsa	60	5	D	1	0	SR	0	Plana	10	Seco	Dicielsa-Ardeñita	R4	17/jun.			
L1.90	6091578	7365729	4558	Dicielsa	87	147	D	2	0	SR	0	Plana	10	Seco	Dicielsa-Ardeñita	R4	17/jun.			
L1.91	6091578	7365729	4558	Dicielsa	68	10	D	1	0	SR	0	Plana	10	Seco	Dicielsa-Ardeñita	R4	17/jun.			
L1.92	6091578	7365729	4558	Dicielsa	49	85	D	3	0	SR	0	Plana	10	Seco	Dicielsa-Ardeñita	R4	17/jun.			
L1.93	6091578	7365729	4558	Dicielsa	68	93	D	1	0	SR	0	Plana	10	Seco	Dicielsa-Ardeñita	R4	17/jun.			
L1.94	6091578	7365729	4558	Dicielsa	50	118	D	2	0	SR	0	Plana	10	Seco	Dicielsa-Ardeñita	R4	17/jun.			
L1.95	6091578	7365729	4558	Dicielsa	50	85	D	1	0	SR	0	Plana	10	Seco	Dicielsa-Ardeñita	R4	17/jun.			
L1.96	6091578	7365729	4558	Dicielsa	89	267	D	2	0	SR	0	Plana	10	Seco	Dicielsa-Ardeñita	R4	17/jun.			
L1.97	6091578	7365729	4558	Dicielsa	51	304	D	1	0	SR	0	Plana	10	Seco	Dicielsa-Ardeñita	R4	17/jun.			
L1.98	6091578	7365729	4558	Dicielsa	79	68	D	4	5	SR	0	Plana	10	Seco	Dicielsa-Ardeñita	R4	17/jun.			
L1.99	6091578	7365729	4558	Dicielsa	80	217	D	2	0	SR	0	Plana	10	Seco	Dicielsa-Ardeñita	R4	17/jun.			
L2.00	6091578	7365729	4558	Dicielsa	83	232	D	1	0	SR	0	Plana	10	Seco	Dicielsa-Ardeñita	R4	17/jun.			
L2.01	6091575	7365743	4558	Dicielsa	85	130	D	5	0	SR	0	Plana	10	Seco	Dicielsa-Ardeñita	R4	17/jun.			
L2.02	6091575	7365743	4558	Dicielsa	60	140	D	1	0	SR	0	Plana	10	Seco	Dicielsa-Ardeñita	R4	17/jun.			
L2.03	6091575	7365743	4558	Dicielsa	60	320	D	1	0	SR	0	Plana	10	Seco	Dicielsa-Ardeñita	R4	17/jun.			
L2.04	6091575	7365743	4558	Dicielsa	85	342	D	2	0	SR	0	Plana	10	Seco	Dicielsa-Ardeñita	R4	17/jun.			
L2.05	6091575	7365743	4558	Dicielsa	84	312	C	3	4	SR	0	Plana	10	Seco	Dicielsa-Ardeñita	R4	17/jun.			
L2.06	6091575	7365743	4558	Dicielsa	83	114	C	2	2	SR	0	Plana	10	Seco	Dicielsa-Ardeñita	R4	17/jun.			
L2.07	6091575	7365743	4558	Dicielsa	85	123	D	1	3	SR	0	Plana	10	Seco	Dicielsa-Ardeñita	R4	17/jun.			
L2.08	6091540	7365741	4618	Dicielsa	70	165	D	1	0	SR	0	Plana	10	Seco	Dicielsa-Ardeñita	R4	17/jun.			
L2.09	6091540	7365741	4618	Dicielsa	79	320	D	2	20	SR	0	Plana	10	Seco	Dicielsa-Ardeñita	R4	17/jun.			
L2.10	6091540	7365741	4618	Dicielsa	88	308	D	1	0	SR	0	Plana	10	Seco	Dicielsa-Ardeñita	R4	17/jun.			
L2.11	6091540	7365741	4618	Dicielsa	45	26	D	3	5	SR	0	Plana	10	Seco	Dicielsa-Ardeñita	R4	17/jun.			
L2.12	6091540	7365741	4618	Dicielsa	80	245	D	2	0	SR	0	Plana	10	Seco	Dicielsa-Ardeñita	R4	17/jun.			
L2.13	6091540	7365741	4618	Dicielsa	56	250	D	1	0	SR	0	Plana	10	Seco	Dicielsa-Ardeñita	R4	17/jun.			
L2.14	6091540	7365741	4618	Dicielsa	60	290	D	1	0	SR	0	Plana	10	Seco	Dicielsa-Ardeñita	R4	17/jun.			
L2.15	6091540	7365741	4618	Dicielsa	65	278	D	2	5	SR	0	Plana	10	Seco	Dicielsa-Ardeñita	R4	17/jun.			
L2.16	6091538	7365658	4556	Dicielsa	83	335	D	1	0	SR	0	Plana	10	Seco	Gimniritas	R3	17/jun.			
L2.17	6091538	7365658	4556	Dicielsa	80	151	D	1	0	SR	0	Plana	10	Seco	Gimniritas	R3	17/jun.			
L2.18	6091538	7365658	4556	Dicielsa	54	260	D	1	10	SR	0	Plana	8	Seco	Gimniritas	R3	17/jun.			
L2.19	6091538	7365658	4556	Dicielsa	61	260	D	2	1	SR	0	Plana	8	Seco	Gimniritas	R3	17/jun.			
L2.20	6091538	7365658	4556	Dicielsa	10	140	D	2	0	SR	0	Plana	8	Seco	Gimniritas	R3	17/jun.			
L2.21	6091538	7365658	4556	Dicielsa	85	280	D	3	30	SR	0	Plana	8	Seco	Gimniritas	R3	17/jun.			
L2.22	6091535	7365658	4554	Dicielsa	87	76	D	2	10	SR	0	Plana	8	Seco	Gimniritas	R3	17/jun.			
L2.23	6091535	7365658	4554	Dicielsa	83	294	D	2	0	SR	0	Plana	8	Seco	Gimniritas	R3	17/jun.			
L2.24	6091535	7365658	4554	Dicielsa	87	165	D	1	0	SR	0	Plana	8	Seco	Gimniritas	R3	17/jun.			
L2.25	6091535	7365658	4554	Dicielsa	89	315	D	1	2	SR	0	Plana	8	Seco	Gimniritas	R3	17/jun.			
L2.26	6091535	7365658	4554	Dicielsa	7	150	D	1	2	SR	0	Plana	8	Seco	Gimniritas	R3	17/jun.			
L2.27	6091535	7365658	4554	Dicielsa	4	163	D	1	2	SR	0	Plana	8	Seco	Gimniritas	R3	17/jun.			
L2.28	6091535	7365658	4554	Dicielsa	89	5	D	2	3	SR	0	Plana	8	Seco	Gimniritas	R3	17/jun.			
L2.29	6091535	7365658	4554	Dicielsa	85	10	D	1	0	SR	0	Plana	8	Seco	Gimniritas	R3	17/jun.			
L2.30	6091535	7365658	4554	Dicielsa	60	75	D	1	0	SR	0	Plana	8	Seco	Gimniritas	R3	17/jun.			
L2.31	6091535	7365658	4554	Dicielsa	65	350	D	2	0	SR	0	Plana	8	Seco	Gimniritas	R3	17/jun.			
L2.32	6091535	7365658	4554	Dicielsa	80	100	D	3	0	SR	0	Plana	8	Seco	Gimniritas	R3	17/jun.			
L2.33	6091535	7365658	4554	Dicielsa	78	290	D	2	0	SR	0	Plana	8	Seco	Gimniritas	R3	17/jun.			
L2.34	6091535	7365658	4554	Dicielsa	60	250	D	1	5	SR	0	Plana	8	Seco	Gimniritas	R3	17/jun.			
L2.35	6091535	7365658	4554	Dicielsa	85	339	D	4	2	SR	0	Plana	8	Seco	Gimniritas	R3	17/jun.			
L2.36	6091535	7365658	4554	Dicielsa	84	110	D	1	1	SR	0	Plana	8	Seco	Gimniritas	R3	17/jun.			
L2.37	6091535	7365658	4554	Dicielsa	87	105	D	4	4	SR	0	Plana	8	Seco	Gimniritas	R3	17/jun.			
L2.38	6091535	7365658	4554	Dicielsa	89	83	D	1	0	SR	0	Plana	8	Seco	Gimniritas	R3	17/jun.			
M2.1	6071622	7365334	4554	Dicielsa	135	82	D	2	2	SR	0	Escalonada	4	Seco	Gimniritas	R3	17/jun.			
M2.2	6071622	7365334	4554	Dicielsa	110	85	D	2	<1	SR	0	Escalonada	6	Seco	Gimniritas	R3	17/jun.			
M2.3	6071622	7365334	4554	Dicielsa	180	47	D	5	2	SR	0	Escalonada	12	Seco	Gimniritas	R3	17/jun.			

Base de datos

DIRECCIÓN TÉCNICA DE PROSPECCIÓN Y EXPLORACIÓN
 "ESTUDIO GEOLOGICO-ESTRUCTURAL DEL ÁREA
 CIRCUNDANTE DEL MANANTIAL DEL SILALA"



PTO.	ESTE	NORTE	ELEV.	TIPO	Az	Bz	DipDir	Pitch	CONTINUIDAD	PERSISTENCIA (30m)	ABERTURA (cm)	RELLENO	FORMA	JRC	AGUA	TIPO ROCA	ALTERACION	DUREZA	FECHA	OBSERVACIONES
M23	607666	7563323	4992	Dioclase	148	74	58		D	3	0	SR	Escalonada	10	Seco	Dacitas		R3	17-jun.	
M23	607666	7563323	4992	Dioclase	138	52	228		D	5	< 1	SR	Plana	6	Seco	Dacitas		R3	17-jun.	
M23	607666	7563323	4992	Dioclase	185	89	370		D	3	< 1	SR	Escalonada	6	Seco	Dacitas		R3	17-jun.	
M24	607696	7563348	4985	Dioclase	190	88	100		D	2	0	SR	Plana	4	Seco	Dacitas		R3	17-jun.	
M24	607696	7563348	4985	Dioclase	152	86	242	C	3	10	SR	Escalonada	14	Seco	Dacitas		R3	17-jun.		
M24	607696	7563348	4985	Dioclase	295	52	205		C	2	0	SR	Plana	12	Seco	Dacitas		R3	17-jun.	
M24	607696	7563348	4985	Dioclase	222	72	150	C	3	6	SR	Plana	6	Seco	Dacitas		R3	17-jun.		
M24	607696	7563348	4985	Dioclase	20	87	110		D	2	7	SR	Plana	4	Seco	Dacitas		R3	17-jun.	
L159	609569	7565775	4590	Falla	82	115		D	1	5	SR	Plana	10	Seco	Dacita-Andesita		R3	17-jun.		
L160	609569	7565775	4590	Falla	72	93		D	1	0	SR	Plana	10	Seco	Dacita-Andesita		R3	17-jun.		
L161	609569	7565775	4590	Falla	82	120		D	1	0	SR	Plana	10	Seco	Dacita-Andesita		R3	17-jun.		
L166	609569	7565775	4590	Falla	68	135	200	D	1	0	SR	Plana	10	Seco	Dacita-Andesita		R4	17-jun.		
L167	609569	7565775	4590	Falla	40	320	185	D	1	0	SR	Plana	10	Seco	Brecha de base		R3	17-jun.		
L168	609569	7565775	4590	Falla	38	324	185	D	1	0	SR	Plana	10	Seco	Brecha de base		R3	17-jun.		
L177	609569	7565775	4590	Falla	56	340		D	1	0	SR	Plana	10	Seco	Dacita-Andesita		R4	17-jun.		
L220	605738	7566568	4566	Falla	76	155	230	D	1	0	SR	Plana	10	Seco	Ignimbritas		R3	17-jun.		
L221	605738	7566568	4566	Falla	89	210		D	1	0	SR	Plana	10	Seco	Ignimbritas		R3	17-jun.		
L222	605738	7566568	4566	Falla	88	190		D	1	0	SR	Plana	10	Seco	Ignimbritas		R3	17-jun.		
L223	605738	7566568	4566	Falla	81	315		D	1	0	SR	Plana	10	Seco	Ignimbritas		R3	17-jun.		
L224	605738	7566568	4566	Falla	87	245		D	1	0	SR	Plana	10	Seco	Ignimbritas		R3	17-jun.		
L225	605738	7566568	4566	Falla	80	260		D	1	0	SR	Plana	10	Seco	Ignimbritas		R3	17-jun.		
L227	605738	7566568	4566	Falla	89	266		D	1	10	SR	Plana	8	Seco	Ignimbritas		R3	17-jun.		
L228	605738	7566568	4566	Falla	88	97		D	1	10	SR	Plana	8	Seco	Ignimbritas		R3	17-jun.		
L229	605738	7566568	4566	Falla	82	335		D	1	10	SR	Plana	8	Seco	Ignimbritas		R3	17-jun.		
L230	605738	7566568	4566	Falla	87	290		D	1	5	SR	Plana	8	Seco	Ignimbritas		R3	17-jun.		
L231	605738	7566568	4566	Falla	65	300		D	1	2	SR	Plana	8	Seco	Ignimbritas		R3	17-jun.		
L233	605545	7566680	4554	Falla	80	20		D	1	0	SR	Plana	8	Seco	Ignimbritas		R3	17-jun.		
L238	605545	7566680	4554	Falla	80	290		D	1	0	SR	Plana	8	Seco	Ignimbritas		R3	17-jun.		
L239	605545	7566680	4554	Falla	77	308		D	1	3	SR	Plana	8	Seco	Ignimbritas		R3	17-jun.		
L240	605545	7566680	4554	Falla	78	280		D	1	8	SR	Plana	8	Seco	Ignimbritas		R3	17-jun.		
L241	605545	7566680	4554	Falla	86	260		D	1	0	SR	Plana	8	Seco	Ignimbritas		R3	17-jun.		
L242	605545	7566680	4554	Falla	88	320		D	1	0	SR	Plana	8	Seco	Ignimbritas		R3	17-jun.		
L243	605545	7566680	4554	Falla	88	316		D	1	0	SR	Plana	8	Seco	Ignimbritas		R3	17-jun.		
L244	605545	7566680	4554	Falla	89	310		D	1	0	SR	Plana	8	Seco	Ignimbritas		R3	17-jun.		
L218	605738	7566568	4566	Falla Inversa	87	140		D	1	0	SR	Plana	10	Seco	Ignimbritas		R3	17-jun.		
L256	605545	7566680	4554	Falla Inversa	86	325		D	1	0	SR	Plana	8	Seco	Ignimbritas		R3	17-jun.		
L176	609569	7565775	4590	Falla Normal	48	160		D	1	2	SR	Plana	10	Seco	Dacita-Andesita		R4	17-jun.		
M22	607672	7563334	4991	Pseudoestratificación	38	33	128	C												
M24	607696	7563348	4985	Pseudoestratificación	240	30	150	C												
E17	610262	7564392	4623	Dioclase	75	295		D	3	2	SR	Plana	12	Seco	Dacitas		R4	18-jun.		
E17	610262	7564392	4623	Dioclase	70	335		D	1	10	SR	Plana	12	Seco	Dacitas		R4	18-jun.		
E18	610033	7564255	4666	Dioclase	134	78	224	C	1	10	SR	Plana	12	Seco	Dacitas		R4	18-jun.		
E19	607120	7561061	5690	Dioclase	26	155		C	4	20	SR	Plana	12	Seco	Dacitas		R4	18-jun.		
E19	607120	7561061	5690	Dioclase	71	21		C	5	< 1	SR	Plana	10	Seco	Andesitas		R4	18-jun.		
E19	607120	7561061	5690	Dioclase	79	85		D	1	1	SR	Plana	4	Seco	Andesitas		R4	18-jun.		
E19	607120	7561061	5690	Dioclase	84	238		C	2	3	SR	Escalonada	12	Seco	Andesitas		R4	18-jun.		
E20	607098	7561059	5691	Dioclase	54	309		C	2	5	SR	Plana	4	Seco	Andesitas		R4	18-jun.		
E20	607098	7561059	5691	Dioclase	76	22		D	1	1	SR	Plana	4	Seco	Andesitas		R4	18-jun.		
E20	607098	7561059	5691	Dioclase	86	14		C	5	7	SR	Plana	14	Seco	Andesitas		R4	18-jun.		
E20	607098	7561059	5691	Dioclase	71	18		C	3	8	SR	Plana	12	Seco	Andesitas		R4	18-jun.		
E21	606972	7561117	5671	Dioclase	42	200		D	2	1	SR	Plana	10	Seco	Andesitas		R4	18-jun.		
E21	606972	7561117	5671	Dioclase	68	30		C	3	2	SR	Plana	14	Seco	Andesitas		R4	18-jun.		
E21	606972	7561117	5671	Dioclase	85	305		D	5	3	SR	Plana	14	Seco	Andesitas		R4	18-jun.		
E22	607180	7561389	5499	Dioclase	62	96		C	3	10	SR	Plana	8	Seco	Andesitas		R4	18-jun.		
E22	607180	7561389	5499	Dioclase	57	159		C	1	2	SR	Plana	14	Seco	Andesitas		R4	18-jun.		
E22	607180	7561389	5499	Dioclase	69	246		D	3	2	SR	Plana	4	Seco	Andesitas		R4	18-jun.		
E22	607180	7561389	5499	Dioclase	74	161		D	1	20	SR	Plana	4	Seco	Andesitas		R4	18-jun.		
E23	607161	7561490	5434	Dioclase	66	139		D	7	0	SR	Plana	2	Seco	Andesitas		R4	18-jun.		
E23	607161	7561490	5434	Dioclase	59	98		D	6	0	SR	Plana	2	Seco	Andesitas		R4	18-jun.		

Annex XVI Appendix B



**DIRECCIÓN TÉCNICA DE PROSPECCIÓN Y EXPLORACIÓN
ESTUDIO GEOLÓGICO-ESTRUCTURAL DEL ÁREA
CIRCUNDANTE DEL MANANTIAL DEL SISALÁ***

PTO.	ESTE	NORTE	ELEV.	TIPO	Az.	Bz.	DipDir	Pitch	CONTINUO	PERSISTENCIA (10m)	ABERTURA (cm)	FORMA	JRC	ACUA	TIPO ROCA	ALTERACION	DUREZA	FECHA	OBSERVACIONES
E2.3	60°161	7361480	5434	Dicielsa	69	332	C	2	SR	Plana	8	Saco	Arribadas	R4	18jun.				
E2.3	60°161	7361480	5434	Dicielsa	84	31	D	2	SR	Plana	6	Saco	Arribadas	R4	18jun.				
E2.3	60°161	7361480	5434	Dicielsa	72	326	C	2	SR	Plana	10	Saco	Arribadas	R4	18jun.				
E2.3	60°161	7361480	5434	Dicielsa	83	42	D	2	SR	Plana	4	Saco	Arribadas	R4	18jun.				
E2.3	60°161	7361480	5434	Dicielsa	138	68	D	3	0.1	SR	Escondido	14	Saco	Arribadas	R4	18jun.			
E2.4	60°0315	7361669	5359	Dicielsa	4	102	C	5	10	Plana	123	Saco	Moreras	R4	18jun.				
E2.4	60°0315	7361669	5359	Dicielsa	72	174	D	3	0.5	SR	Ordeñada	6	Saco	Arribadas	R4	18jun.			
J10	60°138	7361559	5410	Dicielsa	85	190	C	1	4	SR	Escalonada	14	Saco	Arribadas	R4	18jun.			
J11	60°136	7361558	5410	Dicielsa	76	25	D	1	<1	SR	Plana	3	Saco	Arribadas	R4	18jun.			
J12	60°136	7361558	5410	Dicielsa	79	48	C	1	<1	SR	Plana	4	Saco	Arribadas	R4	18jun.			
J14	60°130	7361553	5408	Dicielsa	75	204	C	1	<1	SR	Plana	4	Saco	Arribadas	R4	18jun.			
J15	60°130	7361553	5408	Dicielsa	77	327	D	1	0	SR	Ordeñada	8	Saco	Arribadas	R4	18jun.			
J16	60°134	7361559	5356	Dicielsa	80	200	C	2	0	SR	Escalonada	14	Saco	Arribadas	R4	18jun.			
J17	60°134	7361559	5356	Dicielsa	35	285	D	1	0	SR	Ordeñada	8	Saco	Oxidación	R4	18jun.			
L260	60°2558	7368950	4454	Dicielsa	80	60	D	2	10	SR	Plana	10	Saco	Ducto-Ardestina	R4	18jun.			
L261	60°2558	7368950	4454	Dicielsa	80	295	D	3	0	SR	Plana	10	Saco	Ducto-Ardestina	R4	18jun.			
L262	60°2558	7368950	4454	Dicielsa	80	130	D	2	5	SR	Plana	10	Saco	Ducto-Ardestina	R4	18jun.			
L263	60°2558	7368950	4454	Dicielsa	62	235	C	1	0	SR	Plana	10	Saco	Ducto-Ardestina	R4	18jun.			
L264	60°2558	7368950	4454	Dicielsa	55	290	D	10	0	SR	Plana	10	Saco	Ducto-Ardestina	R4	18jun.			
L265	60°2558	7368950	4454	Dicielsa	60	288	D	5	0	SR	Plana	10	Saco	Oxidación	R4	18jun.			
L266	60°2558	7368950	4454	Dicielsa	62	253	D	10	0	SR	Plana	10	Saco	Ducto-Ardestina	R4	18jun.			
L267	60°2558	7368950	4454	Dicielsa	80	233	D	4	0	SR	Plana	10	Saco	Ducto-Ardestina	R4	18jun.			
L268	60°2239	7368172	4451	Dicielsa	75	285	D	2	4	SR	Plana	10	Saco	Ducto-Ardestina	R4	18jun.			
L269	60°2239	7368172	4451	Dicielsa	80	260	D	1	0	SR	Plana	10	Saco	Ducto-Ardestina	R4	18jun.			
L270	60°2239	7368172	4451	Dicielsa	87	235	D	1	0	SR	Plana	10	Saco	Ducto-Ardestina	R4	18jun.			
L271	60°2239	7368172	4451	Dicielsa	89	257	D	3	0	SR	Plana	10	Saco	Ducto-Ardestina	R4	18jun.			
L272	60°2239	7368172	4451	Dicielsa	85	259	D	3	0	SR	Plana	10	Saco	Ducto-Ardestina	R4	18jun.			
L273	60°2239	7368172	4451	Dicielsa	83	267	D	3	0	SR	Plana	10	Saco	Ducto-Ardestina	R4	18jun.			
L274	60°1454	7368183	4451	Dicielsa	70	185	D	2	2	SR	Plana	10	Saco	Ducto-Ardestina	R4	18jun.			
L275	60°1454	7368183	4451	Dicielsa	84	182	D	1	0	SR	Plana	10	Saco	Ducto-Ardestina	R4	18jun.			
L276	60°1454	7368183	4451	Dicielsa	85	164	D	1	0	SR	Plana	10	Saco	Ducto-Ardestina	R4	18jun.			
L277	60°1454	7368183	4451	Dicielsa	64	187	D	1	0	SR	Plana	10	Saco	Ducto-Ardestina	R4	18jun.			
L278	60°1454	7368183	4451	Dicielsa	73	193	D	2	0	SR	Plana	10	Saco	Ducto-Ardestina	R4	18jun.			
L279	60°1454	7368183	4451	Dicielsa	70	185	D	1	0	SR	Plana	10	Saco	Ducto-Ardestina	R4	18jun.			
L280	60°1584	7368583	4459	Dicielsa	50	135	D	1	0	SR	Plana	10	Saco	Ducto-Ardestina	R4	18jun.			
L281	60°1584	7368583	4459	Dicielsa	88	45	D	4	4	SR	Plana	10	Saco	Ducto-Ardestina	R4	18jun.			
L282	60°1584	7368583	4459	Dicielsa	85	43	D	1	5	SR	Plana	10	Saco	Ducto-Ardestina	R4	18jun.			
L283	60°1584	7368583	4459	Dicielsa	88	47	D	1	5	SR	Plana	10	Saco	Ducto-Ardestina	R4	18jun.			
L284	60°1584	7368583	4459	Dicielsa	80	40	D	1	1	SR	Plana	10	Saco	Ducto-Ardestina	R4	18jun.			
L285	60°1584	7368583	4459	Dicielsa	88	43	D	2	10	SR	Plana	10	Saco	Ducto-Ardestina	R4	18jun.			
L286	60°1584	7368583	4459	Dicielsa	81	39	D	4	5	SR	Plana	10	Saco	Ducto-Ardestina	R4	18jun.			
L287	60°1584	7368583	4459	Dicielsa	83	41	D	3	3	SR	Plana	10	Saco	Ducto-Ardestina	R4	18jun.			
L288	60°1584	7368583	4459	Dicielsa	85	41	D	1	0	SR	Plana	10	Saco	Ducto-Ardestina	R4	18jun.			
L289	60°1578	7368105	4573	Dicielsa	65	265	D	1	0	SR	Plana	10	Saco	Ducto-Ardestina	R4	18jun.			
L290	60°1578	7368105	4573	Dicielsa	68	284	D	1	0	SR	Plana	10	Saco	Ducto-Ardestina	R4	18jun.			
L291	60°1578	7368105	4573	Dicielsa	78	249	D	1	0	SR	Plana	10	Saco	Ducto-Ardestina	R4	18jun.			
L292	60°1498	7365393	4550	Dicielsa	80	281	D	2	20	SR	Plana	10	Saco	Ducto-Ardestina	R4	18jun.			
L293	60°1498	7365393	4550	Dicielsa	85	330	D	1	0	SR	Plana	10	Saco	Ducto-Ardestina	R4	18jun.			
L294	60°1498	7365393	4550	Dicielsa	84	335	D	1	20	SR	Plana	10	Saco	Ducto-Ardestina	R4	18jun.			
L295	60°1578	7365105	4573	Dicielsa	71	248	D	8	0	SR	Plana	10	Saco	Ducto-Ardestina	R4	18jun.			
L296	60°1578	7365105	4573	Dicielsa	76	300	D	1	0	SR	Plana	10	Saco	Ducto-Ardestina	R4	18jun.			
L297	60°1578	7365105	4573	Dicielsa	78	259	D	1	5	SR	Plana	10	Saco	Ducto-Ardestina	R4	18jun.			
L298	60°1578	7365105	4573	Dicielsa	71	191	D	2	0	SR	Plana	10	Saco	Ducto-S	R4	18jun.			
M26	60°0824	7365983	4701	Dicielsa	78	171	D	6	5	SR	Plana	6	Saco	Ductos	R4	18jun.			
M26	60°0824	7365983	4701	Dicielsa	232	48	D	6	-1	SR	Plana	6	Saco	Ductos	R4	18jun.			
M27	60°0824	7365983	4701	Dicielsa	215	90	D	5	45	SR	Plana	6	Saco	Ductos	R4	18jun.			
M27	60°0824	7365983	4701	Dicielsa	155	70	D	4	30	SR	Plana	6	Saco	Ductos	R4	18jun.			
M28	60°0824	7365983	4701	Dicielsa	268	89	D	1	25	SR	Plana	4	Saco	Ductos	R4	18jun.			
M29	60°0824	7365983	4701	Dicielsa	228	89	D	1	0	SR	Plana	4	Saco	Ductos	R4	18jun.			

Base de datos

Página 9

**DIRECCIÓN TÉCNICA DE PROSPECCIÓN Y EXPLORACIÓN
ESTUDIO GEOLÓGICO-ESTRUCTURAL DEL ÁREA
CIRCUNDANTE DEL MANANTIAL DEL SISALÁ***



PTO.	ESTE	NORTE	ELEV.	Az.	Bz.	DipDir	Ptch	CONTINUADO	PERSISTENCIA (km)	ABERTURA (km)	RELLENO	FORMA	JRC	AGUA	TIPO ROCA	ALTERACION	DUREZA	FECHA	NOTAS
M30	60°3177	7561236	55.13	Dicelosa	0	71	90	D	3	<1	SR	Plana	2	Seco	Artesianas	R3	15jun.		
M30	60°3177	7561236	55.13	Dicelosa	200	90	110	D	1	1.5	SR	Plana	4	Seco	Artesianas	R3	15jun.		
M30	60°3177	7561236	55.13	Dicelosa	70	202	70	D	1	<1	SR	Escalonada	2	Seco	Artesianas	R3	15jun.		
M30	60°3177	7561236	55.13	Dicelosa	156	78	156	D	1	2	SR	Ordeñada	8	Seco	Artesianas	R3	15jun.		
M31	60°3175	7561234	55.13	Dicelosa	260	70	150	C	1	1	SR	Plana	4	Seco	Artesianas	R3	15jun.		
M32	60°3176	7561239	55.09	Dicelosa	95	215	95	C	1	1	SR	Plana	4	Seco	Artesianas	R3	15jun.		
M33	60°3176	7561236	55.07	Dicelosa	295	85	205	C	3	30	SR	Plana	14	Seco	Artesianas	R4	15jun.		
M33	60°3197	7561236	55.07	Dicelosa	290	71	70	D	1	2	SR	Rugosa	14	Seco	Artesianas	R4	15jun.		
M34	60°0729	7561216	55.97	Dicelosa	82	31	C	5	10	10	SR	Es calonada	10	Seco	Artesianas	R4	15jun.		
M34	60°0729	7561216	55.97	Dicelosa	78	34	C	4	5	5	SR	Es calonada	8	Seco	Artesianas	R4	15jun.		
M34	60°0729	7561216	55.97	Dicelosa	86	35	C	5	8	SR	Es calonada	10	Seco	Artesianas	R4	15jun.			
M34	60°0729	7561216	55.97	Dicelosa	79	41	C	6	5	SR	Plana	11	Seco	Artesianas	R4	15jun.			
M35	60°153	7561381	54.96	Dicelosa	82	66	C	2	7	SR	Rugosa	8	Seco	Directas	R3	15jun.			
M35	60°153	7561381	54.96	Dicelosa	72	195	70	D	1	<1	SR	Plana	2	Seco	Directas	R3	15jun.		
M36	60°1464	7561402	54.94	Dicelosa	0	90	2	D	1	0	SR	Plana	4	Seco	Directas	R3	15jun.		
M37	60°1299	7561450	54.46	Dicelosa	80	210	200	D	2	2	SR	Es calonada	4	Seco	Directas	R3	15jun.		
M37	60°1299	7561450	54.46	Dicelosa	90	146	146	D	3	8	SR	Es calonada	8	Seco	Directas	R3	15jun.		
M37	60°1299	7561450	54.46	Dicelosa	75	200	200	D	2	2	SR	Es calonada	4	Seco	Directas	R3	15jun.		
M37	60°1299	7561450	54.46	Dicelosa	42	180	180	C	3	4	SR	Plana	4	Seco	Directas	R3	15jun.		
M38	60°1289	7561466	54.63	Dicelosa	23	95	C	2	1	0	SR	Plana	4	Seco	Directas	R4	15jun.		
M39	60°7318	7561480	54.27	Dicelosa	70	245	D	2	2	SR	Es calonada	10	Seco	Directas	R4	15jun.			
M39	60°7318	7561480	54.27	Dicelosa	90	307	C	5	0	SR	Plana	8	Seco	Directas	R4	15jun.			
M39	60°7318	7561480	54.27	Dicelosa	84	180	D	4	4	SR	Plana	8	Seco	Directas	R4	15jun.			
M39	60°7318	7561480	54.27	Dicelosa	86	345	C	1	5	SR	Plana	12	Seco	Directas	R4	15jun.			
E1.7	61.03037	7564437	46.14	Falla	72	160	D	1	0	SR	Plana	12	Seco	Directas	R4	15jun.	Desplazamiento de 15 cm		
E1.9	60°1120	7561061	5690	Falla	81	240	C	2	5	SR	Es calonada	12	Seco	Directas	R4	15jun.	Desplazamiento de 15 cm		
M26	60°0824	7565933	47.01	Falla	96	186	C	1	1	SR	Plana	14	Seco	Directas	R4	15jun.			
E2.3	60°0824	7565933	47.01	Falla	67	170	D	6	5	SR	Plana	12	Seco	Directas	R4	15jun.			
E2.3	60°161	7561490	54.34	Falla formosa	80	67	D	1	2	SR	Ordeñada	14	Seco	Artesianas	R4	15jun.	Desplazamiento de 5 a 20 cm		
E2.0	60°0768	7561059	5691	Falla formosa	68	177	C	3	3	20	SR	Plana	8	Seco	Artesianas	R4	15jun.		
E2.0	60°0768	7561059	5691	Falla formosa	75	266	C	4	10	10	SR	Es calonada	12	Seco	Artesianas	R4	15jun.	Desplazamiento de 15 cm.	
E2.4	60°1260	7561060	53.59	Falla formosa	63	62	C	1	5	SR	Plana	10	Seco	Artesianas	R4	15jun.	Desplazamiento de 5 cm.		
L-28.8	60°1488	7565393	4550	Falla formosa	78	130	D	1	2	SR	Plana	10	Seco	Directas-Artesianas	R4	15jun.	Desplazamiento de 20 cm		
L-28.9	60°1488	7565393	4550	Falla formosa	75	121	D	1	0	SR	Plana	8	Seco	Directas-Artesianas	R4	15jun.			
M25	60°024	7561117	56.71	Psuedostratificación	165	89	295	C	1	0	SR	Plana	8	Seco	Directas	R4	15jun.		
E2.1	60°09172	7561117	56.71	Psuedostratificación	20	315	C	1	1	20	SR	Plana	8	Seco	Directas	R4	15jun.		
E2.3	60°161	7561490	54.34	Psuedostratificación	31	297	C	1	1	20	SR	Plana	8	Seco	Directas	R4	15jun.		
I.1.3	60°1336	7561538	54.10	Psuedostratificación	36	50	C	1	1	20	SR	Plana	8	Seco	Directas	R4	15jun.		
J.9	60°07010	7561116	55.80	Psuedostratificación	194	90	C	1	1	20	SR	Plana	8	Seco	Directas	R4	15jun.		
M26	60°0824	7565933	47.01	Psuedostratificación	138	45	C	1	1	20	SR	Plana	8	Seco	Directas	R4	15jun.		
M27	60°0827	7565944	4694	Psuedostratificación	160	34	70	C	1	1	20	SR	Plana	8	Seco	Directas	R4	15jun.	
M30	60°1348	7561480	54.27	Psuedostratificación	17	96	C	1	1	20	SR	Plana	8	Seco	Directas	R4	15jun.		
M39	60°07318	7561480	54.27	Psuedostratificación	68	365	C	1	1	20	SR	Plana	8	Seco	Directas	R4	15jun.		
E2.3	60°161	7561490	54.34	Psuedostratificación	40	130	C	2	3	SR	Rugosa	14	Seco	Directas	R4	20jun.			
I.2.4	60°09172	7561973	46.13	Psuedostratificación	95	185	D	2	3	10	SR	Plana	14	Seco	Directas	R4	20jun.		
E-25	60°0835	7561557	5333	Psuedostratificación	1.26	87	36	C	6	0.3	SR	Rugosa	6	Seco	Guinieritas	R3	20jun.		
J.1.8	60°0835	7561588	4604	Psuedostratificación	315	79	45	C	4	2	SR	Plana	8	Seco	Directas	R4	20jun.		
J.19	60°0838	7561911	4604	Psuedostratificación	100	78	10	D	3	7	SR	Es calonada	14	Seco	Directas	R4	20jun.		
J.20	60°0839	7561914	4604	Psuedostratificación	5	62	95	D	2	1	SR	Ordeñada	8	Seco	Directas	R4	20jun.		
J.21	60°0839	7561914	4604	Psuedostratificación	45	340	D	2	1	SR	Rugosa	8	Seco	Directas	R4	20jun.			
J.22	60°0830	7561973	46.13	Psuedostratificación	11	44	C	4	1	SR	Es calonada	14	Seco	Directas	R4	20jun.			
J.23	60°0830	7561973	46.13	Psuedostratificación	80	185	D	2	3	SR	Rugosa	8	Seco	Directas	R4	20jun.			
J.24	60°0830	7561973	46.13	Psuedostratificación	85	181	C	3	0.5	SR	Es calonada	14	Seco	Directas	R4	20jun.			
J.25	61.1228	7561657	46.40	Psuedostratificación	85	290	C	2	5	SR	Ordeñada	8	Seco	Guinieritas	R2	20jun.			
J.26	61.1228	7561657	46.40	Psuedostratificación	90	313	C	2	0	SR	Ordeñada	9	Seco	Guinieritas	R2	20jun.			
J.27	61.1228	7561657	46.40	Psuedostratificación	16	60	D	2	0	SR	Ordeñada	8	Seco	Guinieritas	R2	20jun.			
J.28	61.1228	7561659	46.40	Psuedostratificación	36	165	C	3	0.5	SR	Ordeñada	8	Seco	Guinieritas	R2	20jun.			
J.29	61.1228	7561659	46.40	Psuedostratificación	16	283	C	2	1	SR	Ordeñada	8	Seco	Guinieritas	R2	20jun.			
J.30	61.1228	7561662	46.40	Psuedostratificación	90	10	C	6	0.5	SR	Ordeñada	8	Seco	Guinieritas	R2	20jun.			
J.31	61.1228	7561664	46.40	Psuedostratificación	90	328	C	3	0.5	SR	Ordeñada	8	Seco	Guinieritas	R2	20jun.			
J.32	61.1388	7567712	46.46	Psuedostratificación	90	328	C	3	0.5	SR	Ordeñada	8	Seco	Guinieritas	R2	20jun.			

Base de datos

Página 10

Annex XVI Appendix B



**DIRECCIÓN TÉCNICA DE PROSPECCIÓN Y EXPLORACIÓN
"ESTUDIO GEOLÓGICO-ESTRUCTURAL DEL ÁREA
CIRCUNDANTE DEL MANANTIAL DEL SISALÁ"**

PTO.	ESTE	NORTE	ELEV.	TIPO	Az.	Bz.	DipDir	Pitch	CONTINUADO	PERSISTENCIA (10m)	ABERTURA (10m)	FORMA	JRC	AGUA	TIPO ROCA	ALTERACION	DUREZA	FECHA	observaciones
L-33	611.368	7367721	4646	Dicielsa	82	10	C	2	0	SR	Ondulada	S	Saco	Iguminitas		R2	20jun.		
L-34	611.368	7367722	4646	Dicielsa	90	2	C	2	1	SR	Ondulada	S	Saco	Iguminitas		R2	20jun.		
L-35	611.368	7367722	4646	Dicielsa	87	225	C	2	0.5	SR	Ondulada	S	Saco	Dicielsa		R2	20jun.		
L-301	60101988	7364741	4554	Dicielsa	55	248	C	3	0	SR	Plana	S	Saco	Dicielsa-Ardenita		R4	20jun.		
L-302	60101988	7364741	4554	Dicielsa	68	246	C	1	0	SR	Plana	S	Saco	Dicielsa-Ardenita		R4	20jun.		
L-303	60101988	7364741	4554	Dicielsa	65	249	D	2	0	SR	Plana	S	Saco	Dicielsa-Ardenita		R4	20jun.		
L-304	60101988	7364741	4554	Dicielsa	74	238	D	2	0	SR	Plana	S	Saco	Dicielsa-Ardenita		R4	20jun.		
L-305	60101988	7364741	4554	Dicielsa	71	241	C	1	0	SR	Plana	S	Saco	Dicielsa-Ardenita		R4	20jun.		
L-306	60101988	7364741	4554	Dicielsa	50	245	D	2	0	SR	Plana	S	Saco	Dicielsa-Ardenita		R4	20jun.		
L-307	60101988	7364741	4554	Dicielsa	62	255	C	10	2	SR	Plana	S	Saco	Dicielsa-Ardenita		R4	20jun.		
L-308	60202012	7364461	4648	Dicielsa	80	135	D	8	0	SR	Plana	S	Saco	Dicielsa-Ardenita		R4	20jun.		
L-309	60202012	7364461	4648	Dicielsa	88	132	D	2	0	SR	Plana	S	Saco	Dicielsa-Ardenita		R4	20jun.		
L-310	60202012	7364461	4648	Dicielsa	85	142	D	4	0	SR	Plana	S	Saco	Dicielsa-Ardenita		R4	20jun.		
L-311	60202012	7364461	4648	Dicielsa	71	100	D	1	0	SR	Plana	S	Saco	Dicielsa-Ardenita		R4	20jun.		
L-312	60202012	7364461	4648	Dicielsa	72	280	D	4	0	SR	Plana	S	Saco	Dicielsa-Ardenita		R4	20jun.		
L-313	60202012	7364461	4648	Dicielsa	85	134	C	8	0	SR	Plana	S	Saco	Dicielsa-Ardenita		R4	20jun.		
L-314	60202012	7364461	4648	Dicielsa	87	140	C	5	0	SR	Plana	S	Saco	Dicielsa-Ardenita		R4	20jun.		
L-315	60202012	7364461	4648	Dicielsa	76	325	C	3	0	SR	Plana	S	Saco	Dicielsa-Ardenita		R4	20jun.		
L-316	60202012	7364461	4648	Dicielsa	86	315	C	4	0	SR	Plana	S	Saco	Dicielsa-Ardenita		R4	20jun.		
L-317	60202012	7364461	4648	Dicielsa	83	306	D	2	0	SR	Plana	S	Saco	Dicielsa-Ardenita		R4	20jun.		
L-318	60202054	7364305	4656	Dicielsa	64	260	D	1	0	SR	Plana	S	Saco	Dicielsa-Ardenita		R4	20jun.		
L-319	60202054	7364305	4656	Dicielsa	68	246	D	1	0	SR	Plana	S	Saco	Dicielsa-Ardenita		R4	20jun.		
L-320	60202054	7364305	4656	Dicielsa	70	275	D	1	0	SR	Plana	S	Saco	Dicielsa-Ardenita		R4	20jun.		
L-321	60202054	7364305	4656	Dicielsa	72	250	D	1	0	SR	Plana	S	Saco	Dicielsa-Ardenita		R4	20jun.		
L-322	60202054	7364305	4656	Dicielsa	75	270	D	1	0	SR	Plana	S	Saco	Dicielsa-Ardenita		R4	20jun.		
L-323	60202054	7364305	4656	Dicielsa	84	125	D	1	0	SR	Plana	S	Saco	Dicielsa-Ardenita		R4	20jun.		
L-324	60202054	7364305	4656	Dicielsa	84	125	D	1	0	SR	Plana	S	Saco	Dicielsa-Ardenita		R4	20jun.		
L-325	60202054	7364305	4656	Dicielsa	79	128	D	1	0	SR	Plana	S	Saco	Dicielsa-Ardenita		R4	20jun.		
L-326	60202054	7364305	4656	Dicielsa	75	141	D	1	0	SR	Plana	S	Saco	Dicielsa-Ardenita		R4	20jun.		
L-327	60202054	7364305	4656	Dicielsa	86	130	D	3	1	SR	Plana	S	Saco	Dicielsa-Ardenita		R4	20jun.		
L-328	60202054	7364305	4656	Dicielsa	88	140	D	2	2	SR	Plana	S	Saco	Dicielsa-Ardenita		R4	20jun.		
L-329	60202054	7364305	4656	Dicielsa	85	140	D	1	0	SR	Plana	S	Saco	Dicielsa-Ardenita		R4	20jun.		
L-330	60202331	7365022	4653	Dicielsa	85	160	D	1	0	SR	Plana	S	Saco	Dicielsa-Ardenita		R4	20jun.		
L-331	60202331	7365022	4651	Dicielsa	15	265	D	2	3	SR	Plana	S	Saco	Dicielsa-Ardenita		R4	20jun.		
L-332	60202331	7365022	4651	Dicielsa	79	97	D	2	3	SR	Plana	S	Saco	Dicielsa-Ardenita		R4	20jun.		
L-333	60202331	7365022	4651	Dicielsa	49	104	D	1	0	SR	Plana	S	Saco	Dicielsa-Ardenita		R4	20jun.		
L-334	60202331	7365022	4651	Dicielsa	88	103	D	3	0	SR	Plana	S	Saco	Dicielsa-Ardenita		R4	20jun.		
L-335	60202331	7365022	4651	Dicielsa	81	80	C	4	2	SR	Plana	S	Saco	Dicielsa-Ardenita		R4	20jun.		
L-336	60202331	7365022	4651	Dicielsa	70	73	C	3	3	SR	Plana	S	Saco	Dicielsa-Ardenita		R4	20jun.		
L-337	60202331	7365022	4651	Dicielsa	69	276	C	2	4	SR	Plana	S	Saco	Dicielsa-Ardenita		R4	20jun.		
L-338	60202331	7365022	4651	Dicielsa	60	210	D	4	0	SR	Plana	S	Saco	Dicielsa-Ardenita		R4	20jun.		
L-339	60202331	7365022	4651	Dicielsa	62	207	D	4	0	SR	Plana	S	Saco	Dicielsa-Ardenita		R4	20jun.		
L-340	60202331	7365022	4651	Dicielsa	64	209	D	3	0	SR	Plana	S	Saco	Dicielsa-Ardenita		R4	20jun.		
L-341	60202335	7365213	4597	Dicielsa	65	30	D	4	0	SR	Plana	S	Saco	Dicielsa-Ardenita		R4	20jun.		
L-342	60202335	7365213	4597	Dicielsa	77	35	D	2	0	SR	Plana	S	Saco	Dicielsa-Ardenita		R4	20jun.		
L-343	60202335	7365213	4597	Dicielsa	85	54	D	4	2	SR	Plana	S	Saco	Dicielsa-Ardenita		R4	20jun.		
L-344	60202335	7365213	4597	Dicielsa	86	48	D	5	0	SR	Plana	S	Saco	Dicielsa-Ardenita		R4	20jun.		
L-345	60202335	7365213	4597	Dicielsa	62	150	D	3	20	SR	Plana	S	Saco	Dicielsa-Ardenita		R4	20jun.		
L-346	60202338	7365299	4454	Dicielsa	60	260	D	2	10	SR	Plana	S	Saco	Dicielsa-Ardenita		R4	20jun.		
L-347	60202338	7365299	4454	Dicielsa	80	40	D	2	30	SR	Plana	S	Saco	Dicielsa-Ardenita		R4	20jun.		
L-348	60202338	7365299	4454	Dicielsa	77	50	D	1	0	SR	Plana	S	Saco	Dicielsa-Ardenita		R4	20jun.		
L-349	60202338	7365299	4454	Dicielsa	85	146	D	1	20	SR	Plana	S	Saco	Dicielsa-Ardenita		R4	20jun.		
L-350	60202338	7365299	4454	Dicielsa	79	200	D	2	10	SR	Plana	S	Saco	Dicielsa-Ardenita		R4	20jun.		
L-351	60202338	7365299	4454	Dicielsa	86	348	D	4	2	SR	Plana	S	Saco	Dicielsa-Ardenita		R4	20jun.		
L-352	60202340	7365975	4516	Dicielsa	85	15	D	2	0	SR	Plana	S	Saco	Dicielsa-Ardenita		R4	20jun.		
L-353	60202340	7365975	4516	Dicielsa	82	23	D	1	0	SR	Plana	S	Saco	Dicielsa-Ardenita		R4	20jun.		
L-354	60202340	7365975	4516	Dicielsa	85	20	D	1	0	SR	Plana	S	Saco	Dicielsa-Ardenita		R4	20jun.		
M-1	60202355	7365975	4516	Dicielsa	57	2	D	1	10	SR	Plana	S	Saco	Dicielsa		R5	20jun.		
M-2	60202355	7365975	4516	Dicielsa	74	140	D	1	2	SR	Plana	S	Saco	Dicielsa		R5	20jun.		
M-3	60202355	7365975	4516	Dicielsa	65	78	C	3	3	SR	Plana	S	Saco	Dicielsa		R5	20jun.		
M-4	60202355	7365975	4516	Dicielsa	77	80	C	3	5	SR	Plana	S	Saco	Dicielsa		R5	20jun.		
M-5	60202355	7365975	4516	Dicielsa	84	85	C	2	2	SR	Plana	S	Saco	Dicielsa		R5	20jun.		

Base de datos

**DIRECCIÓN TÉCNICA DE PROSPECCIÓN Y EXPLORACIÓN
ESTUDIO GEOLÓGICO-ESTRUCTURAL DEL ÁREA
CIRCUNDANTE DEL MANANTIAL DEL SISALÁ***



PTO.	ESTE	NORTE	ELEV.	TIPO	Az.	Bz.	DipDir	Pitch	CONTINUAD.	PERSISTENCIA	ABERTURA	(mm.)	RELLENO	FORMA	JRC	AGUA	TIPO ROCA	ALTERACION	DUREZA	FECHA	OBSERVACIONES
M43	6090825	73671934	4602	Diciplsa	73	178	D		3	SR			Plana	12	Seco	Ductiles	R5	20-jun.			
M43	6090825	73671934	4602	Diciplsa	80	81	30		2	SR			Escalonada	18	Seco	Ductiles	R5	20-jun.			
M43	6090825	73671934	4602	Diciplsa	65	82	335	C	1	SR			Plana	14	Seco	Ductiles	R5	20-jun.			
M44	61.1200	73671601	4613	Diciplsa	75	186			2	<1			Plana	10	Seco	Umbrineras	R3	20-jun.			
M45	61.1200	73671601	4613	Diciplsa	75	23			1	1	0		Escalonada	16	Seco	Umbrineras	R3	20-jun.			
M46	61.1202	73671627	4614	Diciplsa	10	15	100	C	2	SR			Plana	10	Seco	Umbrineras	R3	20-jun.			
M47	61.1213	73671831	4630	Diciplsa	85	163			2	SR			Plana	6	Seco	Umbrineras	R3	20-jun.			
M47	61.1213	73671831	4630	Diciplsa	87	300			3	0.5			Plana	4	Seco	Umbrineras	R3	20-jun.			
M48	61.1216	73671644	4615	Diciplsa	135	87	225	C	3	SR			Es calonada	5	Seco	Umbrineras	R3	20-jun.			
M48	61.1216	73671644	4615	Diciplsa	88	235	D	2	<1	SR			Es calonada	4	Seco	Umbrineras	R3	20-jun.			
M49	61.1227	73671644	4637	Diciplsa	89	304	C	2	0	SR			Es calonada	4	Seco	Umbrineras	R3	20-jun.			
M49	61.1227	73671644	4637	Diciplsa	86	190	D	2	4	SR			Plana	4	Seco	Umbrineras	R3	20-jun.			
M49	61.1227	73671644	4637	Diciplsa	87	195	C	1	0.2	SR			Plana	4	Seco	Umbrineras	R3	20-jun.			
M50	61.1351	73671700	4640	Diciplsa	86	284	C	1	<1	SR			Escalonada	6	Seco	Umbrineras	R3	20-jun.			
M50	61.1351	73671700	4640	Diciplsa	88	2			2	SR			Plana	8	Seco	Umbrineras	R3	20-jun.			
M51	61.1363	73671703	4650	Diciplsa	90	283	C	1	0.5	SR			Plana	10	Seco	Umbrineras	R3	20-jun.			
M51	61.1363	73671703	4650	Diciplsa	83	25	C	1	0.5	SR			Plana	10	Seco	Umbrineras	R3	20-jun.			
M51	61.1363	73671703	4650	Diciplsa	84	135	C	1	0.5	SR			Plana	10	Seco	Umbrineras	R3	20-jun.			
M51	61.1363	73671703	4650	Diciplsa	83	96	C	2	2	SR			Plana	5	Seco	Umbrineras	R3	20-jun.			
M51	61.1363	73671703	4650	Diciplsa	88	295	C	1	0.5	SR			Plana	1	Seco	Umbrineras	R3	20-jun.			
M51	61.1363	73671703	4650	Diciplsa	81	5	D	1	0.5	SR			Plana	10	Seco	Umbrineras	R3	20-jun.			
M51	61.1363	73671703	4650	Diciplsa	70	145	C	1	0.5	SR			Es calonada	10	Seco	Umbrineras	R3	20-jun.	Desplazamiento 10 cm		
E-25	6090825	73671888	4601	Falla	6	50	C	1	0.5	SR			Plana	10	Seco	Umbrineras	R3	20-jun.	Desplazamiento 5 cm		
E-26	6090825	73671888	4601	Falla	4	53	C	2	0.5	SR			Plana	10	Seco	Umbrineras	R3	20-jun.	Desplazamiento 5 cm		
E-27	6090825	73671888	4601	Falla	4601	588	D	1	0.5	SR			Plana	8	Seco	Umbrineras	R4	20-jun.	Desplazamiento 10 cm		
L-318	60200212	73671451	4648	Falla	88	321	230	D	1	0	SR			Plana	8	Seco	Deslizamiento	R4	20-jun.		
L-325	60200254	73671305	4648	Falla	74	160	80	D	1	0	SR			Plana	8	Seco	Deslizamiento	R4	20-jun.		
L-352	60203466	73671294	4468	Falla	89	80	82	C	1	5	SR			Plana	8	Seco	Deslizamiento	R4	20-jun.		
L-353	60203466	73671294	4468	Falla	80	50	D	1	0	SR			Plana	8	Seco	Deslizamiento	R4	20-jun.			
L-354	6020340	73671095	4516	Falla	65	245	D	1	0	SR			Plana	8	Seco	Deslizamiento	R4	20-jun.			
L-356	6020340	73671095	4516	Falla	70	10	D	1	0	SR			Es calonada	14	Seco	Deslizamiento	R5	20-jun.			
M41	6090825	73671888	4601	Falla inversa	16	67	344	C	1	0.3	SR			Plana	10	Seco	Umbrineras	R3	20-jun.		
M47	61.1213	73671631	4630	Falla inversa	15	20	C	1	0.3	SR			Plana	8	Seco	Umbrineras	R3	20-jun.			
M48	61.1216	73671644	4645	Falla inversa	18	28	C	1	<1	SR			Plana	14	Seco	Umbrineras	R3	20-jun.			
M41	6090825	73671888	4601	Falla Normal	2	84	92	C	1	12	SR			Escalonada	14	Seco	Ductiles	R5	20-jun.		
M43	6090825	73671934	4602	Falla Normal	68	71	139	C	1	4	SR			Escalonada	14	Seco	Ductiles	R5	20-jun.		
M46	61.1202	73671627	4641	Falla Normal	75	80	345	C	1	10	SR			Escalonada	18	Seco	Umbrineras	R3	20-jun.		
M41	6090825	73671888	4601	Permeabilización	130	90	182	C	1	<1	SR			Escalonada	18	Seco	Ductiles	R5	20-jun.		
M51	61.1363	73671703	4650	Permeabilización	15	80	C	1	3	SR			Plana	6	Seco	Umbrineras	R3	20-jun.			
E-29	6010346	73671265	4395	Dicplsa	80	75	C	1	3	SR			Ortigada	14	Seco	Umbrineras	R3	21-jun.			
E-33	6010346	73671887	4396	Dicplsa	264	82	355	C	1	3	SR			Ortigada	12	Seco	Umbrineras	R3	21-jun.		
E-33	6010350	73671887	4394	Dicplsa	76	41	C	1	0.2	SR			Curva	12	Seco	Umbrineras	R3	21-jun.			
E-33	6010350	73671258	4396	Dicplsa	80	55	D	1	0.2	SR			Plana	12	Humedo	Umbrineras	R3	21-jun.			
E-31	6010415	73662633	4390	Dicplsa	227	88	137	D	1	1	SR			Es calonada	13	Humedo	Fujo de aguas termales	R3	21-jun.		
E-31	6010415	73662633	4390	Dicplsa	69	318	D	2	0	SR			Es calonada	14	Humedo	Fujo de aguas termales	R3	21-jun.			
E-33	6010346	73661887	4396	Dicplsa	232	85	142	C	3	4	SR			Plana	14	Seco	Umbrineras	R3	21-jun.		
E-33	6010346	73661887	4396	Dicplsa	84	21	D	1	0.2	SR			Escalonada	12	Seco	Umbrineras	R3	21-jun.			
E-33	6010346	73661887	4396	Dicplsa	220	77	130	D	2	0.2	SR			Escalonada	12	Seco	Umbrineras	R3	21-jun.		
E-33	6010346	73661887	4396	Dicplsa	83	14	129	C	1	1	SR			Curva	12	Seco	Umbrineras	R3	21-jun.		
E-33	6010346	73661887	4396	Dicplsa	80	55	D	1	0.2	SR			Plana	12	Humedo	Umbrineras	R3	21-jun.			
E-33	6010346	73661887	4396	Dicplsa	227	88	137	D	1	1	SR			Es calonada	13	Humedo	Umbrineras	R3	21-jun.		
E-33	6010346	73661887	4396	Dicplsa	7	217	C	2	10	SR			Es calonada	14	Humedo	Fujo de aguas termales	R3	21-jun.			
E-33	6010346	73661887	4396	Dicplsa	8	76	98	C	2	12	SR			Es calonada	14	Humedo	Fujo de aguas termales	R3	21-jun.		
E-33	6010346	73661887	4396	Dicplsa	150	82	60	C	6	15	SR			Es calonada	14	Humedo	Fujo de aguas termales	R3	21-jun.		
E-33	6010346	73661887	4396	Dicplsa	305	53	215	C	4	30	SR			Es calonada	14	Humedo	Fujo de aguas termales	R3	21-jun.		
E-33	6010346	73661887	4396	Dicplsa	110	80	20	C	4	2	SR			Es calonada	14	Humedo	Fujo de aguas termales	R3	21-jun.		
J-11	6010360	73662245	4390	Dicplsa	345	20	265	C	3	2	SR			Es calonada	14	Humedo	Fujo de aguas termales	R3	21-jun.		

Annex XVI Appendix B



**DIRECCIÓN TÉCNICA DE PROSPECCIÓN Y EXPLORACIÓN
"ESTUDIO GEOLÓGICO-ESTRUCTURAL DEL ÁREA
CIRCUNDANTE DEL MANANTIAL DEL SISAL"**

PTO.	ESTE	NORTE	ELEV.	TIPO	Az	Bz	DipDir	Ptch	CONTINUADO	PERSISTENCIA (10m)	ABERTURA (cm)	FORMA	RELLENO	JRC	AGUA	TIPO ROCA	ALTERACION	DUREZA	FECHA	OBSERVACIONES
J42	601.396	75662728	4350	Dicielsa	67	77	337	2	C	2	3	SR	Escalonada	14	Humedo	Flujo de dieritos	R3	21-jun.		
J43	601.404	75662867	4351	Dicielsa	40	81	310	5	C	6	1	SR	Escalonada	14	Humedo	Flujo de dieritos	R3	21-jun.		
J44	601.404	75662850	4351	Dicielsa	230	87	140	5	C	5	3	SR	Escalonada	14	Humedo	Flujo de dieritos	R3	21-jun.		
J45	601.411	75662857	4351	Dicielsa	245	42	155	5	C	1	5	SR	Escalonada	14	Humedo	Flujo de dieritos	R3	21-jun.		
J46	601.422	75662730	4351	Dicielsa	61	85	300	3	C	5	5	SR	Escalonada	14	Humedo	Flujo de dieritos	R3	21-jun.		
J47	601.445	75662769	4358	Dicielsa	5	85	95	3	C	3	3	SR	Escalonada	14	Humedo	Flujo de dieritos	R3	21-jun.		
J48	601.4492	75662548	4355	Dicielsa	245	215	C	1	3	3	3	SR	Escalonada	14	Humedo	Flujo de dieritos	R3	21-jun.		
J49	601.4492	75662548	4355	Dicielsa	70	81	340	5	C	5	10	SR	Escalonada	14	Humedo	Flujo de dieritos	R3	21-jun.		
J50	601.723	75661116	4350	Dicielsa	82	137	C	1	0	SR	Ordeñada	8	Saco	Geomorfos	Ordeñada	R2	21-jun.			
J51	601.723	75661116	4350	Dicielsa	86	66	C	1	0	SR	Ordeñada	8	Saco	Geomorfos	Ordeñada	R2	21-jun.			
J52	601.723	75661111	4350	Dicielsa	83	154	C	3	1	SR	Ordeñada	8	Saco	Geomorfos	Ordeñada	R2	21-jun.			
J53	601.723	75661111	4350	Dicielsa	78	41	C	4	0	SR	Ordeñada	8	Saco	Geomorfos	Ordeñada	R2	21-jun.			
J54	601.723	75661110	4350	Dicielsa	74	285	C	1	0	SR	Ordeñada	14	Saco	Geomorfos	Ordeñada	R2	21-jun.			
J55	601.723	75661110	4350	Dicielsa	90	220	C	3	0	SR	Escalonada	14	Saco	Geomorfos	Escalonada	R2	21-jun.			
J56	601.682	75661348	4350	Dicielsa	68	115	C	6	0	SR	Escalonada	14	Saco	Geomorfos	Escalonada	R2	21-jun.			
J57	601.686	75661513	4350	Dicielsa	87	216	C	2	0	SR	Escalonada	14	Saco	Geomorfos	Escalonada	R2	21-jun.			
J58	601.686	75661513	4350	Dicielsa	68	214	C	2	0	SR	Escalonada	14	Saco	Geomorfos	Escalonada	R2	21-jun.			
J59	601.642	75661716	4352	Dicielsa	10	28	C	2	0	SR	Ordeñada	8	Saco	Geomorfos	Ordeñada	R2	21-jun.			
J60	601.652	75661716	4351	Dicielsa	65	52	D	3	0	SR	Ordeñada	8	Saco	Geomorfos	Ordeñada	R2	21-jun.			
J61	601.6001	75652120	4459	Dicielsa	89	310	D	1	0	SR	Página	8	Saco	Directas	Página	R5	21-jun.			
J62	601.6001	75652120	4459	Dicielsa	79	304	D	2	4	SR	Página	8	Saco	Directas	Página	R5	21-jun.			
J63	601.6001	75652120	4459	Dicielsa	68	306	D	2	5	SR	Página	8	Saco	Directas	Página	R5	21-jun.			
J64	601.6833	75641887	4631	Dicielsa	70	320	D	2	8	SR	Página	8	Saco	Directas	Página	R5	21-jun.			
J65	601.6833	75641887	4631	Dicielsa	68	310	D	1	5	SR	Página	8	Saco	Directas	Página	R5	21-jun.			
J66	601.6833	75641887	4631	Dicielsa	83	280	D	1	3	SR	Página	8	Saco	Directas	Página	R5	21-jun.			
J67	601.6833	75641887	4631	Dicielsa	75	240	D	1	7	SR	Página	8	Saco	Directas	Página	R5	21-jun.			
J68	601.6833	75641887	4631	Dicielsa	60	156	D	2	5	SR	Página	8	Saco	Directas	Página	R5	21-jun.			
J69	601.6832	75645150	4618	Dicielsa	87	150	D	2	3	SR	Página	8	Saco	Directas	Página	R5	21-jun.			
J70	601.6832	75645150	4618	Dicielsa	62	147	D	1	0	SR	Página	8	Saco	Directas	Página	R5	21-jun.			
J71	601.6832	75645150	4618	Dicielsa	70	144	D	1	0	SR	Página	8	Saco	Directas	Página	R5	21-jun.			
J72	601.6832	75645150	4618	Dicielsa	85	135	D	2	0	SR	Página	8	Saco	Directas	Página	R5	21-jun.			
J73	601.6832	75645150	4618	Dicielsa	87	129	D	2	0	SR	Página	8	Saco	Directas	Página	R5	21-jun.			
J74	601.6832	75642123	4778	Dicielsa	88	265	D	2	4	SR	Rugosa	8	Saco	Directas	Rugosa	R5	21-jun.			
J75	601.6830	75642123	4778	Dicielsa	45	150	D	3	5	SR	Rugosa	8	Saco	Directas	Rugosa	R5	21-jun.			
J76	601.6830	75642123	4778	Dicielsa	83	262	D	2	2	SR	Rugosa	8	Saco	Directas	Rugosa	R5	21-jun.			
J77	601.6830	75642123	4778	Dicielsa	87	205	D	1	0	SR	Rugosa	8	Saco	Directas	Rugosa	R5	21-jun.			
J78	601.6830	75642123	4778	Dicielsa	86	192	D	1	3	SR	Página	8	Saco	Directas	Página	R5	21-jun.			
J79	601.6830	75642123	4778	Dicielsa	82	95	D	2	3	SR	Página	8	Saco	Directas	Página	R5	21-jun.			
J80	601.6830	75641214	4550	Dicielsa	72	66	D	1	4	SR	Página	8	Saco	Directas	Página	R5	21-jun.			
J81	601.6830	75641214	4550	Dicielsa	60	70	D	3	6	SR	Página	8	Saco	Directas	Página	R5	21-jun.			
J82	601.6830	75641214	4550	Dicielsa	70	70	D	2	3	SR	Página	8	Saco	Directas	Página	R5	21-jun.			
J83	601.6830	75641214	4550	Dicielsa	60	70	D	1	1	SR	Página	8	Saco	Directas	Página	R5	21-jun.			
J84	601.6830	75641214	4550	Dicielsa	70	70	D	1	1	SR	Página	8	Saco	Directas	Página	R5	21-jun.			
J85	601.6830	75641214	4550	Dicielsa	70	70	D	1	1	SR	Página	8	Saco	Directas	Página	R5	21-jun.			
J86	601.6830	75641214	4550	Dicielsa	70	70	D	1	1	SR	Página	8	Saco	Directas	Página	R5	21-jun.			
J87	601.6830	75641214	4550	Dicielsa	70	70	D	1	1	SR	Página	8	Saco	Directas	Página	R5	21-jun.			
J88	601.6830	75641214	4550	Dicielsa	70	70	D	1	1	SR	Página	8	Saco	Directas	Página	R5	21-jun.			
J89	601.6830	75641214	4550	Dicielsa	70	70	D	1	1	SR	Página	8	Saco	Directas	Página	R5	21-jun.			
J90	601.6830	75641214	4550	Dicielsa	70	70	D	1	1	SR	Página	8	Saco	Directas	Página	R5	21-jun.			
J91	601.6830	75641214	4550	Dicielsa	70	70	D	1	1	SR	Página	8	Saco	Directas	Página	R5	21-jun.			
J92	601.6830	75641214	4550	Dicielsa	70	70	D	1	1	SR	Página	8	Saco	Directas	Página	R5	21-jun.			
J93	601.6830	75641214	4550	Dicielsa	70	70	D	1	1	SR	Página	8	Saco	Directas	Página	R5	21-jun.			
J94	601.6830	75641214	4550	Dicielsa	70	70	D	1	1	SR	Página	8	Saco	Directas	Página	R5	21-jun.			
J95	601.6830	75641214	4550	Dicielsa	70	70	D	1	1	SR	Página	8	Saco	Directas	Página	R5	21-jun.			
J96	601.6830	75641214	4550	Dicielsa	70	70	D	1	1	SR	Página	8	Saco	Directas	Página	R5	21-jun.			
J97	601.6830	75641214	4550	Dicielsa	70	70	D	1	1	SR	Página	8	Saco	Directas	Página	R5	21-jun.			
J98	601.6830	75641214	4550	Dicielsa	70	70	D	1	1	SR	Página	8	Saco	Directas	Página	R5	21-jun.			
J99	601.6830	75641214	4550	Dicielsa	70	70	D	1	1	SR	Página	8	Saco	Directas	Página	R5	21-jun.			
J100	601.6830	75641214	4550	Dicielsa	70	70	D	1	1	SR	Página	8	Saco	Directas	Página	R5	21-jun.			
J101	601.6830	75641214	4550	Dicielsa	70	70	D	1	1	SR	Página	8	Saco	Directas	Página	R5	21-jun.			
J102	601.6830	75641214	4550	Dicielsa	70	70	D	1	1	SR	Página	8	Saco	Directas	Página	R5	21-jun.			
J103	601.6830	75641214	4550	Dicielsa	70	70	D	1	1	SR	Página	8	Saco	Directas	Página	R5	21-jun.			
J104	601.6830	75641214	4550	Dicielsa	70	70	D	1	1	SR	Página	8	Saco	Directas	Página	R5	21-jun.			
J105	601.6830	75641214	4550	Dicielsa	70	70	D	1	1	SR	Página	8	Saco	Directas	Página	R5	21-jun.			
J106	601.6830	75641214	4550	Dicielsa	70	70	D	1	1	SR	Página	8	Saco	Directas	Página	R5	21-jun.			
J107	601.6830	75641214	4550	Dicielsa	70	70	D	1	1	SR	Página	8	Saco	Directas	Página	R5	21-jun.			
J108	601.6830	75641214	4550	Dicielsa	70	70	D	1	1	SR	Página	8	Saco	Directas	Página	R5	21-jun.			
J109	601.6830	75641214	4550	Dicielsa	70	70	D	1	1	SR	Página	8	Saco	Directas	Página	R5	21-jun.			
J110	601.6830	75641214	4550	Dicielsa	70	70	D	1	1	SR	Página	8	Saco	Directas	Página	R5	21-jun.			
J111	601.6830	75641214	4550	Dicielsa	70	70	D	1	1	SR	Página	8	Saco	Directas	Página	R5	21-jun.			
J112	601.6830	75641214	4550	Dicielsa	70	70	D	1	1	SR	Página	8	Saco	Directas	Página	R5	21-jun.			
J113	601.6830	75641214	4550	Dicielsa	70	70	D	1	1	SR	Página	8	Saco	Directas	Página	R5	21-jun.			
J114	601.6830	75641214	4550	Dicielsa	70	70	D	1	1	SR	Página	8	Saco	Directas	Página	R5	21-jun.			
J115	601.6830	75641214	4550	Dicielsa	70	70	D	1	1	SR	Página	8	Saco	Directas	Página	R5	21-jun.			
J116	601.6830	75641214	4550	Dicielsa	70	70	D	1	1	SR	Página	8	Saco	Directas	Página	R5	21-jun.			
J117	601.6830	75641214	4550	Dicielsa	70	70	D	1	1	SR	Página	8	Saco	Directas	Página	R5	21-jun.			
J118	601.6830	75641214	4550	Dicielsa	70	70	D	1	1	SR	Página	8	Saco	Directas	Página	R5	21-jun.			
J119	601.6830	75641214	4550	Dicielsa	70	70	D	1	1	SR	Página	8	Saco	Directas	Página	R5	21-jun.			
J120	601.6830	75641214	4550	Dicielsa	70	70	D	1	1	SR	Página	8	Saco	Directas	Página	R5	21-jun.			
J121	601.6830	75641214	4550	Dicielsa	70	7														

**DIRECCIÓN TÉCNICA DE PROSPECCIÓN Y EXPLORACIÓN
ESTUDIO GEOLÓGICO-ESTRUCTURAL DEL ÁREA
CIRCUNDANTE DEL MANANTIAL DEL SISAL***



PTO.	ESTE	NORTE	ELEV.	TIPO	Az.	Bz.	DipDir	Pitch	CONTINUADO	PERSISTENCIA	ABERTURA	FORMA	JRC	AGUA	TIPO ROCA	ALTERACION	DUREZA	FECHA	OBSERVACIONES
M60	601.404	75662527	43988	Dicielsa	80	100	D		1	0.7	SR	Escalonada	18	Saco	Flujo de dientes	R3	21-jun.		
M61	601.410	75662526	43933	Dicielsa	57	200	C		2	4	SR	Escalonada	18	Saco	Flujo de dientes	R3	21-jun.		
M62	601.418	75662529	43935	Dicielsa	78	315	C		1	4	SR	Escalonada	18	Saco	Flujo de dientes	R2	21-jun.		
M62	601.418	75662529	43935	Dicielsa	75	275	D		2	0	SR	Escalonada	17	Saco	Flujo de dientes	R2	21-jun.		
M62	601.418	75662529	43935	Dicielsa	80	318	D		1	0.3	SR	Escalonada	17	Saco	Flujo de dientes	R2	21-jun.		
M63	601.416	75662529	44038	Dicielsa	234	84	134		1	2	SR	Plana	15	Saco	Flujo de dientes	R2	21-jun.		
M63	601.416	75662527	44038	Dicielsa	63	165	C		2	2	ACilia	Plana	16	Saco	Flujo de dientes	R2	21-jun.		
M63	601.416	75662527	44038	Dicielsa	76	134	C		2	1.5	SR	Plana	16	Saco	Flujo de dientes	R2	21-jun.		
M64	601.424	75662521	43938	Dicielsa	73	314	C		1	0.2	SR	Plana	16	Saco	Flujo de dientes	R2	21-jun.		
M64	601.424	75662521	43938	Dicielsa	76	144	C		1	5	SR	Plana	18	Saco	Flujo de dientes	R2	21-jun.		
M65	601.440	75662521	43935	Dicielsa	66	170	C		1	0.5	SR	Ondulada	18	Saco	Flujo de dientes	R2	21-jun.		
M65	601.440	75662521	43935	Dicielsa	86	322	C		1	0.5	SR	Escalonada	17	Saco	Flujo de dientes	R2	21-jun.		
M65	601.440	75662521	43935	Dicielsa	83	103	C		1	0.3	SR	Plana	18	Saco	Flujo de dientes	R2	21-jun.		
M65	601.440	75662521	43935	Dicielsa	83	172	D		1	0.2	SR	Arenas	18	Saco	Flujo de dientes	R2	21-jun.		
M66	601.482	75662428	43931	Dicielsa	76	160	C		6	3	SR	Plana	14	Saco	Flujo de dientes	R2	21-jun.		
M66	601.482	75662428	43931	Dicielsa	74	223	D		1	1.5	SR	Plana	14	Saco	Flujo de dientes	R2	21-jun.		
M66	601.482	75662428	43931	Dicielsa	85	168	D		2	5	SR	Plana	14	Saco	Flujo de dientes	R2	21-jun.		
M67	601.475	75662521	43931	Dicielsa	82	105	C		3	0.5	SR	Plana	15	Saco	Flujo de dientes	R2	21-jun.		
M67	601.475	75662521	44115	Dicielsa	74	22	C		2	2	ACilia	Plana	16	Saco	Flujo de dientes	R2	21-jun.		
M67	601.475	75662521	44115	Dicielsa	82	44	D		1	3	SR	Plana	16	Saco	Flujo de dientes	R2	21-jun.		
M67	601.475	75662521	44115	Dicielsa	75	329	D		1	2	SR	Plana	16	Saco	Flujo de dientes	R2	21-jun.		
M67	601.475	75662521	44115	Dicielsa	84	125	C		3	3	SR	Plana	16	Saco	Flujo de dientes	R2	21-jun.		
M68	601.504	75662428	43839	Dicielsa	80	107	C		1	11	SR	Plana	14	Saco	Flujo de dientes	R2	21-jun.		
M68	601.504	75662428	43839	Dicielsa	123	78	C		1	0.3	SR	Plana	14	Saco	Flujo de dientes	R2	21-jun.		
M69	601.517	75662426	43935	Dicielsa	83	231	D		3	0.3	SR	Plana	14	Saco	Flujo de dientes	R2	21-jun.		
M69	601.517	75662426	43935	Dicielsa	83	257	C		1	5	ACilia	Plana	14	Saco	Flujo de dientes	R2	21-jun.		
M70	601.521	75662425	43938	Dicielsa	81	257	C		2	2	SR	Plana	16	Saco	Flujo de dientes	R2	21-jun.		
M70	601.521	75662425	43938	Dicielsa	80	169	C		2	2	SR	Plana	16	Saco	Flujo de dientes	R2	21-jun.		
M70	601.521	75662425	43938	Dicielsa	77	279	D		2	3	SR	Plana	16	Saco	Flujo de dientes	R2	21-jun.		
M70	601.521	75662425	43938	Dicielsa	130	85	ACilia		3	3	SR	Plana	16	Saco	Flujo de dientes	R2	21-jun.		
M71	601.521	75662425	43938	Dicielsa	80	208	D		2	0.5	SR	Plana	14	Saco	Flujo de dientes	R2	21-jun.		
M72	601.544	75662321	43931	Dicielsa	165	78	C		1	0	SR	Plana	14	Saco	Flujo de dientes	R2	21-jun.		
M72	601.544	75662328	43930	Dicielsa	84	325	C		2	0.5	SR	Plana	17	Saco	Flujo de dientes	R2	21-jun.		
M72	601.546	75662228	43930	Dicielsa	84	212	C		2	0.1	SR	Plana	17	Saco	Flujo de dientes	R2	21-jun.		
M72	601.546	75662228	43930	Dicielsa	83	175	C		1	0	SR	Plana	17	Saco	Flujo de dientes	R2	21-jun.		
M73	601.584	75662220	43938	Dicielsa	82	175	C		1	0	SR	Plana	17	Saco	Flujo de dientes	R2	21-jun.		
L83	604.350	75661214	45050	Falla	59	73	D		1	2	SR	Plana	8	Saco	Flujo de dientes	R5	21-jun.		
M52	601.320	75662267	43837	Falla inversa	85	285	D		1	25	SR	Ondulada	18	Saco	Flujo de dientes	R3	21-jun.		
M54	601.336	75662627	43133	Falla inversa	84	52	310		1	0	SR	Escalonada	17	Saco	Flujo de dientes	R3	21-jun.		
E32	601.546	75662118	44922	Falla inversa	65	90	D		1	0.4	SR	Cueva	12	Saco	Flujo de dientes	R3	21-jun.		
E32	601.546	75662118	44922	Falla inversa	83	215	C		1	0.2	SR	Plana	12	Saco	Flujo de dientes	R3	21-jun.		
K53	601.559	75661523	43534	Falla inversa	84	73	C		1	3	SR	Ondulada	16	Saco	Flujo de dientes	R3	21-jun.		
W55	601.342	75662522	43935	Falla inversa	68	330	C		1	1	SR	Escalonada	17	Saco	Flujo de dientes	R2	21-jun.		
M71	601.544	75662231	43931	Falla inversa	88	45	C		1	0.5	SR	Plana	14	Saco	Flujo de dientes	R2	21-jun.		
M72	601.546	75662228	43930	Falla inversa	67	284	C		1	0	SR	Plana	14	Saco	Flujo de dientes	R2	21-jun.		
M72	601.546	75662228	43930	Falla inversa	89	215	C		1	0	SR	Plana	17	Saco	Flujo de dientes	R2	21-jun.	Desplazamiento de 10 cm	
M73	601.584	75662220	43938	Falla inversa	165	82	C		3	0	SR	Plana	17	Saco	Flujo de dientes	R2	21-jun.		
L87	604.483	75661857	46311	Pseudotectonicación	9	15	C		0	0	SR	Plana	18	Saco	Flujo de dientes	R3	21-jun.		
M56	601.339	75662621	44044	Pseudotectonicación	310	20	C		3	3	SR	Arenas	16	Saco	Flujo de dientes	R4	22-jun.		
E59	610.663	7566280	46417	Dicielsa	290	85	C		2	10	SR	Cueva	18	Saco	Flujo de dientes	R4	22-jun.		
E59	610.663	7566280	46417	Dicielsa	264	84	ACilia		1	3	SR	Escañón	18	Saco	Flujo de dientes	R4	22-jun.		
E59	610.663	7566280	46417	Dicielsa	10	65	D		1	2	SR	Plana	6	Saco	Flujo de dientes	R4	22-jun.		
E59	610.663	7566280	46417	Dicielsa	70	21	D		2	1	SR	Plana	6	Saco	Flujo de dientes	R4	22-jun.		
E59	610.663	7566280	46417	Dicielsa	4	10	C		3	1	SR	Plana	6	Saco	Flujo de dientes	R4	22-jun.		
E59	610.663	7566280	46417	Dicielsa	87	66	D		1	2	SR	Plana	12	Saco	Flujo de dientes	R4	22-jun.		
E59	610.663	75662819	46533	Dicielsa	63	108	D		3	0.5	SR	Plana	12	Saco	Flujo de dientes	R4	22-jun.		

Base de datos

Página 14

Annex XVI Appendix B



DIRECCIÓN TÉCNICA DE PROSPECCIÓN Y EXPLORACIÓN
ESTUDIO GEOLÓGICO-ESTRUCTURAL DEL ÁREA
CIRCUNDANTE DEL MANANTIAL DEL SISALÁ*

PTO.	ESTE	NORTE	ELEV.	TIPO	Az	Bz	DipDir	Pitch	CONTINUADO	PERSISTENCIA	ABERTURA	(mm)	RELLENO	FORMA	JRC	AGUA	TIPO ROCA	ALTERACION	DUREZA	FECHA	NOTAS
e-596	610,945	7,568,419	4653	Diciplsa	109	86	19		C	1	3		Arenas	Plana	12	Seco	Diciplsa		R4	223un.	
e-596	610,945	7,568,419	4653	Diciplsa	40	323			C	2	1,5		Arenas	Escalonada	10	Seco	Diciplsa		R4	223un.	
e-596	610,945	7,568,419	4653	Diciplsa	60	200			D	3	3		Arenas	Plana	10	Seco	Diciplsa		R4	223un.	
e-597	610,923	7,568,529	4649	Diciplsa	61	94			D	1	0,3		SR	Plana	10	Seco	Diciplsa		R4	223un.	
e-597	610,923	7,568,529	4649	Diciplsa	56	131			D	1	0,2		SP	Escalonada	14	Seco	Diciplsa		R4	223un.	
e-597	610,923	7,568,529	4649	Diciplsa	206	63	246		C	2	5		Arenas	Plana	16	Seco	Diciplsa		R4	223un.	
e-597	610,923	7,568,529	4649	Diciplsa	65	355			C	1	10		Arenas	Plana	10	Seco	Diciplsa		R4	223un.	
e-597	610,923	7,568,529	4649	Diciplsa	40	3			C	1	5		SR	Plana	12	Seco	Diciplsa		R4	223un.	
e-597	610,923	7,568,529	4649	Diciplsa	125	70			D	2	0,3		SR	Plana	14	Seco	Diciplsa		R4	223un.	
e-599	609,848	7,568,700	4669	Diciplsa	75	282			D	1	0,5		SR	Curva	10	Seco	Diciplsa		R4	223un.	
e-599	609,848	7,568,700	4669	Diciplsa	35	73			D	2	1		Arenas	Plana	8	Seco	Diciplsa		R4	223un.	
e-599	609,848	7,568,700	4669	Diciplsa	83	98			D	1	0,5		SR	Plana	8	Seco	Diciplsa		R4	223un.	
e-599	609,848	7,568,700	4669	Diciplsa	185	76			D	2	2		SR	Escalonada	12	Seco	Diciplsa		R4	223un.	
e-599	609,848	7,568,700	4669	Diciplsa	328	72	58		D	2	0,5		SR	Escalonada	14	Seco	Diciplsa		R4	223un.	
i61	610,268	7,567,991	4643	Diciplsa	82	50			C	3	0,8		SR	Escalonada	14	Seco	Diciplsa		R4	223un.	
i61	610,268	7,567,991	4643	Diciplsa	73	212			C	5	5		SR	Escalonada	14	Seco	Diciplsa		R4	223un.	
i61	610,268	7,567,994	4643	Diciplsa	79	18			C	2	7		SR	Escalonada	14	Seco	Diciplsa		R4	223un.	
i61	610,268	7,567,995	4643	Diciplsa	71	370			C	2	30		SR	Escalonada	14	Seco	Diciplsa		R4	223un.	
i61	610,268	7,567,995	4643	Diciplsa	51	78			C	6	0,3		SR	Plana	4	Seco	Diciplsa		R4	223un.	
i62	609,945	7,567,984	4638	Diciplsa	55	308			C	1	1,5		SR	Ondulada	5	Seco	Diciplsa		R4	223un.	
i62	609,945	7,567,984	4638	Diciplsa	78	275			C	1	3		SR	Ondulada	8	Seco	Diciplsa		R4	223un.	
i62	609,945	7,567,984	4638	Diciplsa	82	82			C	3	10		SR	Ondulada	4	Seco	Diciplsa		R4	223un.	
i62	609,945	7,567,984	4638	Diciplsa	37	4			C	2	0,5		SR	Es calonada	14	Seco	Diciplsa		R4	223un.	
i63	609,763	7,568,186	4625	Diciplsa	53	314			C	4	0,5		SR	Ondulada	8	Seco	Diciplsa		R4	223un.	
i63	609,763	7,568,187	4625	Diciplsa	58	80			C	5	1		SR	Plana	4	Seco	Diciplsa		R4	223un.	
i63	609,763	7,568,187	4625	Diciplsa	46	342			C	6	0,5		SR	Ondulada	8	Seco	Diciplsa		R4	223un.	
i63	609,763	7,568,188	4626	Diciplsa	88	154			C	1	10		SR	Ondulada	8	Seco	Diciplsa		R4	223un.	
i63	609,763	7,568,191	4627	Diciplsa	83	194			C	4	15		SR	Escalonada	14	Seco	Diciplsa		R4	223un.	
i63	609,500	7,568,555	4719	Diciplsa	90	150			D	3	0		SR	Plana	8	Seco	Diciplsa		R4	223un.	
i63	609,500	7,568,555	4719	Diciplsa	80	142			D	1	0		SR	Plana	8	Seco	Diciplsa		R4	223un.	
i63	609,500	7,568,555	4719	Diciplsa	64	145			D	2	4		SR	Plana	8	Seco	Diciplsa		R4	223un.	
i63	609,500	7,568,555	4719	Diciplsa	72	165			D	0	0		SR	Plana	8	Seco	Diciplsa		R4	223un.	
i63	609,500	7,568,555	4719	Diciplsa	80	50			D	3	0		SR	Plana	8	Seco	Diciplsa		R4	223un.	
i62	609,500	7,568,555	4719	Diciplsa	88	175			D	2	0		SR	Plana	8	Seco	Diciplsa		R4	223un.	
i62	609,500	7,568,555	4719	Diciplsa	60	25			D	2	0		SR	Plana	8	Seco	Diciplsa		R4	223un.	
i63	609,500	7,568,555	4719	Diciplsa	55	155			D	2	0		SR	Plana	8	Seco	Diciplsa		R4	223un.	
i63	609,500	7,568,555	4719	Diciplsa	82	25			D	1	10		SR	Plana	8	Seco	Diciplsa		R4	223un.	
i63	609,500	7,568,555	4719	Diciplsa	79	335			D	3	3		SR	Plana	8	Seco	Diciplsa		R4	223un.	
i63	609,500	7,568,555	4719	Diciplsa	61	30			D	2	0		SR	Plana	8	Seco	Diciplsa		R4	223un.	
i64	609,642	7,570,190	4779	Diciplsa	315	72			D	3	10		SR	Plana	8	Seco	Diciplsa		R4	223un.	
i64	609,642	7,570,190	4779	Diciplsa	88	164			D	2	25		SR	Plana	8	Seco	Diciplsa		R4	223un.	
i64	609,642	7,570,190	4779	Diciplsa	89	162			D	2	25		SR	Plana	8	Seco	Diciplsa		R4	223un.	
i64	609,642	7,570,190	4779	Diciplsa	79	165			D	0	0		SR	Plana	8	Seco	Diciplsa		R4	223un.	
i64	609,642	7,570,190	4779	Diciplsa	84	169			D	2	0		SR	Plana	8	Seco	Diciplsa		R4	223un.	
i64	609,642	7,570,190	4779	Diciplsa	83	161			D	3	0		SR	Plana	8	Seco	Diciplsa		R4	223un.	
i64	609,642	7,570,190	4779	Diciplsa	82	160			D	2	0		SR	Plana	8	Seco	Diciplsa		R4	223un.	
i64	609,642	7,570,190	4779	Diciplsa	84	155			D	2	0		SR	Plana	8	Seco	Diciplsa		R4	223un.	
i64	609,642	7,570,190	4779	Diciplsa	84	155			D	2	0		SR	Plana	8	Seco	Diciplsa		R4	223un.	
i64	609,642	7,570,190	4779	Diciplsa	84	155			D	2	0		SR	Plana	8	Seco	Diciplsa		R4	223un.	
i64	609,642	7,570,190	4779	Diciplsa	84	155			D	2	0		SR	Plana	8	Seco	Diciplsa		R4	223un.	
i64	609,642	7,570,190	4779	Diciplsa	84	155			D	2	0		SR	Plana	8	Seco	Diciplsa		R4	223un.	
i64	609,642	7,570,190	4779	Diciplsa	84	155			D	2	0		SR	Plana	8	Seco	Diciplsa		R4	223un.	
i64	609,642	7,570,190	4779	Diciplsa	84	155			D	2	0		SR	Plana	8	Seco	Diciplsa		R4	223un.	
i64	609,642	7,570,190	4779	Diciplsa	84	155			D	2	0		SR	Plana	8	Seco	Diciplsa		R4	223un.	
i64	609,642	7,570,190	4779	Diciplsa	84	155			D	2	0		SR	Plana	8	Seco	Diciplsa		R4	223un.	
i64	609,642	7,570,190	4779	Diciplsa	84	155			D	2	0		SR	Plana	8	Seco	Diciplsa		R4	223un.	
i64	609,642	7,570,190	4779	Diciplsa	84	155			D	2	0		SR	Plana	8	Seco	Diciplsa		R4	223un.	
i64	609,642	7,570,190	4779	Diciplsa	84	155			D	2	0		SR	Plana	8	Seco	Diciplsa		R4	223un.	
i64	609,642	7,570,190	4779	Diciplsa	84	155			D	2	0		SR	Plana	8	Seco	Diciplsa		R4	223un.	
i64	609,642	7,570,190	4779	Diciplsa	84	155			D	2	0		SR	Plana	8	Seco	Diciplsa		R4	223un.	
i64	609,642	7,570,190	4779	Diciplsa	84	155			D	2	0		SR	Plana	8	Seco	Diciplsa		R4	223un.	
i64	609,642	7,570,190	4779	Diciplsa	84	155			D	2	0		SR	Plana	8	Seco	Diciplsa		R4	223un.	
i64	609,642	7,570,190	4779	Diciplsa	84	155			D	2	0		SR	Plana	8	Seco	Diciplsa		R4	223un.	
i64	609,642	7,570,190	4779	Diciplsa	84	155			D	2	0		SR	Plana	8	Seco	Diciplsa		R4	223un.	
i64	609,642	7,570,190	4779	Diciplsa	84	155			D	2	0		SR	Plana	8	Seco	Diciplsa		R4	223un.	
i64	609,642	7,570,190	4779	Diciplsa	84	155			D	2	0		SR	Plana	8	Seco	Diciplsa		R4	223un.	
i64	609,642	7,570,190	4779	Diciplsa	84	155			D	2	0		SR	Plana	8	Seco	Diciplsa		R4	223un.	
i64	609,642	7,570,190	4779	Diciplsa	84	155			D	2	0		SR	Plana	8	Seco	Diciplsa		R4	223un.	
i64	609,642	7,570,190	4779	Diciplsa	84	155			D	2	0		SR	Plana	8	Seco	Diciplsa		R4	223un.	
i64	609,642	7,570,190	4779	Diciplsa	84	155			D	2	0		SR	Plana	8	Seco	Diciplsa		R4	223un.	
i64	609,642	7,570,190	4779	Diciplsa	84	155			D	2	0		SR	Plana	8	Seco	Diciplsa		R4	223un.	
i64	609,642	7,570,190	4779	Diciplsa	84	155			D	2	0		SR	Plana	8	Seco	Diciplsa		R4	223un.	
i64	609,642	7,570,190	4779	Diciplsa	84	155			D	2	0		SR	Plana	8	Seco	Diciplsa		R4	223un.	
i64	609,642	7,570,190	4779	Diciplsa	84	155			D	2	0		SR	Plana	8	Seco	Diciplsa				

**DIRECCIÓN TÉCNICA DE PROSPECCIÓN Y EXPLORACIÓN
"ESTUDIO GEOLÓGICO-ESTRUCTURAL DEL ÁREA
CIRCUNDANTE DEL MANANTIAL DEL SISAL"**



PTO.	ESTE	NORTE	ELEV.	Az.	Bz.	DipDir	Ptch	CONTINUADO	PERSISTENCIA	ABERTURA	(mm)	RELLENO	FORMA	JRC	AGUA	TIPO ROCA	ALTERACION	DUREZA	FECHA	OBSERVACIONES
L429	6029309	7365155	7433	Diciplsa	80	300	D	2	4	SR	Orindida	S	Saco	Diciplsa-Ardenita	R4	223u.n.				
L431	6029309	7365155	7433	Diciplsa	80	305	C	1	15	SR	Plana	S	Saco	Diciplsa-Ardenita	R4	223u.n.				
L432	6029309	7365155	7433	Diciplsa	85	326	C	2	30	SR	Plana	S	Saco	Diciplsa-Ardenita	R4	223u.n.				
L433	6029311	7365155	46558	Diciplsa	70	156	D	1	10	SR	Plana	S	Saco	Diciplsa-Ardenita	R4	223u.n.				
L435	6029311	7365155	46558	Diciplsa	84	15	D	2	10	SR	Plana	S	Saco	Diciplsa-Ardenita	R4	223u.n.				
L436	6029305	7365155	46531	Diciplsa	61	5	C	5	20	SR	Plana	S	Saco	Diciplsa-Ardenita	R4	223u.n.				
L437	6029305	7365155	46541	Diciplsa	85	224	C	4	10	SR	Plana	S	Saco	Diciplsa-Ardenita	R4	223u.n.				
M74	6131369	7365155	46542	Diciplsa	84	335	C	3	2	SR	Arenas	S	Saco	Diciplsa-Ardenita	R4	223u.n.				
M74	6131369	7365155	46542	Diciplsa	52	278	C	1	0.5	SR	Plana	S	Saco	Diciplsa-Ardenita	R4	223u.n.				
M75	6131369	7365155	46542	Diciplsa	80	30	C	2	1	SR	Arenas	S	Saco	Diciplsa-Ardenita	R4	223u.n.				
M75	6131361	73651086	46444	Diciplsa	65	122	C	3	1	ACilla	Plana	S	Saco	Diciplsa-Ardenita	R4	223u.n.				
M76	6131320	73651089	46449	Diciplsa	81	45	C	1	0.8	SR	Plana	S	Saco	Diciplsa-Ardenita	R4	223u.n.				
M76	6131320	73651089	46449	Diciplsa	79	149	C	2	0.5	SR	Arenas	S	Saco	Diciplsa-Ardenita	R4	223u.n.				
M77	6010235	73651114	46415	Diciplsa	82	48	D	5	10	SR	Plana	S	Saco	Diciplsa-Ardenita	R4	223u.n.				
M77	6010235	73651114	46415	Diciplsa	82	337	D	2	2	SR	Plana	S	Saco	Diciplsa-Ardenita	R4	223u.n.				
M78	6010235	73651114	46415	Diciplsa	87	235	C	4	0.4	SR	Es calonida	S	Saco	Diciplsa-Ardenita	R4	223u.n.				
M78	6010235	73651134	46415	Diciplsa	43	285	D	4	3	SR	Es calonida	S	Saco	Diciplsa-Ardenita	R4	223u.n.				
M78	6010238	73651134	46439	Diciplsa	72	8	D	3	0.5	SR	Plana	S	Saco	Diciplsa-Ardenita	R4	223u.n.				
M78	6010238	73651134	46439	Diciplsa	74	145	C	3	5	SR	Arenas	S	Saco	Diciplsa-Ardenita	R4	223u.n.				
M78	6010238	73651134	46439	Diciplsa	74	15	C	4	5.5	SR	Plana	S	Saco	Diciplsa-Ardenita	R4	223u.n.				
M79	6029300	73651155	43335	Diciplsa	95	73	C	2	2	SR	Plana	S	Saco	Diciplsa-Ardenita	R4	223u.n.				
M79	6029300	73651155	43335	Diciplsa	165	63	D	2	0.4	SR	Plana	S	Saco	Diciplsa-Ardenita	R4	223u.n.				
M80	6029793	73651183	46331	Diciplsa	52	12	C	3	2	SR	Plana	S	Saco	Diciplsa-Ardenita	R4	223u.n.				
M80	6029793	73651183	46331	Diciplsa	83	260	C	4	3	SR	Plana	S	Saco	Diciplsa-Ardenita	R4	223u.n.				
M80	6029793	73651183	46331	Diciplsa	55	220	D	3	2	SR	Plana	S	Saco	Diciplsa-Ardenita	R4	223u.n.				
M81	6029500	73651555	47119	Diciplsa	76	340	C	5	0	SR	Plana	S	Saco	Diciplsa-Ardenita	R4	223u.n.				
M81	6029500	73651555	47119	Falla	80	5	D	1	80	SR	Plana	S	Saco	Diciplsa-Ardenita	R4	223u.n.				
M82	6029500	73651555	47119	Falla	80	185	D	1	0	SR	Plana	S	Saco	Diciplsa-Ardenita	R4	223u.n.				
M82	6029500	73651555	47119	Falla	85	187	D	1	0	SR	Plana	S	Saco	Diciplsa-Ardenita	R4	223u.n.				
M82	6029500	73651555	47119	Falla	59	40	D	1	0	SR	Plana	S	Saco	Diciplsa-Ardenita	R4	223u.n.				
M82	6029502	73651050	47119	Falla	80	10	20	D	1	15	SR	Plana	S	Saco	Diciplsa-Ardenita	R4	223u.n.			
M82	6029502	73651050	47119	Falla	89	118	D	2	4	SR	Plana	S	Saco	Diciplsa-Ardenita	R4	223u.n.				
M83	6101046	73651444	48522	Falla	42	128	D	1	0	SR	Plana	S	Saco	Diciplsa-Ardenita	R4	223u.n.				
M83	6101046	73651444	48522	Falla	10	212	D	1	0	SR	Plana	S	Saco	Diciplsa-Ardenita	R4	223u.n.				
M83	6101046	73651444	48522	Falla	89	145	D	1	10	SR	Plana	S	Saco	Diciplsa-Ardenita	R4	223u.n.				
M84	6101046	73651444	48522	Falla	45	280	C	320	0.5	SR	Plana	S	Saco	Diciplsa-Ardenita	R4	223u.n.				
M84	6101046	73651444	48522	Falla	41	320	C	320	0.5	SR	Plana	S	Saco	Diciplsa-Ardenita	R4	223u.n.				
M85	6101049	73651419	46533	Peudotraficación	82	131	C	56	68	SR	Plana	S	Saco	Diciplsa-Ardenita	R4	223u.n.				
M85	6101049	73651419	46533	Peudotraficación	245	78	C	315	0.5	SR	Plana	S	Saco	Diciplsa-Ardenita	R4	223u.n.				
M86	6029898	73651700	46659	Peudotraficación	86	17	C	26	0.5	SR	Plana	S	Saco	Diciplsa-Ardenita	R4	223u.n.				
M86	6029898	73651984	46538	Peudotraficación	85	195	D	1	25	SR	Orindida	S	Saco	Diciplsa-Ardenita	R4	223u.n.				
M86	6029898	73651984	46538	Peudotraficación	63	230	C	3	2	SR	Orindida	S	Saco	Diciplsa-Ardenita	R4	223u.n.				
M87	6029890	73651555	47119	Psautodestrificación	75	100	C	45	40	SR	Plana	S	Saco	Diciplsa-Ardenita	R4	223u.n.				
M87	6029890	73651555	47119	Psautodestrificación	52	300	C	5	1	SR	Plana	S	Saco	Diciplsa-Ardenita	R4	223u.n.				
M87	6029890	73651555	47119	Psautodestrificación	62	182	C	4	0.5	SR	Plana	S	Saco	Diciplsa-Ardenita	R4	223u.n.				
M87	6029890	73651555	47119	Psautodestrificación	65	188	D	2	1	SR	Plana	S	Saco	Diciplsa-Ardenita	R4	223u.n.				
M88	6029897	73651444	46538	Psautodestrificación	88	310	C	3	7	SR	Orindida	S	Saco	Aribolitas	R4	123u.jl.				
M88	6029897	73651444	46538	Psautodestrificación	85	195	D	1	25	SR	Orindida	S	Saco	Aribolitas	R4	123u.jl.				
M89	6029111	73651636	45566	Diciplsa	74	320	D	2	0.5	SR	Plana	S	Saco	Diciplsa-Ardenita	R4	123u.jl.				
M89	6029111	73651636	45566	Diciplsa	75	305	D	3	0.5	SR	Rugosa	S	Saco	Diciplsa-Ardenita	R4	123u.jl.				
M90	6029110	73651634	45567	Diciplsa	46417	Peudotraficación	52	300	5	SR	Es calonida	S	Saco	Diciplsa-Ardenita	R4	123u.jl.				
M90	6029110	73651634	45567	Diciplsa	4545	Peudotraficación	62	182	4	SR	Rugosa	S	Saco	Diciplsa-Ardenita	R4	123u.jl.				
M91	6029110	73651634	45567	Diciplsa	4544	Peudotraficación	65	188	2	SR	Es calonida	S	Saco	Diciplsa-Ardenita	R4	123u.jl.				
M91	6029111	73651759	46538	Psautodestrificación	48	35	C	35	0.5	SR	Plana	S	Saco	Diciplsa-Ardenita	R4	123u.jl.				
M92	6029123	73651831	46033	Diciplsa	85	195	D	1	25	SR	Orindida	S	Saco	Aribolitas	R4	123u.jl.				
M92	6029123	73651831	46033	Diciplsa	63	230	C	3	2	SR	Orindida	S	Saco	Aribolitas	R4	123u.jl.				
M93	6029111	73651636	45566	Diciplsa	75	305	D	3	0.5	SR	Plana	S	Saco	Diciplsa-Ardenita	R4	123u.jl.				
M93	6029111	73651636	45566	Diciplsa	45567	Peudotraficación	52	300	5	SR	Rugosa	S	Saco	Diciplsa-Ardenita	R4	123u.jl.				
M94	6131165	73651918	7913	Psautodestrificación	45	40	C	45	40	SR	Plana	S	Saco	Diciplsa-Ardenita	R4	123u.jl.				
M94	6131165	73651918	48522	Psautodestrificación	36	153	C	48	35	SR	Plana	S	Saco	Diciplsa-Ardenita	R4	123u.jl.				
M94	6131165	73651918	48522	Psautodestrificación	48	35	C	48	35	SR	Plana	S	Saco	Diciplsa-Ardenita	R4	123u.jl.				
M95	6131165	73651918	48522	Psautodestrificación	45	40	C	45	40	SR	Plana	S	Saco	Diciplsa-Ardenita	R4	123u.jl.				
M95	6131165	73651918	48522	Psautodestrificación	45	40	C	45	40	SR	Plana	S	Saco	Diciplsa-Ardenita	R4	123u.jl.				
M96	6131165	73651918	48522	Psautodestrificación	45	40	C	45	40	SR	Plana	S	Saco	Diciplsa-Ardenita	R4	123u.jl.				
M96	6131165	73651918	48522	Psautodestrificación	45	40	C	45	40	SR	Plana	S	Saco	Diciplsa-Ardenita	R4	123u.jl.				
M97	6131165	73651918	48522	Psautodestrificación	45	40	C	45	40	SR	Plana	S	Saco	Diciplsa-Ardenita	R4	123u.jl.				
M97	6131165	73651918	48522	Psautodestrificación	45	40	C	45	40	SR	Plana	S	Saco	Diciplsa-Ardenita	R4	123u.jl.				
M98	6131165	73651918	48522	Psautodestrificación	45	40	C	45	40	SR	Plana	S	Saco	Diciplsa-Ardenita	R4	123u.jl.				
M98	6131165	73651918	48522	Psautodestrificación	45	40	C	45	40	SR	Plana	S	Saco	Diciplsa-Ardenita	R4	123u.jl.				
M99	6131165	73651918	48522	Psautodestrificación	45	40	C	45	40	SR	Plana	S	Saco	Diciplsa-Ardenita	R4	123u.jl.				
M99	6131165	73651918	48522	Psautodestrificación	45	40	C	45	40	SR	Plana	S	Saco	Diciplsa-Ardenita	R4	123u.jl.				
M100	6131165	73651918	48522	Psautodestrificación	45	40	C	45	40	SR	Plana	S	Saco	Diciplsa-Ardenita	R4	123u.jl.				
M100	6131165	73651918	48522	Psautodestrificación	45	40	C	45	40	SR	Plana	S	Saco	Diciplsa-Ardenita	R4	123u.jl.				
M101	6131165	73651918	48522	Psautodestrificación	45	40	C	45	40	SR	Plana	S	Saco	Diciplsa-Ardenita	R4	123u.jl.				
M101	6131165	73651918	48522	Psautodestrificación	45	40	C	45	40	SR	Plana	S	Saco	Diciplsa-Ardenita	R4	123u.jl.				
M102	6131165	73651918	48522	Psautodestrificación	45	40	C	45	40	SR	Plana	S	Saco	Diciplsa-Ardenita	R4	123u.jl.				
M102	6131165	73651918	48522	Psautodestrificación	45	40	C	45	40	SR	Plana	S	Saco	Diciplsa-Ardenita	R4	123u.jl.				

PTO.	ESTE	NORTE	ELEV.	Az.	Bz.	DipDir	Pitch	CONTINUADO	PERSISTENCIA (10m)	ABERTURA (10m)	REllENO	FORMA	JRC	Agua	Tipo Rocas	Altitud	Dureza	Fecha	OBSERVACIONES
D-4	6030116	73650259	4552	Diccionaria	86	183	C	3	1	2	SR	Pana/Ondulada	6	Seco	Arribadas	R4	12-ju		
D-4	6030116	73650259	4552	Diccionaria	80	280	D	4	2	SR	Rugosa	8	Seco	Arribadas	R4	12-ju			
D-5	6030105	73650195	4551	Diccionaria	66	15	D	1	0	SR	Plana	5	Seco	Arribadas	R4	12-ju			
D-5	6030105	73650195	4551	Diccionaria	65	35	D	1	0	SR	Plana	4	Seco	Arribadas	R4	12-ju			
D-6	6030047	73650138	4558	Diccionaria	66	215	C	3	0	SR	Rugosa	4	Seco	Arribadas	R4	12-ju			
D-6	6030047	73650138	4558	Diccionaria	66	210	C	1	0	SR	Rugosa	4	Seco	Arribadas	R4	12-ju			
D-8	60303050	73650898	4556	Diccionaria	85	250	C	4	1.5	SR	Ondulada	8	Seco	Arribadas	R4	12-ju			
D-8	60303050	73650898	4556	Diccionaria	85	300	C	2	5	SR	Plana	4	Seco	Arribadas	R4	12-ju			
D-9	6030024	73650653	4554	Diccionaria	72	352	C	4	2	SR	Ondulada	5	Seco	Arribadas	R4	12-ju			
D-9	6030024	73650653	4554	Diccionaria	82	265	D	1	1	SR	Plana	4	Seco	Arribadas	R4	12-ju			
L-39	6020390	73660102	4458	Diccionaria	85	345	D	3	5	SR	Ductiles	6	Seco	Ductiles	R4	12-ju			
L-39	6020390	73660102	4458	Diccionaria	80	340	D	4	2	SR	Ductiles	6	Seco	Ductiles	R4	12-ju			
L-40	6020390	73660102	4458	Diccionaria	87	336	D	2	0	SR	Ondulada	6	Seco	Ductiles	R4	12-ju			
L-41	6020390	73660102	4458	Diccionaria	82	210	D	1	0	SR	Ondulada	6	Seco	Ductiles	R4	12-ju			
L-43	6020390	73660102	4458	Diccionaria	82	176	D	5	0	SR	Ondulada	6	Seco	Ductiles	R4	12-ju			
L-44	6020390	73660102	4458	Diccionaria	80	193	D	0	0	SR	Ondulada	6	Seco	Ductiles	R4	12-ju			
L-45	6020390	73660102	4458	Diccionaria	74	222	D	2	0	SR	Ondulada	6	Seco	Ductiles	R4	12-ju			
L-46	6020390	73660102	4458	Diccionaria	72	318	D	3	0	SR	Plana	6	Seco	Ductiles	R4	12-ju			
L-47	6020390	73660102	4458	Diccionaria	83	327	C	2	5	SR	Ondulada	6	Seco	Ductiles	R4	12-ju			
L-48	6020390	73660102	4458	Diccionaria	86	348	C	6	3	SR	Ondulada	6	Seco	Ductiles	R4	12-ju			
L-49	6020735	7366198	4462	Diccionaria	70	180	D	4	2	SR	Plana	6	Seco	Ductiles	R4	12-ju			
L-50	6020735	7366198	4462	Diccionaria	61	344	D	2	0	SR	Ondulada	6	Seco	Ductiles	R4	12-ju			
L-52	6020735	7366198	4462	Diccionaria	81	110	D	3	2	SR	Ondulada	6	Seco	Ductiles	R4	12-ju			
L-53	6020735	7366198	4462	Diccionaria	88	40	C	2	8	SR	Plana	6	Seco	Ductiles	R4	12-ju			
L-54	6020735	7366198	4462	Diccionaria	72	300	D	3	4	SR	Plana	6	Seco	Ductiles	R4	12-ju			
L-55	6020735	7366198	4462	Diccionaria	80	342	D	2	2	SR	Plana	6	Seco	Ductiles	R4	12-ju			
L-55	6020735	7366198	4462	Diccionaria	72	328	D	1	0	SR	Plana	6	Seco	Ductiles	R4	12-ju			
L-56	6020735	7366198	4462	Diccionaria	86	348	C	6	3	SR	Plana	6	Seco	Ductiles	R4	12-ju			
L-49	6020735	7366198	4462	Diccionaria	70	180	D	4	2	SR	Plana	6	Seco	Ductiles	R4	12-ju			
L-50	6020735	7366198	4462	Diccionaria	61	344	D	2	0	SR	Ondulada	6	Seco	Ductiles	R4	12-ju			
L-52	6020735	7366198	4462	Diccionaria	81	110	D	3	2	SR	Plana	6	Seco	Ductiles	R4	12-ju			
L-53	6020735	7366198	4462	Diccionaria	88	40	C	2	8	SR	Plana	6	Seco	Ductiles	R4	12-ju			
L-54	6020735	7366198	4462	Diccionaria	72	300	D	3	4	SR	Plana	6	Seco	Ductiles	R4	12-ju			
L-55	6020735	7366198	4462	Diccionaria	80	342	D	2	2	SR	Plana	6	Seco	Ductiles	R4	12-ju			
L-55	6020735	7366198	4462	Diccionaria	72	328	D	1	0	SR	Plana	6	Seco	Ductiles	R4	12-ju			
L-56	6020735	7366198	4462	Diccionaria	86	348	C	6	3	SR	Plana	6	Seco	Ductiles	R4	12-ju			
L-57	6020683	7366286	4434	Diccionaria	68	182	D	5	0	SR	Plana	6	Seco	Ductiles	R4	12-ju			
L-61	6020683	7366286	4434	Diccionaria	62	193	D	4	0	SR	Plana	6	Seco	Ductiles	R4	12-ju			
L-62	6020683	7366286	4434	Diccionaria	65	174	D	3	0	SR	Plana	6	Seco	Ductiles	R4	12-ju			
L-63	6020683	7366286	4434	Diccionaria	68	228	D	3	2	SR	Plana	6	Seco	Ductiles	R4	12-ju			
L-64	6020683	7366286	4434	Diccionaria	54	211	D	2	2	SR	Plana	6	Seco	Ductiles	R4	12-ju			
L-65	6020683	7366286	4434	Diccionaria	85	234	D	3	0	SR	Plana	6	Seco	Ductiles	R4	12-ju			
L-66	6020683	7366286	4434	Diccionaria	81	280	D	4	0	SR	Plana	6	Seco	Ductiles	R4	12-ju			
L-67	6020683	7366286	4434	Diccionaria	69	284	D	2	2	SR	Plana	6	Seco	Ductiles	R4	12-ju			
L-68	6020683	7366286	4434	Diccionaria	69	295	D	4	0	SR	Plana	6	Seco	Ductiles	R4	12-ju			
L-69	6020683	7366286	4434	Diccionaria	87	330	D	5	2	SR	Plana	6	Seco	Ductiles	R4	12-ju			
L-70	6020683	7366286	4434	Diccionaria	85	248	D	5	2	SR	Plana	6	Seco	Ductiles	R4	12-ju			
L-71	6020683	7366286	4434	Diccionaria	60	273	D	2	2	SR	Plana	6	Seco	Ductiles	R4	12-ju			
L-72	6020683	7366286	4434	Diccionaria	45	92	D	4	0	SR	Plana	6	Seco	Ductiles	R4	12-ju			
L-73	6020683	7366286	4434	Diccionaria	73	115	D	5	4	SR	Plana	6	Seco	Ductiles	R4	12-ju			
L-74	6020683	7366286	4434	Diccionaria	76	163	D	4	1	SR	Plana	6	Seco	Ductiles	R4	12-ju			
L-75	6020683	7366286	4434	Diccionaria	82	144	D	3	1	SR	Plana	6	Seco	Ductiles	R4	12-ju			
L-76	6020683	7366286	4434	Diccionaria	84	109	D	2	0	SR	Plana	6	Seco	Ductiles	R4	12-ju			
L-77	6020683	7366286	4434	Diccionaria	80	26	D	3	0	SR	Plana	6	Seco	Ductiles	R4	12-ju			
L-78	6020683	7366286	4434	Diccionaria	65	26	D	3	10	SR	Ondulada	6	Seco	Ductiles	R4	12-ju			
L-79	6020683	7366286	4434	Diccionaria	82	39	D	2	1	SR	Plana	6	Seco	Ductiles	R4	12-ju			
L-80	6020683	7366286	4434	Diccionaria	64	75	D	4	2	SR	Plana	6	Seco	Ductiles	R4	12-ju			
L-81	6020683	7366286	4434	Diccionaria	75	136	D	2	0	SR	Plana	6	Seco	Ductiles	R4	12-ju			
L-82	6020683	7366286	4434	Diccionaria	70	30	D	6	0	SR	Plana	6	Seco	Ductiles	R4	12-ju			
L-83	6020683	7366286	4434	Diccionaria	68	150	D	2	0	SR	Plana	6	Seco	Ductiles	R4	12-ju			
L-84	6020683	7366286	4434	Diccionaria	88	146	D	6	0	SR	Plana	6	Seco	Ductiles	R4	12-ju			
L-85	6020683	7366286	4434	Diccionaria	85	174	D	3	4	SR	Plana	6	Seco	Ductiles	R4	12-ju			
L-86	6020683	7366286	4434	Diccionaria	79	172	D	4	1	SR	Plana	6	Seco	Ductiles	R4	12-ju			
L-87	6020683	7366286	4434	Diccionaria	61	3	D	3	0	SR	Plana	6	Seco	Ductiles	R4	12-ju			
L-88	6020683	7366286	4434	Diccionaria	80	91	D	2	2	SR	Plana	6	Seco	Ductiles	R4	12-ju			
L-89	6020683	7366286	4434	Diccionaria	80	9	D	5	3	SR	Plana	6	Seco	Ductiles	R4	12-ju			
L-90	6020683	7366286	4434	Diccionaria	79	10	D	4	3	SR	Plana	6	Seco	Ductiles	R4	12-ju			
L-91	6020683	7366286	4434	Diccionaria	82	362	D	3	0	SR	Plana	6	Seco	Ductiles	R4	12-ju			
L-92	6020683	7366286	4434	Diccionaria	72	145	D	3	0	SR	Plana	7	Seco	Ductiles	R4	12-ju			
L-93	6020683	7366286	4434	Diccionaria	88	362	D	4	3	SR	Plana	6	Seco	Ductiles	R4	12-ju			
L-94	601903	7366630	4460	Diccionaria	72	145	D	3	0	SR	Plana	7	Seco	Ductiles	R4	12-ju			

**DIRECCIÓN TÉCNICA DE PROSPECCIÓN Y EXPLORACIÓN
"ESTUDIO GEOLÓGICO-ESTRUCTURAL DEL ÁREA
CIRCUNDANTE DEL MANANTIAL DEL SISAL"**



PTO.	ESTE	NORTE	ELEV.	TIPO	Az.	Bz.	DipDir	Pitch	CONTINUADO	PERSISTENCIA (10m)	ABERTURA (10m)	RELLENO	FORMA	JRC	ACUA	TIPO ROCA	ALTERACION	DUREZA	FECHA	NOTAS
L495	601.903	75666320	4450	Dicielsa	83	151.	D	5	SR	Plana	7	Seco	Dicielsa	R4	12-ju					
L496	601.903	75666320	4450	Dicielsa	66	285.	D	2	SR	Plana	7	Seco	Dicielsa	R4	12-ju					
L497	601.903	75666320	4450	Dicielsa	87	310.	D	3	SR	Plana	7	Seco	Dicielsa	R4	12-ju					
L498	601.903	75666320	4450	Dicielsa	84	255.	C	2	SR	Plana	7	Seco	Dicielsa	R4	12-ju					
L499	601.903	75666320	4450	Dicielsa	62	150.	C	4	0	SR	Plana	7	Seco	Dicielsa	R4	12-ju				
L500	601.903	75666320	4450	Dicielsa	87	160.	C	4	0	SR	Plana	7	Seco	Dicielsa	R4	12-ju				
L501	601.903	75666320	4450	Dicielsa	88	154.	D	3	0	SR	Plana	7	Seco	Dicielsa	R4	12-ju				
L502	601.903	75666320	4450	Dicielsa	80	154.	D	3	2	SR	Plana	7	Seco	Dicielsa	R4	12-ju				
L503	601.903	75666320	4450	Dicielsa	87	152.	D	2	3	SR	Plana	7	Seco	Dicielsa	R4	12-ju				
L504	601.903	75666320	4450	Dicielsa	75	158.	D	3	2	SR	Plana	7	Seco	Dicielsa	R4	12-ju				
L505	601.903	75666320	4450	Dicielsa	80	210.	D	2	4	SR	Plana	7	Seco	Dicielsa	R4	12-ju				
L506	601.758	75666320	4470	Dicielsa	87	100.	D	5	2	SR	Plana	6	Seco	Dicielsa	R4	12-ju				
L507	601.758	75666320	4470	Dicielsa	89	96.	D	4	1	SR	Plana	6	Seco	Dicielsa	R4	12-ju				
L508	601.758	75666320	4470	Dicielsa	88	92.	D	3	0	SR	Plana	6	Seco	Dicielsa	R4	12-ju				
L509	601.758	75666320	4470	Dicielsa	88	104.	D	2	5	SR	Plana	6	Seco	Dicielsa	R4	12-ju				
L510	601.758	75666320	4470	Dicielsa	85	102.	D	4	4	SR	Plana	6	Seco	Dicielsa	R4	12-ju				
L511	601.277	7567369	4507	Dicielsa	70	220.	D	5	0	SR	Plana	6	Seco	Dicielsa	R4	12-ju				
L512	601.277	7567369	4507	Dicielsa	85	224.	D	6	0	SR	Plana	6	Seco	Dicielsa	R4	12-ju				
L513	601.277	7567369	4507	Dicielsa	87	245.	D	5	15.	SR	Plana	6	Seco	Dicielsa	R4	12-ju				
L514	601.277	7567359	4507	Dicielsa	81	300.	D	4	5.	SR	Plana	6	Seco	Dicielsa	R4	12-ju				
L515	601.277	7567359	4507	Dicielsa	88	120.	D	6	6.	SR	Plana	6	Seco	Dicielsa	R4	12-ju				
L516	601.277	7567359	4507	Dicielsa	85	152.	D	3.	0	SR	Plana	6	Seco	Dicielsa	R4	12-ju				
L517	601.011	7567147	4470	Dicielsa	5	175.	D	1.	0	SR	Plana	6	Seco	Dicielsa	R4	12-ju				
L534	601.013	7567022	4471	Dicielsa	81	210.	D	7	6.	SR	Plana	6	Seco	Dicielsa	R4	12-ju				
L535	601.013	7567022	4471	Dicielsa	73	182.	D	6	8.	SR	Plana	6	Seco	Dicielsa	R4	12-ju				
L536	601.013	7567022	4471	Dicielsa	71	212.	D	4	0.	SR	Plana	6	Seco	Dicielsa	R4	12-ju				
L537	601.013	7567022	4471	Dicielsa	89	234.	D	3.	4.	SR	Plana	6	Seco	Dicielsa	R4	12-ju				
L538	601.013	7567022	4471	Dicielsa	87	214.	D	3.	3.	SR	Plana	6	Seco	Dicielsa	R4	12-ju				
M1	603.367	7568020	4519	Dicielsa	230	68.	D	4.	0.	SR	Plana	6	Seco	Escalonada	R4	12-ju				
M2	603.367	7568020	4519	Dicielsa	234	65.	D	5.	2.	SR	Arenas	6	Seco	Arribadas	R4	12-ju				
M3	603.367	7568016	4516	Dicielsa	237	63.	D	5.	2.	SR	Plana	4	Seco	Arribadas	R4	12-ju				
M4	603.367	7568016	4516	Dicielsa	85	347.	D	4.	1.	SR	Plana	4	Seco	Arribadas	R4	12-ju				
M5	603.367	7568016	4516	Dicielsa	198	108.	D	4.	2.	SR	Rugosa	3	Seco	Arribadas	R4	12-ju				
M6	603.367	7568017	4515	Dicielsa	186	49.	D	3.	1.	SR	Plana	12	Seco	Arribadas	R4	12-ju				
M7	603.367	7568017	4515	Dicielsa	234	324.	C	2.	3.	SR	Curva	12	Seco	Arribadas	R4	12-ju				
M8	603.367	7568017	4515	Dicielsa	231	321.	C	4.	3.	SR	Curva	14	Seco	Arribadas	R4	12-ju				
M9	603.367	7568017	4515	Dicielsa	285	315.	C	3.	2.	SR	Curva	14	Seco	Arribadas	R4	12-ju				
M10	603.367	7568017	4515	Dicielsa	239	74.	C	2.	4.	SR	Curva	12	Seco	Arribadas	R4	12-ju				
M11	603.367	7568017	4515	Dicielsa	198	82.	C	4.	2.	SR	Curva	10	Humedo	Arribadas	R4	12-ju				
M12	603.367	7567748	4509	Dicielsa	260	73.	C	2.	1.	SR	Plana	8	Seco	Arribadas	R4	12-ju				
M13	603.367	7567748	4509	Dicielsa	242	83.	C	3.	2.	SR	Plana	8	Seco	Arribadas	R4	12-ju				
M14	603.367	7567748	4509	Dicielsa	259	77.	C	4.	1.	SR	Plana	8	Seco	Arribadas	R4	12-ju				
M15	603.367	7567748	4509	Dicielsa	307	217.	C	3.	1.	SR	Plana	6	Seco	Arribadas	R4	12-ju				
M16	603.367	7567748	4509	Dicielsa	90	180.	C	10.	2.	SR	Plana	4	Seco	Arribadas	R4	12-ju				
M17	603.367	7567748	4509	Dicielsa	324	234.	C	4.	1.	SR	Plana	8	Seco	Arribadas	R4	12-ju				
M18	603.367	7568177	4540	Dicielsa	265	58.	C	2.	0.5.	SR	Plana	16	Seco	Arribadas	R4	12-ju				
M19	603.367	7568177	4540	Dicielsa	335	82.	C	4.	1.	SR	Plana	16	Seco	Arribadas	R4	12-ju				
M20	603.367	7568177	4540	Dicielsa	347	59.	C	2.	2.	SR	Plana	6	Seco	Arribadas	R4	12-ju				
M21	603.367	7568177	4540	Dicielsa	64.	116.	D	1.	0.	SR	Plana	6	Seco	Arribadas	R4	12-ju				
M22	603.367	7568177	4540	Dicielsa	87.	300.	D	1.	5.	SR	Plana	6	Seco	Arribadas	R4	12-ju				
M23	603.367	7568177	4540	Dicielsa	86.	318.	D	10.	5.	SR	Plana	6	Seco	Arribadas	R4	12-ju				
M24	603.367	7568177	4540	Dicielsa	89.	337.	D	1.	0.	SR	Plana	6	Seco	Arribadas	R4	12-ju				
M25	603.367	7568177	4540	Dicielsa	82.	343.	D	1.	0.	SR	Plana	6	Seco	Arribadas	R4	12-ju				
M26	603.367	7568177	4540	Dicielsa	76.	319.	D	1.	3.	SR	Plana	6	Seco	Arribadas	R4	12-ju				
M27	603.367	7568177	4540	Dicielsa	66.	110.	D	1.	1.	SR	Plana	6	Seco	Arribadas	R4	12-ju				
M28	603.367	7568266	4434	Falla	87.	300.	D	1.	5.	SR	Plana	6	Seco	Arribadas	R4	12-ju				
M29	603.367	7568266	4434	Falla	86.	318.	D	10.	5.	SR	Plana	6	Seco	Arribadas	R4	12-ju				
M30	603.367	7568266	4434	Falla	84.	337.	D	1.	0.	SR	Plana	6	Seco	Arribadas	R4	12-ju				
M31	603.367	7568266	4434	Falla	80.	154.	D	3.	0.	SR	Plana	6	Seco	Arribadas	R4	12-ju				
M32	603.367	7568266	4434	Falla	82.	141.	D	3.	0.	SR	Plana	6	Seco	Arribadas	R4	12-ju				
M33	603.367	7568266	4434	Falla	84.	141.	D	1.	0.	SR	Plana	6	Seco	Arribadas	R4	12-ju				
M34	603.367	7568266	4434	Falla	87.	159.	D	1.	2.	SR	Plana	4	Seco	Arribadas	R4	12-ju				
M35	603.367	7568266	4434	Falla	80.	155.	D	1.	0.	SR	Plana	6	Seco	Arribadas	R4	12-ju				
M36	603.367	7568266	4434	Falla	80.	155.	D	1.	0.	SR	Plana	6	Seco	Arribadas	R4	12-ju				
M37	603.367	7568266	4434	Falla	87.	155.	D	1.	0.	SR	Plana	6	Seco	Arribadas	R4	12-ju				
M38	603.367	7568266	4434	Falla	80.	155.	D	1.	0.	SR	Plana	6	Seco	Arribadas	R4	12-ju				
M39	603.367	7568266	4434	Falla	80.	155.	D	1.	0.	SR	Plana	6	Seco	Arribadas	R4	12-ju				
M40	603.367	7568266	4434	Falla	87.	155.	D	1.	0.	SR	Plana	6	Seco	Arribadas	R4	12-ju				
M41	603.367	7568266	4434	Falla	80.	155.	D	1.	0.	SR	Plana	6	Seco	Arribadas	R4	12-ju				
M42	603.367	7568266	4434	Falla	80.	155.	D	1.	0.	SR	Plana	6	Seco	Arribadas	R4	12-ju				
M43	603.367	7568266	4434	Falla	80.	155.	D	1.	0.	SR	Plana	6	Seco	Arribadas	R4	12-ju				
M44	603.367	7568266	4434	Falla	80.	155.	D	1.	0.	SR	Plana	6	Seco	Arribadas	R4	12-ju				
M45	603.367	7568266	4434	Falla	80.	155.	D	1.	0.	SR	Plana	6	Seco	Arribadas	R4	12-ju				
M46	603.367	7568266	4434	Falla	80.	155.	D	1.	0.	SR	Plana	6	Seco	Arribadas	R4	12-ju				
M47	603.367	7568266	4434	Falla	80.	155.	D	1.	0.	SR	Plana	6	Seco	Arribadas	R4	12-ju				
M48	603.367	7568266	4434	Falla	80.	155.	D	1.	0.	SR	Plana	6	Seco	Arribadas	R4	12-ju				
M49	603.367	7568266	4434	Falla	80.	155.	D	1.	0.	SR	Plana	6	Seco	Arribadas	R4	12-ju				
M50	603.367	7568266	4434	Falla	80.	155.	D</td													

Annex XVI Appendix B



**DIRECCIÓN TÉCNICA DE PROSPECCIÓN Y EXPLORACIÓN
"ESTUDIO GEOLÓGICO-ESTRUCTURAL DEL ÁREA
CIRCUNDANTE DEL MANANTIAL DEL SINALOA"**

PTO.	ESTE	NORTE	ELEV.	TIPO	Az.	Bz.	DipDir	Pitch	CONTINUADO	PERSISTENCIA (10m)	ABERTURA (cm)	FORMA	JRC	AGUA	TIPO ROCA	ALTERACION	DUREZA	FECHA	OBSERVACIONES	
M4	6030372	75686013	4518	Falla inversa	248	55	338		C	1	4	SR	Escalonada	12	Seco	Arribadas	R4	12-3-11	Desplazamiento 10 cm	
L518	60101011	75671497	4470	Falla Normal	70	30	330		D	1	10	SR	Plana	6	Seco	Directas	R4	12-3-11	Desplazamiento 10 cm	
L519	60101011	75671497	4470	Falla Normal	87	304	1		D	1	2	SR	Plana	6	Seco	Directas	R4	12-3-11	Desplazamiento 10 cm	
L520	60101011	75671497	4470	Falla Normal	70	318			D	1	5	SR	Ordillada	6	Seco	Directas	R4	12-3-11	Desplazamiento 10 cm	
L521	60101011	75671497	4470	Falla Normal	89	285			D	1	5	SR	Plana	6	Seco	Directas	R4	12-3-11	Desplazamiento 10 cm	
L522	60101011	75671497	4470	Falla Normal	87	265			D	1	2	SR	Plana	6	Seco	Directas	R4	12-3-11	Desplazamiento 10 cm	
L523	60101011	75671497	4470	Falla Normal	87	325			D	1	20	SR	Plana	6	Seco	Directas	R4	12-3-11	Desplazamiento 5 cm	
L524	60101011	75671497	4470	Falla Normal	90	325			D	1	30	SR	Plana	6	Seco	Directas	R4	12-3-11	Desplazamiento 10 cm	
L525	60101011	75671497	4470	Falla Normal	80	310	62		D	1	0	SR	Plana	6	Seco	Directas	R4	12-3-11	Desplazamiento 5 cm	
L526	60101011	75671497	4470	Falla Normal	88	333			D	1	0	SR	Plana	6	Seco	Directas	R4	12-3-11	Desplazamiento 5 cm	
L527	60101011	75671497	4470	Falla Normal	88	334			D	1	5	SR	Plana	6	Seco	Directas	R4	12-3-11	Desplazamiento 5 cm	
M6	6030508	75686013	4509	Falla Normal	234	74	324		C	1	2	SR	Escalonada	14	Seco	Arribadas	R4	12-3-11	Desplazamiento 40 cm	
D-1	6030213	75686831	4603	Psuedoestratificación	4603	165			C	1	466	SR	Plana	12	Seco	Arribadas	R4	12-3-11	Arribadas	
D-10	60303013	75686631	4553	Psuedoestratificación	54	165			C	1	250	SR	Plana	12	Seco	Arribadas	R4	12-3-11	Arribadas	
D-13	6030342	75686336	4550	Psuedoestratificación	43	165			C	1	250	SR	Plana	12	Seco	Arribadas	R4	12-3-11	Arribadas	
D-7	60303011	75686004	4556	Psuedoestratificación	36	84			C	1	195	SR	Plana	12	Seco	Arribadas	R4	12-3-11	Arribadas	
L442	6030360	75660012	4458	Psuedoestratificación	75	195			C	1	68	SR	Plana	12	Seco	Arribadas	R4	12-3-11	Arribadas	
L51	6030375	75661998	4462	Psuedoestratificación	68	166			C	1	350	SR	Plana	12	Seco	Arribadas	R4	12-3-11	Arribadas	
L78	60303359	75661869	4412	Psuedoestratificación	76	350			C	1	350	SR	Plana	12	Seco	Arribadas	R4	12-3-11	Arribadas	
L85	6030177	75655254	4472	Psuedoestratificación	58	96			C	1	72	SR	Plana	12	Seco	Arribadas	R4	12-3-11	Arribadas	
L341	60301013	75671022	4471	Psuedoestratificación	72	65			C	1	128	SR	Plana	12	Seco	Arribadas	R4	12-3-11	Arribadas	
M1	6030367	7568020	4519	Psuedoestratificación	24	42			C	1	226	SR	Plana	12	Seco	Arribadas	R4	12-3-11	Arribadas	
M5	6030305	7567754	4513	Psuedoestratificación	136	42			C	1	63	SR	Plana	12	Seco	Arribadas	R4	12-3-11	Arribadas	
D-14	6010185	75671630	4529	Discreta	75	85			C	1	4	SR	Plana	14	Seco	Directas	R4	13-3-11	Directas	
D-14	6010185	75671625	4529	Discreta	74	30			D	1	2	SR	Rugosa	12	Seco	Directas	R4	13-3-11	Directas	
D-14	6010185	75671625	4529	Discreta	84	20			D	1	1	SR	Plana	14	Seco	Directas	R4	13-3-11	Directas	
D-16	5993089	75700203	4823	Discreta	248	80	338		D	1	3	SR	Plana	14	Seco	Arribadas	R4	13-3-11	Arribadas	
D-16	5993088	75700201	4823	Discreta	55	70	325		C	1	3	SR	Plana	14	Seco	Arribadas	R4	13-3-11	Arribadas	
D-16	5993088	75700201	4822	Discreta	45	62	315		C	1	3	SR	Ordillada	8	Seco	Arribadas	R4	13-3-11	Arribadas	
D-17	5993139	75705344	4959	Discreta	83	4			C	1	5	SR	Plana	14	Seco	Arribadas	R4	13-3-11	Arribadas	
D-17	5993138	75705444	4959	Discreta	81	302			C	1	3	SR	Es calonada	14	Seco	Arribadas	R4	13-3-11	Arribadas	
D-17	5993136	75705444	4949	Discreta	55	155			C	1	25	SR	Ordillada	8	Seco	Arribadas	R4	13-3-11	Arribadas	
D-17	5993136	75705444	4949	Discreta	53	34			C	1	7	SR	Plana	4	Seco	Arribadas	R4	13-3-11	Arribadas	
D-17	5993136	75705444	4949	Discreta	72	140			C	1	1	SR	Ordillada	8	Seco	Arribadas	R4	13-3-11	Arribadas	
D-18	5993362	75707401	4944	Discreta	73	10			C	1	0.5	SR	Plana	4	Seco	Arribadas	R4	13-3-11	Arribadas	
D-18	5993363	75707401	4944	Discreta	73	95			C	1	3	SR	Plana	4	Seco	Arribadas	R4	13-3-11	Arribadas	
D-18	5993365	75707400	4944	Discreta	76	130			C	1	1	SR	Ordillada	8	Seco	Arribadas	R4	13-3-11	Arribadas	
D-19	5993368	75707396	4940	Discreta	64	255			D	1	0.5	SR	Ordillada	9	Seco	Arribadas	R4	13-3-11	Arribadas	
D-20	5993400	75707396	4931	Discreta	74	231			D	1	1	SR	Plana	4	Seco	Arribadas	R4	13-3-11	Arribadas	
D-20	5993400	75707396	4931	Discreta	90	308			D	1	1	0.5	SR	Es calonada	14	Seco	Arribadas	R4	13-3-11	Arribadas
D-20	5993400	75707396	4931	Discreta	83	255			D	1	2	SR	Plana	4	Seco	Arribadas	R4	13-3-11	Arribadas	
D-20	5993400	75707396	4931	Discreta	70	166			C	1	7	SR	Rugosa	5	Seco	Arribadas	R4	13-3-11	Arribadas	
D-23	5993402	75661959	4468	Discreta	69	348			C	1	5	SR	Rugosa	8	Seco	Arribadas	R4	13-3-11	Arribadas	
L543	6010201	75661959	4468	Discreta	62	362			C	1	0	SR	Plana	8	Seco	Arribadas	R4	13-3-11	Arribadas	
L544	6010201	75661959	4468	Discreta	81	344			D	4	0	SR	Plana	8	Seco	Arribadas	R4	13-3-11	Arribadas	
L545	6010201	75661959	4468	Discreta	72	340			D	6	0	SR	Plana	8	Seco	Arribadas	R4	13-3-11	Arribadas	
L546	6010201	75661959	4468	Discreta	80	160			D	5	0	SR	Plana	8	Seco	Arribadas	R4	13-3-11	Arribadas	
L547	6010201	75661959	4468	Discreta	85	168			D	5	0	SR	Plana	8	Seco	Arribadas	R4	13-3-11	Arribadas	
L548	6010201	75661959	4468	Discreta	88	159			D	10	0	SR	Plana	8	Seco	Arribadas	R4	13-3-11	Arribadas	
L549	6010201	75661959	4468	Discreta	87	172			D	6	0	SR	Plana	8	Seco	Arribadas	R4	13-3-11	Arribadas	
L550	6010201	75661959	4468	Discreta	88	167			D	7	0	SR	Plana	8	Seco	Arribadas	R4	13-3-11	Arribadas	
L551	6010201	75661959	4468	Discreta	80	145			D	4	0	SR	Plana	8	Seco	Arribadas	R4	13-3-11	Arribadas	
L552	6010201	75661959	4468	Discreta	72	160			D	3	0	SR	Rugosa	8	Seco	Arribadas	R4	13-3-11	Arribadas	
L553	6010201	75661959	4468	Discreta	71	166			D	2	0	SR	Rugosa	5	Seco	Arribadas	R4	13-3-11	Arribadas	
L554	6010201	75661959	4468	Discreta	66	327			D	4	0	SR	Plana	5	Seco	Arribadas	R4	13-3-11	Arribadas	
L555	6010201	75661959	4468	Discreta	80	120			D	5	2	SR	Plana	8	Seco	Arribadas	R4	13-3-11	Arribadas	
L556	6010201	75661959	4468	Discreta	62	336			D	5	0	SR	Rugosa	8	Seco	Arribadas	R4	13-3-11	Arribadas	

Base de datos

**DIRECCIÓN TÉCNICA DE PROSPECCIÓN Y EXPLORACIÓN
"ESTUDIO GEOLÓGICO-ESTRUCTURAL DEL ÁREA
CIRCUNDANTE DEL MANANTIAL DEL SISAL"**



PTO.	ESTE	NORTE	ELEV.	TIPO	Az.	Bz.	DipDir	Pitch	CONTINUADO	PERSISTENCIA (100m)	ABERTURA (cm)	FORMA	JRC	AGUA	TIPO ROCA	ALTERACION	DUREZA	FECHA	observaciones
L561	6007119	75661966	4483	Dicelosa	78	87	D		3	20	SR	Rugosa	8	Seco	Dicelosa		R4	13-jul.	
L562	6007119	75661966	4483	Dicelosa	86	345	D		2	10	SR	Rugosa	8	Seco	Dicelosa		R4	13-jul.	
L563	6007119	75661966	4483	Dicelosa	81	359	D		4	3	SR	Rugosa	8	Seco	Dicelosa		R4	13-jul.	
L564	6007119	75661966	4483	Dicelosa	68	345	D		5	5	SR	Rugosa	8	Seco	Dicelosa		R4	13-jul.	
L565	6007119	75661966	4483	Dicelosa	80	165	D		2	4	SR	Rugosa	8	Seco	Dicelosa		R4	13-jul.	
L566	6007119	75661966	4483	Dicelosa	86	135	D		2	8	SR	Rugosa	8	Seco	Dicelosa		R4	13-jul.	
L567	6007119	75661966	4483	Dicelosa	85	164	D		4	5	SR	Rugosa	8	Seco	Dicelosa		R4	13-jul.	
L568	6007119	75661966	4483	Dicelosa	80	160	D		5	2	SR	Rugosa	8	Seco	Dicelosa		R4	13-jul.	
L569	6007119	75661966	4483	Dicelosa	80	153	D		2	6	SR	Rugosa	8	Seco	Dicelosa		R4	13-jul.	
L570	6007119	75661966	4483	Dicelosa	72	185	D		2	6	SR	Rugosa	8	Seco	Dicelosa		R4	13-jul.	
L571	6007119	75661966	4483	Dicelosa	50	3	D		3	10	SR	Rugosa	8	Seco	Dicelosa		R4	13-jul.	
L572	6007119	75661966	4483	Dicelosa	82	154	D		4	10	SR	Rugosa	8	Seco	Dicelosa		R4	13-jul.	
L573	6005118	7567029	4484	Dicelosa	82	285	D		2	6	SR	Rugosa	8	Seco	Dicelosa		R4	13-jul.	
L574	6005118	7567029	4484	Dicelosa	84	35	D		3	4	SR	Rugosa	8	Seco	Dicelosa		R4	13-jul.	
L575	6005118	7567029	4484	Dicelosa	88	170	D		5	3	SR	Rugosa	8	Seco	Dicelosa		R4	13-jul.	
L576	6005118	7567029	4484	Dicelosa	72	136	D		4	8	SR	Rugosa	8	Seco	Dicelosa		R4	13-jul.	
L577	6005118	7567029	4484	Dicelosa	85	182	D		3	10	SR	Rugosa	8	Seco	Dicelosa		R4	13-jul.	
L578	6005118	7567029	4484	Dicelosa	87	246	D		2	0	SR	Rugosa	8	Seco	Dicelosa		R4	13-jul.	
L579	6005118	7567029	4484	Dicelosa	89	165	D		4	0	SR	Rugosa	8	Seco	Dicelosa		R4	13-jul.	
L580	6005118	7567029	4484	Dicelosa	85	224	D		2	0	SR	Rugosa	8	Seco	Dicelosa		R4	13-jul.	
L582	6005118	7567029	4484	Dicelosa	80	150	C		1	0	SR	Rugosa	8	Seco	Dicelosa		R4	13-jul.	
L583	6005118	7567029	4484	Dicelosa	87	284	C		3	2	SR	Rugosa	8	Seco	Dicelosa		R4	13-jul.	
L584	6005118	7567029	4484	Dicelosa	80	356	C		2	4	SR	Rugosa	8	Seco	Dicelosa		R4	13-jul.	
L585	5992887	7571329	5001	Dicelosa	74	120	D		2	2	SR	Rugosa	10	Seco	Dicelosa		R5	13-jul.	
L586	5992887	7571329	5001	Dicelosa	84	100	D		3	0	SR	Ondulada	10	Seco	Dicelosa		R5	13-jul.	
L587	5992887	7571329	5001	Dicelosa	87	105	D		3	0	SR	Ondulada	10	Seco	Dicelosa		R5	13-jul.	
L588	5992887	7571329	5001	Dicelosa	87	118	D		2	5	SR	Ondulada	10	Seco	Dicelosa		R5	13-jul.	
L589	5992887	7571329	5001	Dicelosa	75	95	D		10	5	SR	Ondulada	10	Seco	Dicelosa		R5	13-jul.	
L590	5992887	7571329	5001	Dicelosa	88	350	D		5	5	SR	Ondulada	10	Seco	Dicelosa		R5	13-jul.	
L591	5991169	7571519	5011	Dicelosa	87	80	D		4	0	SR	Plana	8	Seco	Dicelosa-Ardeña		R4	13-jul.	
L592	5991169	7571519	5011	Dicelosa	85	88	D		5	0	SR	Plana	8	Seco	Dicelosa-Ardeña		R4	13-jul.	
L593	5991169	7571519	5011	Dicelosa	70	272	D		4	0	SR	Plana	8	Seco	Dicelosa-Ardeña		R4	13-jul.	
L595	5991169	7571519	5011	Dicelosa	82	100	D		3	0	SR	Plana	8	Seco	Dicelosa-Ardeña		R4	13-jul.	
L596	5991169	7571519	5011	Dicelosa	84	268	D		6	0	SR	Plana	8	Seco	Dicelosa-Ardeña		R4	13-jul.	
L598	5991169	7571519	5011	Dicelosa	68	97	D		8	0	SR	Plana	8	Seco	Dicelosa-Ardeña		R4	13-jul.	
L599	5991169	7571519	5011	Dicelosa	73	110	D		5	0	SR	Plana	8	Seco	Dicelosa-Ardeña		R4	13-jul.	
L600	5991169	7571519	5011	Dicelosa	72	120	D		5	0	SR	Plana	8	Seco	Dicelosa-Ardeña		R4	13-jul.	
L601	5991169	7571519	5011	Dicelosa	64	114	D		10	0	SR	Plana	8	Seco	Dicelosa-Ardeña		R4	13-jul.	
L602	5991169	7571519	5011	Dicelosa	58	93	D		8	2	SR	Plana	8	Seco	Dicelosa-Ardeña		R4	13-jul.	
L604	5991169	7571519	5011	Dicelosa	56	111	D		6	1	SR	Plana	8	Seco	Dicelosa-Ardeña		R4	13-jul.	
L605	5991169	7571519	5011	Dicelosa	70	110	D		7	0	SR	Plana	8	Seco	Dicelosa-Ardeña		R4	13-jul.	
L606	5991169	7571519	5011	Dicelosa	58	165	D		5	0	SR	Plana	8	Seco	Dicelosa-Ardeña		R4	13-jul.	
L607	5991169	7571519	5011	Dicelosa	74	116	D		6	0	SR	Plana	8	Seco	Dicelosa-Ardeña		R4	13-jul.	
L608	5991169	7571519	5011	Dicelosa	80	92	D		6	0	SR	Plana	8	Seco	Dicelosa-Ardeña		R4	13-jul.	
L609	5991169	7571519	5011	Dicelosa	78	115	D		4	0	SR	Plana	8	Seco	Dicelosa-Ardeña		R4	13-jul.	
L610	5991169	7571519	5011	Dicelosa	79	100	D		10	0	SR	Plana	8	Seco	Dicelosa-Ardeña		R4	13-jul.	
L611	5991169	7571519	5011	Dicelosa	73	89	D		8	0	SR	Plana	8	Seco	Dicelosa-Ardeña		R4	13-jul.	
L612	5991169	7571519	5011	Dicelosa	61	99	D		10	0	SR	Plana	8	Seco	Dicelosa-Ardeña		R4	13-jul.	
L613	5991169	7571519	5011	Dicelosa	80	120	D		5	0	SR	Plana	8	Seco	Dicelosa-Ardeña		R4	13-jul.	
L615	5991169	7571519	5011	Dicelosa	79	111	D		7	0	SR	Plana	8	Seco	Dicelosa-Ardeña		R4	13-jul.	
L616	5991169	7571519	5011	Dicelosa	60	93	D		6	0	SR	Plana	8	Seco	Dicelosa-Ardeña		R4	13-jul.	
L617	5991169	7571519	5011	Dicelosa	65	72	D		4	0	SR	Plana	8	Seco	Dicelosa-Ardeña		R4	13-jul.	
L618	5991169	7571519	5011	Dicelosa	60	77	D		4	0	SR	Plana	8	Seco	Dicelosa-Ardeña		R4	13-jul.	
L619	5991169	7571519	5011	Dicelosa	60	77	D		4	0	SR	Plana	8	Seco	Dicelosa-Ardeña		R4	13-jul.	
M11	603537	7567651	4502	Dicelosa	71	1	C		2	0.5	SR	Plana	10	Humedo	Arboladas		R4	13-jul.	
M11	603537	7567651	4502	Dicelosa	263	75	C		3	2	SR	Ondulada	8	Humedo	Arboladas		R4	13-jul.	
M11	603537	7567648	4501	Dicelosa	235	36	D		2	2	SR	Plana	10	Seco	Arboladas		R4	13-jul.	

Base de datos

Página 20

Annex XVI Appendix B



**DIRECCIÓN TÉCNICA DE PROSPECCIÓN Y EXPLORACIÓN
ESTUDIO GEOLÓGICO-ESTRUCTURAL DEL ÁREA
CIRCUNDANTE DEL MANANTIAL DEL SISAL***

PTO.	ESTE	NORTE	ELEV.	TIPO	Az.	Bz.	DipDir	Pitch	CONTINUADO	PERSISTENCIA (100m)	ABERTURA (cm)	RELLENO	FORMA	JRC	AGUA	TIPO ROCA	ALTERACION	DUREZA	FECHA	OBSERVACIONES
M.13	6030540	73671636	4500	Dicielsa	308	64	52		D	3	0.2	SR	Plana	6	Saco	Arribadas	R4	13-jul.		
M.13	6030540	73671636	4500	Dicielsa	336	56	246		C	2	0.5	SR	Plana	12	Saco	Arribadas	R4	13-jul.		
M.14	6030544	73671634	4510	Dicielsa	12	82	282		D	2	0.5	SR	Plana	10	Saco	Arribadas	R4	13-jul.		
M.15	6030289	73671744	4517	Dicielsa	291	87	201		C	4	2	SR	Plana	6	Saco	Arribadas	R4	13-jul.		
M.15	6030289	73671744	4517	Dicielsa	311	66	231		D	2	5	SP	Arenas	8	Saco	Arribadas	R4	13-jul.		
M.15	6030289	73671744	4517	Dicielsa	317	73	227		D	3	3	SP	Arenas	8	Saco	Arribadas	R4	13-jul.		
M.16	6030276	73671736	4519	Dicielsa	60	86	150		C	1	1	SR	Plana	10	Saco	Arribadas	R4	13-jul.		
M.16	6030270	73671736	4519	Dicielsa	31	71	301		C	2	1	SR	Plana	5	Saco	Arribadas	R4	13-jul.		
M.17	6030512	73671701	4507	Dicielsa	210	57	300		D	3	0.5	SR	Plana	10	Saco	Arribadas	R4	13-jul.		
M.17	6030512	73671701	4507	Dicielsa	139	70	289		D	4	0.5	SR	Plana	10	Saco	Arribadas	R4	13-jul.		
M.17	6030512	73671701	4507	Dicielsa	188	66	278		D	5	0.5	SR	Plana	10	Saco	Arribadas	R4	13-jul.		
M.19	6030563	73671527	4494	Dicielsa	216	65	306		C	3	3	SR	Corva	10	Humedo	Arribadas	R4	13-jul.		
M.19	6030563	73671527	4494	Dicielsa	134	69	104		C	3	0.5	SR	Onidiada	2	Humedo	Arribadas	R4	13-jul.		
M.19	6030563	73671527	4494	Dicielsa	201	83	291		C	2	2	SR	Onidiada	6	Humedo	Arribadas	R4	13-jul.		
M.20	6030618	73671365	4494	Dicielsa	284	82	194		D	2	1	SR	Plana	14	Saco	Geomorfos	R3	13-jul.		
M.22	6030690	73671208	4481	Dicielsa	62	95	62		D	2	0.5	SR	Arenas	16	Saco	Geomorfos	R3	13-jul.		
M.22	6030690	73671208	4481	Dicielsa	78	71	275		D	2	5	SP	Buena	12	Humedo	Geomorfos	R3	13-jul.		
M.23	6030690	73671193	4475	Dicielsa	80	212	212		D	2	2	SR	Buena	12	Saco	Geomorfos	R3	13-jul.		
M.23	6030691	73671193	4475	Dicielsa	105	76	75		C	1	8	SR	Onidiada	22	Saco	Geomorfos	R3	13-jul.		
M.24	6030691	73671171	4475	Dicielsa	212	212	212		C	2	2	SR	Onidiada	16	Saco	Geomorfos	R3	13-jul.		
M.24	6030691	73671171	4475	Dicielsa	261	85	191		C	1	2	SR	Corva	6	Saco	Geomorfos	R3	13-jul.		
M.24	6030691	73671171	4475	Dicielsa	22	292	292		C	1	0.2	SR	Onidiada	12	Saco	Geomorfos	R3	13-jul.		
M.25	6030688	73671153	4480	Dicielsa	55	58	58		C	1	10	SR	Plana	12	Saco	Geomorfos	R3	13-jul.		
M.25	6030688	73671153	4480	Dicielsa	75	160	160		C	1	12	SR	Plana	12	Saco	Geomorfos	R3	13-jul.		
M.26	6030686	73671141	4467	Dicielsa	74	15	15		C	1	12	SR	Arenas	14	Saco	Geomorfos	R3	13-jul.		
M.26	6030686	73671141	4467	Dicielsa	52	82	322		C	1	15	SR	Arenas	14	Saco	Geomorfos	R3	13-jul.		
M.28	6030679	7367108	4470	Dicielsa	78	82	82		C	1	4	SR	Onidiada	10	Saco	Geomorfos	R3	13-jul.		
M.28	6030679	7367108	4470	Dicielsa	85	32	32		C	2	5	SR	Arenas	8	Saco	Geomorfos	R3	13-jul.		
M.29	6030545	73671034	4472	Dicielsa	174	63	84		C	1	10	SR	Plana	8	Saco	Arribadas	R4	13-jul.		
M.29	6030545	73671034	4472	Dicielsa	274	72	184		C	2	4	SR	Plana	12	Saco	Arribadas	R4	13-jul.		
M.29	6030545	73671034	4472	Dicielsa	83	262	262		D	3	2	SR	Plana	12	Saco	Arribadas	R4	13-jul.		
M.31	6030406	73661993	4496	Dicielsa	70	345	345		C	5	3	SR	Onidiada	12	Saco	Arribadas	R4	13-jul.		
M.31	6030406	73661993	4496	Dicielsa	320	68	230		C	5	1	SR	Plana	10	Saco	Arribadas	R4	13-jul.		
M.31	6030406	73661993	4496	Dicielsa	319	68	41		C	3	0.5	SR	Plana	12	Saco	Arribadas	R4	13-jul.		
M.32	6030397	73661986	4488	Dicielsa	325	55	35		D	1	3	SR	Plana	8	Saco	Arribadas	R4	13-jul.		
M.33	6030325	73661735	4474	Dicielsa	320	78	230		D	2	0.5	SR	Plana	8	Saco	Arribadas	R4	13-jul.		
M.33	6030325	73661735	4474	Dicielsa	3	79	273		C	4	0.5	SR	Plana	10	Saco	Arribadas	R4	13-jul.		
M.34	6030325	73661735	4474	Dicielsa	338	72	248		D	1	1	SR	Plana	10	Saco	Arribadas	R4	13-jul.		
M.34	6030215	73661686	4479	Dicielsa	77	150	150		C	3	2	SR	Plana	8	Saco	Arribadas	R4	13-jul.		
M.34	6030215	73661686	4479	Dicielsa	86	236	236		D	3	0.5	SR	Plana	6	Saco	Arribadas	R4	13-jul.		
M.34	6030215	73661686	4479	Dicielsa	76	71	70		D	6	1	SR	Plana	12	Saco	Arribadas	R4	13-jul.		
M.34	6030215	73661686	4479	Dicielsa	259	81	349		C	2	3	SR	Arenas	12	Saco	Arribadas	R4	13-jul.		
M.35	6030210	73661683	4480	Dicielsa	254	81	194		D	3	2	SR	Plana	3	Saco	Arribadas	R4	13-jul.		
M.35	6030210	73661683	4480	Dicielsa	72	79	162		C	2	3	SR	Corva	10	Saco	Arribadas	R4	13-jul.		
M.35	6030210	73661683	4480	Dicielsa	39	82	309		C	3	0.5	SR	Arenas	10	Saco	Arribadas	R4	13-jul.		
M.36	6030468	73661330	4459	Dicielsa	233	83	195		D	2	0.5	SR	Plana	8	Saco	Arribadas	R4	13-jul.		
M.36	6030468	73661330	4459	Dicielsa	337	68	23		D	2	0.5	SR	Plana	8	Saco	Arribadas	R4	13-jul.		
M.36	6030468	73661330	4459	Dicielsa	46	80	136		C	3	0.1	SR	Plana	6	Saco	Arribadas	R4	13-jul.		
M.37	6030273	73661605	4466	Dicielsa	233	67	67		C	3	2	SR	Plana	10	Saco	Geomorfos	R3	13-jul.		
M.37	6030273	73661605	4466	Dicielsa	85	145	145		C	3	2	SR	Plana	10	Saco	Geomorfos	R3	13-jul.		
M.38	6030273	73661605	4466	Dicielsa	15	105	105		C	2	5	SR	Arenas	10	Saco	Geomorfos	R3	13-jul.		
M.38	6030273	73661605	4466	Dicielsa	78	302	302		C	3	1	SR	Plana	10	Saco	Geomorfos	R3	13-jul.		
M.38	6030273	73661605	4466	Dicielsa	78	289	289		C	1	1	SR	Plana	10	Saco	Geomorfos	R3	13-jul.		
M.38	602699	73661807	4406	Dicielsa	80	240	c		D	1	1	SR	Plana	10	Saco	Geomorfos	R3	13-jul.		

Base de datos

DIRECCIÓN TÉCNICA DE PROSPECCIÓN Y EXPLORACIÓN
 "ESTUDIO GEOLÓGICO-ESTRUCTURAL DEL ÁREA
 CIRCUNDANTE DEL MANANTIAL DEL SISALÁ"

PTO.	ESTE	NORTE	ELEV.	Az.	Bz.	DipDir	Pitch	CONTINUAD.	PERSISTENCIA (10m)	ABERTURA (10m)	FORMA	JRC	ACUA	TIPO ROCA	ALTERACION	DUREZA	FECHA	OBSERVACIONES
M39	6020690	73651808	4409	Diciembre	85	259		C	2	2	SR		Plana	12	Seco	Iguminitas	R3	13-3 ul.
M39	6020690	73651808	4409	Diciembre	81	235		C	1	2	SR		Escalonada	14	Seco	Iguminitas	R3	13-3 ul.
M39	6020690	73651808	4409	Diciembre	84	295		C	1	0.2	SR		Plana	10	Seco	Iguminitas	R3	13-3 ul.
M39	6020690	73651808	4409	Diciembre	87	82		C	3	1	SR		Escalonada	10	Seco	Iguminitas	R3	13-3 ul.
M40	6020692	73651805	4413	Diciembre	81	50		D	3	10	SR		Brena	16	Seco	Iguminitas	R3	13-3 ul.
M40	6020692	73651805	4413	Diciembre	87	205		C	2	0.5	SR		Brena	12	Seco	Iguminitas	R3	13-3 ul.
M40	6020692	73651805	4413	Diciembre	73	205		C	2	2	SR		Brena	12	Seco	Iguminitas	R3	13-3 ul.
M40	6020692	73651805	4413	Diciembre	79	174		C	3	1	SR		Brena	10	Seco	Iguminitas	R3	13-3 ul.
M40	6020692	73651805	4413	Diciembre	81	240		D	2	2	SR		Brena	12	Seco	Iguminitas	R3	13-3 ul.
M40	6020692	73651805	4413	Diciembre	85	246		C	1	1	SR		Brena	10	Seco	Iguminitas	R3	13-3 ul.
M40	6020692	73651805	4413	Diciembre	87	38		C	2	3	SR		Brena	10	Seco	Iguminitas	R3	13-3 ul.
M40	6020692	73651805	4413	Diciembre	87	45		D	1	12	SR		Plana	10	Seco	Iguminitas	R4	13-3 ul.
M9	6030540	73671694	4501	Diciembre	349	62	259	C	1	1	SR		Plana	12	Seco	Arribadas	R4	13-3 ul.
M9	6030540	73671694	4501	Diciembre	320	70	230	D	4	3	SR		Ordeñada	8	Seco	Arribadas	R4	13-3 ul.
M9	6030540	73671694	4501	Diciembre	63	182		D	2	0.2	SR		Escalonada	8	Seco	Arribadas	R4	13-3 ul.
M9	6030540	73671694	4501	Diciembre	63	67		D	2	2	SR		Plana	2	Seco	Arribadas	R4	13-3 ul.
N10	6030538	73671597	5213	Diciembre	80	172		C	3	2	SR		Plana	2	Seco	Ducto-Ardeña	R4	13-3 ul.
N11	6030538	73671597	5213	Diciembre	83	174		C	3	2	SR		Plana	2	Seco	Ducto-Ardeña	R4	13-3 ul.
N12	6030538	73671597	5213	Diciembre	79	181		C	3	2	SR		Plana	2	Seco	Ducto-Ardeña	R4	13-3 ul.
N13	6030538	73671597	5213	Diciembre	80	179		C	3	2	SR		Plana	2	Seco	Ducto-Ardeña	R4	13-3 ul.
N16	6030538	73711597	5213	Diciembre	86	230		C	3	2	SR		Plana	2	Seco	Arribadas	R4	13-3 ul.
N7	6030538	73711597	5213	Diciembre	81	205		C	3	2	SR		Plana	2	Seco	Arribadas	R4	13-3 ul.
N8	6030538	73711597	5213	Diciembre	89	186		C	3	2	SR		Plana	2	Seco	Arribadas	R4	13-3 ul.
N9	6030538	73711597	5213	Diciembre	80	160		C	3	2	SR		Plana	2	Seco	Arribadas	R4	13-3 ul.
L552	6010291	73661959	4468	Falla	85	85		D	1	1	SR		Plana	8	Seco	Ductos	R4	13-3 ul.
L553	6010291	73661959	4468	Falla	72	34.0		D	1	0	SR		Plana	8	Seco	Ductos	R4	13-3 ul.
M16	6030270	73671736	4509	Falla	347	85	257	C	1	1	SR		Escalonada	14	Seco	Arribadas	R4	13-3 ul.
M18	6030527	73671736	4503	Falla	176	82	266	C	1	6	Greasas		Ordeñada	14	Seco	Arribadas	R4	13-3 ul.
N1	6030538	73711597	5213	Falla de Rumbos	89	185		C	5	1	SR		Plana	2	Seco	Ducto-Ardeña	R4	13-3 ul.
N2	6030538	73711597	5213	Falla de Rumbos	82	245		C	5	1	SR		Plana	2	Seco	Ducto-Ardeña	R4	13-3 ul.
N3	6030538	73711597	5213	Falla de Rumbos	85	265		C	5	1	SR		Plana	2	Seco	Ducto-Ardeña	R4	13-3 ul.
N4	6030538	73711597	5213	Falla de Rumbos	89	215		C	5	1	SR		Plana	2	Seco	Ducto-Ardeña	R4	13-3 ul.
N5	6030538	73711597	5213	Falla de Rumbos	86	235		C	5	1	SR		Plana	2	Seco	Ducto-Ardeña	R4	13-3 ul.
L191	6030538	73711597	5213	Falla de Rumbos	5	120		D	1	0	SR		Plana	8	Seco	Ducto-Ardeña	R4	13-3 ul.
L192	6030538	73711597	5011	Falla de Rumbos	3	109		C	2	2	SR		Cuva	10	Seco	Arribadas	R4	13-3 ul.
M27	6030684	73671351	4474	Falla de Rumbos	79	256		C	1	2	SR		Cuva	6	Seco	Arribadas	R4	13-3 ul.
M10	6030540	73671682	4502	Falla de Rumbos	31	209		C	1	2	SR		Escalonada	12	Seco	Arribadas	R4	13-3 ul.
M14	6030540	73671682	4510	Falla de Rumbos	66	42	336	D	3	1	SR		Plana	12	Seco	Arribadas	R4	13-3 ul.
M22	6030540	73671682	4451	Falla de Rumbos	77	144		C	1	1	SR		Arenas	14	Seco	Arribadas	R4	13-3 ul.
M27	6030684	73671351	4474	Falla de Rumbos	84	47.0		C	1	2	SR		Escalonada	10	Seco	Arribadas	R4	13-3 ul.
M12	6030540	73671351	4501	Falla de Rumbos	62	83		C	1	7	SR		Escalonada	12	Seco	Arribadas	R4	13-3 ul.
M13	6030540	73671351	4500	Falla de Rumbos	340	70	20	D	9	7	SR		Plana	12	Seco	Arribadas	R4	13-3 ul.
M14	6030540	73671351	4510	Falla de Rumbos	10	69	280	C	1	2	SR		Ordeñada	12	Seco	Arribadas	R4	13-3 ul.
M17	6030542	73671351	4507	Falla de Rumbos	146	7.0	166	C	1	2	SR		Arenas	10	Seco	Arribadas	R4	13-3 ul.
M19	6030542	73671351	4507	Falla de Rumbos	81	152		C	2	10	SR		Escalonada	12	Seco	Arribadas	R4	13-3 ul.
M30	6030542	73671351	4494	Falla de Rumbos	211	72	301	C	1	2	SR		Ordeñada	14	Seco	Arribadas	R4	13-3 ul.
M20	6030542	73671351	4494	Falla de Rumbos	258	68	348	C	1	4	SR		Plana	10	Seco	Arribadas	R4	13-3 ul.
M21	6030620	73671353	4494	Falla de Rumbos	290	87	200	C	1	2	SR		Plana	8	Humedo	Arribadas	R4	13-3 ul.
M22	6030620	73671208	4481	Falla de Rumbos	270	88	160	C	1	1	SR		Plana	14	Seco	Arribadas	R4	13-3 ul.
M28	6030679	73671208	4470	Falla de Rumbos	85	150		C	3	4	SR		Plana	12	Seco	Arribadas	R3	13-3 ul.
M28	6030679	73671208	4507	Falla de Rumbos	88	146		C	2	2	SR		Plana	12	Seco	Arribadas	R3	13-3 ul.
M30	6030679	73671208	4494	Falla de Rumbos	81	152		C	1	10	SR		Escalonada	10	Seco	Arribadas	R3	13-3 ul.
M32	6030679	73671208	4494	Falla de Rumbos	319	49	41	C	3	4	SR		Ordeñada	14	Seco	Arribadas	R3	13-3 ul.
M23	6030679	73671208	4494	Falla de Rumbos	4415	86	46	C	1	20	SR		Brena	12	Seco	Arribadas	R3	13-3 ul.
M25	6030679	73671208	4490	Falla de Rumbos	290	90	200	C	1	12	SR		Plana	12	Seco	Arribadas	R3	13-3 ul.
D15	6030162	73671208	4553	Psautoestratificación	53	260		C	1	1	SR		Plana	14	Seco	Arribadas	R4	13-3 ul.
D16	6030162	73671208	4507	Psautoestratificación	48.2	2.3		C	2	2	SR		Plana	12	Seco	Arribadas	R4	13-3 ul.
D17	6030162	73671208	4494	Psautoestratificación	11	22.0		C	1	2	SR		Plana	12	Seco	Arribadas	R4	13-3 ul.
L59	600776	73661999	4484	Psautoestratificación	60	185		C	1	1	SR		Plana	12	Seco	Arribadas	R4	13-3 ul.
L81	600548	73671029	4484	Psautoestratificación	65	84		C	1	1	SR		Plana	12	Seco	Arribadas	R4	13-3 ul.

**DIRECCIÓN TÉCNICA DE PROSPECCIÓN Y EXPLORACIÓN
“ESTUDIO GEOLOGICO-ESTRUCTURAL DEL ÁREA
CIRCUNDANTE DEL MAMANTIL DEL SILALA”**

Base de datos



Punto	Elev.	Norte		Este		Tipo	Az	Eje	Dip	Pitch	Continuidad	Persistencia (0.0m)	Abertura (0.0m)	Relleno	Forma	Agua	Topo Roca	Altura/orden	Dureza	Fecha	Observaciones
		Lat	Long	Lat	Long																
1	597.209	7568.446	53.02	Diciplasa	14	10.15	100	D	3	20	Biogres	0.00	SR	Piana	8	Seco	Dicidas	R4	14.iul.		
2	597.209	7568.446	53.02	Diciplasa	14	87.76	100	D	4	0.5	SR	0.00	SR	Piana	6	Seco	Dicidas	R4	14.iul.		
3	597.541	7568.005	51.04	Diciplasa	14	87.76	65	D	3	1	Arenis	0.00	SR	Ondulada	6	Seco	Dicidas	R4	14.iul.		
4	597.541	7568.005	51.04	Diciplasa	14	86.65	65	D	4	0.2	SR	0.00	SR	Piana	6	Seco	Dicidas	R4	14.iul.		
5	597.541	7568.005	51.04	Diciplasa	14	84	75	D	2	1	Arenis	0.00	SR	Ondulada	6	Seco	Dicidas	R4	14.iul.		
6	597.541	7568.005	51.04	Diciplasa	14	88	250	C	3	0.5	SR	0.00	SR	Piana	6	Seco	Dicidas	R4	14.iul.		
7	597.541	7568.005	51.04	Diciplasa	14	87	75	D	2	0.5	SR	0.00	SR	Piana	6	Seco	Dicidas	R4	14.iul.		
8	597.541	7568.005	51.04	Diciplasa	14	84	264	D	5	0	SR	0.00	SR	Piana	6	Seco	Dicidas	R4	14.iul.		
9	598.782	7567.931	47.52	Diciplasa	14	57	282	D	1	5	SR	0.00	SR	Piana	12	Seco	Dicidas	R4	14.iul.		
10	598.782	7567.931	47.52	Diciplasa	14	74	188	D	2	2	SR	0.00	SR	Curva	12	Seco	Dicidas	R4	14.iul.		
11	598.782	7567.931	47.52	Diciplasa	14	74	12	D	1	2	SR	0.00	SR	Piana	12	Seco	Dicidas	R4	14.iul.		
12	598.782	7567.931	47.52	Diciplasa	14	76	380	D	1	22	SR	0.00	SR	Piana	10	Seco	Dicidas	R4	14.iul.		
13	598.773	7567.919	47.23	Diciplasa	14	85	169	D	2	0	SR	0.00	SR	Ondulada	8	Seco	Dicidas	R4	14.iul.		
14	598.773	7567.919	47.23	Diciplasa	14	80	9	D	2	0	SR	0.00	SR	Ondulada	12	Seco	Dicidas	R4	14.iul.		
15	598.773	7567.919	47.23	Diciplasa	14	82	44	C	1	10	SR	0.00	SR	Piana	4	Seco	Dicidas	R4	14.iul.		
16	598.773	7567.919	47.23	Diciplasa	14	81	325	C	1	12	SR	0.00	SR	Piana	12	Seco	Dicidas	R4	14.iul.		
17	598.776	7567.919	47.42	Diciplasa	14	80	142	C	1	5	SR	0.00	SR	Escalonada	14	Seco	Dicidas	R4	14.iul.		
18	598.776	7567.919	47.42	Diciplasa	14	79	5	C	1	5	SR	0.00	SR	Escalonada	14	Seco	Dicidas	R4	14.iul.		
19	598.775	7567.925	47.43	Diciplasa	14	75	15	D	2	3	SR	0.00	SR	Escalonada	12	Seco	Dicidas	R4	14.iul.		
20	598.775	7567.925	47.43	Diciplasa	14	89	205	C	1	8	SR	0.00	SR	Escalonada	10	Seco	Dicidas	R4	14.iul.		
21	598.775	7567.925	47.43	Diciplasa	14	85	175	C	1	4	SR	0.00	SR	Escalonada	10	Seco	Dicidas	R4	14.iul.		
22	598.775	7567.929	47.38	Diciplasa	14	280	74	D	2	2	SR	0.00	SR	Piana	12	Seco	Dicidas	R4	14.iul.		
23	598.775	7567.929	47.38	Diciplasa	14	30	102	D	1	0	SR	0.00	SR	Escalonada	10	Seco	Dicidas	R4	14.iul.		
24	598.775	7567.929	47.38	Diciplasa	14	77	30	C	1	2	SR	0.00	SR	Piana	10	Seco	Dicidas	R4	14.iul.		
25	598.761	7567.944	47.46	Diciplasa	14	80	352	C	1	1	SR	0.00	SR	Piana	10	Seco	Dicidas	R4	14.iul.		
26	598.761	7567.944	47.46	Diciplasa	14	82	32	C	1	4	SR	0.00	SR	Piana	10	Seco	Dicidas	R4	14.iul.		
27	598.747	7567.972	47.51	Diciplasa	14	86	4	C	6	30	SR	0.00	SR	Piana	8	Seco	Dicidas	R4	14.iul.		
28	598.747	7567.972	47.51	Diciplasa	14	76	178	C	8	5	SR	0.00	SR	Piana	8	Seco	Dicidas	R4	14.iul.		
29	598.747	7567.975	47.51	Diciplasa	14	84	174	C	3	2	SR	0.00	SR	Piana	8	Seco	Dicidas	R4	14.iul.		
30	598.747	7567.975	47.51	Diciplasa	14	125	176	D	1	5	Arenis	0.00	SR	Piana	10	Seco	Dicidas	R4	14.iul.		
31	598.747	7567.975	47.51	Diciplasa	14	115	115	D	3	4	SR	0.00	SR	Piana	12	Seco	Dicidas	R4	14.iul.		
32	598.747	7567.975	47.51	Diciplasa	14	318	178	C	2	0.5	SR	0.00	SR	Piana	6	Seco	Dicidas	R4	14.iul.		
33	598.747	7567.975	47.51	Diciplasa	14	321	178	C	2	0.5	SR	0.00	SR	Piana	4	Seco	Dicidas	R4	14.iul.		
34	598.747	7567.975	47.51	Diciplasa	14	321	178	C	1	1	SR	0.00	SR	Piana	10	Seco	Dicidas	R4	14.iul.		
35	598.747	7567.975	47.51	Diciplasa	14	47	314	C	8	3	SR	0.00	SR	Piana	4	Seco	Dicidas	R4	14.iul.		
36	598.747	7567.975	47.51	Diciplasa	14	41	308	C	8	3	SR	0.00	SR	Piana	4	Seco	Dicidas	R4	14.iul.		
37	598.747	7567.975	47.51	Diciplasa	14	87	200	C	4	1	SR	0.00	SR	Piana	4	Seco	Dicidas	R4	14.iul.		
38	598.747	7567.975	47.51	Diciplasa	14	79	115	C	4	7	SR	0.00	SR	Piana	4	Seco	Dicidas	R4	14.iul.		
39	598.747	7567.975	47.51	Diciplasa	14	88	50	C	4	20	SR	0.00	SR	Piana	4	Seco	Dicidas	R4	14.iul.		
40	598.747	7567.975	47.51	Diciplasa	14	80	351	C	4	2	SR	0.00	SR	Piana	4	Seco	Dicidas	R4	14.iul.		
41	598.747	7567.975	47.51	Diciplasa	14	77	245	C	4	10	SR	0.00	SR	Piana	4	Seco	Dicidas	R4	14.iul.		
42	598.747	7567.975	47.51	Diciplasa	14	88	330	C	3	1	SR	0.00	SR	Piana	4	Seco	Dicidas	R4	14.iul.		
43	598.747	7567.975	47.51	Diciplasa	14	85	290	C	3	0.5	SR	0.00	SR	Piana	4	Seco	Dicidas	R4	14.iul.		
44	598.747	7567.975	47.51	Diciplasa	14	79	312	C	3	2	SR	0.00	SR	Piana	4	Seco	Dicidas	R4	14.iul.		
45	598.747	7567.975	47.51	Diciplasa	14	87	320	C	3	3	SR	0.00	SR	Piana	4	Seco	Dicidas	R4	14.iul.		
46	598.747	7567.975	47.51	Diciplasa	14	88	295	C	3	2	SR	0.00	SR	Piana	4	Seco	Dicidas	R4	14.iul.		
47	598.747	7567.975	47.51	Diciplasa	14	88	329	C	3	1	SR	0.00	SR	Piana	4	Seco	Dicidas	R4	14.iul.		
48	598.747	7567.975	47.51	Diciplasa	14	80	277	C	3	3	SR	0.00	SR	Piana	4	Seco	Dicidas	R4	14.iul.		
49	598.747	7567.975	47.51	Diciplasa	14	81	314	C	3	5	SR	0.00	SR	Piana	4	Seco	Dicidas	R4	14.iul.		
50	598.747	7567.975	47.51	Diciplasa	14	89	285	C	3	3	SR	0.00	SR	Piana	4	Seco	Dicidas	R4	14.iul.		
51	598.747	7567.975	47.51	Diciplasa	14	80	312	C	3	5	SR	0.00	SR	Piana	4	Seco	Dicidas	R4	14.iul.		
52	598.747	7567.975	47.51	Diciplasa	14	81	347	C	3	3	SR	0.00	SR	Piana	4	Seco	Dicidas	R4	14.iul.		
53	598.747	7567.975	47.51	Diciplasa	14	88	312	C	3	5	SR	0.00	SR	Piana	4	Seco	Dicidas	R4	14.iul.		
54	598.747	7567.975	47.51	Diciplasa	14	80	347	C	3	3	SR	0.00	SR	Piana	4	Seco	Dicidas	R4	14.iul.		
55	598.747	7567.975	47.51	Diciplasa	14	81	374	C	3	5	SR	0.00	SR	Piana	4	Seco	Dicidas	R4	14.iul.		
56	598.747	7567.975	47.51	Diciplasa	14	89	347	C	3	3	SR	0.00	SR	Piana	4	Seco	Dicidas	R4	14.iul.		
57	598.747	7567.975	47.51	Diciplasa	14	80	374	C	3	5	SR	0.00	SR	Piana	4	Seco	Dicidas	R4	14.iul.		
58	598.747	7567.975	47.51	Diciplasa	14	81	401	C	3	3	SR	0.00	SR	Piana	4	Seco	Dicidas	R4	14.iul.		
59	598.747	7567.975	47.51	Diciplasa	14	88	374	C	3	5	SR	0.00	SR	Piana	4	Seco	Dicidas	R4	14.iul.		
60	598.747	7567.975	47.51	Diciplasa	14	80	401	C	3	3	SR	0.00	SR	Piana	4	Seco	Dicidas	R4	14.iul.		
61	598.747	7567.975	47.51	Diciplasa	14	81	428	C	3	5	SR	0.00	SR	Piana	4	Seco	Dicidas	R4	14.iul.		
62	598.747	7567.975	47.51	Diciplasa	14	88	401	C	3	3	SR	0.00	SR	Piana	4	Seco	Dicidas	R4	14.iul.		
63	598.747	7567.975	47.51	Diciplasa	14	80	428	C	3	5	SR	0.00	SR	Piana	4	Seco	Dicidas	R4	14.iul.		
64	598.747	7567.975	47.51	Diciplasa	14	81	455	C	3	3	SR	0.00	SR	Piana	4	Seco	Dicidas	R4	14.iul.		
65	598.747	7567.975	47.51	Diciplasa	14	88	428	C	3	5	SR	0.00	SR	Piana	4	Seco	Dicidas	R4	14.iul.		
66	598.747	7567.975	47.51	Diciplasa	14	80	455	C	3	3	SR	0.00	SR	Piana	4	Seco	Dicidas	R4	14.iul.		
67	598.747	7567.975	47.51	Diciplasa	14	81	482	C	3	5	SR	0.00	SR	Piana	4	Seco	Dicidas	R4	14.iul.		
68	598.747	7567.975	47.51	Diciplasa	14	88	455	C	3	3	SR	0.00	SR	Piana	4	Seco	Dicidas	R4	14.iul.		
69	598.747	7567.975	47.51	Diciplasa	14	80	482	C	3	5	SR	0.00	SR	Piana	4	Seco	Dicidas	R4	14.iul.		
70	598.747	7567.975	47.51	Diciplasa	14	81	509	C	3	3	SR	0.00	SR	Piana	4	Seco	Dicidas	R4	14.iul.		
71	598.747	7567.975	47.51	Diciplasa	14	88	482	C	3	5	SR	0.00	SR	Piana	4	Seco	Dicidas	R4	14.iul.		
72	598.747	7567.975	47.51	Diciplasa	14	80	509	C	3												

Annex XVI Appendix B



DIRECCIÓN TÉCNICA DE PROSPECCIÓN Y EXPLORACIÓN
ESTUDIO GEOLÓGICO-ESTRUCTURAL DEL ÁREA
CIRCUNDANTE DEL MANANTIAL DEL SISALÁ*

PTO.	ESTE	NORTE	ELEV.	Az.	Bz.	DipDir	Ptch	CONTINUO	PERSISTENCIA (km)	ABERTURA (cm)	FORMA	JRC	ACUA	TIPO ROCA	ALTERACION	DUREZA	FECHA	NOTAS	
NA2	6020224	7574476	4645	Diclosa	80	304	C	3	4	SR	Plana	4	Seco	Diclosa		R4	14-jul.		
NA3	6020224	7574476	4645	Diclosa	85	316	C	3	3	SR	Plana	4	Seco	Diclosa		R4	14-jul.		
NA4	6020224	7574476	4645	Diclosa	80	330	C	3	1	SR	Plana	4	Seco	Diclosa		R4	14-jul.		
NA5	6020224	7574476	4645	Diclosa	80	321	C	3	0.5	SR	Plana	4	Seco	Diclosa		R4	14-jul.		
NA6	6020224	7574476	4645	Diclosa	73	342	C	3	0.5	SR	Plana	4	Seco	Diclosa		R4	14-jul.		
NA7	6020224	7574476	4645	Diclosa	85	316	C	3	3	SR	Rugosa	4	Seco	Diclosa		R4	14-jul.		
M21	5986017	7585943	5626	Falla	82	89	C	3	10	SR	Ortulada	6	Seco	Arribadas		R4	14-jul.		
L22	5986017	7585943	5626	Falla	88	75	C	1	4	SR	Plana	6	Seco	Arribadas		R4	14-jul.		
M49	5986047	7567972	47151	Falla	78	353	C	2	12	SR	Plana	6	Seco	Diclosa		R4	14-jul.		
M61	5986094	7568530	4953	Falla	80	128	C	2	30	Gravas	Plana	6	Seco	Diclosa		R4	14-jul.		
N15	6011934	7574121	46988	Falla	83	85	C	1	0	SR	Plana	4	Seco	Diclosa		R4	14-jul.		
N16	6011934	7574121	46988	Falla	79	93	C	1	0	SR	Plana	4	Seco	Diclosa		R4	14-jul.		
N18	6020224	7574476	4645	Falla	84	314	C	1	0	SR	Plana	4	Seco	Diclosa		R4	14-jul.		
N48	6020224	7574476	4645	Falla	85	310	C	1	0	SR	Plana	4	Seco	Diclosa		R4	14-jul.		
N49	6020224	7574476	4645	Falla	87	20	C	1	0	SR	Plana	4	Seco	Diclosa		R4	14-jul.		
N17	6011934	7574121	46988	Falla Dextral	21	76	291	C	1	4	SR	Plana	6	Seco	Arribadas		R4	14-jul.	
L337	5986681	7569157	5335	Falla inversa	340	45	C	1	2	SR	Plana	6	Seco	Arribadas		R4	14-jul.	Desplazamiento 10cm	
L440	5986681	7569157	5335	Falla inversa	260	260	C	1	1	SR	Plana	6	Seco	Diclosa		R4	14-jul.		
L345	5987209	7567946	5332	Falla inversa	95	71	325	C	1	0	SR	Plana	4	Seco	Diclosa		R4	14-jul.	
L348	5987209	7567946	5332	Falla inversa	38	71	305	C	1	4	SR	Plana	5	Seco	Diclosa		R4	14-jul.	
M42	598782	7567931	4752	Falla inversa	77	15	C	1	0	SR	Plana	2	Seco	Diclosa		R4	14-jul.		
M44	598778	7567919	47472	Falla inversa	82	292	C	1	5	SR	Plana	6	Seco	Diclosa		R4	14-jul.		
M46	598775	7567928	4737	Falla inversa	68	146	C	1	4	SR	Ortulada	14	Seco	Diclosa		R4	14-jul.		
M48	598761	7567944	47494	Falla inversa	73	152	C	1	25	SR	Escalonada	10	Seco	Diclosa		R4	14-jul.		
M58	598019	7568579	4934	Falla inversa	55	331	C	10	5	SR	Plana	4	Seco	Diclosa		R4	14-jul.		
M63	598019	7568579	4934	Falla inversa	57	337	C	10	6	SR	Plana	4	Seco	Diclosa		R4	14-jul.		
M63	5980194	7568511	4970	Falla inversa	38	125	C	1	0	SR	Cueva	6	Seco	Diclosa		R4	14-jul.		
M63	5980194	7568511	4970	Falla inversa	75	194	D	1	1	SR	Escalonada	6	Seco	Arribadas		R4	14-jul.		
M528	5980194	7568511	4970	Falla inversa	70	64	C	1	2	SR	Ortulada	6	Seco	Arribadas		R4	14-jul.		
M556	5971541	7568605	5104	Falla Normal	82	11	C	2	2	SR	Plana	4	Seco	Diclosa		R4	14-jul.		
M52	598762	7567931	4752	Falla Normal	78	279	C	2	3	SR	Plana	6	Seco	Diclosa		R4	14-jul.		
M42	598762	7567931	4752	Falla Normal	78	280	C	1	2	SR	Plana	6	Seco	Diclosa		R4	14-jul.		
M44	598778	7567931	47472	Falla Normal	77	325	C	1	5	SR	Ortulada	8	Seco	Diclosa		R4	14-jul.		
M51	5986865	7568029	4752	Falla Normal	71	170	C	1	10	SR	Arenas	8	Seco	Diclosa		R4	14-jul.		
M55	5987930	7568029	4752	Falla Normal	80	182	C	1	15	SR	Ortulada	6	Seco	Diclosa		R4	14-jul.		
M60	5980226	7568583	4936	Falla Normal	84	130	C	1	12	SR	Plana	4	Seco	Diclosa		R4	14-jul.		
M60	5980226	7568583	4936	Falla Normal	84	128	C	1	10	SR	Plana	4	Seco	Diclosa		R4	14-jul.		
M62	5980267	7568605	4971	Falla Normal	76	308	C	1	12	SR	Plana	4	Seco	Diclosa		R4	14-jul.		
M62	5980267	7568605	4971	Falla Normal	78	279	C	1	12	SR	Plana	6	Seco	Diclosa		R4	14-jul.		
M63	5980267	7568605	4971	Falla Normal	78	280	C	1	2	SR	Plana	6	Seco	Diclosa		R4	14-jul.		
M14	6011934	7574121	46988	Falla Normal	80	75	C	1	0	SR	Plana	4	Seco	Diclosa		R4	14-jul.		
N18	6011934	7574121	46988	Falla Normal	70	110	C	1	0	SR	Plana	4	Seco	Diclosa		R4	14-jul.		
N20	6011934	7574121	46988	Falla Normal	78	305	C	1	0	SR	Plana	4	Seco	Diclosa		R4	14-jul.		
N28	6011934	7574121	46988	Falla Normal	3	160	C	10	0	SR	Plana	4	Seco	Diclosa		R4	14-jul.		
N29	6011934	7574121	46988	Falla Normal	10	170	C	10	0	SR	Plana	4	Seco	Diclosa		R4	14-jul.		
N30	6020224	7574476	4645	Falla Normal	12	159	C	10	0	SR	Plana	5	Seco	Diclosa		R4	14-jul.		
L626	5980197	7567944	4746	Psuedoestratificación	31	270	C	10	280	C	Seco	Diclosa		Seco	Diclosa		R4	14-jul.	
M48	5980197	7567944	4746	Psuedoestratificación	33	190	C	2	3	SR	Rugosa	12	Seco	Arribadas		R4	15-jul.		
M64	5980267	7570413	53170	Diclosa	70	35	C	1	2	SR	Escalonada	12	Seco	Arribadas		R4	15-jul.		
M64	5980267	7570413	53170	Diclosa	78	48	D	2	1	SR	Ortulada	12	Seco	Arribadas		R4	15-jul.		
M64	5980267	7570413	53170	Diclosa	75	20	C	2	1	SR	Rugosa	14	Seco	Arribadas		R4	15-jul.		
M64	5980267	7570413	53170	Diclosa	78	165	C	3	3	SR	Escalonada	12	Seco	Arribadas		R4	15-jul.		
M65	5980267	7570413	53170	Diclosa	89	62	C	1	1	SR	Plana	5	Seco	Arribadas		R4	15-jul.		
M66	5980267	7570413	53170	Diclosa	82	150	C	4	5	SR	Plana	5	Seco	Arribadas		R4	15-jul.		
M66	5980267	7570413	53170	Diclosa	88	40	C	1	3	SR	Plana	12	Seco	Arribadas		R4	15-jul.		
M66	5980267	7570413	53170	Diclosa	68	338	C	1	2	SR	Ortulada	12	Seco	Arribadas		R4	15-jul.		
M67	5980267	75686400	55522	Diclosa	48	10	D	1	0	SR	Escalonada	12	Seco	Diclosa		R4	15-jul.		

Base de datos

Página 25

**DIRECCIÓN TÉCNICA DE PROSPECCIÓN Y EXPLORACIÓN
"ESTUDIO GEOLÓGICO-ESTRUCTURAL DEL ÁREA
CIRCUNDANTE DEL MANANTIAL DEL SISAL"**



PTO.	ESTE	NORTE	ELEV.	TIPO	Az.	Bz.	DipDir	Pitch	CONTINUADO	PERSISTENCIA (10m)	ABERTURA (cm)	RELLENO	FORMA	JRC	AGUA	TIPO ROCA	ALTERACION	DUREZA	FECHA	NOTAS
M67	5919921	73659420	5552	Diclosa	55	305	D		1	5	SR	Plana	S	Seco	Diclosa	R4	15-jul.			
M67	5919921	73659420	5552	Diclosa	78	285	C		1	0	SR	Plana	10	Seco	Diclosa	R4	15-jul.			
M68	5919920	73659262	5628	Diclosa	52	35	D		2	0.5	SR	Quindela-Escalona	14	Seco	Arenas	R4	15-jul.			
M68	5919920	73659262	5628	Diclosa	76	7	D		1	1	SR	Plana	14	Seco	Arenas	R4	15-jul.			
M68	5919920	73659262	5628	Diclosa	63	268	D		1	3	SR	Escondida	10	Seco	Arenas	R4	15-jul.			
M69	5919921	73659119	5622	Diclosa	80	165	D		3	5	SR	Escondida	14	Seco	Arenas	R4	15-jul.			
M69	5919921	73659119	5622	Diclosa	85	334	D		4	4	SR	Plana	8	Seco	Arenas	R4	15-jul.			
M70	5919923	73659707	5312	Diclosa	82	115	C		4	10	SR	Escalona-Rugosa	14	Seco	Diclosa	R4	15-jul.			
M70	5919923	73659707	5312	Diclosa	67	115	C		3	6	SR	Escalona	14	Seco	Diclosa	R4	15-jul.			
M70	5919923	73659707	5312	Diclosa	85	213	C		2	3	SR	Rugosa	12	Seco	Diclosa	R4	15-jul.			
M70	5919923	73659707	5312	Diclosa	88	145	C		1	10	SR	Plana	4	Seco	Diclosa	R4	15-jul.			
M70	5919923	73659707	5312	Diclosa	78	265	C		3	2	SR	Plana	4	Seco	Diclosa	R4	15-jul.			
M70	5919923	73659707	5312	Diclosa	52	86	C		3	2	SR	Escalonada	14	Seco	Diclosa	R4	15-jul.			
M70	5919923	73659707	5312	Diclosa	61	73	C		2	4	SR	Onidela	12	Seco	Diclosa	R4	15-jul.			
M70	5919923	73659707	5312	Diclosa	90	105	C		2	0	SR	Plana	8	Seco	Diclosa	R4	15-jul.			
M71	59199182	73659888	5306	Diclosa	88	45	C		10	10	SR	Escalonada-Rugosa	14	Seco	Arenas	R4	15-jul.			
M71	59199182	73659888	5306	Diclosa	86	153	C		2	3	SR	Plana	12	Seco	Arenas	R4	15-jul.			
M71	59199182	73659888	5306	Diclosa	90	145	C		5	6	SR	Plana	10	Seco	Arenas	R4	15-jul.			
M72	59197159	73659712	5214	Diclosa	60	1	D		1	10	SR	Quindela-Escalona	14	Seco	Brecha de base	R3	15-jul.			
M72	59197159	73659712	5214	Diclosa	65	178	D		2	3	SR	Patina	5	Seco	Brecha de base	R3	15-jul.			
M72	59197159	73659712	5214	Diclosa	58	283	D		1	8	SR	Escalonada	14	Seco	Diclosa	R4	15-jul.			
M72	59197159	73659712	5214	Diclosa	85	185	C		3	2	SR	Onidela	14	Seco	Diclosa	R4	15-jul.			
M73	5919799	73659599	5149	Diclosa	78	9	D		1	0	SR	Es calonada	10	Seco	Arenas	R3	15-jul.			
M73	5919799	73659599	5149	Diclosa	83	195	C		1	7	SR	Rugosa	12	Seco	Brecha de base	R3	15-jul.			
M65	5919880	73707044	5331	Diclosa	37	212	D		1	0	SR	Plana	8	Seco	Brecha de base	R4	15-jul.			
M66	59198807	73707049	5404	Falla inversa	70	280	C		1	2	SR	Plana	10	Seco	Arenas	R4	15-jul.	Rechazo de 40 cm		
M66	59198807	73707049	5404	Falla inversa	84	323	C		1	7	SR	Plana	10	Seco	Arenas	R4	15-jul.	Rechazo de 18 cm		
M66	59198807	73707049	5404	Falla inversa	255	255	C		3	2	SR	Plana	10	Seco	Arenas	R4	15-jul.			
M66	59198807	73707049	5404	Falla inversa	344	344	C		2	0	SR	Plana	8	Seco	Arenas	R4	15-jul.			
M67	5919921	73659729	5652	Psudotrastricación	32	175	C		1	0	SR	Es calonada	12	Seco	Diclosa	R4	15-jul.			
M68	59199461	73659262	5628	Psudotrastricación	41	151	C		0	0	SR	Plana-Rugosa	8	Seco	Arenas	R4	15-jul.			
M69	5919921	73659710	5622	Psudotrastricación	70	155	C		2	4	SR	Plana-Ordeñada	8	Seco	Arenas	R4	15-jul.			
M71	5919921	73659888	5306	Psudotrastricación	42	0	C		2	0	SR	Rugosa	8	Seco	Arenas	R4	15-jul.			
M72	5919759	73659712	5214	Psudotrastricación	18	292	C		1	3	SR	Rugosa-Ordeñada	12	Seco	Diclosa	R4	15-jul.			
D-29	604290	73757650	4607	Diclosa	45	282	C		2	3.5	SR	Plana-Rugosa	12	Seco	Diclosa	R4	16-jul.			
D-29	604290	73757650	4607	Diclosa	50	168	C		2	0	SR	Plana-Rugosa	10	Seco	Diclosa	R4	16-jul.			
D-29	604290	73757650	4607	Diclosa	70	190	C		2	5	SR	Plana-Rugosa	8	Seco	Diclosa	R4	16-jul.			
D-30	6040418	73757585	4610	Diclosa	66	340	D		1	0	SR	Plana-Ordeñada	12	Seco	Diclosa	R4	16-jul.			
D-30	6040418	73757585	4610	Diclosa	70	305	D		1	0	SR	Plana-Rugosa	8	Seco	Diclosa	R4	16-jul.			
D-30	6040418	73757585	4610	Diclosa	76	290	C		0	0	SR	Plana-Rugosa	8	Seco	Diclosa	R4	16-jul.			
D-30	6040418	73757585	4610	Diclosa	74	295	C		2	4	SR	Plana-Ordeñada	8	Seco	Diclosa	R4	16-jul.			
D-31	6040414	73757585	4610	Diclosa	74	345	C		4	0.5	SR	Arenas	4	Seco	Diclosa	R4	16-jul.			
D-31	6040414	73757585	4610	Diclosa	74	45	D		2	1.5	SR	Rugosa	12	Seco	Diclosa	R4	16-jul.			
D-32	6040418	73757585	4610	Diclosa	83	330	C		2	0	SR	Plana-Ordeñada	6	Seco	Diclosa	R4	16-jul.			
D-32	6040418	73757585	4610	Diclosa	74	180	C		2	0.5	SR	Rugosa	12	Seco	Diclosa	R4	16-jul.			
D-32	6040418	73757585	4610	Diclosa	85	105	C		2	0	SR	Rugosa	8	Seco	Diclosa	R4	16-jul.			
D-33	6040464	73757585	4666	Diclosa	65	38	D		5	0	SR	Plana	4	Seco	Diclosa	R4	16-jul.			
D-33	6040464	73757585	4666	Diclosa	12	245	C		1	2	SR	Plana	4	Seco	Diclosa	R4	16-jul.			
D-34	6040738	73757914	4685	Diclosa	86	244	C		5	1.5	SR	Plana-Ordeñada	8	Seco	Diclosa	R4	16-jul.			
D-34	6040738	73757914	4685	Diclosa	71	315	C		1	1.5	SR	Plana	4	Seco	Diclosa	R4	16-jul.			
D-34	6040738	73757914	4685	Diclosa	52	335	D		1	0.5	SR	Plana	4	Seco	Diclosa	R4	16-jul.			
D-34	6040738	73757914	4685	Diclosa	80	65	C		3	1.5	SR	Banca	8	Seco	Diclosa	R4	16-jul.			
D-34	6040738	73757914	4685	Diclosa	72	175	C		2	0	SR	Plana-Rugosa	9	Seco	Diclosa	R4	16-jul.			
D-35	6040812	73757914	4685	Diclosa	86	95	D		2	0.2	SR	Plana-Ordeñada	8	Seco	Diclosa	R4	16-jul.			
D-35	6040812	73757914	4685	Diclosa	80	295	D		2	3	SR	Arenas	5	Seco	Diclosa	R4	16-jul.			
D-35	6040812	73757914	4685	Diclosa	54	287	C		1	1	SR	Plana-Ordeñada	14	Seco	Diclosa	R4	16-jul.			
D-35	6040812	73757914	4685	Diclosa	66	318	C		2	1.5	SR	Plana-Ordeñada	8	Seco	Diclosa	R4	16-jul.			

Annex XVI Appendix B



DIRECCIÓN TÉCNICA DE PROSPECCIÓN Y EXPLORACIÓN
"ESTUDIO GEOLÓGICO-ESTRUCTURAL DEL ÁREA
CIRCUNDANTE DEL MANANTIAL DEL SISALÁ"

PTO.	ESTE	NORTE	ELEV.	TIPO	Az.	Bz.	DipDir	Pitch	CONTINUADO	PERSISTENCIA (10m)	ABERTURA (cm)	RELLENO	FORMA	JRC	AGUA	TIPO ROCA	ALTERACION	DUREZA	FECHA	OBSERVACIONES
D-35	60404812	7573871	4676	Dicelosa	80	10	C	2	0	5	Arenas	Escarabajo/Rugosa	14	Seco	Dicelosa	12	R4	16-UL		
D-35	60404812	7573871	4676	Dicelosa	68	130	D	1	0	SR	Rugosa/Oniolizada	12	Seco	Dicelosa	12	R4	16-UL			
D-36	60501080	7573882	4666	Dicelosa	75	222	D	0	0	SR	Poco/Oniolizada	8	Seco	Dicelosa	8	R4	16-UL			
D-36	60501080	7573882	4666	Dicelosa	46	28	C	1	1	SR	Oniolizada	8	Seco	Dicelosa	8	R4	16-UL			
D-37	60502584	7574060	4624	Dicelosa	82	240	D	3	1	15	SR	Poco/Oniolizada	8	Seco	Dicelosa	8	R4	16-UL		
D-37	60502584	7574060	4624	Dicelosa	58	210	C	1	1	SR	Poco/Oniolizada	4	Seco	Dicelosa	4	R4	16-UL			
D-37	60502584	7574060	4624	Dicelosa	68	245	D	1	1	SR	Oniolizada	8	Seco	Dicelosa	8	R4	16-UL			
D-37	60502584	7574060	4624	Dicelosa	47	205	D	1	0	SR	Poco/Oniolizada	4	Seco	Dicelosa	4	R4	16-UL			
D-37	60502584	7574060	4624	Dicelosa	80	35	D	2	3.5	SR	Escarabajo/Rugosa	14	Seco	Dicelosa	8	R4	16-UL			
D-37	60502584	7574060	4624	Dicelosa	70	315	C	1	2	Arenas	Poco/Oniolizada	10	Seco	Dicelosa	10	R4	16-UL			
D-38	60501148	7574222	4662	Dicelosa	89	273	C	1	0	SR	Poco/Oniolizada	4	Seco	Dicelosa	4	R4	16-UL			
D-38	60501148	7574222	4662	Dicelosa	78	268	C	1	1	SR	Poco/Oniolizada	8	Seco	Dicelosa	8	R4	16-UL			
D-38	60501148	7574222	4662	Dicelosa	85	5	D	3	0.2	SR	Poco/Oniolizada	4	Seco	Dicelosa	4	R4	16-UL			
D-38	60501148	7574222	4662	Dicelosa	75	185	D	2	0.5	SR	Poco/Oniolizada	8	Seco	Dicelosa	8	R4	16-UL			
D-38	60501148	7574222	4662	Dicelosa	74	26	C	4	0	SR	Poco/Oniolizada	4	Seco	Dicelosa	4	R4	16-UL			
D-39	6040767	7574100	4630	Dicelosa	86	140	C	1	10	Arenas	Poco/Oniolizada	4	Seco	Dicelosa	4	R4	16-UL			
D-39	6040767	7574100	4630	Dicelosa	65	122	C	2	2.5	SR	Poco/Oniolizada	4	Seco	Dicelosa	4	R4	16-UL			
D-39	6040767	7574100	4630	Dicelosa	87	304	C	2	0	SR	Poco/Oniolizada	8	Seco	Dicelosa	8	R4	16-UL			
D-39	6040767	7574100	4630	Dicelosa	56	221	C	2	1	SR	Rugosa/Oniolizada	14	Seco	Dicelosa	14	R4	16-UL			
D-39	6040767	7574100	4630	Dicelosa	80	92	C	2	1.5	SR	Rugosa/Oniolizada	12	Seco	Dicelosa	12	R4	16-UL			
D-39	6040767	7574100	4630	Dicelosa	83	240	D	4	2	SR	Rugosa	10	Seco	Dicelosa	10	R4	16-UL			
L664	6020713	7574969	4620	Dicelosa	78	220	D	7	2	SR	Rugosa	10	Seco	Dicelosa	10	R4	16-UL			
L665	6020713	7574969	4620	Dicelosa	80	200	D	6	1	SR	Rugosa	10	Seco	Dicelosa	10	R4	16-UL			
L666	6020713	7574969	4620	Dicelosa	82	196	D	7	2	SR	Rugosa	10	Seco	Dicelosa	10	R4	16-UL			
L667	6020713	7574969	4620	Dicelosa	81	328	D	4	0	SR	Rugosa	10	Seco	Dicelosa	10	R4	16-UL			
L668	6020713	7574969	4620	Dicelosa	80	335	D	4	4	SR	Rugosa	10	Seco	Dicelosa	10	R4	16-UL			
L669	6020713	7574969	4620	Dicelosa	84	230	D	8	3	SR	Rugosa	10	Seco	Dicelosa	10	R4	16-UL			
L670	6020713	7574969	4620	Dicelosa	81	326	D	6	1	SR	Rugosa	10	Seco	Dicelosa	10	R4	16-UL			
L671	6020713	7574969	4620	Dicelosa	88	306	D	5	0	SR	Rugosa	10	Seco	Dicelosa	10	R4	16-UL			
L672	6020713	7574969	4620	Dicelosa	87	309	D	2	4	Arenas	Rugosa	10	Seco	Dicelosa	10	R4	16-UL			
L673	6020713	7574969	4620	Dicelosa	83	313	D	2	2	SR	Rugosa	10	Seco	Dicelosa	10	R4	16-UL			
L674	6020713	7574969	4620	Dicelosa	87	336	D	3	2	SR	Rugosa	10	Seco	Dicelosa	10	R4	16-UL			
L675	6020713	7574969	4620	Dicelosa	86	336	D	4	0	SR	Rugosa	10	Seco	Dicelosa	10	R4	16-UL			
L676	6020713	7574969	4620	Dicelosa	78	31	D	3	0	SR	Rugosa	8	Seco	Dicelosa	8	R4	16-UL			
L677	6020713	7574969	4620	Dicelosa	80	16	D	2	3	SR	Rugosa	8	Seco	Dicelosa	8	R4	16-UL			
L678	6020713	7574969	4620	Dicelosa	77	328	C	3	4	SR	Rugosa	8	Seco	Dicelosa	8	R4	16-UL			
L679	6020713	7574969	4620	Dicelosa	79	282	D	4	3	SR	Rugosa	8	Seco	Dicelosa	8	R4	16-UL			
L680	6020713	7574969	4620	Dicelosa	85	11	C	2	10	SR	Rugosa	8	Seco	Dicelosa	8	R4	16-UL			
L681	6020713	7574969	4620	Dicelosa	88	357	C	2	12	SR	Rugosa	8	Seco	Dicelosa	8	R4	16-UL			
L682	6020713	7574969	4620	Dicelosa	65	3	D	2	6	SR	Rugosa	8	Seco	Dicelosa	8	R4	16-UL			
L683	6020713	7574969	4620	Dicelosa	85	308	D	4	0	SR	Rugosa	8	Seco	Dicelosa	8	R4	16-UL			
L684	6020713	7574969	4620	Dicelosa	82	296	C	6	0	SR	Rugosa	8	Seco	Dicelosa	8	R4	16-UL			
L685	6020713	7574969	4620	Dicelosa	88	311	C	8	2	SR	Rugosa	4	Seco	Dicelosa	4	R4	16-UL			
L686	6020713	7574969	4620	Dicelosa	80	34	D	2	0	SR	Rugosa	4	Seco	Dicelosa	4	R4	16-UL			
L687	6020713	7574969	4620	Dicelosa	71	264	D	2	0	SR	Rugosa	4	Seco	Dicelosa	4	R4	16-UL			
L688	6020713	7574969	4620	Dicelosa	88	296	D	1	2	SR	Rugosa	4	Seco	Dicelosa	4	R4	16-UL			
L689	6020713	7574969	4620	Dicelosa	80	205	D	2	0	SR	Rugosa	4	Seco	Dicelosa	4	R4	16-UL			
L690	6020713	7574969	4620	Dicelosa	84	213	D	3	2	SR	Rugosa	4	Seco	Dicelosa	4	R4	16-UL			
L691	6020713	7574969	4620	Dicelosa	87	208	D	2	1	SR	Rugosa	4	Seco	Dicelosa	4	R4	16-UL			
L692	6020713	7574969	4620	Dicelosa	89	284	D	4	0	SR	Rugosa	4	Seco	Dicelosa	4	R4	16-UL			
L693	6020713	7574969	4620	Dicelosa	88	294	C	6	0	SR	Rugosa	4	Seco	Dicelosa	4	R4	16-UL			
L695	6020713	7574969	4620	Dicelosa	80	34	D	2	0	SR	Rugosa	4	Seco	Dicelosa	4	R4	16-UL			
L696	6020713	7574969	4620	Dicelosa	71	267	D	2	0	SR	Rugosa	4	Seco	Dicelosa	4	R4	16-UL			
L697	6020713	7574969	4620	Dicelosa	84	267	C	3	0	SR	Rugosa	4	Seco	Dicelosa	4	R4	16-UL			
L698	6020713	7574969	4620	Dicelosa	68	145	C	3	15	SR	Rugosa	4	Seco	Dicelosa	4	R4	16-UL			
L699	6020713	7574969	4620	Dicelosa	78	338	D	2	0	SR	Rugosa	4	Seco	Dicelosa	4	R4	16-UL			
L700	6020713	7574969	4620	Dicelosa	86	15	C	10	5	SR	Rugosa	4	Seco	Dicelosa	4	R4	16-UL			
L701	6020713	7574969	4620	Dicelosa	90	12	C	10	6	SR	Rugosa	4	Seco	Dicelosa	4	R4	16-UL			
L702	6020713	7574969	4620	Dicelosa	80	6	C	10	8	SR	Rugosa	4	Seco	Dicelosa	4	R4	16-UL			
L703	6020713	7574969	4620	Dicelosa	90	358	D	10	10	SR	Rugosa	4	Seco	Dicelosa	4	R4	16-UL			

**DIRECCIÓN TÉCNICA DE PROSPECCIÓN Y EXPLORACIÓN
"ESTUDIO GEOLÓGICO-ESTRUCTURAL DEL ÁREA
CIRCUNDANTE DEL MANANTIAL DEL SISAL"**



PTO.	ESTE	NORTE	ELEV.	Az	Bz	DipDir	Pitch	CONTINUADO	PERSISTENCIA (100m)	ABERTURA (100m)	RELLENO	FORMA	JRC	ACUA	TIPO ROCA	ALTERACION	DUREZA	FECHA	OBSERVACIONES
L704	591.182	7373517	4502	Diclessa	86	16	D	8	0	SR	Plana	4	Seco	Diclessa		R3	16-ul.		
L705	591.182	7373517	4502	Diclessa	82	18	D	6	2	SR	Plana	4	Seco	Diclessa		R3	16-ul.		
L706	591.182	7373517	4502	Diclessa	89	5	D	7	4	SR	Plana	4	Seco	Diclessa		R3	16-ul.		
L707	591.182	7373517	4502	Diclessa	80	3	D	6	20	SR	Plana	4	Seco	Diclessa		R3	16-ul.		
L708	591.182	7373517	4502	Diclessa	85	13	D	5	5	SR	Plana	4	Seco	Diclessa		R3	16-ul.		
L709	591.182	7373517	4502	Diclessa	89	7	D	4	23	SR	Plana	4	Seco	Diclessa		R3	16-ul.		
L710	591.182	7373517	4502	Diclessa	85	8	D	4	5	SR	Plana	4	Seco	Diclessa		R3	16-ul.		
L711	591.182	7373517	4502	Diclessa	89	9	D	10	12	SR	Plana	4	Seco	Diclessa		R3	16-ul.		
M74	604.382	7373651	4605	Diclessa	86	265	D	6	4	SR	Es calonida	14	Seco	Diclessa		R4	16-ul.		
M74	604.382	7373651	4605	Diclessa	78	186	C	3	4	SR	Es calonida	14	Seco	Diclessa		R4	16-ul.		
M74	604.382	7373651	4605	Diclessa	82	340	C	1	2	SR	Plana	12	Seco	Diclessa		R4	16-ul.		
M74	604.382	7373651	4605	Diclessa	89	186	D	4	1	SR	Plana	12	Seco	Diclessa		R4	16-ul.		
M74	604.382	7373651	4605	Diclessa	78	183	D	3	4	SR	Es calonida	12	Seco	Diclessa		R4	16-ul.		
M74	604.382	7373651	4605	Diclessa	82	186	D	4	1	SR	Plana	12	Seco	Diclessa		R4	16-ul.		
M74	604.382	7373651	4605	Diclessa	22	168	D	1	8	SR	Es calonida	14	Seco	Diclessa		R4	16-ul.		
M75	604.383	7373625	4604	Diclessa	78	175	D	3	8	SR	Arenas	16	Seco	Diclessa		R4	16-ul.		
M75	604.383	7373625	4604	Diclessa	55	45	D	3	7	SR	Ortileda	14	Seco	Diclessa		R4	16-ul.		
M75	604.383	7373625	4604	Diclessa	82	105	D	2	2	SR	Ortileda	14	Seco	Diclessa		R4	16-ul.		
M75	604.383	7373625	4604	Diclessa	78	317	D	3	2	SR	Plana	16	Seco	Diclessa		R4	16-ul.		
M75	604.383	7373625	4604	Diclessa	66	211	C	4	5	SR	Arenas	16	Seco	Diclessa		R4	16-ul.		
M75	604.383	7373625	4604	Diclessa	190	88	D	2	2	SR	Plana	14	Seco	Diclessa		R4	16-ul.		
M75	604.383	7373625	4604	Diclessa	76	138	D	2	2	SR	Plana	16	Seco	Diclessa		R4	16-ul.		
M76	604.647	7373936	4653	Diclessa	84	62	D	1	8	SR	Arenas	16	Seco	Diclessa		R4	16-ul.		
M78	604.647	7373948	4671	Diclessa	76	250	C	3	4	SR	Es calonida	16	Seco	Diclessa		R4	16-ul.		
M78	604.647	7373948	4671	Diclessa	81	5	D	3	10	SR	Es calonida	14	Seco	Diclessa		R4	16-ul.		
M78	604.647	7373948	4671	Diclessa	81	290	D	2	6	SR	Es calonida	12	Seco	Diclessa		R4	16-ul.		
M78	604.647	7373948	4671	Diclessa	79	144	C	2	12	SR	Es calonida	10	Seco	Diclessa		R4	16-ul.		
M79	604.709	7373950	4669	Diclessa	104	66	C	4	5	SR	Plana	16	Seco	Diclessa		R4	16-ul.		
M79	604.709	7373950	4669	Diclessa	75	72	C	6	0.5	SR	Ortileda	14	Seco	Diclessa		R4	16-ul.		
M79	604.709	7373950	4669	Diclessa	86	97	C	6	6	SR	Ortileda	14	Seco	Diclessa		R4	16-ul.		
M79	604.709	7373950	4669	Diclessa	83	30	C	6	5	SR	Ortileda	14	Seco	Diclessa		R4	16-ul.		
M79	604.709	7373950	4669	Diclessa	60	72	D	1	3	SR	Plana	14	Seco	Diclessa		R4	16-ul.		
M79	604.709	7373950	4669	Diclessa	80	230	C	3	8	SR	Es calonida	14	Seco	Diclessa		R4	16-ul.		
M80	604.819	7373853	4650	Diclessa	85	248	C	3	5	SR	Ortileda	14	Seco	Diclessa		R4	16-ul.		
M80	604.819	7373853	4650	Diclessa	71	35	D	6	5	SR	Ortileda	16	Seco	Diclessa		R4	16-ul.		
M80	604.819	7373853	4650	Diclessa	84	82	C	4	2	SR	Es calonida	14	Seco	Diclessa		R4	16-ul.		
M80	604.819	7373853	4650	Diclessa	64	312	D	3	6	SR	Es calonida	14	Seco	Diclessa		R4	16-ul.		
M80	604.819	7373853	4650	Diclessa	77	235	C	2	4	SR	Es calonida	14	Seco	Diclessa		R4	16-ul.		
M80	604.819	7373853	4650	Diclessa	84	124	D	1	0	SR	Plana	14	Seco	Diclessa		R4	16-ul.		
M80	604.819	7373853	4650	Diclessa	55	284	D	2	3	SR	Es calonida	14	Seco	Diclessa		R4	16-ul.		
M80	604.819	7373853	4650	Diclessa	70	90	C	1	0	SR	Borsa	10	Seco	Diclessa		R4	16-ul.		
M80	604.819	7373853	4650	Folla	87	125	C	1	0	SR	Borsa	10	Seco	Diclessa		R4	16-ul.		
M80	604.819	7373853	4650	Folla	80	340	C	1	2	SR	Borsa	10	Seco	Diclessa		R4	16-ul.		
M80	604.819	7373853	4650	Folla	41	314	C	1	0.5	SR	Borsa	10	Seco	Diclessa		R4	16-ul.		
M80	604.819	7373853	4650	Folla	20	223	D	3	3	SR	Plana	14	Seco	Diclessa		R4	16-ul.		
M85	604.964	7373948	4671	Folla	86	100	D	1	2	SR	Es calonida	10	Seco	Diclessa		R4	16-ul.		
M77	604.641	7373962	4661	Falla inversa	78	113	C	1	27	SR	Ortileda	10	Seco	Diclessa		R4	16-ul.		
M77	604.641	7373962	4661	Falla inversa	76	82	D	2	4	SR	Corva	14	Seco	Diclessa		R4	16-ul.		
M77	604.641	7373962	4661	Falla inversa	72	98	C	4	4	SR	Es calonida	14	Seco	Diclessa		R4	16-ul.		
M78	604.647	7373948	4671	Falla inversa	200	79	C	3	5	SR	Es calonida	12	Seco	Diclessa		R4	16-ul.		
M78	604.647	7373948	4671	Falla inversa	80	320	C	1	8	SR	Es calonida	14	Seco	Diclessa		R4	16-ul.		
M78	604.647	7373948	4671	Falla inversa	77	204	C	2	3	SR	Plana	14	Seco	Diclessa		R4	16-ul.		
D-29	604.290	7373650	4607	Pseudotratificación	60	154	C	4	0	SR	Es calonida	14	Seco	Diclessa		R4	16-ul.		
D-30	604.448	7373585	4610	Pseudotratificación	40	5	C	4	0	SR	Es calonida	14	Seco	Diclessa		R4	16-ul.		
D-31	604.448	7373585	4610	Pseudotratificación	50	251	C	4	0	SR	Es calonida	14	Seco	Diclessa		R4	16-ul.		
D-33	604.654	7373589	4666	Pseudotratificación	55	140	C	4	4	SR	Es calonida	14	Seco	Diclessa		R4	16-ul.		
D-34	604.654	7373589	4665	Pseudotratificación	55	124	C	4	2	SR	Es calonida	14	Seco	Diclessa		R4	16-ul.		
D-35	605.080	7373852	4666	Pseudotratificación	75	131	C	5	130	C	Plana	14	Seco	Diclessa		R4	16-ul.		
L61	602.713	7373852	4605	Pseudotratificación	85	82	C	4	0	SR	Es calonida	14	Seco	Diclessa		R4	16-ul.		
M74	604.382	7373651	4605	Pseudotratificación	85	82	C	4	0	SR	Es calonida	14	Seco	Diclessa		R4	16-ul.		

Base de datos

Annex XVI Appendix B



DIRECCIÓN TÉCNICA DE PROSPECCIÓN Y EXPLORACIÓN
"ESTUDIO GEOLÓGICO-ESTRUCTURAL DEL ÁREA
CIRCUNDANTE DEL MANANTIAL DEL SINALOA"

PTO.	ESTE	NORTE	ELEV.	TIPO	Az.	Bz.	DipDir	Pitch	CONTINUAD.	PERSISTENCIA	ABERTURA	REllENO	FORMA	JRC	AGUA	TIPO ROCA	ALTERACION	DUREZA	FECHA	observaciones	
M75	604.383	737.625	4604	Psuedoestratificación	87	125			C						Seco	Ductiles		R4	16-jul.		
M76	604.617	737.986	4653	Psuedoestratificación	44	146			C						Seco	Ductiles		R4	16-jul.		
M80	604.819	737.863	4650	Psuedoestratificación	52	120			C						Seco	Ductiles		R4	16-jul.		
D-40	604.589	737.0113	4555	Dicielsa	85	235			C	2	1.5				Ordinada	8			R3	17-jul.	
D-40	604.589	737.0113	4555	Dicielsa	58	175			D	1	3.5				Arenas	Burrosa			R3	17-jul.	
D-40	604.589	737.0113	4555	Dicielsa	58	175			C	1	3.5				Arenas	Burrosa			R3	17-jul.	
D-40	604.589	737.0113	4555	Dicielsa	90	115			C	1	2								R3	17-jul.	
D-40	604.589	737.0113	4555	Dicielsa	70	70			C	3	3.5								R3	17-jul.	
D-41	604.589	736.9716	4553	Dicielsa	65	206			C	2	3								R3	17-jul.	
D-41	604.589	736.9716	4553	Dicielsa	82	110			D	2	0.5								R3	17-jul.	
D-41	604.589	736.9716	4553	Dicielsa	45	225			C	2	2								R3	17-jul.	
D-41	604.589	736.9716	4553	Dicielsa	70	285			D	2	2								R3	17-jul.	
D-42	604.473	736.9716	4593	Dicielsa	81	55			D	1	3.5								R3	17-jul.	
D-43	603.804	736.8412	4611	Dicielsa	45	165			D	1	0								R3	17-jul.	
D-43	603.804	736.8412	4611	Dicielsa	80	185			D	1	0								R3	17-jul.	
D-43	603.804	736.8412	4611	Dicielsa	89	90			D	2	2								R3	17-jul.	
D-43	603.804	736.8412	4611	Dicielsa	66	225			D	1	0								R3	17-jul.	
D-44	604.263	736.0057	4604	Dicielsa	70	240			D	2	1.5								R3	17-jul.	
D-44	604.263	736.0057	4604	Dicielsa	89	260			D	2	2								R3	17-jul.	
D-45	603.288	736.0055	4604	Dicielsa	64	235			D	2	0.5								R3	17-jul.	
D-45	603.288	736.0055	4604	Dicielsa	60	277			C	2	2.5								R3	17-jul.	
D-45	603.288	736.0055	4604	Dicielsa	88	60			C	1	0								R3	17-jul.	
D-45	603.288	736.0055	4604	Dicielsa	44	290			C	2	1								R3	17-jul.	
D-46	606.397	736.9713	4591	Dicielsa	75	245			C	3	9								R3	17-jul.	
D-46	606.397	736.9713	4591	Dicielsa	73	288			C	2	2								R3	17-jul.	
D-46	606.397	736.9713	4591	Dicielsa	76	105			C	1	0.5								R3	17-jul.	
D-46	606.397	736.9713	4591	Dicielsa	82	280			C	2	2								R3	17-jul.	
D-46	606.397	736.9713	4591	Dicielsa	267	1			C	1	1								R3	17-jul.	
D-46	606.397	736.9713	4591	Dicielsa	75	130			C	3	1								R3	17-jul.	
D-46	606.397	736.9713	4591	Dicielsa	85	100			D	1	3								R3	17-jul.	
D-47	603.840	736.6465	4542	Dicielsa	62	325			D	2	1								R3	17-jul.	
D-47	603.840	736.6465	4542	Dicielsa	62	328			D	1	1								R3	17-jul.	
D-47	603.840	736.6465	4542	Dicielsa	48	270			D	2	0								R3	17-jul.	
D-47	603.840	736.6465	4542	Dicielsa	31	322			C	2	2								R3	17-jul.	
D-47	603.840	736.6465	4542	Dicielsa	58	95			D	1	0.5								R3	17-jul.	
D-47	603.840	736.6465	4542	Dicielsa	74	290			C	1	2								R3	17-jul.	
D-48	604.587	736.9403	4573	Dicielsa	73	252			D	1	2.5								R3	17-jul.	
D-48	604.587	736.9403	4573	Dicielsa	61	300			D	1	4								R3	17-jul.	
D-48	604.587	736.9403	4573	Dicielsa	85	104			C	1	6								R3	17-jul.	
D-48	604.587	736.9403	4573	Dicielsa	68	335			D	2	5								R3	17-jul.	
D-48	604.587	736.9403	4573	Dicielsa	76	33			C	4	5								R3	17-jul.	
L-12	602.844	737.5598	4627	Dicielsa	81	260			D	4	1								R3	17-jul.	
L-13	602.844	737.5598	4627	Dicielsa	64	282			D	1	5								R3	17-jul.	
L-14	602.844	737.5598	4627	Dicielsa	70	256			D	5	0								R4	17-jul.	
L-16	602.844	737.5598	4627	Dicielsa	80	320			D	4	2								R4	17-jul.	
L-17	602.844	737.5598	4627	Dicielsa	80	60			C	2	10								R4	17-jul.	
L-19	602.844	737.5598	4627	Dicielsa	87	225			C	2	5								R4	17-jul.	
L-20	602.844	737.5598	4627	Dicielsa	74	85			D	4	2								R4	17-jul.	
L-21	602.844	737.5598	4627	Dicielsa	89	272			D	3	0								R4	17-jul.	
L-22	602.844	737.5598	4627	Dicielsa	85	110			C	4	0								R4	17-jul.	
L-23	602.844	737.5598	4627	Dicielsa	89	100			C	5	1								R4	17-jul.	
L-24	602.844	737.5598	4627	Dicielsa	87	107			C	4	0								R4	17-jul.	
L-25	602.844	737.5598	4627	Dicielsa	88	111			C	3	0								R4	17-jul.	
L-26	602.844	737.5598	4627	Dicielsa	86	114			C	3	0								R4	17-jul.	
L-27	602.844	737.5598	4627	Dicielsa	60	100			D	2	2								R4	17-jul.	
L-28	602.844	737.5598	4627	Dicielsa	62	109			D	1	3								R4	17-jul.	
L-29	602.844	737.5598	4627	Dicielsa	68	124			C	4	0								R4	17-jul.	
L-30	602.844	737.5598	4627	Dicielsa	65	94			D	3	0								R4	17-jul.	
L-31	602.844	737.5598	4627	Dicielsa	83	97			D	2	0								R4	17-jul.	
L-32	602.844	737.5598	4627	Dicielsa	67	109			D	1	3								R4	17-jul.	
L-33	602.844	737.5598	4627	Dicielsa	65	94			D	3	0								R4	17-jul.	
L-34	602.844	737.5598	4627	Dicielsa	68	124			C	4	0								R4	17-jul.	
L-35	602.844	737.5598	4627	Dicielsa	65	94			D	3	0								R4	17-jul.	
L-36	602.844	737.5598	4627	Dicielsa	83	97			D	2	0								R4	17-jul.	

Base de datos

Página 29

**DIRECCIÓN TÉCNICA DE PROSPECCIÓN Y EXPLORACIÓN
"ESTUDIO GEOLÓGICO-ESTRUCTURAL DEL ÁREA
CIRCUNDANTE DEL MANANTIAL DEL SISAL"**



PTO.	ESTE	NORTE	ELEV.	TIPO	Az.	Bz.	DipDir	Pitch	CONTINUIDAD	PERSISTENCIA (10m)	ABERTURA (cm)	RELLENO	FORMA	JRC	AGUA	TIPO ROCA	ALTERACION	DUREZA	FECHA	observaciones
L737	6020844	7573598	4627	Dicielsa	80	90	D	4	SR	Plana	6	Seco	Dicielsa	R4	17-jul.					
L739	6020620	7573443	4670	Dicielsa	88	146	C	4	SR	Rugosa	6	Seco	Dicielsa	R4	17-jul.					
L741	6020620	7573443	4670	Dicielsa	83	75	D	3	SR	Rugosa	6	Seco	Dicielsa	R4	17-jul.					
L742	6020620	7573443	4670	Dicielsa	60	150	C	4	SR	Buena	6	Seco	Dicielsa	R4	17-jul.					
L743	6020620	7573423	4670	Dicielsa	79	156	C	3	SR	Buena	6	Seco	Dicielsa	R4	17-jul.					
L744	6020620	7573423	4670	Dicielsa	87	260	C	2	SR	Rugosa	6	Seco	Dicielsa	R4	17-jul.					
L745	6020620	7573423	4670	Dicielsa	89	126	D	4	SR	Rugosa	6	Seco	Dicielsa	R4	17-jul.					
L746	6020620	7573423	4670	Dicielsa	70	80	D	3	SR	Rugosa	6	Seco	Dicielsa	R4	17-jul.					
L747	6020620	7573423	4670	Dicielsa	87	84	D	2	SR	Rugosa	6	Seco	Dicielsa	R4	17-jul.					
L748	6020620	7573423	4670	Dicielsa	81	72	D	4	SR	Rugosa	6	Seco	Dicielsa	R4	17-jul.					
L749	6020620	7573423	4670	Dicielsa	60	136	C	3	SR	Rugosa	8	Seco	Dicielsa	R4	17-jul.					
L750	6020620	7573423	4670	Dicielsa	88	165	C	3	SR	Ordinada	8	Seco	Dicielsa	R4	17-jul.					
L751	6020620	7573423	4670	Dicielsa	81	320	D	2	SR	Ordinada	8	Seco	Dicielsa	R4	17-jul.					
L752	6020620	7573423	4670	Dicielsa	85	318	C	3	SR	Buena	8	Seco	Dicielsa	R4	17-jul.					
L753	6020620	7573423	4670	Dicielsa	85	345	C	2	SR	Plana	8	Seco	Dicielsa	R4	17-jul.					
L754	6020620	7573423	4670	Dicielsa	87	5	C	1	SR	Plana	8	Seco	Dicielsa	R4	17-jul.					
L755	6020620	7573423	4670	Dicielsa	84	350	D	2	SR	Ordinada	8	Seco	Dicielsa	R4	17-jul.					
L756	6020620	7573423	4670	Dicielsa	87	326	D	4	SR	Plana	8	Seco	Dicielsa	R4	17-jul.					
L757	6020620	7573423	4670	Dicielsa	89	310	D	3	SR	Plana	8	Seco	Dicielsa	R4	17-jul.					
L758	6020625	7569543	4579	Dicielsa	70	105	D	4	SR	Arenas	6	Seco	Dicielsa	R4	17-jul.					
L759	6020625	7569543	4579	Dicielsa	57	99	D	5	SR	Arenas	6	Seco	Dicielsa	R4	17-jul.					
L760	6020625	7569543	4579	Dicielsa	82	115	D	3	SR	Arenas	6	Seco	Dicielsa	R4	17-jul.					
L761	6020625	7569543	4579	Dicielsa	70	126	D	1	SR	Arenas	6	Seco	Dicielsa	R4	17-jul.					
L762	6020625	7569543	4579	Dicielsa	73	120	D	3	SR	Arenas	6	Seco	Dicielsa	R4	17-jul.					
L763	6020625	7569543	4579	Dicielsa	85	123	D	3	SR	Arenas	6	Seco	Dicielsa	R4	17-jul.					
L764	6020625	7569543	4579	Dicielsa	80	103	D	5	SR	Arenas	6	Seco	Dicielsa	R4	17-jul.					
L765	6020627	7569543	4572	Dicielsa	60	104	D	3	SR	Arenas	6	Seco	Dicielsa	R4	17-jul.					
L766	6020627	7569543	4572	Dicielsa	88	45	D	3	SR	Arenas	6	Seco	Dicielsa	R4	17-jul.					
L767	6020627	7569547	4572	Dicielsa	50	97	D	2	SR	Arenas	6	Seco	Dicielsa	R4	17-jul.					
L768	6020627	7569547	4572	Dicielsa	78	100	D	6	SR	Arenas	6	Seco	Dicielsa	R4	17-jul.					
L769	6020627	7569547	4572	Dicielsa	83	104	D	3	SR	Arenas	6	Seco	Dicielsa	R4	17-jul.					
L770	6020627	7569547	4572	Dicielsa	87	395	D	4	SR	Arenas	6	Seco	Dicielsa	R4	17-jul.					
L771	6020627	7569547	4572	Dicielsa	85	138	D	2	SR	Arenas	6	Seco	Dicielsa	R4	17-jul.					
L772	6020627	7569547	4572	Dicielsa	65	326	D	2	SR	Arenas	6	Seco	Dicielsa	R4	17-jul.					
L773	6020502	7570166	4573	Dicielsa	62	260	D	6	SR	Plana	6	Seco	Dicielsa	R4	17-jul.					
L776	6020502	7570166	4573	Dicielsa	87	135	C	3	SR	Plana	6	Seco	Dicielsa	R4	17-jul.					
L779	6020502	7570166	4573	Dicielsa	70	30	D	5	SR	Plana	6	Seco	Dicielsa	R4	17-jul.					
L781	6020502	7570166	4573	Dicielsa	75	27	D	3	SR	Plana	6	Seco	Dicielsa	R3	17-jul.					
L782	6020502	7570166	4573	Dicielsa	81	350	D	4	SR	Plana	12	Seco	Unimritis	R2	17-jul.					
M81	6020548	7570174	4575	Dicielsa	61	220	D	5	SR	Plana	8	Seco	Unimritis	R2	17-jul.					
M82	6020548	7570174	4575	Dicielsa	87	95	D	4	SR	Plana	12	Seco	Unimritis	R2	17-jul.					
M83	6020548	7570174	4575	Dicielsa	39	316	C	1	SR	Plana	12	Seco	Unimritis	R2	17-jul.					
M84	6020548	7570166	4575	Dicielsa	72	214	D	4	SR	Plana	14	Seco	Unimritis	R2	17-jul.					
M85	6020548	7570166	4575	Dicielsa	32	32	C	2	SR	Plana	11	Seco	Unimritis	R2	17-jul.					
M86	6020548	7570166	4575	Dicielsa	40	230	D	4	SR	Plana	10	Seco	Unimritis	R2	17-jul.					
M87	6020505	7570166	4578	Dicielsa	89	295	C	1	SR	Es calonida	14	Seco	Unimritis	R2	17-jul.					
M88	6020505	7570166	4578	Dicielsa	64	330	D	1	SR	Plana	14	Seco	Unimritis	R2	17-jul.					
M89	6020505	7570166	4578	Dicielsa	68	165	D	3	SR	Escalonida	14	Seco	Unimritis	R2	17-jul.					
M90	60205471	7570143	4596	Dicielsa	84	310	D	4	SR	Plana	14	Seco	Unimritis	R2	17-jul.					
M91	60205471	7570143	4596	Dicielsa	72	302	C	0.5	SR	Plana	14	Seco	Unimritis	R2	17-jul.					
M92	60205471	7570143	4596	Dicielsa	63	14	C	1	SR	Plana	14	Seco	Unimritis	R2	17-jul.					
M93	60205471	7570143	4596	Dicielsa	76	134	D	2	SR	Es calonida	14	Seco	Unimritis	R2	17-jul.					
M94	60205471	7570143	4596	Dicielsa	50	287	D	3	SR	Plana	14	Seco	Unimritis	R2	17-jul.					
M95	6020598	7569510	4591	Dicielsa	69	232	D	3	SR	Plana	14	Seco	Unimritis	R2	17-jul.					
M96	6020598	7569510	4591	Dicielsa	74	295	D	1	SR	Arenas	14	Seco	Unimritis	R2	17-jul.					
M97	6020598	7569510	4591	Dicielsa	70	54	C	2	SR	Arenas	14	Seco	Unimritis	R2	17-jul.					
M98	6020598	7569510	4591	Dicielsa	76	256	C	1	SR	Plana	14	Seco	Unimritis	R2	17-jul.					
M99	6020598	7569510	4591	Dicielsa	66	242	C	4	SR	Plana	14	Seco	Unimritis	R2	17-jul.					

Base de datos

Página 30

Annex XVI Appendix B



**DIRECCIÓN TÉCNICA DE PROSPECCIÓN Y EXPLORACIÓN
"ESTUDIO GEOLÓGICO-ESTRUCTURAL DEL ÁREA
CIRCUNDANTE DEL MANANTIAL DEL SISAL"**

PTO.	ESTE	NORTE	ELEV.	TIPO	Az.	Bz.	DipDir	Pitch	CONTINUADO	PERSISTENCIA (100m)	ABERTURA (100m)	FORMA	JRC	AGUA	TIPO ROCA	ALTERACION	DUREZA	FECHA	OBSERVACIONES
M85	6050987	7570082	4559	Diciplasa	62	74	C		3	1	SR	Plana	14	Saco	Iguminitas		R2	17-jul	
M85	6050987	7570082	4559	Diciplasa	81	11	D		3	2	SR	Plana	14	Saco	Iguminitas		R2	17-jul	
M85	6050987	7570082	4559	Diciplasa	82	48	D		2	0	SR	Plana	14	Saco	Iguminitas		R2	17-jul	
M85	6050987	7570082	4559	Diciplasa	75	96	D		1	1	SR	Arenas	14	Saco	Iguminitas		R2	17-jul	
M85	6050987	7570082	4559	Diciplasa	72	27	D		4	3	SR	Arenas	14	Saco	Iguminitas		R2	17-jul	
M85	6050987	7570082	4559	Diciplasa	72	27	D		3	3	SR	Arenas	14	Saco	Iguminitas		R2	17-jul	
M85	6050987	7570082	4559	Diciplasa	45	148	D		3	0	SR	Esalonada	14	Saco	Iguminitas		R2	17-jul	
M85	6050987	7570082	4559	Diciplasa	76	95	C		14	1	SR	Plana	14	Saco	Iguminitas		R2	17-jul	
M85	6050987	7570082	4559	Diciplasa	72	51	C		12	1	SR	Arenas	14	Saco	Iguminitas		R2	17-jul	
M85	6050987	7570082	4559	Diciplasa	78	185	D		3	2	SR	Esalonada	14	Saco	Iguminitas		R2	17-jul	
M85	6050987	7570082	4559	Diciplasa	80	105	C		3	3	SR	Plana	14	Saco	Iguminitas		R2	17-jul	
M85	6050987	7570082	4559	Diciplasa	72	100	C		8	2	SR	Plana	14	Saco	Iguminitas		R2	17-jul	
M87	6030713	75685156	4555	Diciplasa	75	328	C		8	2	SR	Arenas	14	Saco	Iguminitas		R2	17-jul	
M87	6030713	75685156	4555	Diciplasa	66	47	D		2	1	SR	Plana	14	Saco	Iguminitas		R2	17-jul	
M87	6030713	75685156	4555	Diciplasa	82	5	C		10	1	SR	Plana	14	Saco	Iguminitas		R2	17-jul	
M87	6030713	75685156	4555	Diciplasa	73	261	C		1	1	SR	Plana	14	Saco	Iguminitas		R2	17-jul	
M87	6030713	75685156	4555	Diciplasa	83	5	D		6	2	SR	Plana	14	Saco	Iguminitas		R2	17-jul	
M87	6030713	75685156	4555	Diciplasa	85	70	D		4	2	SR	Plana	14	Saco	Iguminitas		R2	17-jul	
M87	6030713	75685156	4555	Diciplasa	68	118	D		2	10	SR	Arenas	14	Saco	Iguminitas		R2	17-jul	
M88	6030715	75685152	4555	Diciplasa	64	170	C		3	8	SR	Plana	14	Saco	Iguminitas		R2	17-jul	
M88	6030715	75685152	4555	Diciplasa	76	181	C		2	1	SR	Plana	14	Saco	Iguminitas		R2	17-jul	
M88	6030715	75685152	4555	Diciplasa	67	26	C		1	1	SR	Plana	14	Saco	Iguminitas		R2	17-jul	
M88	6030715	75685152	4555	Diciplasa	75	345	C		1	2	SR	Arenas	14	Saco	Iguminitas		R2	17-jul	
M88	6030715	75685152	4555	Diciplasa	60	310	C		1	2	SR	Plana	14	Saco	Iguminitas		R2	17-jul	
M88	6030715	75685152	4555	Diciplasa	76	300	C		1	4	SR	Plana	14	Saco	Iguminitas		R2	17-jul	
M88	6030715	75685152	4555	Diciplasa	60	110	D		3	10	SR	Esalonada	14	Saco	Iguminitas		R2	17-jul	
M88	6030715	75685152	4555	Diciplasa	42	340	D		1	3	SR	Plana	14	Saco	Iguminitas		R2	17-jul	
M88	6030715	75685152	4555	Diciplasa	77	170	C		3	2	SR	Arenas	14	Saco	Iguminitas		R2	17-jul	
M88	6030715	75685152	4555	Diciplasa	74	170	C		2	1	SR	Plana	14	Saco	Iguminitas		R2	17-jul	
M89	6040114	75685452	4596	Diciplasa	75	345	C		1	1	SR	Plana	14	Saco	Iguminitas		R2	17-jul	
M89	6040114	75685452	4596	Diciplasa	60	310	C		1	2	SR	Plana	14	Saco	Iguminitas		R2	17-jul	
M89	6040114	75685452	4596	Diciplasa	76	300	C		1	4	SR	Plana	14	Saco	Iguminitas		R2	17-jul	
M89	6040114	75685452	4596	Diciplasa	60	110	D		3	10	SR	Esalonada	14	Saco	Iguminitas		R2	17-jul	
M89	6040114	75685452	4596	Diciplasa	42	340	D		1	3	SR	Plana	14	Saco	Iguminitas		R2	17-jul	
M89	6040114	75685452	4596	Diciplasa	87	160	D		2	5	SR	Arenas	14	Saco	Iguminitas		R2	17-jul	
M89	6040114	75685452	4596	Diciplasa	86	325	C		1	2	SR	Plana	14	Saco	Iguminitas		R2	17-jul	
M89	6040114	75685452	4596	Diciplasa	72	52	D		1	0.5	SR	Plana	14	Saco	Iguminitas		R2	17-jul	
M89	6040114	75685452	4596	Diciplasa	75	285	D		2	2	SR	Plana	12	Saco	Iguminitas		R2	17-jul	
M89	6040114	75685452	4596	Diciplasa	80	269	C		3	0	SR	Plana	12	Saco	Iguminitas		R2	17-jul	
M90	6040114	75685452	4596	Diciplasa	71	260	C		3	10	SR	Plana	14	Saco	Iguminitas		R2	17-jul	
M90	6040114	75685452	4596	Diciplasa	78	25	D		3	4	SR	Arenas	14	Saco	Iguminitas		R2	17-jul	
M90	60401565	75685415	4568	Diciplasa	74	35	C		5	7	SR	Arenas	12	Saco	Iguminitas		R2	17-jul	
M90	60401565	75685415	4568	Diciplasa	80	293	C		1	3	SR	Plana	12	Saco	Iguminitas		R2	17-jul	
M91	6030271	75685381	4580	Diciplasa	80	110	C		3	2	SR	Plana	12	Saco	Iguminitas		R2	17-jul	
M91	6030271	75685381	4580	Diciplasa	75	285	C		3	1	SR	Plana	14	Saco	Iguminitas		R2	17-jul	
M91	6030271	75685381	4580	Diciplasa	82	282	D		2	1	SR	Esalonada	14	Saco	Iguminitas		R2	17-jul	
M91	6030271	75685381	4580	Diciplasa	35	263	D		5	0.5	SR	Plana	12	Saco	Iguminitas		R2	17-jul	
M91	6030271	75685381	4580	Diciplasa	76	310	C		2	0	SR	Plana	12	Saco	Iguminitas		R2	17-jul	
M91	6030271	75685381	4580	Diciplasa	80	155	C		1	0	SR	Plana	8	Saco	Dolomitas		R2	17-jul	
M91	6030271	75685381	4580	Diciplasa	87	310	D		1	0	SR	Plana	6	Saco	Dolomitas		R2	17-jul	
M91	6030271	75685381	4580	Diciplasa	87	155	D		1	0	SR	Plana	6	Saco	Dolomitas		R2	17-jul	
M91	6030271	75685381	4580	Diciplasa	75	155	D		1	4	SR	Plana	6	Saco	Dolomitas		R2	17-jul	
M91	6030271	75685381	4580	Diciplasa	60	128	C		2	0.2	SR	Plana	12	Saco	Iguminitas		R2	17-jul	
M92	6030505	7570166	4578	Falla	85	120	C		2	1	SR	Plana	10	Saco	Iguminitas		R2	17-jul	
M92	6030505	7570166	4578	Falla	84	120	C		2	1	SR	Plana	14	Saco	Iguminitas		R2	17-jul	
M92	6030505	7570166	4578	Falla	77	278	C		1	5	SR	Ornacida	8	Saco	Iguminitas		R2	17-jul	
M92	6030505	7570166	4578	Falla	4604	298	C		1	1	SR	Plana-Ornacida	8	Saco	Iguminitas		R3	17-jul	
D-41	60304972	7568776	4593	Falla inversa	49	282	C		0.5	1	SR	Plana-Ornacida	8	Saco	Iguminitas		R3	17-jul	
D-42	60304972	7568770	4593	Falla inversa	75	302	C		1	0	SR	Plana	12	Saco	Iguminitas		R3	17-jul	
D-43	60304972	7568770	4593	Falla inversa	86	136	C		1	0	SR	Plana	12	Saco	Iguminitas		R3	17-jul	
D-44	60304972	7568770	4593	Falla inversa	315	4515	C		4	4	SR	Plana	12	Saco	Iguminitas		R3	17-jul	
M81	6030498	7570114	4575	Falla inversa	65	210	C		1	5	SR	Plana	2	Saco	Iguminitas		R2	17-jul	
M81	6030498	7570114	4575	Falla inversa	65	231	C		3	0.2	SR	Plana	2	Saco	Iguminitas		R2	17-jul	
M82	6030498	7570114	4575	Falla inversa	64	98	C		0.5	1	SR	Plana	16	Saco	Iguminitas		R2	17-jul	
M82	6030498	7570114	4575	Falla inversa	57	163	C		3	0.5	SR	Plana	16	Saco	Iguminitas		R2	17-jul	
M82	6030498	7570114	4575	Falla inversa	57	163	C		1	5	SR	Plana	4	Saco	Iguminitas		R3	17-jul	
D-44	6030263	7568770	4604	Falla Normal	79	245	C		1	4	SR	Plana	6	Saco	Iguminitas		R3	17-jul	

Base de datos

**DIRECCIÓN TÉCNICA DE PROSPECCIÓN Y EXPLORACIÓN
ESTUDIO GEOLÓGICO-ESTRUCTURAL DEL ÁREA
CIRCUNDANTE DEL MANANTIAL DEL SISALÁ***



PTO.	ESTE	NORTE	ELEV.	Tipo	Az.	Bz.	DipDir	PtchDir	CONTINUADO	PERSISTENCIA (10m)	ABERTURA (10m)	RELLENO	FORMA	JRC	AGUA	TIPO ROCA	ALTERACION	DUREZA	FECHA	OBSERVACIONES
L7'22	002°28'44	7373598	46277	Falla Normal	82	305	C	1	0	SR	Plana	S	Seco	Ductiles	R4	17-jul				
L7'23	002°28'44	7373598	46277	Falla Normal	80	300	C	1	0	SR	Plana	8	Seco	Ductiles	R4	17-jul				
L7'24	002°28'44	7373598	46277	Falla Normal	80	110	C	1	3	SR	Plana	4	Seco	Ductiles	R4	17-jul	Desplazamiento 10cm			
L7'25	002°28'44	7373598	46277	Falla Normal	83	122	75	C	1	20	Briques	Plana	4	Seco	Ductiles	R4	17-jul			
L7'26	002°28'44	7373598	46277	Falla Normal	78	265	D	1	0	SR	Plana	6	Seco	Ductiles	R4	17-jul	Desplazamiento 12cm			
L7'27	002°28'44	7373598	46277	Falla Normal	78	265	D	1	0	SR	Plana	6	Seco	Ductiles	R4	17-jul				
L7'28	002°28'40	7373493	46170	Falla Normal	72	80	C	1	2	SR	Plana	6	Seco	Ductiles	R4	17-jul	Desplazamiento 10cm			
L7'75	002°05'02	7370166	4573	Falla Normal	80	130	D	1	0	SR	Plana	6	Seco	Ductiles	R4	17-jul	Desplazamiento 15 cm			
L7'77	002°05'02	7370166	4573	Falla Normal	65	132	D	1	0	SR	Plana	6	Seco	Ductiles	R4	17-jul	Desplazamiento 15 cm			
M81	002°48'48	7370166	4573	Falla Normal	68	115	C	1	0	SR	Plana	6	Seco	Ductiles	R4	17-jul	Desplazamiento 10 cm			
M82	002°50'05	7370166	4573	Falla Normal	67	140	C	3	1	SR	Arenas	12	Seco	(In)minimistas	R2	17-jul				
M82	002°50'05	7370166	4573	Falla Normal	85	285	C	1	4	SR	Plana	12	Seco	(In)minimistas	R2	17-jul				
M82	002°50'05	7370166	4573	Falla Normal	75	125	C	1	10	SR	Arenas	10	Seco	(In)minimistas	R2	17-jul				
M82	002°50'05	7370166	4573	Falla Normal	71	291	C	1	0	SR	Plana	10	Seco	(In)minimistas	R2	17-jul				
M86	002°05'05	7369340	45716	Falla Normal	76	102	C	1	2.5	SR	Plana	14	Seco	(In)minimistas	R2	17-jul				
M86	002°05'05	7369340	45716	Falla Normal	64	114	C	1	1	SR	Plana	14	Seco	(In)minimistas	R2	17-jul				
M86	002°05'05	7369340	45716	Falla Normal	65	125	C	2	1	SR	Plana	14	Seco	(In)minimistas	R2	17-jul				
M86	002°05'05	7369340	45716	Falla Normal	78	110	C	5	4	SR	Plana	14	Seco	(In)minimistas	R2	17-jul				
M86	002°05'05	7369340	45716	Falla Normal	81	265	C	5	3	SR	Plana	14	Seco	(In)minimistas	R2	17-jul				
M86	002°05'05	7369340	45716	Falla Normal	83	310	C	2	3	SR	Arenas	14	Seco	(In)minimistas	R2	17-jul				
L7'15	002°55'44	7373598	46277	Psiudotratificación	86	345	C	2	0	SR	Plana	10	Seco	(In)minimistas	R4	17-jul				
M86	002°05'05	7369340	45716	Psiudotratificación	26	200	C	2	0	SR	Plana	10	Seco	(In)minimistas	R2	17-jul				
M90	002°56'85	7369340	45716	Psiudotratificación	83	2	C	2	0	SR	Plana	10	Seco	(In)minimistas	R2	17-jul				
L7'84	002°56'90	7373093	5084	Dicelosa	3.27	77	237	D	8	0	SR	Es calonada	8	Seco	Brecha de base	R2	18-juil			
L7'85	002°56'90	7373093	5084	Dicelosa	3.23	68	233	D	8	0	SR	Es calonada	8	Seco	Brecha de base	R2	18-juil			
L7'93	002°56'90	7373093	5084	Dicelosa	64	95	D	4	0	SR	Plana	10	Seco	Brecha de base	R3	18-juil				
L810	002°56'90	7373093	5084	Dicelosa	83	20	C	10	5	SR	Plana	10	Seco	Brecha de base	R4	18-juil				
M92	002°59'49	7373433	4942	Dicelosa	82	180	D	1	0.3	SR	Plana-Rugosa	12	Seco	Arribadas	R4	18-juil				
M92	002°59'49	7373433	4942	Dicelosa	89	230	D	5	2	SR	Plana	10	Seco	Arribadas	R4	18-juil				
M92	002°59'49	7373433	4942	Dicelosa	82	339	D	5	2	SR	Rugosa	10	Seco	Arribadas	R4	18-juil				
M92	002°59'49	7373433	4942	Dicelosa	85	117	C	1	1	SR	Arenas	14	Seco	Arribadas	R4	18-juil				
M92	002°59'49	7373433	4942	Dicelosa	74	239	D	2	0.2	SR	Plana	4	Seco	Arribadas	R4	18-juil				
M92	002°59'49	7373433	4942	Dicelosa	36	224	D	3	1	SR	Plana	8	Seco	Arribadas	R4	18-juil				
M92	002°59'49	7373433	4942	Dicelosa	84	284	D	1	0.2	SR	Rugosa	4	Seco	Arribadas	R4	18-juil				
M92	002°59'49	7373433	4942	Dicelosa	56	300	C	2	0.2	SR	Plana	4	Seco	Arribadas	R4	18-juil				
M93	002°59'36	7373240	50116	Dicelosa	67	182	D	2	0.5	SR	Es calonada-Rugosa	12	Seco	Ductiles	R4	18-juil				
M93	002°59'36	7373240	50116	Dicelosa	87	87	C	1	1.5	SR	Arenas	14	Seco	Ductiles	R4	18-juil				
M93	002°59'36	7373240	50116	Dicelosa	78	17	D	2	1	SR	Es calonada	12	Seco	Ductiles	R4	18-juil				
M93	002°59'36	7373240	50116	Dicelosa	49	90	C	1	0.5	SR	Ondulada	12	Seco	Ductiles	R4	18-juil				
M93	002°59'36	7373240	50116	Dicelosa	70	105	C	2	3	SR	Es calonada	12	Seco	Ductiles	R4	18-juil				
M93	002°59'36	7373240	50116	Dicelosa	86	295	C	1	14	SR	Es calonada	14	Seco	Ductiles	R4	18-juil				
M93	002°59'36	7373240	50116	Dicelosa	78	5	D	3	5	SR	Arenas	14	Seco	Ductiles	R4	18-juil				
M93	002°59'36	7373240	50116	Dicelosa	60	275	C	1	4	SR	Plana	14	Seco	Ductiles	R4	18-juil				
M93	002°59'36	7373240	50116	Dicelosa	53	93	C	1	0.5	SR	Plana	12	Seco	Brecha de base	R3	18-juil				
M93	002°59'36	7373240	50116	Dicelosa	50	195	C	2	0.2	SR	Plana-Ondulada	12	Seco	Brecha de base	R4	18-juil				
M93	002°59'36	7373240	50116	Dicelosa	70	28	D	4	0	SR	Plana	10	Seco	Arribadas	R4	18-juil				
M93	002°59'36	7373240	50116	Dicelosa	82	342	C	1	1	SR	Es calonada	8	Seco	Arribadas	R4	18-juil				
M93	002°59'36	7373240	50116	Dicelosa	73	265	C	2	0.5	SR	Es calonada	14	Seco	Arribadas	R4	18-juil				
M93	002°59'36	7373240	50116	Dicelosa	76	261	C	4	4	SR	Es calonada	14	Seco	Arribadas	R4	18-juil				
M93	002°59'36	7373240	50116	Dicelosa	62	40	C	1	1	SR	Es calonada	14	Seco	Arribadas	R4	18-juil				
M93	002°59'36	7373240	50116	Dicelosa	87	265	C	3	1	SR	Es calonada	14	Seco	Arribadas	R4	18-juil				
M93	002°59'36	7373240	50116	Dicelosa	87	130	D	1	1	SR	Es calonada	12	Seco	Arribadas	R4	18-juil				
M93	002°59'36	7373240	50116	Dicelosa	70	267	D	3	0	SR	Plana	6	Seco	Arribadas	R4	18-juil				
M98	002°59'07	7372838	5176	Dicelosa	88	0	C	4	0.5	Calcare	Plana	10	Seco	Arribadas	R4	18-juil				

Base de datos

Página 32

Annex XVI Appendix B



**DIRECCIÓN TÉCNICA DE PROSPECCIÓN Y EXPLORACIÓN
ESTUDIO GEOLÓGICO-ESTRUCTURAL DEL ÁREA
CIRCUNDANTE DEL MANANTIAL DEL SISALÁ***

PTO.	ESTE	NORTE	ELEV.	Az.	Bz.	Pitch	CONTINUO	PERSISTENCIA (10m)	ABERTURA (10m)	FORMA	JRC	TIPO ROCA	AGUA	TIPO AGUA	ALTERACION	DUREZA	FECHA	NOTAS
M98	519.073	7572.638	517.6	Diciplasa	76	170	C	5	2	SR	Escalonada	12	Saco	Arenas		R4	18 ul.	
M98	519.073	7572.638	517.6	Diciplasa	82	121	C	1	1	SR	Plana	4	Saco	Arenas		R4	18 ul.	
M98	519.073	7572.638	517.6	Diciplasa	75	345	C	2	2	SR	Escalonada	10	Saco	Arenas		R4	18 ul.	
M98	519.073	7572.638	517.6	Diciplasa	64	195	D	3	0.5	Cielita	14	Saco	Arenas		R4	18 ul.		
M98	519.073	7572.638	517.6	Diciplasa	60	245	C	3	0.5	Piso-Ondulado	8	Saco	Arenas		R4	18 ul.		
M98	519.073	7572.638	517.6	Diciplasa	51.16	203.88	D	2	0.5	Cielita	14	Saco	Arenas		R4	18 ul.		
L794	519.5900	757.0793	503.4	Falla	80	215	C	1	2	SR	Es calonada	14	Saco	Arenas		R4	18 ul.	
L795	519.5900	757.0793	503.4	Falla	80	97	C	1	0	SR	Ondulada	10	Saco	Brecha de base		R2	18 ul.	
L796	519.5900	757.0793	503.4	Falla	82	165	C	1	0	SR	Ondulada	10	Saco	Brecha de base		R2	18 ul.	
L797	519.5900	757.0793	503.4	Falla	75	60	C	1	0	SR	Ondulada	10	Saco	Brecha de base		R2	18 ul.	
L798	519.5900	757.0793	503.4	Falla	60	218	C	1	0	SR	Ondulada	10	Saco	Brecha de base		R2	18 ul.	
L799	519.5900	757.0793	503.4	Falla	3.15	87	C	1	0	SR	Ondulada	10	Saco	Brecha de base		R2	18 ul.	
L800	519.5900	757.0793	503.4	Falla	80	50	C	1	0	SR	Ondulada	10	Saco	Brecha de base		R2	18 ul.	
L805	519.5900	757.0793	503.4	Falla	82	37	C	1	0	SR	Ondulada	10	Saco	Brecha de base		R2	18 ul.	
L790	519.5900	757.0793	503.4	Falla inversa	86	180	C	1	0	SR	Escalonada	6	Saco	Brecha de base		R2	18 ul.	
L792	519.5900	757.0793	503.4	Falla inversa	85	201	C	1	0	SR	Escalonada	6	Saco	Brecha de base		R2	18 ul.	
L808	519.369	757.0793	503.4	Falla inversa	3.35	82	C	1	0.5	SR	Curva	10	Saco	Brecha de base		R2	18 ul.	
M98	519.369	757.0793	51.46	Falla inversa	78	70	C	1	0.5	SR	Piso-Ondulado	10	Saco	Arenas		R4	18 ul.	
L786	519.5900	757.0793	503.4	Falla inversa	78	212	D	1	0	SR	Escalonada	8	Saco	Brecha de base		R2	18 ul.	
L787	519.5900	757.0793	503.4	Falla inversa	70	227	D	1	0	SR	Ondulada	10	Saco	Brecha de base		R2	18 ul.	
L788	519.5900	757.0793	503.4	Falla inversa	84	244	C	1	0	SR	Ondulada	6	Saco	Brecha de base		R2	18 ul.	
L789	519.5900	757.0793	503.4	Falla inversa	85	243	C	1	0	SR	Escalonada	6	Saco	Brecha de base		R2	18 ul.	
L790	519.5900	757.0793	503.4	Falla inversa	83	205	C	1	0	SR	Es calonida	6	Saco	Brecha de base		R2	18 ul.	
L791	519.5900	757.0793	503.4	Falla inversa	74	72	C	1	0	SR	Ondulada	10	Saco	Brecha de base		R2	18 ul.	
L797	519.5900	757.0793	503.4	Falla inversa	140	70	C	1	0	SR	Ondulada	10	Saco	Brecha de base		R2	18 ul.	
L801	519.5900	757.0793	503.4	Falla inversa	87	40	C	1	0	SR	Ondulada	10	Saco	Brecha de base		R2	18 ul.	
L802	519.5900	757.0793	503.4	Falla inversa	85	42	C	1	0	SR	Ondulada	10	Saco	Brecha de base		R2	18 ul.	
L803	519.5900	757.0793	503.4	Falla inversa	3.00	75	C	1	0	SR	Ondulada	10	Saco	Brecha de base		R2	18 ul.	
L806	519.5900	757.0793	503.4	Falla inversa	3.10	70	C	1	0	SR	Ondulada	10	Saco	Brecha de base		R2	18 ul.	
L807	519.5900	757.0793	503.4	Falla inversa	80	14	C	1	0	SR	Plana	10	Saco	Brecha de base		R2	18 ul.	
L809	519.5900	757.0793	503.4	Falla inversa	2.20	84	C	1	0	SR	Plana	6	Saco	Arenas		R4	18 ul.	
M92	519.439	757.433	49.42	Falla inversa	42	295	C	1	0.5	SR	Plana	8	Saco	Arenas		R4	18 ul.	
M92	519.439	757.433	49.42	Falla inversa	62	234	C	1	0	SR	Plana	12	Saco	Brecha de base		R3	18 ul.	
M95	519.368	757.186	51.17	Falla inversa	52	153	C	1	0.5	SR	Ondulada	10	Saco	Brecha de base		R4	18 ul.	
M96	519.369	757.186	51.46	Falla inversa	85	188	C	3	0.5	SR	Ondulada-Sesilizada	10	Saco	Brecha de base		R4	18 ul.	
D49	519.369	757.186	51.46	Falla inversa	3.2	44	C	0.5	0.5	SR	Ondulada	8	Saco	Arenas		R4	18 ul.	
L812	519.161	756.867	49.42	Diciplasa	78	215	D	2	0.5	Arena	4	Saco	Dificultad		R4	5-40.		
L813	519.161	756.867	49.42	Diciplasa	89	290	D	3	15	Biques	8	Saco	Dificultad		R4	5-40.		
L814	519.161	756.867	49.42	Diciplasa	90	330	D	4	10	Biques	8	Saco	Dificultad		R4	5-40.		
L815	519.161	756.867	49.42	Diciplasa	250	90	D	4	5	Biques	8	Saco	Dificultad		R4	5-40.		
L816	519.161	756.867	49.42	Diciplasa	80	170	D	2	4	SR	Plana	8	Saco	Dificultad		R4	5-40.	
L826	519.271	756.352	49.46	Diciplasa	75	216	C	5	5	SR	Plana	8	Saco	Dificultad		R4	5-40.	
L827	519.271	756.352	49.46	Diciplasa	76	54	C	5	3	SR	Plana	8	Saco	Dificultad		R4	5-40.	
L828	519.271	756.352	49.46	Diciplasa	81	33	C	6	10	SR	Plana	8	Saco	Dificultad		R4	5-40.	
L830	519.271	756.352	49.46	Diciplasa	75	35	C	2	0	SR	Plana	12	Saco	Dificultad		R4	5-40.	
L832	520.202	756.755	49.24	Diciplasa	88	85	D	4	45	Arena	8	Saco	Dificultad		R4	5-40.		
L833	520.202	756.755	49.24	Diciplasa	89	86	D	3	5	SR	Plana	12	Saco	Dificultad		R4	5-40.	
L834	520.202	756.755	49.24	Diciplasa	85	152	D	2	2	SR	Ondulada	8	Saco	Dificultad		R4	5-40.	
L835	520.202	756.755	49.24	Diciplasa	80	91	D	5	1	SR	Ondulada	8	Saco	Dificultad		R4	5-40.	
L836	520.202	756.755	49.24	Diciplasa	75	35	C	1	1	SR	Plana	12	Saco	Dificultad		R4	5-40.	
M102	519.994	756.356	50.09	Diciplasa	83	65	C	0.5	0.5	SR	Plana	12	Saco	Dificultad		R4	5-40.	
M102	519.994	756.356	50.09	Diciplasa	85	346	C	2	1	SR	Plana	12	Saco	Dificultad		R4	5-40.	
M102	519.994	756.356	50.09	Diciplasa	72	340	C	2	0	SR	Plana	12	Saco	Dificultad		R4	5-40.	
M103	519.300	756.003	49.95	Diciplasa	75	96	C	2	3	SR	Plana	12	Saco	Dificultad		R4	5-40.	
M103	520.070	756.003	49.95	Diciplasa	65	9	D	4	0.2	SR	Plana	12	Saco	Dificultad		R4	5-40.	
M103	520.070	756.003	49.95	Diciplasa	65	11	D	2	0.2	SR	Clavos	10	Saco	Dificultad		R4	5-40.	
M104	520.140	756.342	49.75	Diciplasa	80	185	C	2	3	Arenas	10	Saco	Dificultad		R4	5-40.		
M104	520.140	756.342	49.75	Diciplasa	184	86	D	1	0.5	Arenas	12	Saco	Dificultad		R4	5-40.		

Base de datos

DIRECCIÓN TÉCNICA DE PROSPECCIÓN Y EXPLORACIÓN
 "ESTUDIO GEOLÓGICO-ESTRUCTURAL DEL ÁREA
 CIRCUNDANTE DEL MANANTIAL DEL SISALÁ"

PTO.	ESTE	NORTE	ELEV.	Az.	Bz.	DipDir	Pitch	CONTINUADO	PERSISTENCIA (10m)	ABERTURA (10m)	RELLENO	FORMA	JRC	AGUA	TIPO ROCA	ALTERACION	DUREZA	FECHA	NOTAS
M105	0201177	7463733	4927	Diciembre	73	270	D	4	2	SR	Escalonada	12	Seco	Ductiles		R4	5-90.		
M105	0201177	7463733	4927	Diciembre	42	254	D	1	1	SR	Escalonada	12	Seco	Ductiles		R4	5-90.		
M105	0201177	7463733	4927	Diciembre	76	278	D	2	1	SR	Escalonada	12	Seco	Ductiles		R4	5-90.		
M107	0202237	7463874	4862	Diciembre	85	110	C	2	4	SP	Ondulada	10	Seco	Ductiles		R4	5-90.		
M50	6131801	7463435	4756	Diciembre	42	164	D	1	2	SP	Ondulada	10	Seco	Ductiles		R4	5-90.		
M50	6131801	7463435	4756	Diciembre	74	145	D	1	0.5	SP	Piana	10	Seco	Ductiles		R4	5-90.		
M50	6131801	7463435	4756	Diciembre	70	347	C	2	0.2	SR	Ondulada	12	Seco	Ductiles		R4	5-90.		
M50	6131801	7463435	4756	Diciembre	74	110	C	2	0	SR	Piana	10	Seco	Ductiles		R4	5-90.		
M50	6131801	7463435	4756	Diciembre	81	76	C	1	0.2	SR	Piana	12	Seco	Ductiles		R4	5-90.		
L819	613161	7462167	4932	Falla	70	C	1	0	SR	Piana	8	Seco	Ductiles		R4	5-90.			
D51	613482	7560076	4716	Falla inversa	45	150	D	1	1	SR	Ondulada-Rugosa	12	Seco	Ductiles		R4	5-90.	Rechazo E en otro	
D53	6134848	7569416	4806	Falla inversa	68	228	C	1	1 a 2	Arena	Rugosa-Ondulada	10	Seco	Ductiles		R4	5-90.	Rechazo E en otro	
D54	613230	7558950	4718	Falla inversa	68	273	C	4	1 a 3	SR	Piana-Ondulada	14	Seco	Ductiles		R4	5-90.	Rechazo E en otro	
D54	613230	7558950	4718	Falla inversa	48	267	C	2	0.5	SR	Piana-Rugosa	12	Seco	Ductiles		R4	5-90.	Rechazo E en otro	
D55	613154	7558784	4737	Falla inversa	67	109	C	1	0.5/6	Arena	Piana	4	Seco	Ductiles		R4	5-90.	Rechazo E en otro	
D57	6131784	7558778	4673	Falla inversa	46	330	D	1	0.2	SR	Ondulada	4	Seco	Ductiles		R4	5-90.	Rechazo E en otro	
D58	6131670	7558778	4655	Falla inversa	82	5	C	1	0.5	SR	Rugosa-Escalonada	14	Seco	Ductiles		R4	5-90.	Rechazo E en otro	
D51	6131666	7460221	4614	Falla inversa	70	277	C	1	0.5/3	Arena	Rugosa	10	Seco	Ductiles		R4	5-90.	Rechazo E en otro	
D51	6131666	7460221	4614	Falla inversa	79	111	C	1	1 a 5	Arena	Rugosa-Escalonada	14	Seco	Ductiles		R4	5-90.	Rechazo E en otro	
D51	6131666	7460221	4614	Falla inversa	40	70	C	1	1 a 3	SR	Piana-Ondulada	5	Seco	Ductiles		R4	5-90.	Rechazo E en otro	
M100	6134447	7561488	4936	Falla inversa	87	335	C	1	1	SR	Piana	8	Seco	Ductiles		R4	5-90.	Desplazamiento 5cm	
M106	6132031	7463821	4856	Falla inversa	83	210	C	1	2	SR	Piana	10	Seco	Ductiles		R4	5-90.	Desplazamiento 12cm	
M107	6202387	7463184	4852	Falla inversa	89	33	C	1	2 a 5	Arena	Piana	8	Seco	Ductiles		R4	5-90.	Desplazamiento 14 cm	
D49	6133775	7560372	4641	Falla Normal	79	100	C	1	0.5/5	Arena	Piana	8	Seco	Ductiles		R4	5-90.	Desplazamiento 8 cm	
D50	6131704	7460113	4705	Falla Normal	85	23	C	1	1 a 10	Arena	Piana-Ondulada	8	Seco	Ductiles		R4	5-90.	Desplazamiento 8 cm	
D50	6131704	7460113	4705	Falla Normal	78	204	C	1	10 a 30	Arena	Ondulada-Rugosa	8	Seco	Ductiles		R4	5-90.	Desplazamiento 7 cm	
D52	6131590	7569457	4791	Falla Normal	70	315	C	1	1	SR	Piana-Escalonada	12	Seco	Ductiles		R4	5-90.	Desplazamiento 11 cm	
D52	6131590	7569457	4791	Falla Normal	89	95	C	1	1 a 5	Arena	Ondulada-Escalonada	14	Seco	Ductiles		R4	5-90.	Desplazamiento 8 cm	
D52	6131590	7569457	4791	Falla Normal	75	14	C	1	2	SR	Rugosa	8	Seco	Ductiles		R4	5-90.	Desplazamiento 5cm	
D56	6131195	7568777	4658	Falla Normal	41	303	C	1	2	SR	Rugosa	8	Seco	Ductiles		R4	5-90.	Desplazamiento 4 cm	
D56	6131195	7568777	4658	Falla Normal	74	280	C	1	25/5	Arena	Rugosa-Ondulada	12	Seco	Ductiles		R4	5-90.	Desplazamiento 3 cm	
D59	6131554	7558184	4640	Falla Normal	87	169	C	1	0.3/2	SR	Piana-Ondulada	8	Seco	Ductiles		R4	5-90.	Desplazamiento 6 cm	
D60	6131554	7558184	4640	Falla Normal	67	223	C	1	1 a 2	Arena	Piana-Rugosa	10	Seco	Ductiles		R4	5-90.	Desplazamiento 7 cm	
L818	6131955	7462315	4640	Falla Normal	78	162	C	1	0.5/3	Arena	Ondulada-Rugosa	12	Seco	Ductiles		R4	5-90.	Desplazamiento 5 cm	
L818	6131955	7462315	4640	Falla Normal	50	115	C	1	0	SR	Rugosa	8	Seco	Ductiles		R4	5-90.	Desplazamiento 5 cm	
L820	6131461	7562387	4932	Falla Normal	80	240	C	1	0	SR	Rugosa	8	Seco	Ductiles		R4	5-90.	Desplazamiento 2 a 4 cm	
L822	6131461	7562387	4932	Falla Normal	80	282	C	1	1	SR	Rugosa	8	Seco	Ductiles		R4	5-90.	Desplazamiento 2 a 4 cm	
L823	6131461	7562387	4932	Falla Normal	86	303	C	1	0.5	SR	Rugosa	8	Seco	Ductiles		R4	5-90.	Desplazamiento 2 a 4 cm	
L824	6131461	7562387	4932	Falla Normal	85	266	C	1	2	SR	Rugosa	8	Seco	Ductiles		R4	5-90.	Desplazamiento 2 a 4 cm	
L825	6131461	7562387	4932	Falla Normal	70	310	C	1	1	SR	Rugosa	8	Seco	Ductiles		R4	5-90.	Desplazamiento 2 a 4 cm	
L827	6132302	7462755	4924	Falla Normal	80	145	C	1	0	SR	Ondulada	8	Seco	Ductiles		R4	5-90.	Desplazamiento 3 cm	
L828	6131461	7562387	4932	Falla Normal	82	194	C	3	0.2	SR	Piana	12	Seco	Ductiles		R4	5-90.	Desplazamiento 2 a 4 cm	
L829	6131461	7562387	4932	Falla Normal	82	155	C	1	0.5	SR	Piana	12	Seco	Ductiles		R4	5-90.	Desplazamiento 2 a 4 cm	
L840	6202367	74631920	4848	Falla Normal	80	333	D	1	0.5	SR	Arenas	10	Seco	Ductiles		R4	5-90.	Desplazamiento 4 cm	
L841	6202367	74631920	4848	Falla Normal	81	352	D	1	1.5	SR	Piana	8	Seco	Ductiles		R4	5-90.	Desplazamiento 3 cm	
M100	6131947	7561488	4936	Falla Normal	148	79	C	1	2	SR	Ondulada	10	Seco	Ductiles		R4	5-90.	Desplazamiento 10cm	
M101	6131947	7561521	4942	Falla Normal	70	198	C	1	12	SR	Piana	12	Seco	Ductiles		R4	5-90.	Desplazamiento 15cm	
M102	6131994	7562356	5009	Falla Normal	24	184	C	3	0.2	SR	Piana	10	Seco	Ductiles		R4	5-90.		
M102	6131994	7562356	5009	Falla Normal	82	155	C	1	0.5	SR	Piana	12	Seco	Ductiles		R4	5-90.		
M102	6131994	7562356	5009	Falla Normal	82	155	C	1	0.5	SR	Piana	12	Seco	Ductiles		R4	5-90.		
M105	6202177	7463733	4927	Falla Normal	133	79	C	1	4	SR	Piana	10	Seco	Ductiles		R4	5-90.	Desplazamiento 8 cm	
M107	6202337	74631920	4848	Falla Normal	56	157	C	1	5	SR	Piana	10	Seco	Ductiles		R4	5-90.	Desplazamiento 7 cm	
M108	6131947	7561488	4936	Falla Normal	157	73	C	1	0.5	SR	Piana	10	Seco	Ductiles		R4	5-90.	Desplazamiento 5cm	
M99	6131801	7561435	4786	Falla Normal	160	74	C	1	3	SR	Ondulada	10	Seco	Ductiles		R4	5-90.	Desplazamiento 2cm	
M99	6131801	7561435	4786	Falla Normal	47	140	C	1	12	SR	Piana	12	Seco	Ductiles		R4	5-90.	Desplazamiento 13cm	
L811	613161	7462867	4932	Falla	64	35	C	1	0	SR	Piana	4	Seco	Ductiles		R4	5-90.		

Annex XVI Appendix B



DIRECCIÓN TÉCNICA DE PROSPECCIÓN Y EXPLORACIÓN
ESTUDIO GEOLÓGICO-ESTRUCTURAL DEL ÁREA
CIRCUNDANTE DEL MANANTIAL DEL SISAL*

PTO.	ESTE	NORTE	ELEV.	TIPO	Az.	Bz.	DipDir	Ptch	CONTINUADO	PERSISTENCIA (10m)	ABERTURA (cm)	RELLENO	FORMA	JRC	AGUA	TIPO ROCA	ALTERACION	DUREZA	FECHA	OBSERVACIONES
L817	6131461	74623867	4932	Follicón	58	255	C	1	0	SR	Plana	4	Seco	Ductiles	R4	5-980.				
L829	6130721	74633582	4926	Psuedoestratificación	38	125	C													
L831	6130202	74637755	4924	Psuedoestratificación	72	185	C													
M102	6130984	7462356	5009	Psuedoestratificación	30	216	C													
M103	6132005	7463003	4905	Psuedoestratificación	49	158	C													
M104	6132040	7463342	4915	Psuedoestratificación	32	204	C													
M107	6132027	74631814	4852	Psuedoestratificación	35	250	C													
D53	6130333	73571581	4524	Diciésa	77	178	D	4	0.5	Arena	Plana-Ondulada	8	Seco	Ductiles	R4	5-980.	Desplazamiento 12cm			
D53	613033	73571581	4524	Diciésa	84	11	C	3	1 a 2	Arena	Plana-Ondulada	8	Seco	Ductiles	R4	5-980.				
D53	613033	73571581	4524	Diciésa	55	293	D	3	0.2	Arena	Rugosa Plana	12	Seco	Ductiles	R4	5-980.				
D55	613369	75563982	4547	Diciésa	78	274	C	2	1	Arena	Ondulada-Rugosa	12	Seco	Ductiles	R4	5-980.				
D55	613369	75563982	4547	Diciésa	88	354	D	2	1	Arena	Plana	8	Seco	Ductiles	R4	5-980.				
D55	613369	75563982	4547	Diciésa	83	303	D	5	0.5 a 1	Arena	Ondulada-Rugosa	12	Seco	Ductiles	R4	5-980.				
D56	613451	75565569	4618	Diciésa	78	214	D	4	0.2 a 2	Arena	Plana	10	Seco	Ductiles	R4	5-980.				
D56	613451	75565569	4618	Diciésa	82	153	D	1	1 a 2	Arena	Rugosa	12	Seco	Ductiles	R4	5-980.				
D56	613451	75565569	4618	Diciésa	87	132	D	2	6 a 10	Arena	Rugosa-Escalonada	14	Seco	Ductiles	R4	5-980.				
D56	613451	75565569	4618	Diciésa	82	271	D	2	0.5 a 3	Arena	Rugosa	4	Seco	Arenosas	R4	5-980.				
D59	6131396	75562024	4652	Diciésa	83	212	D	2	5	Arena	Ondulada-Rugosa	14	Seco	Arenosas	R4	5-980.				
D59	6131396	75562024	4652	Diciésa	83	209	C	2	1	Arena	Rugosa-Escalonada	14	Seco	Arenosas	R4	5-980.				
D75	6131788	7555334	4712	Diciésa	72	58	C	2	0.5 a 1	Arena	Ondulada-Rugosa	12	Seco	Ductiles	R4	5-980.				
D75	6131788	7555334	4712	Diciésa	70	40	D	2	0.2 a 2	Arena	Ondulada	10	Seco	Ductiles	R4	5-980.				
L842	6131309	73577748	4616	Diciésa	59	218	C	3	2	SR	Plana	10	Seco	Traquea-Arenosa	R4	5-980.				
L843	6131309	73577748	4616	Diciésa	70	245	D	2	1 a 2	SR	Plana	10	Seco	Ductiles	R4	5-980.				
L844	6131309	73577748	4616	Diciésa	88	290	D	4	0	SR	Plana	10	Seco	Traquea-Arenosa	R4	5-980.				
L845	6131309	73577748	4616	Diciésa	72	308	D	2	30	Arena	Plana	10	Seco	Traquea-Arenosa	R4	5-980.				
L846	6131309	73577748	4616	Diciésa	89	178	D	6	3	Arena	Plana	10	Seco	Traquea-Arenosa	R4	5-980.				
L847	6131309	73577748	4616	Diciésa	85	174	D	5	2	Arena	Plana	10	Seco	Traquea-Arenosa	R4	5-980.				
L848	6131309	73577748	4616	Diciésa	89	176	D	4	5	Arena	Plana	10	Seco	Traquea-Arenosa	R4	5-980.				
L849	6131309	73577748	4616	Diciésa	80	156	D	4	2	SR	Plana	10	Seco	Traquea-Arenosa	R4	5-980.				
L850	6131307	73575545	4644	Diciésa	86	168	D	3	2	Arena	Plana	10	Seco	Traquea-Arenosa	R4	5-980.				
L851	6131307	73575545	4644	Diciésa	72	162	D	3	4	Arena	Plana	10	Seco	Traquea-Arenosa	R4	5-980.				
L852	6131307	73575545	4644	Diciésa	58	150	D	3	2	Arena	Plana	10	Seco	Traquea-Arenosa	R4	5-980.				
L853	6131307	73575545	4644	Diciésa	60	130	D	6	1	Arena	Plana	10	Seco	Traquea-Arenosa	R4	5-980.				
L854	6131307	73575545	4644	Diciésa	85	174	D	4	3	Arena	Plana	10	Seco	Traquea-Arenosa	R4	5-980.				
L855	6134626	7357052	4618	Diciésa	76	60	D	3	3	Arena	Plana	10	Seco	Traquea-Arenosa	R4	5-980.				
L855	6134626	7357052	4618	Diciésa	70	210	D	4	0	SR	Plana	10	Seco	Traquea-Arenosa	R4	5-980.				
L857	6134626	7357052	4618	Diciésa	87	224	D	5	3	Arena	Plana	10	Seco	Traquea-Arenosa	R4	5-980.				
L858	6134626	7357052	4618	Diciésa	78	100	C	5	3	SR	Plana	10	Seco	Traquea-Arenosa	R4	5-980.				
L859	6134626	7357052	4618	Diciésa	68	249	C	4	10	Arena	Plana	10	Seco	Traquea-Arenosa	R4	5-980.				
L860	6134626	7357052	4618	Diciésa	72	244	C	4	15	Arena	Plana	10	Seco	Traquea-Arenosa	R4	5-980.				
L861	6134626	7357052	4618	Diciésa	70	211	C	3	0	Arena	Plana	10	Seco	Traquea-Arenosa	R4	5-980.				
L862	6134626	7357052	4618	Diciésa	69	192	C	8	0	SP	Ondulada	10	Seco	Traquea-Arenosa	R4	5-980.				
L866	6131308	73577748	4632	Diciésa	60	160	C	3	5	SR	Ondulada	10	Seco	Traquea-Arenosa	R4	5-980.				
L873	6131307	73575545	4836	Diciésa	65	300	D	2	2	SR	Ondulada	12	Seco	Ductiles	R4	5-980.				
L876	6131217	7356193	4826	Diciésa	61	154	C	3	2	SR	Ondulada	12	Seco	Ductiles	R4	5-980.				
L877	6131217	7356193	4826	Diciésa	50	60	C	2	0	SR	Ondulada	12	Seco	Ductiles	R4	5-980.				
L880	6131306	73575545	4678	Diciésa	60	114	C	2	5	SR	Plana	8	Seco	Ductiles	R4	5-980.				
L881	6131306	73575545	4678	Diciésa	80	104	D	3	1	SR	Plana	8	Seco	Ductiles	R4	5-980.				
L882	6131306	73575545	4678	Diciésa	78	357	D	3	0.5	Arena	Plana	8	Seco	Ductiles	R4	5-980.				
L883	6131306	73575545	4678	Diciésa	62	346	C	1	0	SR	Plana	8	Seco	Ductiles	R4	5-980.				
L885	6131306	73575545	4678	Diciésa	45	140	C	1	2	SR	Plana	8	Seco	Ductiles	R4	5-980.				
L870	6131306	73575545	4678	Diciésa	58	150	C	1	1	SR	Plana	8	Seco	Ductiles	R4	5-980.				
L871	6131306	73575545	4678	Diciésa	51	240	C	1	1	SR	Plana	8	Seco	Ductiles	R4	5-980.				
L872	6131306	73575545	4678	Diciésa	35	90	C	1	0	SR	Plana	8	Seco	Ductiles	R4	5-980.				
L874	6131306	73575545	4678	Diciésa	65	178	C	1	0	SR	Plana	8	Seco	Ductiles	R4	5-980.				
M109	6131815	7357193	4826	Falla	71	200	C	1	0	SR	Ondulada	12	Seco	Ductiles	R4	5-980.				
M110	6131681	73561887	4791	Falla	133	78	C	1	5	SR	Plana	8	Seco	Ductiles	R4	5-980.				
M108	6131250	7357802	4676	Falla	162	84	C	1	1	SR	Plana	10	Seco	Ductiles	R4	5-980.				

Base de datos

Página 35

**DIRECCIÓN TÉCNICA DE PROSPECCIÓN Y EXPLORACIÓN
"ESTUDIO GEOLÓGICO-ESTRUCTURAL DEL ÁREA
CIRCUNDANTE DEL MANANTIAL DEL SISAL"**



PTO.	ESTE	NORTE	ELEV.	TIPO	Az	Bz	DipDir	Pitch	CONTINUADO	PERSISTENCIA (km)	ABERTURA (km)	RELLENO	FORMA	JRC	AGUA	TIPO ROCA	ALTERACION	DUREZA	FECHA	OBSERVACIONES
M109	61.2815	7357.642	4711	Falla	215	75	125	1	C	1	0.2 a 1.5	Arena	Escalonada	8	Seco	Ductil-Ardeña	R4	6-980.		
D54	61.1822	7357.116	4531	Falla inversa	85	226	82	176	C	1	1	SR	Rugosa	12	Seco	Ductil-S	R4	6-980.	Rechazo 2 cm	
D70	61.3573	7356.2157	4631	Falla inversa	82	176	82	176	C	1	1	Arena	Plan-Ordeñada	4	Seco	Atresitas	R4	6-980.	Rechazo 0 cm	
D71	61.1501	7355.5841	4618	Falla inversa	71	365	86	25	C	1	4	Arena	Plana	4	Seco	Brecha de base	R3	6-980.	Rechazo 1 cm	
D73	61.1887	7356.1517	4655	Falla inversa	86	25	86	1	C	1	14	Arena	Resaca-Escalonada	12	Seco	Atresitas	R4	6-980.	Rechazo 5 cm	
D73	61.1887	7356.1517	4655	Falla inversa	86	25	86	1	C	1	6	Arena	Resaca-Escalonada	14	Seco	Atresitas	R4	6-980.	Desplazamiento 17 cm	
D74	61.1505	7355.5931	4704	Falla inversa	87	280	87	1	C	1	0.2	SR	Ordeñada	14	Seco	Atresitas	R4	6-980.	Rechazo 15 cm	
D74	61.1505	7355.5931	4704	Falla inversa	58	330	D	1	D	1	7	SR	Rugosa-Escalonada	14	Seco	Atresitas	R4	6-980.	Rechazo 20 cm	
D76	61.1516	7355.5150	4658	Falla inversa	64	240	C	1	C	1	7 a 15	Arena	Escalonada	14	Seco	Brecha de base	R3	6-980.	Desplazamiento 3 cm	
D66	61.1887	7356.793	4573	Falla Kormai	55	304	C	1	C	1	4	SR	Ordeñada-Rugosa	12	Seco	Brecha de base	R3	6-980.	Desplazamiento 3 cm	
D72	61.6186	7356.673	4633	Falla Kormai	74	143	C	1	C	1	1 a 5	Arena	Rugosa-Escalonada	14	Seco	Brecha de base	R3	6-980.	Desplazamiento 3 cm	
D72	61.6172	7355.554	4676	Falla Kormai	78	15	D	1	D	1	1	SR	Plana	4	Seco	Brecha de base	R3	6-980.		
E641	61.1122	7356.009	5035	Falla Kormai	148	75	58	1	C	1	10	SR	Escalonada	12	Seco	Atresitas	R4	6-980.		
E641	61.1122	7356.009	5035	Falla Kormai	71	342	C	1	C	1	3	SR	Plana	6	Seco	Atresitas	R4	6-980.		
L864	61.1928	7356.7779	4632	Falla Kormai	58	175	260	1	C	1	0	SR	Ordeñada	10	Seco	Traguilla-Ardesita	R4	6-980.		
L867	61.1737	7356.4719	4645	Falla Kormai	59	120	C	1	C	1	0	SR	Ordeñada	10	Seco	Traguilla-Ardesita	R4	6-980.	Desplazamiento 7 cm	
L868	61.1737	7356.4719	4645	Falla Kormai	44	85	185	C	C	1	0	SR	Plana	9	Seco	Traguilla-Ardesita	R4	6-980.	Desplazamiento 7 cm	
L870	61.1826	7357.5606	4678	Falla Kormai	89	165	C	1	C	1	2	Arena	Es-Ordeñada	10	Seco	Atresitas	R4	6-980.	Desplazamiento 10 cm	
M108	61.1826	7357.5602	4676	Falla Kormai	140	83	90	1	C	2	4	SR	Es-Ordeñada	10	Seco	Ductil-Ardeña	R4	6-980.		
M110	61.1651	7355.8857	4751	Falla Kormai	67	352	C	1	C	1	1	SR	Es-Ordeñada	12	Seco	Atresitas	R4	6-980.		
M111	61.1566	7355.8857	4751	Falla Kormai	82	84	330	1	C	1	2	SR	Es-Ordeñada	10	Seco	Atresitas	R4	6-980.		
E641	61.1122	7356.009	5035	Falla Kormai	67	352	C	1	C	1	2	SR	Es-Ordeñada	12	Seco	Atresitas	R4	6-980.		
L863	61.1928	7356.7779	4632	Pseudotrastricación	50	220	C	1	C	1	14	SR	Plana	10	Seco	Traguilla-Ardesita	R4	6-980.		
L878	61.1626	7357.506	4678	Pseudotrastricación	52	125	C	1	C	1	125	SR	Plana	10	Seco	Atresitas	R4	6-980.		
M110	61.1651	7356.8857	4791	Pseudotrastricación	29	161	C	1	C	1	161	SR	Plana	10	Seco	Atresitas	R4	6-980.		
M111	61.1566	7355.5520	4791	Pseudotrastricación	24	168	C	1	C	1	157	SR	Plana	4	Seco	Atresitas	R4	6-980.		
D78	61.0167	7355.1507	4896	Diclosa	51	157	C	1	C	1	0.2	SR	Plana	4	Seco	Atresitas	R4	7-980.		
D79	61.0167	7356.996	4918	Diclosa	78	162	D	3	D	3	0.1	SR	Plana	8	Seco	Ductil-Ordeñada	R4	7-980.		
D79	61.0167	7356.996	4918	Diclosa	80	60	D	3	D	3	0.5	Arena	Plana	8	Seco	Ductil-Ordeñada	R4	7-980.		
D79	61.0167	7356.996	4918	Diclosa	82	155	D	1	D	1	0.2	SR	Plana	4	Seco	Ductil-Ordeñada	R4	7-980.		
D80	61.0167	7356.652	5112	Diclosa	85	143	D	3	D	3	0.2	SR	Plana	4	Seco	Atresitas	R4	7-980.		
D80	61.0167	7356.652	5112	Diclosa	70	24	D	1	D	1	0.2 a 1.1	SR	Plana	4	Seco	Atresitas	R4	7-980.		
D82	61.0167	7356.652	5112	Diclosa	48	242	C	1	C	1	1 a 3	Arena	Plana	4	Seco	Atresitas	R4	7-980.		
D82	61.0167	7357.115	5318	Diclosa	80	112	C	1	C	1	0	SR	Plana	10	Seco	Ductil-Ordeñada	R4	7-980.		
L884	61.1039	7353.1589	4620	Diclosa	80	88	D	6	D	6	3	SR	Plana	10	Seco	Ductil-Ordeñada	R4	7-980.		
L885	61.1039	7353.1589	4620	Diclosa	89	60	D	5	D	5	1	SR	Plana	10	Seco	Ductil-Ordeñada	R4	7-980.		
L886	61.1039	7353.1589	4620	Diclosa	82	65	D	5	D	5	2	SR	Plana	10	Seco	Ductil-Ordeñada	R4	7-980.		
L887	61.1039	7353.1589	4620	Diclosa	85	67	D	5	D	5	3	SR	Plana	10	Seco	Ductil-Ordeñada	R4	7-980.		
L888	61.1039	7353.1589	4620	Diclosa	70	60	D	3	D	3	0	SR	Plana	10	Seco	Ductil-Ordeñada	R4	7-980.		
L889	61.1039	7353.1589	4620	Diclosa	60	330	C	6	C	6	0	SR	Plana	10	Seco	Ductil-Ordeñada	R4	7-980.		
L895	61.1039	7353.1589	4620	Diclosa	79	319	C	6	C	6	3	SR	Plana	10	Seco	Ductil-Ordeñada	R4	7-980.		
L897	61.1039	7353.1589	4620	Diclosa	87	327	C	6	C	6	0	SR	Plana	10	Seco	Ductil-Ordeñada	R4	7-980.		
L898	61.1039	7353.1589	4620	Diclosa	72	320	D	5	D	5	2	SR	Plana	10	Seco	Ductil-Ordeñada	R4	7-980.		
L899	61.1039	7353.1589	4620	Diclosa	70	327	D	5	D	5	3	SR	Plana	10	Seco	Ductil-Ordeñada	R4	7-980.		
L904	61.0788	7352.551	4650	Diclosa	79	212	D	2	D	2	6	Orificio-de Fe	SR	Ordeñada	10	Seco	Ductil-Ordeñada	R4	7-980.	
L905	61.0788	7352.551	4650	Diclosa	89	325	D	2	D	2	0	SR	Ordeñada	10	Seco	Ductil-Ordeñada	R4	7-980.		
L906	61.0788	7352.551	4650	Diclosa	88	350	D	2	D	2	0	SR	Ordeñada	10	Seco	Ductil-Ordeñada	R4	7-980.		
L907	61.0788	7352.551	4650	Diclosa	87	307	D	2	D	2	0	SR	Ordeñada	12	Seco	Ductil-Ordeñada	R4	7-980.		
L908	61.0172	7353.947	4744	Diclosa	88	141	C	6	C	6	5	SR	Ordeñada	12	Seco	Ductil-Ordeñada	R4	7-980.		
L909	61.0172	7353.947	4744	Diclosa	85	136	C	6	C	6	10	SR	Ordeñada	12	Seco	Ductil-Ordeñada	R4	7-980.		
L910	61.0172	7353.947	4744	Diclosa	86	140	C	6	C	6	2	SR	Ordeñada	12	Seco	Ductil-Ordeñada	R4	7-980.		
L911	61.0172	7353.947	4744	Diclosa	42	346	D	2	D	2	0	SR	Plana	6	Seco	Ductil-Ordeñada	R4	7-980.		
L920	61.0162	7352.546	4758	Diclosa	70	150	D	2	D	2	0	SR	Plana	6	Seco	Ductil-Ordeñada	R4	7-980.		
L923	61.0142	7352.259	4626	Diclosa	87	266	D	3	D	3	2	SR	Plana	10	Seco	Ductil-Ordeñada	R4	7-980.		
L925	61.0142	7352.259	4626	Diclosa	89	280	D	3	D	3	0	SR	Plana	10	Seco	Ductil-Ordeñada	R4	7-980.		
L926	61.0142	7352.259	4626	Diclosa	89	320	D	3	D	3	2	SR	Plana	10	Seco	Ductil-Ordeñada	R4	7-980.		
L927	61.0142	7352.259	4626	Diclosa	85	316	D	3	D	3	2	SR	Plana	10	Seco	Ductil-Ordeñada	R4	7-980.		

PTO.	ESTE	NORTE	ELEV.	Az.	Bz.	DipDir	Pitch	CONTINUADO	PERSISTENCIA (10m)	ABERTURA (cm)	RELLENO	FORMA	JRC	TIPO ROCA	AGUA	DUREZA	ALTERACION	FECHA	OBSERVACIONES
L928	610,042	7564,259	4626	Diciembre	68	350	D	2	4	SR	Plana	10	Seco	Ductiles	R4	7-980.			
L929	610,042	7564,259	4626	Diciembre	76	306	D	3	0,5	SR	Plana	10	Seco	Ductiles	R4	7-980.			
L930	610,042	7564,259	4626	Diciembre	68	80	D	2	0	SR	Plana	10	Seco	Ductiles	R4	7-980.			
L932	610,042	7564,259	4626	Diciembre	65	114	C	2	2	SR	Plana	10	Seco	Ductiles	R4	7-980.			
M112	611,150	7564,364	4718	Diciembre	280	42	150	1	1	8	SR	Brena	14	Seco	Aristadas	R4	7-980.		
M112	611,150	7564,364	4718	Diciembre	232	80	142	C	1	6	SR	Escalonada	12	Seco	Aristadas	R4	7-980.		
M112	611,150	7564,364	4718	Diciembre	243	33	C	1	2	SR	Escalonada	14	Seco	Aristadas	R4	7-980.			
M112	611,150	7564,364	4718	Diciembre	240	81	150	C	4	0,5	Arena	Plana	6	Seco	Aristadas	R4	7-980.		
M113	609,050	7560,900	5029	Diciembre	60	165	C	1	1	2	SR	Escalonada	14	Seco	Aristadas	R4	7-980.		
M113	609,050	7560,900	5029	Diciembre	78	130	C	1	2	SR	Plana	12	Seco	Aristadas	R4	7-980.			
M114	609,095	7560,829	5023	Diciembre	220	70	130	C	2	3	SR	Escalonada	12	Seco	Aristadas	R4	7-980.		
M114	609,095	7560,829	5023	Diciembre	226	74	136	C	2	3	SR	Plana	12	Seco	Aristadas	R4	7-980.		
M114	609,095	7560,829	5023	Diciembre	193	71	283	C	1	1	SR	Plana	12	Seco	Aristadas	R4	7-980.		
M115	609,335	7560,314	51,54	Diciembre	160	82	250	D	1	2	SR	Escalonada	12	Seco	Bruchos de base	R4	7-980.		
M117	609,451	7560,271	51,23	Diciembre	262	75	172	D	4	2	SR	Escalonada	8	Seco	Aristadas	R4	7-980.		
M117	609,451	7560,271	51,23	Diciembre	270	76	180	D	2	4	SR	Escalonada	8	Seco	Aristadas	R4	7-980.		
M112	609,801	7560,090	4714	Falla	70	135	C	1	1	2	SR	Ortulada	12	Seco	Bruchos de base	R3	7-980.		
M113	609,801	7560,092	4714	Falla	62	147	C	1	1	0	SR	Ortulada	12	Seco	Bruchos de base	R3	7-980.		
M114	609,801	7560,092	4714	Falla	72	130	C	1	1	0	SR	Ortulada	12	Seco	Bruchos de base	R3	7-980.		
M115	609,801	7560,092	4714	Falla	88	100	C	1	1	0	SR	Ortulada	12	Seco	Bruchos de base	R3	7-980.		
M116	609,801	7560,092	4714	Falla	75	122	C	1	1	0	SR	Ortulada	12	Seco	Bruchos de base	R3	7-980.		
M118	609,612	7562,546	4758	Falla	55	100	D	1	1	0	SR	Plana	6	Seco	Ductiles	R4	7-980.		
M119	609,612	7562,546	4758	Falla	32	80	D	1	1	0	SR	Plana	6	Seco	Ductiles	R4	7-980.		
M122	609,612	7560,900	5029	Falla	84	197	C	1	1	1	SR	Arena	10	Seco	Aristadas	R4	7-980.		
M113	609,090	7560,900	5029	Falla	73	134	D	1	1	2	SR	Escalonada	14	Seco	Aristadas	R4	7-980.		
L903	610,078	7562,551	4650	Falla Dextral	28	135	D	1	2	SR	Plana	10	Seco	Ductiles	R4	7-980.	Desplazamiento 5 cm		
D78	610,0637	7557,189	4896	Falla inversa	85	257	D	3	0,2 a 1,5	SR	Rugosa-Escalonada	12	Seco	Ductiles	R4	7-980.	Rechazo 0 cm		
D78	610,0637	7557,189	4896	Falla inversa	57	262	C	1	0,5	SR	Burros	12	Seco	Ductiles	R4	7-980.	Rechazo 0 cm (microfallo)		
D82	609,962	7557,145	53,15	Falla inversa	38	305	D	1	1	1	SR	Rugosa-Planillada	12	Seco	Aristadas	R4	7-980.		
E656	609,104	7560,634	5004	Falla inversa	74	285	122	D	1	5	SR	Escalonada	12	Seco	Aristadas	R4	7-980.	Desplazamiento 8 cm	
M115	609,335	7560,314	51,54	Falla inversa	160	70	D	1	1	5	SR	Ortulada	12	Seco	Bruchos de base	R3	7-980.	Aristadas	
M116	609,335	7560,314	51,54	Falla inversa	161	64	C	1	1	0,5	SR	Milofita	6	Seco	Aristadas	R4	7-980.	Rechazo 8 cm	
M116	609,332	7560,327	51,57	Falla inversa	43	275	C	1	1	0	SR	Plana	14	Seco	Aristadas	R4	7-980.	Rechazo 10 cm	
M119	609,936	7560,189	5036	Falla inversa	203	54	C	1	1	12	SR	Rugosa	12	Seco	Ductiles	R4	7-980.	Desplazamiento 2 cm	
D80	609,278	7556,652	51,72	Falla Normal	78	98	D	1	0,5	SR	Arena	10	Seco	Ductiles	R4	7-980.	Desplazamiento 2 cm		
D81	609,738	7556,900	53,55	Falla Normal	45	240	C	1	0,5 a 1,0	SR	Rugosa-Escalonada	14	Seco	Aristadas	R4	7-980.			
D85	609,104	7556,074	5004	Falla Normal	50	58	C	1	0,5 a 2	SR	Plana	10	Seco	Ductiles	R4	7-980.			
L890	61,039	7563,189	4620	Falla Normal	79	62	C	1	15	SR	Ortulada	10	Seco	Ductiles	R4	7-980.	Desplazamiento 1 cm		
L891	61,039	7563,189	4620	Falla Normal	84	60	C	1	7	SR	Ortulada	10	Seco	Ductiles	R4	7-980.	Desplazamiento 1 cm		
L892	61,039	7563,189	4620	Falla Normal	80	70	C	1	0	SR	Ortulada	10	Seco	Ductiles	R4	7-980.	Desplazamiento 1 cm		
L893	61,039	7563,189	4620	Falla Normal	75	51	C	1	7	SR	Ortulada	10	Seco	Ductiles	R4	7-980.	Desplazamiento 5 cm		
L894	61,039	7563,189	4620	Falla Normal	86	45	C	1	1	5	SR	Ortulada	10	Seco	Ductiles	R4	7-980.	Desplazamiento 5 cm	
L901	61,039	7563,189	4620	Falla Normal	70	20	D	3	0	SR	Ortulada	10	Seco	Ductiles	R4	7-980.	Desplazamiento 15 cm		
L902	61,039	7563,189	4620	Falla Normal	70	23	D	1	0	SR	Ortulada	10	Seco	Ductiles	R4	7-980.	Desplazamiento 15 cm		
L921	610,442	7564,289	4758	Falla Normal	44	10	D	1	15	SR	Plana	6	Seco	Ductiles	R4	7-980.	Desplazamiento 10 cm		
L931	610,442	7564,289	4758	Falla Normal	87	122	C	1	1	1	SR	Plana	10	Seco	Ductiles	R4	7-980.	Desplazamiento 5 cm	
M113	609,090	7560,900	5029	Falla Normal	200	110	C	1	7	SR	Escalonada	12	Seco	Aristadas	R4	7-980.	Desplazamiento 2 cm		
M113	609,090	7560,900	5029	Falla Normal	265	61	C	1	1	10	SR	Plana	10	Seco	Aristadas	R4	7-980.	Desplazamiento 2 cm	
M114	609,095	7560,059	5023	Falla Normal	230	140	C	1	4	SR	Plana	10	Seco	Aristadas	R4	7-980.	Desplazamiento 9 cm		
M114	609,095	7560,059	5023	Falla Normal	315	76	C	1	2	SR	Plana	8	Seco	Aristadas	R4	7-980.	Desplazamiento 2 cm		
M115	609,335	7560,314	51,54	Falla Normal	250	86	C	1	340	SR	Escalonada	9	Seco	Aristadas	R4	7-980.	Desplazamiento 3 cm		
M115	609,335	7560,314	51,54	Falla Normal	95	59	C	1	1	2	SR	Escalonada	8	Seco	Aristadas	R4	7-980.	Desplazamiento 3 cm	
M116	609,335	7560,314	51,54	Falla Normal	76	64	C	1	1	1	SR	Escalonada	14	Seco	Aristadas	R4	7-980.	Desplazamiento 2 cm	
M116	609,335	7560,314	51,54	Falla Normal	82	93	C	1	2	SR	Escalonada	12	Seco	Aristadas	R4	7-980.	Desplazamiento 15 cm		
M117	609,335	7560,271	51,23	Falla Normal	43	45	C	1	10	SR	Escalonada	14	Seco	Aristadas	R4	7-980.	Desplazamiento 2 cm		
M118	609,840	7560,260	5042	Falla Normal	183	83	C	1	5	SR	Escalonada	8	Seco	Aristadas	R4	7-980.			

**DIRECCIÓN TÉCNICA DE PROSPECCIÓN Y EXPLORACIÓN
ESTUDIO GEOLÓGICO-ESTRUCTURAL DEL ÁREA
CIRCUNDANTE DEL MANANTIAL DEL SISAL***



PTO.	ESTE	NORTE	ELEV.	Tipo	Az	Bz	DipDir	Pitch	CONTINUADO	PERSISTENCIA (10m)	ABERTURA (cm)	FORMA	JRC	Agua	Tipo Roca	ALTERACION	DUREZA	FECHA	OBSERVACIONES
M118	6080840	7560260	5042	Falla Normal	180	68	90		C	1	8	SR	Escalonada	14	Seco	Artesianas	R4	7-ago.	Desplazamiento 3 cm
M119	6080936	7560247	5036	Falla Normal	190	65	100		C	1	2	SR	Escalonada	12	Seco	Artesianas	R4	7-ago.	Desplazamiento 8 cm
D79	6101050	7560986	4918	Falla Estriatal	73	148			C	1	0.2	SR	Poco-Ondulada	4	Seco	Artesianas	R4	7-ago.	Desplazamiento 1 cm
M119	6080936	7560247	5036	Falla Estriatal	66	144			C	1	10	SR	Plana	14	Seco	Artesianas	R4	7-ago.	
D80	6080228	7560682	5172	Brusquedad-Fracaso	55	232			C	1		SR	Plana	14	Seco	Artesianas	R4	7-ago.	
D82	6080842	7557115	5318	Perforación-Erosión	21	195			C	1		SR	Plana	14	Seco	Artesianas	R4	7-ago.	
M113	6080936	7560190	5009	Posterior-Erosión	33	87			C	1		SR	Orlada-Rugosa	12	Seco	Artesianas	R4	7-ago.	
D84	6080855	7574238	4746	Dicelosa	87	160			D	2		SR	Orlada-Rugosa	12	Seco	Ignimritis	R3	8-ago.	
D84	6080855	7574238	4746	Dicelosa	80	40			D	2		SR	Rugosa	10	Seco	Ignimritis	R3	8-ago.	
D85	6080371	7574022	4722	Dicelosa	74	145			C	6	1	SR	Rugosa	10	Seco	Ignimritis	R3	8-ago.	
D85	6080371	7574022	4722	Dicelosa	84	340			C	2		SR	Poco-Ondulada	8	Seco	Ignimritis	R3	8-ago.	
D87	607313	75731578	4615	Dicelosa	73	25			C	2		SR	Plana-Rugosa	10	Seco	Ignimritis	R3	8-ago.	
D87	607313	75731578	4615	Dicelosa	46	312			D	3		SR	Orlada-Rugosa	12	Seco	Ignimritis	R3	8-ago.	
D88	607318	75731582	4615	Dicelosa	87	308			C	3		SR	Plana-Rugosa	10	Seco	Ignimritis	R3	8-ago.	
D89	6080189	75727805	4654	Dicelosa	69	22			C	2	1	SR	Orlada-Rugosa	8	Seco	Ignimritis	R3	8-ago.	
D89	6080189	75727805	4654	Dicelosa	87	109			C	2	3.5	SR	Plana-Rugosa	8	Seco	Ignimritis	R3	8-ago.	
D89	6080189	75727805	4654	Dicelosa	70	35			D	2	4	SR	Plana-Rugosa	10	Seco	Ignimritis	R3	8-ago.	
D89	6080189	75727805	4654	Dicelosa	88	305			C	3		SR	Plana-Rugosa	10	Seco	Ignimritis	R3	8-ago.	
D91	6080805	7573005	4744	Dicelosa	85	105			C	4	0.5	SR	Plana-Rugosa	10	Seco	Ignimritis	R3	8-ago.	
D91	6080805	7573005	4744	Dicelosa	64	287			C	1		SR	Plana-Rugosa	10	Seco	Ignimritis	R3	8-ago.	
D92	6080034	75751516	4933	Dicelosa	62	92			C	4	5	SR	Plana-Ondulada	8	Seco	Ductilas	R4	8-ago.	
D92	6080034	75751516	4933	Dicelosa	88	285			D	3		SR	Plana-Ondulada	8	Seco	Ductilas	R4	8-ago.	
D92	6080034	75751516	4933	Dicelosa	60	45			C	5	1	SR	Plana-Ondulada	8	Seco	Ductilas	R4	8-ago.	
D94	6080703	75758688	4938	Dicelosa	50	51			D	4	1 a 3	SR	Plana-Ondulada	8	Seco	Artesianas	R4	8-ago.	
D94	6080703	75758688	4938	Dicelosa	84	160			D	2	1 a 3	SR	Arena	12	Seco	Artesianas	R4	8-ago.	
D94	6080703	75758688	4938	Dicelosa	84	112			D	2	0.5	SR	Rugosa	12	Seco	Artesianas	R4	8-ago.	
D95	6080547	7576002	4853	Dicelosa	70	210			C	2		SR	Orlada-Rugosa	14	Seco	Artesianas	R4	8-ago.	
D95	6080547	7576002	4853	Dicelosa	86	40			D	1		SR	Rugosa	12	Seco	Artesianas	R4	8-ago.	
E666	6080841	75727368	4801	Dicelosa	51	202			D	4	0.2	SR	Orlada	12	Seco	Artesianas	R4	8-ago.	
E666	6080841	75727368	4801	Dicelosa	74	50			D	3	3	SR	Plana	4	Seco	Artesianas	R4	8-ago.	
E666	6080841	75727368	4801	Dicelosa	83	340			D	2	1	SR	Plana	4	Seco	Artesianas	R4	8-ago.	
E668	6080841	75727368	4801	Dicelosa	86	77			C	1	4	SR	Plana	4	Seco	Artesianas	R4	8-ago.	
E668	6080878	7573144	4700	Dicelosa	86	129			C	3	2	SR	Plana	4	Seco	Ignimritis	R3	8-ago.	
I337	611730	75691645	4838	Dicelosa	79	315			C	5	0	SR	Plana	10	Seco	Ductilas	R4	8-ago.	
I338	611730	75691645	4838	Dicelosa	72	310			C	4		SR	Plana	10	Seco	Ductilas	R4	8-ago.	
I339	611730	75691645	4838	Dicelosa	260	170			D	2	0	SR	Plana	10	Seco	Ductilas	R4	8-ago.	
I340	611730	75691645	4838	Dicelosa	65	284			D	3	1	SR	Plana	10	Seco	Ductilas	R4	8-ago.	
I341	611730	75691645	4838	Dicelosa	74	278			D	3	1	SR	Plana	10	Seco	Ductilas	R4	8-ago.	
L922	6090326	7571795	4807	Dicelosa	80	330			C	6	1	SR	Plana	10	Seco	Ductilas	R4	8-ago.	
L933	6090326	7571795	4807	Dicelosa	83	319			C	6	1	SR	Plana	10	Seco	Ductilas	R4	8-ago.	
L944	6090326	7571795	4807	Dicelosa	80	370			C	5	2	SR	Plana	10	Seco	Ductilas	R4	8-ago.	
L944	6090326	7571795	4807	Dicelosa	80	370			C	5	0	SR	Plana	10	Seco	Ductilas	R4	8-ago.	
L945	6090326	7571795	4807	Dicelosa	78	110			C	5	0	SR	Plana	10	Seco	Ductilas	R4	8-ago.	
L946	6090326	7571795	4807	Dicelosa	84	365			C	2		SR	Plana	10	Seco	Ductilas	R4	8-ago.	
L947	6090326	7571795	4807	Dicelosa	88	165			C	3		SR	Plana	10	Seco	Ductilas	R4	8-ago.	
L947	6090326	7571795	4807	Dicelosa	80	330			C	2	4	SR	Plana	10	Seco	Ductilas	R4	8-ago.	
L948	6090326	7571795	4807	Dicelosa	85	300			C	2	10	SR	Plana	10	Seco	Ductilas	R4	8-ago.	
L949	6090326	7571795	4807	Dicelosa	80	159			D	2	0	SR	Plana	10	Seco	Ductilas	R4	8-ago.	
L950	6090326	7571795	4807	Dicelosa	85	200			D	2	7	SR	Plana	10	Seco	Ductilas	R4	8-ago.	
L951	6090326	7571795	4807	Dicelosa	87	315			D	1		SR	Plana	10	Seco	Ductilas	R4	8-ago.	
L952	6090326	7571795	4807	Dicelosa	68	330			D	2	0	SR	Plana	10	Seco	Ductilas	R4	8-ago.	
L953	6090326	7571795	4807	Dicelosa	184	94			D	4		SR	Orlada	16	Seco	Ductilas	R4	8-ago.	
M120	611107	7573414	4807	Dicelosa	280	88			C	4	3	SR	Orlada	12	Seco	Ductilas	R4	8-ago.	
M121	610086	7573402	4805	Dicelosa	195	86			C	1	2	SR	Orlada	14	Seco	Ductilas	R4	8-ago.	
M121	610086	7573402	4805	Dicelosa	80	150			C	1	3	SR	Orlada	14	Seco	Ductilas	R4	8-ago.	
M122	610086	7573402	4805	Dicelosa	215	76			C	2	2	SR	Escañadas	14	Seco	Ductilas	R4	8-ago.	
M122	610086	7573402	4805	Dicelosa	84	38			D	1	1	SR	Escañadas	12	Seco	Ductilas	R4	8-ago.	
M122	610086	7573402	4805	Dicelosa	73	91			D	1	5	SR	Plana	10	Seco	Ductilas	R4	8-ago.	
M122	610086	7573402	4805	Dicelosa	68	341			D	2	1	SR	Plana	8	Seco	Ductilas	R4	8-ago.	
M122	610305	7572478	4803	Dicelosa	71	333			C	1	2	SR	Plana	12	Seco	Ductilas	R4	8-ago.	

Base de datos

Página 38



**DIRECCIÓN TÉCNICA DE PROSPECCIÓN Y EXPLORACIÓN
"ESTUDIO GEOLÓGICO-ESTRUCTURAL DEL ÁREA
CIRCUNDANTE DEL MANANTIAL DEL SISALÁ"**

PTO.	ESTE	NORTE	ELEV.	Az.	Bz.	DipDir	Pitch	CONTINUO	PERSISTENCIA (10m)	ABERTURA (cm)	RELLENO	FORMA	JRC	AGUA	TIPO ROCA	ALTERACION	DUREZA	FECHA	OBSERVACIONES
M123	6090298	7577282	4831	Diciembre	80	354		D	1	2	SR	Cuva	6	Seco	Ductiles		R4	8-90.	
M124	6090120	7577404	4821	Diciembre	72	314		C	1	3	SR	Plana	12	Seco	Ductiles		R4	8-90.	
M124	6090120	7577404	4821	Diciembre	54	50		C	1	1	SR	Plana	12	Seco	Ductiles		R4	8-90.	
M124	6090120	7577404	4821	Diciembre	83	44		C	1	3	SR	Plana	12	Seco	Ductiles		R4	8-90.	
M125	6090867	7577711	46954	Diciembre	90	195		C	5	2	SR	Página	10	Seco	Grumitos		R3	8-90.	
M125	6090867	7577711	46954	Diciembre	76	324		C	1	1	SR	Página	10	Seco	Grumitos		R3	8-90.	
M126	6090523	7577524	46588	Diciembre	78	320		C	2	10	SR	Página	10	Seco	Grumitos		R3	8-90.	
M126	6090523	7577524	46588	Diciembre	70	255		C	1	5	SR	Página	10	Seco	Grumitos		R3	8-90.	
M126	6090523	7577524	46588	Diciembre	78	200		C	1	5	SR	Página	10	Seco	Grumitos		R3	8-90.	
M127	6090516	7577804	4650	Diciembre	70	54		C	2	4	SR	Página	10	Seco	Grumitos		R3	8-90.	
M127	6090516	7577804	4650	Diciembre	66	145		C	3	1	Atena	Plana	8	Seco	Ductiles		R4	8-90.	
M128	6090329	7576347	4652	Diciembre	80	140		C	2	2	SR	Página	8	Seco	Ductiles		R4	8-90.	
M128	6090329	7576347	4652	Diciembre	79	150		C	2	0.5	SR	Página	4	Seco	Grumitos		R3	8-90.	
M129	609164	7579290	4822	Diciembre	82	210		C	2	10	Atena	Escalonada	4	Seco	Grumitos		R3	8-90.	
M129	609164	7579290	4822	Diciembre	75	213		D	1	5	SR	Página	8	Seco	Grumitos		R3	8-90.	
M130	6091691	7580515	4929	Diciembre	86	344		C	1	1	SR	Página	9	Seco	Monocristales		R4	8-90.	
M130	6091691	7580515	4929	Diciembre	85	265		C	1	1	SR	Página	10	Seco	Ductiles		R4	8-90.	
M133	6111730	7586645	4338	Falla	395	173		C	1	1	Atena	Alma	10	Seco	Ductiles		R4	8-90.	
M134	6111730	7586645	4338	Falla	75	168		C	1	0	Atena	Página	10	Seco	Ductiles		R4	8-90.	
M135	6111730	7586645	4338	Falla	50	166		C	1	2	SR	Página	10	Seco	Ductiles		R4	8-90.	
M134	6111730	7586645	4338	Falla	88	165		C	1	2	SR	Rugosa	14	Seco	Ductiles		R4	8-90.	
M134	6111730	7586645	4338	Falla	60	176		C	1	3	SR	Rugosa	14	Seco	Ductiles		R4	8-90.	
M134	6111730	7586645	4338	Falla	79	282		C	1	0	SR	Rugosa	14	Seco	Ductiles		R4	8-90.	
M134	6111730	7586645	4338	Falla	75	284		C	1	0	SR	Rugosa	14	Seco	Ductiles		R4	8-90.	
M134	6111730	7586645	4338	Falla	83	244		C	1	0	SR	Rugosa	14	Seco	Ductiles		R4	8-90.	
M134	6111730	7586645	4338	Falla	83	244		C	1	0	SR	Rugosa	10	Seco	Ductiles		R4	8-90.	
M135	6111730	7586645	4338	Falla	75	168		C	1	0	SR	Página	10	Seco	Ductiles		R4	8-90.	
M134	6111730	7586645	4338	Falla	80	255		C	1	2	SR	Rugosa	14	Seco	Ductiles		R4	8-90.	
M134	6111730	7586645	4338	Falla	88	165		C	1	2	SR	Rugosa	14	Seco	Ductiles		R4	8-90.	
M134	6111730	7586645	4338	Falla	60	176		C	1	3	SR	Rugosa	14	Seco	Ductiles		R4	8-90.	
M134	6111730	7586645	4338	Falla	79	282		C	1	0	SR	Rugosa	14	Seco	Ductiles		R4	8-90.	
M134	6111730	7586645	4338	Falla	83	244		C	1	0	SR	Rugosa	10	Seco	Ductiles		R4	8-90.	
M134	6111730	7586645	4338	Falla	83	244		C	1	0	SR	Rugosa	14	Seco	Ductiles		R4	8-90.	
M135	6111730	7586645	4338	Falla	80	210		C	1	0	SR	Página	10	Seco	Ductiles		R4	8-90.	
M135	6111730	7586645	4338	Falla	43	198		C	1	0	SR	Página	10	Seco	Ductiles		R4	8-90.	
M135	6111730	7586645	4338	Falla	52	112		C	1	0	SR	Página	10	Seco	Ductiles		R4	8-90.	
M135	6111730	7586645	4338	Falla	33	97		C	1	2	SR	Página	10	Seco	Ductiles		R4	8-90.	
M135	6111730	7586645	4338	Falla	87	132		C	1	2	SR	Página	10	Seco	Ductiles		R4	8-90.	
M135	6111730	7586645	4338	Falla	89	148		D	1	10	SR	Página	10	Seco	Ductiles		R4	8-90.	
M135	6111730	7586645	4338	Falla	83	356		C	1	3	SR	Página	10	Seco	Ductiles		R4	8-90.	
M136	6111730	7577795	4807	Falla	83	322		C	1	8	Atena	Escalonada	16	Seco	Artesitas		R4	8-90.	
M136	6111730	7577795	4807	Falla	54	199		C	1	4	SR	Página	12	Seco	Grumitos		R3	8-90.	
M136	6111730	7577795	4807	Falla	57	115		D	1	3.5	SR	Rugosa	4	Seco	Grumitos		R4	8-90.	
M136	6111730	7577795	4807	Falla	81	200		C	1	0.5	SR	Página-Rugosa	8	Seco	Grumitos		R3	8-90.	
M136	6111730	7577795	4807	Falla	89	55		C	1	0.5	SR	Página-Rugosa	12	Seco	Grumitos		R3	8-90.	
M136	6111730	7577795	4807	Falla	82	94		C	1	1	SR	Ortodoxa-Rugosa	12	Seco	Grumitos		R3	8-90.	
M137	6090343	7577501	4743	Falla	4743	173		C	1	0.5	SR	Página-Rugosa	10	Seco	Grumitos		R3	8-90.	
M137	6090343	7577501	4743	Falla	4645	173		C	1	0.5	SR	Página-Rugosa	15	Seco	Grumitos		R3	8-90.	
M137	6090343	7577501	4743	Falla	50	230		C	1	4	SR	Página	4	Seco	Grumitos		R3	8-90.	
M137	6090343	7577501	4743	Falla	64	85		D	1	0.5	SR	Página	4	Seco	Grumitos		R3	8-90.	
M137	6090343	7577501	4743	Falla	45	105		D	1	1	SR	Página	4	Seco	Grumitos		R3	8-90.	
M137	6090343	7577501	4743	Falla	65	182		C	1	0	SR	Página	10	Seco	Ductiles		R4	8-90.	
M137	6090343	7577501	4743	Falla	79	295		C	1	2	SR	Escalonada	4	Seco	Grumitos		R3	8-90.	
M137	6090343	7577501	4743	Falla	22	268		C	1	2	SR	Escalonada	4	Seco	Grumitos		R3	8-90.	
M137	6090343	7577501	4743	Falla	25	264		C	1	2	SR	Escalonada	4	Seco	Grumitos		R3	8-90.	
M137	6090343	7577501	4743	Falla	10	170		C	2	1	SR	Página	4	Seco	Grumitos		R3	8-90.	
M137	6090343	7577501	4743	Falla	83	187		D	1	0.5	SR	Página	4	Seco	Grumitos		R3	8-90.	
M137	6090343	7577501	4743	Falla	85	62		D	1	0.2	SR	Arena	12	Seco	Grumitos		R3	8-90.	
M137	6090343	7577501	4743	Falla	85	185		D	1	5	SR	Ortodoxa-Rugosa	14	Seco	Grumitos		R3	8-90.	
M137	6090343	7577501	4743	Falla	56	215		D	1	2	SR	Ortodoxa-Rugosa	8	Seco	Grumitos		R3	8-90.	
M137	6090343	7577501	4743	Falla	68	270		D	1	1	SR	Página-Rugosa	12	Seco	Grumitos		R3	8-90.	
M137	6090343	7577501	4743	Falla	4744	174		C	1	1.4	SR	Página-Rugosa	4	Seco	Grumitos		R3	8-90.	
M137	6090343	7577501	4743	Falla	65	140		C	1	0.5	SR	Página	6	Seco	Artesitas		R4	8-90.	
M137	6090343	7577501	4743	Falla	167	81		C	1	1.3	SR	Página	4	Seco	Grumitos		R3	8-90.	
M137	6090343	7577501	4743	Falla	212	59		C	1	0.5	SR	Página	4	Seco	Grumitos		R3	8-90.	
M137	6090343	7577501	4743	Falla	81	122		C	1	0.5	SR	Página	10	Seco	Ductiles		R4	8-90.	
M137	6090343	7577501	4743	Falla	10	170		C	1	0.5	SR	Página	10	Seco	Ductiles		R4	8-90.	
M137	6090343	7577501	4743	Falla	83	187		D	1	0.5	SR	Página	10	Seco	Ductiles		R4	8-90.	
M137	6090343	7577501	4743	Falla	85	62		D	1	0.2	SR	Página	10	Seco	Ductiles		R4	8-90.	
M137	6090343	7577501	4743	Falla	85	185		D	1	5	SR	Ortodoxa-Rugosa	14	Seco	Grumitos		R3	8-90.	
M137	6090343	7577501	4743	Falla	56	215		D	1	2	SR	Ortodoxa-Rugosa	8	Seco	Grumitos		R3	8-90.	
M137	6090343	7577501	4743	Falla	68	270		D	1	1	SR	Página-Rugosa	12	Seco	Grumitos		R3	8-90.	
M137	6090343	7577501	4743	Falla	4744	174		C	1	1.4	SR	Página-Rugosa	4	Seco	Grumitos		R3	8-90.	
M137	6090343	7577501	4743	Falla	65	140		C	1	0.5	SR	Página	6	Seco	Artesitas		R4	8-90.	
M137	6090343	7577501	4743	Falla	167	81		C	1	1.3	SR	Página	4	Seco	Grumitos		R3	8-90.	
M137	6090343	7577501	4743	Falla	212	59		C	1	0.5	SR	Página	4	Seco	Grumitos		R3	8-90.	
M137	6090343	7577501	4743	Falla	10	170		C	1	0.5	SR	Página	10	Seco	Ductiles		R4	8-90.	
M137	6090343	7577501	4743	Falla	83	187		D	1	0.5	SR	Página	10	Seco	Ductiles		R4	8-90.	
M137	6090343	7577501	4743	Falla	85	62		D	1	0.2	SR	Página	10	Seco	Ductiles		R4	8-90.	
M137	6090343	7577501</																	

**DIRECCIÓN TÉCNICA DE PROSPECCIÓN Y EXPLORACIÓN
ESTUDIO GEOLÓGICO-ESTRUCTURAL DEL ÁREA
CIRCUNDANTE DEL MANANTIAL DEL SISALÁ***



PTO.	ESTE	NORTE	ELEV.	TIPO	Az.	Bz.	DipDir	Pitch	CONTINUO	PERSISTENCIA (10m)	ABERTURA (10m)	RELLENO	FORMA	JRC	ACUA	TIPO ROCA	ALTERACION	DUREZA	FECHA	OBSERVACIONES
L944	61.1135	737.642	4859	Falla Normal	65	266	C	1	0	SR	Rugosa	14	Saco	Ductiles	R4	8-ago.	Desplazamiento 15 cm			
L949	61.1135	737.642	4859	Falla Normal	62	268	C	1	0	SR	Rugosa	14	Saco	Ductiles	R4	8-ago.	Desplazamiento 15 cm			
L954	61.1280	737.5012	4769	Falla Normal	88	10	C	1	0	SR	Plana	6	Saco	Igmnititas	R3	8-ago.	Desplazamiento 5 cm			
L955	61.1280	737.5012	4769	Falla Normal	70	8	C	1	0	SR	Plana	6	Saco	Igmnititas	R3	8-ago.	Desplazamiento 10 cm			
L956	61.1280	737.5012	4769	Falla Normal	85	166	C	1	0	SR	Plana	6	Saco	Igmnititas	R3	8-ago.	Desplazamiento 3 cm			
L957	61.1280	737.5012	4769	Falla Normal	62	260	C	1	0	SR	Plana	6	Saco	Igmnititas	R3	8-ago.	Desplazamiento 5 cm			
L958	61.1280	737.5012	4769	Falla Normal	84	10	C	1	0	SR	Okobido Fe	6	Saco	Igmnititas	R3	8-ago.	Desplazamiento 5 cm			
L959	61.1280	737.5012	4769	Falla Normal	55	23	C	1	2	SR	Plana	6	Saco	Igmnititas	R3	8-ago.	Desplazamiento 10 cm			
L960	61.1280	737.5012	4769	Falla Normal	63	360	D	1	2	SR	Plana	6	Saco	Igmnititas	R3	8-ago.	Desplazamiento 80 cm			
M123	609.6398	737.282	4831	Falla Normal	264	66	174	C	1	2	Arena	Plana	12	Saco	Ductiles	R4	8-ago.	Desplazamiento 3 cm		
M125	608.6357	737.711	46934	Falla Normal	72	120	D	1	0.5	SR	Plana	10	Saco	Igmnititas	R3	8-ago.	Desplazamiento 15 cm			
M126	608.6352	737.711	46934	Falla Normal	68	232	C	1	0.5	SR	Plana	10	Saco	Igmnititas	R3	8-ago.	Desplazamiento 15 cm			
M126	608.6352	737.7124	46938	Falla Normal	82	330	C	1	0	SR	Plana	10	Saco	Igmnititas	R3	8-ago.	Desplazamiento 10 cm			
M127	608.6352	737.7124	46938	Falla Normal	76	315	C	1	0	SR	Plana	10	Saco	Igmnititas	R4	8-ago.	Desplazamiento 15 cm			
M128	608.6352	737.7124	46938	Falla Normal	69	104	C	1	0	SR	Ortigado	8	Saco	Ductiles	R3	8-ago.	Desplazamiento 15 cm			
M128	608.6352	737.7124	46938	Falla Normal	80	146	C	1	0.5	SR	Corva	4	Saco	Igmnititas	R3	8-ago.	Desplazamiento 5 cm			
M128	608.6352	737.7124	46938	Falla Normal	85	144	C	1	0.5	SR	Plana	4	Saco	Igmnititas	R3	8-ago.	Desplazamiento 5 cm			
M130	608.6351	737.7124	46938	Falla Normal	87	210	C	1	0.5	SR	Arena	6	Saco	Arribadas	R4	8-ago.	Desplazamiento 5 cm			
D66	61.0305	737.4025	4725	Falla Horizontal	78	159	C	1	0.5	SR	Plana-Rugosa	12	Saco	Igmnititas	R3	8-ago.	Desplazamiento 5 cm			
M122	61.0305	737.4025	4725	Falla Horizontal	146	53	C	1	0.5	SR	Plana	10	Saco	Igmnititas	R4	8-ago.	Desplazamiento 30 cm			
D34	61.0301	737.7124	4938	Psuedoestratificación	72	184	C	1	0.5	SR	Plana	12	Saco	Arribadas	R4	8-ago.	Desplazamiento 10 cm			
L961	61.0302	737.7124	48007	Psuedoestratificación	265	50	C	1	0.5	SR	Plana	8	Saco	Igmnititas	R2	8-ago.	Desplazamiento 10 cm			
M121	61.0306	737.7124	48935	Psuedoestratificación	73	264	C	1	0.5	SR	Plana	8	Saco	Ductiles	R4	8-ago.	Desplazamiento 10 cm			
M123	61.0306	737.7124	48933	Psuedoestratificación	62	2	C	1	0.5	SR	Plana	8	Saco	Ductiles	R4	8-ago.	Desplazamiento 10 cm			
M124	61.0306	737.7124	48931	Psuedoestratificación	60	260	C	1	0.5	SR	Plana	8	Saco	Ductiles	R4	8-ago.	Desplazamiento 10 cm			
M124	61.0306	737.7124	48931	Psuedoestratificación	60	358	C	1	0.5	SR	Plana	8	Saco	Ductiles	R4	8-ago.	Desplazamiento 10 cm			
M127	604.5156	737.6804	46520	Psuedoestratificación	205	205	C	1	0.5	SR	Plana	8	Saco	Ductiles	R3	8-ago.	Desplazamiento 10 cm			
D100	61.1290	737.6807	48922	Diclessa	72	65	C	1	0.5	SR	Plana	8	Saco	Ductiles	R4	8-ago.	Desplazamiento 10 cm			
D102	61.1291	737.6807	48922	Diclessa	87	18	C	1	0.5	SR	Plana	8	Saco	Ductiles	R4	8-ago.	Desplazamiento 10 cm			
D102	61.1291	737.6807	48922	Diclessa	77	197	C	1	0.5	SR	Plana	8	Saco	Ductiles	R4	8-ago.	Desplazamiento 10 cm			
D103	61.1291	737.6808	48924	Diclessa	74	162	D	14	2	SR	Es calonida	12	Saco	Arribadas	R4	8-ago.	Desplazamiento 10 cm			
D103	61.1291	737.6808	48924	Diclessa	81	198	D	14	1	SR	Es calonida	12	Saco	Arribadas	R4	8-ago.	Desplazamiento 10 cm			
D104	61.1291	737.6808	48924	Diclessa	66	195	D	14	3	SR	Es calonida	8	Saco	Arribadas	R4	8-ago.	Desplazamiento 10 cm			
D104	61.1291	737.6808	48924	Diclessa	66	87	D	5	1	SR	Es calonida	14	Saco	Arribadas	R3	8-ago.	Desplazamiento 10 cm			
D96	61.1291	737.6808	48924	Diclessa	71	97	D	6	1	SR	Es calonida	12	Saco	Arribadas	R2	9-ago.	Desplazamiento 10 cm			
D96	61.1291	737.6808	48924	Diclessa	56	300	D	2	0.2	SR	Ortigado-Rugosa	10	Saco	Igmnititas	R2	9-ago.	Desplazamiento 10 cm			
D96	61.1291	737.6808	48924	Diclessa	85	180	D	1	0.5	SR	Plana-Rugosa	4	Saco	Igmnititas	R2	9-ago.	Desplazamiento 10 cm			
D96	61.1291	737.6808	48924	Diclessa	87	300	D	2	0.2	SR	Plana	4	Saco	Igmnititas	R2	9-ago.	Desplazamiento 10 cm			
D96	61.1291	737.6808	48924	Diclessa	78	220	D	1	0.5	SR	Plana	4	Saco	Igmnititas	R2	9-ago.	Desplazamiento 10 cm			
D96	61.1291	737.6808	48924	Diclessa	79	110	C	2	0.2	SR	Plana-Rugosa	8	Saco	Arribadas	R2	9-ago.	Desplazamiento 10 cm			
D96	61.1291	737.6808	48924	Diclessa	42	160	C	3	1.2	SR	Plana	4	Saco	Arribadas	R2	9-ago.	Desplazamiento 10 cm			
D97	61.1291	737.6808	48925	Diclessa	89	255	C	5	1	SR	Plana-Doblada	8	Saco	Arribadas	R2	9-ago.	Desplazamiento 10 cm			
D97	61.1291	737.6808	48925	Diclessa	84	320	C	2	0.2	SR	Plana-Doblada	14	Saco	Arribadas	R2	9-ago.	Desplazamiento 10 cm			
D98	61.1291	737.6808	48925	Diclessa	88	90	C	4	2	SR	Plana	4	Saco	Arribadas	R2	9-ago.	Desplazamiento 10 cm			
D99	61.1291	737.6808	48924	Diclessa	71	140	C	3	1.5	SR	Plana-Rugosa	12	Saco	Arribadas	R3	9-ago.	Desplazamiento 10 cm			
D99	61.1291	737.6808	48924	Diclessa	44	30	C	2	0.2	SR	Plana-Doblada	8	Saco	Arribadas	R3	9-ago.	Desplazamiento 10 cm			
D104	61.1291	737.6808	48924	Diclessa	60	260	D	3	0.5 a 1.5	SR	Plana-Doblada	10	Saco	Arribadas	R4	9-ago.	Desplazamiento 10 cm			
D104	61.1291	737.6808	48924	Diclessa	88	130	C	5	10	SR	Plana	8	Saco	Arribadas	R4	9-ago.	Desplazamiento 10 cm			
L977	61.1291	737.6808	48924	Diclessa	87	146	C	4	5	SR	Plana	8	Saco	Arribadas	R4	9-ago.	Desplazamiento 10 cm			
L979	61.1291	737.6808	48924	Diclessa	89	182	C	5	4	SR	Plana	8	Saco	Arribadas	R4	9-ago.	Desplazamiento 10 cm			
L980	61.1291	737.6808	48924	Diclessa	80	126	C	5	6	SR	Plana	8	Saco	Arribadas	R4	9-ago.	Desplazamiento 10 cm			
L981	61.1291	737.6808	48924	Diclessa	72	135	C	5	2	SR	Plana	9	Saco	Arribadas	R4	9-ago.	Desplazamiento 10 cm			
L982	61.1291	737.6808	48924	Diclessa	85	144	C	5	4	SR	Plana	9	Saco	Arribadas	R4	9-ago.	Desplazamiento 10 cm			
L983	61.1291	737.6808	48924	Diclessa	88	150	C	3	3	SR	Plana	8	Saco	Arribadas	R4	9-ago.	Desplazamiento 10 cm			
L985	61.1291	737.6808	48925	Diclessa	65	205	C	7	0	SR	Plana	5	Saco	Arribadas	R4	9-ago.	Desplazamiento 10 cm			
L986	61.1291	737.6808	48925	Diclessa	50	208	C	5	0	SR	Plana	5	Saco	Arribadas	R4	9-ago.	Desplazamiento 10 cm			
L987	61.1291	737.6808	48925	Diclessa	63	182	D	5	0	SR	Plana	8	Saco	Arribadas	R4	9-ago.	Desplazamiento 10 cm			
L988	61.1291	737.6808	48925	Diclessa	70	180	C	5	0	SR	Plana	8	Saco	Arribadas	R4	9-ago.	Desplazamiento 10 cm			



**DIRECCIÓN TÉCNICA DE PROSPECCIÓN Y EXPLORACIÓN
"ESTUDIO GEOLÓGICO-ESTRUCTURAL DEL ÁREA
CIRCUNDANTE DEL MANANTIAL DEL SISALÁ"**

PTO.	ESTE	NORTE	ELEV.	Az.	Bz.	DipDir	Pitch	CONTINUADO	PERSISTENCIA (10m)	ABERTURA (cm)	RELLENO	FORMA	JRC	TIPO ROCA	AGUA	ROTAZION	DUREZA	FECHA	NOTAS
L989	614.992	7381.319	497.95	Diáclisis	74	186		C	5	2	SR	Plana	8	Seco	Rotação	R4	9-980.		
L990	614.992	7381.319	497.95	Diáclisis	61	188		C	5	2	SR	Plana	8	Seco	Rotação	R4	9-980.		
L991	614.948	7380.994	504.97	Diáclisis	70	160		C	6	0	SR	Plana	8	Seco	Rotação	R4	9-980.		
L992	614.948	7380.994	504.97	Diáclisis	80	162		C	6	4	SR	Plana	8	Seco	Rotação	R4	9-980.		
L993	614.948	7380.994	504.97	Diáclisis	83	156		C	6	2	SR	Plana	8	Seco	Rotação	R4	9-980.		
L994	614.948	7380.994	504.97	Diáclisis	84	164		C	6	5	SR	Plana	8	Seco	Rotação	R4	9-980.		
L995	614.948	7380.994	504.97	Diáclisis	79	168		C	6	4	SR	Plana	8	Seco	Rotação	R4	9-980.		
L996	614.948	7380.994	504.97	Diáclisis	4	105		C	5	0	SR	Plana	8	Seco	Rotação	R4	9-980.		
M131	613.975	7377.096	4727	Diáclisis	325	74		C	1	1	SR	Plana	14	Seco	Rodante	R2	9-980.		
M131	613.975	7377.096	4727	Diáclisis	70	255		D	2	2	Arena	Rugosa	14	Seco	Rodante	R2	9-980.		
M131	613.975	7377.096	4727	Diáclisis	67	310		C	4	2	SR	Plana	12	Seco	Rodante	R2	9-980.		
M131	613.975	7377.096	4727	Diáclisis	61	192		D	2	4	SR	Corva	12	Seco	Rodante	R2	9-980.		
M131	613.975	7377.096	4727	Diáclisis	49	25		C	2	2	SR	Plana	12	Seco	Rodante	R2	9-980.		
M131	613.975	7377.096	4727	Diáclisis	28	270		C	1	3	SR	Plana	10	Seco	Rodante	R2	9-980.		
M132	613.951	7377.123	4738	Diáclisis	85	225		C	1	3	SR	Plana	10	Seco	Igumítritas	R2	9-980.		
M132	613.951	7377.123	4738	Diáclisis	77	295		C	10	0.5	SR	Corva	8	Seco	Igumítritas	R2	9-980.		
M135	613.949	7377.096	4752	Diáclisis	78	65		C	3	9	SR	Plana	14	Seco	Dolinado-Aqueduto	R4	9-980.		
M135	613.949	7377.096	4752	Diáclisis	61	227		C	4	2	SR	Alma	12	Seco	Dolinado-Aqueduto	R4	9-980.		
M135	613.949	7377.096	4752	Diáclisis	60	225		D	3	1	SR	Es calonida	14	Seco	Dolinado-Aqueduto	R4	9-980.		
M136	613.949	7377.096	4752	Diáclisis	74	28		D	4	7	SR	Plana	8	Seco	Rodante	R4	9-980.		
M136	613.949	7377.096	4752	Diáclisis	24	155		C	2	1	SR	Ondulada	8	Seco	Arribadas	R4	9-980.		
M137	613.949	7377.096	4752	Diáclisis	85	55		C	6	1	SR	Plana	6	Saco	Igumítritas	R2	9-980.		
M137	613.949	7377.096	4752	Diáclisis	60	170		D	1	6	SR	Plana	10	Saco	Igumítritas	R2	9-980.		
M137	613.949	7377.096	4752	Diáclisis	72	233		C	2	3	SR	Ondulada	8	Saco	Igumítritas	R2	9-980.		
M137	613.949	7377.096	4752	Diáclisis	71	288		D	3	3	SR	Rugosa	12	Saco	Igumítritas	R2	9-980.		
M138	613.949	7377.096	4752	Diáclisis	87	285		C	3	3	SR	Plana-Rugosa	10	Saco	Igumítritas	R2	9-980.		
M138	613.949	7377.096	4752	Diáclisis	60	225		D	3	7	SR	Plana	10	Saco	Igumítritas	R2	9-980.		
M138	613.949	7377.096	4752	Diáclisis	74	28		D	4	1	SR	Plana	14	Saco	Arribadas	R4	9-980.		
M138	613.949	7377.096	4752	Diáclisis	85	55		C	6	1	SR	Plana	6	Saco	Arribadas	R4	9-980.		
M138	613.949	7377.096	4752	Diáclisis	60	170		D	1	6	SR	Plana	12	Saco	Arribadas	R2	9-980.		
M138	613.949	7377.096	4752	Diáclisis	72	233		C	2	3	SR	Ondulada	8	Saco	Igumítritas	R2	9-980.		
M138	613.949	7377.096	4752	Diáclisis	71	288		D	3	3	SR	Rugosa	12	Saco	Igumítritas	R2	9-980.		
M138	613.949	7377.096	4752	Diáclisis	84	335		C	2	1	SR	Plana	12	Saco	Igumítritas	R2	9-980.		
M138	613.949	7377.096	4752	Diáclisis	45	270		D	2	1	SR	Plana	14	Saco	Arribadas	R2	9-980.		
M138	613.949	7377.096	4752	Diáclisis	32	95		D	4	1	SR	Plana	8	Saco	Igumítritas	R2	9-980.		
M138	613.949	7377.096	4752	Falla	211	84	131	C	1	10	SR	Alma	12	Saco	Rodante	R3	9-980.		
M138	613.949	7377.096	4752	Falla	86	30	290	C	1	1	SR	Plana	5	Saco	Rodante	R4	9-980.		
M138	613.949	7377.096	4752	Falla	5	265	C	1	0	SR	Plana	8	Saco	Rodante	R4	9-980.			
M138	613.949	7377.096	4752	Falla	6	260	C	1	0	SR	Plana	8	Saco	Rodante	R4	9-980.			
M139	613.949	7377.096	4752	Falla	4893	4893		C	1	0	SR	Plana	8	Saco	Rodante	R4	9-980.		
M139	613.949	7377.096	4752	Falla	4893	4893		C	2	1	SR	Plana	12	Saco	Rodante	R3	9-980.		
M139	613.949	7377.096	4752	Falla	4893	4893		D	1	1	SR	Plana	12	Saco	Rodante	R2	9-980.		
M139	613.949	7377.096	4752	Falla	4893	4893		C	1	0.5	SR	Plana	10	Saco	Igumítritas	R2	9-980.		
M139	613.949	7377.096	4752	Falla	4893	4893		C	1	0.5	SR	Plana	10	Saco	Igumítritas	R2	9-980.		
M139	613.949	7377.096	4752	Falla	4893	4893		D	1	1	SR	Plana	8	Saco	Igumítritas	R2	9-980.		
M139	613.949	7377.096	4752	Falla	4893	4893		C	1	5	SR	Alma	5	Saco	Rodante	R4	9-980.		
M139	613.949	7377.096	4752	Falla	4893	4893		D	1	2.5	SR	Plana-Escalonada	12	Saco	Rodante	R3	9-980.		
M139	613.949	7377.096	4752	Falla	4893	4893		C	1	1	SR	Plana-Ondulada	8	Saco	Igumítritas	R2	9-980.		
M139	613.949	7377.096	4752	Falla	4893	4893		D	1	4	SR	Plana	12	Saco	Rodante	R2	9-980.		
M139	613.949	7377.096	4752	Falla	4893	4893		C	1	0.5	SR	Plana	10	Saco	Igumítritas	R2	9-980.		
M139	613.949	7377.096	4752	Falla	4893	4893		D	1	0.5	SR	Plana	10	Saco	Igumítritas	R2	9-980.		
M139	613.949	7377.096	4752	Falla	4893	4893		C	1	3	SR	Plana	10	Saco	Igumítritas	R2	9-980.		
M139	613.949	7377.096	4752	Falla	4893	4893		D	1	2	SR	Plana	8	Saco	Igumítritas	R2	9-980.		
M139	613.949	7377.096	4752	Falla	4893	4893		C	1	5	SR	Alma	5	Saco	Igumítritas	R4	9-980.		
M139	613.949	7377.096	4752	Falla	4893	4893		D	1	2	SR	Plana	8	Saco	Igumítritas	R2	9-980.		
M139	613.949	7377.096	4752	Falla	4893	4893		C	1	0.5	SR	Alma	5	Saco	Igumítritas	R4	9-980.		
M139	613.949	7377.096	4752	Falla	4893	4893		D	1	0.5	SR	Plana	8	Saco	Igumítritas	R2	9-980.		
M139	613.949	7377.096	4752	Falla	4893	4893		C	1	3	SR	Plana	10	Saco	Igumítritas	R2	9-980.		
M139	613.949	7377.096	4752	Falla	4893	4893		D	1	2	SR	Plana	8	Saco	Igumítritas	R2	9-980.		
M139	613.949	7377.096	4752	Falla	4893	4893		C	1	0.5	SR	Alma	5	Saco	Igumítritas	R4	9-980.		
M139	613.949	7377.096	4752	Falla	4893	4893		D	1	0.5	SR	Plana	8	Saco	Igumítritas	R2	9-980.		
M139	613.949	7377.096	4752	Falla	4893	4893		C	1	3	SR	Plana	10	Saco	Igumítritas	R2	9-980.		
M139	613.949	7377.096	4752	Falla	4893	4893		D	1	2	SR	Plana	8	Saco	Igumítritas	R2	9-980.		
M139	613.949	7377.096	4752	Falla	4893	4893		C	1	0.5	SR	Alma	5	Saco	Igumítritas	R4	9-980.		
M139	613.949	7377.096	4752	Falla	4893	4893		D	1	0.5	SR	Plana	8	Saco	Igumítritas	R2	9-980.		
M139	613.949	7377.096	4752	Falla	4893	4893		C	1	3	SR	Plana	10	Saco	Igumítritas	R2	9-980.		
M139	613.949	7377.096	4752	Falla	4893	4893		D	1	2	SR	Plana	8	Saco	Igumítritas	R2	9-980.		
M139	613.949	7377.096	4752	Falla	4893	4893		C	1	0.5	SR	Alma	5	Saco	Igumítritas	R4	9-980.		
M139	613.949	7377.096	4752	Falla	4893	4893		D	1	0.5	SR	Plana	8	Saco	Igumítritas	R2	9-980.		
M139	613.949	7377.096	4752	Falla	4893	4893		C	1	3	SR	Plana	10	Saco	Igumítritas	R2	9-980.		
M139	613.949	7377.096	4752	Falla	4893	4893		D	1	2	SR	Plana	8	Saco	Igumítritas	R2	9-980.		
M139	613.949	7377.096	4752	Falla	4893	4893		C	1	0.5	SR	Alma	5	Saco	Igumítritas	R4	9-980.		
M139	613.949	7377.096	4752	Falla	4893	4893		D	1	0.5	SR	Plana	8	Saco	Igumítritas	R2	9-980.		
M139	613.949	7377.096	4752	Falla	4893	4893		C	1	3	SR	Plana	10	Saco	Igumítritas	R2	9-980.		
M139	613.949	7377.096	4752	Falla	4893	4893		D	1	2	SR	Plana	8	Saco	Igumítritas	R2	9-980.		
M139	613.949	7377.096	4752	Falla	4893	4893		C	1	0.5	SR	Alma	5	Saco	Igumítritas	R4	9-980.		
M139	613.949	7377.096	4752	Falla	4893	4893		D	1	0.5	SR	Plana	8	Saco	Igumítritas	R2	9-980.		
M139	613.949	7377.096	4752	Falla	4893	4893		C	1	3	SR	Plana	10	Saco	Igumítritas	R2	9-980.		
M139	613.949	7377.096	4752	F															

DIRECCIÓN TÉCNICA DE PROSPECCIÓN Y EXPLORACIÓN
 "ESTUDIO GEOLÓGICO-ESTRUCTURAL DEL ÁREA
 CIRCUNDANTE DEL MANANTIAL DEL SISALÁ"

PTO.	ESTE	NORTE	ELEV.	Az.	Bz.	DipDir	Pitch	CONTINUADO	PERSISTENCIA (100m)	ABERTURA (100m)	RELLENO	FORMA	JRC	ACUA	TIPO ROCA	ALTERACION	DUREZA	FECHA	OBSERVACIONES
L.010	61.1364	7367270	4630	Diciplasa	86	284		C	1	0	SR	Plana	6	Saco	Iguminitas		R3	10-ago-00.	
L.011	61.1364	7367270	4630	Diciplasa	87	276		C	2	0	SR	Plana	6	Saco	Iguminitas		R3	10-ago-00.	
L.012	61.1364	7367270	4630	Diciplasa	89	31		C	3	0	SR	Plana	6	Saco	Iguminitas		R3	10-ago-00.	
L.014	61.1364	7367270	4630	Diciplasa	89	26		C	3	0	SR	Plana	6	Saco	Iguminitas		R3	10-ago-00.	
L.015	61.1364	7367270	4630	Diciplasa	89	10		C	2	0	SR	Plana	6	Saco	Iguminitas		R3	10-ago-00.	
L.016	61.1364	7367270	4630	Diciplasa	89	27		C	2	0	SR	Plana	6	Saco	Iguminitas		R3	10-ago-00.	
L.017	61.1364	7367270	4630	Diciplasa	89	25		C	2	0	SR	Plana	6	Saco	Iguminitas		R3	10-ago-00.	
L.003	61.1364	7367270	4630	Diciplasa	80	154		C	1	2	SR	Plana	5	Saco	Iguminitas		R3	10-ago-00.	
L.012	61.1364	7367270	4630	Falla Dextral	10	18		C	1	0	SR	Plana	6	Saco	Iguminitas		R3	10-ago-00.	Desplazamiento .10 cm
L.018	61.1364	7367270	4630	Falla Dextral	5	37		C	1	0	SR	Plana	6	Saco	Iguminitas		R3	10-ago-00.	
L.019	61.1364	7367270	4630	Falla Dextral	4	340		C	1	0	SR	Plana	6	Saco	Iguminitas		R3	10-ago-00.	
L.020	61.1364	7367270	4630	Falla Dextral	9	18		C	1	0	SR	Plana	6	Saco	Iguminitas		R3	10-ago-00.	
L.001	622.233	7367330	4605	Falla normal	55	295		C	1	10	SR	Plana	8	Saco	Iguminitas		R3	10-ago-00.	Desplazamiento .02 cm
D.005	61.813	7357987	4545	Diciplasa	85	173		C	2	0	SR	Plana	12	Saco	Iguminitas		R3	11-ago-00.	
D.005	61.813	7357987	4545	Diciplasa	35	280		D	3	0.2	Arena	Ortoblada-Rugosa	10	Saco	Ductiles		R3	11-ago-00.	
D.005	61.813	7357987	4545	Diciplasa	52	250		D	1	0.3-1	Arena	Plana	8	Saco	Ductiles		R3	11-ago-00.	
D.005	61.813	7357987	4545	Diciplasa	74	213		D	1	1	Arena	Plana	4	Saco	Ductiles		R3	11-ago-00.	
D.005	61.813	7357987	4545	Diciplasa	91	363		D	2	2.5	SR	Ortoblada	14	Saco	Ductiles		R3	11-ago-00.	
D.008	61.745	7359504	4556	Diciplasa	72	246		C	1	1	Arena	Ortoblada-Higosa	12	Saco	Iguminitas		R2	11-ago-00.	
D.008	61.745	7359504	4552	Diciplasa	90	226		D	1	1	Arena	Ortoblada-Higosa	10	Saco	Iguminitas		R2	11-ago-00.	
D.009	61.951	6360385	4616	Diciplasa	76	338		C	1	1	Arena	Ortoblada-Higosa	4	Saco	Iguminitas		R2	11-ago-00.	
D.010	61.951	6360385	4616	Diciplasa	84	226		C	2	0.5	SR	Plana	4	Saco	Iguminitas		R2	11-ago-00.	
D.110	6.67.87	7367791	4632	Diciplasa	78	160		D	2	0.5	SR	Ortoblada	8	Saco	Iguminitas		R2	11-ago-00.	
D.110	6.67.87	7367791	4632	Diciplasa	80	272		C	3	0	SR	Plana	4	Saco	Iguminitas		R2	11-ago-00.	
D.110	6.67.87	7367791	4632	Diciplasa	86	70		C	1	0	SR	Plana	4	Saco	Iguminitas		R2	11-ago-00.	
D.110	6.67.87	7367791	4632	Diciplasa	21	25		C	4	0	SR	Plana	4	Saco	Iguminitas		R2	11-ago-00.	
D.111	6.67.87	7367791	4632	Diciplasa	76	3		C	3	0	SR	Plana-Rugosa	10	Saco	Iguminitas		R2	11-ago-00.	
D.111	6.67.87	7367791	4632	Diciplasa	69	237		C	7	1 a 2	SR	Rugosa-Escalonada	12	Saco	Iguminitas		R2	11-ago-00.	
D.111	6.67.87	7367791	4632	Diciplasa	82	65		C	2	0	SR	Rugosa-Escalonada	4	Saco	Iguminitas		R2	11-ago-00.	
D.111	6.67.87	7367791	4632	Diciplasa	68	0		C	2	0	SR	Rugosa-Escalonada	3	Saco	Iguminitas		R2	11-ago-00.	
D.111	6.67.87	7367791	4632	Diciplasa	69	324		C	3	0.2 a 2	SR	Plana	4	Saco	Iguminitas		R2	11-ago-00.	
D.113	6.52.277	7365386	4638	Diciplasa	68	135		D	1	2	Arena	Ortoblada	14	Saco	Ductiles		R2	11-ago-00.	
D.114	6.52.277	7365386	4638	Diciplasa	87	25		D	1	0.5	SR	Plana	4	Saco	Iguminitas		R2	11-ago-00.	
D.114	6.52.277	7365386	4639	Diciplasa	88	133		C	3	0.5	SR	Plana	4	Saco	Iguminitas		R2	11-ago-00.	
D.114	6.52.277	7365386	4639	Diciplasa	90	148		C	2	0.5	SR	Plana	4	Saco	Iguminitas		R2	11-ago-00.	
D.114	6.52.277	7365386	4639	Diciplasa	52	94		C	1	0.5	SR	Plana	10	Saco	Ductiles		R2	11-ago-00.	
D.108	6.77.57	7359906	4559	Falla inversa	78	184		C	1	4.5	SR	Plana	14	Saco	Ductiles		R3	11-ago-00.	Recharo 20 cm
D.112	6.15.012	7362867	4707	Falla inversa	79	222		C	1	3	SR	Plana	14	Saco	Ductiles		R2	11-ago-00.	Recharo 25 cm
D.112	6.15.012	7362867	4707	Falla inversa	12	315		C	1	0.5	SR	Plana	12	Saco	Ductiles		R2	11-ago-00.	Recharo 25 cm
D.112	6.15.012	7362867	4707	Falla inversa	78	280		C	1	0.5	SR	Plana	12	Saco	Ductiles		R2	11-ago-00.	Recharo 25 cm
D.107	6.15.757	7359906	4559	Falla Normal	50	200		D	1	1 a 3	Arena	Rugosa-Escalonada	14	Saco	Ductiles		R3	11-ago-00.	
D.008	6.15.949	7360044	4552	Falla Normal	84	320		C	1	0.5 a 5	Arena	Rugosa-Escalonada	12	Saco	Iguminitas		R2	11-ago-00.	Desplazamiento 1 cm
D.008	6.15.949	7360044	4552	Falla Normal	72	164		C	1	0.5	SR	Plana	4	Saco	Iguminitas		R2	11-ago-00.	
D.009	6.15.951	6360385	4615	Falla Normal	88	140		C	1	1.2	SR	Plana	4	Saco	Iguminitas		R2	11-ago-00.	Desplazamiento 3 cm
D.009	6.15.951	6360385	4615	Falla Normal	88	138		C	1	5	SR	Plana	4	Saco	Iguminitas		R2	11-ago-00.	Desplazamiento 3 cm
D.111	6.15.951	6360385	4615	Falla Normal	84	245		C	1	6	SR	Plana	4	Saco	Iguminitas		R2	11-ago-00.	Desplazamiento 3 cm
D.111	6.15.951	6360385	4615	Falla Normal	90	50		C	1	0.2	Arena	Plana	4	Saco	Iguminitas		R2	11-ago-00.	Desplazamiento 1 cm
D.008	6.15.757	7359906	4556	Falla Normal	88	227		C	1	0.5	SR	Rugosa-Escalonada	12	Saco	Ductiles		R2	11-ago-00.	Desplazamiento 6 cm
D.008	6.15.757	7359906	4556	Falla Normal	87	312		C	1	3	SR	Plana	8	Saco	Iguminitas		R2	11-ago-00.	
D.113	6.15.277	7362868	4638	Falla Normal	88	28		D	1	0.7	SR	Plana	4	Saco	Iguminitas		R2	11-ago-00.	Desplazamiento 1.5 cm
D.113	6.15.277	7362868	4638	Falla Normal	88	130		D	1	0.5	SR	Plana	4	Saco	Iguminitas		R2	11-ago-00.	
D.114	6.15.291	7360042	4559	Falla Normal	88	140		C	1	0.2	SR	Plana	4	Saco	Iguminitas		R2	11-ago-00.	
D.114	6.15.291	7360042	4559	Falla Normal	88	138		C	1	5	SR	Plana	4	Saco	Iguminitas		R2	11-ago-00.	
D.114	6.15.291	7360042	4559	Falla Normal	84	245		C	1	6	SR	Plana	4	Saco	Iguminitas		R2	11-ago-00.	
D.114	6.15.291	7360042	4559	Falla Normal	70	54		C	1	0.2	Arena	Plana	4	Saco	Iguminitas		R2	11-ago-00.	Desplazamiento 1 cm
D.112	6.15.902	7362247	4641	Falla Normal	90	305		C	1	0.5	SR	Plana	4	Saco	Ductiles		R2	11-ago-00.	Desplazamiento 6 cm
D.112	6.15.902	7362247	4641	Falla Normal	87	312		C	1	3	SR	Plana	4	Saco	Iguminitas		R2	11-ago-00.	
D.005	6.15.163	7362867	4556	Falla Normal	88	28		D	1	0.7	SR	Plana	4	Saco	Ductiles		R2	11-ago-00.	
D.005	6.15.163	7362867	4556	Falla Normal	87	260		C	2	0.5	SR	Plana	8	Saco	Robusta		R3	12-ago-00.	
D.023	6.20.053	7365389	4944	Diciplasa	51	300		C	2	0.5	SR	Rugosa	12	Saco	Robusta		R3	12-ago-00.	
D.027	6.20.164	7367362	4937	Diciplasa	75	149		C	2	0	SR	Rugosa	12	Saco	Robusta		R3	12-ago-00.	
D.028	6.20.164	7367362	4937	Diciplasa	73	170		D	2	1	SR	Rugosa	12	Saco	Robusta		R3	12-ago-00.	

Base de datos

Página 42

**DIRECCIÓN TÉCNICA DE PROSPECCIÓN Y EXPLORACIÓN
ESTUDIO GEOLÓGICO-ESTRUCTURAL DEL ÁREA
CIRCUNDANTE DEL MANANTIAL DEL SISAL***

PTO.	ESTE	NORTE	ELEV.	TIPO	Az.	Bz.	DipDir	Ptch	CONTINUADO	PERSISTENCIA (10m)	ABERTURA (cm)	RELLENO	FORMA	JRC	AGUA	TIPO ROCA	ALTERACION	DUREZA	FECHA	OBSERVACIONES
L1.029	6193936	7568104	4937	Diciélsa	79	330	C	2	10	SR	Ortoblada	14	Saco	Rodante	R3	12-480.				
L1.031	6193936	7568104	4937	Diciélsa	55	73	D	2	1.5	SR	Plana	4	Saco	Rodante	R3	12-480.				
L1.033	6120642	7567784	4837	Diciélsa	62	275	D	3	3	SR	Plana	8	Saco	Rodante	R3	12-480.				
L1.034	6120642	7567784	4837	Diciélsa	53	200	D	3	0	SR	Ortoblada	8	Saco	Rodante	R3	12-480.				
L1.035	6120716	7567637	4930	Diciélsa	50	105	C	2	1	SR	Bonosa	13	Saco	Rodante	R3	12-480.				
L1.036	6120716	7567637	4930	Diciélsa	78	100	C	2	1.5	SR	Bonosa	12	Saco	Rodante	R3	12-480.				
L1.038	6121142	7567015	4939	Diciélsa	85	34	C	2	7	SR	Plana	5	Saco	Rodante	R3	12-480.				
L1.039	6121142	7567015	4939	Diciélsa	42	260	D	3	0	SR	Plana	5	Saco	Rodante	R3	12-480.				
L1.040	6121142	7567015	4939	Diciélsa	50	255	D	3	0.5	SR	Ortoblada	8	Saco	Rodante	R3	12-480.				
L1.042	6121516	7566044	4947	Diciélsa	78	175	D	2	1	SR	Ortoblada	10	Saco	Rodante	R3	12-480.				
L1.043	6121516	7566044	4947	Diciélsa	73	102	D	2	4	SR	Ortoblada	8	Saco	Rodante	R3	12-480.				
M1.42	6161556	7564328	4750	Diciélsa	70	83	C	3	0.2±1	Arena	Ortoblada	8	Saco	Igumintitas	R2	12-480.				
M1.42	6161556	7564328	4750	Diciélsa	66	45	D	1	1	SR	Ortoblada	12	Saco	Igumintitas	R2	12-480.				
M1.43	6161243	7567374	4639	Diciélsa	88	232	C	2	2	SR	Plana	4	Saco	Igumintitas	R2	12-480.				
M1.44	6161281	7568025	4638	Diciélsa	88	280	C	2	0.5	SR	Escalonada	14	Saco	Igumintitas	R2	12-480.				
M1.46	6161579	7572268	4717	Diciélsa	75	161	C	1	0.1	SR	Plana	4	Saco	Igumintitas	R2	12-480.				
M1.46	6161579	7572268	4717	Diciélsa	74	167	C	1	0.1	SR	Ortoblada-Escalona	14	Saco	Igumintitas	R2	12-480.				
M1.45	6161562	7570194	4763	Falla de Roca	77	160	C	2	0.1±5	SR	Es calonada	12	Saco	Rodante	R3	12-480.	Desplazamiento 6 cm			
L1.022	6120553	7566569	4944	Falla de Roca	37	145	C	1	0.5	SR	Es calonada	10	Saco	Rodante	R3	12-480.	Desplazamiento 2 cm			
M1.39	6161508	7561596	4559	Falla de Roca	50	130	C	1	0.2±1	Arena	Ortoblada	10	Saco	Igumintitas	R2	12-480.	Rechazo 10 cm			
M1.39	6161508	7561596	4559	Falla de Roca	89	253	C	1	0.5±1	Arena	Plana	4	Saco	Igumintitas	R2	12-480.	Rechazo 15 cm			
M1.41	6161604	7562198	4632	Falla de Roca	87	88	C	1	1.3	SR	Plana	4	Saco	Igumintitas	R2	12-480.	Rechazo 10 cm			
M1.41	6161604	7562198	4632	Falla de Roca	73	183	C	1	1.2	SR	Ortoblada	12	Saco	Igumintitas	R2	12-480.	Rechazo 10 cm			
M1.42	612181	7568025	4638	Falla de Roca	45	20	C	1	3	SR	Plana-Ortoblada	12	Saco	Rodante	R3	12-480.	Desplazamiento 2 cm			
L1.024	6120523	7566569	4944	Falla de Roca	80	250	C	1	2.5	SR	Es calonada	12	Saco	Rodante	R3	12-480.	Desplazamiento 1 cm			
L1.025	6120523	7566569	4944	Falla de Roca	79	90	C	1	1	SR	Es calonada	12	Saco	Rodante	R3	12-480.	Desplazamiento 4 cm			
L1.026	6161934	7567362	4937	Falla de Roca	78	198	C	1	1	SR	Es calonada	12	Saco	Rodante	R3	12-480.	Desplazamiento 5 cm			
M1.42	6161936	7568104	4937	Falla de Roca	4937	145	D	1	2	SR	Es calonada	12	Saco	Rodante	R3	12-480.	Desplazamiento 7 cm			
M1.032	6120642	7567784	4837	Falla de Roca	85	92	C	1	3.5	SR	Plana	8	Saco	Rodante	R3	12-480.	Desplazamiento 3 cm			
M1.037	6120716	7567637	4930	Falla de Roca	66	65	C	1	0	SR	Plana	12	Saco	Rodante	R2	12-480.	Desplazamiento 3 cm			
L1.041	6121516	7566044	4939	Falla de Roca	61	150	D	1	2.5	SR	Ortoblada	14	Saco	Rodante	R3	12-480.	Desplazamiento 3 cm			
M1.39	6161508	7561596	4559	Falla de Roca	62	81	C	1	1	SR	Plana	4	Saco	Igumintitas	R2	12-480.	Desplazamiento 2 cm			
M1.40	6161483	7561752	4556	Falla de Roca	74	300	C	1	0.5	Arena	Plana-Ortoblada	8	Saco	Igumintitas	R2	12-480.	Desplazamiento 4 cm			
M1.40	6161483	7561752	4556	Falla de Roca	84	295	C	1	0.5	SR	Plana	4	Saco	Igumintitas	R2	12-480.	Desplazamiento 2.5 cm			
M1.41	6161604	7562198	4632	Falla de Roca	67	89	C	2	0.5±2	SR	Plana	4	Saco	Igumintitas	R2	12-480.	Desplazamiento 1 cm			
M1.41	6161243	7567374	4639	Falla de Roca	75	70	C	1	0.3±3	Arena	Plana-Rugosa	8	Saco	Igumintitas	R2	12-480.	Desplazamiento 3 cm			
M1.44	6161281	7568025	4638	Falla de Roca	78	232	C	1	1.5	SR	Ortoblada-Rugosa	12	Saco	Igumintitas	R2	12-480.	Desplazamiento 4.5 cm			
M1.44	6161281	7568025	4638	Falla de Roca	103	192	C	1	0.5±2	SR	Plana	12	Saco	Igumintitas	R4	13-480.	Desplazamiento 2 cm			
L1.046	6120521	7584802	4751	Diciélsa	52	154	C	4	0.5	SR	Plana	8	Saco	Arestadas	R3	12-480.				
L1.050	6000821	7583743	4553	Diciélsa	75	186	D	2	0	SR	Plana-Rugosa	12	Saco	Igumintitas	R3	12-480.				
L1.051	6000821	7583743	4553	Diciélsa	82	208	C	4	1	SR	Arena	12	Saco	Igumintitas	R3	12-480.				
L1.052	6000821	7583743	4553	Diciélsa	80	260	C	1	1	SR	Plana	12	Saco	Arestadas	R4	13-480.				
M1.45	6161243	7567474	4639	Diciélsa	81	180	D	2	0.5	SR	Rugosa	12	Saco	Arestadas	R4	13-480.				
M1.45	6161243	7567474	4639	Diciélsa	84	135	D	5	1	SR	Rugosa	12	Saco	Arestadas	R4	13-480.				
L1.056	6036811	7574752	4636	Diciélsa	89	151	C	3	2	SR	Plana	12	Saco	Igumintitas	R3	12-480.				
L1.056	6036940	7577810	4735	Diciélsa	86	26	C	2	0	SR	Plana	12	Saco	Igumintitas	R3	13-480.				
L1.051	6036940	7577810	4735	Diciélsa	81	27	D	2	0	SR	Plana-Rugosa	12	Saco	Arestadas	R4	13-480.				
M1.47	6196847	7576184	4752	Diciélsa	53	35	D	3	0.5±1	SR	Ortoblada	8	Saco	Arestadas	R4	13-480.				
M1.47	6196847	7576184	4752	Diciélsa	59	45	C	2	0.5	SR	Ortoblada	12	Saco	Arestadas	R4	13-480.				
M1.48	6197729	7588067	4552	Diciélsa	81	180	D	2	0.5	SR	Rugosa	12	Saco	Arestadas	R4	13-480.				
M1.48	6197729	7588067	4552	Diciélsa	84	135	D	5	1	SR	Rugosa	12	Saco	Arestadas	R4	13-480.				
M1.49	600731	7583586	4552	Diciélsa	77	187	C	3	0.5	SR	Plana	4	Saco	Igumintitas	R2	13-480.				
M1.49	600731	7583586	4552	Diciélsa	84	244	D	6	0.5	SR	Plana	4	Saco	Igumintitas	R2	13-480.				
M1.50	601635	7575560	4577	Diciélsa	84	315	C	1	10	SR	Arena	12	Saco	Igumintitas	R2	13-480.				
M1.50	601635	7575560	4577	Diciélsa	74	285	C	3	13	SR	Plana-Escalonada	12	Saco	Igumintitas	R2	13-480.				
M1.51	601635	7575560	4577	Diciélsa	42	164	D	2	0.5	SR	Plana-Rugosa	8	Saco	Igumintitas	R2	13-480.				
M1.51	601635	7577194	4624	Diciélsa	88	143	C	2	0.5	SR	Plana-Escalonada	8	Saco	Igumintitas	R2	13-480.				
M1.51	601635	7577194	4624	Diciélsa	85	95	D	1	1	SR	Plana-Escalonada	10	Saco	Igumintitas	R2	13-480.				

Base de datos

Página 43

**DIRECCIÓN TÉCNICA DE PROSPECCIÓN Y EXPLORACIÓN
ESTUDIO GEOLÓGICO-ESTRUCTURAL DEL ÁREA
CIRCUNDANTE DEL MANANTIAL DEL SISAL***



PTO.	ESTE	NORTE	ELEV.	TIPO	Az.	Bz.	DipDir	Ptch	CONTINUO	PERSISTENCIA (km)	ABERTURA (km)	FORMA	RELLENO	JRC	AGUA	TIPO ROCA	ALTERACION	DUREZA	FECHA	OBSERVACIONES
M152	604.390	737.7400	4650	Dicelosa	85	202	C	1	0.5	SR	Plana-Rugosa	10	Saco	Iguminitas		R2	13-380-			
M152	604.390	737.7400	4650	Dicelosa	60	330	D	1	0.5	SR	Plana	4	Saco	Iguminitas		R2	13-380-			
M152	604.390	737.7400	4650	Dicelosa	88	164	C	3	0.5	SR	Plana	4	Saco	Iguminitas		R2	13-380-			
M154	604.865	737.6273	4652	Dicelosa	48	225	C	3	0.5	SR	Nieve-Escalonada	8	Saco	Iguminitas		R2	13-380-			
M154	604.865	737.6273	4652	Dicelosa	61	154	C	5	0.5	SR	Nieve-Escalonada	4	Saco	Iguminitas		R2	13-380-			
M157	609.867	737.6194	4752	Falla Interna	87	204	D	1	0.8	SR	Plana-Rugosa	8	Saco	Arribadas		R4	13-380-			
L1044	599.770	738.6802	4571	Falla Interna	87	170	C	2	1	SR	Plana-Ondulada	8	Saco	Arribadas		R4	13-380-	Desplazamiento 5 cm		
L1047	599.770	738.6802	4571	Falla Interna	77	347	C	1	1	SR	Plana	8	Saco	Arribadas		R4	13-380-	Desplazamiento 0.5 cm		
L1057	603.811	737.5729	4636	Falla Interna	83	166	C	1	0	SR	Plana-Rugosa	12	Saco	Iguminitas		R3	13-380-	Desplazamiento 0 cm		
L1059	604.905	737.5727.1	46557	Falla Interna	65	290	C	3	0	SR	Rugosa	12	Saco	Iguminitas		R3	13-380-	Desplazamiento 1 cm		
L1059	604.905	737.5727.1	4710	Falla Interna	82	0	C	1	0	SR	Plana-Escalonada	14	Saco	Iguminitas		R2	13-380-	Re-hazo 1 cm		
L1049	599.770	738.6766	4710	Falla Interna	68	150	C	1	0	SR	Plana-Rugosa	12	Saco	Arribadas		R4	13-380-	Desplazamiento 15 cm		
L1053	601.652	737.6247.8	4550	Falla Interna	82	348	C	8	1	SR	Plana-Rugosa	10	Saco	Iguminitas		R3	13-380-	Desplazamiento 2 cm		
L1055	601.652	737.6247.8	4550	Falla Interna	60	51	C	2	0	SR	Plana-Rugosa	14	Saco	Iguminitas		R3	13-380-	Desplazamiento 4 cm		
M149	600.9305	737.6271	46537	Falla Interna	80	10	C	2	2	SR	Plana-Burra	12	Saco	Arribadas		R2	13-380-	Desplazamiento 2.5 cm		
M150	600.9305	737.6271	738.5586	Dicelosa	4552	10	C	1	1	SR	Escalonada	10	Saco	Iguminitas		R2	13-380-	Desplazamiento 2 cm		
M155	601.635	737.5650	4577	Falla Interna	89	237	D	1	6	SR	Ondulada-Rugosa	12	Saco	Iguminitas		R2	13-380-	Desplazamiento 1 cm		
L1048	599.770	738.6822	4710	Falla Interna	80	217	C	1	1	SR	Ondulada-Rugosa	12	Saco	Arribadas		R4	13-380-	Desplazamiento 10 cm		
L1048	599.770	738.6822	4571	Falla Interna	78	213	C	1	0	SR	Ondulada	12	Saco	Arribadas		R4	13-380-	Desplazamiento 10 cm		
L1045	599.729	738.68067	4571	Falla Interna	17	212	C	2	2	SR	Arena	4	Saco	Iguminitas		R4	13-380-	Patagonia-Estratificación		
M148	599.729	738.68067	4572	Falla Interna	22	225	C	2	2	SR	Rugosa	8	Saco	Iguminitas		R4	13-380-	Patagonia-Estratificación		
M153	604.484	737.6564	46533	Falla Interna	68	70	C	3	1	SR	Ondulada-Escalonada	8	Saco	Iguminitas		R4	13-380-	Patagonia-Estratificación		
D115	598.469	736.2589	5004	Dicelosa	62	8	D	2	2	SR	Ondulada-Ondulada	8	Saco	Arribadas		R4	13-380-	Patagonia-Estratificación		
D115	598.469	736.2589	5004	Dicelosa	86	105	D	6	1 a 3	SR	Plana-Escalonada	10	Saco	Arribadas		R3	14-380-	Patagonia-Estratificación		
D117	599.724	736.6162	5192	Dicelosa	89	225	C	3	6	SR	Ondulada-Rugosa	10	Saco	Bricha de base		R3	14-380-	Patagonia-Estratificación		
D118	599.724	736.6170	5310	Dicelosa	73	163	C	4	3	SR	Ondulada-Rugosa	12	Saco	Bricha de base		R3	14-380-	Patagonia-Estratificación		
D118	599.724	736.6170	5310	Dicelosa	25	125	C	4	3	SR	Ondulada-Rugosa	12	Saco	Bricha de base		R3	14-380-	Patagonia-Estratificación		
D119	598.9579	736.6170	48310	Dicelosa	74	305	C	2	2	SR	Ondulada	8	Saco	Arribadas		R4	14-380-	Patagonia-Estratificación		
D120	598.736	736.6181	4904	Dicelosa	82	109	C	4	5.5	SR	Plana-Ondulada	10	Saco	Arribadas		R4	14-380-	Patagonia-Estratificación		
D121	599.239	736.6187	4765	Dicelosa	85	360	C	2	2	SR	Plana-Ondulada	9	Saco	Bricha de base		R3	14-380-	Patagonia-Estratificación		
D121	599.239	736.6187	4765	Dicelosa	84	192	D	1	0	SR	Plana-Ondulada	10	Saco	Bricha de base		R3	14-380-	Patagonia-Estratificación		
J64	599.748	736.6187	4765	Dicelosa	50	330	D	1	1	SR	Plana	4	Saco	Bricha de base		R3	14-380-	Patagonia-Estratificación		
J66	598.037	736.6182	51453	Dicelosa	88	264	C	3	0.5	SR	Plana	8	Saco	Arribadas		R3	14-380-	Patagonia-Estratificación		
J68	598.175	736.6186	4930	Dicelosa	88	302	C	3	0.2	SR	Plana-Ondulada	4	Saco	Bricha de base		R3	14-380-	Patagonia-Estratificación		
J68	598.175	736.6186	4935	Dicelosa	58	100	C	2	0.5	SR	Plana	12	Saco	Arribadas		R4	14-380-	Patagonia-Estratificación		
L121	602.641	736.6186	4410	Dicelosa	68	220	C	6	30	SR	Plana	12	Saco	Iguminitas		R2	14-380-			
L122	602.641	736.6186	4410	Dicelosa	87	216	C	3	3	SR	Plana	12	Saco	Iguminitas		R2	14-380-			
L123	602.641	736.6186	4410	Dicelosa	85	240	C	4	0	SR	Plana	12	Saco	Iguminitas		R2	14-380-			
L124	602.641	736.6186	4410	Dicelosa	60	110	C	6	1	SR	Escalonada	6	Saco	Iguminitas		R3	14-380-			
M156	597.494	736.6193	5216	Dicelosa	81	91	C	3	0.5	SR	Escalonada	6	Saco	Iguminitas		R3	14-380-			
M157	597.494	736.6193	5216	Dicelosa	78	240	D	3	3	SR	Plana	6	Saco	Ductiles		R2	14-380-			
M158	597.494	736.6193	5216	Dicelosa	88	165	C	3	0.5	SR	Escalonada	6	Saco	Ductiles		R2	14-380-			
L122	598.451	736.6193	4755	Dicelosa	79	35	D	3	12	SR	Plana	12	Saco	Reducto		R3	14-380-			
M163	598.451	736.6193	4755	Dicelosa	82	238	D	1	10	SR	Ondulada	16	Saco	Reducto		R3	14-380-			
M163	598.451	736.6193	4755	Dicelosa	60	245	D	1	5	SR	Escalonada Plana	12	Saco	Reducto		R3	14-380-			
L163	601.012	736.6210	4317	Falla	84	232	C	1	1	SR	Plana	12	Saco	Falla de lechos		R2	14-380-			
L164	601.012	736.6210	4317	Falla	84	151	C	1	0.5	SR	Ondulada	8	Saco	Ductiles		R3	14-380-			
L165	601.012	736.6210	4317	Falla	84	350	C	1	1	SR	Cova	16	Saco	Reducto		R3	14-380-			
M161	598.442	736.6190	4710	Dicelosa	82	115	D	4	0.5	SR	Ondulada	14	Saco	Reducto		R3	14-380-			
M161	598.442	736.6190	4710	Dicelosa	77	232	C	2	12	SR	Plana	12	Saco	Reducto		R3	14-380-			
M162	598.442	736.6190	4710	Dicelosa	81	205	C	3	3	SR	Plana	12	Saco	Reducto		R3	14-380-			
M160	598.281	736.6193	4921	Dicelosa	74	210	C	1	1	SR	Plana	12	Saco	Falla de lechos		R2	14-380-			
M160	598.281	736.6193	4921	Dicelosa	84	151	C	1	5	SR	Plana	4	Saco	Ductiles		R3	14-380-			
L165	601.012	736.6210	4317	Falla	83	160	C	1	2	SR	Plana	12	Saco	Falla de lechos		R2	14-380-			
L167	601.012	736.6210	4317	Falla	85	120	C	1	0	SR	Rugosa	14	Saco	Falla de lechos		R2	14-380-			
L167	601.012	736.6210	4317	Falla	70	156	C	1	1	SR	Rugosa	14	Saco	Falla de lechos		R3	14-380-			
L168	601.012	736.6210	4317	Falla	88	96	C	1	0	SR	Plana	10	Saco	Iguminitas		R3	14-380-			

Base de datos

**DIRECCIÓN TÉCNICA DE PROSPECCIÓN Y EXPLORACIÓN
"ESTUDIO GEOLÓGICO-ESTRUCTURAL DEL ÁREA
CIRCUNDANTE DEL MANANTIAL DEL SISAL"**

PTO.	ESTE	NORTE	ELEV.	TIPO	Az.	Bz.	DipDir	Pitch	CONTINUADO	PERSISTENCIA (10m)	ABERTURA (10m)	FORMA	JRC	ACUJA	TIPO ROCA	ALTERACION	DUREZA	FECHA	OBSERVACIONES
L1.085	-601.1583	75662209	4397	Falla	85	80	C	1	0	SR	Plana	10	Saco	Igumintitas	R3	14-480-			
L1.086	-601.1583	75662209	4397	Falla	48	125	C	1	0	SR	Onidizada	10	Saco	Igumintitas	R3	14-480-			
L1.087	-601.1583	75662209	4397	Falla	88	86	C	1	0	SR	Plana	10	Saco	Igumintitas	R3	14-480-			
L1.091	-601.1583	75662209	4397	Falla	87	94	C	1	0	SR	Plana-abusada	12	Saco	Igumintitas	R3	14-480-			
L1.092	-601.1583	75662209	4397	Falla	69	134	C	1	0	SR	Plana-abusada	12	Saco	Igumintitas	R3	14-480-			
L1.096	-601.1583	75662209	4397	Falla	89	130	C	1	0	SR	Plana-abusada	12	Saco	Igumintitas	R3	14-480-			
L1.099	-601.1583	75662209	4397	Falla	85	300	C	1	0	SR	Plana-abusada	12	Saco	Igumintitas	R3	14-480-			
L1.101	-601.1583	75662209	4397	Falla	59	344	C	1	0	SR	Plana-abusada	12	Saco	Igumintitas	R3	14-480-			
L1.102	-601.1583	75662209	4397	Falla	89	144	C	1	0	SR	Plana-abusada	12	Saco	Igumintitas	R3	14-480-			
L1.103	-601.1583	75662209	4397	Falla	89	330	C	1	0	SR	Plana-abusada	12	Saco	Igumintitas	R3	14-480-			
L1.104	-602.190	75658686	4400	Falla	80	43	C	1	2	SR	Plana	10	Saco	Flujo de dientes	R2	14-480-			
L1.105	-602.190	75658686	4400	Falla	84	79	C	1	1	SR	Plana	10	Saco	Flujo de dientes	R2	14-480-			
L1.106	-602.190	75658686	4400	Falla	76	265	C	1	0	SR	Plana	10	Saco	Flujo de dientes	R2	14-480-			
L1.107	-602.190	75658686	4400	Falla	89	335	C	1	0	SR	Plana	10	Saco	Flujo de dientes	R2	14-480-			
L1.108	-602.190	75658686	4400	Falla	89	286	C	1	3	SR	Micro brecha	10	Saco	Flujo de dientes	R2	14-480-			
L1.109	-602.190	75658686	4400	Falla	86	340	C	1	1	SR	Micro brecha	10	Saco	Flujo de dientes	R2	14-480-			
L1.110	-602.190	75658686	4400	Falla	73	160	C	1	4	SR	Micro brecha	12	Saco	Flujo de dientes	R2	14-480-			
L1.113	-602.190	75658686	4400	Falla	85	334	C	1	1	SR	Plana	12	Saco	Flujo de dientes	R2	14-480-			
L1.114	-602.190	75658686	4400	Falla	83	68	C	1	1	SR	Plana	12	Saco	Flujo de dientes	R2	14-480-			
L1.115	-602.190	75658686	4400	Falla	83	160	C	1	0	SR	Plana	12	Saco	Flujo de dientes	R2	14-480-			
L1.116	-602.190	75658686	4400	Falla	88	352	C	1	6	SR	Micro fracta	6	Saco	Flujo de dientes	R2	14-480-			
M1.56	597.494	75659893	5216	Falla	225	70	135	C	1	0.5	SR	Plana	6	Saco	Ductos	R3	14-480-		
M1.57	597.510	75659894	5216	Falla	88	70	C	6	2	SR	Escalonada	8	Saco	Ductos	R3	14-480-			
M1.59	597.926	75659007	5012	Falla	180	78	C	1	1	SR	Onidizada	14	Saco	Flujo de dientes	R2	14-480-			
L1.075	-601.373	75662277	4381	Falla	87	330	C	1	0	SR	Rugosa	8	Saco	Ductos	R3	14-480-			
M1.58	597.748	75658625	5930	Falla	192	84	282	C	1	1	SR	Escalonada	8	Saco	Ductos	R3	14-480-		
M1.59	597.748	75658625	5930	Falla	88	115	C	1	1	SR	Escalonada	8	Saco	Ductos	R3	14-480-	Desplazamiento 14 cm		
M1.60	597.926	75660007	5012	Falla	270	54	180	C	1	0.5	SR	Plana-Cava	4	Saco	Ductos	R3	14-480-		
M1.61	597.926	75660007	5012	Falla	82	158	C	1	6	SR	Plana	12	Saco	Redondeo	R2	14-480-			
D1.062	-601.070	75662210	4378	Falla Ductos	85	30	C	1	1.5	SR	Plana	12	Saco	Flujo de dientes	R2	14-480-	Desplazamiento 100 cm		
L1.077	-601.1583	75662209	4397	Falla Ductos	80	25	C	1	2	SR	Rugosa	14	Saco	Igumintitas	R3	14-480-			
D1.13	-597.724	75658710	5310	Falla Ductos	43	320	D	1	0.5	SR	Ortoblasto-Argiles a	12	Saco	Brich de la base	R3	14-480-			
L1.20	-598.724	75658710	4904	Falla Ductos	78	320	D	1	1.5	SR	Plana-Onidizada	10	Saco	Arribes	R4	14-480-	Recinto c/m		
L1.078	-601.1583	75662209	4397	Falla Ductos	89	350	C	1	0	SR	Plana	10	Saco	Igumintitas	R3	14-480-	Desplazamiento 180 cm		
L1.100	-601.1583	75662209	4397	Falla Ductos	85	340	C	1	1	SR	Plana	12	Saco	Flujo de dientes	R2	14-480-	Desplazamiento 45 cm		
L1.111	-602.190	75658686	4400	Falla Ductos	89	80	C	1	0	SR	Plana	10	Saco	Flujo de dientes	R2	14-480-	Desplazamiento 10 cm		
D1.15	597.469	75658625	5024	Falla Ductos	71	175	C	1.5	1	SR	Arena	4	Saco	Arribes	R4	14-480-			
D1.16	597.535	75658622	5161	Falla Ductos	62	305	C	2	1	SR	Onidizada-Escalonada	12	Saco	Brich de la base	R3	14-480-			
D1.17	597.535	75658622	5161	Falla Ductos	76	285	C	1	0.5 a 10	SR	Plana-Onidizada	8	Saco	Brich de la base	R3	14-480-			
D1.17	597.826	75658622	5192	Falla Ductos	72	210	D	1	1	SR	Onidizada	12	Saco	Brich de la base	R3	14-480-			
D1.19	598.559	75658606	4895	Falla Ductos	89	195	C	1	1.5	SR	Onidizada	8	Saco	Ductos	R4	14-480-	Desplazamiento 8 cm		
D1.20	598.559	75658606	4895	Falla Ductos	43	43	C	1	2	SR	Plana	12	Saco	Arribes	R4	14-480-	Desplazamiento 3 cm		
J34	597.748	75658625	5143	Falla Ductos	85	25	C	1	0.2	SR	Plana	4	Saco	Arribes	R4	14-480-	Desplazamiento 3 cm		
J35	597.730	75658615	5035	Falla Ductos	50	310	C	1	1	SR	Onidizada	14	Saco	Brich de la base	R3	14-480-	Desplazamiento 2 cm		
J66	598.087	75658556	4930	Falla Ductos	86	185	C	1	1.3	SR	Plana-Escalonada	14	Saco	Brich de la base	R3	14-480-	Desplazamiento 2 cm		
J67	598.170	75658758	4965	Falla Ductos	85	121	D	1	2 a 5	SR	Plana-Escalonada	14	Saco	Brich de la base	R3	14-480-	Desplazamiento 20 cm		
J68	598.175	75658758	4965	Falla Ductos	69	140	C	1	3 a 5	SR	Onidizada-Escalonada	14	Humedo	Arribes	R4	14-480-	Desplazamiento 5 cm		
J70	598.305	75662209	4397	Falla Ductos	70	310	C	1	0.5	SR	Plana	4	Saco	Arribes	R4	14-480-	Desplazamiento 15 cm		
L1.066	-601.106	75662245	4372	Falla Ductos	88	234	C	1	2	SR	Plana	12	Saco	Flujo de dientes	R2	14-480-			
L1.067	-601.106	75662245	4382	Falla Ductos	84	80	D	1	0	SR	Plana	12	Saco	Igumintitas	R2	14-480-			
L1.069	-601.182	75662260	4382	Falla Ductos	4351	Falla Ductos	67	226	C	1	3	SR	Rugosa	14	Saco	Flujo de dientes	R2	14-480-	
L1.071	-601.173	75662277	4382	Falla Ductos	40	214	C	1	0	SR	Rugosa	14	Saco	Flujo de dientes	R2	14-480-			
L1.072	-601.173	75662277	4382	Falla Ductos	82	94	C	1	3	SR	Rugosa	14	Saco	Flujo de dientes	R2	14-480-			
L1.074	-601.173	75662277	4382	Falla Ductos	84	280	C	1	1	SR	Rugosa	14	Saco	Flujo de dientes	R2	14-480-			
L1.076	-601.173	75662267	4397	Falla Ductos	80	86	C	1	0	SR	Plana	10	Saco	Igumintitas	R3	14-480-	Desplazamiento 15 cm		
L1.079	-601.1583	75658629	4397	Falla Ductos	88	16	C	1	0	SR	Plana	10	Saco	Igumintitas	R3	14-480-			
L1.080	-601.1583	75658629	4397	Falla Ductos	72	70	C	1	0	SR	Plana	10	Saco	Igumintitas	R3	14-480-			
L1.081	-601.1583	75662209	4397	Falla Ductos	84	320	C	1	0	SR	Plana	10	Saco	Igumintitas	R3	14-480-	Desplazamiento 20 cm		

Base de datos

**RECREACIÓN TÉCNICA DE PROSPECCIÓN Y EXPLORACIÓN
ESTUDIO GEOLOGICO-ESTRUCTURAL DEL ÁREA
CIRCUNDANTE DEL MANANTIAL DEL SILALA***

Nº.	ESTE	NORTE	ELEV.	TIPO	Az	Bz	Dipol	Pitch	CONTINUO	PERIODICO	RELEÑO	FORMA	JRC	AGUA	TIPO ROCA	ALTURA CON	DUREZA	FECHA	OBSERVACIONES
PRESISTENCIA EN CM	ALTAZON	RELEÑO	FORMA	PERIODICO															
24	601583	7566209	4397	Falla Normal	8	30	C	2	0	SR	Plana-Rugosa	10	Seco	Iginimurtas	R3	14-ago	Despilazamiento 40 cm		
	601583	7566209	4397	Falla Normal	8	130	C	1	0	SR	Plana-Rugosa	10	Seco	Iginimurtas	R3	14-ago	Despilazamiento 20 cm		
39	601583	7566209	4397	Falla Normal	89	154	C	1	0	SR	Plana-Rugosa	10	Seco	Iginimurtas	R3	14-ago	Despilazamiento 10 cm		
33	601583	7566209	4397	Falla Normal	88	105	C	2	0	SR	Plana-Rugosa	12	Seco	Iginimurtas	R3	14-ago	Despilazamiento 5 cm		
34	601583	7566209	4397	Falla Normal	89	21	C	2	0	SR	Plana-Rugosa	12	Seco	Iginimurtas	R3	14-ago	Despilazamiento 30 cm		
36	601583	7566209	4397	Falla Normal	89	110	C	1	0	SR	Plana-Rugosa	12	Seco	Iginimurtas	R3	14-ago	Despilazamiento 15 cm		
37	601583	7566209	4397	Falla Normal	89	34	C	1	0	SR	Plana-Rugosa	12	Seco	Iginimurtas	R3	14-ago	Despilazamiento 2 cm		
12	601583	7566209	4397	Falla Normal	89	34	C	2	0	SR	Plana-Rugosa	12	Seco	Iginimurtas	R3	14-ago	Despilazamiento 30 cm		
19	601583	7566209	4400	Falla Normal	70	150	C	1	0	SR	Ondulada	10	Seco	Efluo de hierros	R2	14-ago	Despilazamiento 5 cm		
30	601583	7566209	4401	Falla Normal	97	160	C	1	0	SR	Plana	12	Seco	Efluo de hierros	R2	14-ago	Despilazamiento 5 cm		
19	601583	7566209	4401	Falla Normal	88	260	C	1	1.5	SR	Plana	12	Seco	Efluo de hierros	R2	14-ago	Despilazamiento 6 cm		
34	601583	7566209	4401	Falla Normal	89	110	C	1	0	SR	Plana-Rugosa	12	Seco	Efluo de hierros	R2	14-ago	Despilazamiento 30 cm		
35	601583	7566209	4410	Falla Normal	86	175	C	1	0	SR	Plana	12	Seco	Iginimurtas	R2	14-ago	Despilazamiento 10 cm		
35	601583	7566209	4410	Falla Normal	86	60	D	1	0	SR	Plana	8	Seco	Iginimurtas	R3	14-ago	Despilazamiento 1 cm		
8	597748	7569125	5930	Falla Normal	170	77	260	C	1	5	SR	Plana	6	Seco	Ductiles	R3	14-ago	Despilazamiento 42 cm	
8	597748	7569125	5930	Falla Normal	205	79	115	C	1	10	SR	Plana-Cuva	4	Seco	Ductiles	R3	14-ago	Despilazamiento 5 cm	
8	597748	7569125	5930	Falla Normal	61	175	C	1	0.5	SR	Plana-Cuva	4	Seco	Ductiles	R3	14-ago	Despilazamiento 5 cm		
8	597748	7569125	5930	Falla Normal	68	164	C	1	10	SR	Plana	4	Seco	Ductiles	R4	14-ago	Despilazamiento 3 cm		
9	598579	7568175	4931	Falla intestinal	59	108	C	1	2	SR	Plana	4	Seco	Anisotropas	R5	14-ago	Ductiles		
9	598579	7568175	4935	Peurdestratificación	52	342	C	1	0	SR	Plana	4	Seco	Anisotropas	R4	14-ago	Ductiles		
6	598579	7568175	4934	Peurdeestratificación	34	55	C	1	0	SR	Plana	4	Seco	Anisotropas	R3	14-ago	Ductiles		
6	598579	7568175	4934	Peurdeestratificación	18	200	C	1	0	SR	Plana	4	Seco	Anisotropas	R3	14-ago	Ductiles		
1	598579	7568175	4935	Peurdeestratificación	35	215	C	1	1	Arena	Plana-Rugosa	10	Seco	Ductiles	R3	14-ago	Ductiles		
4	603207	75751500	46399	Diceliosa	74	316	C	1	1	1.5	Arena	Plana-Rugosa	12	Seco	Ductiles	R3	15-agosto	Ductiles	
5	603202	75751500	4710	Diceliosa	71	106	D	2	1	0.4±1	SR	Plana	4	Seco	Ductiles	R3	15-agosto	Ductiles	
5	603202	75751500	4710	Diceliosa	60	254	D	2	1	SR	Plana-Rugosa	12	Seco	Ductiles	R3	15-agosto	Ductiles		
6	603202	75751500	4710	Diceliosa	90	168	C	4	1.3	SR	Plana	4	Seco	Ductiles	R3	15-agosto	Ductiles		
6	603202	75751500	4736	Diceliosa	74	221	C	2	4	Arena	Plana	14	Seco	Ductiles	R3	15-agosto	Ductiles		
6	603202	75751500	4736	Diceliosa	83	315	D	2	0.5±2	Arena	Rugosa-Escalonada	14	Seco	Ductiles	R3	15-agosto	Ductiles		
6	603202	75751500	4736	Diceliosa	74	125	C	1	0	SR	Rugosa-Escalonada	14	Seco	Ductiles	R3	15-agosto	Ductiles		
4	603207	75751500	4736	Diceliosa	83	195	C	1	0	SR	Rugosa	14	Seco	Iginimurtas	R3	15-agosto	Ductiles		
9	603206	75751500	4736	Diceliosa	85	36	C	1	1	SR	Plana	4	Seco	Iginimurtas	R3	15-agosto	Ductiles		
9	603206	75751500	4736	Diceliosa	83	105	C	3	1	SR	Plana-Rugosa	12	Seco	Iginimurtas	R3	15-agosto	Ductiles		
33	603036	7564425	4385	Falla	20	347	C	1	0	SR	Plana	12	Seco	Efluo de hierros	R2	15-agosto	Despilazamiento 30 cm		
33	603036	7564425	4385	Falla	87	308	C	1	0	SR	Plana	12	Seco	Iginimurtas	R3	15-agosto	Despilazamiento 10 cm		
35	603036	7564425	4385	Falla	88	17	C	1	0	SR	Plana	12	Seco	Iginimurtas	R3	15-agosto	Despilazamiento 5 cm		
35	603036	7564425	4385	Falla	87	297	C	1	0.5	SR	Plana-Rugosa	12	Seco	Efluo de hierros	R3	15-agosto	Recalado a ch		
35	603036	7564425	4385	Falla	1	1.5	SR	Plana	12	Seco	Iginimurtas	R3	15-agosto	Recalado a ch					
37	603036	7564425	4385	Falla	87	330	C	1	1	SR	Plana	12	Seco	Efluo de hierros	R2	15-agosto	Despilazamiento 5 cm		
37	603036	7564425	4385	Falla	50	330	C	1	0	SR	Plana	12	Seco	Efluo de hierros	R2	15-agosto	Despilazamiento 5 cm		
37	603036	7564425	4385	Falla	75	233	C	1	0	SR	Plana	12	Seco	Efluo de hierros	R2	15-agosto	Despilazamiento 5 cm		
37	603036	7564425	4385	Falla	75	186	C	1	0	SR	Plana	12	Seco	Efluo de hierros	R2	15-agosto	Despilazamiento 5 cm		
37	603036	7564425	4385	Falla	75	187	C	1	0	SR	Plana	12	Seco	Efluo de hierros	R2	15-agosto	Despilazamiento 5 cm		
37	603036	7564425	4385	Falla	75	188	C	1	0	SR	Plana	12	Seco	Efluo de hierros	R2	15-agosto	Despilazamiento 5 cm		
37	603036	7564425	4385	Falla	75	189	C	1	0	SR	Plana	12	Seco	Efluo de hierros	R2	15-agosto	Despilazamiento 5 cm		
37	603036	7564425	4385	Falla	75	190	C	1	0	SR	Plana	12	Seco	Efluo de hierros	R2	15-agosto	Despilazamiento 5 cm		
37	603036	7564425	4385	Falla	75	191	C	1	0	SR	Plana	12	Seco	Efluo de hierros	R2	15-agosto	Despilazamiento 5 cm		
37	603036	7564425	4385	Falla	75	192	C	1	0	SR	Plana	12	Seco	Efluo de hierros	R2	15-agosto	Despilazamiento 5 cm		
37	603036	7564425	4385	Falla	75	193	C	1	0	SR	Plana	12	Seco	Efluo de hierros	R2	15-agosto	Despilazamiento 5 cm		
37	603036	7564425	4385	Falla	75	194	C	1	0	SR	Plana	12	Seco	Efluo de hierros	R2	15-agosto	Despilazamiento 5 cm		
37	603036	7564425	4385	Falla	75	195	C	1	0	SR	Plana	12	Seco	Efluo de hierros	R2	15-agosto	Despilazamiento 5 cm		
37	603036	7564425	4385	Falla	75	196	C	1	0	SR	Plana	12	Seco	Efluo de hierros	R2	15-agosto	Despilazamiento 5 cm		
37	603036	7564425	4385	Falla	75	197	C	1	0	SR	Plana	12	Seco	Efluo de hierros	R2	15-agosto	Despilazamiento 5 cm		
37	603036	7564425	4385	Falla	75	198	C	1	0	SR	Plana	12	Seco	Efluo de hierros	R2	15-agosto	Despilazamiento 5 cm		
37	603036	7564425	4385	Falla	75	199	C	1	0	SR	Plana	12	Seco	Efluo de hierros	R2	15-agosto	Despilazamiento 5 cm		
37	603036	7564425	4385	Falla	75	200	C	1	0	SR	Plana	12	Seco	Efluo de hierros	R2	15-agosto	Despilazamiento 5 cm		
37	603036	7564425	4385	Falla	75	201	C	1	0	SR	Plana	12	Seco	Efluo de hierros	R2	15-agosto	Despilazamiento 5 cm		
37	603036	7564425	4385	Falla	75	202	C	1	0	SR	Plana	12	Seco	Efluo de hierros	R2	15-agosto	Despilazamiento 5 cm		
37	603036	7564425	4385	Falla	75	203	C	1	0	SR	Plana	12	Seco	Efluo de hierros	R2	15-agosto	Despilazamiento 5 cm		
37	603036	7564425	4385	Falla	75	204	C	1	0	SR	Plana	12	Seco	Efluo de hierros	R2	15-agosto	Despilazamiento 5 cm		
37	603036	7564425	4385	Falla	75	205	C	1	0	SR	Plana	12	Seco	Efluo de hierros	R2	15-agosto	Despilazamiento 5 cm		
37	603036	7564425	4385	Falla	75	206	C	1	0	SR	Plana	12	Seco	Efluo de hierros	R2	15-agosto	Despilazamiento 5 cm		
37	603036	7564425	4385	Falla	75	207	C	1	0	SR	Plana	12	Seco	Efluo de hierros	R2	15-agosto	Despilazamiento 5 cm		
37	603036	7564425	4385	Falla	75	208	C	1	0	SR	Plana	12	Seco	Efluo de hierros	R2	15-agosto	Despilazamiento 5 cm		
37	603036	7564425	4385	Falla	75	209	C	1	0	SR	Plana	12	Seco	Efluo de hierros	R2	15-agosto	Despilazamiento 5 cm		
37	603036	7564425	4385	Falla	75	210	C	1	0	SR	Plana	12	Seco	Efluo de hierros	R2	15-agosto	Despilazamiento 5 cm		
37	603036	7564425	4385	Falla	75	211	C	1	0	SR	Plana	12	Seco	Efluo de hierros	R2	15-agosto	Despilazamiento 5 cm		
37	603036	7564425	4385	Falla	75	212	C	1	0	SR	Plana	12	Seco	Efluo de hierros	R2	15-agosto	Despilazamiento 5 cm		
37	603036	7564425	4385	Falla	75	213	C	1	0	SR	Plana	12	Seco	Efluo de hierros	R2	15-agosto	Despilazamiento 5 cm		
37	603036	7564425	4385	Falla	75	214	C	1	0	SR	Plana	12	Seco	Efluo de hierros	R2	15-agosto	Despilazamiento 5 cm		
37	603036	7564425	4385	Falla	75	215	C	1	0	SR	Plana	12	Seco	Efluo de hierros	R2	15-agosto	Despilazamiento 5 cm		
37	603036	7564425	4385	Falla	75	216	C	1	0	SR	Plana	12	Seco	Efluo de hierros	R2	15-agosto	Despilazamiento 5 cm		
37	603036	7564425	4385	Falla	75	217	C	1	0	SR	Plana	12	Seco	Efluo de hierros	R2	15-agosto	Despilazamiento 5 cm		
37	603036	7564425	4385	Falla	75	218	C	1	0	SR	Plana	12	Seco	Efluo de hierros	R2	15-agosto	Despilazamiento 5 cm		
37	603036	7564425	4385	Falla	75	219	C	1	0	SR	Plana	12	Seco	Efluo de hierros	R2	15-agosto	Despilazamiento 5 cm		
37	603036	7564425	4385	Falla	75	220	C	1	0	SR	Plana	12	Seco	Efluo de hierros	R2	15-agosto	Despilazamiento 5 cm		
37	603036	7564425	4385	Falla	75	221	C	1	0	SR	Plana	12	Seco	Efluo de hierros	R2	15-agosto	Despilazamiento 5 cm		
37	603036	7564425	4385	Falla	75	222	C	1	0	SR	Plana	12	Seco	Efluo de hierros	R2	15-agosto	Despilazamiento 5 cm		
37	603036	7564425	4385	Falla	75	223	C	1	0	SR	Plana								

Base de datos

DIRECCIÓN TÉCNICA DE PROSPECCIÓN Y EXPLORACIÓN
"ESTUDIO GEOLÓGICO-ESTRUCTURAL DEL ÁREA
CIRCUNDANTE DEL MANANTIAL DEL SILALA"



PTO.	ESTE	NORTE	ELEV.	TIPO	Az	Bz	DipDir	Pitch	CONTINUIDAD	PERSISTENCIA (30m)	ABERTURA (cm)	RELLENO	FORMA	JRC	AGUA	TIPO ROCA	ALTERACION	DUREZA	FECHA	OBSERVACIONES
L1147	600188	7565406	4327	Falla Normal		70	45		C	1	0	SR	Plana	12	Seco	Ignimbritas		R3	15-agosto.	Desplazamiento 6 cm
L1148	600188	7565406	4327	Falla Normal		89	52		C	1	0	SR	Plana	12	Seco	Ignimbritas		R3	15-agosto.	Desplazamiento 5 cm
L1149	600188	7565406	4327	Falla Normal		87	62		C	1	0	SR	Plana	12	Seco	Ignimbritas		R3	15-agosto.	Desplazamiento 10 cm
L1150	600188	7565406	4327	Falla Normal		88	58		C	1	0	SR	Plana	12	Seco	Ignimbritas		R3	15-agosto.	Desplazamiento 10 cm
L1142	600587	7565829	4320	Falla Sinestral		89	5		C	1	0	SR	Plana	12	Seco	Ignimbritas		R3	15-agosto.	Desplazamiento 30 cm
D124	605207	7575500	4699	Pseudoestratificación		42	142		C							Seco	Dacitas	R3	15-agosto.	
D125	605202	7575087	4710	Pseudoestratificación		65	238		C							Seco	Dacitas	R3	15-agosto.	

CONVENIO DE COOPERACIÓN INTERINSTITUCIONAL Y
CONTRATO DE CONSULTORIA DIREMAR - SERGEOMIN



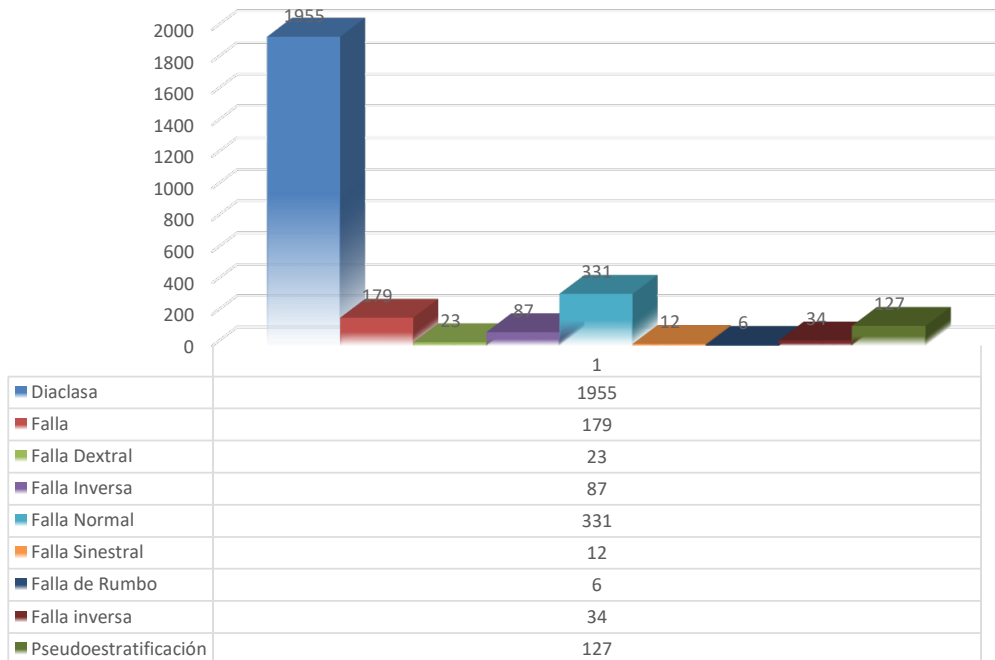
**ESTADÍSTICA CUANTITATIVA Y
CUALITATIVA DE
ESTRUCTURAS**

Calle Federico Suazo N° 1673 Esquina Reyes Ortiz – La Paz - Bolivia
Telf. (591 – 2) 2330981 – 2331236 - Fax 2391725 – 2318295
www.sergeomin.gob.bo

Anexo

Estadística cuantitativa y cualitativa del proyecto “Estudio Geológico-Estructural del área Circundante al Manantial Silala”

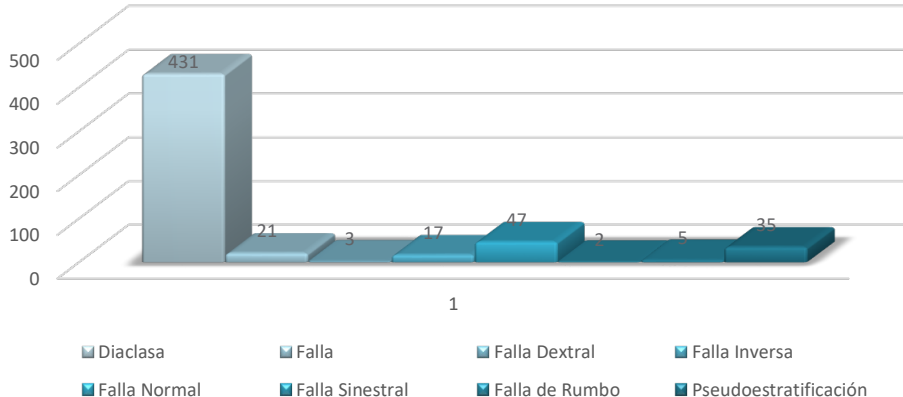
ESTRUCTURAS GEOLOGICAS-PROYECTO SILALA



ESTRUCTURAS	CANTIDAD
Diaclase	1955
Falla	179
Falla Dextral	23
Falla Inversa	87
Falla Normal	331
Falla Sinestral	12
Falla de Rumbo	6
Falla inversa	34
Pseudoestratificación	127
Total Estructuras	2754

Cerro Inacaliri

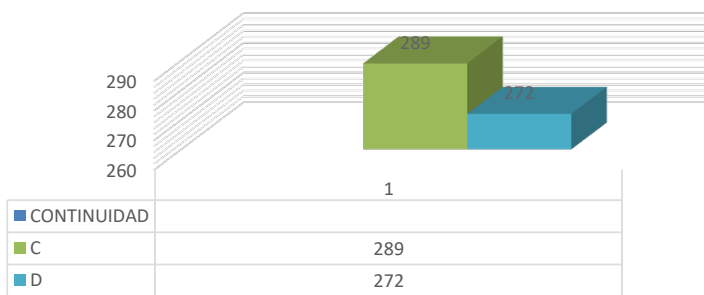
Estructuras Cerro Inacaliri



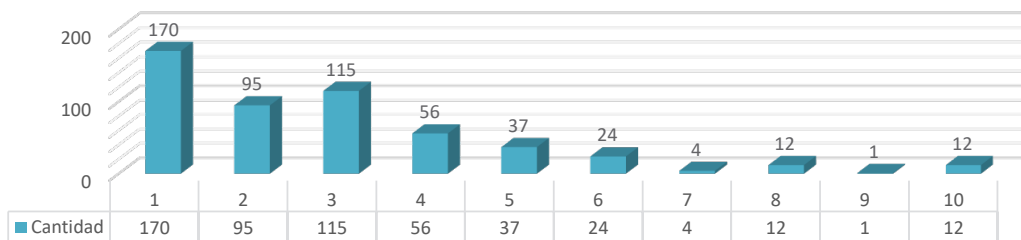
ESTRUCTURAS

Diaclasa	431
Falla	21
Falla Dextral	3
Falla Inversa	17
Falla Normal	47
Falla Sinestral	2
Falla de Rumbo	5
Pseudoestratificación	35

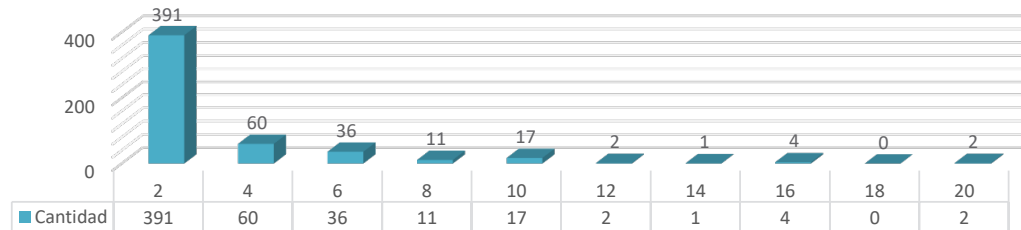
Continuidad



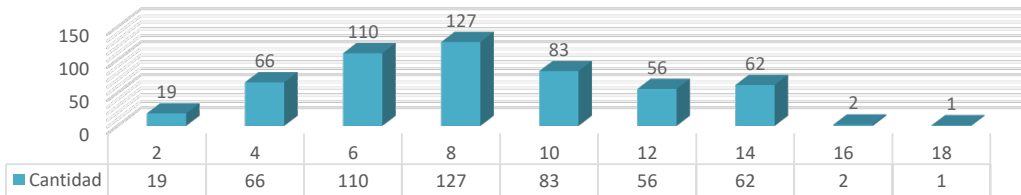
Persistencia



Abertura

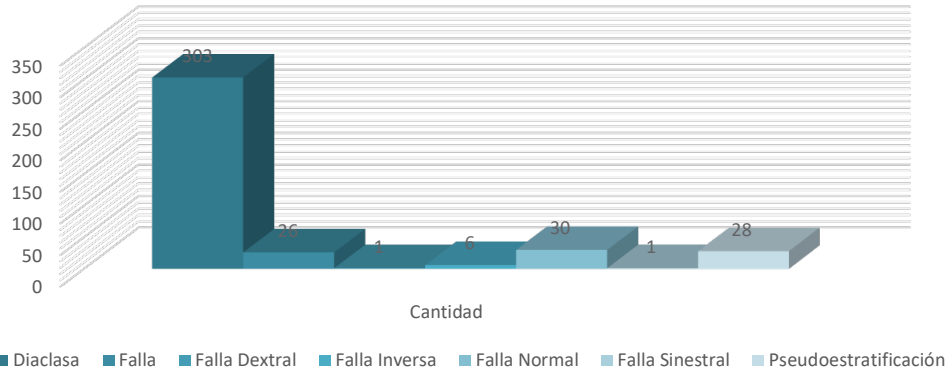


Rugosidad JRC



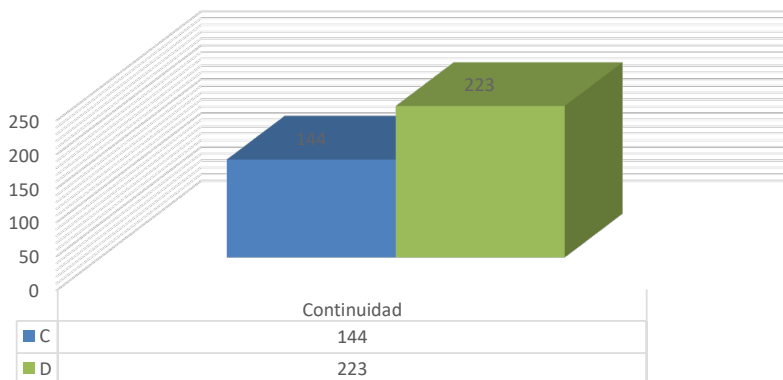
Silala Grande

Estructuras Silala Grande



Estructuras	Cantidad
Diaclasa	303
Falla	26
Falla Dextral	1
Falla Inversa	6
Falla Normal	30
Falla Sinestral	1
Pseudoestratificación	28

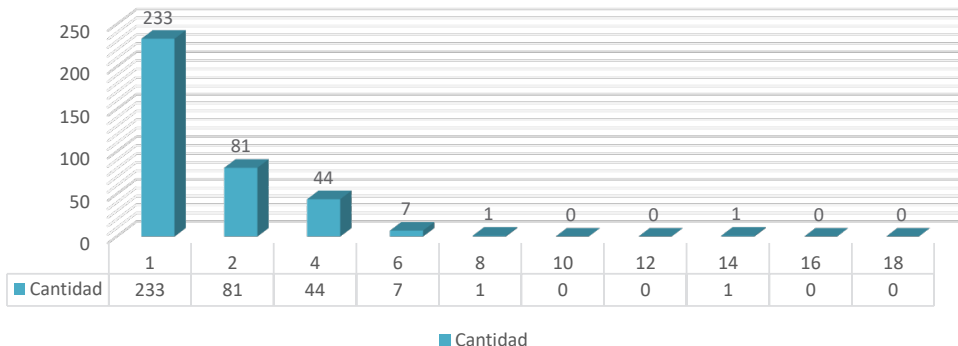
Continuidad



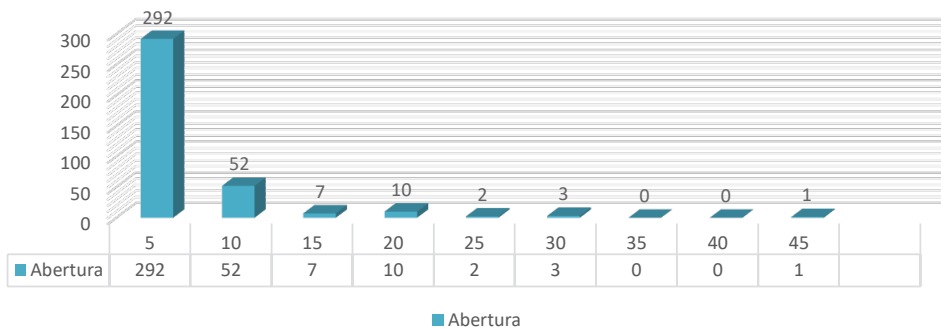
DIRECCIÓN TÉCNICA DE PROSPECCIÓN Y EXPLORACIÓN
“ESTUDIO GEOLÓGICO-ESTRUCTURAL DEL ÁREA
CIRCUNDANTE DEL MANANTIAL DEL SILALA”



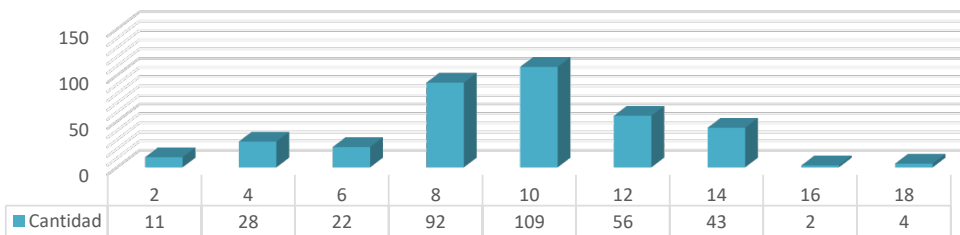
Persistencia



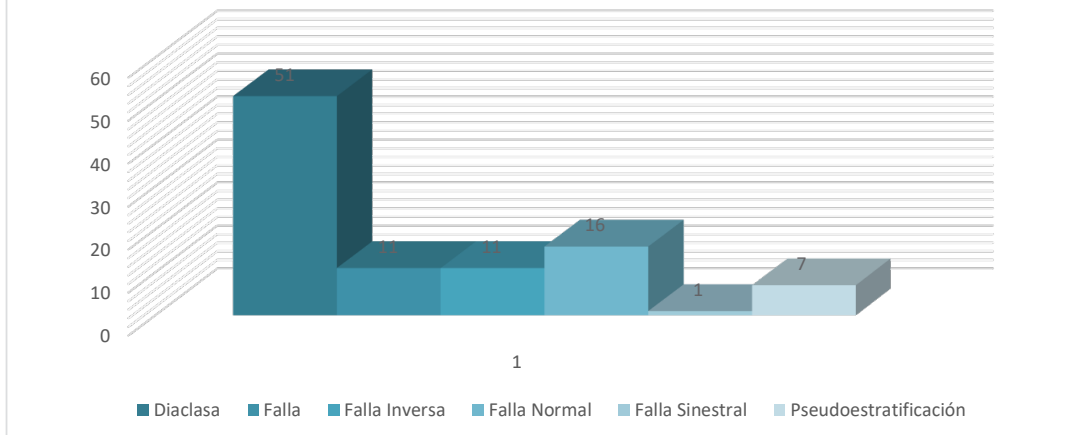
Abertura



Rugosidad JRC

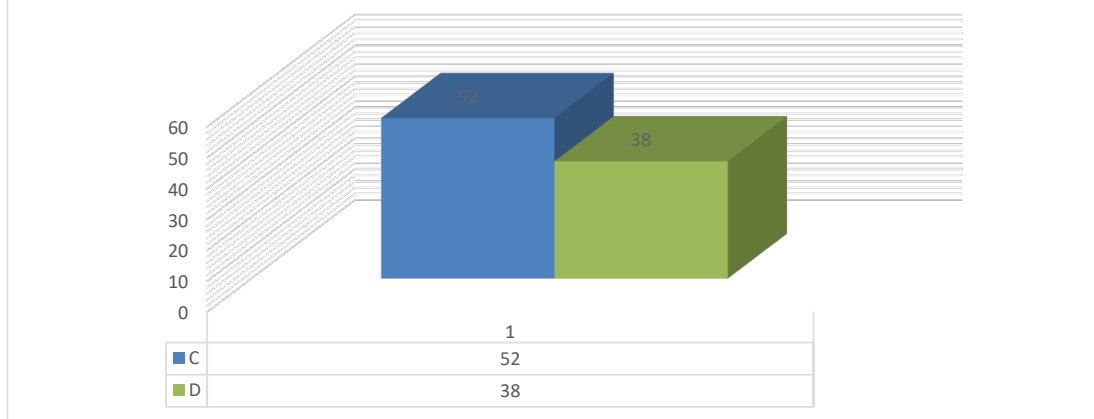


Estructuras Cerro Cahuana



Estructuras	Cantidad
Diaclasa	51
Falla	11
Falla Inversa	11
Falla Normal	16
Falla Sinestral	1
Pseudoestratificación	7

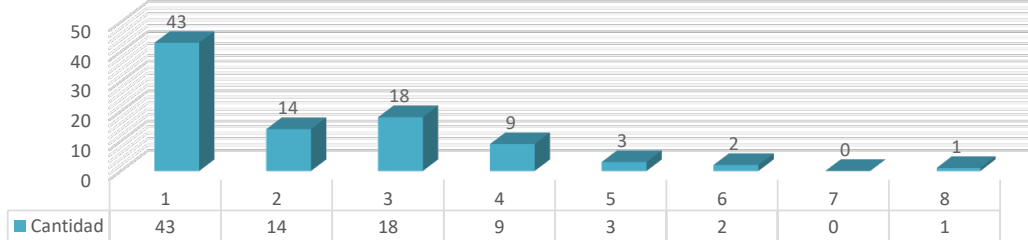
Continuidad



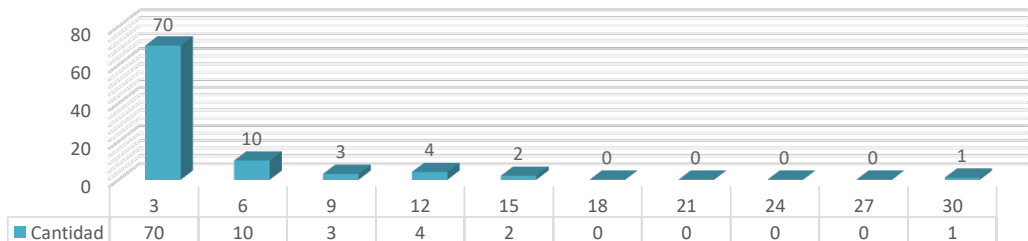
DIRECCIÓN TÉCNICA DE PROSPECCIÓN Y EXPLORACIÓN
“ESTUDIO GEOLÓGICO-ESTRUCTURAL DEL ÁREA
CIRCUNDANTE DEL MANANTIAL DEL SILALA”



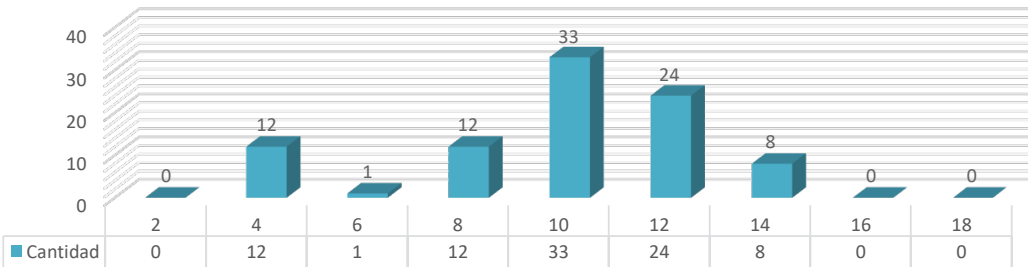
Persistencia



Abertura

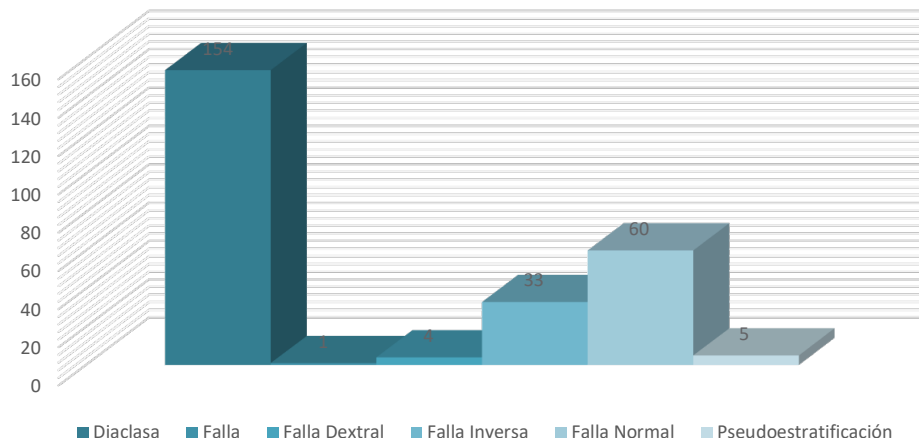


Rugosidad JRC



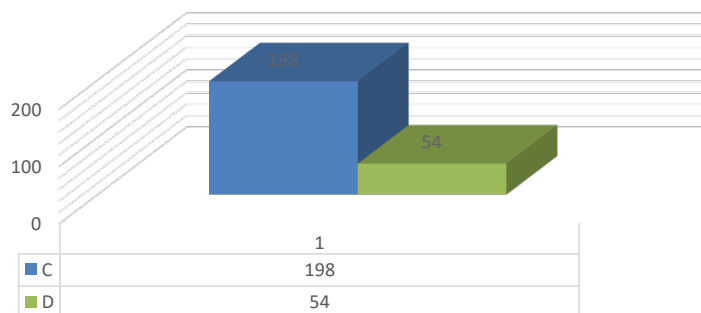
Pastos Grandes

Estructuras Pastos Grandes

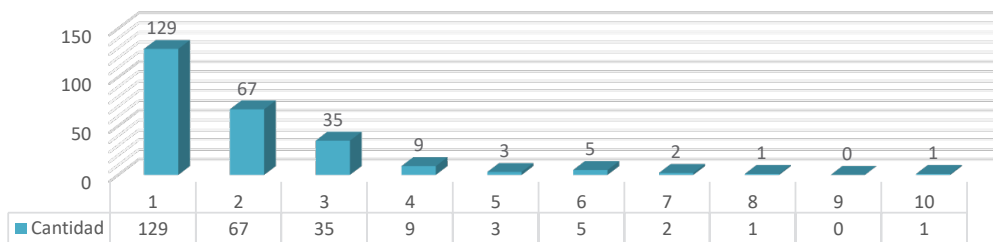


Estructuras	Cantidad
Diaclasa	154
Falla	1
Falla Dextral	4
Falla Inversa	33
Falla Normal	60
Pseudoestratificación	5

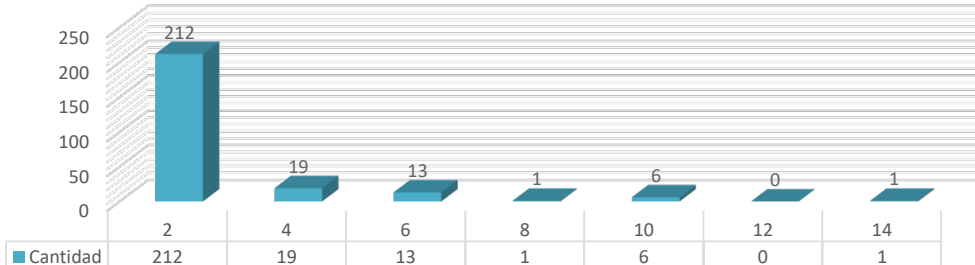
Continuidad



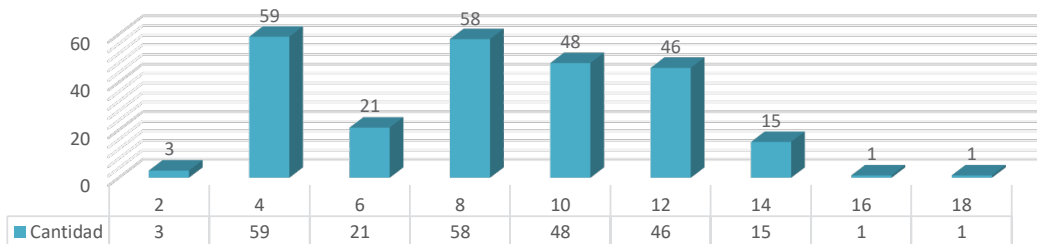
Persistencia



Abertura

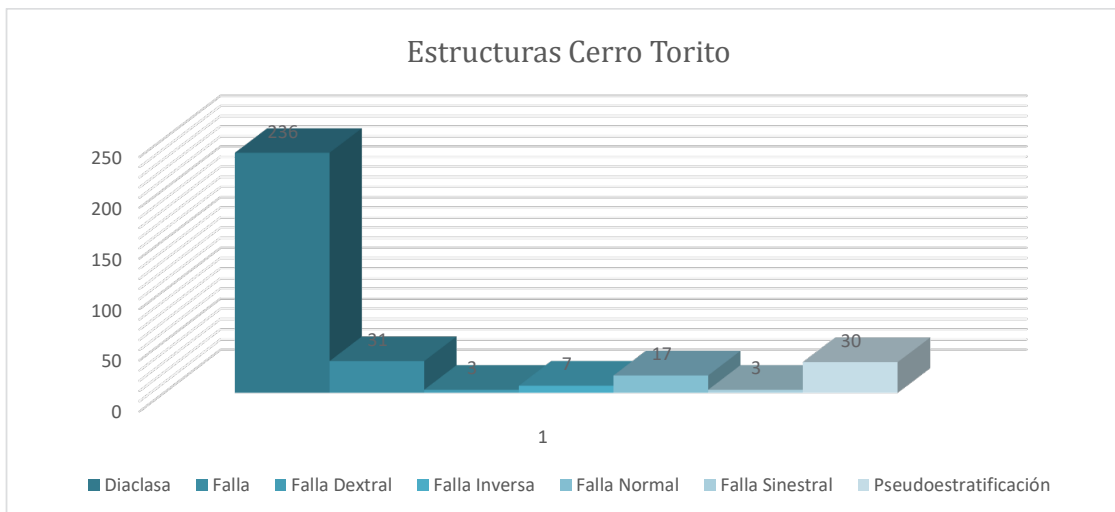


Rugosidad JRC



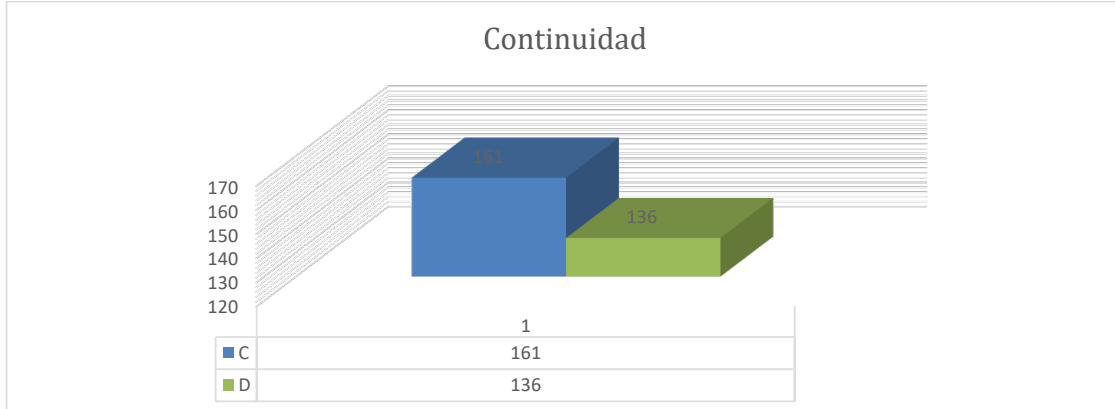
Cerro Torito

Estructuras Cerro Torito

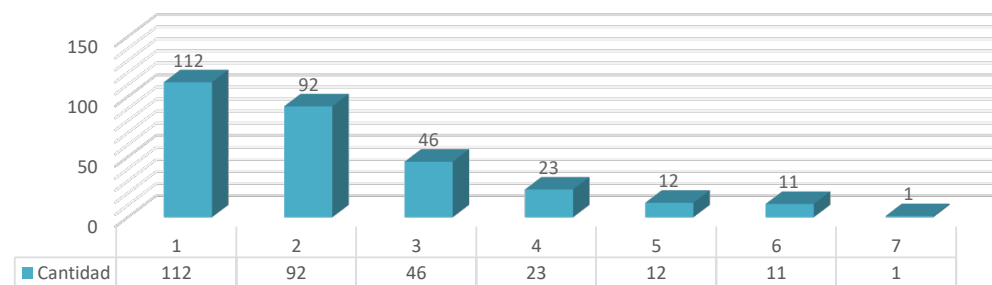


Estructura	Cantidad
Diaclasa	236
Falla	31
Falla Dextral	3
Falla Inversa	7
Falla Normal	17
Falla Sinistral	3
Pseudoestratificación	30

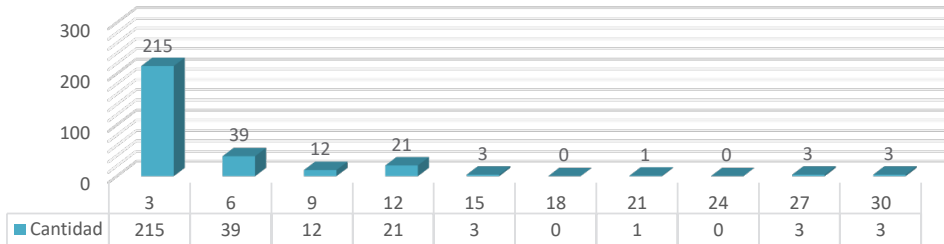
Continuidad



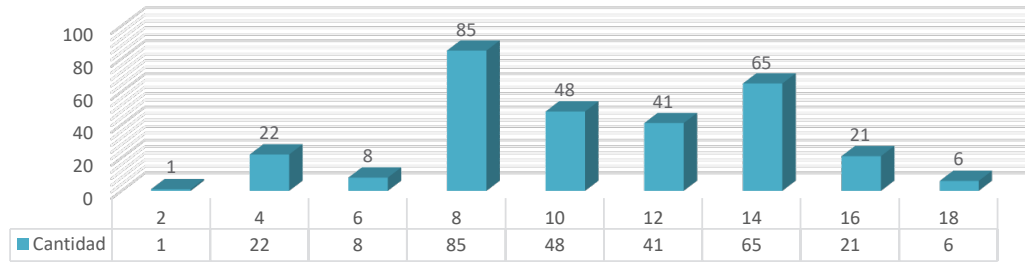
Persistencia



Abertura

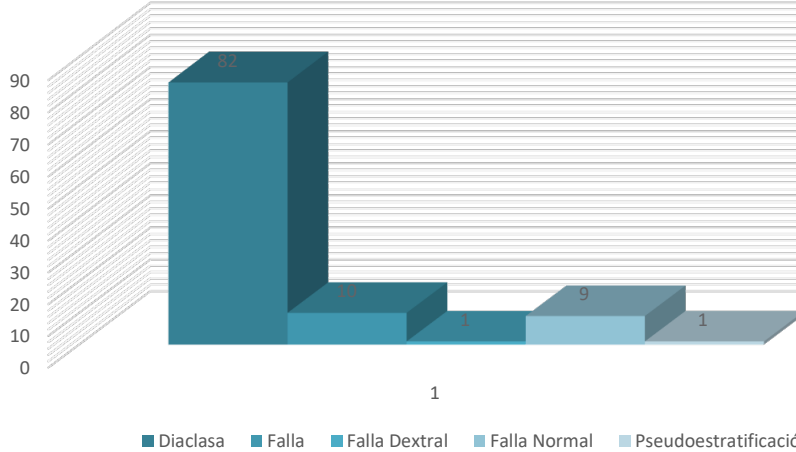


Rugosidad JRC



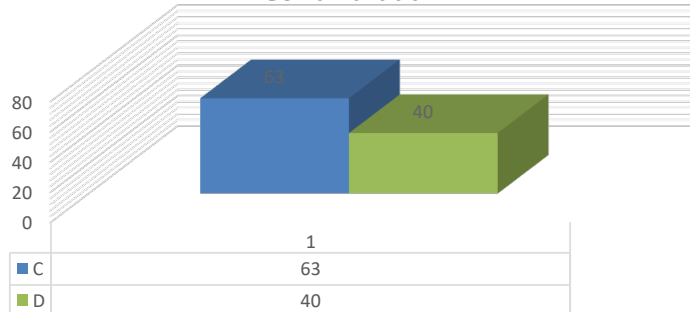
Cerro Negro

Estructuras Cerro Negro

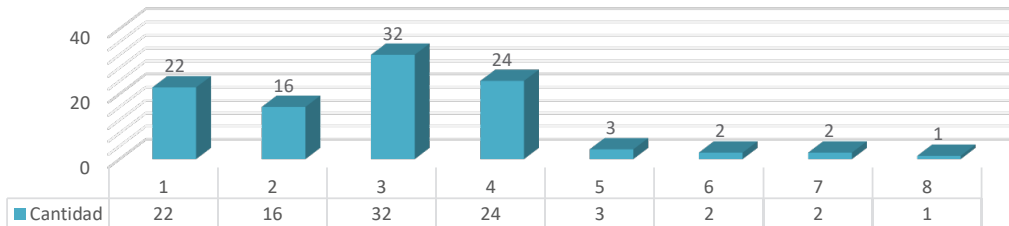


Estructuras	Cantidad
Diaclasa	82
Falla	10
Falla Dextral	1
Falla Normal	9
Pseudoestratificación	1

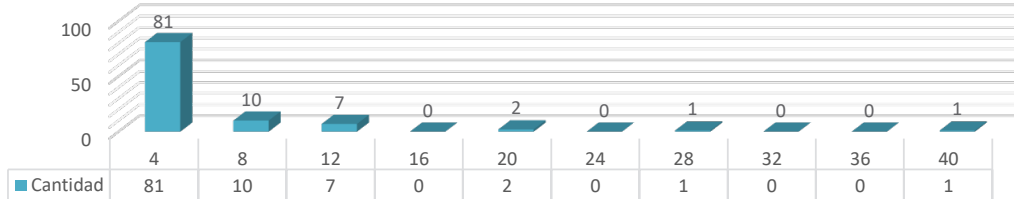
Continuidad



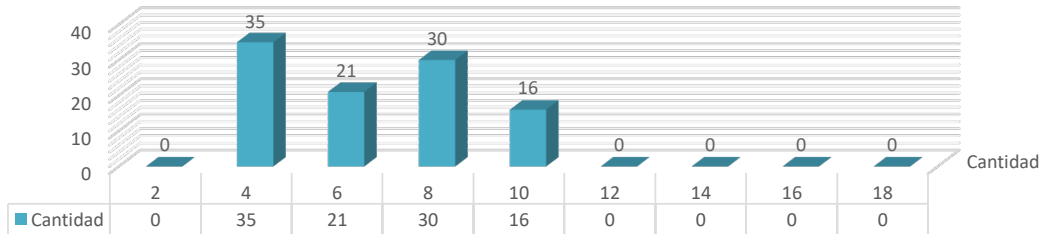
Persistencia



Abertura

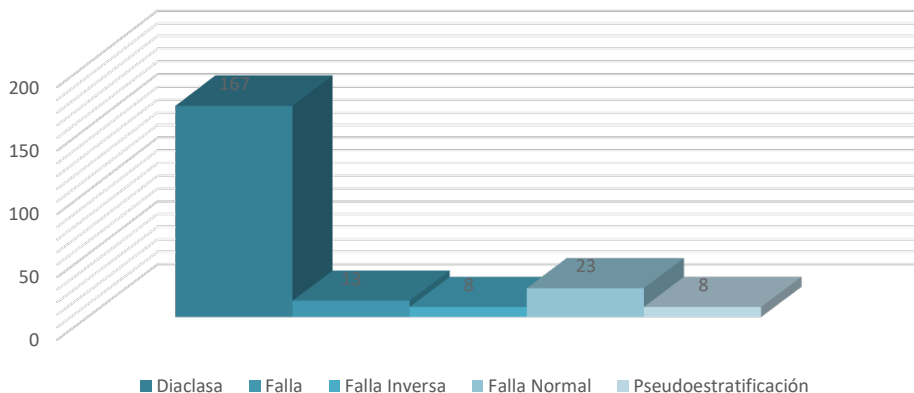


Rugosidad JRC



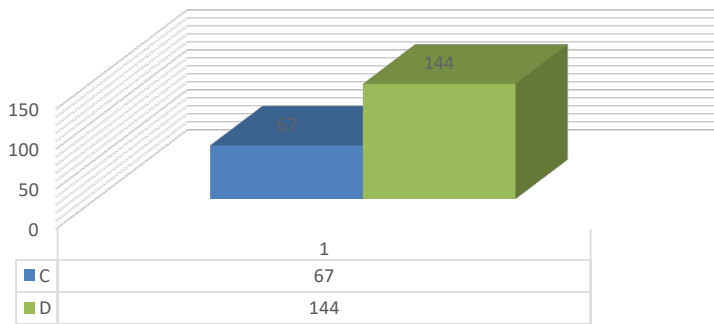
Silala Chico

Estructuras Silala Chico

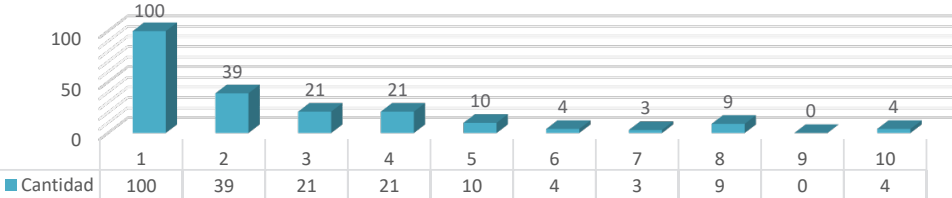


Estructuras	Continuidad
Diaclasa	167
Falla	13
Falla Inversa	8
Falla Normal	23
Pseudoestratificación	8

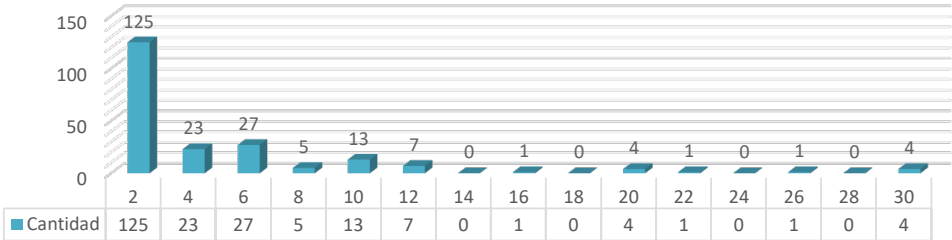
Continuidad



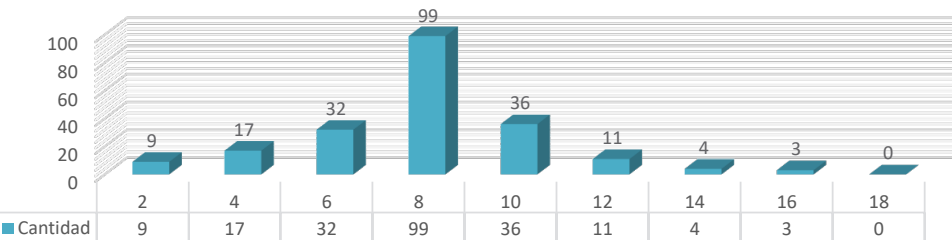
Persistencia



Abertura

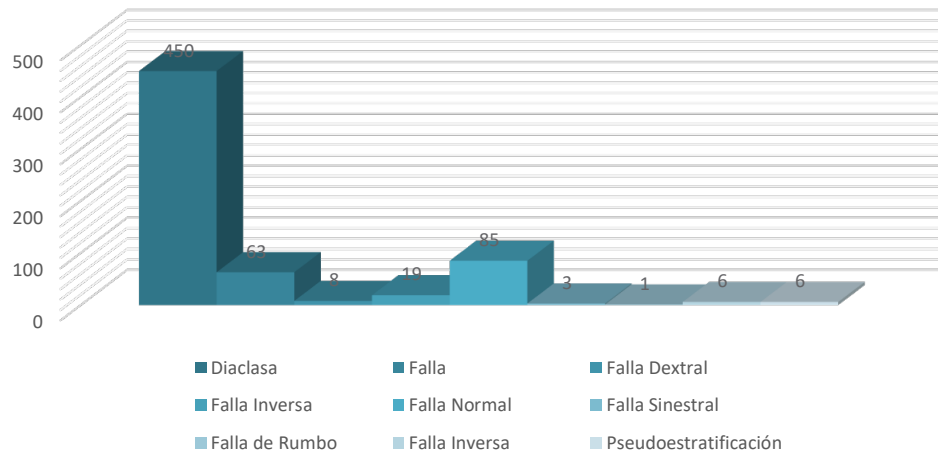


Rugosidad JRC



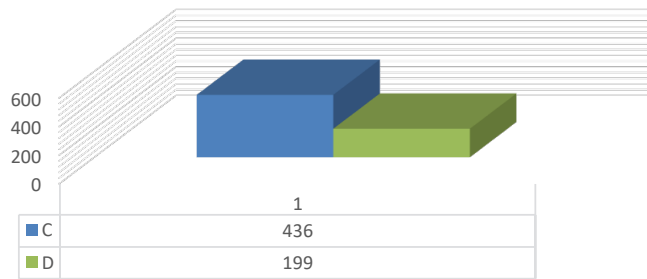
Ignimbritas Silala

Estructuras Ignimbritas Silala



ESTRUCTURAS	Cantidad
Dioclase	450
Falla	63
Falla Dextral	8
Falla Inversa	19
Falla Normal	85
Falla Sinestral	3
Falla de Rumbo	1
Falla Inversa	6
Pseudoestratificación	6

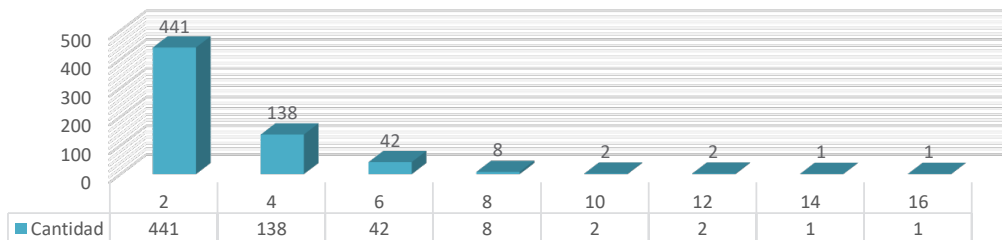
Continuidad



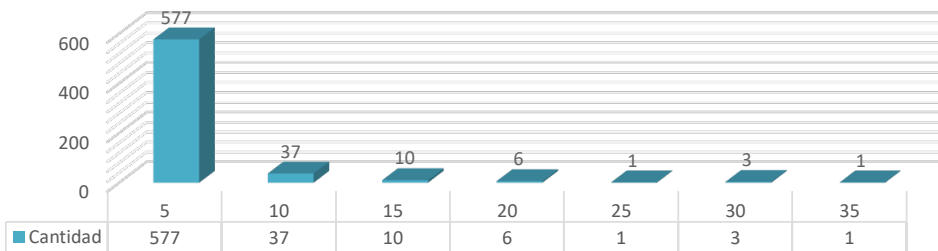
DIRECCIÓN TÉCNICA DE PROSPECCIÓN Y EXPLORACIÓN
“ESTUDIO GEOLÓGICO-ESTRUCTURAL DEL ÁREA
CIRCUNDANTE DEL MANANTIAL DEL SILALA”



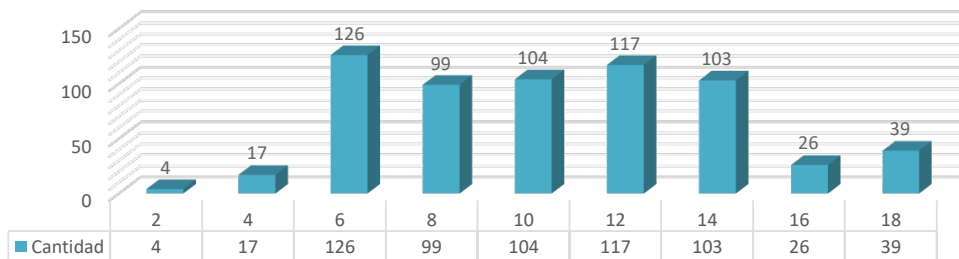
Persistencia



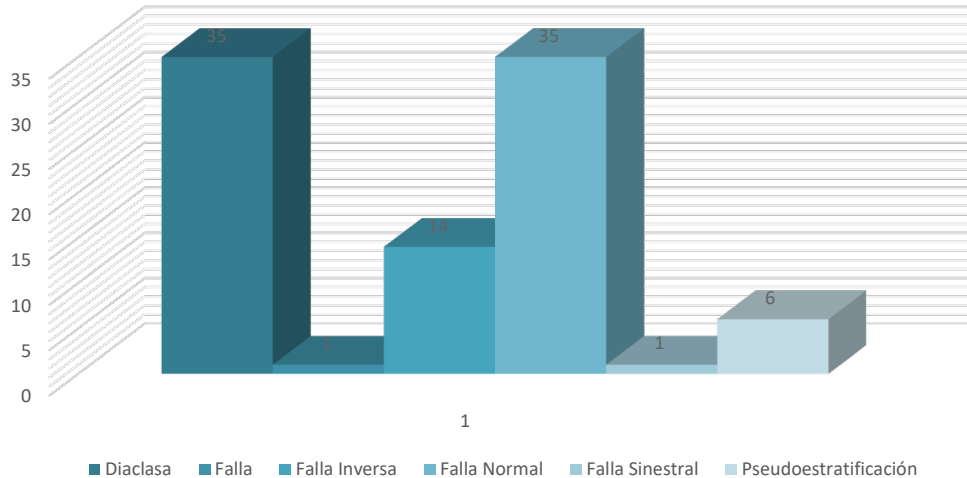
Abertura



Rugosidad JRC



Estructuras Cerro El Meson



Estructuras

Cantidad

Diaclasa
 Falla
 Falla Inversa
 Falla Normal
 Falla Sinistral
 Pseudoestratificación

35

1

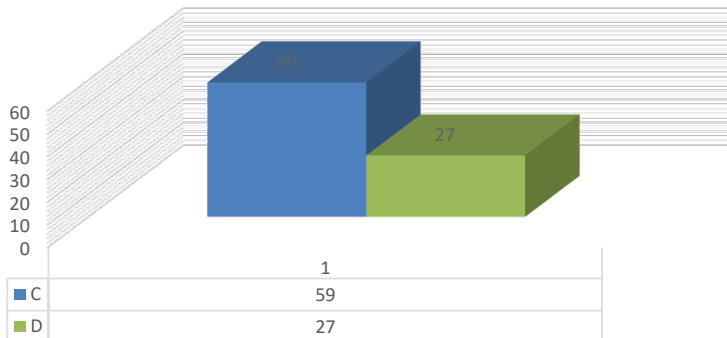
14

35

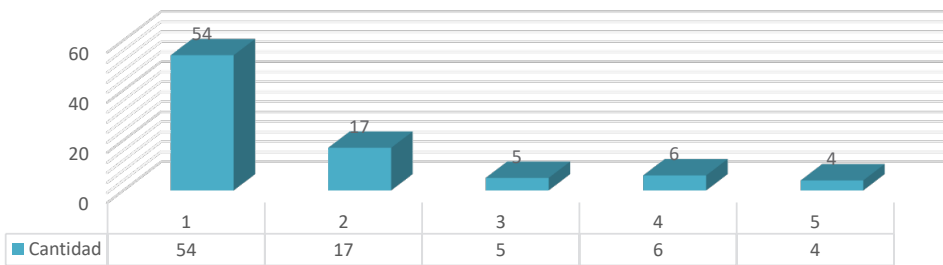
1

6

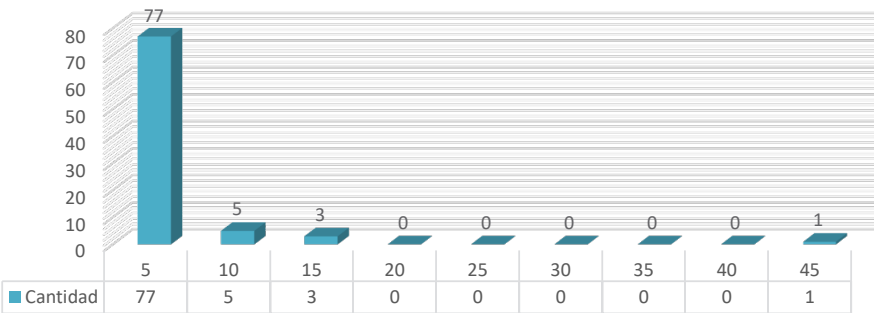
Continuidad



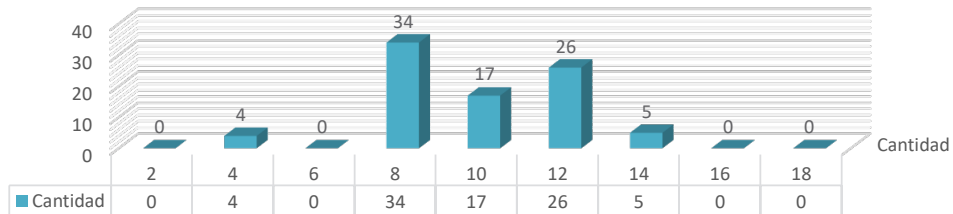
Persistencia



Abertura

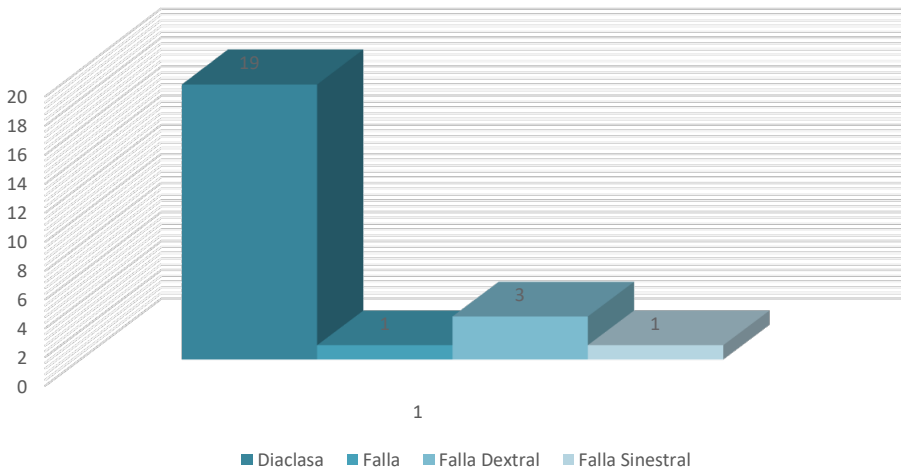


Rugosidad JRC



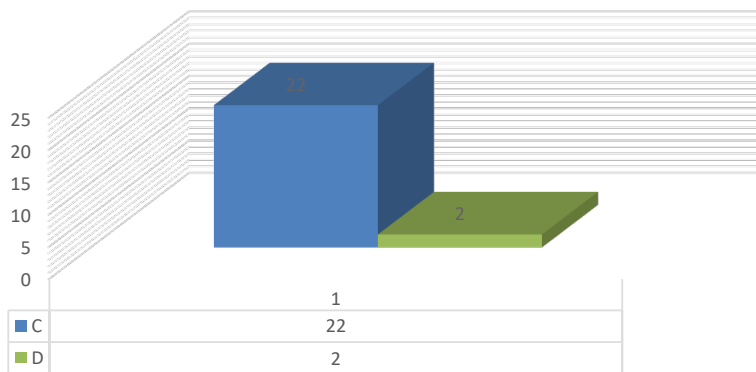
Cerro Chascón

Estructuras Cerro Chascon

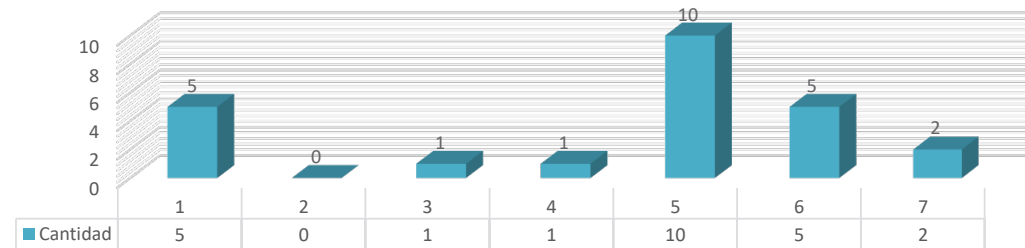


ESTRUCTURAS	Cantidad
Diaclasa	19
Falla	1
Falla Dextral	3
Falla Sinestral	1

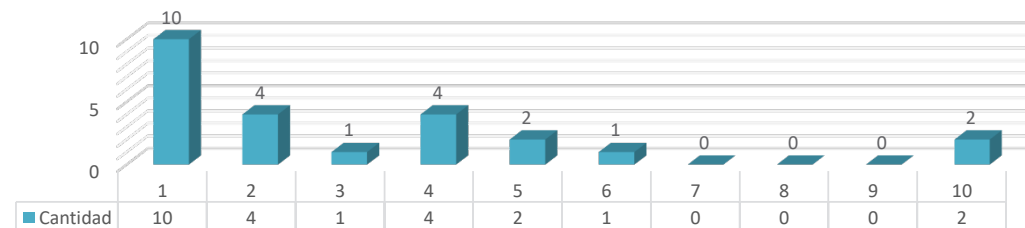
Continuidad



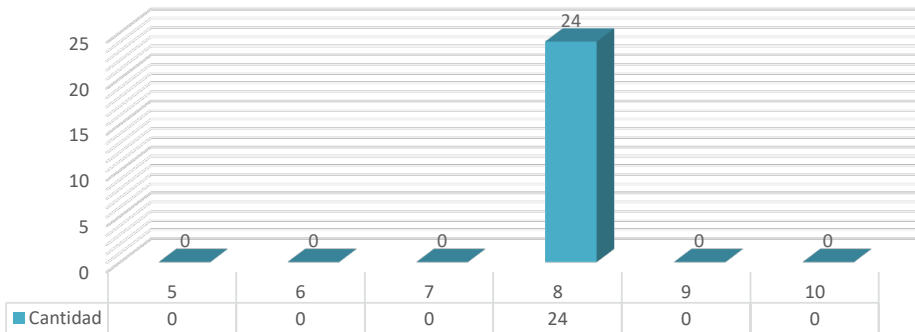
Persistencia



Abertura

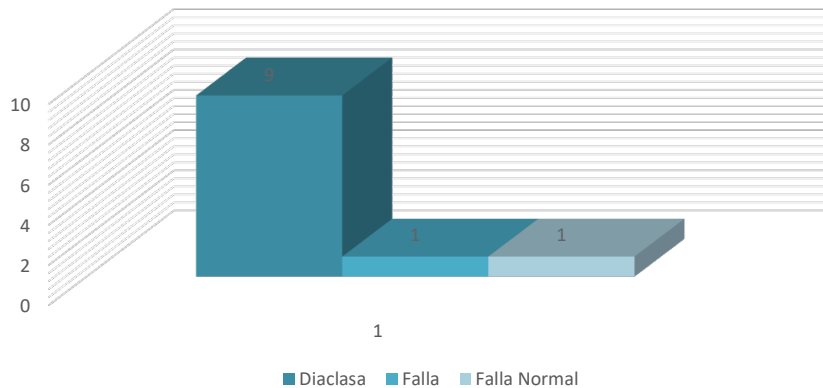


Rugosidad JRC



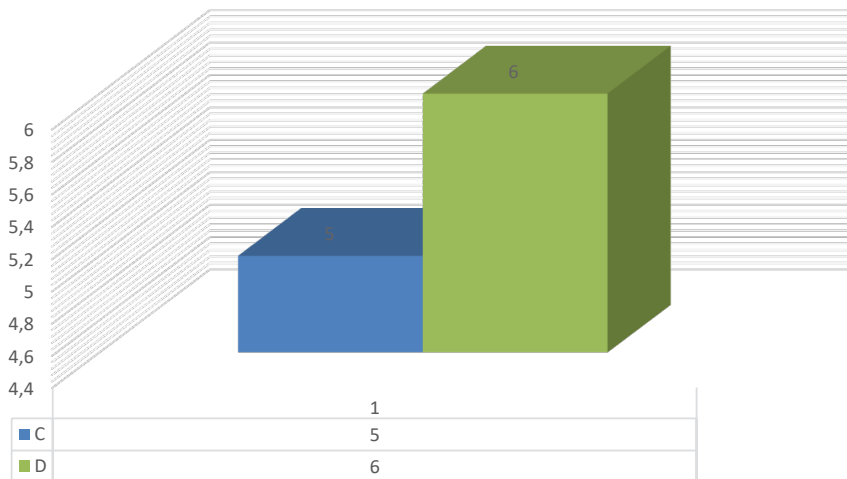
Cerro Capina

Estructuras Cerro Capina

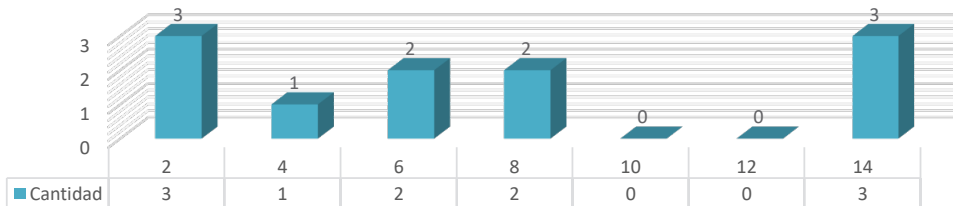


ESTRUCTURAS	Cantidad
Diaclasa	9
Falla	1
Falla Normal	1

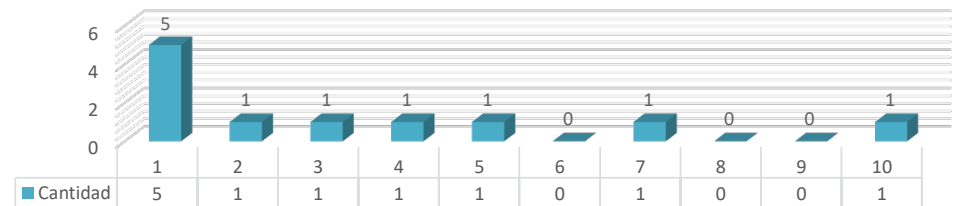
Continuidad



Persistencia



Abertura



Rugosidad JRC

